Identification of Astrocytic Factors That Could Play a Role in Myelination

Hülya Kıray
(B.Sc, M.Res)

A thesis submitted in fulfilment of the requirements of the University of Glasgow for the degree of Doctor of Philosophy

College of Medical, Veterinary and Life Sciences
Institute of Infection, Immunity and Inflammation
University of Glasgow

April 2015

Knowledge should mean a full grasp of knowledge:

Knowledge means to know yourself, heart and soul.

If you have failed to understand yourself,

Then all of your reading has missed its call.

Yunus Emre

(1240-1321, Eskisehir, Turkey)

Acknowledgments

I would like to thank to all those who helped me complete this PhD project despite its ups and downs throughout the years. It has been a long journey for me and I am truly proud of myself for being able to finish this great responsibility.

Firstly, I would like to thank the Wellcome Trust 4-Year PhD Programme for funding my studies and hence making it possible for me to take part in a PhD programme in the UK. I would like to thank the leaders of the Programme, Prof Darren Monckton and Dr. Olwyn Byron, and Prof Bill Cushley, the former head of the Programme, for giving me the chance to take part in this Programme. They were not just welcoming upon our arrival at the University but have continued to support us throughout the years whenever we needed help and courage.

I would like to extend my thanks to my supervisor, Prof Sue Barnett, for her help and support and for giving me the opportunity to study what I wanted to study in the Glial Cell Biology Group, consisting of friendly and helpful researchers. Besma Nash, Jennifer Higginson, Kalliopi Ioannidou, Michael McGrath, Michael Whitehead, Paul O'Neill, Peter Donoghue, Rebecca Lamond, Stephanie Boomkamp, Steven Johnstone and Susan Lindsay deserve special thanks for each teaching me something new (science-related or not), for the creative and very artistic birthday decorations, the chatty lunches that had to end with the horoscopes every day, reminding me of the things I kept forgetting and much more. Thanks to Stephanie also for our castle trips, a hobby that we acquired to lighten our dull weekends. Thanks especially to Besma, whose completed project gave inspiration for mine and thereby provided ideas. Her collecting some culture samples to be used in my project was invaluable. I would also like to thank the members of the groups of Prof Chris Linington and Prof Hugh Willison for allowing us to borrow their reagents and to use their instruments, for contributing a lot to our discussions in the lab meetings, the crowded Christmas lunches and much more. Thanks to our collaborators Dr Martin McBride and Dr John McClure, as well, for their enormous help with the microarray experiment.

The staff of Univeristy of Glasgow Biological Services Central Research Unit deserve the warmest thanks, as well. The head of the Unit, Colin Hughes, and his great team; Anthony McDermott, Craig Begley, Dennis Duggan, Douglas Robertson, Joanne Battersby, John Pearson and Stuart Lannigan, thank you all for your enormous help.

Thanks also to the other students of the Wellcome Trust PhD Programme 2009. We started this journey together. Charlie Scott, Daniela Pajek Michlmayr, David Rodgers,

Kate Beckham, and Lenka Richterova, thank you all for helping me have a smoother settling-in period in Glasgow. I would like to thank especially Daniela and Lenka for letting us create such a sincere and strong bond that will hopefully last forever.

I would also like to thank my friends, some of whom I have known for more than ten years. Bagdeser Akdogan, Benura Azeroglu, Esra Yalcin, Melis Duner, Ozge Korukmez, Sermin Meliha Paksoy Kucuk, and Yesim Yigit Fidan were always there for me when I needed their support and comforting words despite the long distances between us. I can write a separate essay for each of them but the space limitations do not allow that. Thanks girls! Benura, special thanks go to you for so many reasons I cannot list in here but to summarise it all, thanks for feeding me with your own hands when I was too weak to do so and for repeating your motto in such a charismatic way: “Everything will be alright.”

I cannot forget my previous teachers, who have inspired me in many ways. Thanks Ms. Aysel Oztemizer for encouraging me to go further and apply to a very prestigious school that I had never thought it possible for myself to enter there until then. Thanks Mr. Louis Ungemach for giving your Biology lessons with such enthusiasm and creativity throughout our high-school years. My undergrad years introduced me to Prof Avni Kuru, whose friendship and unique personality motivated me to continue asking my never-ending “But why?” questions. Thanks for trying to answer them as patiently as you could.

Lastly, my family and my beloved one deserve the most special thanks for their support, patience and purely for their presence.

Table of Contents

List of Figures

CHAPTER 1

CHAPTER 2

CHAPTER 3

CHAPTER 4

CHAPTER 5

CHAPTER 6

APPENDIX

List of Tables

CHAPTER 6

CHAPTER 7

APPENDIX

List of Abbreviations

ANOVA	Analysis of variance
AP-1	activator protein-1
BBB	blood brain barrier
cAMP	cyclic adenosine monophosphate
cDNA	complementary deoxyribonucleic acid
CNTF	ciliary neurotrophic factor
CNS	central nervous system
Cre	Cre recombinase
CREB	cAMP responsive element binding protein
cRNA	complementary ribonucleic acid
CSF	cerebrospinal fluid
Ct	threshold cycle
CTGF	connective tissue growth factor
DIV	days *in vitro*
DMEM	Dulbecco's Modified Eagle's Medium
DMEM-BS	Dulbecco's Modified Eagle's Medium modified from Bottenstein and Sato, 1979
dNTP	deoxynucleotide triphosphate
EAE	experimental autoimmune encephalomyelitis
ECM	extracellular matrix
EDTA	ethylenediamine tetraacetic acid
EGF	epidermal growth factor
FBS	fetal bovine serum
Gapdh	glyceraldehyde-3-phosphate dehydrogenase
GFAP	glial fibrillary acidic protein
Gp130	glycoprotein 130
HBSS	Hank's balanced salt solution
ICER	inducible cAMP early repressor
ILMN	Illumina
IPA	Ingenuity pathway analysis
KO	knocokout
LoxP	locus of crossover in P1
LPS	lipopolysaccharide
MBP	myelin basic protein
Mmp	matrix metalloproteinase
mRNA	messenger ribonucleic acid
MS	multiple sclerosis
NsM	neurosphere media
OPC	oligodendrocyte progenitor cell
PAI-2	plasminogen activator inhibitor 2
PANTHER	protein analysis through evolutionary relationships
PBS	phosphate-buffered saline
PDGF	platelet-derived growth factor beta
PLL	poly-L-lysine
PLP	myelin proteolipid protein
PM	plating medium

qRT-PCR	quantitative reverse transcriptase-polymerase chain reaction
RCF	relative centrifugal force
rpm	revolutions per minute
SD	Sprague Dawley
SLC	solute carrier
Th1	T helper cell type 1
TnC	tenascin C

Abstract

Multiple sclerosis (MS) is generally considered to be an autoimmune disease; it results in areas of focal demyelination known as plaques, where astrocytes are the main constituent and appear hypertrophic and stellate with increased expression of glial fibrillary acidic protein (GFAP). Although these reactive astrocytes can be beneficial for encapsulating areas of tissue necrosis within the glial scar, the pro-inflammatory cytokines and extracellular molecules they secrete are thought to be inhibitors of remyelination. Conversely, astrocytes can secrete anti-inflammatory cytokines in their less activated state and thereby can be beneficial for remyelination; although the mechanisms involved are not clearly understood. We have developed myelinating cultures of embryonic rat mixed spinal cord cells that are plated on neurosphere-derived astrocyte monolayers, which allow us to manipulate their reactive state and determine any effects of these astrocytes on myelination. To identify any differences in gene expression profiles of several purified astrocyte phenotypes we carried out a microarray analysis using myelinating cultures plated on astrocytes on poly-L-lysine (PLL-astrocytes) or on tenascin C (TnC-astrocytes), untreated or treated with ciliary neurotrophic factor (CNTF) since it was previously shown that CNTF could stimulate myelination in these myelinating cultures and that TnC-astrocytes supported myelination less than PLL-astrocytes. The microarray analysis suggested CCL2, CCL7 and SERPINB2 as potential myelination regulators, which were validated by qRT-PCR but failed to affect axonal ensheathment in myelinating cultures. A metabolomics analysis was also carried out using untreated or CNTF-treated PLL- and TnC-astrocytes. A list of metabolites were associated with different astrocyte phenotypes and highlighted the importance of lipid metabolism, which might be crucial for stimulating myelination. These *in vitro* astrocyte phenotypes were compared with previously identified *in vivo* astrocyte reactivity markers, which suggested that PLL- and TnC-astrocytes could reflect *in vivo* astrocytes to some extent and that TnC-astrocytes might not be as "quiescent" as currently considered. It is possible that TnC-astrocytes suppress myelination by creating an extracellular matrix (ECM) rich environment, while CNTF dissolves the ECM and thus creates a more regenerative environment. Despite similar stimulatory effects of CNTF on mixed neural cells on PLL and TnC, CNTF appears to affect them via different mechanisms showing that distinct reactive astrocytes could react to the same stimulus in different ways as also presented in *in vivo* studies.

Author's Declaration

I declare that, except where explicit references is made to the contribution of others, that this dissertation is the result of my own work and has not been submitted for any other degree at the University of Glasgow or any other institution.

Signature _____

Printed name _____

Chapter 1

Introduction

1.1 Anatomy and function of the central nervous system with a specific focus on glial cells

The central nervous system (CNS) consists of the brain and the spinal cord, which are both separated from the rest of the body by the blood-brain barrier (BBB) that regulates the diffusion of molecules between the two tissues (Bradbury, 1993; Engelhardt, 2003). The CNS is derived from neuroepithelium, which consists of stem-like progenitor cells that give rise to immature neurons, basal progenitors, and radial glia (Gotz and Huttner, 2005). Radial glia cells not only can generate radial glia and immature neurons or basal progenitors through asymmetric cell divisions but also provide the progenitors that eventually differentiate into mature glial cells; namely, oligodendrocytes, ependymal cells, and astrocytes (Miyata et al., 2001; Noctor et al., 2001; Shimojo et al., 2011). Microglia, also a glial cell type, are not derived from neurepithelial cells unlike the rest of the CNS structures (Nayak et al., 2014).

Glial cells are found nearly in one to one ratio to neurons in human brains despite regional differences presenting lower glia/neuron ratio in the cerebellum and grey matter of the cerebral cortex as opposed to the rest of brain where glial cells outnumber neurons by a ratio of 10 (Azevedo et al., 2009; Herculano-Houzel, 2014). Unlike neurons that provide electrical transmissions, which allow for both conscious and autonomic behaviours (Zoidi and Dermietzel, 2002; Burdakov, 2004); glial cells were considered as the structural “glue” in the extracellular matrix to physically support neural networks rather than play active roles in the CNS (Virchow, 1859). Glial cells have gained more importance lately with their vital roles shown in brain physiology, metabolism, development and neurological diseases (Barres, 2008). Glial cells consist of the following cell types: astrocytes, microglia, oligodendrocytes, and ependymal cells (Somjen, 1988). Ependymal cells take place at the interface between the brain parenchyma and ventricles and are suggested to regulate the flow of substances through both sides of the interface (Jimenez et al., 2014): while, other glial cells take part in various crucial cellular functions such as regulation of synapse formation (Ullian et al., 2001) and synapse transmission (Fields and Stevens-Graham, 2002), providing neurons with metabolites as a source of energy (Wender et al., 2000; Magistretti, 2006; Lee et al., 2012), modulation of neuronal activity through the release of gliotransmistters (Volterra and Meldolesi, 2005), regulation of blood flow (Koehler et al., 2009) and many other developmental and homeostatic functions, some of which will be explained below in more detail.

1.1.1 Oligodendrocytes

Oligodendrocyte (OL) progenitor cells (OPCs) in the spinal cord are initially generated from ventral neuroepithelial cells (NECs) that take place at a specific domain of the ventricular zone termed pMN (Sun et al., 1998; Takebayashi et al., 2002) and also from dorsal NECs (Fogarty et al., 2005). The proliferating OPCs migrate away from these sites of origin and populate the entire spinal cord before differentiating into mature OLs. OPC production in the brain occur from ventral to dorsal regions in three waves, which are initiated in ventral neuroepithelium, lateral and the caudal ganglionic eminences (LGE/CGE), and cortex, respectively (Kessaris et al., 2006, 2008). While the first OPCs generated in the ventral forebrain almost disappear during postnatal period and are replaced by progenitors migrating from LGE/CGE; the majority of OPCs in most regions of the postnatal and adult telencephalon consist of LGE/CGE-derived populations and the cortex-derived populations that primarily inhabit cortex (Kessaris et al., 2006).

OLs go through several maturation stages, in which they show different morphology mostly in terms of their process numbers and expression profile (reviewed in Zhang, 2001; in Barateiro et al., 2014, Fig 1.1). OPCs take place at the very early stages of differentiation with their increased proliferation and migration capacity (Grinspan et al., 1995; Miller et al., 1998). As the OPCs differentiate into preoligodendrocytes, they increase the number of their cell processes, which increase even more and become ramified in immature oligodendrocytes that develop into post-mitotic cells (Armstrong et al., 1992; Grinspan et al., 1995). In the final stages of OL development, mature oligodendrocytes present extensive secondary branching, and extend membranes that contain myelin proteins and enwrap the neuronal axons tightly to provide their insulating myelin sheath. In cell cultures, where they do not have contact with axons, leaflets of flattened membrane stay connected to soma, which can be seen in Fig 1.1 (Gard et al., 1989).

The main function of OLs is to produce myelin sheaths that wrap axons in several layers and thus support the axonal signal conduction (Fig 1.2). One OL can extend multiple processes to the same or different axons to generate the myelin segments known as internodes (Fig 1.2). This ensheathment not only protects the axons and hence the neurons from the external chemical/physical insults but also facilitates axonal conduction by restricting the membrane depolarisation to the areas in between the internodes (Sherman et al., 2005). Thus, these areas, called nodes of Ranvier, provide rapid and saltatory nerve conduction (Fig 1.2). Both the nodal and the paranodal proteins are important for forming the right axo-glial junctions in order to initiate the myelination (Poliak et al., 2003). The myelination also depends on the presence of the

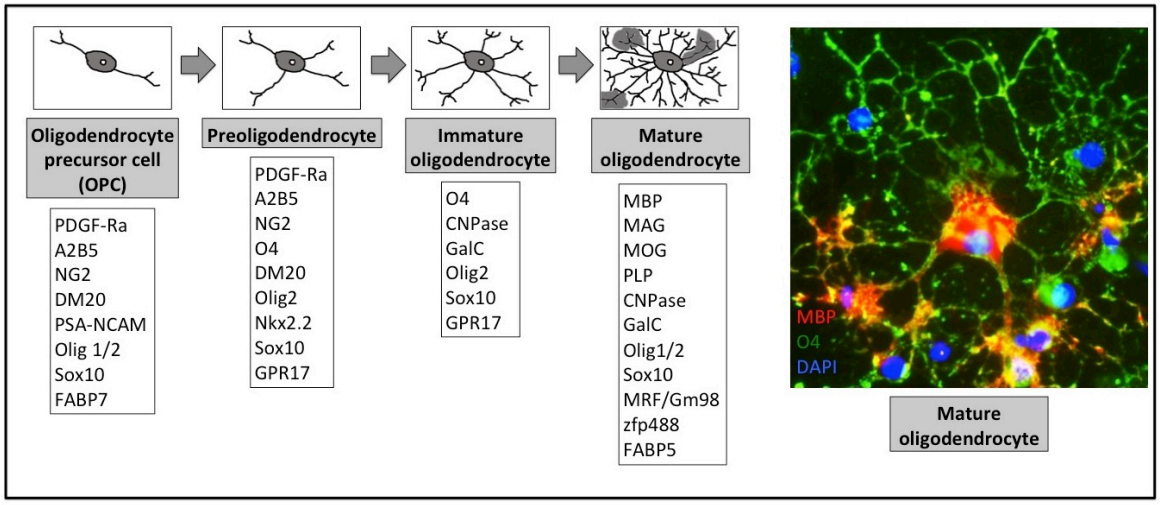

Figure 1. 1 The major maturation stages of oligodendroglial cells.
The basic morphology and the markers known to be expressed along the differentiation stages in the oligodendrocyte lineage are presented in the figure. An example of a mature oligodendrocyte, purified from primary rat cortical astrocyte cultures, is shown in the image on the right, where the markers MBP and the O4 antibody are shown in red and green, respectively. The cell nuclei are visualised by DAPI in blue. The schematic image was modified from Barateiro and Fernandes, 2014. CNPase: 2',3'-cyclic nucleotide 3'-phosphodiesterase; FABP: fatty-acid-binding proteins; GalC: galactocerebroside C; GPR17: G protein-coupled receptor; MAG: myelin associated glycoprotein; MBP: myelin basic protein; MOG: myelin oligodendrocyte glycoprotein; MRF: myelin gene regulatory factor; Nkx2.2: NK2 homeobox 2; PDGF-R: platelet-derived growth factor; PLP: proteolipid protein; PSA-NCAM: polysialic acid-neural cell adhesion molecule; zfp: zinc finger proteins.

type of extracellular ligands on the axons and the secreted molecules in the environment. For example, the axonal ligands Jagged, PSA-NCAM, LINGO-1 have been shown to inhibit either OPC differentiation or myelination; while, some others such as neuregulin and Wnt signaling have shown controversial effects on axonal ensheathment (Reviewed in Emery, 2010). Several oligodendroglial transcription factors such as Olig1/2, Ascl1, Nkx2.2, Sox6/10, YY1, Tcf4, Id2/4, Hes5, and Myrf have also emerged as intrinsic regulators of OPC differentiation and/or myelination (Emery, 2010).

Neuronal activity also appears to play a role in the capacity of OLs to myelinate axons. The presence of a crosstalk between neurons and OLs can regulate both the differentiation of OLs and myelination. For instance, active axons secrete adenosine, which then activates purinergic receptors on OPCs and promote their differentiation and myelination (Stevens et al., 2002). The crosstalk sometimes even includes astrocytes that for example can respond to axonal release of ATP by secreting the cytokine LIF, which in turn stimulates OLs to enhance myelination (Ishibashi et al., 2006). Moreover, the ionotropic glutamate receptors on OLs have been shown to respond to glutamate, exogenously added to the system, as well as to that released by neuronal activity (Yamazaki et al., 2007). Other types of neurotransmitter receptors are also present on

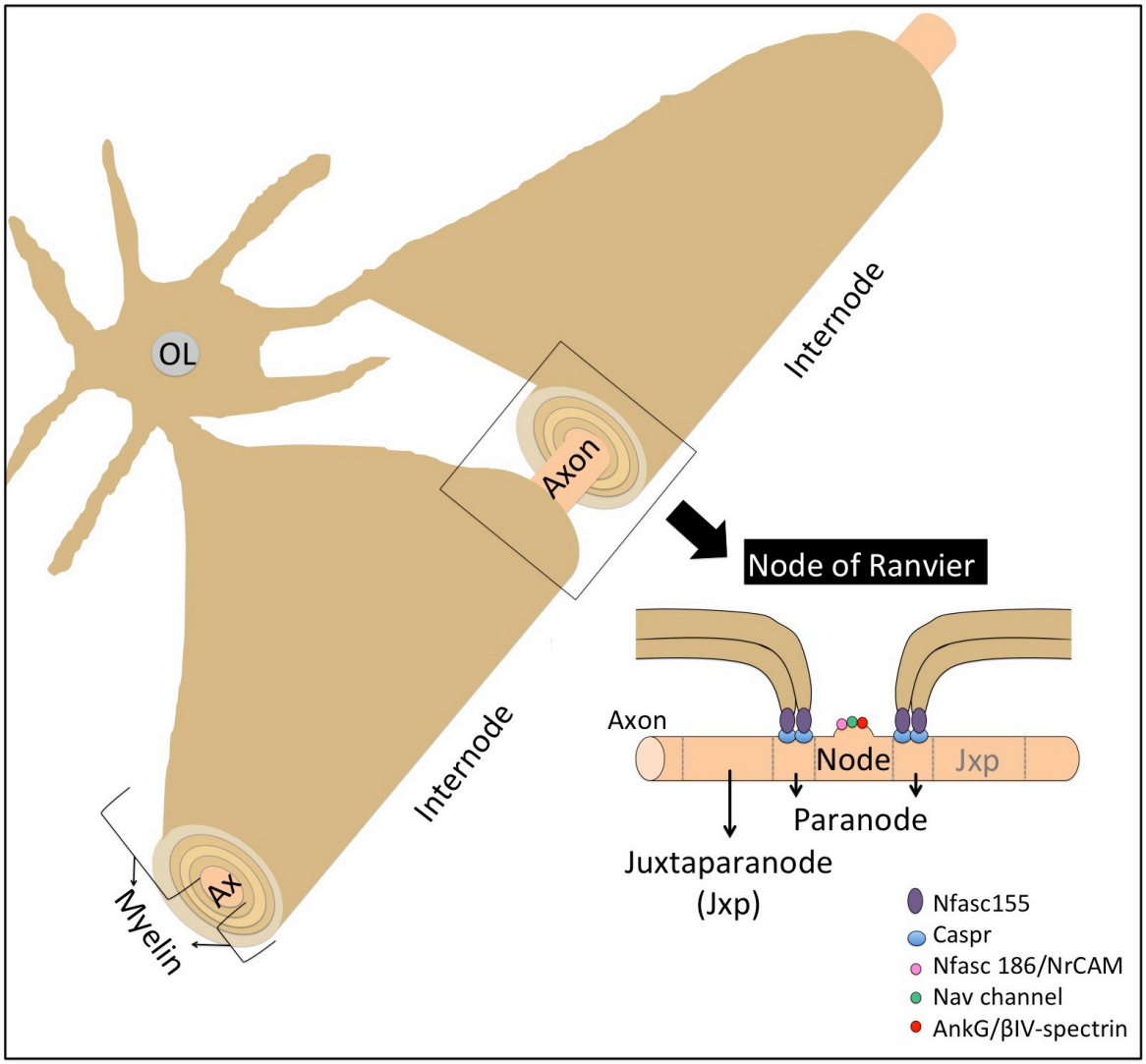

Figure 1. 2 The schematic of ensheathment of an axon by an oligodendrocyte.
An oligodendrocyte extends its processes that wrap the neighbouring axons in several layers. This membranious structure that encapsulates the oligodendrocyte (OL) cytoplasm has channels in between the layers that forms the myelin sheaths. Axons are myelinated intermittently forming internodes that can be seen above in the figure. The structures between the internodes are termed nodes of Ranvier and are also shown above in detail. The nodal and paranodal surface proteins contribute to the generation of healthy myelin sheaths. The figure was modified from Sherman and Brophy, 2005. AnkG: ankyrin G; Ax: axon; Caspr: contactin-associated protein; Nav channel: voltage-gated sodium channel; Nfasc: neurofascin

OLs such as ionotropic γ- aminobutyric acid (GABA) receptors that also initiate depolarisation in OLs upon activation (Gilbert et al., 1984; Berger et al., 1992; Yamazaki et al., 2010). The ion influx across the plasma membrane following the activation of such receptors is suggested to change the structure of the OL processes due to osmotic swelling. The tightness of the insulation, provided by myelin sheaths, might increase or decrease depending on those structural changes and thus facilitate or slow down the axonal conduction velocity, respectively (Karadottir et al., 2005; reviewed in Yamazaki et al., 2010). The conduction velocity might also be affected by the ability of OLs to dynamically and rapidly extend/retract their processes depending on the stimuli in the vicinity (Paez et al., 2007; Yamazaki et al., 2010). Consequently, OLs not only function in myelination but also appear to take part in the maintenance and regulation of it in later stages.

In addition to playing a role in myelination, OLs have also been reported to participate in neuronal survival and development. Targeted ablation of OLs in mice using diphtheria toxin have resulted in symptoms such as spastic paralysis, motor deficits, tremor, and ataxia, which have been associated with severe axonal injury detected as the accumulation of non-phosphorylated neurofilaments and amyloid precursor proteins (Ghosh et al., 2011; Pohl et al., 2011; Oluich et al., 2012). Secondary immune reaction and demyelination have been ruled out as causes for axonal injury in these animal models, which has left the lack of OLs as the primary cause. In addition, studies with transgenic animals showing abnormal expression of an oligodendroglial myelin protein (PLP, proteolipid protein) have presented axon degeneration that has been linked to decreased axonal transport of the proteins from soma (Griffiths et al., 1998; Gotow et al., 1999; Edgar et al., 2004; Edgar et al., 2010). Axon injury and motor neuron cell loss has also been observed in spinal cord organotypic cultures that were treated with an inhibitor to an extracellular membrane channel (MCT1), which is expressed predominantly in OLs and is suggested to function in the transport of lactate mainly out of cells (Lee et al., 2012b). Because extracellular lactate is important for the neuronal energy supply (Wyss et al., 2011) and because conditional down-regulation of *Mct1* in OLs has also lead to axon degeneration in mice, OLs are proposed to play role in the survival of neuronal cells (Lee et al., 2012b). The neurotrophins OLs produce also provide trophic support for both OLs and local neurons (Byravan et al., 1994; Dai et al., 2001).

Degeneration of OLs have been observed in some demyelinating diseases such as multiple sclerosis (MS), which presents symptoms such as numbness/tingling, weakness, spasticity, vertigo, and walking difficulties (Ozawa et al. 1994). Post-mortem tissue from MS patients and several animal models of MS have shown increased numbers of

early OL progenitors in the subventricular zone with the presence of certain progenitor markers and morphology that suggests that OPCs potentially migrate to the lesions to renew the lost OL numbers (Nait-Oumesmar et al., 2007; reviewed in Maki et al., 2013) and to provide remyelination (Prineas et al., 1993; Raine and Wu, 1993). Despite the presence of OPCs and pre-myelinating OLs in MS lesions, myelin repair is often insufficient or absent especially during chronic stages of the disease (Wolswijk, 1998; Chang et al., 2002), which is why studies are conducted to discover methods that provide a more regenerative environment allowing remyelination in these lesions (Huang et al., 2010; Rodgers et al., 2013). This and above-mentioned functions show how important OLs are and what a major role they play in the CNS.

1.1.2 Microglia

Microglia are the CNS-resident innate immune cells that constantly survey their local microenvironment with their dynamic processes and react rapidly to various pathologies. They constitute 10-15% of all glial cells in the CNS. Microglia were first considered to be of hematopoietic origin due to their phenotypic resemblance to peripheral monocytes/macrophages and dendritic cells (Hickey and Kimura, 1988; Eglitis and Mezey, 1997; Simard and Rivest 2004). Later it has been shown that they are derived from erythromyeloid progenitors cells in the yolk sac and migrate into the brain with the help of the circulatory system in early embryonic stages (Cuadros et al., 1993; Alliot et al., 1999; Schulz et al., Ginhoux et al., 2010; 2012; Kierdorf et al., 2013). During neonatal development, these microglial progenitors appear similar to macrophages morphologically but they eventually proliferate and differentiate into mature microglia with ramified processes. Their morphology presents differences mainly in terms of the length and number of their processes depending on their location in the adult brain showing that these cells are sensitive to their milieu (Lawson et al., 1990).

Microglia play a role in neuronal survival, neuronal apoptosis, synaptogenesis, defence against pathogens and clearing all the metabolic products and the debris of dying cells. They secrete growth factors such as IGF-1, FGF, NGF, BDNF, which play roles in neuronal development, maintenance and function (Araujo et al., 1992; Yamagata et al., 1995; Nakajima et al., 2001; Trang et al., 2011; Ueno et al., 2013). On the other hand, they can also stimulate the programmed cell death of neurons that show transient functions or are faulty due to defective differentiation or migration (Frade et al., 1998; Marin-Teva et al., 2004; Wakselman et al. 2008). In addition to that, microglia clean the resultant cellular debris through phagocytosis (Takahashi et al., 2005; Hristova et al., 2010). Microglia also secrete factors that are important for synaptic function and plasticity (Roumier et al., 2004; Wake et al., 2009; Paolicelli et al., 2011; Ji et al.,

2013). They can change their morphology and location in relation to synapses upon exposure to a sensory stimulus (Tremblay et al., 2010). In order to perform their functions, the resting (quiescent) microglia survey the CNS parenchyma and become activated upon encountering unhealthy cells, cellular debris, and any foreign antigens they cannot recognise such as those on pathogens (Garg et al., 2005; Morgan et al., 2005; Esen and Kielian, 2006; Herber et al., 2006; Faustino et al., 2011). The change in their morphology after the activation starts with extension of microglial processes towards the target, which is followed by migration of their cell bodies and phagocytosis (Catalin et al., 2013). They can even surround the lesion sites in various CNS injuries to protect the healthy CNS from the injured tissue in the vicinity (Dibaj et al., 2010).

Microglial dysfunction has been associated with some CNS diseases. For example, obsessive-compulsive disorder and Rett syndrome have been linked to mutations in some microglial transcriptions factors (Greer et al., 2002; Chen et al., 2010; Derecki et al., 2012). Other than that, functional microglia can sometimes exacerbate neurodegenerative conditions, where they initially play positive roles. They can phagocytose the toxic proteins that accumulate in patients with Alzheimer's and Parkinson's diseases but their production of pro-inflammatory cytokines at later stages can cause the pathology and hence the cognitive decline to progress (McGeer et al., 1988; Hickman et al., 2008; Heneka et al., 2010; Stefanova et al., 2011; Vom Berg et al., 2012; Krabbe et al., 2013). Similarly, microglia clear the myelin debris during the demyelination in multiple sclerosis but they can later present antigens to the infiltrating T-cells from periphery and also produce reactive-oxygen species and pro-inflammatory cytokines, which would aggravate the disease (Boyle and McGeer, 1990; Hao et al., 2010; reviewed in Ciccarelli et al., 2014). In addition, they can also secrete metalloproteinase proteins that would disrupt the blood brain barrier (BBB) integrity and elevate the inflammation (Yong et al., 1998; Maeda and Sobel, 1996).

These detrimental roles of microglia have been associated with their "classically activated M1 state", during which they are able to recognise harmful stimuli using various immune receptors such as toll-like receptors (TLRs), nucleotide-binding oligomerisation domains (NODs), CD68, Fcy, and many scavenger receptors; and react by secreting inflammatory cytokines such as TNFα, IL-6, IL-1β, IFNγ, and several chemokines (Ransohoff and Perry, 2009; Ransohoff and Brown, 2012; Boche et al., 2013). If M1 response is not down-regulated once the pathological stimulus is eradicated and persists for longer than normal, chronic inflammation can lead to tissue destruction as mentioned above (Perry and Teeling, 2013). The pro-inflammatory M1 response is usually followed by "alternatively activated M2" response, where microglia express cytokines and receptors to inhibit inflammation and restore homeostasis (Martinez et

al., 2009, Varin and Gordon, 2009). Therefore, the dysregulation of the transition from M1 state to M2 state might be contributing to disease progress in multiple sclerosis by prolonging the detrimental effects of pro-inflammatory cytokines in the CNS (Tanner et al., 2011; Cherry et al., 2014). M2-promoting cytokines such as IL-33 and IL-10 have been shown to decrease demyelination levels and improve clinical scores in an animal model of MS (Yang et al., 2009; Jiang et al., 2012), which can be attributed to the production of neurotrophic mediators such as IGF1, PDGFα, TGFß, and SPP1 that might support remyelination and regeneration as predicted from their up-regulation in M2 microglia during recovery (Olah et al., 2012). Therefore, the equilibrium between the resting microglia and their polarised states, M1 and M2; and the spatial and temporal regulation of these phenotypes appears to be important for the amelioration of CNS pathologies.

1.1.3 Astrocytes

Astrocytes are the most abundant glial cells in the CNS. They are distinguished from other glial cells by their stellate morphology, which is mainly divided into two subtypes. Protoplasmic astrocytes reside in gray matter and they morphologically have several stem branches which branch further into many fine processes; whereas, fibrous astrocytes reside throughout all white matter and have long fiber-like processes (Cajal, 1909). Astrocytes are found throughout the whole healthy CNS in a non-overlapping, highly well organized manner (Bush et al., 1999).

Astrocytes originate from neuroectoderm like other CNS cells apart from microglia. Neuroepithelial cells generate radial glial cells, which differentiate first into neurons and later become gliogenic to produce astrocytes (McConnel et al., 1992; Cepko et al., 1996). JAK-STAT signaling pathway, which is regulated by IL-6 family cytokines, is associated with the switch from the neurogenesis to astrogenesis in the progenitor cells (Barnabe-Heider et al., 2005; He et al., 2005). In mouse spinal cord, astrocyte progenitors appear between embryonic days (E) 13.5-15.5 in three subpopulations, VA1-3 (ventral astrocytes 1-3), which show differential expression of transcription factors that regulate the astrogenesis (Hochstim et al., 2008). The functional importance of these astrocyte subpopulations is not clear. In the cerebral cortex, astrocyte production from radial glial cells begins around E18.5 in the cortical subventrical zone, from where astrocytes migrate to other brain regions (Hochstim et al., 2008). In the adult cortex, fibrous and protoplasmic astrocytes have been recently shown to be derived from separate lineages (Garcia-Marques and Lopez-Mascaraque, 2013). Moreover, an additional astrocyte subtype, named pial astrocytes due to their presence at the pial surface, has also been shown to present a different developmental origin, morphology,

location and thus has been suggested to have a distinct function (Garcia-Marques and Lopez-Mascaraque, 2013). Such regional astrocyte subtypes are suggested to have different roles during development and most likely in adulthood (Molofsky et al., 2014; reviewed in Bayraktar, et al., 2015).

Despite the diverse functions of astrocytes (Section 1.2), there is one major immunostaining marker used in general for these cells. That marker is glial fibrillary acid protein (GFAP), which is an intermediate filament protein (Sofroniew and Vinters, 2010). Other markers have been used for immunohistochemical detection of astrocytes such as glutamine synthetase and S100β; however unlike GFAP, they are also expressed in neural cells such as neurons or oligodendrocytes (Norenberg, 1979; Cammer, 1990; Wang and Walz, 2003; Goncalves et al., 2008). GFAP was first isolated from multiple sclerosis patients' demyelinated plaques, where it was found in high concentrations (Eng et al., 1970). This led to the immunohistochemical association of GFAP with reactive astrocytes. GFAP expression is considered as a sensitive marker that labels most reactive astrocytes present in CNS injury sites although it does not label all non-reactive astrocytes in healthy CNS tissue or distant from CNS lesions (Sofroniew and Vinters, 2010). GFAP might still be expressed in these astrocytes in low levels but the current immunohistochemical techniques might not be sensitive enough to detect any such expressions.

Transcriptomic analyses recently carried out by comparing primary cultures of astrocytes, neurons, and oligodendrocytes in an attempt to detect cell type-specific transcriptional regulations have identified some other proteins highly expressed in astrocytes (Lovatt et al., 2007; Cahoy et al., 2008). For example, aldehyde dehydrogenase 1 L1 (Aldh1L1) enzyme has been proposed by Cahoy et al. (2008) as a more sensitive and reliable new immunohistochemical astrocyte marker. Their study has shown that Aldh1L1 is expressed specifically by astrocytes in the CNS, not being expressed in neurons, oligodendrocyets or in OPCs, and that it can label both astrocyte perikarya and processes throughout both grey and white matter unlike GFAP, which labels mainly thick main processes of astrocytes (Cahoy et al., 2008). In addition, all GFAP positive cells are also labelled with Adh1L1; whereas, the latter one potently labels many more astrocytes (Cahoy et al., 2008). These findings suggest that GFAP, the conventional, common marker for labelling astrocytes immunohistochemically, might be displaced with Adh1L1 in the near future.

1.2 Astrocytes and their roles in the CNS

1.2.1 The functions of astrocytes in the healthy CNS

1.2.1.1 Transport of ions and molecules into/out of cells

Astrocytes are suggested to form astroglial networks via their expression of membrane proteins connexins (Cxs) to provide intercellular communication (Giaume, 2010). Astrocytes are connected to each other at the very distal tips of their processes via gap junctions that can be detected at an ultrastructural level (Ogata and Kosaka, 2002). Gap junction channels (GJCs), constructed from connexin monomers, constitute a direct pathway between the cytoplasm of two adjacent astrocytes and allow the transport of amino acids, metabolites, second messengers, and ions such as K^+, Ca^{2+}, and Na^+ (Ransom and Ye, 2005; Tabernero et al., 2006; Ransom and Giaume, 2012). Hemichannels (HCs), another connexin-based channel type, do not take part in astroglial networks directly. Nevertheless, they regulate the transport between the cell cytoplasm and extracellular space, which in turn provides paracrine and/or autocrine signaling that could be considered as a form of cell-to-cell communication, as well. HCs, unlike GJCs, are generally closed at resting membrane potential and normal concentrations of the intra/extracellular cations. However, a change in these conditions and/or the presence of other signals such as pro-inflammatory agents can activate these channels to allow the transport of molecules such as glutamate, ATP, and glucose (Spray et al., 2006; Retamal et al., 2007; Orellana et al., 2009, 2012).

Heterocellular coupling, provided by GJCs, has also been observed between astrocytes and other cells such as oligodendrocytes and neurons (Ransom and Kettenmann, 1990; Robinson et al., 1993; Venance et al., 1995; Maglione et al., 2010; Wasseff and Scherer, 2011). However, these couplings appear to be more restricted and developmentally regulated (Froes et al., 1999; Alvarez-Maubecin et al., 2000; Bittman et al., 2002; Pakhotin and Verkhratsky, 2005). They have been detected in developing tissues but not in adult animals, where functional astrocyte-astrocyte and neuron-neuron couplings are present (Cotrina et al., 2001; Peters et al., 2009; Cruz et al., 2010). These heterocellular couplings might therefore be important primarily for development.

Studies with knockout animals, where various connexin expressions are inhibited, suggest the importance of the communication between astrocytes, and between astrocytes and oligodendrocytes on myelin integrity. Myelin damage has been observed in Cx47, Cx43/Cx30, Cx30/Cx47 single/double knockout mice (Menichella et al., 2003; Odermatt et al., 2003; Lutz et al., 2009; Tress et al., 2012). Moreover, connexin

channels and hence connexin proteins have been demonstrated to play a role in the regulation of neuronal activity and survival (Barnett et al., 2001). For example, astroglial connexins decrease neuronal excitability by removing extracellular K+ and glutamate; while, they provide metabolic supply to neurons (Wallraff et al., 2006; Rouach et al., 2008; Froger et al. 2010; Pannasch et al., 2011). On the other hand, the elevation of connexin expression at lesion sites in CNS pathologies might also be associated with other (possibly protective) roles (Nagy et al., 1996; Koulakoff et al., 2008; Kuchibhotla et al., 2009; Mei et al., 2010; Karpuk et al., 2011).

More recently, another membrane channel family, pannexins (Panxs), has been identified (Panchin et al., 2000) and has been shown to form HCs-like channels but not any GJCs (Giaume et al., 2013). Even though less has been revealed about currently known two pannexins, Panx1 and Panx2, they have been both shown to be expressed in astrocytes (Zappala et al., 2007; Iglesias et al., 2009) in addition to Panx1 expression also in microglia and oligodendrocytes (Domercq et al., 2010; Orellana et al., 2011a). Panx channels (PCs) can be activated by positive transmembrane voltages and by increased intracellular free Ca^{2+} concentrations similar to HCs (Bennet et al., 2003; Locovei et al., 2006; Kienitz et al., 2011; Ma et al., 2012b). Both HCs and PCs provide the release of precursor and signaling molecules (e.g., NAD+, ATP, adenosine, inositol triphosphate, glutamate), uptake of second messengers (e.g., cyclic-ADP-ribose, nitric oxide, Ca^{2+}) and metabolites (e.g., glucose, glutathione, ascorbate, reviewed in Giaume et al., 2013). The opening/closing of these channels is also regulated by extracellular signals such as **1)** integral membrane proteins (e.g., stomatin), **2)** growth factors (EGF and FGF1/2), and **3)** pro-inflammatory agents (e.g.,TNF-α, IL-1ß, ß-amyloid peptide) *in vitro* (Morita et al., 2007; Retamal et al., 2007; Garre et al., 2010; Orellana et al., 2011b; Zhan et al., 2012) in addition to the **4)** difference between intra/extracellular concentrations of mono/divalent cations, **5)** pH, **6)** mechanical stress, **7)** protein kinases and phosphatases, and **8)** oxidant and reducing agents (reviewed in Sarz et al., 2010; Wang et al., 2013). Consequently, astrocytes appear to maintain water, pH, ion, and metabolite homeostasis in the CNS and to provide intercellular communication with each other and with neurons and other glial cells utilising their GJCs and elaborately controlled HCs, as explained above.

1.2.1.2 Energy and metabolism

Glucose enters the brain via cells lining the blood brain barrier. Unlike these endothelial cells, neurons and other glial cells can phosphorylate glucose efficiently and thus allow it to be trapped inside these cells. Astrocytes can perform several steps of reactions to transform glucose into glycogen, the principal source of stored energy in both the brain

and the body (Pellegri et al., 1996; Pfeiffer- Guglielmi et al., 2003). Astrocytes appear to utilise both i) oxidative aerobic reactions to produce high-yield energy and ii) anaerobic reactions to produce lactate, which presents increased levels upon glucose treatment in cultured astrocytes in aerobic conditions (Walz and Mukerji, 1988). In addition to that, astrocytes have been suggested to increase extracellular lactate levels to provide energy substrate for nearby neurons based on following pieces of evidence: 1) Lactate transporters are present on neuronal membranes (Dringen et al., 1993), 2) Elevated neurotransmitter (glutamate) uptake causes glucose to be converted into lactate in cultured astrocytes (Pellerin and Magistretti, 1994), 3) Lactate levels increase in parallel with stimulated neuronal activity in different brain regions (reviewed in Figley and Stroman, 2011), 4) The cytoarchitectural arrangement of astrocytes is such that their processes surround both synapses and capillaries, which deliver glucose and oxygen to the brain (reviewed in Agulhon et al., 2008). As an alternative to this 'astrocyte-neuron lactate shuttle' hypothesis, it has been proposed that energy demands in regions surrounding synapses could be met by mitochondria, recently-discovered in astrocyte processes (Lovatt et al., 2007; Pardo et al., 2011; Derouiche et al., 2015). However, the fact that glucose and glutamate stimulate lactate production in astrocytes despite the presence of mitochondria in aerobic conditions still favours the initial hypothesis.

Astrocytes are also proposed to be primary cellular sources of cholesterol in the CNS (reviewed in Pfrieger and Ungerer, 2011), which is surrounded by the blood- brain barrier that does not allow the transport of hepatic or dietary supply of cholesterol to enter inside. It is crucial for the cholesterol to be synthesised in the CNS since it is a major component of biological membranes and is a precursor to many signaling molecules such as steroid hormones. Astrocytic expression of several apolipoproteins, which can mediate the secretion of cholesterol, has strengthened the suggestion that astrocytes can provide cholesterol to other cells in the CNS (Boyles et al., 1985; Lin et al., 1986; Xu et al., 2006; Kurumada et al., 2007). Both *in vitro* and *in vivo* studies have revealed that neurons can take up lipoproteins via specific receptors (Rothe and Muller, 1991; Narita et al., 1997; Sun et al., 1998; Liu et al., 2007). The neuron-specific knockout of one of these proteins has led to age-dependent loss of spines and synapses, and impairment of motor function and memory (May et al., 2004; Liu et al., 2010), emphasising the vital role of cholesterol uptake by neurons. Additionally, sterol synthesis has been detected at higher levels in astrocytes compared to in neurons of the developing rat brain (Nieweg et al., 2009. Therefore, in addition to their roles in providing energy for neurons, astrocytes also emerge as cholesterol-suppliers in the CNS.

1.2.1.3 Neuronal support and synapse formation/function

Astrocytes do not create or transmit action potentials like neurons do even though they express potassium and sodium channels (Kang et al., 1998). However, they can contribute to neuronal signal transmission in various ways. They can regulate the neuronal excitability by releasing gliotransmitters such as glutamate, purine, GABA and D-serine into the synaptic cleft upon being excited by changes in neuronal synaptic activity (Parpura et al., 1994; Bezzi et al., 1998; Mothet et al., 2000; Coco et al., 2003; reviewed in Halassa et al., 2007). The neurotransmitter released from the synapse can reach adjacent glial cells, stimulating increases in intracellular Ca^{2+} concentrations, which then leads to the secretion of gliotransmitters (Porter and McCarthy, 1996). These regulatory molecules then feed back to presynaptic nerve terminal to modulate synaptic neurotransmission (Araque et al., 1998). These observations have even given rise to the currently accepted 'tripartite synapse' hypothesis, where astrocytes form an active, integral regulatory component of the synapse (Fig 1.3, reviewed in Araque et al., 1999; in Halassa et al., 2007). It is predicted that processes of one astrocyte can contact with over 100,000 synapses (Bushong et al., 2002), which could explain how groups of pyramidal neurons within approximately 100 μm can be synchronously excited by glutamatergic gliotransmission (Guthrie et al., 1999; Fellin et al., 2004). Recently, microglia have also been shown to interact with neuronal synapses (Fig 1.3) using electron microscopy (Tremblay et al., 2010) and to play a role in synapse maturation, synaptic remodelling, and synaptic activity (reviewed in Ji et al., 2013), suggesting the complexity of crosstalk between neural cells.

In addition to playing a role in synaptic signal transmission, astrocytes can also actively remove excitotoxic glutamate from the extracellular space and convert it to glutamine by increasing their levels of glutamate transporters and glutamine synthetase (Faden et al., 1989; Eng et al., 1997; Krum et al., 2002). Thereby, they prevent neuronal cell death in case of brain pathology. Moreover, astrocytes secrete molecules that might be required for the formation, function and pruning of developing synapses (Ullian et al., 2001; Christopherson et al., 2005). Such growth factors and other molecules might also be functional in synaptic remodelling and pruning in healthy or diseased adult CNS (reviewed in Barres, 2008).

Another way in which astrocytes contribute to the synaptic transmission is by supporting maintenance of fluid, ion, pH and transmitter homeostasis of the synaptic interstitial fluid. Astrocyte processes contain transporters for K^+ uptake and aquaporin 4 water channels (Nielsen et al.; 1997; Rash et al., 1998; Amiry-Moghaddam et al., 2003; Solenov et al., 2004). These channels are especially clustered along processes that

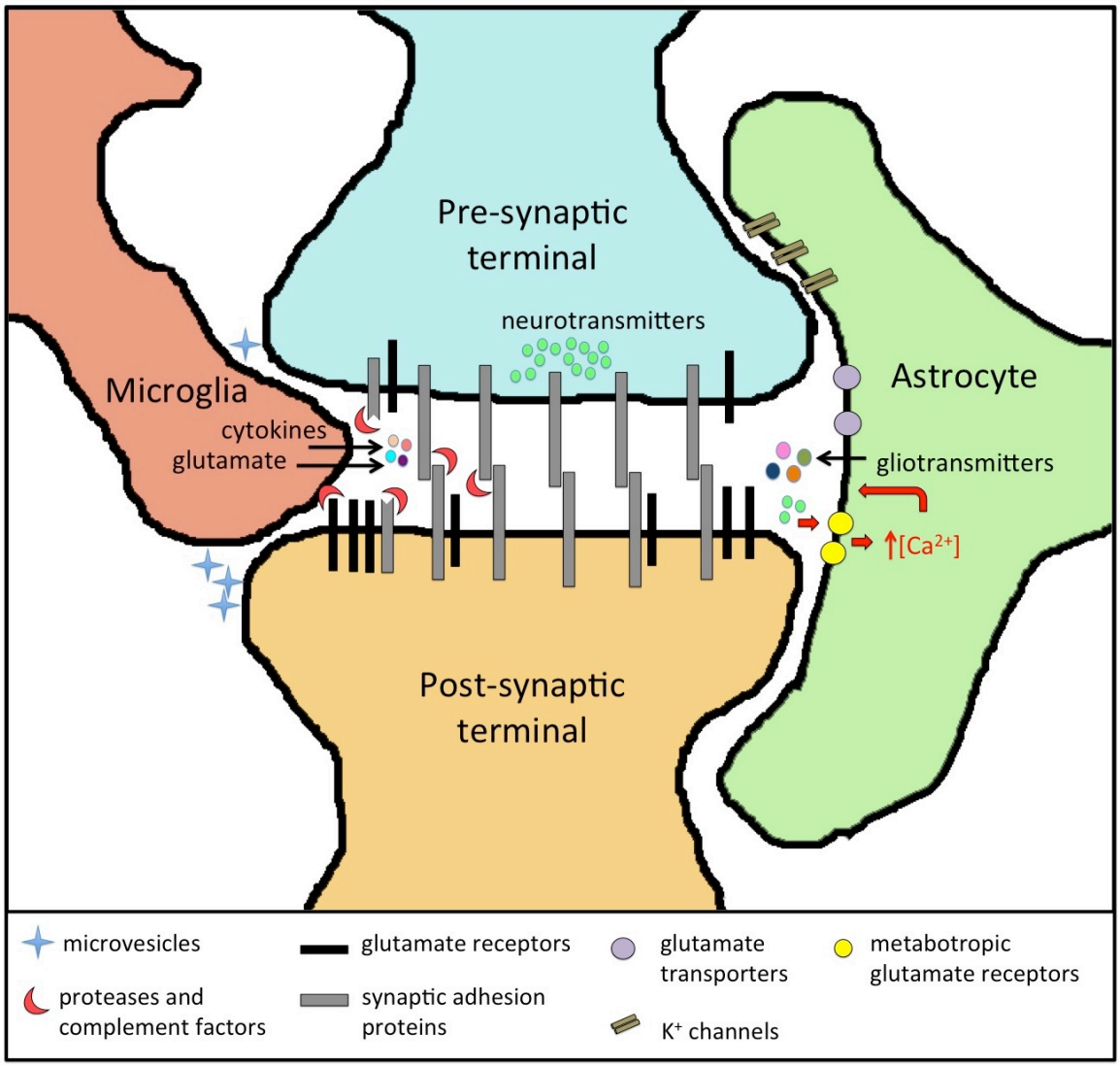

Figure 1. 3 A schematic of interaction of an astrocyte and microglia with a neuronal synapse.

The schematic presents a model for the interaction of astrocytic and microglial ends with a neuronal synapse based on the evidence provided by electron microscopy using *in vivo* tissue. The astrocytic process enwraps the pre-synaptic and post-synaptic neuronal terminals, forming the "tripartite synapse". Astrocytes clear K^+ ions that accumulate after neuronal activity in the synaptic cleft using their K^+ channels and remove the synaptic transmitter glutamate by the activity of plasma-membrane glutamate transporters. Neurotransmitters secreted from the pre-synaptic terminal can activate astrocytic metabotropic glutamate receptors, which in turn induces an increase in intracellular Ca^{2+} levels and thereby triggers the release of gliotransmitters into the synaptic cleft. Microglia processes in proximity to neuronal synapses can secrete proteases that will modulate the stability of synaptic adhesion proteins, which in turn affects synaptic transmission, or remove complement-tagged structures to provide synaptic pruning or remodelling. Microglia can also secrete cytokines and glutamate into the milieu and thus induce neurotransmission. They can release ectosomes (microvesicles) that directly interact with neuronal membranes and can play a role in signaling cascades. Locations of transporters and receptors in this schematic do not necessarily represent their exact spatial distribution. The image was modified from Halassa et al., 2007 and Ji et al., 2013.

contact blood vessels and function in regulation of fluid homeostasis in the healthy CNS (reviewed in Sofroniew and Vinters, 2010). Astrocyte processes also express high levels of transporters for neurotransmitters and thus maintain the transmitter homeostasis of the synaptic interstitial fluid (Steinhauser et al., 1994; Gundersen et al., 1996; Mennerick et al., 1996; Bergles and Jahr, 1997; Fujita et al., 1999). The harmful effects of accumulation of some small molecules like potassium or glutamate could be eliminated by the spreading of these molecules into the linked astrocytes via gap junctions (reviewed in Seifert et al., 2006; in Sofroniew and Vinters, 2010).

Astrocytes support neuronal survival not only by removing excitotoxic molecules from the extracellular space but also by providing energy for neurons. They contact blood vessels with some of their processes while they also have contacts with neuronal cell body, axons and synapses. Such a positioning allows uptake of glucose from blood vessels and transfer energy metabolites to neurons, which might be established again via gap junctions (Rouach et al., 2008). In addition, astrocytes are main storage places for glycogen granules in the CNS and astrocytic glycogen accumulates the most in areas of high synaptic density (Phelps, 1972; Peters et al., 1991). The utilization of astrocytic glycogen by neurons maintains the neural activity during hypoglycemia and during high neuronal activity (Brown and Ransom, 2007; Suh et al., 2007). This is provided by astrocyte-neuron lactate shuttle that has been explained above.

1.2.1.4 Blood-brain barrier integrity

The blood-brain barrier (BBB) is a physical barrier consisting of mainly ependymal cells that regulate the transport of ions and molecules via their tight junctions, which render the necessity of membrane transporters (solute carriers) to provide the brain-blood traffic. Brain nutrients such as glucose and amino acids enter the brain through this barrier; whereas, potentially toxic and metabolic waste products are removed away from the brain into the blood to be decomposed. The BBB is present as three sites: 1) the middle layer of the meninges, which surrounds the brain and the spinal cord as a whole, 2) the choroid plexus epithelium, which separates brain parenchyma from ventricles, and 3) brain endothelium that is the barrier between the brain cells and the capillaries (Reviewed in Abbott et al., 2006). This endothelium is covered by enlarged astrocytes processes, named ‘end feet’, showing the close relationship of astrocytes with the BBB. Indeed, primary brain endothelial cells can form tight endothelial barriers with closer similarities to the BBB *in vivo* when co-cultured with astrocytes compared to when grown alone (Candela et al., 2010; Skinner et al., 2009). Moreover, several astrocytic growth factors such as TGFα and GDNF have been shown to stimulate the formation of tight junctions in cultured endothelial cells, as well (Abbott, 2002).

Lineage-specific inhibition of early postnatal astrogliosis in mouse cortex delays vessel growth and branching; while, the astrogliosis that is allowed to proceed in later stages can rescue these delays (Ma et al., 2012a). Therefore, it is clear that astrocytes are important for the development of a healthy BBB.

Astrocytes not only transport water, ions and molecules between the CNS tissue and the BBB but also appear to control the dilation and contraction of the arteriols upon synaptic transmission. Glutamate released during signal transduction can activate the astrocytic Ca^{2+} signaling, which has been associated with the secretion of vasoactive cyclooxygenase that can dilate the arteriol and thus increase the local blood flow (Anderson and Nedergaard, 2003; Zonta et al., 2003). Consequently, astrocytes contribute to the homeostasis in the CNS by playing a role in the development, maintenance, and function of the BBB in addition to their other homeostatic roles, explained above.

1.2.1.5 Crosstalk between astrocytes and other neural cells

Astrocytes can communicate with other neural cells in the CNS and thereby alter their functions. An example for the crosstalk between astrocytes and other neural cells in the CNS is the tripartite synapse as explained above (Fig 1.3, Araque et al., 1999; Halassa et al., 2007). Neurotransmitters secreted into the pre-synaptic cleft can stimulate astrocytes to increase their intracellular Ca^{2+} levels, which would initiate the release of gliotransmitters into the synapse (Fig 1.3). Gliotransmitters can regulate the neuronal excitability in return (Parpura et al., 1994; Bezzi et al., 1998; Mothet et al., 2000; Coco et al., 2003; reviewed in Halassa et al., 2007). Heterocellular couplings, provided by gap junction channels, between astrocytes and other cells such as oligodendrocytes and neurons (Ransom and Kettenmann, 1990; Robinson et al., 1993; Venance et al., 1995; Maglione et al., 2010; Wasseff and Scherer, 2011) present another example for the crosstalk including astrocytes. The astrocytic crosstalk is sometimes more complex and takes part in the communication between two different cell types such as seen in responding to axonal release of ATP by secreting the cytokine LIF, which in turn stimulates oligodendrocytes to enhance myelination (Ishibashi et al., 2006).

1.2.2 Astrocyte phenotypes and their reactivity

Astrocytes are suggested to inhabit the CNS at various degrees of reactivity, which is likely to exist as a whole spectrum rather than a few different types (Sofroniew and Vinters, 2010; Nash et al., 2011a). Astrocytes have presented differences in morphology, proliferation rate, and secretion profile in various CNS pathologies

compared to in health. In healthy CNS tissue, there are few proliferating or newly generated astrocytes; whereas, actively dividing reactive astrocytes in human specimens have been particularly reported in association with infection and acute demyelinating lesions (Colodner et al., 2005). The source of these proliferating cells may be mature astrocytes that re-enter the cell cycle and/or progenitor cells in the local parenchyma or periventricular regions (Buffo et al., 2008; Gadea et al., 2008; Magnus et al., 2008; Carlen et al., 2009). These observations have divided astrocytes initially into quiescent and reactive astrocytes. Reactive astrocytes have been shown to play a role in reactive astrogliosis, which includes mainly four elements: **i)** astrocytes show molecular, cellular and functional changes in response to all forms and severities of CNS injury, **ii)** the type and level of changes the astrocytes undergo depend on the severity of the injury, **iii)** the changes in this process are moderated in a context-specific manner by inter- and intracellular signalling molecules, **iv)** the changes the astrocytes go through in this process could be seen as gain or loss of function of their activities and these can affect the surrounding neural or non-neural cells positively or negatively (Reviewed in Sofroniew, 2009). Reactive astrogliosis has further been categorised as **1)** mild, **2)** severe diffuse and **3)** severe with glial scar formation (reviewed in Sofroniew and Vinters, 2010), which will be explained below

1.2.2.1 Mild astrogliosis

Mild astrogliosis is also termed as isomorphic astrogliosis or as astrocyte activation. These activated astrocytes show a low level of increase in GFAP expression, cell hypertrophy, little or no cell proliferation (Wilhelmsson et al., 2006; reviewed in Sofroniew, 2009). This type of astrogliosis generally occurs due to mild non-penetrating, non-contusive trauma and due to diffuse innate activation that could be caused by viral or bacterial infections. It is also seen in sites distal to CNS lesions. The possible mechanisms causing this phenomenon are summarised in four elements by Malhotra and Shintka (2002): **i)** cytokines released in the injury site might diffuse into a large area, **ii)** activated astrocytes might migrate from the lesion to distant sites, **iii)** neuronal degeneration at the lesion might lead to fibre degeneration that will affect distal astrocytes or **iv)** direct astrocyte injury at the site of injury might release molecules that will be carried to distal astrocytes via gap junctions. Although the cell body and processes of the astrocytes enlarge, processes of neighbouring astrocytes still do not overlap with each other, maintaining the neatly ordered cell network organisation (Wilhelmsson et al., 2006). Because there is little change in the organisation of the tissue architecture, activated astrocytes have the potential to return to their healthy appearance if the pathological mechanism is eliminated or reversed.

1.2.2.2 Severe diffuse reactive astrogliosis

The reorganisation in tissue architecture is more severe, long-lasting and can spread around in a large area in severe diffuse reactive astrogliosis compared to that in mild astrogliosis (Sofroniew and Vinters, 2010). It is seen as explicit hypertrophy of the cell body and processes and astrocyte proliferation, which result in intermingling and overlapping of neighbouring astrocyte processes. The GFAP expression is up regulated to higher levels compared to that seen in mild astrogliosis. This glial reaction usually occurs in areas around severe focal lesions, infections or in areas responding to chronic neurodegenerative insults.

1.2.2.3 Severe astrogliosis with glial scar formation

Another severe reactive astrogliosis type presents up-regulation in GFAP expression, extensive astrocyte proliferation and hypertrophy of the cell body and processes to a higher extent such that astrocyte processes overlap with each other considerably and dense glial scars form (Fig 1.4). These glial scars consist of mostly astrocytes (reviewed in Silver and Miller, 2004) and they function as compact barriers along borders to severe tissue damage, necrosis, infection or autoimmune-stimulated inflammatory infiltration (Bush et al., 1999; Fisher, 2008; Herrmann et al., 2008; Voskuhl et al., 2009). This type of reactive astrogliosis occurs in cases of penetrating or contusive trauma, invasive infections, neoplasm, chronic degeneration and systemically triggered inflammatory challenges (Sofroniew and Vinters, 2010). The dense collagenous extracellular matrix, deposed in these areas, contain molecular cues that inhibit axonal and cellular migration, which can prevent or complicate the axonal regeneration in CNS lesions (in Silver and Miller, 2004). Nevertheless, these scars have been shown to protect neurons from the damages of inflammatory cells and infectious agents. In the study carried by Bush et al. (1999), the ablation of scar-forming reactive astrocytes in transgenic mice has led to increased outgrowth of nerve fibers in injured CNS parenchyma as expected but also has resulted in a prolonged increase in leukocyte infiltration, failure of BBB repair with the presence of vasogenic edema, and neuronal degeneration. Such observations have disproved the stereotyped views that reactive astrogliosis and glial scar formation are uniformly negative processes and that the total inhibition of them can be considered as a potential therapeutic strategy.

1.2.2.4 Pros and cons of reactive astrocytes

The beneficial roles of reactive astrocytes in protecting CNS cells and tissue have been summarized by Sofroniew and Vinters (2010) as **1)** taking up potentially excitotoxic glutamate and converting it to non-toxic precursors (Rothstein et al., 1996),

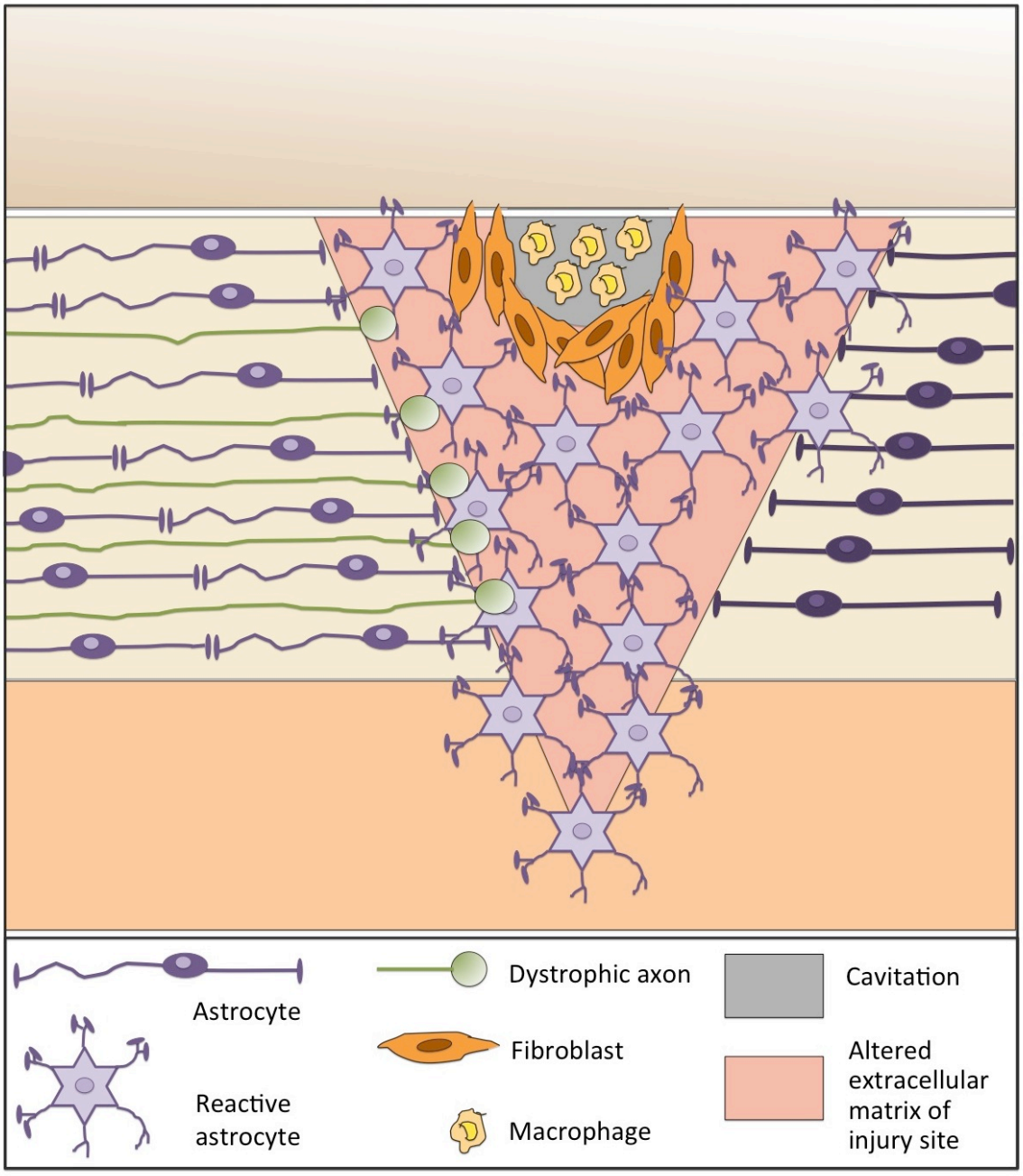

Figure 1. 4 Schematic representation of a glial scar in a large spinal cord lesion following stab injury.

Stab lesion disrupts the blood-brain barrier by penetrating the meninges and allows the invasion of fibroblasts and macrophages into the central nervious system. Astrocytes proliferate and undergo hypertrophy, which forms a dense network of reactive cells at the lesion site. Axons are repelled by elevated levels of inhibitory molecules in the milieu such as sulphate proteoglycans of chondroitin and keratan, which are produced by reactive astrocytes. The glial scar forms a physical and chemical barrier to regenerating axons. Astrocytes around the lesion (seen on the right of the figure) are mildly-activated as opposed to highly reactive astrocytes at the lesion site and to relatively “quescient” astrocytes outside the lesion (seen on the left of the figure). The image was modified from Silver and Miller, 2004.

2) protecting from oxidative stress via glutathione production (Chen et al., 2001; Shih et al., 2003), **3)** protecting neurons by releasing adenosine (Lin et al., 2008) and by degrading amyloid-beta peptides (Koistinaho et al., 2004), **4)** protecting from NH_4^+ toxicity (Rao et al., 2005), **5)** expediting the repair of the BBB (Bush et al., 1999), **6)** reducing vasogenic edema after trauma, stroke or obstructive hydrocephalus (Bush et al., 1999; Zador et al., 2009), **7)** stabilising extracellular fluid and ion balance (Zador et al., 2009), and **8)** preventing the spread of inflammatory cells or infectious agents from CNS lesions into healthy CNS parenchyma by forming a glial barrier (Faulkner et al., 2004; Myer et al., 2006; Okada et al., 2006; Li et al., 2008a).

Reactive astrocytes also exhibit various detrimental effects upon being stimulated by specific signalling cascades. They can **i)** deteriorate inflammation via cytokine production (Brambilla et al., 2005; 2009), **ii)** produce reactive oxygen species at neurotoxic levels (Swanson et al., 2004; Hamby et al., 2006), **iii)** release excitotoxic glutamate (Takano et al., 2005), **iv)** disrupt the BBB function due to VEGF production (Argaw et al., 2009), **v)** initiate cytotoxic edema during trauma and stroke because of over activity of aquaporin 4 channels, **vi)** potentially contribute to the formation of seizure and chronic pain (Jansen et al., 2005; Tian et al., 2005; Milligan et al., 2009). The fact that reactive astrocytes can play both beneficial and detrimental roles in CNS lesions might be explained by their secreting pro- or anti-inflammatory cytokines depending on types of molecules that stimulate these astrocytes (Eddleston and Mucke, 1993; John et al., 2003). Their stimulation by certain types of molecules might depend on particular time frames after the insult or on different locations in relation to lesions. The observations so far suggest that astrocytes would exhibit pro-inflammatory effects in or nearby CNS lesion shortly after the lesion has started to form; whereas, they would exhibit anti-inflammatory effects at later times and more distant locations from the lesions (reviewed in Sofroniew, 2005; 2009).

Although astrocytes playing a role in each type of astrogliosis have been defined as reactive astrocytes in paragraphs above, it is important to mention that an attempt has also been made by others to distinguish between the terminology used to define astrocytes taking place in mild astrogliosis (isomorphic astrogliosis) and those in severe astrogliosis (anisomorphic astrogliosis, Liberto et al., 2004). Nash et al. (2011a) have recently defined mild astrogliosis as “astrocyte activation” and severe astrogliosis as “astrocyte reactivity”. So in terms of level of activation, quiescent astrocytes are followed by “activated astrocytes”, which are followed by “reactive astrocytes”. In order to eliminate confusion, these new terms will be used below when these two phenotypes will be required to be differentiated. Otherwise, astrocytes in any kind of reactive astrogliosis will be referred to as ‘reactive astrocytes’ in general.

1.2.2.5 Activation of astrocytes in astrogliosis

Many intercellular signalling molecules can trigger reactive astrogliosis or can regulate some aspects of it. These molecules include large polypeptide growth factors and cytokines (John et al., 2003; Di Giorgio et al., 2007), mediators of innate immunity such as lipopolysaccharide and other Toll-like receptor ligands (Farina et al., 2007), neurotransmitters (Bekar et al., 2008), purines, reactive oxygen species (Swanson et al., 2004), molecules related to hypoxia and glucose deprivation (Swanson et al., 2004), products associated with neurodegeneration and with systemic metabolic toxicity (Simpson et al., 2010; Norenberg et al., 2009), and regulators of cell proliferation. Such molecules can be produced and released by both other astrocytes and other cell types in the CNS such as neurons, oligodendrocyte lineage cells, microglia, pericytes and endothelia. For example, in response to injury, microglia become activated and release the cytokine IL-1β (Herx et al., 2000), which is an early and dominant injury signal (Auron, 1998). Since astrocyte activation is delayed in mice lacking IL-1β as well as in mice lacking IL-1 type 1 receptor, it could be concluded that microglial activation is necessary for the activation of astrocytes (Herx et al., 2000).

Astrocytes have also been shown to react to other cytokines and growth factors. For instance, fibroblast growth factor (FGF), epidermal growth factor (EGF) and insulin-like growth factor-1 (IGF-1) increase the expression of glutamine transporters in astrocytes *in vitro* (Zelenaia et al., 2000; Suzuki et al., 2001), which might be a sign of astrocyte activation since the expression of these receptors is also increased in cultured traumatized astrocytes and in astrocytes obtained from traumatized rat cortex (Eng et al., 1979; Faden et al., 1989; Krum et al., 2002). Moreover, activated astrocytes up-regulate the expression of glutamine synthetase, whose levels can be regulated also by cytokines, including nerve growth factor (NGF) and FGF-2, which are downstream of IL-1 stimulation (Loret et al., 1989; Kazazoglu et al., 1996). So the pro-inflammatory cytokine IL-1 secreted in the case of a brain injury could stimulate the production and/or secretion of growth factors, which then could up-regulate the expression of enzymes and transporters in reactive astrocytes as mentioned above to remove the potential exocytotoxic glutamate. In contrast to that, TGFß, an anti-inflammatory cytokine that has been shown to be elevated in neurodegenerative diseases (Masliah et al., 2001; Pasquali et al., 2015), impairs astrocytic glutamine synthetase function in astroglial cultures and stimulates neurotoxicitiy in neuronal/astrocyte mixed cultures (Toru-Delbauffe et al., 1990; Chao et al., 1992), which might be associated with detrimental roles of highly reactive astrocytes as opposed to mildly activated beneficial astrocytes.

CNTF stands out as a well-known IL-6 family cytokine that has been demonstrated to activate astrocytes both *in vitro* and *in vivo* as observed by the increase in the astrocytic expression of reactivity markers such as GFAP, vimentin, and clusterin; cellular and nuclear hypertrophy; and cell proliferation (Winter et al., 1995; Levison et al., 1996; 1998; Hudgins and Levison, 1998). Like CNTF, pro-inflammatory cytokines such as TNFα and INFγ have also been shown to potentiate reactive astrogliosis (Yong et al., 1991; Balasingam et al., 1994; Corbin et al., 1996; reviewed in John et al., 2003). This could be especially important in inflammatory neurodegenerative diseases such as multiple sclerosis as will be explained below.

1.2.3 Astrocytic roles on myelination in general

Several studies have demonstrated that astrocytes can have promoting effects on myelination (Moore et al., 2011). *In vitro* studies, where conditioned medium was collected from primary astrocytes to treat other cultures, have shown that secreted astrocytic factors can act as mitogens for oligodendrocyte precursor cells, can protect oligodendrocytes against various kinds of stress and neurons from injury, and can support neuronal survival better than non-conditioned medium (Noble and Murray, 1984; Yoshida et al., 1995; Yamamuro et al., 2003; Zhu et al., 2006; Arai and Lo, 2010). Astrocytes can also secrete factors that increase the number of myelinated axons in response to axon firing (Ishibashi et al., 2006) and that influence the rate of axonal ensheathment *in vitro* (Watkins et al., 2008). In contrary to their stimulatory effects on myelination, astrocytes can generate an extracellular matrix inhibitory to the axonal outgrowth due to chondroitin sulphates they secrete (Canning et al., 1996; Filous et al., 2010). The fact that whether astrocytes will behave in a positive or negative way in neuronal support and myelination could be related to the degree of the astrocyte reactivity; i.e., 'activated astrocytes' could be providing a stimulatory environment unlike 'reactive astrocytes' do (reviewed in Nash et al., 2011a; in Barnett and Linington, 2013). Additionally, the difference between levels and activities of stimulatory and inhibitory secreted astrocytic-factors could be important to determine the overall astrocytic effect in the microenvironment.

Interestingly, rat spinal cords, where myelination was followed over a postnatal time period, have presented a direct ratio between the immunereactivity for myelin basic protein (MBP) and the number of GFAP positive astrocytes (Dziewulska et al., 1999). Moreover, transplantation of astrocytes into lesions has enhanced remyelination in rat spinal cords (Franklin et al., 1991). Knockout studies presented abnormal myelination, nonmyelinated axons in the optic nerve, and reduced myelin thickness in spinal cords of older (18-24 months of age as opposed to 2 months) GFAP null mice (Liedtke et al.,

1996). Non-conservative mutations in *GFAP* gene have also been linked to a white matter brain disorder named Alexender disease (Brenner et al., 2001; Li et al., 2002). Therefore, the evidence for direct or indirect astrocytic roles on re/myelination has been established both at *in vitro* and *in vivo* studies.

1.2.4 The effects of cytokine-activated astrocytes on neurogenesis, neuronal survival, and re/myelination

Cytokine-activated astrocytes can promote neuronal survival potentially by secreting various neurotrophic and growth factors (GFs) into the vicinity of neurons. Neurotrophic factors (NFs) secreted by astrocytes in response to injury, disease, and activation of cytokine receptors include nerve GF (NGF), brain-derived NF (BDNF), activity dependent NF (ADNF), hepatocyte GF (HGF), ciliary NF (CNTF), leukemia inhibitory factor (LIF) and fibroblast GF-2 (FGF-2) (Schwartz et al., 1994; Rudge et al., 1995; Uchida et al., 1998; Dreyfus et al., 1999; Messersmith et al., 2000; Albrecht et al., 2002). For example, IL-1β potently increases astrocytic expression of NGF, which then can promote neuronal survival (Friedman et al., 1990; Spranger et al., 1990). Primary rat astrocytes have also been shown to increase their expression of NGF in response to a fusion protein of IL-6 and soluble IL-6 receptor (Marz et al., 1999). Activation by another cytokine, vasoactive intestinal peptide (VIP), promotes ADNF secretion from astrocytes, which has been shown to promote the survival of spinal cord neurons and cortical neurons (Gozes et al., 1999). In addition, it protects rat cerebral cortical cultures from ß-amyloid peptide neurotoxicity (Brenneman et al., 1996; Gozes et al., 1996). CNTF also activates astrocytes to promote neuronal survival. Cultured spinal cord astrocytes, activated with CNTF, support the survival of a significantly greater number of ventral spinal motor neurons and promote neurite outgrowth better than compared to unstimulated astrocytes (Albrecht et al., 2002). IL-1β can induce the production of astrocytic CNTF, which likely presents its above-mentioned effects by increasing the production of astrocytic neurotrophic factors such as FGF-2 (Herx et al., 2000; Liberto et al., 2004).

Accumulating evidence show that cytokine-activated astrocytes can promote neurogenesis possibly by stimulating the differentiation of neural stem cells (NSCs), which are present in the subventricular zone and the dentate gyrus of the hippocampus in adult animals (Liberto et al., 2004). Because these multipotent cells can migrate beyond their sites of origin and can later differentiate into neurons and microglia, they carry the potential to enhance recovery from CNS injury and disease. FGF-2 and other factors, which can be secreted by cytokine-activated astrocytes (Albrecht et al., 2002), have been shown to stimulate NSCs to proliferate both *in vitro* and *in vivo* (Kuhn et al., 1997). Moreover, co-culturing adult NSCs with primary hippocampal astrocytes increases

the number of newly formed neurons 10-fold (Song et al., 2002), which suggests that astrocyte-derived factors must be regulating neurogenesis.

CNTF also plays a role in remyelination process of demyelinated CNS lesions. Mice infected with the A-59 strain of the mouse hepatitis virus (MHV-A59), another useful animal model for MS (Jordan et al., 1989, Messersmith et al., 2000), have presented IL-1β production early during the course of infection, when demyelination takes place; whereas levels of CNTF have increased later, during the remyelination phase (Albrecht et al., 2003). In the same animal model, *Cntf* mRNA, but not *Il-1β* mRNA, has been found to be induced in remyelinating regions and to be present in cells exhibiting astrocytic features. It is suggested that the increase in IL-1β levels at early stages of the pathology stimulates the induction of CNTF mRNA and protein in astrocytes (Stockli et al., 1991; Guthrie et al., 1997; Dallner et al., 2002; Liberto et al., 2004), a phenomenon which appears to be important for remyelination stages (Herx et al., 2000). Moreover, CNTF treatment elevates astrocytic levels of *Fgf-2* mRNA significantly; whereas, IL-1β shows no effect (Albrecht et al., 2003). Since FGF-2 can enhance oligodendrocyte precursor cell (OPC) proliferation (Albrecht et al., 2003), it is likely that CNTF-activated-astrocytic release of FGF-2 stimulates OPC proliferation (Redwine et al. 1997; Messersmith et al., 2000) and thus provides remyelination in demyelinated CNS lesions. Similarly, IL-1β can stimulate the astrocytic production of another IL-6 family cytokine, LIF (Aloisi et al., 1994), which has been shown to promote survival and differentiation of oligodendrocytes and expression of mature myelin protein in different studies (Kahn and De Vellis, 1994; Mayer et al., 1994; Bugga et al., 1998).

Above-mentioned beneficial effects of astrocytes on myelination could be associated with mild astrogliosis rather than more severe reactive astrogliosis types as discussed by several groups of investigators (reviewed in White and Jakeman, 2008; in Sofroniew and Vinters, 2010; in Nash et al., 2011a). Astrocytes can impede myelination probably depending on their activation phenotype (Moore et al., 2011). The word 'phenotype' here represents the change in their several properties such as morphology, and antigenic and physiological characteristics obtained after injury. As it is argued by Nash et al. (2011a), activated astrocytes could promote remyelination; whereas, reactive astrocytes could suppress remyelination after injury.

Reactive astrocytes are functional in severe astrogliosis as mentioned above (Section 1.2.2.3). Various pro-inflammatory cytokines can activate astrocytes in such CNS pathologies, where reactive astrocytes will in turn secrete other cytokines and/or chemokines (reviewed in John et al., 2003). One of the cytokines, secreted by reactive

astrocytes, with detrimental effects is tumor necrosis factor-α (TNFα), which induces myelin and oligodendrocyte damage *in vitro* (Selmaj et al., 1988). Its expression in MS plaques positively correlates with the extent of demyelination (Bitsch et al., 2000). Since one of the major targets for TNFα is the maturation of oligodendrocytes (Cammer and Zhang, 1999), the remyelination failure present in CNS lesions could be because TNFα prevents the differentiation of oligodendrocytes in these sites. Reactive astrocytes also secrete CXCL10 (Ransohoff et al., 1993), a chemokine that has also been shown to be expressed by reactive astrocytes around active MS lesions (Omari et al., 2005; Carter et al., 2007). *Cxcl10* mRNA expression increases significantly during peak disease and decreases during the recovery phases in animal models of MS (Godiska et al., 1995; Glabinski et al., 1997; Fife et al., 2001). In a very recent *in vitro* study, astrocytes with increased expression of *Cxcl10* failed to promote myelination, which was reversed by the neutralisation of CXCL10 by using antibodies (Nash et al., 2011b). CXCL10 might express this effect by binding to its receptor CXCR3, expressed by oligodendrocytes. Therefore, reactive astrocytes appear also to be capable of initiating myelination-inhibiting crosstalk with other cells unlike their stimulatory roles, explained above.

As seen above, astrocytes appear to play important roles not just in myelination in embryonic CNS tissues but also in remyelination in adult tissue after CNS injury in addition to their various functions stimulated following CNS damage. Their functions might be related to their 'phenotype' and hence it is important to test different phenotypes of astrocytes in follow-up studies to elucidate the molecular mechanisms how astrocytes play a role in myelination. Such studies might reveal novel treatments for MS patients, who currently lack a treatment that will reverse their disabilities.

1.2.5 Astrocytes in multiple sclerosis

Multiple sclerosis is an autoimmune, neurodegenerative disease, affecting the CNS. The highest prevalence for this disease has been detected so far in Scotland which ranges from 145 to 193 per 100 000 (Pugliatti et al., 2001). The initial symptoms of the disease often include weakness in one or more limbs, inflammation of the optic nerve, paraesthesiae (sensation of tingling, pricking, numbness), diplopia (double vision), vertigo, and bladder dysfunction (McAlpine et al., 1972). The age of onset of the disease may vary usually between 10 and 50 years (Noseworthy et al., 1983; Sindern et al., 1992). The disease can have a progressive or a relapsing-remitting course, where periods of worsening neurologic functions (exacerbations) are followed by partial or complete recovery periods (remissions, Fig 1.5). The progressive subtype is named as primary progressive if the progression has been present from the onset; whereas,

secondary progressive MS shows progression after an initial period of relapsing-remitting course (Fig 1.5, reviewed in McDonnell and Hawkins, 1996). As the disease progresses, disabilities might accumulate and might produce immobility, lack of protective pharyngeal reflexes and bladder problems, making the patient more susceptible to infection.

The main pathological mechanisms leading to an initiation or increase in the disease activity could be summarized as T-cell reactivity to a myelin antigen or another CNS antigen, disruptions in the BBB permeability and increase in the expression of cell adhesion molecules, which would affect the cell trafficking across the BBB (McFarland and Martin, 2007). Two major occurrences of MS are relapses and progression. Relapses are considered to be clinical presentation of acute inflammation and demyelination in the CNS; whereas, progression is considered to reflect the presence of axonal loss and neurodegeneration (Fitzner and Simons, 2010). The loss of myelin in MS can lead to severe loss of function as mentioned above and thus it is very important to find treatments to prevent the myelin damage from occurring in the first place or to find ways to facilitate the remyelination process.

Astrocytes in MS plaques have been suggested to secrete cytokines that are either stimulatory or inhibitory for myelination. TNFα and INFγ not only can activate astrocytes but they can also be secreted by reactive astrocytes both in MS and experimental autoimmune encephalomyelitis (EAE), a mouse MS model, where demyelination is induced by myelin antigens, administered together with adjuvant that contains bacterial components (Traugott and Lebon, 1988; Tsukada et al., 1991; Villarroya et al., 1996; Meeuwsen et al., 2003). The level of TNFα expression in MS has been correlated with the extent of demyelination (Bitsch et al., 2000). Similarly, INFγ has been shown to suppress remyelination and to delay disease recovery in transgenic EAE mice, where INFγ expression was stimulated temporally in recovery stage in astrocytes (Lin et al., 2006b). On the other hand, another astrocytic-cytokine, LIF, decreases disease severity when exogenously administered in both chronic EAE and relapsing-remitting EAE mice (Aloisi et al., 1994; Butzkueven et al., 2002; Ishibashi et al., 2006). Promoting effects of LIF on the survival and maturation of oligodendrocytes also support the positive roles of LIF on remyelination (Khan and De Vellis, 1994; Mayer et al., 1994; Bugga et al., 1998).

Reactive astrocytes have been observed both in acute and chronic plaques in MS with increased expressions of markers such as GFAP, vimentin, nestin, eNCAM, FGFR4, EGFR, NGF, bFGF, TnR, and CTGF (Holley et al., 2003). The failed axonal regeneration in MS

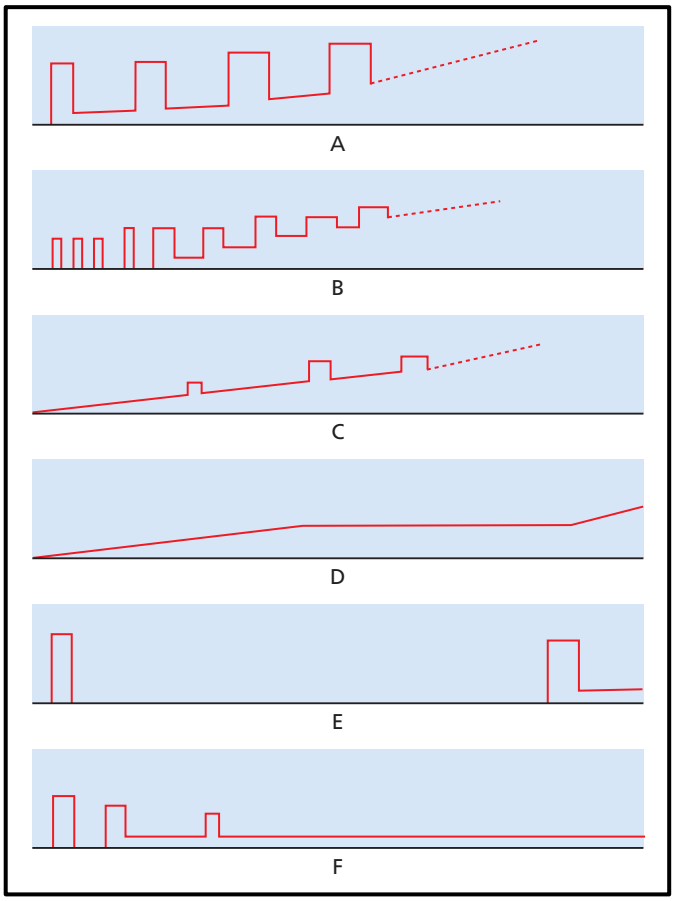

Figure 1. 5 Multiple sclerosis (MS) subtypes
A) Secondary progressive MS. Iniitial relapsing-remitting MS that suddenly begins to present increased disability without periods of remission. **B)** Relapsing-remitting MS with many short attacks that tend to increase in duration and severity. These unpredictable attacks are followed by periods of remission. **C)** Progressive-relapsing MS. Slow and steady progression since onset with superimposed relapse and increasing disability. **D)** Primary progressive MS. Slow and steady progression from onset without relapses. **E)** Abrupt onset with good remission followed by long latent phase. **F)** Relapses of diminishing frequency and severity; slight residual disability only. Image was taken from Compston et al., 2006.

lesions has been correlated with dense glial scars that consist primarily of enlarged and entangled reactive astrocytes and that surround non-regenerating fibers closely (reviewed in Silver and Miller, 2004). However, this glial scar has later gained attention also with its protective roles in lesions. Targeted depletion of the group of reactive astrocytes that proliferate immediately around the core of the lesion in mouse brains and spinal cords has resulted in increased levels of failure in BBB repair, inflammatory response and cellular degeneration (Bush et al., 1999; Faulkner et al., 2004). Therefore, the glial scar is now also considered as a protective barrier that separates the injury from healthy tissue and thus prevents the damage and the immune response from spreading around and invading the normal CNS. Nevertheless, astrocytes going through astrogliosis can still be seen as harmful due to their secretion of toxic factors and glutamate-mediated excitotoxicity in addition to taking part in compact glial scars (Bannerman et al., 2007; Cambron et al., 2012). The most recent opinion is that

'reactive astrocytes' could be responsible for detrimental effects in the CNS lesions; while, 'activated astrocytes' might play beneficial roles and promote CNS repair (reviewed in Barnett and Linington, 2012).

1.3 CNS myelinating culture systems

1.3.1 Organotypic slice cultures

The first attempt to generate brain slice cultures involved tissue from embryonic chick rhomboencephalon and was not very successful as the cultures could not be mainted for a long period of time (Levi and Meyer, 1941). Myelin formation was later observed in culture of mammalian CNS, where it was visualised by its refractive pattern on light microscopy (Hild, 1956). Cerebellar sections from neonatal mice have provided an *ex vivo* system to observe myelination when optic nerve explants were transplanted onto them (Stanhope et al., 1986). It has later been shown that these slice cultures also have the capacity to support myelination in the absence of any transplantation (Seil and Herndon, 1991). They have also provided a model to study effects of a treatment on myelination. For example, progesterone stimulated myelination, which was assessed by immunofluorescence of MBP (myelin basic protein) in both mouse and rat cerebellar slice cultures (Ghoumari et al., 2003). However, MBP expression does not appear to reflect solely the amount of axonal ensheathment around axons. To assess the myelination more precisely, electron microscopy has been utilised in many other studies including those in embryonic spinal cord slice cultures (Bunge and Wood, 1973; Billing-Gagliardi et al., 1980; Shrager and Novakovic, 1995). An automated way has been used recently to quantify myelination levels in mouse cerebellar slice cultures. The images obtained via fluorescence microscopy were analysed by a software, which quantified the colocalisation of MBP (representing myelin) and NFH (neurofilament, representing axons) immunofluorescence (Huang et al., 2011; Zhang et al., 2011). Despite these new improvements, slice cultures still remain laborious especially due to the requirement of tissue slicing using special equipment like microtome or vibratome.

1.3.2 Cocultures containing dorsal root ganglion neurons

Dissociated embryonic rodent spinal cord cells or glial cells, which are isolated from spinal cord cell suspensions, are added onto 3-4 weeks old dorsal root ganglion (DRG) neuronal cultures to generate cocultures that will present CNS myelination in the following 4-6 weeks (Mithen et al., 1983; Wood and Williams, 1984; Wood and Bunge, 1986). Watkins et al. (2008) have shortened this period by seeding oligodendrocyte precursor cells on retinal ganglion cells, where the generation of compact myelin has

been observed within six days. Because DRG neurons are primarily considered to be part of peripheral nervous system due to their roles in conveying peripheral signals to the CNS and regulating vascular and other tissue functions in the area of their peripheral terminations (reviewed in Holzer and Maggi, 1998), it cannot be guaranteed that they will behave similar to CNS neurons under all circumstances even if they are cultured in the presence of CNS spinal cord cells or purified astrocytes (Chan et al., 2004). Therefore, other culture types could be more convenient for the purposes of studying CNS myelination.

1.3.3 Dissociated mixed CNS cultures

Dissociated cells from an embryonic CNS region such as the forebrain, cerebellum, or spinal cord can be used to prepare mixed cultures to observe myelination. The number of myelinated fibres per unit of surface increased gradually in cerebral hemisphere cultures from embryonic day 15 (E15) mice between days 13 and 22 as observed by electron microscopy after immunocytochemistry (Lubetzki et al., 1993). Unlike mouse cerebral cultures, embryonic rat cerebellar cultures have presented continuous myelination at least up to 3 months, where cultures were dense and axonal ensheathment was abundant (Svenningsen et al., 2003). On the other hand, Thomson et al. (2006) developed embryonic mouse spinal cord myelinating cultures that could be maintained in defined media rather than serum, which contains undefined components. Additionally, they showed that these cultures provided robust myelination when a supportive monolayer of neurosphere-derived mouse astrocytes was used, which could also allow the study of the effect of different astrocyte phenotypes on myelination. Their protocol was later adapted to rats by Sorensen et al. (2008).

Embryonic rat spinal cord cultures are prepared from dissociated rat spinal cord cells, obtained from embryonic day 15 Sprague Dawley rats. Dissociated spinal cord cells are plated onto a confluent monolayer of astrocytes, derived from postnatal day 1 rat striatum neurospheres. The cultures develop over 24-28 days. They allow the study of neuronal survival and neurite outgrowth in the first 12 days, which are followed by oligodendrocyte precursor proliferation and oligodendrocyte process extension to axons in the following 6 days. At days 22-28, the formation of myelin internodes and nodes of Ranvier can be observed (Sorensen et al., 2008).

Applying immunocytochemistry to spinal cord myelinating cultures allows the observation of morphological properties such as oligodendrocyte development, and axon and myelin sheath integrity by using specific antibodies. Neurites are usually visualised using an antibody against phosphorylated neurofilament SMI-31 and neurite density is

measured using Image J software, where the pixel value of SMI-31 fluorescence reactivity is measured as a percentage of the total pixel value in one image, taken using a fluorescent microscope. Mature myelin is visualized using the AA3 antibody, which labels PLP/DM20 proteins, present both in myelin sheaths and in oligodendrocyte cell bodies. Therefore, to calculate the percentage of myelination, the myelinated axons have to be manually identified on images using Adobe Photoshop software (Sorensen et al., 2008).

Astrocytes, which are used as a feeder monolayer underneath embryonic rat spinal cord cultures, are plated on poly-L-lysine (PLL)-coated coverslips to obtain a control condition. These spinal cord myelinating cultures on PLL-astrocytes (PLL-myelinating cultures) are considered to be the control phenotype *in vitro*, but it cannot be assumed that they represent quiescent (inactivated) astrocytes present in the healthy CNS *in vivo*. For instance, primary rat astrocytes grown on a 3D collagen gel system express lower levels of reactivity markers like GFAP, vimentin and aquaporin 4 compared to those grown in a monolayer (East et al., 2009). Cultural processes such as dissection and enzymatic dissociation might induce an activated cell phenotype. Moreover, cultured astrocytes are exposed to foetal bovine serum; whereas those in normal human brain are not. Therefore, artificial culture conditions might cause astrocyte monolayers to have a different state of activation compared to that at their tissue source and thus affect activities of spinal cord myelinating cultures. Nevertheless, PLL-myelinating cultures can still be used as controls to compare effects of different treatments on cell proliferation, differentiation and myelination.

Alternatively, rat astrocytes can be plated on tenascin C (TnC)-coated coverslips (Nash et al., 2011b). TnC is an extracellular matrix (ECM) glycoprotein that has been shown to induce a quiescent phenotype in cultured adult human astrocytes (Holley et al., 2005). Among other tested ECM molecules, including laminin, collagen IV, fibronectin, vitronectin and proteoglycans, TnC reduced the expression of activated/reactive astrocyte markers (e.g., nestin, neural cell adhesion molecule, EGF receptor, and basic FGF) and slowed down the proliferation of astrocytes the greatest (Holley et al., 2005). Thus, plating astrocytes on TnC-coated coverslips is currently considered as a method to generate a more quiescent phenotype compared to reactive phenotypes. It could be argued that the phenotype of TnC-astrocytes resembles that of astrocytes in the healthy CNS because the expression level of astrocyte reactivity markers in TnC-astrocytes were comparable to those of astrocytes in normal cerebral white matter *in vivo* (Holley et al., 2005). Therefore, TnC-astrocytes and hence TnC-myelinating cultures could also be preferred as the control conditions. However, further studies are required to validate this view.

1.4 The roles of cytokines and chemokines in the CNS

Cytokines are a group of small glycoproteins that may function as membrane-bound complexes or be secreted into the microenvironment by various cells. Cytokine superfamily includes several groups of signaling protein families such as chemokines, interferons, interleukins, lymphokines, and tumor necrosis factors. Chemokines are divided into four classes based on the positions of key cysteine residues: C, CC, CXC, and CX3C (Bajetto et al., 2001). The main function that differentiates chemokines from other cytokines is their roles in cell recruitment, which they provide through both specific and shared G-protein coupled receptors. Both chemokines and other cytokines have been shown to take part in various functions in the CNS as will be explained below.

1.4.1 The roles of cytokines in the development of the CNS

Both *in vitro* and *in vivo* experiments have suggested important roles for several cytokines in the CNS development. Among them, IL-6 family cytokines (**IL-6, IL-11, IL-27, CLC, CNTF, CT-1, LIF, NP,** and **OSM**) appear to regulate **1)** the self-renewal of radial glial cells (RGCs) that can generate neurons and glia during embryogenesis, **2)** the shift from neuronogenesis to astrogliosis at early stages of development, **3)** determination of neuronal identity, and **4)** cell survival (reviewed in Deverman and Patterson, 2009). Essential components of their signaling pathway such as **i)** the common receptor subunit GP130 that binds all IL-6 family members (Fig 1.6), **ii)** more specific receptor subunits LIFRβ and CNTFRα, and **iii)** STAT3 that is a transcription factor primarily mediating GP130 signaling are all expressed in the early ventricular zone, which is populated by RGCs (Yoshimatsu et al., 2006; Alfonsi et al., 2008) and the cytokines CT-1, CNTF, NP, LIF are also expressed in the embryonic brain (Derouet et al., 2004; Barnabe-Heider et al., 2005; Gregg and Weiss, 2005). The stimulation of the crosstalk between STAT3 and Notch signaling, which can be activated by CNTF (Chojnacki et al., 2003), is suggested to inhibit neuronal differentiation and to promote the RGC fate (Kamakura et al., 2004; Yoshimatsu et al., 2006). On the other hand, GP130 family cytokines induce GFAP expression at later stages of embryogenesis as can be seen in the impaired astrogliogenesis of *Gp130* or *LifrB* knockout embryos (Koblar et al., 1998; Nakashima et al., 1999). It is suggested that they do not promote a full maturation of astrocytes but rather contribute to the generation of GFAP positive multipotent astroglial progenitors that will occupy adult subventricular zone. The involvement of LIF signaling in control of the neuronal subtype identity; and the increased motor neuron loss in knockout animals lacking an IL-6 family cytokine or receptor present other examples of present IL-6 family cytokine roles in CNS development (reviewed in Deverman et al., 2009).

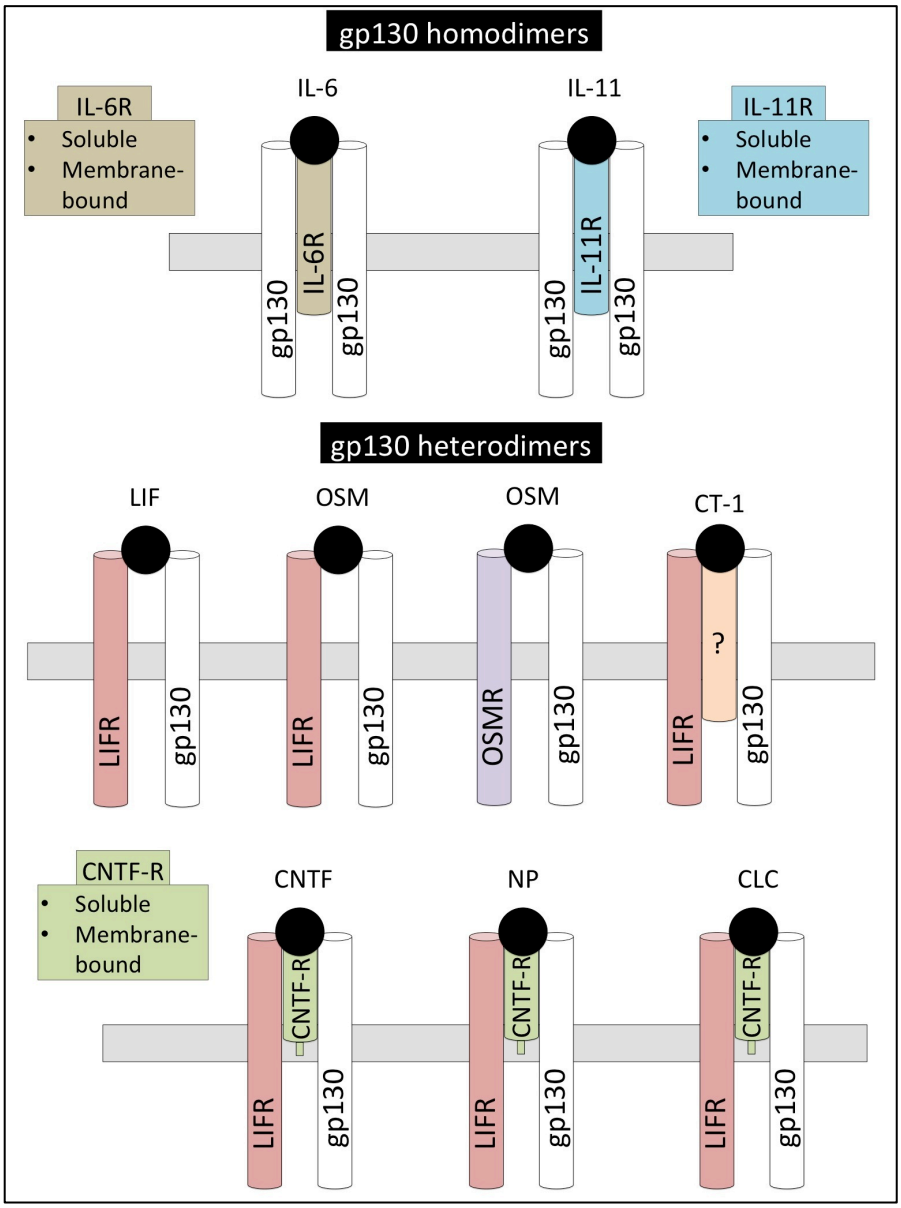

Figure 1. 6 Interleukin-6 (IL-6) family of cytokines and their receptors.

IL-6 family cytokines bind to their respective α-receptors (IL-6R, IL-11R, CNTF-R) that induce the dimerisation of gp130, LIFR, or OSMR to conduct their signaling. IL-6 and IL-11 bind their corresping α-receptors that can be either membrane-bound or found in the soluble form, and signal through a gp130 homodimer. LIF and OSM do not require an α-receptor and signal through a heterodimer of LIF receptor (LIFR) and OSM receptor (OSMR). OSM can also use a heterodimer of OSMR and gp130. CT-1 also uses a heterodimer of LIFR/gp130 but requires an α-receptor, currently not known. CNTF, NP, and CLC all signal through a heterodimer of LIFR/gp130 after binding CNTF α-receptor (CNTFR). The image was modified from Kraakman et al., 2013. CLC: cardotrophin-like cytokine-like factor; CNTF: ciliary neurotrophic factor; CT-1: cardiotrophin 1; LIF: leukamia inhibitory factor; NP: neuropoietin; OSM: oncastatin M; R: receptor

Other cytokines such as granulocyte colony stimulating factor (**G-CSF**) and **IL-1ß** are also expressed in embryonic CNS tissue and are suggested to promote neurogenesis. Moreover, **TGFß**, **TNFα**, and **IL-9** cytokines have been associated with functions such as neuronal subtype differentiation, regulation of cell survival, and synaptic modulation and elimination; while, bone morphogenetic proteins (BMPs), a subgroup of TGFß cytokine family, suppress neurogenesis (reviewed in Deverman et al., 2009).

1.4.2 The role of cytokines in the adult CNS

Even though cytokines have been suggested to be secreted by all neuronal and glial cells, astrocytes and microglia appear as the major cellular source of cytokines in the CNS. Cytokines in the healthy CNS can regulate various functions including synthesis of neurotrophic factors, neurogenesis, astrogenesis and astrocytic survival, oligodendroglial maturation, neurotransmission, synaptic maturation and plasticity, and myelination (reviewed in Camacho-Arroyo et al., 2009; in Schmitz and Chew, 2009). **IL-1ß, IL-2, IL-6** cytokines can promote γ-aminobutyric acid (GABA)-mediated inhibitory signal transduction; while, **IFNγ** decreases GABAergic neuron activation and **IFNα** treatment changes the balance between excitatory and inhibitory neurotransmission by reducing the former and increasing the latter (Vikman et al., 2001; Brask et al., 2004). In addition to its neuroprotective roles and its effects on neurotransmitters, **IL-3** can also play a role in differentiation and maintenance of cholinergic neurons (Tabira et al., 1998; Wen et al., 1998).

CNTF, an IL-6 family cytokine, and CNTF receptor alpha (CNTFRα), which is a specific component of its receptor complex, are constitutively expressed in astrocytes of white matter and grey matter, respectively, of normal mouse brain (Stockli et al., 1991; Dallner et al., 2002). Microglia also present CNTFRα expression unlike astrocytes in mixed glial cultures, which might be due to the brain region dissociated to set up the cultures (Krady et al., 2008). Therefore, it is likely that this spatial control of CNTF ligand and receptor expression determines which cells will respond to CNTF that will be important for final CNTF effects in the brain. CNTF knockout mice present increased degeneration in spinal motor neurons with increasing age, which shows the role of CNTF in neuroprotection (Masu et al., 1993). CNTF also stimulates oligodendrocyte survival and maturation *in vitro* and *in vivo* (Stankoff et al., 2002; Cao et al., 2010), enhances migration of subventricular zone-derived progenitors (Vernerey et al., 2013), and protects oligodendrocytes from apoptosis and decreases myelin destruction in demyelinating pathological conditions (Linker et al., 2002).

1.4.3 The role of cytokines in CNS pathology

CNTF has presented up-regulated mRNA levels during remyelination phase of a cuprizone-induced demyelinating disease model, which has suggested association between this cytokine and re/myelination (Gudi et al., 2011). In parallel with that, subcutaneous CNTF injection at the remyelination phase of the same animal model has shown increased myelin oligodendrocyte glycoprotein (MOG) expression in cerebral cortex (Salehi et al., 2013). Moreover, intraperitoneal injections of CNTF and intravenously transplanted mesenchymal stem cells that overexpress CNTF have both led to reduced loss of neurons and disease severity, and increased neuronal functional recovery in EAE mice, an animal model for multiple sclerosis (Kuhlman et al., 2006; Lu et al., 2009).

Pro-inflammatory cytokines have been seen to play roles in many CNS pathologies (reviewed in Schmitz et al., 2009). For instance, IL-1ß, IL-6, IL-18, and IFNγ cytokine levels are related with the development or presence of white matter disease and impaired neurologic development in preterm infants. IL-1ß, IL-6, and TNFα take place among induced cytokines upon the inflammatory response initiated in cerebral ischemia. Additional cytokines such as IL-1ß, IL-6, IL-8, TNFα, IL-4, and IL-10 are observed in traumatic CNS injury. Positive correlation can be seen for some of these pro-inflammatory cytokines with the severity of disease symptoms; e.g., TNFα expression in MS lesions is linked to clinical course; and the concentrations of IL-6 in the serum and cerebrospinal fluid (CSF) of acute stroke patients are associated with brain infarct volume and stroke severity. As discussed by Schmitz et al. (2009), cytokines can present both beneficial and detrimental effects in CNS pathophysiology and lead to cell damage and death on one hand, and promote tissue repair on the other.

1.4.4 The chemokines and their roles in the CNS

Chemokines are usually associated with the immune system due to their ability to regulate cell trafficking of immune system cells. However, constitutively expressed chemokines have been detected in healthy CNS in addition to inflammatory chemokines that can either be secreted by activated glial cells, mainly astrocytes and microglia, or by leucocytes that enter the CNS upon a CNS injury. All of these homeostatic and inflammatory chemokines belonging to four classes (C, CC, CXC, and CX3C) generate a complex signaling network together with their receptors, many of which have been shown to be promiscuous and to lead to chemokine redundancy (Fig 1.7).

Constitutive CNS expressions have been reported for several chemokines including CCL2, CCL3, CCL19, CCL21, CXCL12, and CX3CL1 (reviewed in Jaerve and Muller, 2012). Cellular sources for such chemokines appear to be activated/reactive astrocytes and/or microglia, endothelial cells, and/or neurons, which also express corresponding receptors. Depending on the severity of the injury, expressions of chemokines and chemokine receptors can be up-regulated in the CNS within minutes to hours and remain for several days after trauma. Many chemokines such as CCL2-5, CCL7-8, CCL12, CCL20-21, CXCL1-3, CXCL5, CXCL8, CXCL10, CXCL12, and CX3CL1 have been shown to be up-regulated in spinal cord injury, traumatic brain injury and/or stroke (Jaerve and Muller, 2012).

The lymphoid chemokines, CCL19, CCL21, and CXCL13, can also be induced in the CNS upon inflammatory processes such as autoimmune demyelinating disease or non-inflammatory insults in addition to their role in the development and maintenance of secondary lymphoid tissues (reviewed in Lalor and Segal, 2010). Increased glutamate mediated excitotoxicity in ischemia is suggested to stimulate neuronal production and secretion of CCL21, which in turn activates microglia. In addition to their suggested protective roles in CNS infections, the lymphoid chemokines have been proposed to take part in lymphocyte recruitment, B cell maintenance or expansion, and microglial activation/ chemotaxis in MS. Elevated chemokine expressions have been detected in EAE spinal cords in parallel with clinical relapses and chronic progression and in both active and inactive MS lesions. While CCL19 and CCL21 are constitutively expressed in cerebrovascular endothelium and choroid plexus and are responsible for the immune surveillance of the subarachnoid and perivascular spaces of healthy CNS; CXCL13 presence is in the CNS detected upon autoimmune demyelination. Infiltrating myeloid dendritic cells are suggested as possible cellular source for this chemokine that presents increased expression during EAE relapses and possibly contributes to encephalitogenic T cell migration towards dendritic cells in the CNS (McMahon et al., 2005; Bagaeva et al., 2006). Both CXCL13 deficiency and neutralisation reduce the severity of EAE early clinical course. Several other chemokines and their receptors are expressed in EAE and/or MS, where they are suggested to mediate trafficking of inflammatory cells in the CNS, regulate the migration of regulatory cells, and/or restrict the spreading of the inflammation (reviewed in Hamann et al., 2008). Therefore, chemokines appear to be beneficial with their homeostatic immune surveillance and clearance of immune infections; while, they may show detrimental effects with their ectopic expressions in CNS injury or autoimmune demyelination.

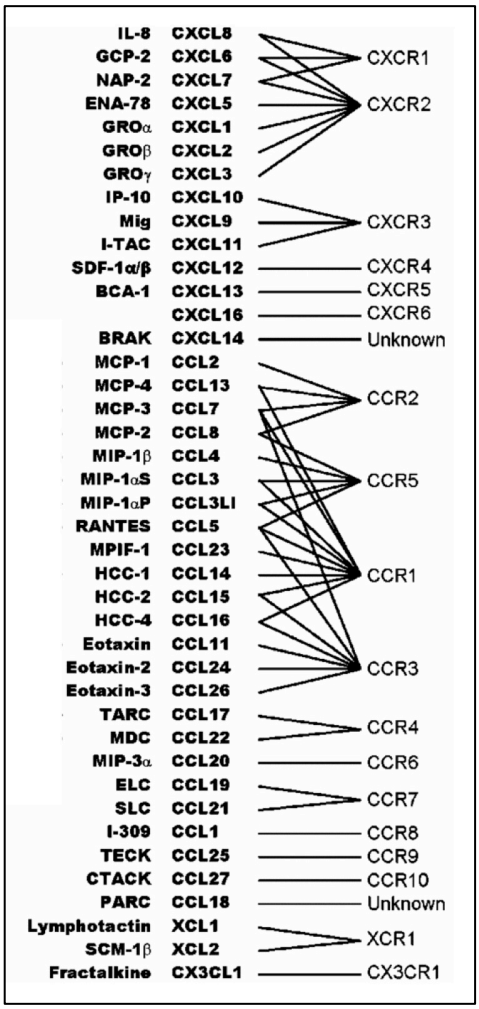

Figure 1. 7 A list of chemokines and their receptors.
Currently known chemokines are listed above with their old acronyms (on the left) and their names based on the new nomenclature (in the middle). A chemokine receptor (on the right) can bind more than one chemokine and a chemokine can signal through multiple chemokine receptors as shown in the figure. This is associated with the redundancy observed in functions of the chemokine system. The image was taken from Borroni et al., 2006.

1.5 The use of 'omic' studies to detect the differential mechanisms in distinct astrocyte phenotypes

'Omic' technologies provide detailed information about different molecules that make up a cell. They can be categorised as genomics, transcriptomics, proteomics, and metabolomics that target the universal detection of genes, mRNA, proteins and metabolites, respectively, in a specific biological sample (Horgan and Kenny, 2011). They can be integrated to form systems biology, which usually would require collaborations between investigators from different research areas or can be followed individually to obtain insights about one particular complex system at a time. Two examples, transcriptomics and metabolomics, will be explained in more detail below in

their relation to distinguishing different astrocyte phenotypes; whereas, genomics and proteomics will be skipped as they are beyond the scope of this thesis.

1.5.1 Transcriptomics

The transcriptome reflects the genes that are actively expressed at any given moment in the cells analysed. Currently, a high-scale analysis is carried out by means of gene expression microarrays that allow the observation of changes in expressions of thousands of genes in one experimental run. The microarrays consist of basically probes that are attached on glass slides, often named chips. The probes could be in the form of complementary DNA (cDNA) or an oligonucleotide, both of which allow the binding of the sample cDNA to assess the amount of mRNA for each gene in a specific condition compared to that in a control condition. Because of the very high numbers of variables in microarray experiments, the statistics become more complicated and the possibility of false positives increases. Therefore, the microarray gene expression profiling analyses are usually followed by other experiments such as real-time PCR in an attempt to validate those changes in gene expressions. Some other validating experiments can also be preferred depending on the purposes of the investigation, for which the examples will be given below.

Microarrays have been utilised to identify astrocytic markers that present either very low or no expression in other cell types such as oligodendrocytes and neurons, isolated from mouse forebrain (Cahoy et al., 2008) or olfactory ensheathing cells and Schwann cells from rats (Vincent et al., 2005). Astrocytes positive for ALDH1L1 and GLT1, two astrocytic markers, have also been compared by means of microarray gene expression profiling analysis, which presented highly similar expression profiles for astroglial genes but also showed the expression of some neuronal genes in GLT1 positive astrocytes (Yang et al., 2011). Differences have also been observed between cultured astrocytes that were plated on either poly-l-lysine (PLL)-coated or tenascin C (TnC)-coated glass coverslips (Nash et al., 2011b). Because PLL-astrocytes have been shown to be more supportive for myelination in embryonic rat spinal cord myelinating cultures compared to TnC-astrocytes, the differentially expressed genes between PLL- and TnC-astrocytes have been associated with regulation of myelination. After selecting several candidates to continue to work with, the expressional change has been validated for *Cxcl10* that was up-regulated in TnC-astrocytes. The follow-up *in vitro* studies also presented decreased levels of myelination in the presence of CXCL10 treatment and increased myelination levels in cultures with TnC-astrocytes that were treated with anti-CXCL10 neutrilising antibodies, both of which validated the results of the microarray (Nash et al., 2011b).

Astrocytes with different properties can also be studied using other strategies. Cytokine-treated cultured human astrocytes, which were isolated from healthy adult donors, have been compared against their controls using a lower-scale cDNA array that contained probes for a relevant functional group of 268 genes encoding cytokines, chemokines, growth factors and their receptors (Meeuwsen et al., 2003). The genes that were induced by pro-inflammatory cytokines (TNFα, IL-1β, or IFN-γ) have been listed in a way presenting the fold changes for all three separate treatments to provide basis for future studies. On the other hand, Zamanian et al. (2012) have carried out a more extensive study using reactive mouse astrocytes isolated at various time points after the onset of ischemic stroke or neuroinflammation induced by middle cerebral artery occlusion or intraperitoneal LPS injection, respectively. The heat map, generated by hierarchical clustering using the genes that were differentially expressed between the astrocytes from the two injury models, suggested that these astrocytes could present different expression profiles despite the presence of reactive gliosis in both types of CNS damage. They have identified two reactivity markers based on the most highly increased expressions in both injury models and have validated the results by immunohistrochemistry. The lists of top 50 changes in astrocytes from the two injuries compared to their controls and Gene Ontology grouping of these genes have provided further insights into understanding the common and differential mechanisms between reactive astrocytes from distinct CNS traumas.

1.5.2 Metabolomics

The information obtained from transcriptomics can provide the basis for a targeted metabolomics study investigating the differences between distinct astrocyte subpopulations or between astrocytes and other CNS cell types (Lovatt et al., 2007). A microarray gene expression profiling analysis has shown enhanced expression of genes encoding glycogenic and glycolytic enzymes in mouse cortical astrocytes, which has lead to mass spectrometry analysis to detect the levels of radioactively-labelled glucose-derived metabolites (Lovatt et al., 2007). The results from microarray and mass spectrometry experiments have confirmed each other in that particular study, where active oxidative metabolism has been identified and validated in protoplasmic astrocytes.

Another metabolomics approach has been applied on lipid samples isolated from whole-brain extracts from neonatal and adult mice (Camargo et al., 2012). Transgenic mice that lacked the astrocytic expression of SCAP (sterol regulatory element-binding protein cleavage-activating protein) have been used to observe the effects of the inhibition of astrocytic lipid synthesis. Lipid chromatography tandem mass spectrometry (LC-MS/MS)

has played role in the detection of relative levels of different types of lipids and fatty acids between wild type and conditional knockout animals. Therefore, this method has not only formed a way to validate the suppression of lipid synthesis *in vivo* but has also provided detailed information about astrocyte lipid metabolism.

It is also possible to follow untargeted analytical methods in metabolomics if different conditions are compared without extensive knowledge of which metabolites could be expressed in certain cell types and/or under certain conditions (reviewed in Dunn et al., 2012). The samples collected from the cells and the spent medium of astrocyte cultures can be analysed with LC-MS/MS to reveal several hundreds of putative metabolites that could highlight the differences between quiescent and reactive astrocytes or between astrocytes with other distinctive properties. Such a study has not been published yet to my knowledge.

1.6 Conclusions

Astrocytes are now accepted to present a continuum of phenotypes ranging from quiescent to reactive. Even though reactive astrocytes are mostly associated with various CNS pathologies, they have been shown to exhibit beneficial roles in addition to their previously established detrimental effects. The mechanisms that lead a specific astrocyte reactivity phenotype to exert protective and stimulatory or inhibitory roles under particular conditions are not yet fully understood. Cytokines and chemokines appear to be important regulators of astrocyte activation, which is usually observed as increased GFAP and nestin expression in astrocytes, cell hypertrophy, and increased cell proliferation rate. Regardless of the fact that whether these morphological changes appear or not, these signaling molecules and other environmental changes such as the use of a different cell culture-adhering substrate can still alter the astrocyte properties and allow them to be supportive or cause them to be inhibitory depending on circumstances (Nash et al., 2011b). Therefore, it would be crucial to find out what explicit changes occur in astrocytes in relation to their positive or negative roles. Once identified, these mechanisms could later be exploited for therapeutic discoveries to be used in neurodegenerative diseases like multiple sclerosis, where there is a dynamic regulation of extracellular matrix and cytokine secretion.

1.7 Aims

The main aim of this thesis is to address how various astrocyte phenotypes can influence myelination and identify their mechanism of action. This will be carried out by continuing previous studies on microarray gene profiling (Array 1) of various phenotypes

of monocultures of astrocytes with the addition of complex neuronal cultures plated on top (Array 2). Thus we are now considering how the crosstalk of neural cells can affect astrocyte gene expression.

i) To address if any identified proteins are important in the astrocyte regulation for myelination, genes identified in the array will be validated in our embryonic rat spinal cord myelinating cultures.

ii) To identify mechanism of action of CNTF on astrocyte reactivity and myelination, we will use a web-based program that will identify putative transcription factors involved in the transcriptional regulation of the molecules detected in Array 2.

iii) To address if CNTF plays a role in astrocyte metabolism, lipid chromatography tandem mass spectrometry will be carried out using samples from astrocyte monolayers plated on different coating substrates (PLL or TnC).

Chapter 2

Materials and Methods

2.1 Animals and animal care

All experimental animals were bred at the facility of University of Glasgow Biological Services (UGBS). All procedures were carried out in accordance with the guidelines, set forth by the Animal Scientific Procedures Act, under a project license (No: 6003895) granted by the UK Home Office with the approval of the University of Glasgow Ethical Review Process Applications Panel. Sprague Dawley (SD) rats and C57BL/6 mice were bred and killed according to UK Home Office standards by the trained staff of UGBS. The animals used for the experiments were either time-mated and embryos were collected on embryonic day 13.5 (E13.5) or 15.5, the day of plugging being E0.5, or were dissected at postnatal day 1 (P1).

All Sprague Dawley rats used were wild type. C57BL/6 mice consisted of three genotypes, one of them being the wild type and the other two both carrying the *Gp130* gene, flanked by two loxP sites that would allow the binding of Cre recombinase to these sites and hence the excision and inactivation of the target gene (Lakso et al., 1992; Betz et al., 1998; Bajenrau et al., 2002; Drogemuller et al., 2008). One strain was GFAP-$Cre^{-/-}$gp$130^{fl/fl}$, which did not contain the expression of Cre recombinase; whereas, GFAP-$Cre^{+/-}$gp$130^{fl/fl}$ mice showed constitutive Cre recombinase expression, controlled by *Gfap* promoter, and thus had their astrocytic *Gp130* gene inactivated (Haroon et al., 2011). GFAP-$Cre^{-/-}$gp$130^{fl/fl}$ mice were used as controls compared to GFAP-$Cre^{+/-}$gp$130^{fl/fl}$ mice in the experiments as these animals have been shown to resemble the wild type phenotype (Drogemuller et al., 2008; Haroon et al., 2011). Gp$130^{fl/fl}$ colonies were maintained by breeding GFAP-$Cre^{-/-}$gp$130^{fl/fl}$ with GFAP-$Cre^{+/-}$ gp$130^{fl/fl}$ animals (Fig 2.1). The colony was started using animals, obtained from Schluter Lab, Germany (Institut für Medizinische Mikrobiologie, Otto-von-Guericke Universität Magdeburg, Leipziger).

2.2 Cell culture

All cultures were maintained in a humidified incubator at 37°C of 7% CO_2/93% air. All media and reagents were filtered through a 0.22 μm filter.

2.2.1 Neurosphere-derived astrocyte cultures

Neurospheres were generated using the dissociated striata of Sprague Dawley rats aged 16-36 hours (Postnatal day 1). The tissue was mechanically dissociated using a glass Pasteur pipette in 1-2 ml of L-15 media (Invitrogen, Paisley, UK). The suspension was

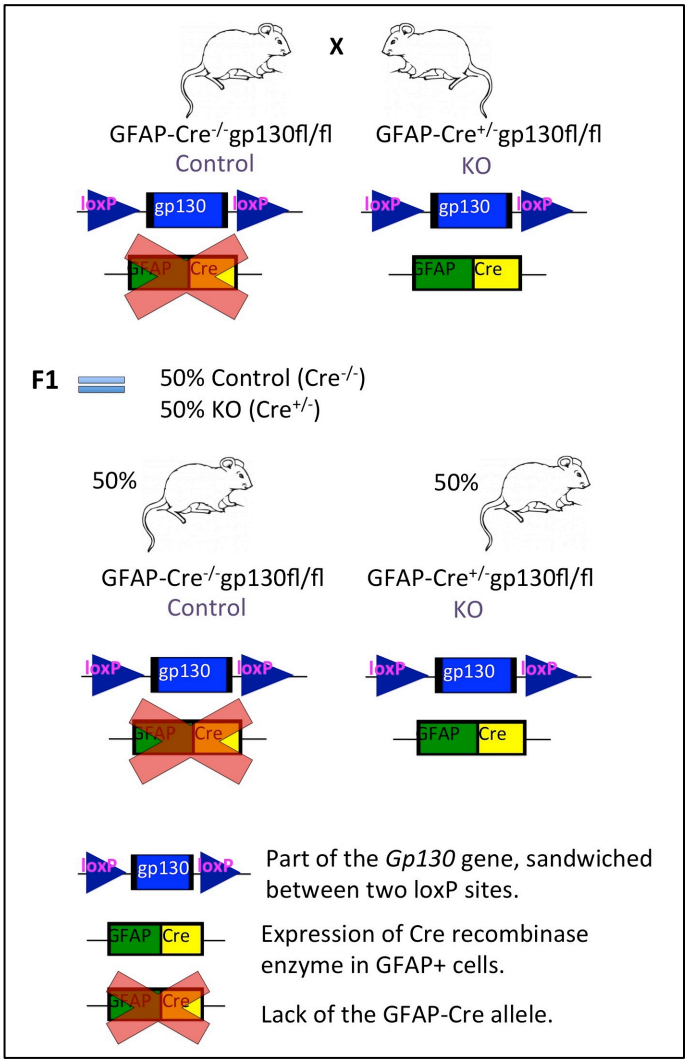

Figure 2. 1 C57BL/6 gp130$^{fl/fl}$ mouse colony was maintained by crossing GFAP-Cre$^{+/-}$ gp130$^{fl/fl}$ with GFAP-Cre$^{-/-}$gp130$^{fl/fl}$.

Astrocytic gp130 knockout (KO) mice were bred as shown above so that a litter would provide both the Cre recombinase (-) controls and the Cre recombinase (+) KO mouse pups. Cre-lox recombination system, used to generate astrocytic gp130 KO mice, allows the site-specific nucleotide sequence excision to inactivate a target gene. This system was targeted to function in astrocytes under the control of *Gfap* promoter and the *Gp130* gene was flanked with two loxP sites. The Cre recombinase enzyme in the astrocytes of GFAP-Cre$^{+/-}$ gp130$^{fl/fl}$ mice would, thus, inactivate the *Gp130* gene; whereas, this inactivation could not take place in GFAP-Cre$^{-/-}$gp130$^{fl/fl}$ control mice due to the lack of Cre expression. GFAP-Cre$^{+/-}$gp130$^{fl/fl}$ mice and GFAP-Cre$^{-/-}$gp130$^{fl/fl}$ mice were crossed to provide new generations, where the possibility of obtaining the animals from each genotype was 50% as seen in the diagram. GFAP: glial fibrillary acidic protein.

then centrifuged at 800 rpm (136 RCF) for 5 min. The pellet was resuspended in 1-2 ml of neurosphere media (NsM) consisting of Dulbecco's Modified Eagle Medium:Nutrient Mixture F-12 supplemented with other reagents seen in Table 2.1. The cell pellet was then mechanically dissociated again with a glass Pasteur pipette and placed into a 75 cm^3 tissue culture flask (Greiner, Gloucestershire, UK) containing 20 ml of NsM. The cell suspension was supplemented with 20 ng/ml recombinant human epidermal growth

factor (EGF, R&D Systems). Every 2 days, 5 ml NsM and 4 μl EGF (20 ng/ml) were added into the flask. When 60-70% of spheres were large enough (>200 μm), the spheres were differentiated into astrocytes as described by Thomson et al. (2006). Briefly, the spheres were plated onto poly-L-lysine-coated-coverslips (13 mm diameter, VWR International, Leicestershire, UK) with 10% FBS in DMEM (Table 2.1) for 5-10 days until a confluent monolayer formed. The coverslips were coated either with poly-L-lysine (PLL) or tenascin C (TnC). For PLL-coating, the coverslips were kept in PLL solution (13.3 μg/ml in distilled water, Sigma) for 1-24 hr at 37°C, washed in distilled water and left to air dry in the tissue culture hood before being used. For TnC-coating, each coverslip was incubated in 75 μl of TnC solution (5 μg/ml, CC065, Millipore) for 1-2 hr at 37°C. TnC solution was then removed and the coverslips were left to dry. For experiments that would compare PLL and TnC conditions, PLL-coated coverslips were also prepared using 75 μl of PLL solution per coverslip but the coverslips were washed with PBS unlike TnC-coated coverslips.

A modified version of the above-mentioned protocol was followed when tissue from $gp130^{fl/fl}$ neonatal mice were used because cultures had to be made from single pups prior to genotyping. Since the genotype from each pup from a litter of the breeding of GFAP-$Cre^{-/-}$$gp130^{fl/fl}$ with GFAP-$Cre^{+/-}$$gp130^{fl/fl}$ could not be known until tissue was genotyped by PCR, each striatal tissue had to be treated in separate microcentrifuge tubes due to the possibility of their genotypes being different from one another. Thus mechanical dissociation of the tissue samples was carried out using a 21-gauge (G) needle in 1 ml of L15 as this was more practical when dealing with an increased number of microcentrifuge tubes. The samples were centrifuged in a microcentrifuge, where centrifugation at 1200 rpm for 6 min generated less delicate pellets. The samples were then resuspended in 1 ml of L15 media again using a 21G needle. This 1 ml of cell suspension and 1 μl of EGF were added into 4 ml of NsM in 25 cm^3 tissue culture flask. The cultures were fed with 1 ml of fresh NsM and 1 μl of EGF every 2 days until the spheres were large enough to be used for the next stage of cell plating (5-9 days). The coverslips to be coated with astrocytes were coated with PLL solution, prepared using boric acid (0.25% boric acid and 0.38% sodium tetraborate in distilled water, all from Sigma) instead of water (13.3 μg/ml PLL, Sigma). This is believed to be more optimal for mouse cell attachment.

The astrocyte cultures were treated with various reagents by removing 250 μl of their culture medium and replacing it with 250 μl of fresh medium containing appropriate reagent at a concentration, twice the amount intended, to account for dilution once added to the total volume each coverslip was maintained in. For example, if cultures

Table 2. 1 The list of principal medium types and their ingredients used for cell culture.

Medium	Ingredients	Source
Neurosphere Medium (NsM)	Dulbecco's Modified Eagle Medium:Nutrient Mixture F-12 (DMEM/F12 containing 3,151 mg/L glucose, #21331)	Life Tech.
	0.1% $NaHCO_3$, 2 mM L-glutamine, 5,000 IU/ml penicillin, 5 μg/ml streptomycin, 5 mM HEPES, 0.01% bovine serum albumin	Life Tech.
	0.6% glucose (#G7021), 25 μg/ml insulin, 100 μg/ml apotransferrin, 60 μM putrescine (P-7505), 20 nM progesterone (P-6149) and 30 nM sodium selenite (S-9133)	Sigma
10% FBS in DMEM	low glucose (1000 mg/L) DMEM (#21885-025)	Life Tech.
	10% foetal bovine serum, 2 mM L-glutamine	Sigma
Plating Medium (PM)	50% high-glucose (4,500 mg/L) DMEM (#41966), 25% horse serum (#26050-088), 25% Hank's Balanced Salt Solution (HBSS, #14170-088)	Life Tech.
Differentiation Medium (DM)	high-glucose (4,500 mg/L) DMEM (#41966)	Life Tech.
	10 ng/ml biotin, 50 nM hydrocortisone, 0.5 mg/ml insulin, and 0.5% hormone mixture (1 mg/ml apotransferrin, 20 mM putrescine, 4 μM progesterone and 6 μM selenium, formulation based on N2 mix of Bottenstein and Sato, 1979)	Sigma

The table shows the ingredients of neurosphere medium (NsM), 10% FBS in DMEM, plating medium (PM) and differentiation medium (DM). NsM is used to culture striatum-derived neurospheres and 10% FBS in DMEM is a medium for the maintenance of neurosphere-derived astrocyte cultures. Embryonic spinal cord myelinating cultures are initiated in PM and are maintained in DM from then on. The catalogue numbers and the company source are also presented above for the reagents. DMEM: Dulbecco's Modified Eagle Medium; FBS: foetal bovine serum; Life Tech.: Life Technologies.

were going to be treated with 10 ng/ml of a reagent, a solution was prepared at 20 ng/ml and 250 μl of that was added into each well during the treatment.

2.2.2 Embryonic spinal cord myelinating cultures

The method of generating myelinating embryonic mixed spinal cord cultures is based on that developed for mice (Thomson et al., 2008) and rat cultures (Sorensen et al., 2008). The spinal cords of embryonic day 15.5 (E15.5) SD rats or E13.5 C57BL/6 wild type mice were dissociated and the meninges were removed before placing the tissue in a bijou containing L-15 on wet ice. The spinal cords (4-5) were dissociated mechanically using Pasteur pipettes and then enzymatically using trypsin (100 μl of 2.5%, Invitrogen, Paisley, Scotland) and collagenase (100 μl of 1.33%, ICN Pharmaceuticals, UK) for 15 min at 37°C. Enzymatic activity was stopped by adding 1 ml of a solution containing 0.52

mg/ml soybean trypsin inhibitor (T-9003), 3.0 mg/ml bovine serum albumin (A2153) and 0.04 mg/ml DNase (D-4263, all from Sigma). The cells were triturated using a Pasteur pipette and centrifuged at 1200 rpm for 5 min. The cell pellet was resuspended in plating medium (PM, Table 2.1). The coverslips, covered in a confluent monolayer of astrocytes, were placed in a dry 35 mm Petri dish and the mixed spinal cord cell suspension was plated on top as a droplet at a density of 150,000 cells per 100 μl. Two coverslips were placed in each dish and they were incubated at 37°C for 2 hours to allow for stable attachment. A mixture of 400 μl of PM and 600 μl of differentiation medium (DM, Table 2.1) was added into each dish. The insulin was removed from DM after 12 days in culture to prevent excessive proliferation of non-myelinating oligodendrocytes that could obscure the myelin sheaths (Thomson et al., 2006, 2008). Cultures were fed every other day by removing 400 μl of media and replacing it with fresh 500 μl DM to avoid the possible decrease in volume of medium that could occur over time due to evaporation at 37°C. The cultures were maintained for 24-28 days *in vitro* (DIV).

This protocol was also modified for generation of myelinating cultures of spinal cord tissue from C57BL/6 gp130$^{fl/fl}$ mouse embryos (E13.5) as each embryo obtained from the same litter would have to be treated separately since they could not be genotyped until the myelinating cultures were set up. Each spinal cord was placed in 500 μl of L15 media. Mechanical dissociations and titrations were made using 1000 μl and 200 μl pipette tips respectively. Enzymatic dissociation was stopped by adding 500 μl of the solution containing soybean trypsin inhibitor, bovine serum albumin and DNase solution. The samples were centrifuged using a microcentrifuge at 1200 rpm for 6 min. The cell suspension, ready to be used in plating medium, was either plated on glass coverslips, previously coated with PLL, dissolved in boric acid buffer, or on coverslips, each containing a confluent monolayer of GFAP-Cre$^{-/-}$gp130$^{fl/fl}$ or GFAP-Cre$^{+/-}$gp130$^{fl/fl}$ mouse astrocytes. Immediately after adding a mixture of PM and DM media into the Petri dish, the coverslips were pressed down gently at the edges using a 200 μl pipette tip to avoid them from floating later on. The process was repeated 2 days later, during the second feeding of the cultures. If any coverslips were seen to float from then on, they were again pinned down using a pipette tip.

The embryonic spinal cord myelinating cultures were treated with various reagents starting from 12 DIV, by removing 400 μl of the used medium and replacing it with 500 μl of fresh medium containing such a reagent at the appropriate concentration, 2.4 fold of the amount intended, as it would be halved once dissolved in the total volume in the dish (1.2 ml).

2.2.3 Oligondendrocyte cultures

Cortical astrocytes were isolated from cerebral cortices of 1 day old SD rats as described in Noble and Murray (1984). Briefly, the cortex was dissected from P1 pups and enzymatically dissociated. The cells were maintained in 10% FBS in DMEM (Table 2.1) and grown to confluency in a 75 cm^3 flask for 5-8 days. The flasks were shaken at 37^oC for 4-5 hours to remove the more lightly attached oligodendrocyte precursor cells (OPCs). The detached cells were removed from the intact astrocyte monolayer and placed into a 15 cm Petri dish and incubated at 37^oC for 15 min to allow the microglia to attach to the dish. The remaining cell suspension was then centrifuged at 1200 rpm for 3 min. The pellet was resuspended in 2.5 ml of DMEM-BS media (Bottenstein and Sato, 1979) containing 10 ng/ml of PDGF and 10 ng/ml of FGF2 (both from Peprotech, UK), known OPC mitogens (Bogler et al., 1990). The cells were plated onto PLL-coated coverslips in a 24-well plate at a volume of 100 μl and incubated at 37^oC for 15 min to allow the cells to attach. Then an additional 400 μl of DMEM-BS media with PDGF and FGF2 was added into each well. The cells were fed every other day. The growth factors were removed from the media for some of the cells after 4-5 days so as to treat with various reagents. The cells were fed every other day for 8 days by removing 250 μl of the original media and replacing it with 250 μl of fresh media. OPC cultures were treated with various reagents as described in the treatment of astrocyte cultures (Section 2.2.1).

2.2.4 Reagents used for treatments

Astrocytes, oligodendrocytes and embryonic spinal cord myelinating cultures were treated with various reagents. These are rat recombinant CNTF (#557-NT-010, R&D Systems, USA), anti-CNTF neutralising antibody (MAB557, R&D Systems), recombinant rat CCL2 (3144-JE-025/CF, R&D Systems), recombinant rat CCL7 (CHM-280, Prospec, USA), recombinant human CTGF (#120-19, Peprotech, UK), and recombinant human SERPINB2 (ab69515, Abcam, UK).

2.3 Immunocytochemistry

Coverslips, on which cells were plated, were taken out of 24-well plates or 35 mm dishes using forceps and excess media was blotted against tissue paper and placed on a staining tray which lifts the coverslip off the surface and is receptive for a small amount of antibody for staining. For cell surface markers, antibodies were diluted in culture media; whereas, for intracellular markers antibodies were diluted in blocking buffer (BB) consisting of 0.1% Triton-X-100 and 0.2% gelatine in PBS. If only external markers

were used, cells were treated first with primary antibodies followed by fluorochrome labeled class specific secondary antibodies, each step for 20 min, followed by mounting in Vectashield with or without DAPI. If intracellular markers were to be used in combination with a cell surface marker, after the treatment with its class specific antibody cells were fixed and permeabilised with ice cold methanol at -20°C for 10 min. Some primary antibodies required fixation with 4% paraformaldehyde (Para, Table 2.2), which was then followed by permeabilisation with 0.5% Triton-X-100 for 15 min. Cells were blocked in BB for 15 min. Primary antibodies of internal markers were incubated for 40-60 min and secondary fluorochrome class specific antibodies were incubated for 30-40 min. The coverslips were then mounted in Vectashield. All the reagents and antibodies were added as 50 μl onto each coverslip at room temperature (RT) unless otherwise stated. Coverslips were washed between each subsequent staining step 2-3 times in PBS. The primary and secondary antibodies used are listed in Tables 2.2 and 2.3.

Table 2. 2 The list of primary antibodies used for immunocytochemistry.

Antigen	Raised in	Istotype	Dilution	Fixation method	Internal/ cell surface	Source
A2B5	Mouse	IgM	1:1	n/a	Cell surface	Hybridoma
PLP (AA3)	Rat	IgG	1:100	4% Para/ ice cold methanol	Internal	Hybridoma
GFAP	Rabbit	IgG	1:500	4% Para/ ice cold methanol	Internal	DAKO
MOG	Mouse	IgG_{2a}	1:100	n/a	Cell surface	Hybridoma
MBP	Mouse	IgG_{2a}	1:100	Ice cold methanol	Internal	Hybridoma
Nestin	Mouse	IgG_1	1:200	Ice cold methanol	Internal	Abcam
O4	Mouse	IgM	1:1	n/a	Cell surface	Hybridoma
SMI-31	Mouse	IgG1	1:1500	4% Para/ ice cold methanol	Internal	Covance

Table of the primary antibodies used to detect the listed antigens for immunocytochemistry with animal species they were raised in, their isotypes, the optimum dilution of use, the fixation method, the type of detection they would provide (internal or external) and the company they were purchased from. Some primary antibodies could be fixed using 4% Para or ice cold 100% methanol, both of which revealed similar results. A2B5: oligodendrocyte progenitor marker; GFAP: glial fibrillary acidic protein; Ig: immunoglobulin; MBP: myelin basic protein; MOG: myelin oligodendrocyte glycoprotein; n/a: not applicable; O4: oligodendrocyte marker; Para: paraformaldehyde; PLP: myelin proteolipid protein; SMI-31: phosphorylated neurofilament.

Table 2. 3 The list of secondary antibodies used for immunocytochemistry.

Antibody	Conjugate	Dilution	Source
Goat anti-mouse IgG1	Alexa Fluor:555	1:600	Molecular Probes
Goat anti-mouse IgM	Alexa Fluor:555	1:600	Molecular Probes
Goat anti-rat IgG	Alexa Fluor:488	1:600	Molecular Probes
Goat anti-rat IgG	FITC	1:100	Southern Biotech
Goat anti-mouse IgM	TRITC	1:100	Southern Biotech
Goat anti-mouse IgG_{2a}	FITC	1:100	Southern Biotech
Goat anti-rabbit IgG	FITC	1:100	Southern Biotech

Shown in the table are the secondary antibodies used in immunocytochemistry. They were conjugated to the fluorochromes to allow indirect visualisation of the antigens using fluorescent microscopy. Their optimum dilution and company source are also listed in the table. FITC: fluorescein isothiocyanate; Ig: immunoglobulin; TRITC: tetramethylrhodamine.

2.4 Microarray gene expression profiling

2.4.1 Sample description

Embryonic rat spinal cord myelinating cultures (Section 2.2.2) were used for microarray gene expression profiling. These cultures were plated on astrocytes, seeded either on PLL- or TnC-coated coverslips. At 12 DIV, they were either fed with standard medium (control) or treated with recombinant rat CNTF (1ng/ml, R&D systems, 557-NT-010) and total RNA was extracted from these cultures 4 hr or 24 hr after the feeding or the treatment. Thus, 8 different conditions were generated to test: 1) PLL-control-4 hr, 2) PLL-CNTF-4hr, 3) TnC-control-4hr, 4) TnC-CNTF-4hr, 5) PLL-control-24 hr, 6) PLL-CNTF-24hr, 7) TnC-control-24hr, 8) TnC-CNTF-24hr. The cultures were generated and maintained by Dr. Besma Nash in three biological replicates.

2.4.2 RNA extraction

Total RNA was extracted from embryonic rat spinal cord myelinating cultures 4 hr and 24 hr after standard medium feeding or CNTF-treatment using a Qiagen Kit. The samples were then frozen at -20^{o}C in RNAse free microcentrifuge tubes. The RNA extraction was performed together with Dr. Besma Nash.

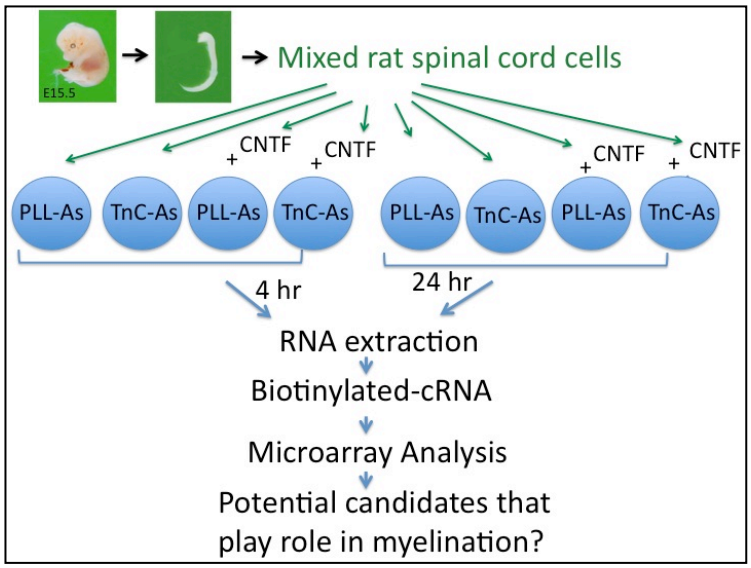

Figure 2. 2 A microarray gene expression profiling analysis was carried out using embryonic rat spinal cord myelinating cultures, at different conditions.
The spinal cords of E15.5 Sprague Dawley rat embryos were mechanically and enzymatically dissociated and seeded on astrocyte monolayers, plated on coverslips coated with PLL or TnC. After 12 days *in vitro* some of these cultures were additionally treated with 1 ng/ml of recombinant rat CNTF while sister cultures were fed with standard medium. Total RNA was extracted from these cultures 4 hr and 24 hr after the standard medium feeding or CNTF treatment. Using the RNA samples, biotinylated cRNA samples were prepared for microarray gene expression profiling analysis. The analysis of differentially expressed transcripts between cultures at different conditions provided suggestions for potential regulators of myelination. The cultures were prepared in three biological replicates. CNTF: ciliary neurotrophic factor; PLL: Poly-L-lysine; TnC: Tenascin C.

2.4.3 Checking the RNA integrity

The integrity of the total RNA from these samples was assessed using the Agilent 2100 Bioanalyser before the process of RNA amplification and biotinylation. Agilent 2100 Bioanalyser uses microfluidics/capillary electrophoresis to analyse nucleic acids. It compares the fluorescence of the sample, to which an RNA-specific dye has been added, with that of a standard. High quality total RNA is presented with the presence of two distinct bands for 28S and 18S subunits, with a ratio of 2:1, respectively, in the electropherograms (see Fig 2.3 for example) obtained from Agilent 2100 Bioanalyser analyzing software. In order to provide a more quantitative data for RNA integrity, a software algorithm (Expert 2100 software, starting with Rev 02.01) calculates the RNA integrity number (RIN). RIN is not influenced by instrument, sample integration and concentration variability. Examples for several RINs are presented in Fig 2.3. The RIN values and electropherograms of the total RNA samples used for microarray gene expression profiling are shown in Appendix I. The RIN values for our samples ranged between 8.9-10.

2.4.4 RNA amplification and biotinylation

RNA was amplified to maximise the complementary RNA (cRNA) yield and biotinylated using an Illumina Total Prep RNA Amplification Kit (AMIL1791, Ambion, Life Technologies, UK) following the manufacturer's guideline that included the following major steps: Total RNA was reverse-transcribed to synthesize first strand cDNA, the second strand cDNA was synthesized following that, cDNA was purified, cDNA was transcribed *in vitro* to synthesize cRNA, and cRNA was purified. cRNA was biotinylated during the *in vitro* transcription (IVT) step. 250 ng of total RNA in 11 μl was used to start the RNA amplification process. The purity of biotinylated cRNA samples was assessed again using the Agilent 2100 Bioanalyser and its software (Appendix II), where the ribosomal contamination can be detected as two distinct peaks as shown in the example electropherogram in Fig 2.4. Since the concentration of one particular cRNA sample (#8, Appendix III) was very low (13.5 ng/μl) compared to others, the amplification and biotinylation steps were repeated for that one sample only (new concentration 75 ng/μl) to avoid further expenditure of other total RNA. Because the concentration of some cRNA were lower than the required 150 ng/μl for the direct hybridisation assay, all the samples were centrifuged in a high-speed vacuum centrifuge for 40 (2 x 20) min. The cRNA integrity was assessed again using the Agilent 2100 Bioanalyser and the concentrations were measured using a Nanodrop 2000 spectrophotometer. cRNA concentrations are listed in Appendix III. The electropherograms, showing the cRNA quality of the samples before the vacuum centrifugation, presented some contamination for two samples (Appendix II, samples #2 and #12), although this was not considered to be high enough to exclude them in the microarray gene expression profiling analysis. Electropherograms after the vacuum are not presented, as the Agilent 2100 Bioanalyser does not produce any sensible readings at highly increased concentrations such as those above 250-300 ng/μl. Only the electropherogram for sample #8 is shown both before and after vacuum centrifugation due to the above-mentioned reason (Appendix II).

2.4.5 Direct hybridisation assay

Two Sentrix Beadchip RatRef-12 v1 arrays (serial numbers: #5842733044, #5842733065, Illumina, USA) were used to carry out the direct hybridisation assay. Each of these gene expression Beadchip arrays contain over 22,000 oligonucleotide probes targeting all known genes and known alternative splice variants. These probe sequences are attached to 3-micron beads that are assembled into the microwells of the BeadChip substrate. The main purpose of the direct hybridisation assay is thus to hybridise the cRNA sequences to the beads.

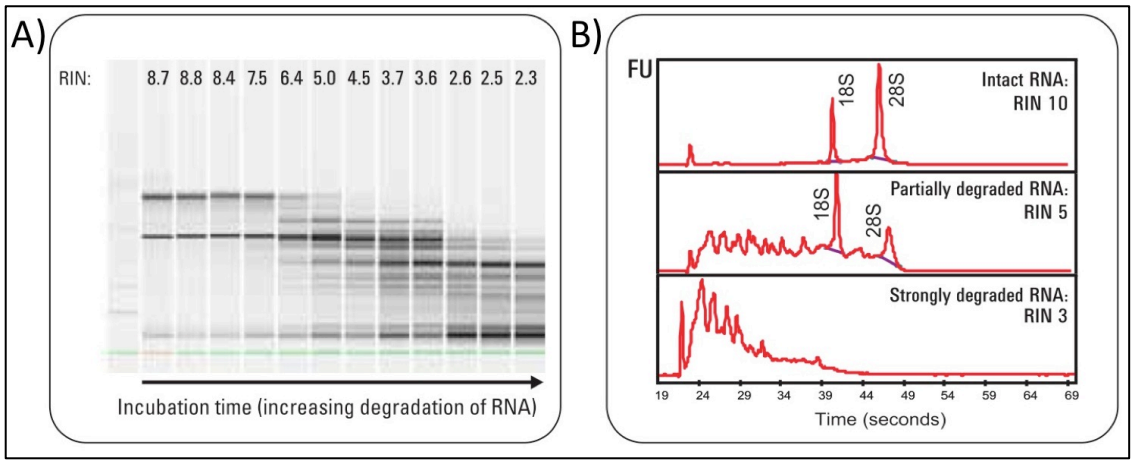

Figure 2. 3 Examples of RNA integrity using the results obtained from the Agilent 2100 Bioanalyser.

A software algorithm (Expert 2100 software, starting with Rev 02.01) is used to calculate the RNA integrity number (RIN) for each RNA sample entered into Agilent 2100 Bioanalyser. A higher RIN presents a sample with higher quality. Good quality RNA samples are expected to present two distinct bands 18S and 28S subunits, with a ratio of 1:2, respectively. **A)** Samples with higher RINs present two clear bands for those subunits; while, those with lower RINs present less clear bands due to increased RNA degradation. **B)** The expected ratio for the subunits is observed clearly for a RIN of 10; whereas, this ratio is disturbed for lower RINs such as 5 and 3. (Image taken from Agilent 2100 bioanalyser, application compendium, http://www.chem.agilent.com/Library/applications/5989-3542EN.pdf)

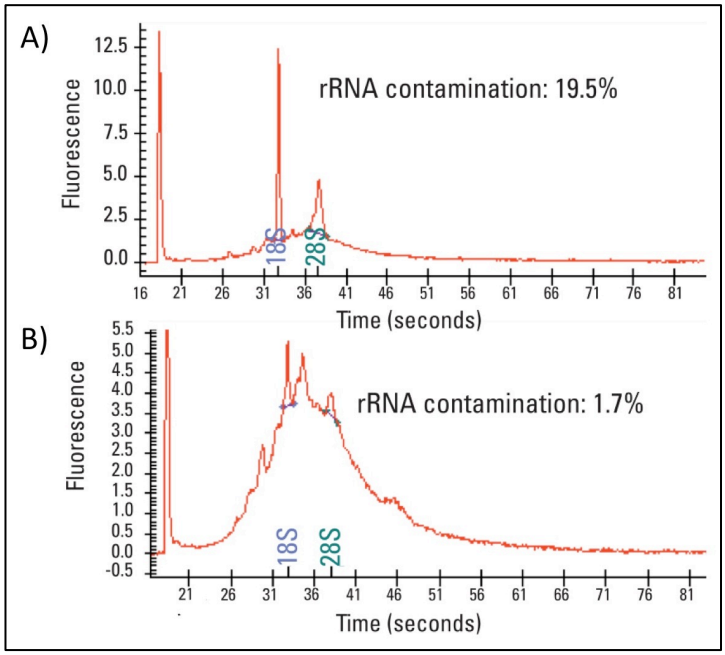

Figure 2. 4 Examples of ribosomal RNA (rRNA) contamination detected by the Agilent 2100 Bioanalyser in mRNA samples.

Shown in the image is the analysis of mRNA quality of two commercially available RNA samples by Agilent 2100 Bioanalyser and its software. A) The contamination with two rRNA subunits present themselves as clear peaks in the electropherogram; whereas, B) such peaks are less visible or not existent in samples with less or no contamination. (Image taken from Agilent 2100 Bioanalyser, application compendium, http://www.chem.agilent.com/Library/applications/5989-3542EN.pdf)

The hybridisation process was carried out following the manufacturer's guidelines. Briefly, 10 µl of Hybridisation (Hyb) Mix, provided in the kit, was mixed with 5 µl of cRNA at 150 ng/µl. The mixture was heated at 65°C for 5 min and then applied on the arrays that have previously been placed in a Hyb Chamber Insert. The samples were loaded into the BeadChip arrays in the order shown in Table 2.4 (designed by the statistician Dr. John Mcclure, Mcbride Lab, Institute of Cardiovascular and Medical Sciences, University of Glasgow) to maximise the randomness in the system to provide a higher level of significance in the end. The inserts containing the arrays were then loaded into a BeadChip Hyb Chamber. The Chamber lid was closed and locked securely and the arrays were left in the 58°C Illumina Hybridisation Oven overnight. The following day the coverseal of each array slide was removed and the arrays were washed in several steps using ethanol and other washing solutions provided by the manufacturer. After the washes, the arrays were incubated with streptavidin-Cy3 for 10 min at RT to develop the signal provided by hybridisation and washed again. They were then dried by centrifugation at 275 rcf for 4 min at RT. Once ready, the BeadChip arrays were scanned on the Illumina BeadArray Reader on the same day. Ms. Wendy Crawford (Mcbride Lab, Institute of Cardiovascular and Medical Sciences, University of Glasgow) was of great help on all steps of the direct hybridisation assay and scanning the arrays. Please see the manufacturer's manual for further details (*http://support.illumina.com/content/dam/illumina-support/documents/myillumina/3466bf71-78bd-4842-8bfc-393a45d11874/wggex_direct_hybridization_assay_guide_11322355_a.pdf*).

Table 2. 4 The order of the biotinylated cRNA samples loaded into the BeadChip Arrays.

BeadChip #5842733044				BeadChip #5842733065			
Lane	**Group**	**Time Point**	**Biological repeat (n)**	**Lane**	**Group**	**Time Point**	**Biological repeat (n)**
1	PLL + CNTF	4 hr	1	1	TnC + CNTF	24 hr	3
2	TnC + CNTF	24 hr	1	2	TnC Control	4 hr	2
3	TnC Control	4 hr	1	3	PLL + CNTF	24 hr	2
4	PLL Control	4 hr	3	4	TnC + CNTF	24 hr	2
5	PLL + CNTF	24 hr	3	5	PLL Control	4 hr	2
6	TnC + CNTF	4 hr	1	6	PLL Control	24 hr	3
7	TnC Control	24 hr	1	7	PLL + CNTF	4 hr	3
8	PLL Control	24 hr	1	8	TnC + CNTF	4 hr	2
9	TnC + CNTF	4 hr	3	9	PLL Control	24 hr	2
10	PLL + CNTF	24 hr	1	10	TnC Control	4 hr	3
11	PLL Control	4 hr	1	11	TnC Control	24 hr	2
12	TnC Control	24 hr	3	12	PLL + CNTF	4 hr	2

Total RNA was isolated from embryonic rat spinal cord cultures plated on astrocyte monolayers on PLL or TnC, 4 hr or 24 hr after standard medium feeding (control) or recombinant rat CNTF feeding (+CNTF). The cultures were maintained in three biological replicates (n). Total RNA was amplified in means of *in vitro* transcription reactions and was biotinylated using the same RNA amplification kit (AMIL1791, Ambion), the

processes of which generated hundreds to thousands copies of biotinylated cRNA. These samples were then loaded in the order, shown in the table, into two Sentrix BeadChip RatRef-12 v1 arrays (Illumina) for the direct hybridisation assay. This order was designed by Dr. John Mcclure (Univeristy of Glasgow). CNTF: ciliary neurotrophic factor.

2.4.6 Analysis of BeadChip data

Data was quantile normalised in BeadStudio (Illumina, San Diego, USA) and Rank Products (RP, Breitling et al., 2004) was used to assess the statistical significance of pairwise intergroup differences. A false discovery rate (FDR) cut-off value of 5% was used to determine significances by means of FDR multiple testing correction method (Benjamin and Hochberg, 1995). Venn diagrams were generated to look at the differences in gene expressions between embryonic rat spinal cord myelinating cultures at different conditions as explained in detail in Chapter 3.

2.5 Quantitative real time polymerase chain reaction (qRT-PCR)

2.5.1 RNA extraction

Total RNA was extracted from primary cell cultures using PureLink RNA Mini Kit (Ambion, Life Technologies, UK) following the manufacturer's guideline. Briefly, cells were washed with PBS and then lysed with a Lysis Buffer, included in the kit, containing 2-mercaptoethanol. This was then homogenised by passing through a 21G syringe needle 5-10 times, treated with 70% ethanol and the microcentrifuge tubes were flicked to disperse any remaining precipitates. Samples were centrifuged in spin cartridges for RNA to bind to the filters during the following RNA-purifying, washing steps. Finally, total RNA was collected in 14 µl of RNA-se free water and stored at -20^{o}C until future use. The concentrations of the samples were measured using the RNA setting of the NanoDrop 2000.

2.5.2 cDNA synthesis

Total RNA, extracted from the cell cultures as described above, was used as a starting material for reverse transcription to generate cDNA. The process was carried out using TaqMan Reverse Transcription Reagents kit (N808-0234, Applied Biosystems, Life Technologies, UK) and following the manufacturer's guideline. Basically, 7.7 µl or 15.4 µl of total RNA was added into a mixture of TaqMAN reverse transcription (RT) buffer, magnesium chloride, deoxy nucleoside triphosphates (dNTPs), oligodeoxythymidylic acid (oligo-dT) primers (or random hexamers), RNase inhibitor and MultiScribe reverse

transcriptase, creating a total volume of 20 µl or 40 µl, respectively, for each reaction mix. To increase the cDNA yield, the reactions were prepared mostly in 40 µl even if the volumes of the total RNA samples were not large enough, in which case RNA-se free water was added to make its volume up to 15.4 µl. An imporatn point was to insure that the total RNA used should not be greater than 2 µg, which was never the case in our samples as their concentrations never reached to such high levels. Samples were incubated at 25°C for 10 min, at 48°C for 30 min, and at 95°C for 5 min using a previously set-up program in Veriti 96-well Thermal Cycler (#9902, Applied Biosystems). Their concentrations were measured using the 'single stranded (ss) DNA' setting of NanoDrop 2000 spectrophotometer. The cDNA samples were stored at -20°C until further analysis by qRT-PCR.

2.5.3 Running the qRT-PCR plate

qRT-PCR reactions were run in 384-well plates (Axygen PCR-384M2-C-BC,Thistle Scientific, UK). Each reaction consisted of 2 µl of TaqMan Gene Expression Master Mix (#4369016, Applied Biosystems), 0.25 µl of rat *Gapdh* endogenous control primer (the housekeeping gene, # 4352338E, Applied Biosystems), 0.25 µl of the probe (primer set) and 2 µl of the cDNA sample (at 50 ng/µl). All the probes were also from Applied Biosystems with the following catalogue numbers shown in brackets: Ccl2 (Rn00580555_m1), Ccl7 (Rn01467286_m1), Ctgf (Rn01537279_g1), Cxcl11 (Rn00788262_g1), Cxcl13 (Rn01450028_m1), Lcn2 (Rn00590612_m1), Serpinb2 (Rn00572553_m1), Thbs2 (Rn02111874_s1), and Wif1 (Rn00586968_m1). A master mix was prepared for each probe to speed up the process and to minimise the technical variations in the system. Each reaction was run in three technical replicates. Control reactions were also prepared, where cDNA was not added, to check whether the probes were free of contamination. The 384-well plate then was sealed with an optical adhesive film (4360954, Applied Biosystems) and centrifuged briefly at 500-600 rpm for 40-60 sec. Once ready, it was run using the 7900HT Instrument (Applied Biosystems), controlled by the SDS 2.4 software, where real time PCR was carried out with VIC-MGB and FAM-MGB dyes selected to show the expressions of *Gapdh* and the probes, respectively. During the run, samples were incubated at 50°C for 2 min, at 95°C for 10 min and 40 cycles of the following program was performed: 15 sec at 95°C and 1 min at 60°C.

2.5.4 Analysing the qRT-PCR data

Once the qRT-PCR run was completed, data was exported from the SDS 2.4 software in Microsoft Excel sheets as Ct (cycle threshold) values. Ct is the number of cycles

required for the fluorescent signal to cross the threshold, i.e. to exceed the background level. ΔCt value was calculated as the subtraction of the VIC (Gapdh) Ct from the FAM (probe) Ct. Then the mean ΔCt was calculated by taking the average of three technical repeats per sample. The average of the mean ΔCt values of three biological replicates formed another mean ΔCt (mean ΔCt 2 in Table 2.5). Mean ΔCt 2 value for PLL-control-4 hr cultures was substracted from the mean ΔCt 2 values of other samples to obtain ΔΔCt values standardised to PLL-control-4 hr samples. Relative quantification was calculated by using the formula "POWER(2, -ΔΔCt)" in Microsoft Excel as seen in Table 2.5. Standard error of mean for relative quantification values were calculated separately for plus and minus error bars as shown in Table 2.5. One way repeated measures ANOVA test was used to determine any possible significance between the three mean ΔCt values of one culture condition (n=3) and those of another.

Table 2. 5 The calculation of relative quantification and standard error of mean at the end of qRT-PCR analysis

		A	B	C	D	E	F	G	H	I	J
	Sample	**Mean ΔCt**	**Mean ΔCt 2**	**Standard Deviation**	**Standard Error**	**ΔΔCt**	**RQ**			**Error Bar (Minus)**	**Error Bar (Plus)**
1	PLL-con-4 hr n=1	4.65									
2	PLL-con-4 hr n=2	12.0									
3	PLL-con-4 hr n=3	7.67									
4			=Avg (A1:A3)	=Stdev (A1:A3)	=C4/ SQRT(3)	=B4-B4	=Power(2, E4)	=Power(2, -(E4+D4)	=Power(2, -(E4-D4)	=F4-G4	=F4-H4
5			8.09	3.67	2.12	0.00	1.00	0.23	4.344	0.770	3.344
6	TnC-con-4 hr n=1	11.2									
7	TnC-con-4 hr n=2	11.9									
8	TnC-con-4 hr n=3	12.6									
9			=Avg (A6:A8)	=Stdev (A6:A8)	=C9/ SQRT(3)	=B9-B4	=Power(2, E9)	=Power(2, -(E9+D9)	=Power(2, -(E9-D9)	=F9-G9	=F9-H9
10			11.9	0.73	0.42	3.80	0.07	0.05	0.096	0.018	0.024

An example is given in the table above for the calculations carried away to obtain relative quantification (RQ) and standard error of mean values at the end of qRT-PCR experiments. The values presented are from the 1st qRT-PCR experiment carried away using the probe for *Serpinb2* expression. Mean ΔCt values for three biological repeats for the culture conditions of PLL-control-4 hr and TnC-control-4hr are used to begin the calculations in the example above. The formulas shown in the table were used in Microsoft Excel to calculate the relevant values.

2.6 Analysing the microarray gene expression profiling data using oPPOSUM

The genes that were found to be differentially expressed in the microarray gene expression profiling analysis, where total RNA from embryonic rat spinal cord myelinating cultures at different conditions was collected (Array 2), were also used to determine any possible transcription factors that could be regulating the expressions of these genes. The genes that were differentially regulated at one direction (up or down) in a comparison of two culture conditions (e.g. PLL-control-4 hr vs TnC-control-4 hr) were entered into oPOSSUM 3.0 (Kwon et al., 2012; *http://opossum.cisreg.ca/oPOSSUM3*), a web-based program that allows single site analysis (SSA), which detects over-represented conserved transcription factor binding sites in a set of human, mouse, fly, worm or yeast genes. As mouse is the closest species to rat, we had to use the mouse SSA in our analysis. The conservation cut off value was left as 0.40 and matrix score threshold as 85%. It was selected that all the results to be displayed at the end. These results were copied to Microsoft Excel to produce scatter (XY) plots, showing Fisher score vs Z-score values of the hits for transcription factor binding sites. The values with Z-score≥10 and Fisher score≥7 were considered statistically significant as directed by the developers of the program (Kwon et al., 2012). The analysis was run for all the possible upstream/ downstream sequence lengths (2000/0, 2000/2000, 5000/2000, 5000/5000, 10000/5000, 10000/10000).

2.7 Metabolomics

2.7.1 Preparation of cells

When neurospheres were being isolated from postnatal day 1 rats as described above in Section 2.2.1, three brains from one litter (usually of 6-12 pups) were prepared separately to culture in one of 3 x 75 cm^3 tissue flask of neurospheres, and were considered as one 'n'. When the neurospheres were large enough, which is approximately at 7 DIV, each flask of neurospheres was used for preparing two 24-well plates of astrocytes, one with PLL-coated coverslips and one with TnC-coated coverslips. Half a millilitre of triturated neurosphere suspension was seeded on the coverslips at a density of 250,000 cells/ml. Four days later, half of the coverslips in each plate were treated with rat recombinant CNTF (ciliary neurotrophic factor) of a final concentration of 1 ng/ml and at 7 DIV they were treated again. Six coverslips of astrocytes for each condition were used for isolating metabolites at 9 DIV. So the four culture conditions for each n were: PLL-Control, PLL+CNTF, TnC-Control, and

TnC+CNTF. The extra sister coverslips from each plate were used for immunocytochemistry.

2.7.2 Extracting the metabolites

The cells were cooled down rapidly to 4°C by being placed on wet ice. From each condition 5 µl of spent media was collected and added into 200 µl of ice cold chloroform/methanol/water (in 1:3:1 ratio), mixed well, placed on ice for the time being and then frozen at -80°C. It was important to mix vigorously during cooling stage to avoid freezing and possible cell lysis. The rest of the spent media was removed and the cells were washed twice in ice cold PBS. Then 250 µl of ice cold chloroform/methanol/water (in 1:3:1 ratio) was added into each well containing a coverslip. The 24-well plates were then placed on a shaker at 4°C for 1 hr. The lysate was then removed and centrifuged for 3 min at 13000g at 4°C. The supernatant was then removed and stored at -80°C. A sample of non-spent media was also prepared as a control by adding 5 µl of fresh media into 200 µl of chloroform/methanol/water (in 1:3:1 ratio) and freezing it at -80°C. The samples were sent on dry ice to the Metabolomics Facility of University of Glasgow to be processed in Q-Exactive Hybrid Quadrupole-Orbitrap mass spectrometer (Thermo Scientific, USA). A list of data was sent to us as an IDEOM file, which is a Microsoft Excel template with a collection of VBA (Visual Basic for Applications) macros that enable automated data processing of mass spectrometry data (Creek et al., 2012). Each putative metabolite detected was presented with mean peak intensity relative to control condition (PLL-control) in this IDEOM file. The list also contained Student's t-test significance values, obtained by comparing the data sets of each two culture conditions.

2.8 Genotyping the gp130 transgenic C57BL/6 mice

2.8.1 DNA isolation

Genomic DNA was isolated from E13.5 brains of GFAP-Cre$^{-/-}$gp130$^{fl/fl}$ and GFAP-Cre$^{+/-}$ gp130$^{fl/fl}$ C57BL/6 mice using PureLink Genomic DNA Mini Kit (K1820-01, Invitrogen, Life Technologies) and following the manufacturer's guideline. The brains were frozen at -20°C on the day the embryos were used for setting up spinal cord myelinating cultures and were thawed on another day on ice to be used for DNA extraction. The extraction was carried out briefly by 1) incubating the samples in Digestion Buffer with Proteinase K at 55°C overnight, 2) treating them with RNAse A, Lysis/Binding Buffer, 96-100% ethanol, respectively, 3) washing them in Spin Columns with Washing Buffers, and 4)

eluting the samples in 100 µl of Elution Buffer, also provided in the kits like the above-mentioned other buffers and reagents. The purified DNA was stored at -20°C.

A faster and less expensive technique was used to obtain the genomic DNA from tails samples of neonatal animals (P1) and of animals aged 3 weeks or older (teenage/adult). Tail clips were performed by the experienced staff of University of Glasgow Biological Services. The tail samples were incubated in 250 µl of alkaline lysis buffer (25 mM NaOH, 0.2 mM EDTA, pH=12) at 95°C for 1 hr, which was followed by the addition of 250 µl of neutralising buffer (40 mM Tris, pH=5), after which the samples were ready to be used for PCR without the need of further purification steps. This same method was also applied on embryonic tissue but it was discontinued because the processes of PCR and agarose gel electrophoresis did not reveal consistent, reproducible, and reliable results for embryonic samples, which was not the case seen for postnatal/adult tail samples. The samples could also be stored at -20°C after the neutralisation step.

2.8.2 Polymerase chain reaction (PCR) and agarose gel electrophoresis

Genomic DNA, extracted from embryonic or adult mouse tissue, was used for PCR to check samples for the presence of GFAP-Cre transgene or of loxP site-flanked exon 16 of *Gp130* gene (gp130fl). Each PCR reaction consisted of a total volume of 25 µl, which included 5 µl of 5X GoTaq DNA polymerase buffer (M3171, Promega, USA), 0.5 µl of forward primer (20 µM stock), 0.5 µl of reverse primer (20 µM stock), 0.5 µl of dNTPs (10 mM stock, N0447S, New England BioLabs, USA), 0.25 µl GoTaq DNA polymerase (5u/µl, M3171, Promega, USA), RNAse-free water and genomic DNA, whose volumes were calculated according to the stock genomic DNA concentrations available so that the initial DNA amount would be 100-200 ng per sample. The samples were run according to the following program: 1) 15 sec at 95°C, 2) 38 cycles of 45 sec at 95°C, 45 sec at 65°C, 30 sec at 72°C, 3) 30 sec at 72°C, and 4) finish at 4°C. The GFAP-Cre transgene was detected as a 850 bp band (Fig 2.5) using the primers 5´-GAC ACC AGA CCA ACT GGT AAT GGT AGC GAC – 3` and 5´-GCA TCG AGC TGG GTA ATA AGC GTT GGC AAT-3`. Gp130fl was detected as a 400 bp band (Fig 2.5) using the primers 5´- GTG AAC AGT CAC CAT GTA CAT CTG TAC GC-3` and 5´- TGG CTT GAG CCT CAG CTT GGC TAG-3`. All primers were purchased from Sigma-Aldrich. The samples were incubated in Veriti 96-well Thermal Cycler (#9902, Applied Biosystems) and either were used immediately in agarose gel electrophoresis or were stored at 4°C up to 72 hours. The agarose gel was prepared using UltraPure Agarose (#16500-500, Life Technologies) as 1.5-2% and run at 60-80 V for 45-60 min. The samples were run in the gel along with 1 Kb Plus DNA Ladder

(#10787-018, Life Technologies) at a concentration of 0.042 µg/µl. The gel was later visualised using the instrument and the software Alpha Imager (Alpha Innotech).

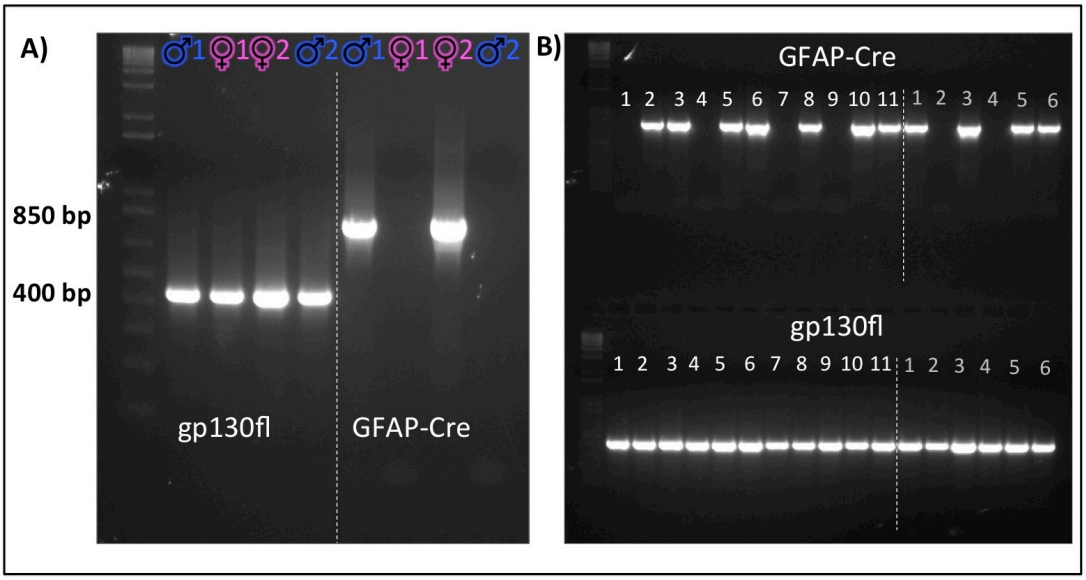

Figure 2. 5 GFAP-Cre$^{-/-}$gp130$^{fl/fl}$ and GFAP-Cre$^{+/-}$gp130$^{fl/fl}$ transgenic mice were genotyped using PCR followed by agarose gel electrophoresis.
A) The tail DNA from 4 transgenic mice (2 females and 2 males) obtained from Schluter Lab, Germany (Institut fur Medizinische Mikrobiologie, Otto-von-Guericke Universitat Magdeburg, Leipziger) presented a 850 bp band for GFAP-Cre transgene and a 400 bp band for the loxP site-flanked exon 16 of *Gp130* gene (gp130fl), which was in accordance with the findings of Schluter et al. **B)** Presented is an example for the genotyping of the litters generated from the crossing of the original breeders in A. Both litters (litter size 11 and 6) consisted of pups positive for the loxP site-flanked gp130. Some pups were positive for GFAP-Cre while the others were not. All the GFAP-Cre animals used in this project carried a flanked *Gp130*.

2.9 Microscopy and image analysis

Cells were imaged using an Olympus BX51 fluorescent microscope and Image-Pro software. An image of each channel (red, green or blue) was taken individually. They were merged to create a composite image. Experiments were performed in triplicate. For the quantification of neurite density and myelination, 10-15 images were taken at random at 10x magnification from each coverslip. Each condition was performed at least in two 35 mm Petri dishes, each containing two coverslips. Therefore, 40-60 images were analysed on average per condition in one experiment..To quantify the cell numbers for OPCs and astrocytes, 15-20 images were taken at random at 20x magnification from each coverslip. Each condition was performed at least in duplicate and therefore 30-40 images were analysed per condition in one experiment.

2.9.1 Neurite density and myelin quantification

Neurite density and myelination level of the myelinating spinal cord cultures plated on each glass cover slip were quantified using the “myelin.cp” pipeline of the software Cell

Profiler (Carpenter et al., 2006). The pipeline separates the red and green channels from the composite image and applies the necessary adjustments as described in *https://github.com/muecs/cp*. The axons are shown in the red channel, detected by the SMI-31 antibody, and the myelin is shown in the green channel, stained by the PLP antibody. Data is quantified for the percentage of SMI31 positive fibres that are ensheathed by myelin. The quantification results are exported to Microsoft Excel sheets and represent the number of pixels as the percentage of the total number of pixels.

2.9.2 Cell number quantification

The pipeline "dapi.cp" (*https://github.com/muecs/cp)* of Cell Profiler software was used to detect the total number of DAPI positive cells (seen in blue channel) on each glass coverslip of astrocytes or OPCs. The positive cells for a particular marker (seen in green and/or red channel) were counted using the Cell Counter function of the Image J software and they were expressed as percentage of the total number of cells. This percentage per coverslip was calculated by the division of the total number of specific-marker-positive cells in 10-15 images by the total number of cells in all those images. Then the overall percentage was calculated by taking the average of percentages found for all coverslips with the same condition.

2.9.3 Quantification of GFAP and nestin immunofluorescence intensity

Image J was used to measure mean brightness of the fluorescence detected in green (GFAP) and red (nestin) channels per image for each coverslip of astrocyte cultures used. The mean brightness of fluorescence value was multiplied by the whole image area to calculate the total intensity of GFAP or nestin fluorescence per field of view. Total intensity of fluorescence was divided by the DAPI positive cell number per field of view to obtain the average GFAP and nestin intensity per cell per field of view.

2.10 Statistical analysis

Graphpad Prism software was used to analyse data when multiple conditions were compared. One-way repeated measures ANOVA test was applied to data followed by either Bonferroni correction or Dunnett's test in an attempt to detect any significance. Paired Student's t-test was used when only two conditions were compared to each other. All values were expressed as means ±the standard error of the mean (SEM). Values were designated as significant if $p \leq 0.05$, which was presented using asterisks.

Chapter 3

Identification of secreted factors that may play a role in myelination

3.1 Introduction

A common pathological feature of CNS injury and disease is reactive astrocytes (Sofroniew and Vinters, 2010). Astrocytes have been shown to exist in different reactivity states both *in vivo* and *in vitro*. Astrocyte phenotypes are now believed to exist as a continuum of reactivity status rather than a specific defined phase, namely quiescent, activated and reactive. As explained in Section 1.2.2, such different states have been shown to exist *in vitro,* and Nash et al. (2011b) have exploited this phenomenon using embryonic rat myelinating spinal cord cultures to demonstrate that different astrocyte phenotypes can have distinct effects on axonal ensheathment, the final stage of myelination. The definitions of the cultures they used are shown in Table 3.1. They demonstrated that myelinating cultures plated on TnC-astrocytes (TnC-As) resulted in less myelination than those plated on PLL-astrocytes (PLL-As). On the other hand, CNTF (ciliary neurotrophic factor), a method to activate astrocytes (Winter et al., 1995; Levison et al., 1996; Hudgins and Levison, 1998; Levison et al., 1998; reviewed in Liberto et al. 2004), increased the percentage of axons myelinated both in cultures plated on PLL- and on TnC.

The above-mentioned observations are in accordance with the previously reported CNTF functions, i.e., **1)** to enhance the survival of neurons (Barbin et al., 1984; Hagg and Varon, 1993; Naumann et al., 2003; Krady et al, 2008), **2)** to promote the differentiation of glial progenitors into astrocytes, and **3)** to stimulate the maturation and survival of oligodendrocytes (Barres et al., 1996; Marmur et al., 1998; Sleeman et al., 2000; Stankoff et al., 2002; Albrecht et al., 2007; Cao et al., 2010) and **4)** to decrease the severity of disease course, to increase the neuronal functional recovery, and to be up-regulated during the remyelination phases of neurodegenerative disease models (Butzkueven et al., 2002; Linker et al., 2002; Albrecht et al., 2003; Kuhlmann et al., 2006; Lu et al, 2009; Gudi et al., 2011).

Previously in the lab, Nash et al. (2011b) compared differentially regulated genes using an Illumina array for the astrocyte treatments and thus phenotypes, shown in Table 3.2, to reveal several astrocytic factors that could affect axonal ensheathment (**Array 1**). The validation of the expressional changes of these factors narrowed down the list to *Cxcl10* chemokine only. Since *Cxcl10* expression was down-regulated in PLL-astrocytes when comparison was made to the less myelination-supportive TnC-astrocytes, this has suggested CXCL10 as a negative regulator of myelination. Embryonic rat spinal cord myelinating cultures plated on PLL-astrocytes and treated with this factor myelinated less when compared to untreated controls (Nash et al., 2011b). Thus, the authors have

produced a validated method from gene profiling of monolayers of different astrocyte phenotypes to identify potential astrocytic factors that could play a role in myelination.

Table 3. 1 Definitions of cultures that were used in this project.

Culture Name	Definition
PLL-astrocytes (PLL-As)	Neurosphere-derived astrocytes are plated on cover slips, coated with PLL.
TnC-astrocytes (TnC-As)	Neurosphere-derived astrocytes are plated on cover slips, coated with TnC.
PLL-myelinating cultures	Embryonic mixed spinal cord cells are plated on PLL-As.
TnC-myelinating cultures	Embryonic mixed spinal cord cells are plated on TnC-As.

PLL: poly-l-lysine; TnC: tenascin C.

Table 3. 2 The conditions of the astrocyte cultures used for the microarray gene expression profiling analysis 1 (Array 1, Nash et al., 2011b).

Array 1		
Astrocyte cultures	**Treatment**	**Time Point (hr)**
PLL-As	control	4
PLL-As	control	24
PLL-As	CNTF	4
PLL-As	CNTF	24
TnC-As	control	4

Rat neurospheres obtained from postnatal day 1 striata were plated on glass coverslips, previously coated with PLL (poly-L-lysine) or TnC (tenascin C) to generate astrocyte cultures as monolayers. PLL-astrocytes and TnC-astrocytes were either untreated or treated with rat CNTF (ciliary neurotrophic factor) to generate astrocytes with different reactivity phenotypes. Total RNA lysates were collected from these cultures 4 or 24 hr after standard medium feeding or CNTF treatment to be used for Array 1. RNA samples were obtained from three biological replicates.

Despite the fact that Nash et al. (2011b) identified a negative regulator of myelination, they could not find a factor that increased myelination (positive for myelination). The promyelinating condition was CNTF treatment of astrocytes and under these conditions very few genes were differentially regulated upon CNTF treatment compared to controls. The fact that few possible candidates to promote myelination were identified in the comparisons of CNTF treatment of astrocytes to the conditions that led to lower myelination levels in culture (no treatment) led to the hypothesis that crosstalk between the astrocytes and the other cell types in the spinal cord mixed cultures will be required to activate astrocytes to influence myelination. Thus, another microarray gene expression profiling analysis was set up using embryonic mixed spinal cord myelinating cultures plated on astrocyte monolayers on different substrates and treated or not treated with CNTF to identify potential positive regulators of myelination. This second microarray (**Array 2**) and its analysis is the basis of this chapter.

For our microarray gene expression profiling analysis (Array 2), RNA samples were harvested from embryonic rat mixed spinal cord cultures plated on the various astrocyte monolayers at 12 days *in vitro* (DIV), 4 hr or 24 hr after the CNTF treatment or standard medium feeding. The eight culture conditions used were as shown in Table 3.3. For the purpose of this chapter, I will refer to these embryonic rat spinal cord cultures as "**myelinating cultures**". Even though it is possible to observe different stages of myelination in these cultures (Sherman and Brophy, 2005; Nash et al., 2010), I will suggest the effects of different candidates on the regulation of axonal ensheathment, which is the initial stage of myelination and can be observed at 22-28 DIV.

Table 3. 3 The conditions of the embryonic mixed spinal cord myelinating cultures used for the microarray gene expression profiling analysis 2 (Array 2).

Array 2			
Myelinating spinal cord cultures plated on the following astrocytes (As)	**Treatment**	**Myelination Degree**	**Time Point (hr)**
PLL-As	control	++	4
PLL-As	control	++	24
PLL-As	CNTF	+++	4
PLL-As	CNTF	+++	24
TnC-As	control	+	4
TnC-As	control	+	24
TnC-As	CNTF	+++	4
TnC-As	CNTF	+++	24

Dissociated and enzyme-treated embryonic rat spinal cords were plated on neurosphere-derived rat astrocyte monolayers, previously plated on PLL- or TnC-coated glass coverslips to generate embryonic rat mixed spinal cord myelinating cultures. These myelinating cultures were either untreated or treated with rat CNTF (ciliary neurotrophic factor) to generate cultures with different levels of axonal ensheathment. Total RNA was collected from these cultures 4 or 24 hr after standard medium feeding or CNTF treatment to be used for Array 2. RNA samples were obtained from three biological replicates. The myelination levels these myelinating cultures present are shown relative to each other based on the study of Nash et al. (2011b). + is the lowest level and +++ shows the highest level of myelination.

3.2 Aims

The overall aim of this chapter is to identify secreted astrocytic factors that modulate myelination. This was carried out as follows:

- A microarray gene expression profiling analysis was performed using dissociated spinal cord cells (Array 2) plated on a range of astrocytes to determine whether the crosstalk between astrocytes and these neural cells affects the expression profiles of astrocytes and the secretion of myelination-regulating factors.

- Comparison was made between the transcriptional profiles of astrocyte monolayers (Array 1) and myelinating spinal cord cultures plated on astrocytes

(Array 2) under different conditions in an attempt to validate the previous findings of Array 1 (Nash et al., 2011b) and thus the current findings of Array 2. This comparison was also necessary for identification of potential myelination-regulating transcripts, stimulated by the above-mentioned crosstalk and not detected in the astrocyte monolayers alone.

- Array 2 was analysed by identifying the expressional changes between the myelinating cultures at different conditions that were grouped mainly as coating-substance (PLL or TnC), treatment (CNTF or none), and time point (4 or 24 hr). To simplify the analysis, expressional changes were analysed in binary comparisons to identify the effects of CNTF in PLL-myelinating cultures and in TnC-myelinating cultures and to determine the effect of the coating-substance on the untreated myelinating cultures. Such analysis was required for establishing the expression profiles of the myelinating cultures with varying degrees of myelination as seen in Table 3.3.

3.3 Results

3.3.1 Comparison of the expression profiles of astrocyte monolayers (Array 1) with those of the myelinating spinal cord cultures (Array 2)

The microarray gene expression profiling analysis using myelinating cultures plated on neurosphere-derived astrocyte monolayers (Array 2) revealed a higher number of genes that were differentially expressed between different conditions compared to those detected in Array 1. As seen in Fig 3.1 A, there were 32 genes differentially regulated between PLL- and TnC- untreated (control) astrocytes (Array 1); as opposed to the 131 genes in the myelinating cultures (Array 2).

There were 7 genes shared between the comparisons of PLL- and TnC- conditions of astrocyte monolayers and myelinating cultures (Fig 3.1 A). These genes were ***Aldh1a1***, ***Cxcl10***, ***Fn1***, ***Igfbp2***, ***Krt19***, ***Tagln***, and an unidentified gene locus. Six of them showed the same direction of regulation. *Aldh1a1* was up-regulated in cultures on PLL compared to those on TnC, but *Cxcl10*, *Fn1*, *Krt19*, *Tagln* genes and the gene locus *Loc497841* were all down-regulated on PLL in both arrays. *Igfbp2* was up-regulated in PLL-astrocytes but was down-regulated in PLL-myelinating cultures compared to TnC conditions.

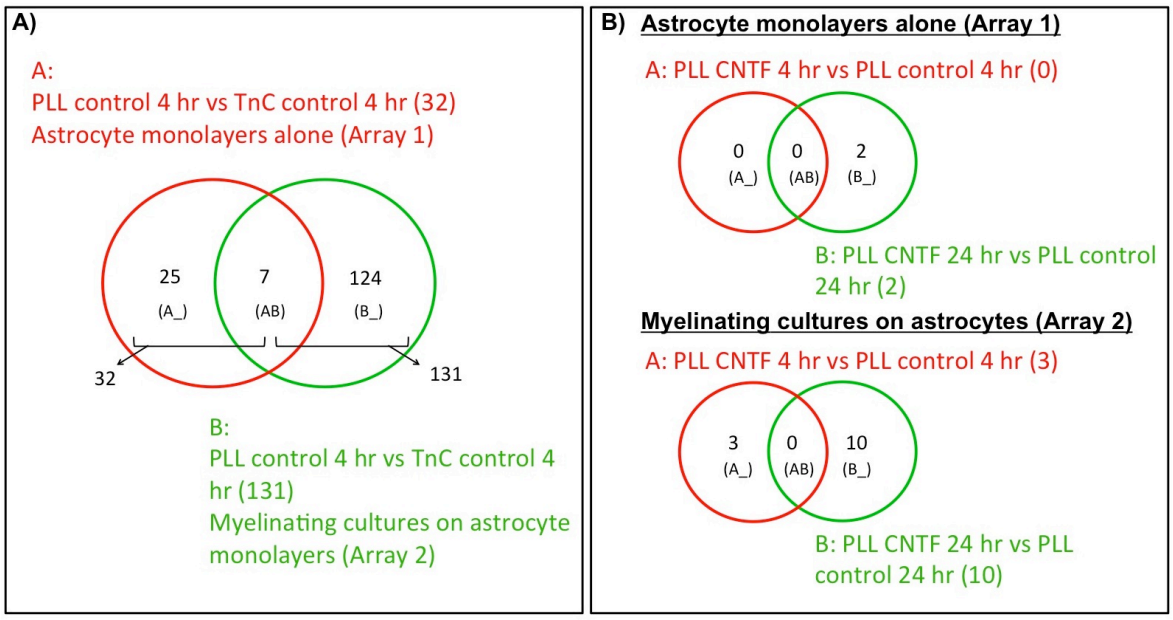

Figure 3. 1 A higher number of differentially regulated transcripts was detected in embryonic rat spinal cord myelinating cultures (Array 2) compared to in astrocyte monolayers (Array 1, Nash et al., 2011b).
Venn diagrams present the number of differentially regulated transcripts in cultures at different conditions in Array 1 and Array 2. Microarray gene expression profiling analysis was carried out using samples from astrocyte monolayers (Array 1, Nash et al., 2011b) and myelinating cultures, plated on astrocyte monolayers (Array 2). Both arrays were prepared using astrocytes, which were seeded on glass coverslips coated with poly-L-lysine (PLL) or tenascin C (TnC). Both culture types used for these arrays were either untreated (control) or treated with ciliary neurotrophic factor (CNTF) and total RNA was collected from the cultures 4 hr or 24 hr after standard medium feeding or CNTF treatment. Three biological replicates were prepared for each array and each biological replicate was run in three technical replicates in both arrays. False discovery rate was designated as 5%. **A)** There were 32 differentially regulated transcripts between PLL-control and TnC-control astrocyte monolayers (Array 1) and 131 transcripts detected between PLL-control and TnC-control myelinating cultures. There were 7 common genes detected in both of these comparisons. **B)** There were 2 transcripts differentially regulated upon CNTF treatment in PLL-astrocyte monolayers and they were detected at 24 hr (Array 1); whereas, 13 transcripts were differentially regulated in total upon CNTF treatment in PLL-myelinating cultures (Array 2), with 3 of them detected at 4 hr and 10 of them detected at 24 hr.

Identifying common factors that were differentially regulated in the same direction in both simple and complex culture systems not only validates the results of the previous microarray analysis (Array 1) but also confirms the Array 2 results. Nash et al. (2011b) identified CXCL10 as a potential negative regulator of myelination since its expression was down-regulated in PLL-control astrocyte monolayers compared to TnC-control astrocytes, which the authors have shown to be less supportive for myelination. Thereafter, CXCL10 treatment of myelinating spinal cord cultures on PLL-astrocytes lowered the myelination levels when compared to non treated controls. The down-regulation of *Cxcl10* mRNA in myelinating cultures on PLL-astrocytes (Array 2) also correlates with previous findings of Nash et al. (2011b).

Previously in Array 1, it was expected to identify a candidate molecule, which would potentially stimulate myelination, by comparing the differentially regulated genes between the PLL-control astrocytes and the PLL+CNTF astrocytes that show higher levels of myelination. However, only two genes were differentially regulated upon CNTF treatment on PLL-astrocytes (Fig 3.1 B). As these genes, *Gdf15* and *Cd93*, from the

literature did not appear to be candidates that could have specifically a direct role in myelination; they were not considered as potential myelination regulators. On the other hand, three genes were differentially regulated upon CNTF treatment in PLL-myelinating cultures at 4 hr and 10 genes at 24 hr in Array 2 (Fig 3.1 B). It is possible that these new 13 genes were predominantly expressed by the other cell types and not astrocytes in the myelinating cultures. However, it is also possible that the crosstalk between the astrocyte monolayers and the spinal cord cells induced their expression in astrocytes.

The differentially regulated genes between the PLL- and TnC-control conditions in astrocyte monolayers (Array 1) and in the myelinating spinal cord cultures (Array 2) were also used in PANTHER Classification System (*http://www.pantherdb. org*), which can generate pie charts based on Gene Ontology categorisation, i.e. by molecular function, biological process, cellular component, protein class and pathway. The number of genes that were found to be associated with pathways and/or biological processes is shown in Table 3.4. The percentages of genes assigned to each category of pathway or biological process are presented in Fig 3.2. There appears to be a higher variety of pathways detected for the myelinating spinal cord cultures (Array 2) compared to astrocyte monolayers (Array 1). Immune system pathways constitute 32-33% of the pathways detected in both culture types, suggesting the importance of the immune system elements in these cultures. In addition, several different immune system pathway subcategories were detected in myelinating cultures (Array 2) in agreement with their higher complexity compared to astrocyte monolayers (Array 1). The substrate difference (PLL vs TnC) appears to affect apoptotic and localisation processes in both culture types in similar ratios (Fig 3.2). On the other hand, a higher percentage of genes appears to be associated with biological regulation and metabolic, immune system, response to stimulus and multicellular organismal processes in myelinating cultures as opposed to a lower percentage of genes associated with developmental, biological adhesion and cellular processes, which could also be due to their complexity.

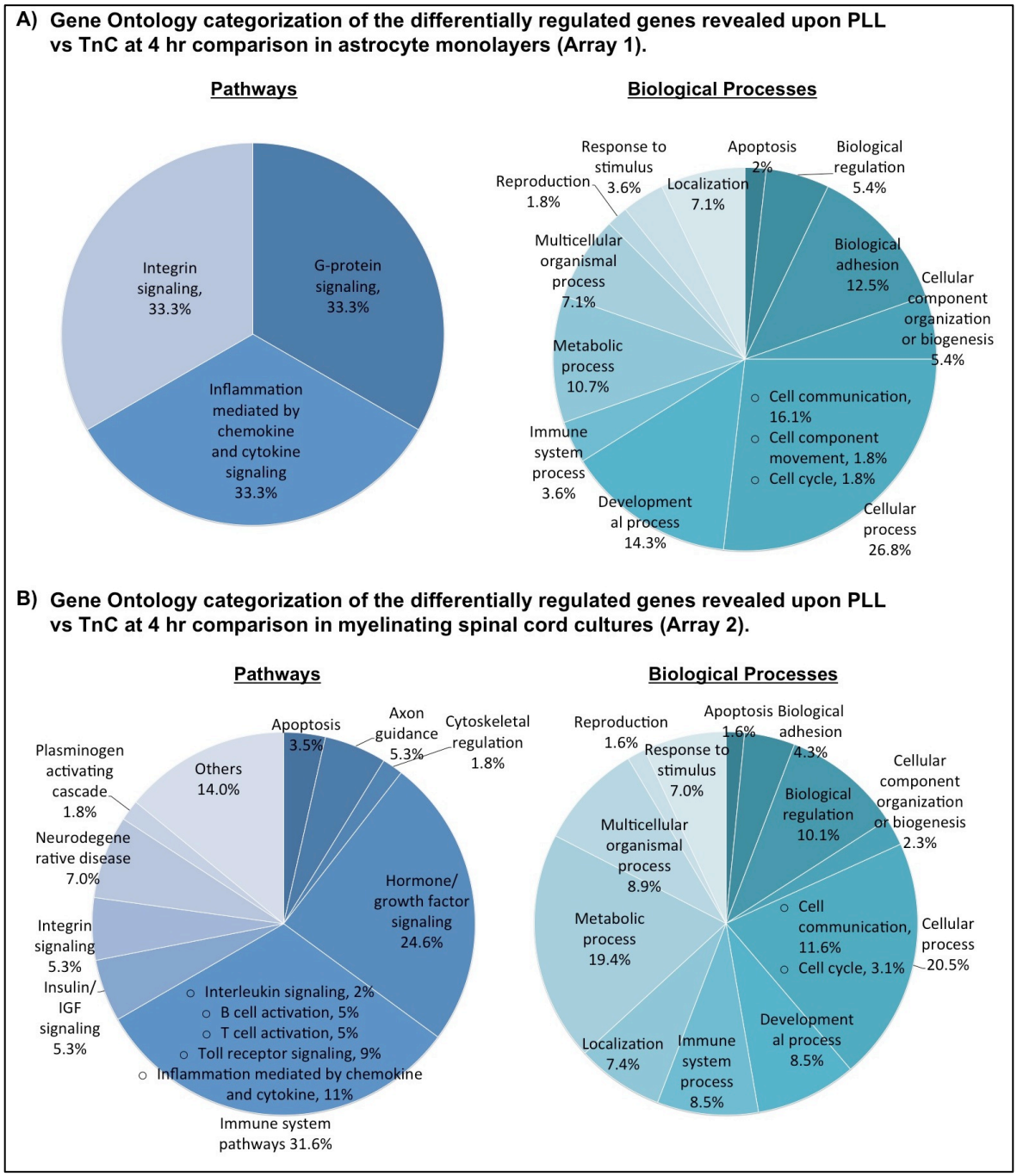

Figure 3. 2 Gene Ontology categorizations of the differentially regulated transcripts detected in Array 1 and Array 2.

Microarray gene expression profiling analysis was carried out using samples from astrocyte monolayers (Array 1, Nash et al., 2011b) and embryonic rat spinal cord myelinating cultures, plated on astrocyte monolayers (Array 2). Both arrays were prepared using astrocytes, which were seeded on glass coverslips coated with poly-L-lysine (PLL) or tenascin C (TnC). Total RNA was collected from the cultures 4 hr after standard medium feeding. Three biological replicates were prepared for each array and each biological replicate was run in three technical replicates in both arrays. False discovery rate was designated as 5%. The lists of transcripts differentially regulated between the cultures on PLL and TnC were entered into PANTHER Classification System (*http://www.pantherdb.org*) to generate pie charts, showing the percentages of transcripts associated with the presented pathways and biological processes in **A)** Array 1, and **B)** Array 2.

Table 3. 4 PANTHER Classification analysis of the differentially regulated genes between PLL and TnC control conditions in Array 1 (astrocytes) and 2 (myelinating cultures).

	# of differentially regulated genes	# of genes included in PANTHER analysis	Total # of pathway hits	Total # of biological process hits
Array 1	32	28	6	56
Array 2	131	105	57	258

Genes identified in the expressional comparisons of PLL and TnC control (untreated) conditions in Array 1 and 2 were entered into PANTHER online analysis program, which revealed the genes associated with various cellular processes and pathways and calculated the percentages for each subcategory. The numbers of transcripts originally detected in the microarray gene expression profiling between the PLL and TnC control conditions are shown in the 1st column and the number of genes, for which PANTHER could detect any associations are presented in the 2nd column. There were 6 and 57 genes associated with pathways shown in Fig 3.2 in Array 1 and Array 2, respectively. The total numbers of genes associated with the biological processes shown in Fig 3.2 are 56 and 258 for Array 1 and 2, respectively. Different pathways and biological processes detected in the analysis shared some of the genes, which increased the total number of biological process hits above the initial numbers of genes entered into the PANTHER program.

3.3.2 CNTF appears to show its pro-myelinating effect on PLL and on TnC via different mechanisms (Array 2)

CNTF has been shown to promote myelination in myelinating cultures plated on PLL-astrocytes and on TnC-astrocytes (Nash et al., 2011b). Since it had a supportive effect on myelination in both cultures, the anticipation was that CNTF would trigger similar expressional changes on both substrates. Surprisingly, some unexpected differences were observed upon CNTF treatment in PLL- and TnC-myelinating cultures (Array 2), which led to the suggestion that CNTF might be stimulating myelination in PLL- and TnC-cultures via different mechanisms. Supporting evidences are explained below.

3.3.2.1 The transcriptional changes in PLL- and TnC-myelinating cultures upon CNTF treatment at 4 hr and 24 hr

One piece of evidence suggesting the differential effect of CNTF in PLL- and TnC-myelinating cultures is the difference in the percentage of the differentially regulated genes at early and late time points (Fig 3.3). The majority of the expressional changes appeared to occur at the later time point in PLL-cultures in contrast to that seen for TnC-cultures (Fig 3.3). Nevertheless, the possibility that CNTF triggers the same changes at different rates on the two substrates cannot be excluded.

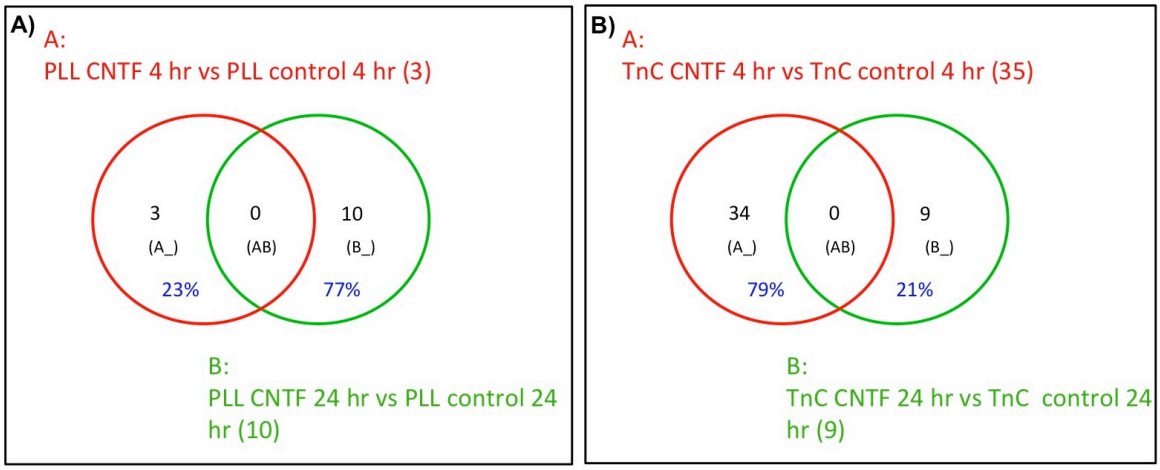

Figure 3. 3 Majority of the transcriptional changes upon CNTF treatment appears to occur at 24 hr in PLL-myelinating cultures but at 4 hr in TnC-myelinating cultures.
Microarray gene expression profiling analysis (Array 2) was carried out using samples from embryonic rat spinal cord myelinating cultures, plated on astrocyte monolayers on glass coverslips, coated with poly-L-lysine (PLL) or tenascin C (TnC). The cultures were either untreated (control) or treated with ciliary neurotrophic factor (CNTF) and total RNA was collected from the cultures 4 hr or 24 hr after standard medium feeding or CNTF treatment. Three biological replicates were prepared for the array and each biological replicate was run in three technical replicates. False discovery rate was designated as 5%. Shown in the figure are the Venn diagrams, presenting the number of differentially regulated transcripts upon CNTF treatment in PLL- and TnC-myelinating cultures. **A)** Majority of the transcriptional changes upon CNTF treatment appears to occur at 24 hr in PLL-myelinating cultures (77%); whereas, **B)** CNTF treatment appears to trigger majority of such changes at 4 hr in TnC-myelinating cultures (79%). There were not any common transcripts that were differentially regulated upon CNTF treatment between the two time points (4 hr and 24 hr) in either of the cultures.

Interestingly, there were two common genes that were differentially regulated in the same direction upon CNTF treatment on both substrates; however, those on TnC were detected at the earlier time point while those on PLL were detected at the later time point (Fig 3.4 D). ***Fmod*** was down-regulated and ***Crem*** was up-regulated on both substrates upon CNTF treatment. Thus these two candidates, FMOD and CREM, could be playing essential roles in the promotion of myelination by CNTF. Ingenuity Pathway Analysis (IPA) showed that these two candidates interact with different proteins in PLL- and TnC-myelinating cultures (Figs 3.5, 3.6). For example, FMOD appeared to intearact with collagens on TnC, which was not observed on PLL (Figs 3.5, 3.6). This also suggests a differential CNTF-initiated mechanism in these two cultures. Please see discussion (Section 3.4) for further explanation.

Apart from *Fmod* and *Crem*, there was one other common gene locus, *Loc499554*, differentially expressed at the later time point in both PLL- and TnC- cultures (Fig 3-4, B). If the changes occurring after 24 hr reflect the changes that would affect the biological processes in the cells more closely compared to those after 4 hr, the above-mentioned comparison and hence the common gene revealed from this comparison will be more relevant as a candidate to regulate myelination. However, it is also possible that metabolic changes, initiated by the expressional changes at the earlier time point, will have a long-lasting effect on the cell functions and since these will be metabolic changes, they will not be detected by microarray gene expression profiling. Whatever the case is, *Loc499554* might be an interesting locus to study in the future. As this is not an established gene yet, it is difficult to speculate whether this transcript could have an effect on myelination or not. However, it was down-regulated in both PLL- and TnC-cultures 24 hr after the CNTF treatment (Fig 3.4 B), which Nash et al. (2011b) have shown to be more supportive for axonal ensheathment. Its down-regulation in more supportive conditions suggests a possible negative role on axonal ensheathment. Once the gene function is characterised, a role in myelination could also be considered in the future.

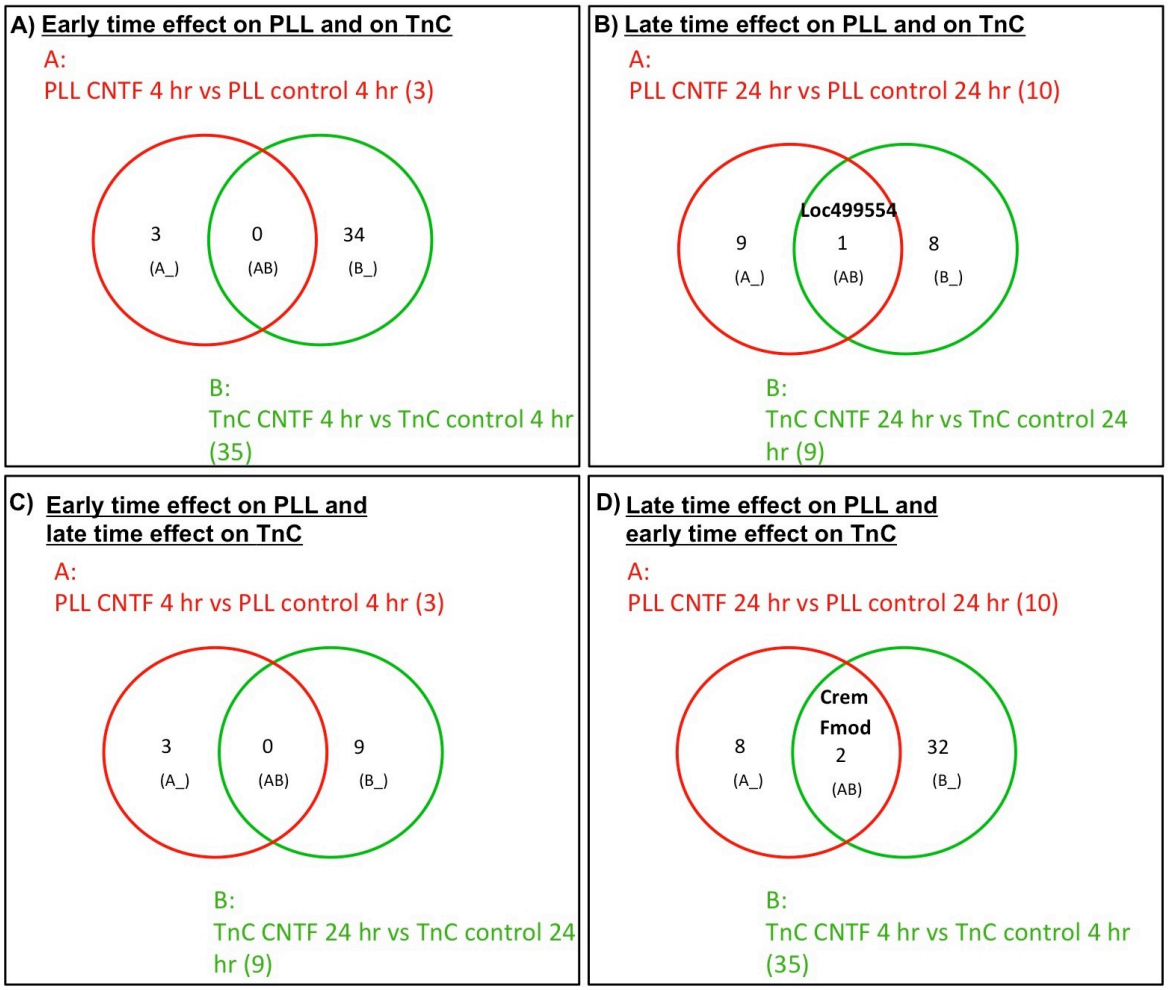

Figure 3. 4 Exogenous CNTF appears to trigger the differential expression of *Crem*, *Fmod* and *Loc499544* in both PLL- and TnC-myelinating cultures.

Microarray gene expression profiling analysis (Array 2) was carried out using samples from embryonic rat spinal cord myelinating cultures, plated on astrocyte monolayers, on glass coverslips, coated with poly-L-lysine (PLL) or tenascin C (TnC). The cultures were either untreated (control) or treated with ciliary neurotrophic factor (CNTF) and total RNA was collected from the cultures 4 hr or 24 hr after standard medium feeding or CNTF treatment. Three biological replicates were prepared for the array and each biological replicate was run in three technical replicates. False discovery rate was designated as 5%. In an attempt to determine the early and late effect of CNTF in both PLL- and TnC-myelinating cultures, the transcripts differentially regulated upon CNTF treatment on one substrate at one time point were compared with those on the other substrate at the same or different time point. **A)** Early effects of CNTF in PLL- and TnC-myelinating cultures did not cause a common change between the cultures. **B)** The CNTF treatment after 24 hr decreased the expression of *Loc499554* in both PLL- and TnC-myelinating cultures, revealing a gene locus that could be important for myelination, triggered by CNTF treatment. **C)** In the comparison of the early CNTF effect in PLL-myelinating cultures and the late CNTF effect in TnC-myelinating cultures, there was not a common transcript revealed. **D)** In the comparison of the late CNTF effect in PLL-myelinating cultures and the early CNTF effect in TnC-myelinating cultures, *Fmod* was found to be down-regulated and *Crem* was seen to be up-regulated in both cultures. Thus, *Crem*, *Fmod* and *Loc499554* appear to be among the common transcripts affected by exogenous CNTF treatment in myelinating cultures on PLL or TnC.

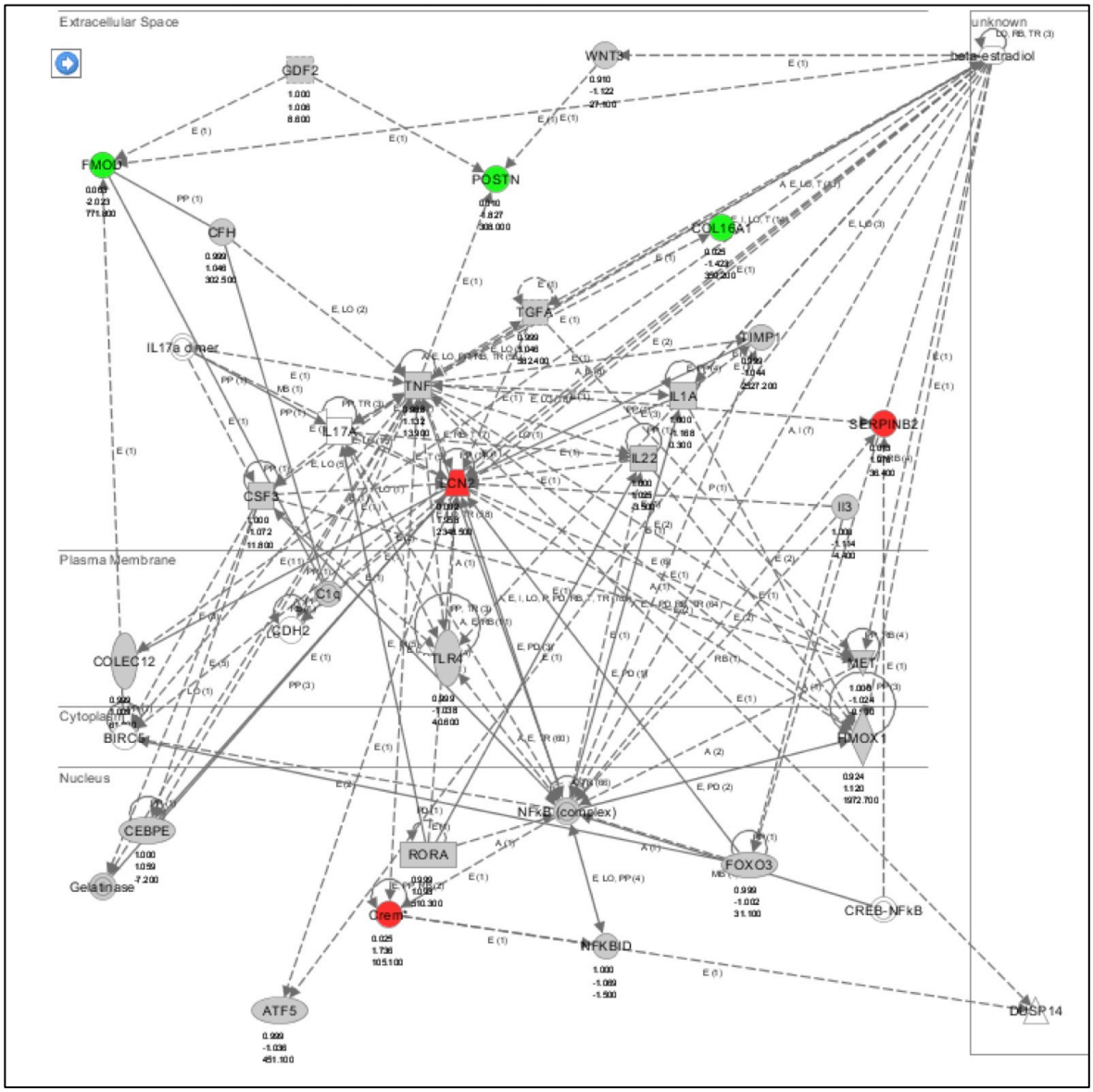

Figure 3. 5 Ingenuity Pathway Analysis (IPA) diagram showing the interactions of the molecules in PLL-myelinating cultures upon CNTF treatment (PLL+CNTF vs PLL-control) at 24 hr.

Microarray gene expression profiling analysis (Array 2) was carried out using samples from embryonic rat spinal cord myelinating cultures, plated on astrocyte monolayers on glass coverslips, coated with poly-L-lysine (PLL). The cultures were either untreated (control) or treated with ciliary neurotrophic factor (CNTF) and total RNA was collected from the cultures 24 hr after standard medium feeding or CNTF treatment. Three biological replicates were prepared for the array and each biological replicate was run in three technical replicates. False discovery rate was designated as 5%. There were 10 transcripts differentially regulated upon CNTF treatment in PLL-myelinating cultures at 24 hr. The diagram shows the pathway network consisting of the highest number (6) of molecules. Red and green represent up- and down-regulated transcripts, respectively, upon CNTF treatment. *Crem*, *Lcn2*, and *Serpinb2* were up-regulated but *Col16a1*, *Fmod* and *Postn* were down-regulated upon CNTF treatment in PLL-myelinating cultures at 24 hr, affecting the possible interactions shown in the diagram. Col16a1: collagen type XVI, alpha 1; Crem: cAMP responsive element modulator; Fmod: fibromodulin; Lcn2: lipocalin 2, neutrophil gelatinase-associated lipocalin; Postn: periostin; Serpinb2: serpin peptidase inhibitor.

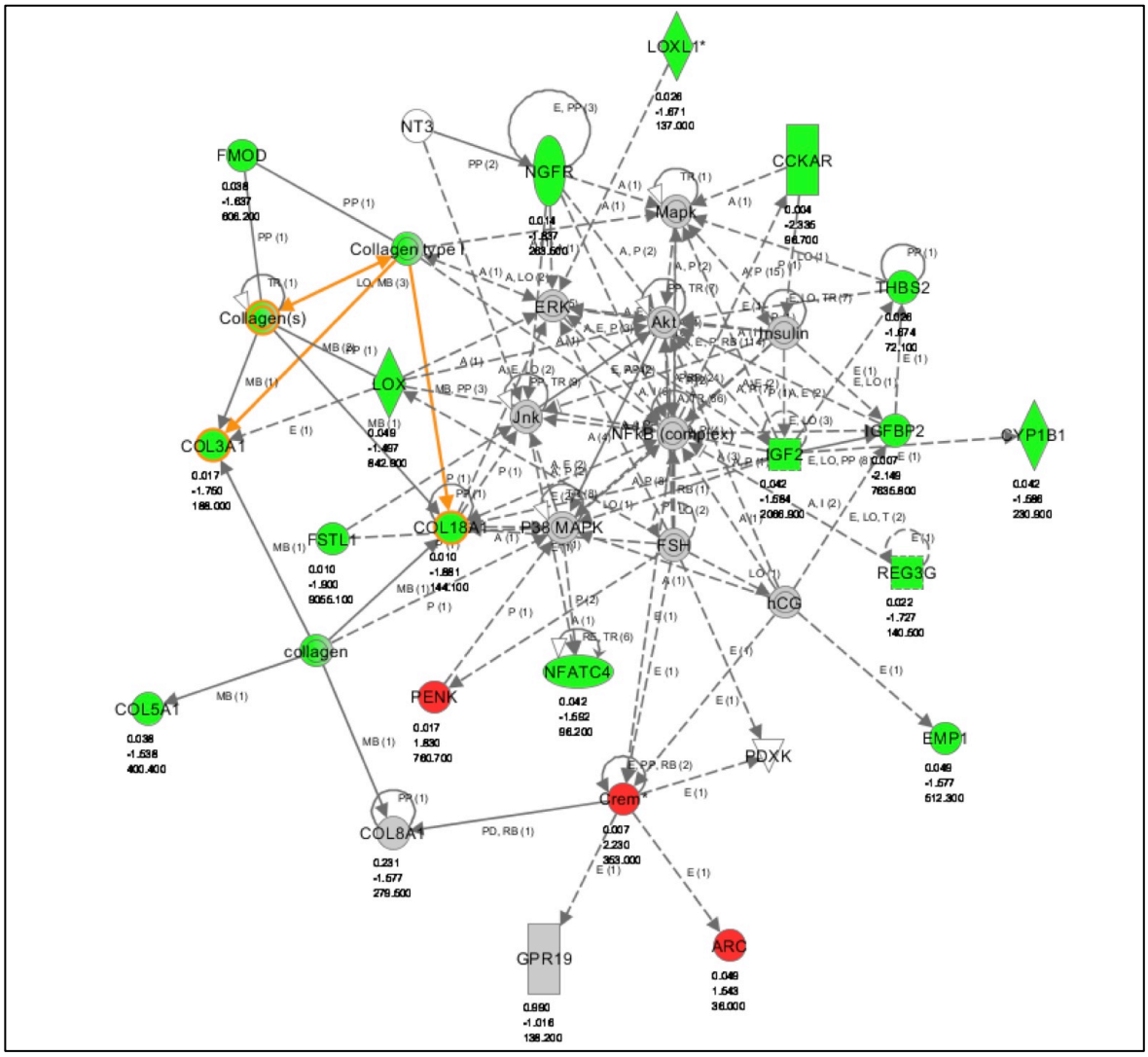

Figure 3. 6 Ingenuity Pathway Analysis (IPA) diagram showing the interactions of the molecules in TnC-myelinating cultures upon CNTF treatment (TnC+CNTF vs TnC-control) at 4 hr.

Microarray gene expression profiling analysis (Array 2) was carried out using samples from embryonic rat spinal cord myelinating cultures, plated on astrocyte monolayers on glass coverslips, coated with tenascin C (TnC). The cultures were either untreated (control) or treated with ciliary neurotrophic factor (CNTF) and total RNA was collected from the cultures 4 hr after standard medium feeding or CNTF treatment. Three biological replicates were prepared for the array and each biological replicate was run in three technical replicates. False discovery rate was designated as 5%. There were 37 transcripts differentially regulated upon CNTF treatment in TnC-myelinating cultures at 4 hr. The diagram shows the pathway network consisting of the highest number (19) of molecules. Red and green represent up- and down-regulated transcripts, respectively, upon CNTF treatment. *Arc*, *Crem* and *Penk* were up-regulated but *Cckar*, *Col18a1*, *Col3a1*, *Col5a1*, *Cyp1b1*, *Emp1*, *Fmod*, *Fstl1*, *Igf2*, *Igfbp2*, *Lox*, *Loxl1*, *Nfatc4*, *Ngfr*, *Reg3g*, and *Thbs2* were down-regulated upon CNTF treatment in TnC-myelinating cultures at 4 hr, affecting the possible interactions shown in the diagram. Arc: activity-regulated cytoskeleton-associated protein; Cckar: cholecystokinin A; Col18a1: collagen type XVIII alpha 1; Col3a1: collagen type III alpha 1; Col5a1: collagen type VI alpha I; Crem: cAMP responsive element modulator; Cyp1b1: cytochrome P450 family 1 subfamily B; Emp: epithelial membrane protein 1; Fmod: fibromodulin; Fstl: follistatin; Igf2: insulin-like growth factor 2; Igfbp2: insulin-like growth factor-binding protein 2; Lox: lysyl oxidase; Lox1: lipoxygenase 1; Nfatc4: nuclear factor of activated T cells; Ngfr: nerve growth factor receptor; Penk: preproenkephalin; Reg3g: regenerating islet-derived 3 gamma; Thbs2: thrombospondin 2.

3.3.2.2 CNTF treatment in PLL- and TnC-myelinating cultures over time

The data of expressional changes over time hint as well that CNTF might be acting in PLL- and TnC-myelinating cultures via different mechanisms. It is possible to exclude the expressional changes over time in control conditions from the ones in CNTF-treated conditions on both substrates separately (Fig 3.7, grey areas). The common genes between the 39 and 14 genes differentially regulated specifically upon CNTF treatment over time on PLL and TnC, respectively, would have the potential of having essential roles in the CNTF effect on both substrates. Interestingly, there were no such common genes, suggesting again a difference in the CNTF mechanism in PLL- and TnC-myelinating cultures. The differentially regulated genes specifically upon CNTF treatment over time in PLL- and TnC-myelinating cultures are presented in Table 3.5.

Even though similar types of gene categories are seen in both culture conditions (Table 3.5), the members of these groups are quite different. For example, the metalloprotease (MMP), *Mmp12* was down-regulated over time in PLL+CNTF myelinating cultures. CNTF appears to trigger the up-regulation of *Mmp12* in PLL-myelinating cultures temporarily at 4 hr, an effect that is lost at 24 hr (Table 3.8). No expressional changes of *Mmp12* were seen in TnC-myelinating cultures at all.

On the other hand, another metalloprotease, *Mmp3,* was up-regulated over time both in PLL-control and PLL+CNTF myelinating cultures (Table 3.6). Its levels remained constant over time in TnC-control myelinating cultures but increased in TnC+CNTF cultures (Table 3.7). These changes suggest that the up-regulation of *Mmp3* in TnC-myelinating cultures is triggered by CNTF; whereas, apparently, this up-regulation occurs in PLL-cultures without exogenous induction over time. Similarly, the members of the cytokines and chemokines listed under the secreted factors and the directions of their regulation were different in PLL- (*Ccl6, Ccl12, Cxcl1, Cxcl9*) and TnC-cultures (*Cxcl13*, Table 3.5).

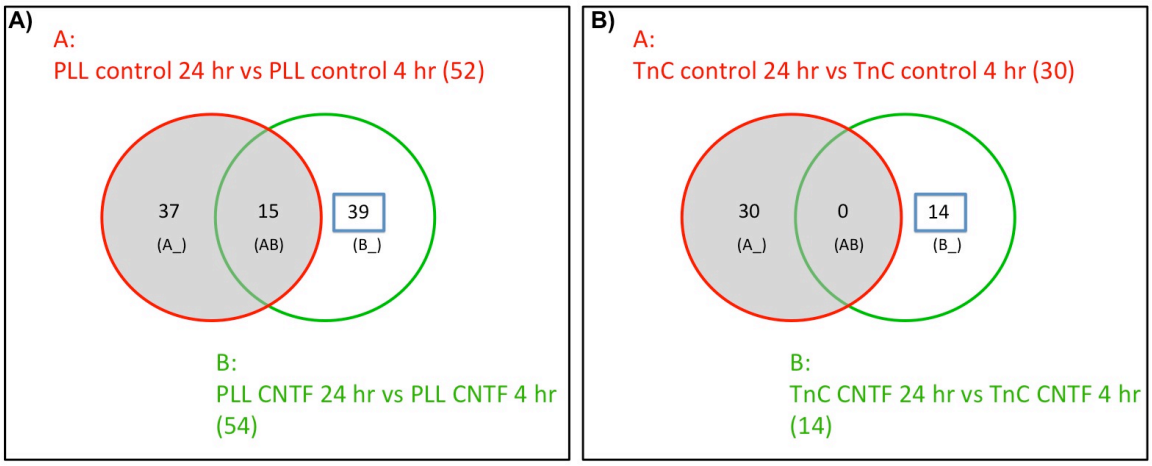

Figure 3. 7 Exogenous CNTF appears to trigger distinct mechanisms over time in PLL- and TnC-myelinating cultures.

Microarray gene expression profiling analysis (Array 2) was carried out using samples from embryonic rat spinal cord myelinating cultures, plated on astrocyte monolayers on glass coverslips, coated with poly-L-lysine (PLL) or tenascin C (TnC). The cultures were either untreated (control) or treated with ciliary neurotrophic factor (CNTF) and total RNA was collected from the cultures 4 hr or 24 hr after standard medium feeding or CNTF treatment. Three biological replicates were prepared for the array and each biological replicate was run in three technical replicates. False discovery rate was designated as 5%. The grey areas represent the differentially regulated transcritps over time (24 hr vs 4 hr) in **A)** PLL-control myelinating cultures and in **B)** TnC-control myelinating cultures. Those transcripts were excluded from the list of transcripts, differentially expressed over time in **A)** PLL+CNTF and in **B)** TnC+CNTF myelinating cultures to obtain the transcripts, whose expression was significantly changed over time only in the presence of exogenous CNTF. The numbers of such transcripts were 39 and 14 in PLL- and TnC-myelinating cultures, respectively. There were not any common transcripts between the lists of those 39 and 14 transcripts, which suggested a distinct mechanism for the exogenous CNTF effect in PLL- and TnC-myelinating cultures.

Table 3. 5 Categorisation of differentially regulated genes upon CNTF treatment over time in PLL- and TnC-myelinating cultures (Array 2), excluding the genes differentially expressed over time also in control conditions.

	PLL	TnC
Categories	**Differentially regulated genes**	**Diff. reg. genes**
Chemokines	*Ccl6*, *Ccl12*, *Cxcl1*, *Cxcl9*	*Cxcl13*
Coenzyme	-	*Coq10b*, *Slamf9*
Enzymes	*Acot1*, *Cyp1b1*, *Mat2a*, *Mmp12*, *Adcy8*, *Agpat7*, *Cbs*, *Nqo1*, *Pkm2*, *Plcd4*, *Ppp1r1b*, *Ptprn*	*Hmox1*, *Mmp3*, *Oas1a*
Growth factor	-	*Bdnf*
Hormones	*Adcyap1*, *Crh*	-
Lipid-binding protein	*Fabp4*	-
Membrane proteins	*Emp1*, *Rilp*, *Slco1c1*	-
Neuropeptides	*Hcrt*, *Penk1*	-
Other nuclear proteins	*Rbm3*, *Rilp*	*Zbp1*
Receptor	*Cckar*	*Slamf9*
Secreted factors	*Ccl6*, *Ccl12*, *Cxcl1*, *Cxcl9*, *Igfbp2*, *Mmp12*, *Adcyap1*, *Crh*, *Penk1*	*Bdnf*, *Cxcl13*, *Mmp3*
Signaling protein	*Arhgef19*	*Mx1*
Solute carrier	*Slco1c1*	-
Transcription factors	*Msx1*, *Npas4*, *Plagl1*, *Scg2*	*Crem*, *Fos*, *Irf7*

Microarray gene expression profiling analysis was carried out using embryonic myelinating spinal cord cultures (Array 2). Illustrated in the table are the differentially expressed transcripts over time in PLL+CNTF and TnC+CNTF myelinating cultures. The transcripts differentially regulated over time in PLL- and TnC-control (untreated) myelinating cultures were excluded from this list. The transcripts up-regulated over time are shown in red and those down-regulated over time are shown in green. The transcripts were categorised based on the classification in UniProt (*http://www.uniprot.org/*).

Table 3. 6 Differentially regulated genes over time in PLL-control and PLL+CNTF-myelinating cultures (Array 2).

PLL-control-myelinating cultures			
		24 hr vs 4 hr	
PROBE_ID	ILMN_GENE	False Discovery Rate	Fold Change
ILMN_1349555	COQ10B	0.000	-4.64
ILMN_1375922	NR4A3	0.000	-4.61
ILMN_1376694	CREM	0.002	-3.93
ILMN_1375583	CREM	0.002	-3.62
ILMN_1375833	CREM	0.002	-3.27
ILMN_2039673	ARC	0.004	-2.84
ILMN_1365302	SNF1LK	0.003	-2.69
ILMN_1355906	NR4A2	0.003	-2.57
ILMN_1371574	GEM_PREDICTED	0.004	-2.47
ILMN_1367486	DUSP1	0.010	-2.47
ILMN_1650285	HMOX1	0.004	-2.36
ILMN_1369914	RASD1	0.004	-2.34
ILMN_1357229	CCL2	0.004	-2.29
ILMN_1368356	FOS	0.004	-2.27
ILMN_1356140	LOC501170	0.015	-2.21
ILMN_1360447	BDNF	0.009	-2.06
ILMN_1361968	RGD1560523_PREDICTED	0.029	-1.95
ILMN_1360615	LOC503409	0.010	-1.94
ILMN_1351429	SERPINB2	0.010	-1.91
ILMN_1358226	USP2	0.010	-1.91
ILMN_1375203	PTP4A1	0.015	-1.86
ILMN_1369005	EGR1	0.042	-1.86
ILMN_1367740	MT1A	0.015	-1.85
ILMN_1364929	BAMBI	0.038	-1.80
ILMN_1374218	RIBC2	0.030	-1.77
ILMN_1363606	LCN2	0.031	-1.76
ILMN_1354131	PORF1	0.034	-1.75
ILMN_1357783	HBEGF	0.021	-1.73
ILMN_1349422	PTGS2	0.042	-1.71
ILMN_1364972	AGTR1A	0.034	-1.71
ILMN_1353835	RGD1310149_PREDICTED	0.039	-1.71
ILMN_1356628	NFKBIA	0.038	-1.63
ILMN_1371918	AFF4_PREDICTED	0.004	-1.62
ILMN_1363228	ELL2	0.011	-1.62
ILMN_1350498	FGF2	0.046	-1.52
ILMN_1354272	LOC310926	0.046	-1.51
ILMN_1376421	MRPS10	0.048	-1.50
ILMN_1360188	NFIL3	0.030	-1.44
ILMN_1367288	PQLC1	0.039	-1.41
ILMN_1366196	NEGR1	0.015	-1.40
ILMN_1372032	RGD1307986_PREDICTED	0.013	-1.33
ILMN_1357093	TPM4	0.038	-1.31
ILMN_2040245	MAP1B	0.029	-1.24
ILMN_1349593	SRRM2_PREDICTED	0.010	1.34
ILMN_1350091	G0S2	0.022	1.35
ILMN_1356608	LOC499201	0.034	1.40
ILMN_1367525	RGD1308141_PREDICTED	0.024	1.46
ILMN_1364931	ADORA2A	0.010	1.48
ILMN_1366294	GSTP2	0.013	1.51

ILMN_1371684	LOC499103	0.003	1.51
ILMN_1375744	KCNC2	0.029	1.55
ILMN_1376443	ASCL1	0.034	1.62
ILMN_1353353	ALK	0.006	1.68
ILMN_1361666	MMP3	0.000	1.80

PLL+CNTF- myelinating cultures

		24 hr vs 4 hr	
PROBE_ID	**ILMN_GENE**	**False Discovery Rate**	**Fold Change**
ILMN_1375922	NR4A3	0.000	-5.38
ILMN_1349555	COQ10B	0.001	-3.01
ILMN_1357890	MMP12	0.001	-2.96
ILMN_1350836	CCKAR	0.001	-2.45
ILMN_1368356	FOS	0.002	-2.45
ILMN_1365302	SNF1LK	0.002	-2.18
ILMN_1355906	NR4A2	0.001	-2.17
ILMN_1349422	PTGS2	0.009	-2.07
ILMN_1361968	RGD1560523_PREDICTED	0.010	-2.00
ILMN_1361869	LOC690943	0.034	-1.90
ILMN_1353833	ACOT1	0.038	-1.90
ILMN_1363228	ELL2	0.013	-1.84
ILMN_1376635	CYP1B1	0.022	-1.81
ILMN_1350180	EMP1	0.011	-1.80
ILMN_1359095	MAT2A	0.031	-1.75
ILMN_1372537	MSX1	0.038	-1.73
ILMN_1530238	LOC684681	0.021	-1.71
ILMN_1368224	CCL12_PREDICTED	0.039	-1.71
ILMN_1353835	RGD1310149_PREDICTED	0.017	-1.68
ILMN_2039673	ARC	0.006	-1.68
ILMN_1363453	NPAS4	0.026	-1.67
ILMN_1364222	PLAGL1	0.038	-1.66
ILMN_1355237	CXCL1	0.044	-1.64
ILMN_1353336	RBM3	0.020	-1.60
ILMN_1369914	RASD1	0.032	-1.57
ILMN_1369168	CCL6	0.038	-1.52
ILMN_1363606	LCN2	0.011	-1.49
ILMN_1367600	RGD1565540_PREDICTED	0.033	-1.30
ILMN_1376344	FABP4	0.043	-1.14
ILMN_1360048	IGFBP2	0.009	-1.06
ILMN_1361632	CXCL9	0.010	-1.05
ILMN_1373954	RGD1560030_PREDICTED	0.047	-1.04
ILMN_1355694	LOC363492	0.041	1.01
ILMN_1362918	LOC361912	0.031	1.16
ILMN_1370261	RGD1566401_PREDICTED	0.017	1.20
ILMN_1366004	PLCD4	0.044	1.34
ILMN_1353874	CBS	0.014	1.39
ILMN_1366452	PKM2	0.010	1.40
ILMN_1351683	RILP_PREDICTED	0.028	1.49
ILMN_1372370	AGPAT7_PREDICTED	0.049	1.50
ILMN_1355146	HCRT	0.043	1.52
ILMN_1350196	ADCY8	0.031	1.56
ILMN_1376782	ADCYAP1	0.020	1.58
ILMN_1352810	ARHGEF19_PREDICTED	0.016	1.60

ILMN_1360716	SCG2	0.011	1.64
ILMN_2039396	NQO1	0.011	1.69
ILMN_2040370	PPP1R1B	0.002	1.70
ILMN_1352410	PENK1	0.006	1.74
ILMN_1353353	ALK	0.004	1.88
ILMN_1351429	SERPINB2	0.004	1.89
ILMN_1358429	CRH	0.002	2.04
ILMN_1363020	PTPRN	0.010	2.22
ILMN_1357978	SLCO1C1	0.001	2.42
ILMN_1361666	MMP3	0.001	7.16

An Illumina array was carried out on myelinating spinal cord cultures of different phenotypes (Array 2). The genes differentially expressed over time (24 hr vs 4 hr) in PLL-control and PLL+CNTF myelinating cultures are listed in the table. RNA samples were collected from myelinating cultures, at 12 DIV, 4 hr and 24 hr after standard medium feeding. Three biological replicates were used for the experiment. Gene fold changes are shown in the table. Negative and positive values represent the down-regulations and up-regulations, respectively. False discovery rate was designated as 5%. The genes highlighted in grey are common between PLL-control and PLL+CNTF cultures.

Table 3. 7 Differentially regulated genes over time in TnC-control and TnC+CNTF myelinating cultures (Array 2).

TnC-control-myelinating cultures			
		24 hr vs 4 hr	
PROBE_ID	ILMN_GENE	False Discovery Rate	Fold Change
ILMN_1375909	SLC14A2	0.002	-3.40
ILMN_1372537	MSX1	0.002	-2.63
ILMN_1350576	LOC290704	0.012	-2.55
ILMN_1372919	CYR61	0.021	-2.50
ILMN_1360048	IGFBP2	0.024	-2.47
ILMN_1350836	CCKAR	0.021	-2.05
ILMN_1371407	FMOD	0.021	-2.04
ILMN_1354884	FSTL1	0.024	-1.99
ILMN_1360481	PLEC1	0.040	-1.87
ILMN_1650537	GPC4	0.040	-1.87
ILMN_1351900	FCNB	0.012	-1.82
ILMN_1350180	EMP1	0.023	-1.70
ILMN_1375922	NR4A3	0.021	-1.69
ILMN_1357452	GDA	0.023	-1.65
ILMN_1367695	TMEM37	0.026	-1.64
ILMN_1356721	CCR1	0.026	-1.64
ILMN_1366649	LOC501087	0.040	1.55
ILMN_1354725	LOC500490	0.032	1.57
ILMN_1350958	LOC498644	0.039	1.61
ILMN_1371124	LOC500960	0.021	1.63
ILMN_1348840	SNAP25	0.021	1.66
ILMN_1371063	LOC498048	0.013	1.74
ILMN_1352230	LOC362543	0.012	1.80
ILMN_1373694	LOC362315	0.012	1.80
ILMN_1361190	RGD1559917_PREDICTED	0.040	1.81
ILMN_1369444	LOC361942	0.013	1.88
ILMN_1355694	LOC363492	0.021	1.92
ILMN_1650120	CLDN11	0.004	1.92
ILMN_1363606	LCN2	0.040	2.01
ILMN_1375194	LOC500867	0.004	2.08

TnC+CNTF-myelinating cultures			
		24 hr vs 4 hr	
PROBE_ID	ILMN_GENE	False Discovery Rate	Fold Change
ILMN_1375833	CREM	0.017	-2.08
ILMN_1650285	HMOX1	0.002	-2.01
ILMN_1376694	CREM	0.016	-2.01
ILMN_1360447	BDNF	0.029	-1.94
ILMN_1368356	FOS	0.016	-1.80
ILMN_1349555	COQ10B	0.012	-1.77
ILMN_1369833	LOC501538	0.043	-1.53
ILMN_1356758	CXCL13	0.016	1.27
ILMN_1368490	LOC24906	0.022	1.31
ILMN_1358414	ZBP1	0.016	1.49

ILMN_1373648	MX1	0.016	1.63
ILMN_1367846	SLAMF9_PREDICTED	0.022	1.66
ILMN_1362908	OAS1A	0.018	1.81
ILMN_1352469	IRF7	0.016	1.93
ILMN_1361666	MMP3	0.016	3.13

An Illumina array was carried out on myelinating spinal cord cultures of different phenotypes (Array 2). The genes differentially expressed over time (24 hr vs 4 hr) in TnC-control and TnC+CNTF myelinating cultures are listed in the table. RNA samples were collected from myelinating cultures, at 12 DIV, 4 hr and 24 hr after standard medium feeding or CNTF treatment. Three biological replicates were used for the experiment. Gene fold changes are shown in the table. Negative and positive values represent the down-regulations and up-regulations, respectively. False discovery rate was designated as 5%. The genes highlighted in grey are common between TnC -control and TnC+CNTF cultures.

3.3.3 Binary comparisons reveal potential candidates that could regulate axonal ensheathment (Array 2)

CNTF is likely to show its effect in PLL- and TnC-myelinating cultures via different mechanisms, as explained above. Therefore, the expressional changes occurring upon CNTF treatment in PLL- and TnC- myelinating cultures were analysed separately as the next step of the Array 2 analysis. Another binary comparison was necessary to analyse the expressional changes between PLL-control and TnC-control myelinating cultures as they also were demonstrated to exhibit different levels of myelination (Nash et al., 2011b).

3.3.3.1 PLL+CNTF vs PLL-control myelinating cultures

There were only three genes differentially regulated upon CNTF treatment in PLL-myelinating cultures at 4 hr, and 10 genes/gene loci at 24 hr with no genes overlapping between the two time points (Table 3.8). At 4 hr, the metalloproteinase ***Mmp12*** and the chemokine ligand ***Cxcl13*** were up-regulated and ***Ribc2*** was down-regulated upon CNTF treatment in PLL-myelinating cultures (Table 3.8). The expression of *Mmp12* was down-regulated over time in PLL-CNTF cultures (Table 3.6) back to control levels. Its temporary up-regulation might be triggering signalling pathways that would eventually have a positive effect on myelination as explained in Section 3.4. As for *Cxcl13*, such a down-regulation over time in PLL+CNTF myelinating cultures or up-regulation over time in PLL-control myelinating cultures was not seen, making it more difficult to explain the lack of its differential expression between PLL-control and PLL+CNTF cultures at 24 hr (Table 3.8). It is possible that *Cxcl13* expression naturally increases on PLL slowly over a long period of time without any exogenous treatment and at 24 hr reaches the same levels as those in CNTF-treated cultures. This could be interpreted as CNTF facilitates the up-regulation of *Cxcl13* in PLL-myelinating cultures. This increase at a specific early time point could influence the cell biology in the myelinating cultures in a way that

would positively affect myelination since PLL+CNTF myelinating cultures exhibit higher myelination levels compared to untreated PLL-cultures (Nash et al., 2011b).

Table 3. 8 Differentially regulated genes detected 4 hr and 24 hr after CNTF treatment in PLL-myelinating cultures (Array 2).

at 4 hr			
		PLL CNTF vs PLL control	
PROBE_ID	**ILMN_GENE**	**False Discovery Rate**	**Fold Change**
ILMN_1374218	RIBC2	0.006	-2.10
ILMN_1357890	MMP12	0.009	1.59
ILMN_1356758	CXCL13	0.035	1.69
at 24 hr			
		PLL CNTF vs PLL control	
PROBE_ID	**ILMN_GENE**	**False Discovery Rate**	**Fold Change**
ILMN_1371407	FMOD	0.003	-2.02
ILMN_1360313	POSTN_PREDICTED	0.010	-1.83
ILMN_1364416	COL16A1	0.025	-1.11
ILMN_1363227	LOC499554	0.013	-1.08
ILMN_1375194	LOC500867	0.045	1.01
ILMN_1362918	LOC361912	0.018	1.02
ILMN_1355694	LOC363492	0.018	1.12
ILMN_1363606	LCN2	0.002	1.56
ILMN_1376694	CREM	0.037	1.69
ILMN_1375833	CREM	0.025	1.74
ILMN_1351429	SERPINB2	0.013	1.98

An Illumina array was carried out on myelinating spinal cord cultures of different phenotypes (Array 2). The genes differentially expressed upon CNTF (cilliary neurotrophic factor) treatment in PLL-myelinating cultures are listed in the table. RNA samples were collected from myelinating cultures, at 12 DIV, 4 hr and 24 hr after standard medium feeding or treatment. The transcripts highlighted in a black box were selected as potential regulators of myelination. Three biological replicates were used for the experiment. Gene fold changes are shown in the table. Negative and positive values represent the down-regulations and up-regulations, respectively. False discovery rate was designated as 5%.

Unlike *Mmp12* and *Cxcl13*, *Ribc2* was down-regulated upon CNTF treatment in PLL-myelinating cultures at 4 hr. Its expression was also down-regulated over time in PLL-control cultures (Table 3.6) explaining the lack of its differential expression at 24 hr (Table 3.8). It is difficult to speculate whether the faster drop in its expression upon CNTF treatment will have an effect on myelination as there is very little known about this gene in the literature. Ribc2 stands for RIB43A domain with coiled-coils 2 and seems to be an uncharacterised microtubule ribbon protein, which might be important for the proper segregation of chromosomes during cell proliferation (Arango et al., 2004). Other than that, not much is known about this protein in mammals. It might help process

extension in oligodendrocytes as a cytoskeleton protein but it is difficult to reach a definite conclusion at this stage.

Down-regulation of the extracellular matrix (ECM) organisation proteins 24 hr after the CNTF treatment in PLL-myelinating cultures (Table 3.9) could provide a more suitable environment for axonal ensheathment by providing ample space for oligodendrocyte processes to extend and wrap around axons. Fibromodulin (*Fmod*) was down-regulated upon CNTF treatment also in TnC-myelinating cultures. Since CNTF has been suggested to increase axonal ensheathment also on TnC (Nash et al., 2011b), down-regulation of *Fmod* expression upon CNTF would present FMOD as a negative regulator of axonal ensheathment as explained in Section 3.4.

On the other hand, up-regulation of ***Lcn2*** (lipocalin 2, neutrophil gelatinase-associated lipocalin), ***Serpinb2*** (serpin peptidase inhibitor) and ***Crem*** (cAMP responsive element modulator) upon CNTF treatment in PLL-myelinating cultures (Table 3.8) would suggest them as positive regulators of axonal ensheathment. Serpinb2 continued to present itself as a possible stimulator of myelination when its differential expressions in other comparisons were observed. It was also up-regulated in PLL-control myelinating cultures compared to TnC-control cultures at 4 hr (Table 3.14). Its expression was down-regulated over time in PLL-control cultures but this was reversed upon CNTF treatment (Table 3.6). Thus, CNTF treatment maintained the 4 hr *Serpinb2* levels until at least 24 hr after the onset of the treatment and also elevated them by a fold change of 1.89.

Table 3. 9 Categorisation of differentially regulated genes 4 hr and 24 hr after CNTF treatment in PLL-myelinating cultures (Array 2).

	4 hr	24 hr
Categories	**Differentially regulated genes**	**Diff. reg. genes**
Chemokine	*Cxcl13*	-
Enzymes	Mmp12	Serpinb2
Extracellular matrix proteins	*Mmp12*	*Fmod, Col16a1, Postn*
Others	*Ribc2*	-
Secreted factors	*Cxcl13*, *Mmp12*	*Fmod, Col16a1, Postn, Lcn2*, *Serpinb2*
Transcription factor	-	*Crem*

Microarray gene expression profiling analysis was carried out using embryonic myelinating spinal cord cultures (Array 2). Illustrated in the table are the differentially expressed transcripts 4 hr and 24 hr after CNTF (cilliary neurotrophic factor) treatment in PLL-myelinating cultures. The transcripts up-regulated upon CNTF treatment are shown in red and the ones down-regulated are shown in green. The transcripts were categorised based on the classification in UniProt (*http://www.uniprot.org/).* Diff: differentially; reg: regulated.

SERPINB2, also named PAI-2, is a member of the serine protease inhibitor superfamily. It can play a role in cell survival and differentiation, innate immune response, and neuroprotection (Masos and Miskin, 1997; Sharon et al., 2002; Fan et al., 2004; reviewed in Medcalf, 2011). *PAI-2* promoter contains a CRE-site, which could be controlled by the transcriptional factor CREM (Zhang et al., 2009). The up-regulation of *Crem* upon CNTF treatment in PLL-cultures at 24 hr, and in PLL-control cultures compared to TnC-cultures at 4 hr is in parallel with the change seen for *PAI-2*. Thus, CREM could be playing a role in the up-regulation of *Serpinb2* in these conditions. Interestingly, no change is detected for *Serpinb2* upon CNTF treatment in TnC-cultures despite the up-regulation of *Crem* at 4 hr, which suggests that CREM is not enough on its own to affect the expression of *Serpinb2* upon CNTF treatment. FOS has also been suggested to affect *Serpinb2* expression via AP-1 site binding (Stringer et al., 2012). The up-regulation of *Fos* in PLL-cultures compared to TnC-cultures at 4 hr is again in accordance with that finding.

Even though *Lcn2* (Lipocalin-2) was suggested to have a positive effect on myelination due to its up-regulation upon CNTF treatment in PLL-cultures at 24 hr (Table 3.8), its down-regulation in PLL-control cultures when compared to TnC-cultures (3.14) poses a contradiction since PLL-control cultures have been shown to have higher levels of myelination (Nash et al., 2011b). Unlike the case seen for *Serpinb2*, CNTF treatment did not sustain or increase the *Lcn2* levels in PLL-cultures over time (Table 3.6). On the other hand, *Lcn2* expression was elevated in TnC-control cultures over time, the opposite of what was seen for PLL-control cultures. The association of LCN2 with disease onset and/or progression in spinal cord injury, EAE, MS and neuromyelitis optica (NMO) (Rathore et al., 2011; Berard et al., 2012; Marques et al., 2012; Howe et al., 2014) and of LCN2 deficiency with myelin sparing at the spinal cord epicentre (Rathore et al., 2011) appear to contradict the suggestion that LCN2 could have a positive role in myelination. However, its role in promotion of neuronal processes and neuron migration (Bi et al., 2013) and the removal of the damaged or unhealthy cells in nervous system (Lee et al., 2012a) might be important in our relatively young myelinating cultures (12 DIV) for a healthy development. These contradictory observations make it difficult to propose a steady, solid effect of LCN2 on myelination; however, they do not exclude the possibility of LCN2 playing a role in myelination, either.

After this detailed analysis of transcriptional changes in PLL+CNTF vs PLL-control myelinating cultures, **CXCL13**, **LCN2** and **SERPINB2** were chosen to study further as potential positive regulators of axonal ensheathment in biological validation assays (Table 3.10). The fact that they are secreted proteins was important, as they would

need to be exogenously added to the embryonic rat spinal cord myelinating cultures plated on PLL-astrocytes to prove they had any effects on axonal ensheathment (Nash et al., 2011b). ECM proteins (FMOD, COL16A1), CREM and MMP12 were not selected despite being secreted factors since studying them in the myelinating cultures would be more difficult than studying the other selected candidates. The ECM proteins may be negative regulators of myelination due to their down-regulation upon CNTF treatment on PLL. Thus, their removal from the cultures would possibly be necessary to observe increased myelination levels rather than adding exogenous ECM proteins to the cultures where they may not be able to reduce myelination further. Working with CREM, a transcription factor, and MMP12 that might require zymographic assays would also be more complicated. Additionally, to keep the list of genes of interest short, priority was given to CXCL13, LCN2, SERPINB2.

Table 3. 10 Candidates selected from the comparison of PLL+CNTF vs PLL-control myelinating cultures to study further.

Cand.	Suggested Effect on Myelination	Supporting/Contradicting Evidence	References
Cxcl13	supportive	○ Elevated levels detected in the spinal cords of mice with EAE and the CNS of MS patients. ○ Rituximab, a drug that is used in MS treatment, has been shown to reduce CXCL13 levels in the CSF and serum of MS patients ○ Promoted CNS myelination in cerebellar slice cultures.	Magliozzi et al., 2004; Bagaeva et al., 2006; Krumbholz et al., 2006; Piccio et al., 2010; Yuen et al., 2013
Lcn2	supportive	○ Induced cortical neuron death in a time- and dose-dependent manner in primary cultures but was not toxic to glia *in vitro*. ○ Increased the number of neuronal processes and promoted neuron migration in primary mouse neuronal cultures.	Lee et al., 2012a; Bi et al., 2013
SB2	supportive	○ Its expression increased in mouse neurons where neuronal survival was promoted. ○ It was shown to inhibit/regulate the levels of uPA, whose degrading activity against MBP has been detected in conditioned media from primary rat microglia.	Kawano et al., 1970; Nakajima et al., 1992; Zhang et al., 2009

Microarray gene expression profiling analysis was carried out using embryonic rat spinal cord cultures plated on astrocyte monolayers on coverslips, coated with PLL (PLL-myelinating cultures). Illustrated in the table are the candidates selected as potential regulators of myelination based on their differential expression between the untreated and CNTF-treated PLL-myelinating cultures. Basic facts, which are/could be related to myelination-regulating roles, are also presented for these candidates with their references. Cand.: candidates; CNS: central nervous system; CNTF: cilliary neurotrophic factor; Cxcl13: chemokine 13; Lcn2: lipocalin2; PLL: poly-L-lysine; SB2: serpinb2; uPA: urokinase-type plasminogen activator.

3.3.3.2 TnC+CNTF vs TnC-control myelinating cultures

Similar to the case seen in PLL-myelinating cultures, there were no common genes that were differentially regulated upon CNTF treatment in TnC-myelinating cultures at both time points (Table 3.11). Thus, the effects of CNTF treatment on gene expression in TnC-myelinating cultures appear to be different at the early and later time points.

There were 34 genes that were differentially regulated at 4 hr after CNTF treatment in TnC-myelinating cultures as opposed to 9 differentially regulated genes at 24 hr (Table 3.11). Some of the genes that were down-regulated upon CNTF treatment at 4 hr were also down-regulated over time in TnC-control cultures. These genes were *Msx1* (Msh homeobox 1), *Cckar* (cholecystokinin A receptor), *Igfbp2* (insulin-like growth factor binding protein 2), *Fstl1* (follistatin-like 1), *Slc14a2* (urea transporter member 2), *Fmod* (fibromodulin) and *Emp1* (epithelial membrane protein 1, Table 3.7). Even though their down-regulation upon CNTF treatment at 4 hr may suggest that they are inhibitory to axonal ensheathment, the facts that they were not down-regulated at 24 hr and that they were also down-regulated over time in control cultures without any CNTF treatment show that they may not be highly related to CNTF functions in these cultures. If we exclude such genes from the down-regulated genes upon CNTF treatment at 4 hr (Table 3.11), the secreted myelination-inhibiting candidates (Table 3.12) will be the collagens ***Col18a1***, ***Col3a1*** and ***Col5a1***, ***Fbn2*** (fibrillin 2), ***Igf2*** (insulin-like growth factor 2), lysyl oxidase-like proteins ***Loxl1*** and ***Loxl2***, ***Megf6*** (multiple EGF-like-domains 6), ***Reg3b*** (regenerating islet-derived 3 beta), ***Thbs2*** (thrombospondin 2), and ***Wif1*** (WNT inhibitory factor 1*)*. After excluding the ECM proteins from this list due the above-mentioned reasons, we selected ***Thbs2*** and ***Wif1*** to study further (Table 3.13). The matricellular protein THBS2 especially was interesting as THBS4 was also suggested as a negative myelination-regulator at the end of the microarray analysis carried away using astrocyte monolayers alone (Array1, Nash et al., 2011b). The down-regulation of *Thbs2* and *Wif1* upon CNTF treatment in TnC-cultures suggested that these could be negative regulators of myelination.

Table 3. 11 Differentially regulated genes detected 4 hr and 24 hr after CNTF treatment in TnC-myelinating cultures (Array 2).

at 4 hr			
		TnC CNTF vs TnC control	
PROBE_ID	ILMN_GENE	False Discovery Rate	Fold Change
ILMN_1372537	MSX1	0.004	-2.38
ILMN_1350836	CCKAR	0.004	-2.34
ILMN_1360048	IGFBP2	0.007	-2.15
ILMN_1351352	LOXL2_PREDICTED	0.014	-1.91
ILMN_1354884	FSTL1	0.010	-1.90
ILMN_1375909	SLC14A2	0.010	-1.89
ILMN_1364899	COL18A1	0.010	-1.88
ILMN_1365512	NGFR	0.014	-1.84
ILMN_1354941	COL3A1	0.017	-1.75
ILMN_1357508	REG3B	0.022	-1.73
ILMN_1376260	MEGF6	0.022	-1.71
ILMN_1650153	THBS2	0.026	-1.67
ILMN_1376846	LOXL1	0.026	-1.67
ILMN_1364986	WIF1	0.036	-1.64
ILMN_1371407	FMOD	0.038	-1.64
ILMN_1366296	PRPH1	0.038	-1.64
ILMN_1351076	FBN2	0.026	-1.63
ILMN_1370683	NFATC4	0.042	-1.59
ILMN_1376635	CYP1B1	0.042	-1.59
ILMN_1359301	IGF2	0.042	-1.58
ILMN_1359457	COLEC12	0.042	-1.58
ILMN_1350180	EMP1	0.049	-1.58
ILMN_1360227	BOC_PREDICTED	0.049	-1.56
ILMN_1353887	COL5A1	0.038	-1.54
ILMN_1530405	LOXL1	0.042	-1.53
ILMN_1369190	PDLIM7	0.042	-1.52
ILMN_1371773	CD248_PREDICTED	0.049	-1.50
ILMN_1376823	LOX	0.049	-1.50
ILMN_1362820	SSG1	0.049	-1.49
ILMN_1651027	RGD1566042_PREDICTED	0.017	1.52
ILMN_2039673	ARC	0.049	1.54
ILMN_1349555	COQ10B	0.049	1.62
ILMN_1361431	RPE65	0.026	1.74
ILMN_1375833	CREM	0.026	1.76
ILMN_1352410	PENK1	0.017	1.83
ILMN_1375583	CREM	0.017	1.88
ILMN_1376694	CREM	0.007	2.23
at 24 hr			
		TnC CNTF vs TnC control	
PROBE_ID	ILMN_GENE	False Discovery Rate	Fold Change
ILMN_1650120	CLDN11	0.011	-1.80
ILMN_1350345	LOC499638	0.048	-1.23
ILMN_1361494	LOC498901	0.041	-1.20
ILMN_1363227	LOC499554	0.040	-1.08
ILMN_1356110	KLF4	0.011	1.25

ILMN_1364113	CTGF	0.016	1.37
ILMN_1367546	TBX15_PREDICTED	0.044	1.97
ILMN_1372919	CYR61	0.016	2.74
ILMN_1361666	MMP3	0.011	3.31

An Illumina array was carried out on myelinating spinal cord cultures of different phenotypes (Array 2). The genes differentially expressed upon CNTF (cilliary neurotrophic factor) treatment in TnC-myelinating cultures are listed in the table. RNA samples were collected from myelinating cultures, at 12 DIV, 4 hr and 24 hr after standard medium feeding or treatment. The transcripts highlighted in a black box were selected as potential regulators of myelination. Three biological replicates were used for the experiment. Gene fold changes are shown in the table. Negative and positive values represent the down-regulations and up-regulations, respectively. False discovery rate was designated as 5%. TnC: tenascin C.

Thbs2 encodes for thrombospondin-2 (TSP2), a matricellular protein that is involved in a variety of cellular processes in the extracellular matrix rather than contributing to the physical properties of structural elements in tissues (Sage and Bornstein, 1991). Elevated levels of TSP2 in CNS pathology (Lin et al., 2003; Liauw et al., 2008, Huang et al., 2013) could be attributed to an inhibitory function of TSP2 in the CNS; however, TSP2 has also been shown to contribute to synaptic recovery, axonal sprouting and behavioural recovery after stroke (Liauw et al., 2008). On the other hand, TSP2 was also postulated as a clearance factor for MMP2 that is associated with the regulation of PNS myelination (Lehmann et al., 2009). As MMP2 is also present in the CNS (Cuzner et al., 1996; Heo et al., 1999), it could be important for CNS myelination despite its proteolytic activity against MBP *in vitro* (Latronico et al., 2013). In spite of some positive roles of TSP2, our results showed that its transcript is down-regulated in cultures that has been shown to be more supportive of myelination, i.e. TnC-CNTF- cultures (Table 3.11) and was thus suggested as a negative regulator of myelination.

Wif1 was also down-regulated in PLL-control myelinating cultures compared to TnC-contol myelinating cultures, suggesting once more a negative role for WIF1 in myelination. Wnt inhibitor factor (WIF1) is an extracellular antagonist of Wnt secreted proteins. Therefore, Wnt signalling would be expected to have a positive role on axonal ensheathment once it is not inhibited by WIF1. Despite the supporting evidence in Table 3.13, there are also some contradictory results presented. As Tawk et al. (2011) remind the readers, Wnt signalling components so far examined in oligodendrocyte development are all shared between the canonical Wnt and other major signalling pathways, such as PI3/AKT pathway. In addition, Wnt signalling could have a distinct effect on oligoglial cell differentiation based on their differentiation stage, e.g., stimulating PLP expression in oligodendrocyte-enriched cultures but not in primary OPC cultures (Shimizu et al., 2005; Feigenson et al., 2009; Li and Richardson, 2009; Ye et al., 2009; Fancy et al., 2011; Tawk et al., 2011; Zhong et al., 2011). The interception of Wnt signalling components with other signalling pathways (Tawk et al., 2011) and their

possible distinct actions at different developmental stages (Xie et al., 2013) create a very complex system. Nevertheless, there is clear evidence suggesting involvement of Wnt signalling in oligodendrocyte maturation and myelination (Fancy et al., 2009; Tawk et al., 2011).

Table 3. 12 Categorisation of differentially regulated genes 4 hr and 24 hr after CNTF treatment in TnC-myelinating cultures (Array 2).

	4 hr	24 hr
Categories	**Differentially regulated genes**	**Diff. reg. genes**
Cell junction protein	-	*Cldn11*
Coenzyme	*Coq10b*	-
Developmental proteins	*Pdlim7*, *Arc*	-
Enzymes	*Boc*, *Cyp1b1*, *Fbn2*, *Loxl2*, *Rpe65*	*Mmp3*
Extracellular matrix proteins	*Col18a1*, *Col3a1*, *Col5a1*, *Fbn2*, *Fmod*, *Loxl1*, *Ssg1*, *Thbs2*	-
Growth factor	*Igf2*	*Ctgf*
Membrane proteins	*Cd248*, *Colec12*, *Emp1*, *Lox*	-
Neuropeptide	*Penk1*	-
Others	*Igfbp2*	*Cyr61*
Receptors	*Cckar*, *Ngfr*	-
Secreted factors	*Col18a1*, *Col3a1*, *Col5a1*, *Fbn2*, *Fmod*, *Fstl1*, *Igf2*, *Igfbp2*, *Lox*, *Loxl1*, *Loxl2*, *Megf6*, *Penk1*, *Reg3b*, *Ssg1*, *Thbs2*, *Wif1*	*Ctgf*, *Cyr61*, *Mmp3*
Signaling protein	*Wif1*	-
Solute carrier	*Slc14a2*	-
Structural protein	*Prph1*	-
Transcription factors	*Msx1*, *Nfatc4*, *Crem*	*Klf4*, *Tbx15*

Microarray gene expression profiling analysis was carried out using embryonic myelinating spinal cord cultures (Array 2). Illustrated in the table are the differentially expressed transcripts 4 hr and 24 hr after CNTF (cilliary neurotrophic factor) treatment in TnC-myelinating cultures. The transcripts up-regulated upon CNTF treatment are shown in red and the ones down-regulate are shown in green. The transcripts were categorised based on the classification in UniProt (*http://www.uniprot.org/).* Diff: differentially; reg: regulated.

Table 3. 13 Candidates selected from the comparison of TnC+CNTF vs TnC-control myelinating cultures to study further.

Cand.	Suggested Effect on Myelination	Supporting/Contradicting Evidence	References
Thbs2	inhibitory	○ Its expression increased in neurons, microglia and As in CNS pathology. ○ It promoted neurite growth and synaptic formation *in vitro* and *in vivo*. ○ It was shown to regulate the levels of MMP2 whose inhibition leads to incomplete myelin formation.	Bornstein, 2001; Yang et al., 2001; Lin et al., 2003; Christopherson et al., 2005; Liauw et al., 2008; Eroglu et al., 2009; Lehmann et al., 2009; Huang et al., 2013;
Wif1	inhibitory	○ Inhibits Wnt signalling, known to act in axon regeneration after SCI, neurogenesis, axon and dendrite development, differentiation of neural progenitors, axon synaptogenesis during development, support of the viability of neurons in adult brain. ○ Wnt could promote olig maturation and myelination in zebrafish. ○ Dominant active Wnt signalling led to hypomyelination in P15 mouse CNS.	Lee et al., 2004; Li et al., 2005; Gao et al., 2007, Liu et al., 2008b; Salinas and Zou, 2008, Toledo et al., 2008, Fancy et al., 2009; Yang et al., 2010; Zhang and Ma, 2010; Hanafy and Sloane, 2011; Tawk et al., 2011; Wu et al., 2012, Chen et al., 2013
Ctgf	supportive	○ Ctgf/CTGF levels were increased in different types of rat, mouse and human CNS pathology. ○ Suggested to play a role in differentiation of As and oligs *in vitro*. ○ Inhibited olig maturation *in vitro* and *in vivo*. ○ CTGF treatment decreased the level of myelination in embryonic rat myelinating cultures.	Hertel et al., 2000; Schwab et al., 2001; Meeuwsen et al., 2003; Spliet et al., 2003; Ueberham et al., 2003; Conrad et al., 2005; Zhao et al., 2005b; McClain et al., 2009; Obayashi et al., 2009; Stritt et al., 2009; Lu and Ramanan, 2012; Zamanian et al., 2012; Lamond et al., 2013

Microaray gene expression profiling analysis was carried out using embryonic rat spinal cord cultures plated on astrocyte monolayers on coverslips, coated with TnC (TnC-myelinating cultures). Illustrated in the table are the candidates selected as potential regulators of myelination based on their differential expression between the untreated and CNTF-treated TnC-myelinating cultures. Basic facts, which are/could be related to myelination-regulating roles, are also presented for these candidates with their references. As: astrocytes; Cand.: candidates; CNS: central nervous system; CTGF: connective tissue growth factor; Olig: oligodendrocyte; Thbs2: Thrombospondin 2; TnC: tenascin C; Wif1: WNT inhibitory factor 1.

Among the transcripts differentially regulated upon CNTF treatment in TnC-cultures at 24 hr were the transcripts of the secreted proteins *Ctgf*, *Cyr61* and *Mmp3* (Table 3.12), which were all up-regulated in the presence of CNTF and thus could be suggested as positive regulators of myelination. MMP3 was not selected as a myelination-regulating candidate to work with due to the above-mentioned reasons (Section 3.3.3.1). Ctgf and Cyr61, both members of the matricellular protein family CCN (CYR61/CTGF/NOV, Jones and Bouvier, 2014), are expressed in the human CNS (Schwab et al., 2001; Goodwin et al., 2010). Cyr61 has been studied mainly in terms of its effects in cancer (Sin et al., 2008; Young et al., 2009; Goodwin et al., 2010; Haseley et al., 2012); whereas, CTGF (connective tissue growth factor) has been implicated to play a role in oligodendrocyte development and hence in myelination even though its effect appeared to be a negative one rather than a positive one (Table 3.13). Nash et al. (2011b) have also suggested CTGF as a negative regulator of myelination at the end of their microarray gene expression analysis (Array 1). They used neither exogenous THBS4 nor CTGF, though, to prove their possible negative effects on axonal ensheathment in myelinating cultures since the differential expression of the endogenous transcripts were not found to be significant by means of qRT-PCR. My results were based on myelinating cultures on astrocytes (Array 2), though, a more complex system compared to astrocyte monolayers alone (Array 1), where different results could thus be seen. The study showing the inhibitory effect of CTGF in axonal ensheathment (Lamond et al., 2013) had not been published yet at the time I chose the candidates to work with. Lamond et al (2013) have recently published that CTGF is secreted by Schwann cells at high levels, which inhibits myelination. However, it is possible that unlike the high levels of CTGF in Schwann cells, embryonic rat spinal cord myelinating cultures present lower levels of CTGF and that exogenous CTGF treatment of these cultures at different concentrations will show different results as protein levels may affect function. Thus, CTGF stood out as a strong candidate to show some effect on myelination, which required further investigation.

Consequently, after detailed analysis of the comparison of TnC+CNTF vs TnC-control myelinating cultures, the following candidates were selected as possible myelination regulators to work with: **CTGF**, **THBS2**, and **WIF1** (Table 3.13).

3.3.3.3 PLL-control vs TnC-control myelinating cultures

The comparisons that revealed the highest numbers of differentially regulated hits were PLL-control vs TnC-control myelinating cultures at both time points. At the early time point (4 hr) 131 genes and at the late time point (24 hr) 59 genes were differentially regulated (Table 3.14). There were 24 hits common between the two time points. Thus, approximately 64.5% of the changes took place only at 4 hr, leaving 21% to happen at 24

hr alone and 14.5% at both time points. Similar to the case seen for CNTF treatment in TnC-myelinating cultures, most of the expressional changes occurred at the early time point between PLL- and TnC-control cultures.

Interestingly, ***Wif1*** was among the down-regulated genes in PLL-control myelinating cultures compared to TnC-control ones at 4 hr, which would suggest that it is a negative regulator of myelination; whereas, ***Serpinb2*** was up-regulated on PLL compared to on TnC, which proposed the likelihood of Serpinb2 being a positive myelination regulator. These observations are in accordance with the conclusions drawn after the above-mentioned comparisons of PLL-control vs PLL+CNTF and TnC-control vs TnC+CNTF myelinating cultures. This provided stronger evidence for the possibility of these genes being associated with a negative effect on myelination.

Penk1 (proenkephalin), *Crh* (corticotropin releasing hormone) and *Vgf* (neurosecretory protein VGF) were the up-regulated secreted factors in PLL-control cultures with the highest fold changes at 24 hr (3.39, 2.93, 2.62 respectively) and with less but still moderately high levels at 4 hr (3.34, 2.53, 1.90, respectively, Tables 3.14, 3.16). The differential regulation of *Vgf* was not seen at the end of any other comparisons. *Crh* was seen to be up-regulated over time in PLL+CNTF myelinating cultures (Table 3.6) but this expressional change did not appear to be directly related to CNTF treatment due to lack of significant expressional change of *Crh* upon CNTF treatment at either time points or over time in PLL-control myelinating cultures. *Penk1*, however, was significantly up-regulated upon CNTF treatment in TnC-myelinating cultures at 4 hr (Table 3.11) with the second highest fold change among the up-regulated genes on that list. Consequently, **PENK1** appears to be an essential candidate for a positive regulator of myelination. In contrast, there does not seem to be any proof in the literature to back up this theory, as it is a part of the opioid system, involved mainly in pain perception, cognitive functions, affective behaviours and locomotion (Diaz and Asai, 1990; Konig et al., 1996; Roques et al., 2000).

Table 3. 14 Differentially regulated genes detected at 4 hr and 24 hr between PLL- and TnC-control myelinating cultures.

at 4 hr			
		PLL control vs TnC control	
PROBE_ID	ILMN_GENE	False Discovery Rate	Fold Change
ILMN_1373199	KRT19	0.006	-3.53
ILMN_1363606	LCN2	0.006	-2.96
ILMN_1357368	LOC497841	0.005	-2.36
ILMN_1368490	LOC24906	0.004	-2.28
ILMN_1351900	FCNB	0.005	-1.99
ILMN_1364008	KCNN4	0.006	-1.93
ILMN_1359301	IGF2	0.006	-1.90
ILMN_1360484	TBC1D17_PREDICTED	0.011	-1.86
ILMN_1352911	PLEK	0.010	-1.84
ILMN_1349895	RGD1565140_PREDICTED	0.010	-1.83
ILMN_1348956	FN1	0.018	-1.82
ILMN_1360038	CD37	0.020	-1.82
ILMN_1348883	TREM2_PREDICTED	0.026	-1.79
ILMN_1354712	COL1A2	0.011	-1.77
ILMN_1364986	WIF1	0.020	-1.76
ILMN_1374014	SLC2A5	0.012	-1.75
ILMN_1353896	TLR2	0.019	-1.74
ILMN_1376550	H19	0.011	-1.71
ILMN_1376842	TAGLN	0.017	-1.70
ILMN_1376635	CYP1B1	0.017	-1.69
ILMN_1371535	CXCL11	0.018	-1.69
ILMN_1358836	SLCO2B1	0.042	-1.67
ILMN_1367546	TBX15_PREDICTED	0.005	-1.65
ILMN_1356721	CCR1	0.023	-1.62
ILMN_1374661	LIPA	0.026	-1.58
ILMN_1371160	TRAF4AF1	0.022	-1.58
ILMN_1368619	ANXA3	0.026	-1.56
ILMN_1376740	GLIPR1	0.023	-1.55
ILMN_1363050	BUB1_PREDICTED	0.035	-1.55
ILMN_1355463	TLR3	0.045	-1.55
ILMN_1350851	P2RY14	0.035	-1.54
ILMN_1367421	CH25H	0.011	-1.54
ILMN_1357053	LPL	0.038	-1.53
ILMN_1355260	MSR2_PREDICTED	0.036	-1.52
ILMN_1361476	KIF11	0.021	-1.52
ILMN_1366430	LOC498363	0.042	-1.51
ILMN_1374846	MRC1_PREDICTED	0.043	-1.50
ILMN_1364335	CXCL10	0.033	-1.50
ILMN_1365800	RAC2	0.046	-1.50
ILMN_1376765	LCP1	0.028	-1.49
ILMN_1372349	ARHGDIB	0.047	-1.49
ILMN_1352748	SOSTDC1	0.030	-1.48
ILMN_1359219	AIF1	0.034	-1.46
ILMN_1357030	LAPTM5	0.040	-1.46
ILMN_1353170	RGD1309107	0.028	-1.44
ILMN_1371182	TLR7_PREDICTED	0.034	-1.43
ILMN_1359930	PAX3	0.035	-1.43
ILMN_1359086	FCGR3A	0.014	-1.43
ILMN_1650502	LOC362792	0.034	-1.37
ILMN_1365447	CRYAB	0.014	-1.36

ILMN_1366566	CD68	0.044	-1.30
ILMN_1354506	ICAM1	0.046	-1.29
ILMN_1357508	REG3B	0.029	-1.29
ILMN_1360048	IGFBP2	0.014	-1.07
ILMN_1372919	CYR61	0.016	-1.06
ILMN_1350836	CCKAR	0.003	1.05
ILMN_1371407	FMOD	0.003	1.16
ILMN_1371285	MAFF_PREDICTED	0.034	1.18
ILMN_1366540	LOC500721	0.020	1.24
ILMN_1353486	SLC38A1	0.035	1.29
ILMN_1365894	SERPINF1	0.020	1.31
ILMN_1371252	RGD1563002_PREDICTED	0.046	1.37
ILMN_1354748	OSGIN1	0.036	1.40
ILMN_1369005	EGR1	0.020	1.44
ILMN_1370682	ACSBG1	0.049	1.45
ILMN_1352960	SPAG4	0.048	1.45
ILMN_1352810	ARHGEF19_PREDICTED	0.044	1.46
ILMN_1360188	NFIL3	0.020	1.47
ILMN_1357605	RGD1564664_PREDICTED	0.043	1.48
ILMN_1354070	ISG12(B)	0.035	1.51
ILMN_1350597	DLX2	0.034	1.52
ILMN_1368902	YPEL4	0.034	1.52
ILMN_1650120	CLDN11	0.028	1.54
ILMN_1366187	BAALC	0.026	1.54
ILMN_1370171	NMBR	0.046	1.55
ILMN_1360404	STC1	0.027	1.56
ILMN_1356628	NFKBIA	0.026	1.57
ILMN_1368246	NPTX2_PREDICTED	0.024	1.58
ILMN_1373804	GPR103	0.023	1.59
ILMN_1375203	PTP4A1	0.023	1.60
ILMN_1370828	CTH	0.022	1.61
ILMN_1349422	PTGS2	0.022	1.63
ILMN_1363228	ELL2	0.035	1.63
ILMN_1363020	PTPRN	0.021	1.63
ILMN_1373113	RAB27B	0.020	1.65
ILMN_1355386	LOC246266	0.020	1.65
ILMN_1353839	PER1	0.020	1.65
ILMN_1354991	LOC499837	0.022	1.66
ILMN_1370796	RGD1565064_PREDICTED	0.019	1.67
ILMN_1362093	EMD	0.018	1.68
ILMN_1650285	HMOX1	0.011	1.70
ILMN_1373449	TNNC2	0.009	1.72
ILMN_1365302	SNF1LK	0.009	1.72
ILMN_1359665	CHGB	0.040	1.74
ILMN_1360716	SCG2	0.014	1.75
ILMN_1367103	ADAMTS1	0.024	1.76
ILMN_1372537	MSX1	0.019	1.82
ILMN_1370567	LOC363410	0.012	1.83
ILMN_1363468	OXNAD1_PREDICTED	0.017	1.83
ILMN_1356902	CARTPT	0.026	1.84
ILMN_1364821	LOC500720	0.009	1.86
ILMN_1357783	HBEGF	0.011	1.87
ILMN_1364414	VGF	0.011	1.90
ILMN_1368356	FOS	0.011	1.92
ILMN_1356140	LOC501170	0.029	1.93
ILMN_1367475	ALDH1A1	0.005	2.02
ILMN_1376258	DDIT4L	0.009	2.02
ILMN_1369914	RASD1	0.008	2.04

ILMN_1351517	VIP	0.007	2.07
ILMN_1354131	PORF1	0.006	2.09
ILMN_1358226	USP2	0.008	2.11
ILMN_1366467	DLX1	0.011	2.11
ILMN_1367180	RGD1562092_PREDICTED	0.006	2.15
ILMN_1364960	LOC497675	0.005	2.17
ILMN_2039673	ARC	0.005	2.27
ILMN_1367486	DUSP1	0.005	2.30
ILMN_1357890	MMP12	0.004	2.34
ILMN_1355906	NR4A2	0.005	2.36
ILMN_1376782	ADCYAP1	0.005	2.39
ILMN_1351429	SERPINB2	0.004	2.42
ILMN_1358429	CRH	0.005	2.53
ILMN_1360447	BDNF	0.004	2.57
ILMN_1357978	SLCO1C1	0.005	2.74
ILMN_1357229	CCL2	0.004	2.78
ILMN_1366023	CCL7	0.004	2.88
ILMN_1374218	RIBC2	0.004	2.90
ILMN_1375922	NR4A3	0.005	3.20
ILMN_1371574	GEM_PREDICTED	0.003	3.24
ILMN_1352410	PENK1	0.004	3.34
ILMN_1375833	CREM	0.003	3.78
ILMN_1375583	CREM	0.003	3.94
ILMN_1376694	CREM	0.002	4.41
ILMN_1349555	COQ10B	0.003	4.74

at 24 hr

		PLL control vs TnC control	
PROBE_ID	**ILMN_GENE**	**False Discovery Rate**	**Fold Change**
ILMN_1376740	GLIPR1	0.018	-2.42
ILMN_1349895	RGD1565140_PREDICTED	0.029	-2.39
ILMN_1364744	LOC294942	0.007	-2.32
ILMN_1376635	CYP1B1	0.009	-2.25
ILMN_1376550	H19	0.011	-2.21
ILMN_1368490	LOC24906	0.011	-2.13
ILMN_1373199	KRT19	0.034	-1.99
ILMN_1361248	LOC500428	0.015	-1.97
ILMN_1374789	LOC497804	0.032	-1.92
ILMN_1364008	KCNN4	0.018	-1.91
ILMN_1372861	ZDHHC20	0.034	-1.91
ILMN_1360484	TBC1D17_PREDICTED	0.029	-1.87
ILMN_1367877	FCGR3	0.029	-1.86
ILMN_1348883	TREM2_PREDICTED	0.029	-1.86
ILMN_1361190	RGD1559917_PREDICTED	0.030	-1.84
ILMN_1370152	RGD1565785_PREDICTED	0.047	-1.83
ILMN_1357973	LOC500829	0.032	-1.82
ILMN_1354725	LOC500490	0.032	-1.82
ILMN_1370302	LOC500755	0.038	-1.78
ILMN_1649797	LOC499560	0.040	-1.76
ILMN_1369211	LOC500949	0.041	-1.74
ILMN_1649767	LOC498896	0.042	-1.74
ILMN_1361017	LOC500398	0.042	-1.73
ILMN_1353994	P2RY12	0.044	-1.72
ILMN_1359301	IGF2	0.047	-1.70
ILMN_1368071	UBE1C	0.047	-1.70
ILMN_1362483	AXL	0.047	-1.70

ILMN_1367541	S100A13_PREDICTED	0.047	1.59
ILMN_1363716	SORL1_PREDICTED	0.042	1.61
ILMN_1359665	CHGB	0.041	1.63
ILMN_1358491	GSTM7	0.034	1.68
ILMN_1365716	GSTM1	0.039	1.68
ILMN_1353193	GLDC_PREDICTED	0.034	1.68
ILMN_1355484	ROM1	0.040	1.68
ILMN_1366467	DLX1	0.032	1.70
ILMN_1361016	AGT	0.042	1.70
ILMN_1360716	SCG2	0.032	1.71
ILMN_1376782	ADCYAP1	0.032	1.72
ILMN_1371684	LOC499103	0.039	1.73
ILMN_1367453	GADD45G	0.030	1.73
ILMN_1367475	ALDH1A1	0.028	1.76
ILMN_1364960	LOC497675	0.041	1.76
ILMN_1376443	ASCL1	0.032	1.77
ILMN_1365068	S100A3	0.029	1.80
ILMN_1368575	LGI4	0.018	1.82
ILMN_1364821	LOC500720	0.017	1.87
ILMN_1353696	HBB	0.014	1.87
ILMN_1351517	VIP	0.011	1.95
ILMN_1359976	GPR37L1	0.032	1.96
ILMN_1368643	THRSP	0.011	2.00
ILMN_1353353	ALK	0.014	2.17
ILMN_1363020	PTPRN	0.011	2.33
ILMN_1357978	SLCO1C1	0.004	2.47
ILMN_1364414	VGF	0.011	2.62
ILMN_1358429	CRH	0.011	2.93
ILMN_1372537	MSX1	0.018	3.02
ILMN_2040370	PPP1R1B	0.004	3.12
ILMN_1352410	PENK1	0.003	3.39
ILMN_1361666	MMP3	0.000	5.38

An Illumina array was carried out on myelinating spinal cord cultures of different phenotypes (Array 2). The genes differentially expressed between PLL- and TnC-control (untreated) myelinating cultures are listed in the table. RNA samples were collected from myelinating cultures, at 12 DIV, 4 hr and 24 hr after standard medium feeding. The transcripts highlighted in a black box were selected as potential regulators of myelination. Three biological replicates were used for the experiment. Gene fold changes are shown in the table. Negative and positive values represent the down-regulations and up-regulations, respectively. False discovery rate was designated as 5%. The genes highlighted in grey were differentially regulated at both time points.

Some of the secreted factors, differentially expressed at 4 hr between PLL-control and TnC-control myelinating cultures (Table 3.14), appeared to be temporarily up- or down-regulated on specific substrates. Among the transcripts that were up-regulated only at 4hr on PLL compared to those on TnC some were down-regulated over time in PLL-cultures but not differentially expressed over time in TnC- cultures (Table 3.15 A). Thus, these transcripts appeared to be related more with the changes occurring in PLL-cultures rather than those in TnC-cultures as they clearly occurred on PLL alone when no treatments were present. These genes (Table 3.15 A1) formed a potential list of candidates that could be responsible for higher levels of axonal ensheathment on PLL cultures compared to TnC ones. On the other hand, the transcripts down-regulated only at 4 hr in PLL-control cultures compared to TnC-control cultures and down-regulated over time in TnC- cultures (Table 3.15 B2) represented the ones associated with the TnC-cultures and hence with the lower myelination levels seen in them compared to PLL-cultures in the absence of any treatments. We concentrated on the transcripts that could be associated with positive regulation of myelination (Table 3.15 A1).

BDNF has been excluded from the list of genes of interest as it has previously been studied extensively. Its positive effects on myelin formation have been proposed in many studies before (Mitew et al., 2013; Song et al., 2013; From et al., 2014). PORF1 and USP2 do not appear to be closely related to myelination functions as according to UniProt Database, PORF1 is a precursor for a gonadotropin regulatory hormone, a primary regulator in the neuroendocrine control of reproduction, (Krsmanovic et al., 2003) and USP2 is listed to function in muscle organ and skeletal muscle tissue development, protein deubiquitination and stabilisation, myogenesis and transcription. The functions of HBEGF have been suggested as enhancement of the invasion of cancer cells (Bos et al., 2009), heart and embryonic development (Hope et al., 2004; Kimber et al., 2008), gonadotropin-related activation (Shah et al., 2004) and promoting astrocyte survival in serum-free culture (Foo et al., 2011). Finally, ***Serpinb2*** and ***Ccl2*** have been chosen to continue to work with from the list in Table 3.15 A1 based on the evidence suggesting that they may be playing a role in myelination (Table 3.16).

CCL2 is a chemokine associated with the migration of macrophages and leukocytes into the CNS during pathology. CCL2 expression has been shown to be raised in a cuprizone-induced demyelination model, where putative second inflammatory response generated both pro- and anti-inflammatory cytokines and increased the expression of CCR2, the CCL2 receptor, within a short time window (Biancotti et al., 2008). The authors suggested that this might present a microenvironment conductive for recruitment of astrocytes, neural progenitors and OPCs for the process of further injury or repair (Biancotti et al., 2008). The balance between further injury and repair could be one of

Table 3. 15 Temporary expressional changes detected between PLL-control and TnC-control myelinating cultures.

	Explanation		Explanation
A) ↑PLL vs TnC at 4 hr	64 transcripts were up-regulated in PLL-control cultures compared to TnC-control cultures at 4 hr , not at 24 hr.	**B)** ↓PLL vs TnC at 4 hr	45 transcripts were down-regulated in PLL-control cultures compared to TnC-control cultures at 4 hr , not at 24 hr.
1) PLL ↓ or **2)** TnC↑ over time	In order for these 64 transcripts to reach similar levels of expression between PLL- and TnC-cultures at 24 hr, they must be either **1)** down-regulated over time on PLL or **2)** up-regulated over time on TnC.	**1)** PLL ↑ or **2)** TnC↓ over time	In order for these 42 transcripts to reach similar levels of expression between PLL- and TnC-cultures at 24 hr, they must be either **1)** up-regulated over time on PLL or **2)** down-regulated over time on TnC.
Transcripts		**Transcripts**	
A1) **Bdnf** (brain-derived neurotrophic factor), **Ccl2** (chemokine ligand 2) , **Hbegf** (heparin-binding EGF-like growth factor), **Porf1** (preoptic regulatory factor 1), **Serpinb2** (serpin peptidase inhibitor), **Usp2** (ubiquitin specific peptidase 2)		**B1)** none	
A2) none		**B2)** **Cyr61** (cysteine-rich, angiogenic inducer, 61), **Fcnb** (ficolin B), **Igfbp2** (insulin-like growth factor binding protein 2)	

Microarray gene expression profiling analysis was carried out using embryonic myelinating spinal cord cultures (Array 2). RNA samples were collected 4 hr and 24 hr after standard medium feeding from PLL- and TnC- control (untreated) myelinating cultures. The transcripts that were differentially regulated between PLL- and TnC-control myelinating cultures at both time points (4 hr, 24 hr) were excluded from those at 4 hr. Their differential expression at 4 hr but not at 24 hr meant that they were up/down-regulated at the early time point temporarily. In order for these transcripts to reach similar expressional levels at 24 hr between PLL- and TnC-cultures, the changes explained above should have taken place. The transcripts that were up-regulated at 4 hr in PLL-cultures compared to TnC-cultures but were down-regulated over time in PLL-cultures are shown in **A1**. Those that were down-regulated at 4 hr on PLL compared to that on TnC and were down-regulated over time on TnC are presented in **B2**. There were no transcripts up-regulated over time to overcome the initial differential expression between PLL- and TnC-cultures (**A2** and **B1**).

the reasons for contradicting results for the effect of CCL2 in CNS pathologies (Table 3.17), e.g., exacerbating the disease in EAE mice (Glabinski et al., 2003) but helping the EAE mice to recover faster when overexpressed (Elhofy et al., 2005). In addition, the deteriorating effect of CCL2 in EAE onset and development could be that it provides adherence of leukocytes to the pia mater vasculature and thus increases the BBB permeability rather than recruiting the phagocytic immune cells from the periphery or than having a direct effect on axonal ensheathment or repair (Huang et al., 2005; Dos Santos et al., 2005; Yao and Tsirka, 2011). In addition, another chemokine CXCL13 has been shown to enhance myelination despite its elevated levels in EAE spinal cords and CNS of MS patients (Yuan et al., 2013). The contradicting results suggest how complicated the role of CCL2 could be in EAE. It might be crucial for the right concentrations of CCL2 to be obtained in the microenvironment to prevent and/or recover from pathology.

Ccl7 was another chemokine up-regulated in PLL-control cultures at 4 hr (Table 3.14), suggesting a possible positive role in myelination. CCL7 expression might be affected by Th1 (activated helper T cell) response since the pro-inflammatory cytokines IL-1β and TNF-α have been shown to increase the levels of both *Ccl2* and *Ccl7* in primary rat and macaque astrocyte cultures (Thompson and Eldik, 2009; Renner et al., 2011). It is likely that CCL7 plays a role in chemotaxis of peripheral mononuclear cells into the CNS in pathology (Okada et al., 2009; Renner et al., 2011). In accordance with that suggestion, the expression of *Ccr1*, a CCL7 receptor, was detected in the infiltrating macrophages but not in astrocytes, microglia or T-cells in EAE mice (Sunnemark et al., 2003). *Ccr1* expression correlated with the clinical symptom severity probably related to the higher numbers of infiltrating cells due to higher CCR1 levels (Sunnemark et al., 2003). CCL7 has also been suggested as a factor that influences neuronal differentiation and neuritogenesis (Edman et al., 2008). Despite its predominant immune system-related functions in the CNS, CCL7 is still likely to affect axonal ensheathment directly or indirectly as seen in the case of CXCL10 (Nash et al., 2011b).

Among the differentially regulated secreted factors between PLL- and TnC-cultures, the other two interesting candidates were the chemokines ***Cxcl10*** and ***Cxcl11***. Cxcl10 has been shown before to be inhibitory to myelination in embryonic rat spinal cord cultures (Nash et al., 2011b). Cxcl11, however, has not been studied in such circumstances before. Its down-regulation in PLL-myelinating cultures compared to TnC-cultures suggests an inhibitory role for CXCL11 in myelination. The potential role of CXCL11 in MS pathogenesis has been suggested to be related to its capability to recruite the activated CXCR3+ Th1 cells to the sites of inflammation (Szczucinski et al., 2007), a

Table 3. 16 Categorisation of the differentially regulated genes at 4 hr and 24 hr between PLL- and TnC-control myelinating cultures.

	4 hr	24 hr
Categories	**Differentially regulated genes**	**Diff. reg. genes**
Cell junction protein	*Cldn11*	-
Coenzyme	*Coq10b*	-
Developmental proteins	*Arc*, *Dlx1*	*Ascl1*, *Dlx1*, *Gadd45g*
Enzymes	*Bub1*, *Ch25h*, *Cyp1b*, *Kif11*, *Lipa*, *Lpl*, *Rac2*, *Tbc1d17*, *Acsbg1*, *Adamts1*, *Aldh1a1*, *Cth*, *Dusp1*, *Emd*, *Hmox1*, *Mmp12*, *Oxnad1*, *Per1*, *Ptgs2*, *Ptp4a1*, *Ptprn*, *Serpinb2*, *Serpinf1*, *Snf1lk*, *Usp2*	*Axl*, *Cyp1b*, *Tbc1d17*, *Ube1c*, *Agt*, *Aldh1a1*, *Alk*, *Gldc*, *Gstm1*, *Gstm7*, *Mmp3*, *Ppp1r1b*, *Ptprn*
Extracellular matrix proteins	*Col1a2*, *Fcnb*, *Fn1*, *Fmod*	*Mmp3*
Growth factor	*Igf2*, *Hbegf*, *Vgf*	*Igf2*, *Vgf*
Hormones and neuropeptides	*Adcyap1*, *Bdnf*, *Cartptp*, *Chgb*, *Crh*, *Porf1*, *Penk1*, *Stc1*, *Vip*	*Adcyap1*, *Chgb*, *Crh*, *Vip*, *Penk1*
Immune system proteins	*Ccr1*, *Cd37*, *Cxcl10*, *Cxcl11*, *Fcgr3a*, *Lcn2*, *Reg3b*, *Tlr2*, *Tlr3*, *Tlr7*, *Ccl2*, *Ccl7*, *Kcnn4*	*Fcgr3*, *Kcnn4*
Membrane proteins	*Cd68*, *Glipr1*, *Laptm5*, *Isg12(b)*, *Spag4*	*Glipr1*, *Rom1*
Others	*Anxa3*, *H19*, *Icam1*, *Kcnn4*, *Plek*, *Traf4af1*, *Baalc*, *Dlx2*, *Ddit4l*, *Nptx2*, *Osgin1*, *Ribc2*, *Ypel4*	*H19*, *Zdhhc20*, *Hbb*, *Lgi4*, *S100a13*, *S100a3*, *Thrsp*
Receptors	*Ccr1*, *Fcgr3a*, *Mrc1*, *Msr2*, *P2ry14*, *Tlr2*, *Tlr3*, *Tlr7*, *Trem2*, *Cckar*, *Gpr103*, *Nmbr*	*P2ry12*, *Trem2* *Gpr37l1*, *Sorl1*
Secreted factors	*Col1a2*, *Cxcl10*, *Cxcl11*, *Cyr61*, *Fcnb*, *Fn1*, *Igf2*, *Igfbp2*, *Lcn2*, *Reg3b*, *Wif1*, *Adamts1*, *Adcyap1*, *Bdnf*, *Cartpt*, *Ccl2*, *Ccl7*, *Chgb*, *Crh*, *Fmod*, *Hbegf*, *Mmp12*, *Nptx2*, *Penk1*, *Porf1*, *Serpinb2*, *Serpinf1*, *Stc1*, *Usp2*, *Vgf*, *Vip*	*Igf2*, *Adcyap1*, *Chgb*, *Crh*, *Gldc*, *Gstm1*, *Lgi4*, *Mmp3*, *Penk1*, *S100a13*, *Vgf*, *Vip*
Signaling protein	*Arhgdib*, *Sostdc1*, *Wif1*, *Arhgef19*, *Gem*, *Nfkbia*, *Rab27b*, *Rasd1*	-
Solute carrier	*Slc2a5*, *Slco2b1*, *Slc38a1*, *Slco1c1*	*Slco1c1*
Structural protein	*Aif1*, *Cryab*, *Krt19*, *Lcp1*, *Tagln*, *Tnnc2*	*Krt19*
Transcription factors	*Pax3*, *Tbx15*, *Crem*, *Ell2*, *Egr1*, *Fos*, *Maff*, *Msx1*, *Nfil3*, *Nr4a2*, *Nr4a3*, *Scg2*	*Ascl1*, *Msx1*, *Scg2*

Microarray gene expression profiling analysis was carried out using embryonic myelinating spinal cord cultures (Array 2). Illustrated in the table are the differentially expressed transcripts 4 hr and 24 hr after standard medium feeding between PLL- and TnC- control (untreated) myelinating cultures. The transcripts up-regulated on PLL are shown in red and the ones down-regulated are shown in green. The transcripts were categorised based on the classification in UniProt (http://www.uniprot.org/). Diff: differentially; reg: regulated.

Table 3. 17 Candidates selected from the PLL-control vs TnC-control myelinating cultures comparison to study further.

Cand.	Suggested Effect on Myelination	Supporting/Contradicting Evidence	References
Ccl2	supportive	○ Elevated levels in the CNS of EAE mice and in MS lesions. ○ Inhibition of its expression in mouse As reduced EAE severity. ○ Treatment of the animals with a malfunctioning CCL2 protein delayed the onset of EAE and decreased demyelination and axonal loss. ○ Th1 response compromised in mice constitutively expressing CCL2 in their As. These mice exhibited less severe EAE despite the presence of enhanced numbers of mononuclear cells infiltrates into the CNS compared to wild types.	McManus et al., 1998; Vorn et al., 1999; Glabinski et al., 2003; Elhofy et al., 2005; Dos santos et al., 2005; Tanuma et al., 2006; Biancotti et al., 2008; Dogan et al., 2008; Brini et al., 2009 Zaheer et al., 2012; Hidaka et al., 2014 Paul et al., 2014
Ccl7	supportive	○ Elevated in MS lesions and in some EAE rat models. ○ Inlfuences neuronal differentiation and neuritogenesis.	McManus et al., 1998; Edman et al., 2008; Zheng and Zhang, 2014
Cxcl11	inhibitory	○ Elevated levels present in the CSF and sera of MS patients. ○ Its expression was increased in the CNS of EAE mice.	Hamilton et al., 2002; McColl et al., 2004; Szczucinski et al., 2007; Jernas et al., 2012;
Lcn2	inhibitory	○ See Table 3-11.	See Table 3-11.
Serpinb2	supportive	○ See Table 3-11.	See Table 3-11.
Wif1	inhibitory	○ See Table 3-14.	See Table 3-14.

Microaray gene expression profiling analysis was carried out using embryonic rat spinal cord cultures plated on astrocyte monolayers on coverslips, coated with PLL or TnC (PLL-myelinating cultures, TnC-myelinating cultures). Illustrated in the table are the candidates selected as potential regulators of myelination based on their differential expression between the untreated PLL- and TnC-myelinating cultures. Basic facts, which are/could be related to myelination-regulating roles for these candidates are also presented in the table with their references. As: astrocytes; Cand.: candidates; CCL2: chemokine (C-C motif) ligand 2; CCL7: chemokine (C-C motif) ligand 7; CNS: central nervous system; factor 1; CSF: cerebrospinal fluid; CXCL11: chemokine (C-X-C motif) ligand 11; EAE: Experimental autoimmune encephalomyelitis; Lcn2: lipocalin 2; MS: multiple sclerosis; Serpinb2: serpin peptidase inhibitor clade B member 2; Wif1: Wnt inhibitory factor 1.

hypothesis that was contradicted by another study (Liu et al., 2006). The increased expression of this chemokine in EAE and MS lesions could suggest a negative role for it in terms of myelination. This suggestion is in agreement with its proposed effect on myelination revealed by Array 2 analysis.

Based on the comparison of differentially regulated genes between PLL- and TnC-untreated myelinating cultures, ***Ccl2***, ***Ccl7*** **and** ***Serpinb2*** were selected as potential positive regulators and ***Cxcl11***, ***Lcn2*** **and** ***Wif1*** were selected as potential negative regulators of myelination (Table 3.17).

3.4 Conclusions and discussion

3.4.1 Astrocyte monolayers (Array 1) vs embryonic spinal cord myelinating cultures (Array 2)

The only common analysis between the microarray gene expression profiling of astrocyte monolayers (Array 1, Nash et al., 2011b) and the myelinating cultures (Array 2) is the comparison of PLL-control vs TnC-control conditions at 4 hr (Tables 3.2 and 3.3). Only 22% (7 genes/gene loci) of the differentially regulated astrocytic transcripts found in Array 1 were also differentially expressed in myelinating cultures (Array 2, Table 3.18). Failure to detect the differential expression of the rest of the transcripts could be due to the crosstalk between the astrocytes and the other CNS cell types, namely astrocytes, oligodendrocytes or their precursors, microglia, and neurons from the spinal cords.

One example for such a crosstalk is the tripartite synapses, where astrocyte processes can interact with both presynaptic and postsynaptic elements of the synapse and hence with the neurons (Araque et al., 1999). The neurotransmitters in the synaptic cleft can trigger astrocytic signalling pathways that would result in the secretion of gliotransmitters, which can activate the receptors at the pre- and post-synaptic neuron (Reviewed in Haydon et al., 2007 and in Orellana and Stehberg, 2014). The solute carrier (SLC) transport proteins at the membranes of both astrocytes and neurons are indispensable for such a complex functioning. Interestingly, the SLCs up-regulated in PLL-control astrocytes (Array 1) are *Slc22a3* and *Slc4a4*, which were not differentially regulated between PLL- and TnC-control myelinating cultures (Array 2). Slc4a4 could contribute to acid/base homeostasis and glycolysis regulation in astrocyte monolayers (Array 1, Ruminot, 2011; Theparambil et al., 2014), which could be a possible intrinsic attempt of the astrocytes to prepare a homeostatic environment for themselves, neurons and other CNS cells. Slc22a3, as well, could contribute to such a homeostasis by

regulating the concentrations of all four amines (Vialou et al., 2008). The loss of their differential regulation in Array 2 could be because the older astrocytes (12 DIV as opposed to 7-8 DIV cells in Array 1) in myelinating cultures adapt different functions or because the crosstalk between astrocytes and neurons leads the astrocytes to new functions, leaving the ones involved in the maintenance of homeostasis at minimal levels. In addition, new SLCs were found to be differentially regulated in myelinating cultures (Array 2), where it is likely that CNS cell types other than astrocytes express them. However, for example *Slco1c1* has been shown to be expressed predominantly in astrocytes in the brain and to be responsible for the transport of thyroxin and prostaglandins across the BBB (Baklaushev, 2013), a complex function, for which the astrocytes in the myelinating cultures could be becoming ready despite the lack of any vasculature in these cultures.

Astrocytes could also have crosstalk with microglia or oligodendrocytes in myelinating cultures (Array 2). Astrocytes express a variety of pattern recognition receptors (PRRs) that include Toll-like receptors (TLRs), mannose receptors, scavenger receptors and complement receptors (Farina et al., 2007). Following the activation of such receptors, astrocytes secrete cytokines, chemokines and neurotrophins that target other CNS cells (Farina et al., 2007; Tian et al., 2012). Those other cells can re-activate or inhibit the astrocytic receptors in return, which would affect the secretion profile of astrocytes. The initial activation of the receptors could also be influenced by the factors expressed by the CNS cells other than astrocytes. In astrocyte monolayers (Array 1), only *Cxcl10* was seen to be differentially regulated between PLL- and TnC-control conditions; however, in myelinating cultures (Array 2), *Ccl2*, *Ccl7* and *Cxcl11* were also differentially expressed in addition to *Cxcl10*. The differential expression of these three chemokines in Array 2 could be due to the astrocyte-CNS cells' crosstalk mentioned above.

There were seven transcripts that were differentially regulated between PLL- and TnC-conditions in both astrocyte monolayers (Array 1) and in myelinating cultures (Array 2, Table 3.18). *Igfbp2* was the only transcript that showed a different direction of change in each array, i.e. up-regulated in astrocyte monolayers and down-regulated in myelinating cultures. This suggests that either the mixed spinal cord cells in the myelinating cultures are expressing *Igfbp2* in an opposite dominant way to that expressed by astrocytes in the supporting astrocyte monolayer underneath or that the presence of these cells has an effect on the astrocyte monolayer resulting in a down-regulation of *Igfbp2* instead of up-regulating it on PLL. One explanation for this difference could be the change of medium in which the cultures are maintained. The astrocyte monolayers are maintained in a medium with 10% serum; while, the medium

Table 3. 18 The common transcripts that were differentially regulated in the comparison of PLL-cultures vs TnC-cultures at 4 hr in astrocyte monolayers (Array 1) and in myelinating cultures (Array 2).

Transcripts	Change	Key features	References
Aldh1a1 (Aldehyde dehydrogenase 1 family, member A1)	Up	○ Catalyses the conversion of aldehydes to the corresponding acids. Can produce 9-cis-retinoic acid, shown to be stimulatory for myelination. ○ More highly expressed in As from P17-30 mice compared to in neurons, OPCs and oligs. ○ Its expression increases during the development of the human CNS. ○ Highly expressed in mature human As but not in neurons or oligs.	Niederreither et al., 2002; Cahoy et al., 2008; Huang et al., 2011 Adam et al., 2012 Paterson et al., 2013
Igfbp2 (Insulin-like growth factor binding protein 2)	As: Up MC: Down	○ The predominant insulin-like growth factor binding protein in the CNS and CSF. ○ Expressed in some neurons, microglia, oligs and As. ○ Can bind to the growth factors IGF1 and IGF2, present in the CNS. ○ Prevents IGF2 signaling by inhibiting the interaction of IGF2 with its receptor. ○ IGF1/2-IGFBP2 binding will prolong the half-life of IGFs and will help them to be carried and released in the vicinity of the target cells.	Baxter and Martin, 1989; Ocrant et al., 1990; Roghani et al., 1991; Jones and Clemmons, 1995; Collett-Solberg and Cohen, 1996; Baxter, 2000; O'donnell et al., 2002; Chesik et al., 2004; Chesik et al., 2007; Sim et al, 2009; Fletcher et al., 2013
Cxcl10 (Chemokine ligand 10)	Down	○ Is a microglia/macrophage attractant. ○ Highly expressed at the rim of demyelinating MS plaques. ○ As were suggested as the major source of *Cxcl10* mRNA expression in cuprizone-induced demyelination. ○ Is also expressed by microglia upon INFγ treatment. ○ Inhibited myelination levels in embryonic rat spinal cord MC.	Tanuma et al., 2006; Carter et al., 2007; Van zwam et al., 2010; Nash et al., 2011; Skripuletz et al., 2013
Fn1 (Fibronectin 1)	Down	○ Extracellular matrix glycoprotein. ○ Specifically localises in areas of demyelination in MS and EAE. Injection of FN1 aggregates into lesions and inhibits olig differentiation and remyelination. ○ Expression is increased in microglia/macrophages and reactive As in the rat brain upon cryoinjury. ○ FN1 expressed in As of injured CNS may play a role in the formation of the glial scar.	Camand et al., 2004; Stenzel et al., 2011; Kim et al., 2013; Stoffels et al., 2013
Krt19	Down	○ Intermediate filament protein, expressed in epithelia, such as the small	Omary et al., 2009

(Keratin 19)		intestine, colon, exocrine pancreas, bladder, gallbladder, and ductal cells of liver.	
Loc497841	Down	○ Unidentified, hypothetical gene	NCBI/Gene
Tagln (Transgelin)	Down	○ Suggested to play a role in neuroprotection of ischemic rat cortical neurons. ○ Increased expression in rat spinal cord after SCI was interpreted as a possible role in the response to tissue damage or the repair following SCI.	Lin et al., 2005; Prasad et al., 2012;

Microarray gene expression profiling analysis was carried out using astrocyte monolayers (Array 1, Nash et al., 2011b) and embryonic myelinating spinal cord cultures (Array 2). RNA was collected 4 hr after standard medium feeding from 7-8 DIV old astrocyte monolayers (Array 1) or 12 DIV old embryonic spinal cord myelinating cultures (Array 2). The differentially regulated transcripts between PLL- and TnC-astrocyte monolayers were compared with those between PLL- and TnC-myelinating cultures. Illustrated in the table are the 7 common transcripts detected in that comparison. As: astrocytes; Change: Direction of differential regulation; MC=myelinating cultures; olig: oligodendrocyte; SCI: spinal cord injury.

for myelinating cultures have defined hormones in the absence of serum (Table 2.1). Chesik et. al.(2004) have demonstrated that 10% serum could enhance IGFBP2 expression in astrocytes as opposed to those maintained in chemically defined, insulin- and serum-free medium. Thus, it is possible that the factors in the media affect the astrocyte reactivity and in addition alter their gene expressions on different substrates in a different way. Interestingly, *Igfbp2* expression is induced upon CNS injury in reactive astrocytes and reactive microglia (Chesik et al., 2004; O'donnell et al., 2002; Fletcher et al., 2013). Since PLL-astrocytes have been indicated to be more reactive than TnC-astrocytes due to their increased GFAP expression (Nash et al., 2011b), the up-regulation of *Igfbp2* in PLL-astrocyte monolayers is in accordance with the previous studies. Therefore, the down-regulation of *Igfbp2* in PLL-myelinating cultures compared to TnC-myelinating cultures (Array 2) could also suggest that these two culture types are reversed in terms of astrocyte reactivity compared to astrocyte monolayers alone (Array 1).

In young astrocyte cultures (as in Array 1), the primary role of IGFBP2 could be preventing IGF1, the major insulin growth factor in fetal tissues (Bondy et al., 1992), from degradation and thereby preparing a more suitable environment for healthy cultures that will support myelination in the future since IGF1 has been shown to stimulate migration and differentiation of oligodendrocyte precursor cells and promote remyelination (Kuhl et al, 2002; Yao et al., 1996; Li et al., 1998). In this case, the increased IGFBP2 levels in PLL-astrocytes will contribute towards a more myelination-supportive phenotype compared to TnC-astrocytes.

Both IGFBP2 and IGF2 have been detected in the myelin sheaths of individual myelinated fibers of all of the major nerve tracts in adult rats (Logan et al., 1994). Conversely, in the later stages of the cultures (as in Array 2), the predominant function of IGFBP2 could be blocking the IGF1/2 signalling maybe to prevent myelination or further maturation of oligodendrocytes at a time when the axons or other components in the environment are not yet ready for myelination. It is possible that in the myelinating spinal cord cultures, IGFBP2 binding to IGFs prevents their positive effects on myelination. So it could be considered that the suppression of IGFBP2 will allow a supportive phenotype in PLL-myelinating cultures (Array 2). The lowered *Igfbp2* levels in PLL-myelinating cultures could also be to accompany depressed *Igf2* levels (Table 3.14). In either case, despite its proven roles on myelination, the controversial roles of IGFBP2 make it a difficult candidate to use in the myelinating cultures.

Detection of the differentially regulated astrocytic factors between PLL- and TnC-myelinating cultures (Table 3.18) confirmed the previous study that was done using astrocyte monolayers alone (Array 1, Nash et al., 2011b). The up-regulation of *Aldh1a1* in PLL-cultures compared to TnC-cultures would suggest that it has a stimulatory effect on myelination based on the previous findings showing higher levels of myelination in PLL-cultures (Nash et al., 2011b). On the other hand, down-regulation of *Cxcl10*, *Fn1*, *Krt19* and *Tagln* in PLL-cultures would suggest a negative role for these molecules on myelination. Indeed, the supporting evidences are in agreement with most of these findings (Table 3.18). *Krt19* has not been reported to be expressed in the CNS to our knowledge. Thus, its detection in the astrocyte monolayers in Array 1 (Nash et al., 2011b) and in the myelinating cultures in Array 2 is very interesting. Because astrocytes on PLL and TnC can present different morphologies, the differential regulation of this intermediate filament protein could be one of the factors playing a role in this difference (Holley et al., 2005). Therefore, out of these seven common transcripts (Table 3.18), differentially regulated in astrocyte monolayers and in myelinating cultures on different substrates, ***Aldha1a1, Fn1 and Tagln*** stand out as potential candidates to play a role in myelination and require further investigation.

3.4.2 Candidates that appear to be important for myelination in both PLL- and TnC-myelinating cultures

The analysis of the expressional changes in PLL- and TnC-myelinating cultures upon CNTF treatment revealed FMOD and CREM as common possible myelination-regulators stimulated by the CNTF effect (Section 3.3.2.1). IPA diagrams presented interactions of *Fmod* and *Crem* with different types of molecules in these cultures (Fig 3.5, 3.6),

suggesting distinct CNTF-initiated mechanisms between myelinating cultures on PLL and TnC.

Fibromodulin (FMOD) is a proteoglycan that plays a role in organising the structure of type I and II collagen fibrils in extracellular matrix (Vogel, K.G. et al., 1984; Olberg, A. et al., 1989; Svensson, L. et al., 2000). If FMOD contributes towards a more inhibitory environment for axonal ensheathment as suggested by its down-regulation upon CNTF treatment on both PLL and TnC substrates (Tables 3.8, 3.11), it is contradictory to see its up-regulation in PLL-myelinating cultures compared to TnC-myelinating cultures (Table 3.14), where the amount of myelination has been shown to be lower (Nash et al., 2011b). Different pathways could be related with FMOD function on these two substrates. Looking at the PLL-control vs TnC-control comparison, there seems to be an association between *NFκBIα* (also up-regulated on PLL) and *Fmod*, which might include the involvement of JNK signalling (Lee et al., 2011) that does not appear to be affected by CNTF treatment as *NFκBIα* was differentially regulated neither on PLL nor on TnC upon CNTF treatment.

Considering the roles of FMOD reported in other studies, it is possible that FMOD is active in cell survival/apoptosis, antigen presentation, cell fate determination, cell attachment and cytoskeletal reorganisation in the myelinating cultures (Mayr et al., 2004; Bi et al., 2007; Zheng et al., 2008; Choudhury et al., 2010; Lee et al., 2011; Zheng et al., 2011; Zheng et al., 2012; Jian et al., 2013). Its role in PLL-myelinating cultures might be one that promotes axonal ensheathment maybe by stimulating cell survival and differentiation in relatively young cultures (12 DIV). Perhaps FMOD functions start to focus on ECM organisation once the cultures are more mature creating a less permissive environment for axonal ensheathment. CNTF signalling might be targeting this presumably myelination-inhibitory function of FMOD, an action perhaps programmed to occur at later stages of the cultures upon possible increased endogenous CNTF levels (Stockli et al., 1991; Kirsch et al., 1997; Eddie et al., 2012). In addition, the IPA analysis suggests that different pathways that include FMOD are present in PLL- and TnC-myelinating cultures. On TnC, FMOD appears to be related mostly to collagens and lysysl oxidases (LOXes), indicating clearly a role in ECM organisation (Fig 3.6). On the other hand, FMOD is linked to complement factor H (CFH), colony stimulating factor (CSF) and tumor necrosis factor (TNF) in PLL-cultures upon CNTF treatment, suggesting a role in immunity more than in ECM organisation (Fig 3.5).

In parallel with the suggestion of Lee et al. (2011) that there could be a functional link between **FMOD and LOX**, *Fmod* and *Lox* were both down-regulated upon CNTF treatment in TnC-myelinating cultures (Table 3.11). Moreover, several collagens

(*Col18a1*, *Col3a1*, *Col5a1*) and *Fbn2* (fibrillin-2) were also down-regulated upon CNTF treatment in TnC-myelinating cultures. Because microfibrils are made up of fibrillins and because microfibril-associated glycoproteins serve as scaffolds for extracellular matrix protein monomers to be polymerised by LOX or a LOXL (Kielty et al., 2002), decreased quantities of such scaffolds would eventually lead to a less stable, less dense extracellular matrix. Thus, it appears that the myelination-stimulatory role of CNTF treatment in TnC-cultures might be due to the fact that CNTF creates a less densely-packed extracellular environment that presumably provides a more suitable setting for oligodendrocytes to extend their processes that would myelinate the axons nearby. In parallel with that, other members of the LOX family, *Loxl1* that plays a role in elastin polymerisation and Loxl2 were also down-regulated upon CNTF treatment in TnC-myelinating cultures (Table 3.11). LOXL1 has been shown to be expressed in the adult mouse brain, in the neural tube of fetal mice, and to surround the axon fibers (Hayashi et al., 2004). A lower expression of LOXL1, thus, could provide a less compact extracellular matrix around axon fibers, which might promote axon-oligodendrocyte process interaction. In conclusion, I think it would be worthwhile considering LOX family members as potential regulators of myelination in future studies even though they may not be astrocytic factors as suggested by Gilad et al. (2001).

In contrast to *Fmod*, ***Crem*** was up-regulated on both substrates upon CNTF treatment (Tables 3.8, 3.11), suggesting a positive role in myelination. CREM is a member of the transcription regulating family CREB/CREM/ATF that bind to cAMP-response elements (CREs) in the promoters of cAMP-regulated genes (reviewed in De Cesare and Sassone-Corsi, 2000). The *Crem* gene encodes for several transcripts due to initiation of translation from different internal promoters and due to alternative splicing (Mioduszewska et al., 2003). Some of these proteins are translation activators; whereas, the others, mostly ICER proteins, are associated with translation inhibition. In Array 2, the probe used for *Crem* (ILMN_1376694) can detect the eight validated *Crem* transcripts (*Crem* 2-9), listed in NCBI Gene Database. It is, therefore, very difficult to comment on the possible functions of CREM in the myelinating cultures since we cannot be sure which *Crem* isoforms were up-regulated. There are some indicators as to what type of CREM proteins these could be, however. For example, it is known that ICER expression peaks around 2-6 hr after stimulation, depending on types of stimulation and cell types (Luckman and Cox, 1995; Maronde et al., 1999; Pfeffer et al., 1999; Storvik et al., 2000; Liu et al, 2006b; Hu et al., 2008). As *Crem* up-regulation in TnC-myelinating cultures was observed at 4 hr upon CNTF treatment, this transcript might be an ICER. On the other hand, the expressional change of *Crem* in PLL-myelinating cultures was detected at 24 hr, suggesting this may not be an ICER. In addition, ICER has been shown to repress c-FOS (Monaco and Sassone-Corsi, 1997; Misund et al., 2007; Kojima et al.,

2008); however, both *Crem* and *Fos* were up-regulated in PLL-cultures compared to TnC-cultures at 4 hr. Therefore, it is possible that CNTF enhances the expression of a translation-activating *Crem* isoform in PLL-myelinating cultures as opposed to a translation-inhibiting *Crem* in TnC-myelinating cultures.

Crem expression was down-regulated over time in untreated PLL-cultures (Table 3.6), suggesting that CNTF maintains the on-going *Crem* expression in PLL-cultures rather than initiating it from the start. This could be obtained, for example, if CREM provides a negative feedback by acting as a transcriptional repressor of its own gene when it eventually reaches a certain expression level. CNTF could be triggering a potent transcriptional activator that would compete with the CREM protein for the promoter or enhancer region of the *Crem* gene. In contrast, *Crem* expression in untreated TnC-myelinating cultures appeared to be stable over time (Table 3.7). It was up-regulated upon CNTF treatment at 4hr and decreased at 24 hr back to the level seen at 4 hr (Table 3.11). So, in this case CNTF must be triggering mechanisms that would enhance Crem expression possibly via transcriptional activators in TnC-cultures. These transcriptional activators may not be dominant enough in competing for the *Crem* promoter or their half-life might not be long enough to support *Crem* expression further as the increased expression is down-regulated over time.

Interestingly, another difference between the PLL- and TnC-myelinating cultures seems to be the apparent association of CREM with CREB-NFkB complex upon CNTF treatment on PLL but not on TnC, as seen in the IPA analysis (Fig 3.5, 3.6). It is possible for CREB phosphorylation (activation) to be associated with myelin formation and oligodendrocyte maturation (Sato-Bigbee and DeVries, 1996). **CREB** has been shown 1) to take part in the stimulation of MBP expression by cAMP in primary rat oligodendrocyte cultures (Afshari et al., 2001), 2) to be immunolabeled in a way to be continuous with oligodendrocyte processes in chicken cerebella, where overlapping p-CREB and MBP staining was also observed (Kim et al., 2005), 3) to be present in its phosphorylated (active) state at higher levels in the rat spinal cord at the peak stage of EAE (Kim et al., 2007), where it could be contributing towards remyelination apart from leading to the occurrence of reactive astrogliosis (Kim et al., 2007). In that sense, it is interesting that CREB appears as a potential factor among the network of molecules, playing a role in the CNTF effect in PLL-myelinating cultures, which does not appear to be the case in TnC-myelinating cultures.

It is also interesting that *Snf1lk*, a kinase responsible for negative regulation of CREB activity, was up-regulated in untreated PLL-myelinating cultures compared to TnC-cultures at 4 hr (Table 3.14). *Snf1lk* was down-regulated over time both in untreated

and treated PLL-cultures, suggesting that the decreased levels of this p-CREB inhibitor at the late time point allowed the p-CREB activity in PLL-cultures. This change at 24 hr in PLL-cultures could be one of the reasons why there were more genes differentially regulated in PLL+CNTF myelinating cultures at 24 hr as opposed to at 4hr (Fig 3.3) since CREB would then be able to regulate the expressions of genes including CREs in their promotors.

3.4.3 The CNTF effect in PLL- and TnC-myelinating cultures over time

Genes differentially regulated over time in PLL+CNTF and TnC+CNTF myelinating cultures were compared after the expressional changes that occurred in the untreated conditions were excluded from the lists (Fig 3.7, areas shown in blue boxes). This analysis showed that there were different members of chemokines/cytokines, enzymes, and transcription factors differentially regulated in PLL- and TnC-myelinating cultures (Tables 3.6, 3.7).

The chemokines/cytokines identified in PLL-myelinating cultures (*Ccl6*, *Ccl12, Cxcl1* and *Cxcl9*) were all down-regulated over time upon CNTF treatment (Table 3.6), which could suggest a negative effect on myelination. However, the absence of any significant expressional change for these transcripts between control and CNTF-treated cultures at any time point weakens this suggestion. On the other hand, *Cxcl13* was up-regulated over time in TnC+CNTF myelinating cultures, a fact that could be interpreted as a possible positive effect on myelination according to the previous findings (Nash et al., 2011b). Additionally, *Cxcl13* was up-regulated upon CNTF treatment in PLL-cultures at 4 hr. So its differential expression does not seem to be specific to TnC-cultures. Therefore, CXCL13 appears to have the potential to play a positive role in myelination in both cultures. The fact that CXCL13 can promote CNS myelination in cerebellar slice cultures from newborn mice (Yuen et al., 2013) also supports the suggestion for a positive CXCL13 effect in myelination. However, CXCL13 has also been proposed to show a negative effect in neurodegenerative diseases such as MS by maintaining pathogenic T cell responses (Bagaeva et al., 2006; Rainey-Barger et al., 2011). Since the myelinating cultures do not contain any B- or T-cells, CXCL13 could be expressed by microglia or astrocytes as they are known to secrete chemokines. CNTF might be initiating an immune-like response in PLL-cultures and leading to secretion of CXCL13, which in turn could activate other signalling pathways. Because both microglia and astrocytes express the CXCL13 receptor, CXCR5, it is possible that the secreted CXCL13 in turn affects microglia and/or astrocytes (Flynn et al., 2003).

There was a higher number of **enzyme transcripts** differentially regulated over time in PLL+CNTF myelinating cultures compared to in TnC+CNTF cultures (Table 3.5). Out of 12 enzyme transcripts differentially regulated in PLL+CNTF cultures, three transcripts showed changes in other comparisons, as well. ***Ppp1r1b*** and **Ptprn** were not only up-regulated over time in CNTF-treated PLL-cultures, but they were also up-regulated in PLL-control cultures compared to TnC-control cultures, which suggested that they could be potential enhancers of myelination. PPP1R1B could possibly enhance myelination by inactivating protein phosphatase PP1 that has been shown to contribute to oligodendrocyte loss and hypomyelination in mice expressing INF-γ in their CNS and in cultured rat hippocampal slices upon INF-γ treatment (Lin et al., 2008). Similarly, the protein tyrosine phosphatase PTPRN could be playing a role in cellular processes such as growth and differentiation in such a way that would stimulate myelination. However currently less is known about this transmembrane receptor enzyme that is highly expressed in rat primary hippocampal neurons (Chiang and Flanagan, 1996; Jiang et al., 1998; Jiang et al., 2006). On the other hand, the results indicated ***Cyp1b1*** as a negative regulator of myelination since it was down regulated 1) over time in PLL+CNTF cultures, 2) upon CNTF treatment in TnC-cultures at 4 hr, 3) in PLL-control cultures compared to TnC-cultures both at 4 and 24 hr. CYP1B1 is one of the cytochrome P450 monooxygenases, expressed in the human CNS (Rieder et al., 1998). Even though cerebral P450 enzymes can detoxify foreign toxic compounds and are thus important for cell homeostasis, they can also metabolise endogenous compounds such as steroids and eicosanoids and generate reactive oxygen radicals and lipid peroxides that could cause cellular damage or cell death (Mesnil et al., 1984; Guengerich et al., 1985; Anandatheerthavarada et al., 1990; Mills et al., 1995; Montoliu et al., 1995; Rieder et al., 1998). Interestingly, *CYP1B1* has been found to be highly associated with *BDNF* and *MBP (*Luo et al., 2013). Higher reactive oxygen species generation by this enzyme may cause apoptotic changes that lead to glaucoma development (Luo et al., 20013) and maybe to reduction in myelination levels.

A subgroup of enzymes, namely **matrix metalloproteinases** (MMPs), was also identified in the analysis. *Mmp-3* was not only up-regulated over time in TnC+CNTF myelinating cultures (Table 3.5), but also in PLL-control and in PLL+CNTF cultures (Table 3.6). Its expression level at 24 hr was the lowest in TnC-control cultures, higher in PLL-control cultures, and the highest in TnC+CNTF cultures. As Nash et al. (2011b) have observed increased levels of myelination in this same order, our data suggest a positive correlation between MMP-3 and myelination. Similarly, the expression level of *Mmp-12* at 4 hr was the lowest in TnC-control cultures, higher in PLL-control cultures, and the highest in PLL+CNTF cultures. Based on these expressional changes, **MMP-3 and MMP-12**

appear to be playing positive roles in myelination. Even though MMP-12 protein and *Mmp-3* mRNA expressions have been shown to be elevated in MS lesions (Lindberg et al., 2001; Vos et al., 2003); MMP-12 has also been associated with myelination in mouse CNS (Laersen et al., 2006) and a positive role has been suggested for MMP-3 in remyelination due to its proteolytic activity required for releasing growth factors like IGF-1, heparin binding EGF-like factor (HBEGF) and transforming growth factor-β (Dubois-Dalcq and Murray, 2001; McCawley and Matrisian, 2001; Fowlkes et al.,2004) and due to its expressional association with remyelination in a cuprizone-induced demyelination model (Skuljec et al., 2011). The expression of Mmp-3 increased over time in PLL-cultures both before and after the CNTF treatment; however, it was up-regulated in TnC-cultures only upon CNTF treatment at 24 hr. The enhancement of different MMP transcripts upon CNTF treatment on different substrates could account for distinct mechanisms CNTF triggers on these substrates.

As for the **transcriptional factor** transcripts detected in the analysis, ***Msx1***, ***Npas4***, ***Plagl1***, ***Scg2*** were differentially regulated over time in PLL+CNTF cultures and ***Crem***, ***Fos***, ***Irf7*** were differentially expressed over time in TnC+CNTF cultures (Table 3.5). *Msx1* (msh homeobox 1) and Scg2 (secretogranin II) were both up-regulated in PLL-control cultures compared to TnC-control cultures at both time points, suggesting a positive role for these transcription factors in myelination. As **SCG-2** has been shown to play a role in neuronal protection and differentiation and inflammatory responses, it is possible for this neuropeptide precursor to be involved in increase of myelination (Wiedermann, 2000; Taupenot et al., 2003; Hung and Porter, 2008; Shyu et al., 2008). Its involvement in Stat3 signalling also correlates with its up-regulation over time in the presence of CNTF, which has also been shown to signal via Stat3 (Shyu et al., 2008). On the other hand, the down-regulation of *Msx1* in PLL-CNTF cultures over time and in TnC-cultures upon CNTF treatment contradicts the above-mentioned suggestion for a positive role of MSX1 in myelination. On the other hand, *Irf7* was up-regulated but *Crem* and *Fos* were down-regulated over time in TnC+CNTF cultures (Table 3.5). CREM has been discussed above extensively in Section 3.4.2. Even though the up-regulation of *Irf7* could be interpreted as a possible positive effect on myelination especially when its putative roles on myelin stability and remyelination are considered (Salem et al., 2011), the absence of any significant expressional changes for *Irf7* in other comparisons in Array 2 makes it difficult to draw such a conclusion.

Fos, on the other hand, did not appear to be a TnC-specific transcript like *Irf7*. It was down-regulated over time in PLL-control cultures, in PLL+CNTF cultures, and in TnC+CNTF cultures. Its change in TnC-cultures appears to be CNTF-dependent and this might be explained with the dominant enhancing effect of CNTF on oligodendrocyte

differentiation (Tanaka et al., 2013). Since FOS levels are lowered in later stages of differentiating oligodendrocyte cultures with the levels decreased to almost 50% at 24 hr (Bichenkov and Ellingson, 2009), CNTF could stimulate oligodendrocyte maturation that would lead to *Fos* down-regulation over time, which could then allow MBP transcription since the repression of FOS on MBP promoter would be lifted (Miskimins and Miskimins, 2001). Apparently this occurs in PLL-cultures naturally over time; whereas, a stimulating-agent like CNTF is needed in TnC-cultures to induce the *Fos* reduction. If down-regulation of *Fos* by CNTF allows increased myelination levels, what would be the explanation for higher *Fos* expression in PLL-cultures compared to TnC-cultures at 4hr? Even though *Fos* was down-regulated over time in PLL-cultures and reached similar levels of expression with TnC-cultures at 24 hr, the initial high levels of *Fos* in PLL-cultures could be one of the factors that leads to the stimulation or inhibition of different transcripts upon CNTF treatment on the two substrates.

3.4.4 General Conclusions and Summary

The microarray gene expression profiling analysis was carried out using samples from embryonic rat spinal cord myelinating cultures, plated on PLL- or TnC-astrocyte monolayers. Detection of differentially expressed common astrocytic factors in myelinating cultures, plated on various astrocyte phenotypes (Array 2) and in astrocyte monolayers (Array 1, Nash et al., 2011b) confirmed candidates identified in the original study and therefore the second array. The differentially regulated genes associated with CNTF treatment and with different substrates used were mainly chemokines and other immune system proteins, ECM proteins and ECM-modifying proteins, enzymes, growth factors/hormones, membrane proteins, neuropeptides, receptors, signalling proteins, solute carriers, structural proteins, and transcription factors. Thus, it appears that exogenous recombinant CNTF or changing the coverslip-coating agent from PLL to TnC, or vice versa, are enough to initiate or repress the expression of a wide range of genes that could very well be part of different pathways that would eventually lead to the difference in myelination levels observed in these cultures (Nash et al., 2011b).

It is interesting to observe many differentially regulated chemokines in these CNS cultures despite the lack of any lymphoid cells such as lymphocytes, macrophages, B- and T-cells. It is likely that these chemokines were expressed by microglia and/or astrocytes as shown previously (reviewed in Williams et al., 2014). For example, astrocytes and microglia can be activated by LCN2 (lipocalin-2) in an autocrine manner, which leads to the secretion of pro-inflammatory cytokines and makes the astrocytes and microglia secrete higher levels of LCN2, creating a loop of positive feedback (Jang

et al., 2013a; Jang et al., 2013b). Thus, LCN2 could be one of the factors that contribute to an inflammatory response in the myelinating cultures.

There were mainly four pieces of evidence, suggesting that CNTF could initiate different mechanisms in PLL- and TnC-myelinating cultures despite its common positive effect on myelination in these cultures; **1)** Detection of the majority of the differentially regulated transcripts upon CNTF treatment at different time points (Fig 3.3), **2)** IPA diagrams, showing the interaction of common transcripts with different molecules in distinct pathways in CNTF-treated cultures on different substrates (Figs 3.5 and 3.6), **3)** lack of any common genes differentially regulated over time in CNTF+cultures on PLL and TnC (Fig 3.7), and **4)** differential expression of distinct members of gene function categories upon CNTF treatment in PLL- and TnC-cultures. The effect of CNTF in TnC-cultures could be specifically to create a more permissive extracellular environment for oligodendrocyte process extension and axonal ensheathment as interpreted from its effects on the expressions of ECM and ECM-modifying proteins. Its positive effect in PLL-cultures does not appear to be as clear.

Following the conclusion that CNTF could be exerting its myelination-promoting effect in PLL- and TnC-myelinating cultures (Array 2) via different mechanisms, the differentially expressed transcripts were analysed in the following binary comparisons: 1) PLL-control vs PLL+CNTF, 2) TnC-control vs TnC+CNTF, 3) PLL-control vs TnC-control. The candidates selected from these comparisons as potential regulators that might play a role in myelination are shown in Fig 3.8. The selection was made based on the previous observation that the myelination level is the lowest in TnC-myelinating cultures, followed by PLL-myelinating cultures and the highest in both PLL+CNTF and TnC+CNTF myelinating cultures (Nash et al., 2011b). Thus, the transcripts up-regulated in 1) CNTF-treated conditions compared to untreated (control) cultures and in 2) PLL-control cultures compared to in TnC-control cultures could be candidates that play positive roles in myelination; whereas, those down-regulated could be the ones that play negative roles. The selection of the potential regulators of myelination was based on the facts that the candidates 1) would be small secreted molecules, whose effects on myelination could be observed by treating the cultures for a specific period of time and 2) could be associated with myelination based on their reported roles in the literature such as neuronal survival, neurite extension, oligodendrocyte proliferation and/or maturation, elevated/lowered expressions in demyelinated lesions in CNS diseases like multiple sclerosis. The next step would be to validate the expressional changes for the selected candidates by means of qRT-PCR and continue with tissue culture experiments to observe their possible effects on myelination levels in embryonic rat spinal cord myelinating cultures (Chapter 4).

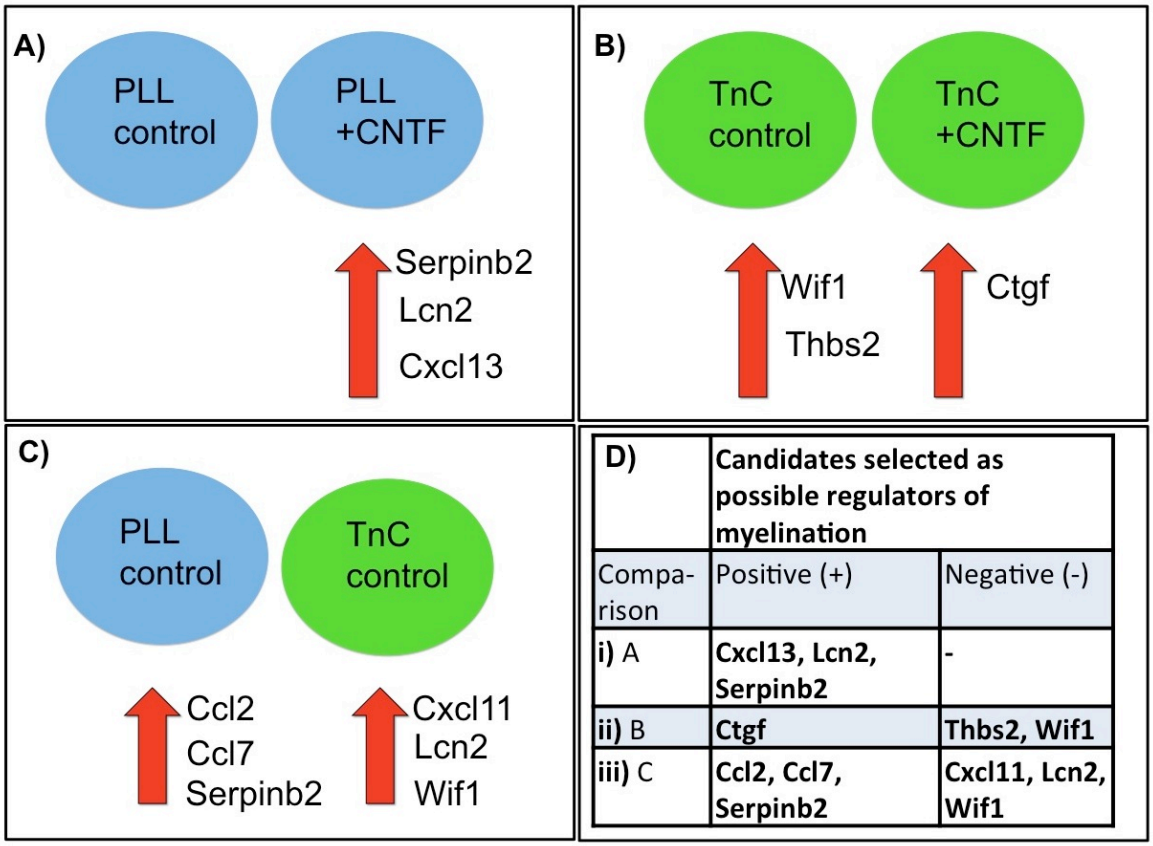

D)	Candidates selected as possible regulators of myelination	
Compa-rison	Positive (+)	Negative (-)
i) A	**Cxcl13, Lcn2, Serpinb2**	-
ii) B	**Ctgf**	**Thbs2, Wif1**
iii) C	**Ccl2, Ccl7, Serpinb2**	**Cxcl11, Lcn2, Wif1**

Figure 3. 8 The potential myelination-regulating candidates selected for further analysis following the binary comparisons of lists of differentially regulated genes in myelinating cultures at different conditions.

Microarray gene expression profiling analysis (Array 2) was carried out using samples from embryonic rat spinal cord myelinating cultures, plated on astrocyte monolayers on glass coverslips, coated with poly-L-lysine (PLL) or tenascin C (TnC). The cultures were either untreated (control) or treated with ciliary neurotrophic factor (CNTF) and total RNA was collected from the cultures 4 hr or 24 hr after standard medium feeding or CNTF treatment. Three biological replicates were prepared for the array and each biological replicate was run in three technical replicates. False discovery rate was designated as 5%. The differentially regulated transcripts between the conditions shown in the diagram were compared in an attempt to identify potential regulators of myelination based on the previous finding that myelination level is the lowest in TnC-control myelinating cultures, higher in PLL-control myelinating cultures, and the highest in PLL+CNTF and in TnC+CNTF myelinating cultures (Nash et al., 2011) **A)** Serpinb2, Lcn2, Cxcl13 were selected as potential positive regulators of myelination due to their up-regulation upon CNTF treatment in PLL-cultures. **B)** Wif1 and Thbs2 were selected as potential negative regulators of myelination and Ctgf was selected as a potential positive regulator of myelination due to their up-regulations in the conditions shown in the diagram. **C)** The analysis of the differentially regulated genes between PLL- and TnC-control cultures revealed Ccl2, Ccl7, and Serpinb2 as potential positive regulators of myelination and Cxcl11, Lcn2, Wif1 as potential negative regulators. **D)** The table presents a summary of the selected candidates from the binary comparisons shown in A, B, and C. Ccl2: chemokine (C-C) ligand 2; Ccl7: chemokine (C-C) ligand 7; Ctgf: connective tissue growth factor; Cxcl11: chemokine (C-X-C) ligand 11; Cxcl13: chemokine (C-X-C) ligand 13; Lcn2: lipocalin-2; Serpinb2: serpin peptidase inhibitor; Thbs2: thrombospondin 2; Wif1: WNT inhibitory factor 1.

Chapter 4

Validation of the putative protein candidates that modulate myelination

4.1 Introduction

Our microarray gene expression profiling analysis (Array 2) was carried out using embryonic rat spinal cord mixed cultures, which were referred to as "myelinating cultures", to identify factors that could play a role in axonal ensheathment that is observed at later stages (24-30 DIV) of these cultures. The microarray analysis identified CCL2, CCL7, CTGF, CXCL11, CXCL13, LCN2, SERPINB2, THBS2, and WIF1 as possible regulators of myelination (Chapter 3). Because the possibility of false positives is increased in transcriptomics due to high numbers of variables analysed, the up/down-regulations of the expression of the selected candidates at different conditions were required to be validated by quantitative real-time polymerase chain reaction (qRT-PCR). The following validation step would be to treat the myelinating cultures with the selected candidates to observe their possible effects on myelination. Neurite density and myelination level of the myelinating cultures were quantified using the "myelin.cp" pipeline of the software Cell Profiler (Carpenter et al., 2006). This method of quantification has recently been validated to be sensitive enough to detect changes in myelination percentages (Lindner et al., 2015).

4.2 Aims

The overall aim of this chapter was to validate candidates obtained from the microarray as modulators of myelination. This will be carried out as follows:

- Performing qRT-PCR using RNA samples **i)** from the stock solutions that were used for Array 2 and **ii)** that were isolated from another set of three biological replicates of embryonic rat spinal cord myelinating cultures at different conditions (PLL-control, PLL+CNTF, TnC-control, TnC+CNTF). Selecting the candidates, which present significant expressional changes that validate the results of Array 2, to treat the myelinating cultures with.

- Assessing effects of candidates on myelination by treating the embryonic rat spinal cord myelinating cultures from an early time point (10 or 12 DIV onwards) with recombinant proteins at various concentrations. Assessing their effects on myelination in myelinating cultures set up on various astrocyte phenotypes plated on PLL (PLL-As) or on TnC (TnC-As) substrates since these astrocyte monolayers have distinct capacities to support myelination and since this difference could affect the way and/or the magnitude of the effects of the exogenous proteins on myelination.

4.3 Results

4.3.1 Validation of the expressional changes detected in Array 2 by means of qRT-PCR

Nine potential myelination-regulating candidates were chosen after the three main comparisons were made, i.e. PLL+CNTF vs PLL-control, TnC+CNTF vs TnC-control and PLL-control vs TnC-control myelinating cultures, whose results were also related with changes that occurred over time. The candidates that were suggested as potential positive regulators were CCL2, CCL7, CTGF, CXCL13, and SERPINB2; whereas, CXCL11, THBS2, and WIF1 were suggested as negative regulators. LCN2 was associated both with more and less supportive myelination phenotypes due to its increased expression upon CNTF treatment in PLL-myelinating cultures and reduced expression in PLL-myelinating cultures compared to TnC-myelinating cultures, respectively.

4.3.1.1 qRT-PCR using cDNA samples from Array 2 (1st qRT-PCR)

In order to validate the expressional changes detected by microarray analysis, cDNA prepared from the same RNA samples used for Array 2 was used to perform a second set of qRT-PCR experiments. *Gapdh* was used as the experimental housekeeping control gene. In addition, measuring the expression of the gene of interest and the expression of *Gapdh* in the same reaction well by means of TaqMan assay provided more accuracy for these experiments.

Significances were calculated by the application of repeated-measures one-way ANOVA test. The Bonferroni correction of a multiple comparison was applied later to detect any significant comparisons. It was important to exclude the comparisons that were not biologically relevant from the analysis because the higher the number of comparisons are the more difficult it is to obtain significance with Bonferroni test. Due to the presence of three variables in the cultural conditions, i.e. substrate, treatment and time point, there were 8 (2^3) different conditions, which would form 28 possible binary comparisons ($^8C_2$ = the number of ways 8 items can be combined, taking 2 at a time). For the ANOVA analysis with Bonferroni's correction 16 comparisons (Table 4.1) that were considered to be biologically relevant were included. One variable was compared for most of the comparisons, i.e. the substrate (PLL or TnC, #1, 5, 11, 14), the treatment (control or CNTF, #2, 8, 12, 16) or the time point (4 hr or 24 hr, #3, 6, 9, 10), to be able to identify the effect of each factor on the expression of the gene of interest. There were four comparisons where both substrates and treatments were different (#4, 7, 13 and 15 in Table 4.1) but these were biologically relevant as

myelination phenotypes were compared at the same time point. As mentioned earlier, PLL+CNTF and TnC+CNTF myelinating cultures have shown similar levels of axonal ensheathment which was higher than that in PLL-control cultures and than in TnC-control cultures, with the lowest level (Nash et al., 2011b). For example, the transcripts up-regulated in TnC-CNTF cultures compared to PLL-control cultures (#4 and 13 in Table 4.1) at early and late time points would be associated with increased myelination levels. On the other hand, comparisons of different conditions over time (e.g., PLL-con-4 hr vs TnC-con-24 hr, TnC-con-4 vs PLL-CNTF-24) were not considered biologically relevant because the transcriptional changes detected in those comparisons would be associated with both the myelination phenotype and the change over time preventing to conclude what those transcriptional changes reflected.

Table 4. 1 The comparisons included in repeated measures one-way ANOVA test with Bonferroni correction to analyse the significance of transcriptional changes detected by qRT-PCR.

	Substrate	Treatment	Time Point (hr)		Substrate	Treatment	Time Point (hr)
1	PLL	control	4	vs	TnC	control	4
2	PLL	control	4	vs	PLL	CNTF	4
3	PLL	control	4	vs	PLL	control	24
4	PLL	control	4	vs	TnC	CNTF	4
5	PLL	CNTF	4	vs	TnC	CNTF	4
6	PLL	CNTF	4	vs	PLL	CNTF	24
7	PLL	CNTF	4	vs	TnC	control	4
8	TnC	control	4	vs	TnC	CNTF	4
9	TnC	control	4	vs	TnC	control	24
10	TnC	CNTF	4	vs	TnC	CNTF	24
11	PLL	control	24	vs	TnC	control	24
12	PLL	control	24	vs	PLL	CNTF	24
13	PLL	control	24	vs	TnC	CNTF	24
14	PLL	CNTF	24	vs	TnC	CNTF	24
15	PLL	CNTF	24	vs	TnC	control	24
16	TnC	control	24	vs	TnC	CNTF	24

Microarray gene expression profiling analysis was carried out using embryonic myelinating spinal cord cultures (Array 2). Illustrated in the table is a list of comparisons of the myelinating cultures at different conditions. Out of the 28 possible comparisons, 16 comparisons were used in the Bonferroni's method of one-way ANOVA analysis since these comparisons were considered to be biologically relevant.

After Bonferroni's test, Dunnett's post-hoc test was run by including all conditional datasets for each gene of interest by designating one of four possible control conditions: 1) PLL-control 4 hr, 2) PLL-control 24 hr, 3) TnC-control 4 hr, 4) TnC-control 24 hr. Although untreated PLL-astrocytes condition was previously used as a control in a similar study (Nash et al., 2011b), it is also possible to assign TnC-control condition as a reference for comparison because the lowest myelination level is seen on TnC-control myelinating cultures. It has also been suggested that PLL-cultures could be more representative of activated astrocytes and hence more distant to what *in vivo* CNS environment would be like (Holley et al., 2005; Nash et al., 2011b). In parallel with that, SERPINB2 protein, which has been detected in the astrocytes of injured brains but not in those of healthy control brains (Dietzmann et al., 2000), was up-regulated in PLL-control myelinating cultures compared to TnC-control myelinating cultures. Therefore, TnC-myelinating cultures could be more representative of the healthy CNS *in vivo* in some aspects compared to PLL-myelinating cultures.

As seen in Figures 4.1 and 4.2, the only candidates that showed significant expressional changes were *Serpinb2*, *Ccl2* and *Ccl7*. Surprisingly, the up-regulation of *Serpinb2* in PLL-control cultures compared to TnC-control cultures was significant only for the 24 hr time point; whereas this up-regulation was detected significant at 4 hr in the microarray analysis. However, the mean value of TnC-control 4 hr condition was indeed much lower than the mean value of PLL-control 4 hr as seen in Fig 4.1 C. The significance appeared to be lost due to the biological variance between the three biological repeats of PLL-control 4 hr condition since the Ct values for *Gapdh* and *Serpinb2* expressions were within one cycle between the technical replicates. The mean ΔCt values between the technical replicates were also within one cycle. Thus, it appeared that *Serpinb2* expression in PLL- control myelinating cultures prepared from different animals could be quite variable 4 hr after feeding with fresh media. Such variation was lost at 24 hr. Treating with CNTF appeared to cause less variation between different biological replicates of PLL cultures at 4 hr but this variation rose at 24 hr (Fig 4.1 C). In TnC conditions, however, the variations were much lower due to the fact that *Serpinb2* expression was also very low (below 0.1 fold) here. Due to the above-mentioned variations, the Bonferroni test including the 16 comparisons in Table 4.1 revealed no significant changes.

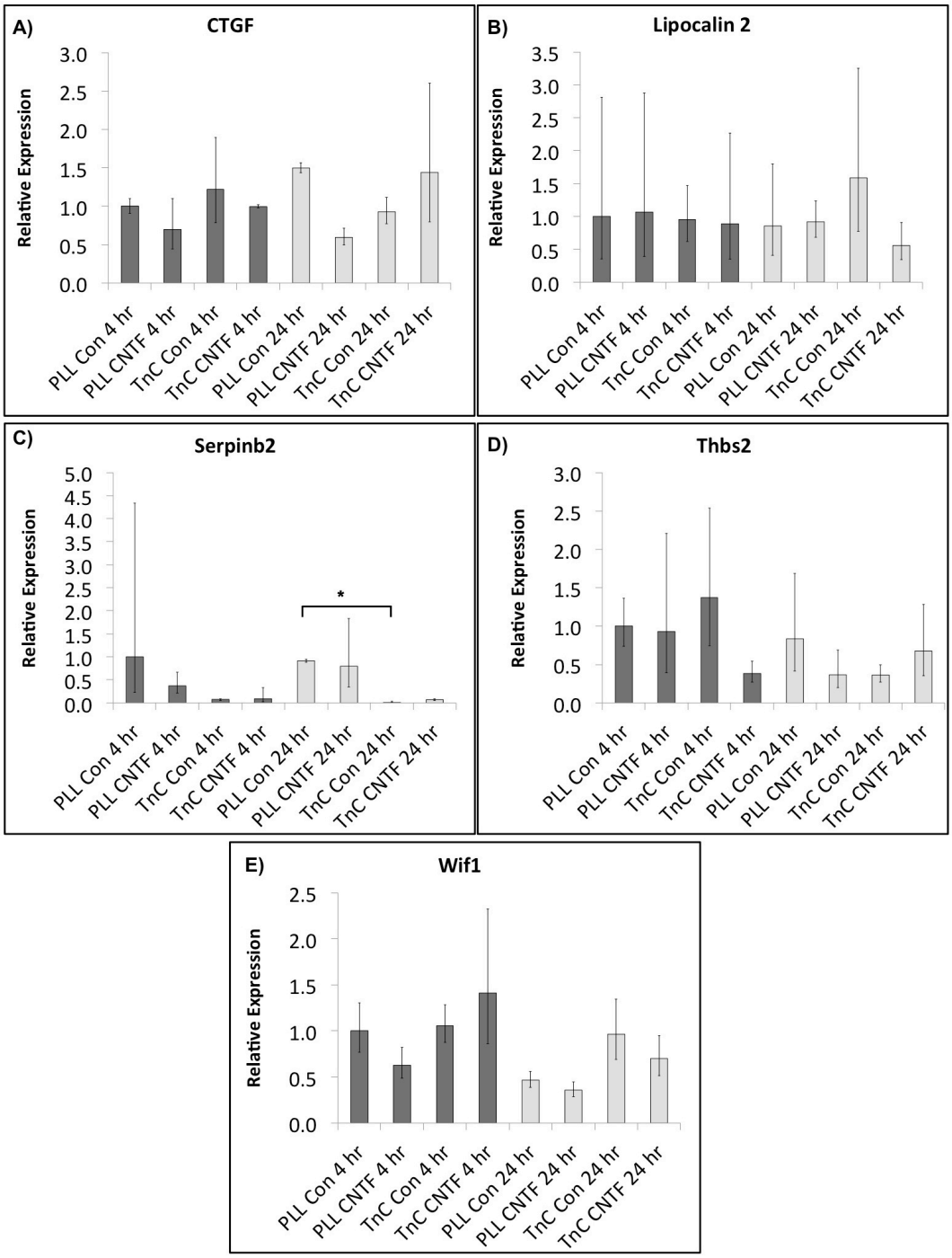

Figure 4. 1 The 1st qRT-PCR results for the possible myelination-regulating candidates selected at the end of Array 2.

Microarray gene expression profiling analysis was carried out using samples from embryonic rat spinal cord myelinating cultures, plated on astrocyte monolayers on glass coverslips, coated with poly-L-lysine (PLL) or tenascin C (TnC). The cultures were either untreated (control) or treated with ciliary neurotrophic factor (CNTF) and total RNA was collected from the cultures 4 hr or 24 hr after standard medium feeding or CNTF treatment. Three biological replicates were prepared for the array and each biological replicate was run in three technical replicates. False discovery rate was designated as 5%. The RNA samples used were from the same batches used for Array 2. Relative expressions were normalised to PLL-control-4hr levels for each transcript. The significance seen for differential *Serpinb2* expression ($p<0.05$) in the graph was detected using repeated measures of one-way ANOVA test. The error bars represent ± standard error of the mean relative to the housekeeping gene *Gapdh*. Darker and lighter bars represent the 4 hr and 24 hr samples, respectively. Ctgf: connective tissue growth factor; Lcn2: lipocalin-2; Serpinb2: serpin peptidase inhibitor; Thbs2: thrombospondin 2; Wif1: WNT inhibitory factor 1.

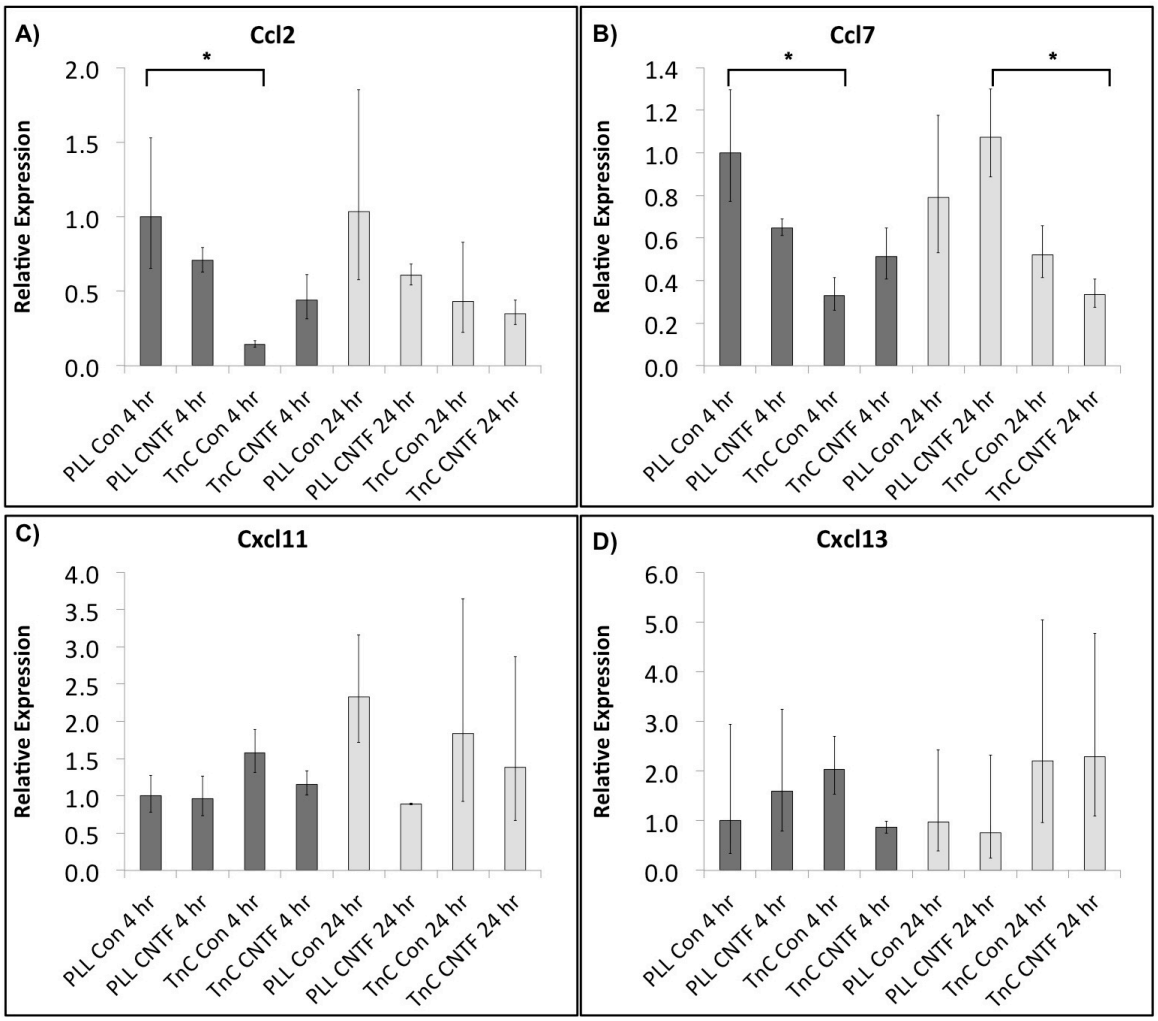

Figure 4. 2 The 1st qRT-PCR results for the possible myelination-regulating chemokines selected at the end Array 2.

Array 2 was carried out using samples from embryonic rat spinal cord myelinating cultures, plated on astrocyte monolayers on glass coverslips, coated with poly-L-lysine (PLL) or tenascin C (TnC). The cultures were either untreated (control) or treated with ciliary neurotrophic factor (CNTF) and total RNA was collected from the cultures 4 hr or 24 hr after standard medium feeding or CNTF treatment. Three biological replicates were prepared for the array and each biological replicate was run in three technical replicates. False discovery rate was designated as 5%. The RNA samples used for the 1st qRT-PCR were from the same batches used for Array 2. Relative expressions were normalised to PLL-control-4hr levels for each transcript. The significance seen for differential *Ccl2 and Ccl7* expression (*, $p \leq 0.05$) in the graph was detected using repeated measures of one-way ANOVA test. The error bars represent ± standard error of the mean relative to the housekeeping gene *Gapdh*. Darker and lighter bars represent the 4 hr and 24 hr samples, respectively. Ccl2: chemokine (C-C) ligand 2; Ccl7: chemokine (C-C) ligand 7; Cxcl11: chemokine (C-X-C) ligand 11; Cxcl13: chemokine (C-X-C) ligand 13.

Nevertheless, Dunnett's test presented the expressional change between PLL-control 24 hr vs TnC-control- 24 hr as significant when the control condition was designated as PLL-control-24 hr or TnC-control-24 hr. This result was still in accordance with the microarray assay results. Carrying out qRT-PCR validated the increase of *Serpinb2* expression in cultures, with a higher level of axonal ensheathment. Thus, there was further proof to support the suggestion of SERPINB2 as a positive regulator of myelination.

As for the chemokines checked, *Ccl2* and *Cc7* were the only ones that showed significant expressional changes in qRT-PCR results (Fig 4.2). The Bonferroni test demonstrated the increased *Ccl2* expression to be significant in PLL-control cultures compared to TnC-control cultures at 4 hr (Fig 4.2 A). This significance was confirmed by the Dunnett's test, as well, where PLL-control-4 hr or TnC-control-4 hr values were designated as the control. This significance of raised *Ccl2* expression in PLL-control cultures compared to TnC-control cultures at 4 hr was in accordance with the microarray assay results. Similarly, this expressional change supported the suggestion of CCL2 as a positive regulator of axonal ensheathment.

The Bonferroni test for *Ccl7*, however, revealed the expressional change in a different binary comparison as significant. Unexpectedly, *Ccl7* was up-regulated in PLL+CNTF cultures compared to TnC+CNTF cultures at 24 hr (Fig 4.2 B). This significance was not detected in the microarray assay and was difficult to interpret in terms of the effect of CCL7 on myelination as both PLL+CNTF and TnC+CNTF cultures have been shown to have similar levels of myelination (Nash et al., 2011b). The Dunnett's test, on the other hand, validated the up-regulation in PLL-control cultures compared to TnC-control cultures at 4 hr when the control was designated as PLL-control 4 hr or TnC-control 4 hr values. Therefore, *Ccl7* was also validated as a candidate for positive regulation of axonal ensheathment.

The expressional changes for the other candidates were not found to be significant with one-way ANOVA. However, the relative quantification graphs showed some differential expression tendencies in accordance with the ones found in the microarray analysis. For example, *Thbs2* expression was down-regulated in TnC+CNTF cultures compared to TnC-control cultures at 4 hr (Fig 4.1 D). *Cxcl11* expression was down-regulated in PLL-control samples compared to TnC-control ones at 4 hr (Fig 4.2 C). *Cxcl13* expression was up-regulated over time in TnC-CNTF samples (Fig 4.12 D). *Wif1* was up-regulated on TnC compared to on PLL at 24 hr without treatment (Fig 4.1 E). None of these changes were found to be significant.

Ctgf was suggested as a potential positive regulator of axonal ensheathment as it was up-regulated upon CNTF treatment in TnC cultures at 24 hr in Array2. This expressional change was not significant in qRT-PCR analysis (Fig 4.1 A). There was an expressional change that was found to be significant for *Ctgf* with unpaired Student's T-test, a test that is used only to compare two conditions and that has less power in an experiment with multiple conditions. *Ctgf* was down-regulated upon CNTF treatment on PLL at 24 hr, which would indicate it as a negative regulator of axonal ensheathment. Nash et al. (2011b) have indeed suggested it is a negative regulator since their microarray analysis have indicated *Ctgf* to be up-regulated in TnC-control cultures compared to both PLL-control cultures and the PLL+CNTF cultures at 4 hr (Array 1). Their qRT-PCR results for *Ctgf* were also not significant but there was a tendency for down-regulation in PLL+CNTF-24 hr compared to TnC-control-4 hr, which again could be interpreted as a possible negative effect on axonal ensheathment. These controversial facts about CTGF either could be artefacts of a variable culture system or of possible technical errors or they could imply a highly complex mechanism for CTGF in these cultures. Therefore, it would be interesting to further investigate the role of CTGF in these myelinating cultures especially at different concentrations.

In conclusion, there were significant changes detected in the expression of *Ccl2*, *Ccl7* and *Serpinb2* by means of qRT-PCR using the cDNA samples synthesised from the original RNA samples that were extracted from the myelinating cultures used for Array 2 analysis. Even though, there was not any significance detected for *Ctgf*, it was also selected for further study as explained above.

4.3.1.2 qRT-PCR using new cDNA samples, not used in Array 2 (2nd qRT-PCR)

Total RNA was also collected from three different biological replicates of the embryonic rat spinal cord myelinating cultures 4 hr after standard medium feeding or treatment, forming the following four conditions: PLL-control, TnC-control, PLL+CNTF, and TnC+CNTF. The cDNA obtained from these RNA samples were used for another qRT-PCR analysis also in attempt to validate the transcriptional changes observed in Array 2. The significances were calculated by repeated measures one-way ANOVA statistical analysis, followed by Bonferroni's multiple comparison and/or Dunnett's tests.

As seen in Fig 4.3 and 4.4, significant transcriptional changes were observed for *Ccl2*, *Ccl7*, and *Cxcl11*. The significance detected for increased Serpinb2 expression in PLL-

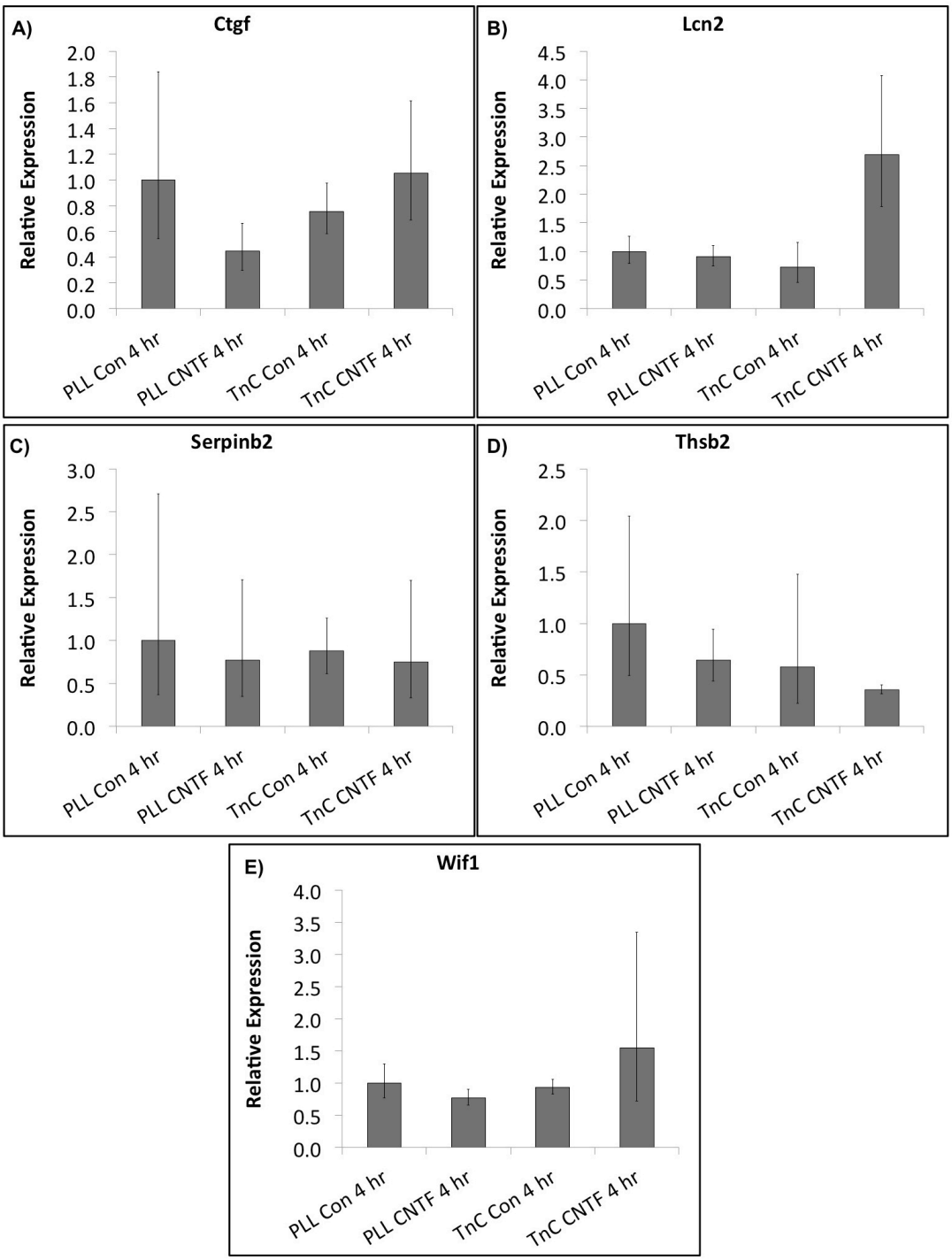

Figure 4. 3 The 2nd qRT-PCR results for the possible myelination-regulating candidates selected at the end Array 2.

The RNA samples used for the 2nd qRT-PCR were not from the same batches used for Array 2. Three biological replicates of embryonic rat spinal cord myelinating cultures, plated on astrocyte monolayers on glass coverslips, coated with poly-L-lysine (PLL) or tenascin C (TnC) were cultured until 12 days *in vitro*. The cultures were then either treated with ciliary neurotrophic factor (CNTF) or fed with standard medium. Total RNA was harvested from the cultures 4 hr after standard medium feeding or CNTF feeding. Relative expressions were normalised to PLL-control levels for each transcript. The error bars represent ± standard error of the mean relative to the housekeeping gene *Gapdh*. Repeated measures of one-way ANOVA test was applied to the results to detect any possible significances. There were not any significances observed for the candidates shown in the graphs above. Ctgf: connective tissue growth factor; Lcn2: lipocalin-2; Serpinb2: serpin peptidase inhibitor; Thbs2: thrombospondin 2; Wif1: WNT inhibitory factor 1.

myelinating cultures compared to that in TnC-myelinating cultures at 24 hr in the previous qRT-PCR (Fig 4.1) was not seen in the one where new cDNA samples were used (Fig 4.3). This could be because only 4 hr samples were used this time and that the standard error was also very high for PLL-control-4 hr myelinating cultures in the second qRT-PCR (Fig 4.3) similar to the case seen previously (Fig 4.1). On the other hand, there were significant expressional changes observed for *Cxcl11* (Fig 4.4) unlike the first qRT-PCR (Fig 4.2). Dunnett's test revealed that *Cxcl11* was up-regulated upon CNTF treatment in PLL-myelinating cultures and it was also up-regulated in PLL+CNTF myelinating cultures compared to TnC-control cultures (Fig 4.4). In addition, the Bonferroni's multiple comparison test presented that *Cxcl11* was up-regulated in TnC+CNTF cultures compared to in PLL-control cultures (Fig 4.4). All of these significant changes suggested that CXCL11 might be a positive regulator of myelination due to its increased expression in myelinating cultures with a higher capacity of myelination. However, CXCL11 was proposed as a possible negative regulator of myelination after Array 2 due to its down-regulation in PLL-control myelinating cultures compared to TnC-control cultures. Such a down-regulation was also detected in the second qRT-PCR (Fig 4.4) but was not found to be significant. The lack of any significant differential expression of Cxcl11 in the first qRT-PCR (Fig 4.2) and the above-mentioned controversial results of the second qRT-PCR weakened the argument that CXCL11 could be a strong candidate that could be effective in myelination.

Similar to the results of the first qRT-PCR (Fig 4.2), significant up-regulations were seen for *Ccl2* and *Ccl7* in myelinating cultures that have been shown to present higher levels of myelination (Fig 4.4). *Ccl2* was up-regulated both in PLL+CNTF and TnC+CNTF myelinating cultures compared to TnC-control cultures, where significances were detected both by Bonferroni's multiple comparison and Dunnett's tests (Fig 4.4). Ccl7 was up-regulated in TnC+CNTF cultures compared to PLL-control cultures; and also in PLL+CNTF cultures compared to TnC-control myelinating cultures (Fig 4.4), which were detected by Dunnett's test only. Even though these specific differential expressions for *Ccl2* and *Ccl7* were not detected in Array 2, they were still in agreement with the suggestion that these factors could have a positive role in myelination as indicated by the up-regulation of *Ccl2* and *Ccl7* in PLL-control cultures compared to TnC-control cultures in Array 2.

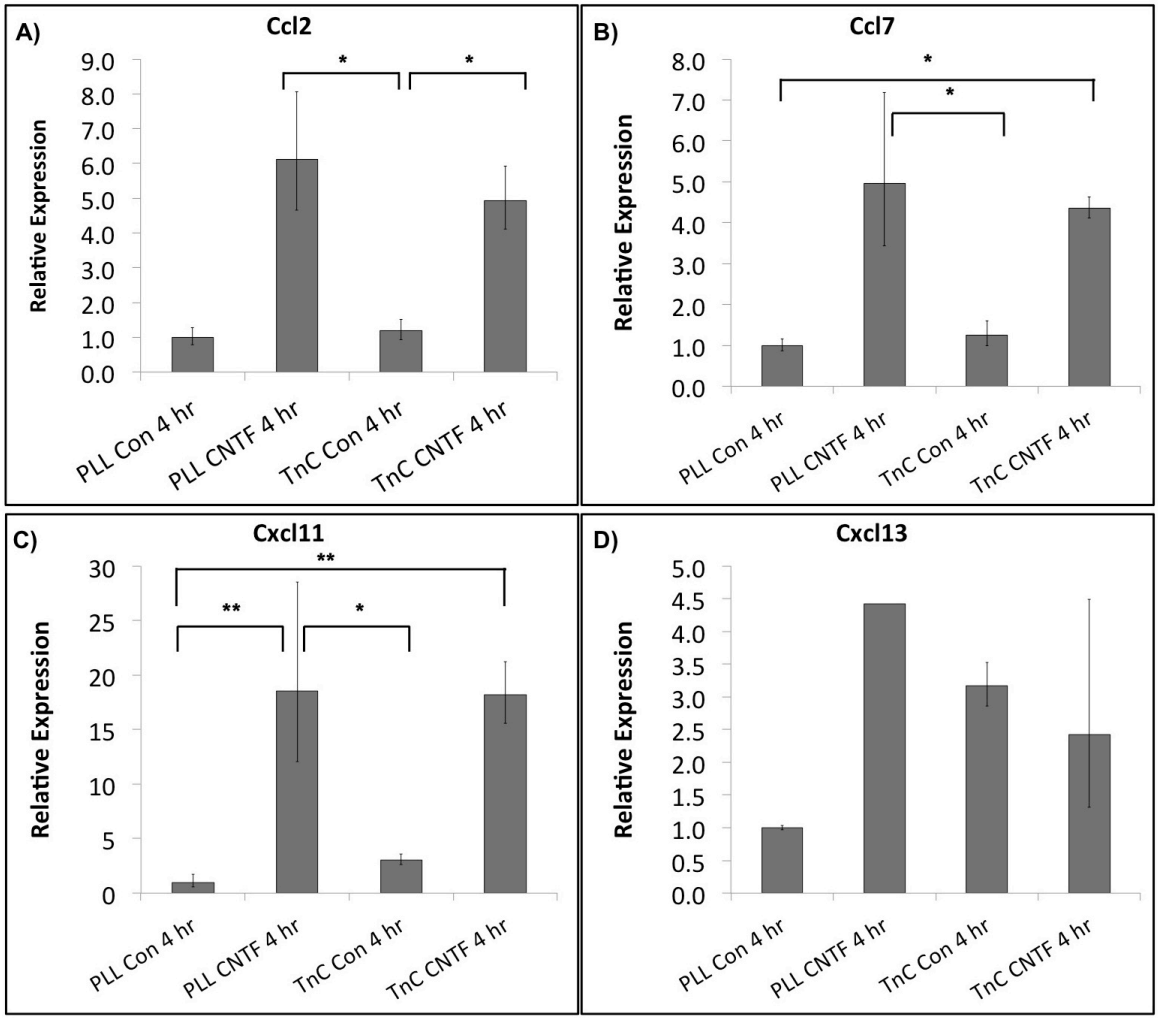

Figure 4. 4 The 2nd qRT-PCR results for the possible myelination-regulating chemokines selected at the end of microarray gene expression profiling analysis (Array 2).
The RNA samples used for the 2nd qRT-PCR were not from the same batches used for Array 2. Three biological replicates of embryonic rat spinal cord myelinating cultures, plated on astrocyte monolayers on glass coverslips, coated with poly-L-lysine (PLL) or tenascin C (TnC) were cultured until 12 days *in vitro*. The cultures were then either treated with ciliary neurotrophic factor (CNTF) or fed with standard medium. Total RNA was harvested from the cultures 4 hr after standard medium feeding or CNTF feeding. Relative expressions were normalised to PLL-control levels for each transcript. The error bars represent ± standard error of the mean relative to the housekeeping gene *Gapdh*. Repeated measures of one-way ANOVA test was applied to the results to detect any possible significances. Significances were observed for *Ccl2*, *Ccl7* and *Cxcl11* (*, $p \leq 0.05$; **, $p \leq 0.01$). Ccl2: chemokine (C-C) ligand 2; Ccl7: chemokine (C-C) ligand 7; Cxcl11: chemokine (C-X-C) ligand 11; Cxcl13: chemokine (C-X-C) ligand 13.

In conclusion of both qRT-PCRs, the chemokines CCL2 and CCL7, and SERPINB2 were selected as the potential candidates that could play a positive role in myelination in embryonic rat spinal cord myelinating cultures. The next step would be to test their exogenous effects on axonal ensheathment in these cultures.

4.3.2 Treatment of myelinating cultures with myelination-regulating candidates identified in Array 2

The expressional changes detected in Array 2 were validated for *Ccl2*, *Ccl7*, and *Serpinb2* out of the nine candidates that were suggested to regulate myelination after the microarray analysis. Even though the up- and down- regulations of *Ctgf* seen in Array 2 could not be validated by qRT-PCR, CTGF was also included in the list of candidates to be tested in myelinating cultures since it was also previously suggested to play a role in myelination due to its increased expression in astrocyte monolayers that have been shown to be less supportive for myelination (Nash et al., 2011b). Therefore, embryonic rat myelinating cultures were treated separately with recombinant CCL2, CCL7, CTGF and SERPINB2 proteins and the myelination levels under different conditions were later visualised and calculated.

4.3.2.1 CTGF did not lead to any significant changes in myelination levels

The myelinating cultures were treated with recombinant human CTGF (#120-19, Peprotech, UK) starting from 12 DIV onwards once every other day until they were used for immunocytochemistry on day 24-28 *in vitro*. In the first set of experiments (1st titration), the myelinating cultures were treated with CTGF at concentrations ranging between 0.05-50 ng/ml (Fig 4.5 A&B). Even though one-way repeated measures ANOVA statistical test did not reveal any significance for the changes in myelination level in the cultures treated with different concentrations of CTGF, the decrease at 12.5 ng/ml was investigated further. The 2nd titration consisted of five concentrations between 4 and 20 ng/ml, which did not lead to any significant changes in the level of myelination or neurite density in myelinating cultures, either (Fig 4.5 C&D).

The myelination percentages were standardised to the control (no treatment) within each biological repeat to avoid high variations when the average raw myelination values were taken. A specific range of myelination percentages has not been identified yet to reflect clearly the health of these myelinating cultures; however, as the myelination percentage drops below 1-2%, the neurite density tends to decrease leading to a sparse culture, and the myelin stained with the antibody against PLP tends to appear less organised in neat long tubular sheaths, which are normally the shapes detected and

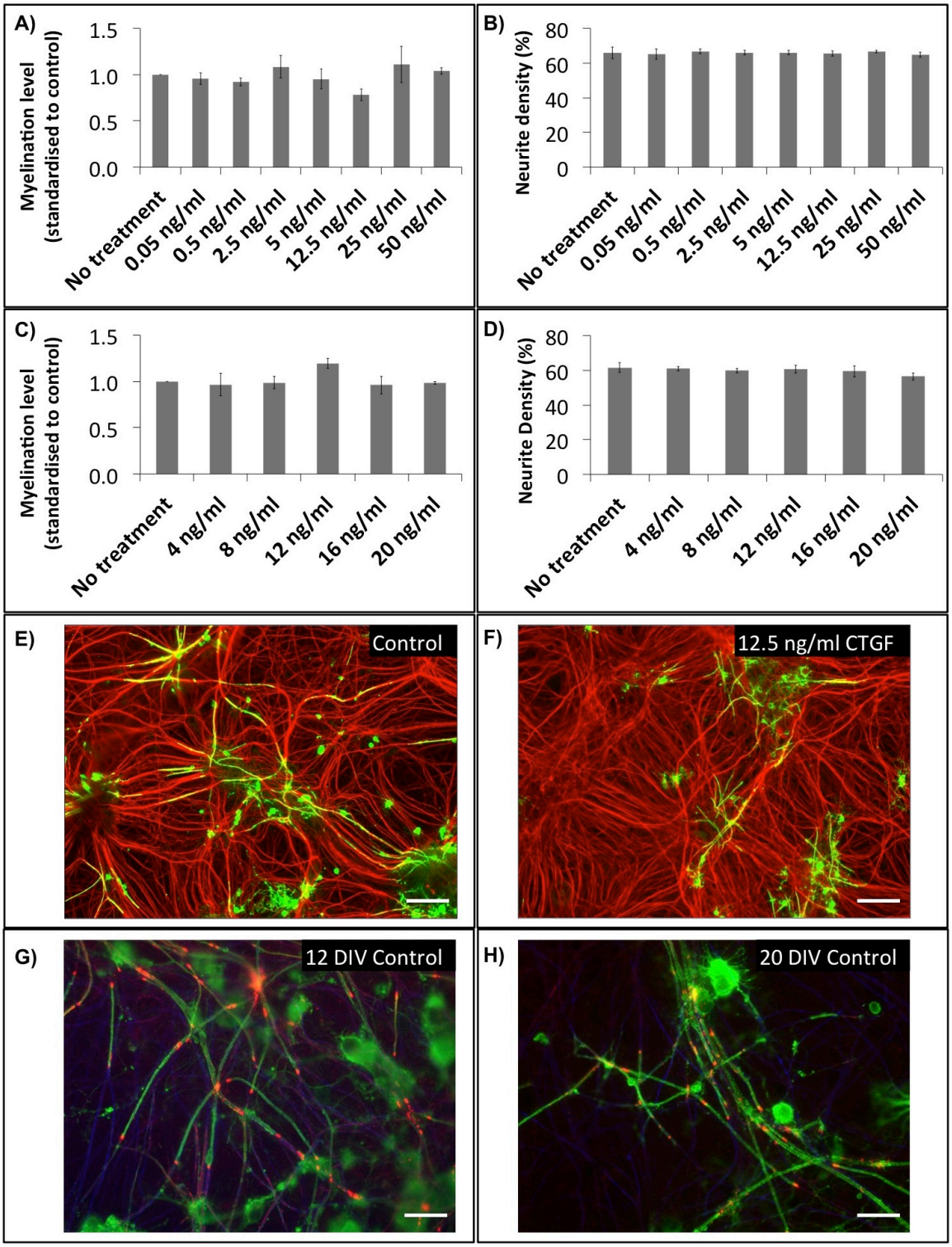

Figure 4. 5 CTGF does not have a significant effect on myelination levels in rat myelinating cultures.

Embryonic rat spinal cord myelinating cultures, set up using PLL-astrocytes, were treated with recombinant rat CTGF from 12 DIV onwards every other day at the concentrations shown in the graphs above. The cultures were immunostained at 24-28 DIV using AA3 antibody to detect PLP green and hence myelin and using SMI-31 to detect neurites. Myelination percentage is shown as standardised to control (no treatment) condition. CTGF was applied to the cultures in two titrations as seen above (A&B, C&D). Neither of them showed any significance for myelination percentage or neurite density. Representative images from the control and CTGF-treated cultures are presented in E and F, respectively, where PLP is shown in green and neurites in red. The staining for PLP (green) and the paranodal protein Caspr (red) suggested the profile of healthy axonal ensheathment (G&H). Each titration was carried out in three experimental repeats. One-way repeated measures ANOVA test was used to detect any possible significance. The error bars represent ± standard error of the mean. All scale bars represent 25 µm. PLL: poly-L-lysine; PLP: proteolipid protein.

quantified by the Cell Profiler. The raw myelination level values varied between 2.8-7.8% for CTGF treatments. The representative images also presented healthy-looking myelinating cultures (Fig 4.5 E&F), which was also supported by the presence of Caspr, a paranodal protein, in the cultures (Fig 4.5 G&H). Therefore, the failure to show an expected positive effect on myelination using recombinant CTGF seemed not to be related at least to the health of the cultures used.

4.3.2.2 SERPINB2 did not affect myelination in rat embryonic spinal cord myelinating cultures

Full-length human SERPINB2 protein (ab69515, Abcam, UK) was added into the medium of the rat myelinating cultures in two sets of titration. In the first one, the cultures were treated with 1, 10 and 100 ng/ml of SERPINB2, which did not appear to affect the myelination levels as no significant changes were detected for the concentrations used (Fig 4.6 A&B). Therefore, a second titration was carried out using the concentrations equal to and below 1 ng/ml (Fig 4.6 C&D) in case SERPINB2 could show an effect specifically at lower concentrations rather than at higher concentrations like 10 and 100 ng/ml. Similarly, there were no significant changes observed using one-way repeated measures ANOVA test. As *Serpinb2* expression was detected to be higher in PLL-myelinating cultures compared to in TnC-myelinating cultures (Array 2, Chapter 3), it was possible that the exogenously added SERPINB2 did not affect myelination any further due to the comparatively higher levels of endogenous SERPINB2 in PLL-myelinating cultures. Therefore, TnC-myelinating cultures that were set up using astrocytes plated on TnC-coated coverslips (TnC-As) were also treated with SERPINB2 starting from 12 DIV onwards at a concentration range of 0.01-10 ng/ml (Fig 4.6 E&F), which did not reveal a significant effect of SERPINB2 on axonal ensheathment. No significant difference was detected in the myelination level or the neurite density of the untreated PLL- and TnC-cultures (Fig 4.6 E&F).

Despite a lower neurite density observed in the myelinating cultures used for SERPINB2 treatments compared to that seen in cultures used for CTGF treatments above, the representative images showed the presence of long and solid myelin sheaths (Fig 4.6 G&H) as expected from healthy cultures. The raw values for myelination levels were also all above 3% in these cultures. Consequently, the lack of any apparent effect of SERPINB2 on axonal ensheathment in these myelinating cultures did not appear to be related to the quality of the cultures.

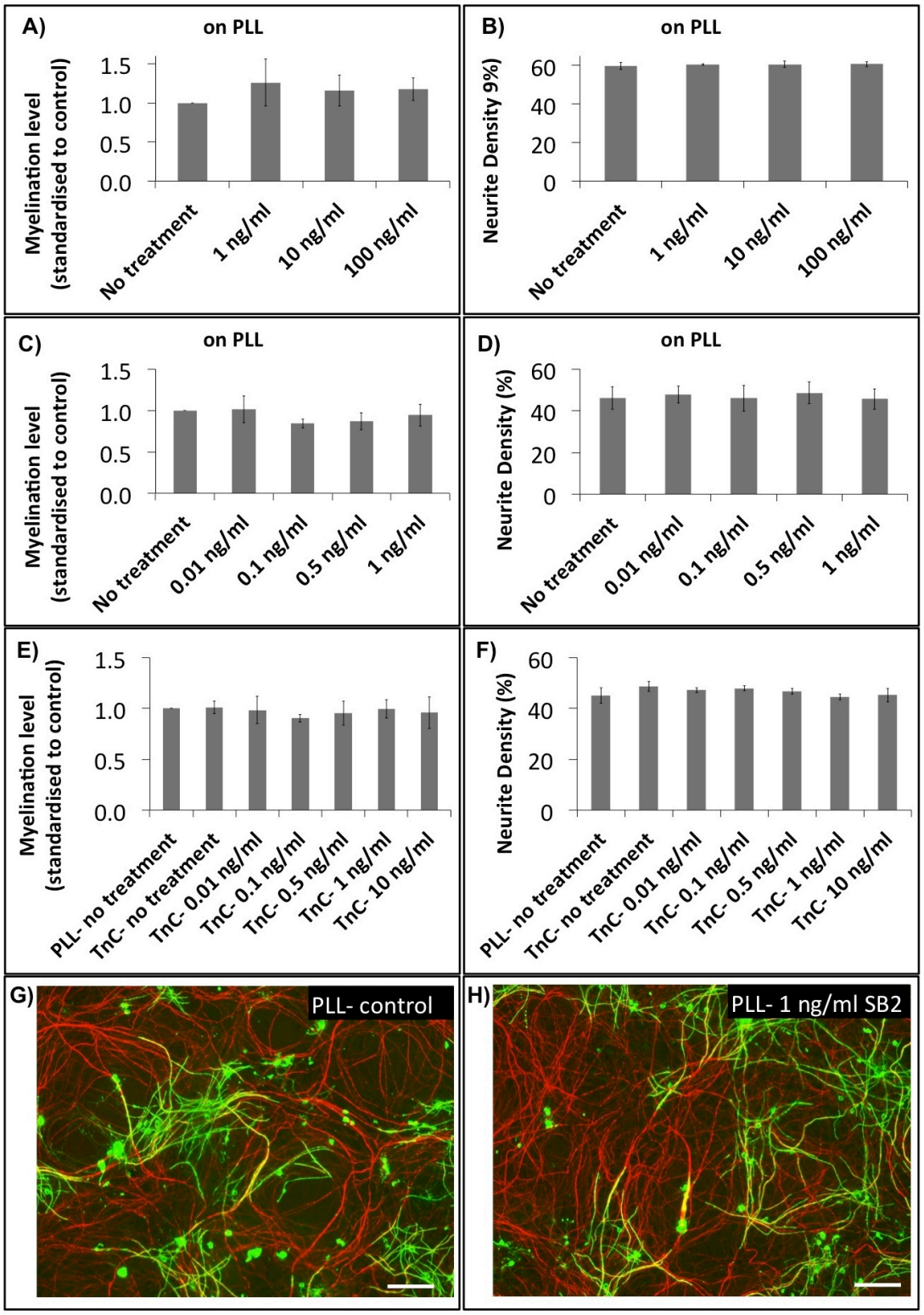

Figure 4. 6 SERPINB2 does not affect myelination levels in rat myelinating cultures Embryonic rat spinal cord myelinating cultures were treated with recombinant human SERPINB2 from 12 DIV onwards every other day at the concentrations shown in the graphs above. The cultures were set up using astrocytes, plated on either PLL or TnC. The cultures were immunostained at 24-35 DIV using AA3 (PLP) antibody to detect myelin and using SMI-31 to detect neurites. Myelination percentage is shown as standardised to control (no treatment) condition. SERPINB2 was applied to the cultures in two titrations as seen above (**A&B, C&D**). Neither of them showed any significance for myelination percentage or neurite density. The 2nd titration of concentrations was also applied to TnC-myelinating cultures, where SERPINB2 did not show any significant effect (**E&F**). Representative images show PLP in green and SMI-31 in red (**G&H**). Each titration was carried out in three experimental repeats. One-way repeated measures ANOVA test was used to detect any possible significance. The error bars represent ± standard error of the mean. DIV: days *in vitro*; PLL: poly-L-lysine; PLP: proteolipid protein; TnC: tenascin C.

4.3.2.3 CCL2 did not affect myelination

Recombinant rat CCL2 (3144-JE-025/CF, R&D Systems, USA) was used for treatments at five different concentrations ranging between 0.1-100 ng/ml (Fig 4.7). There were not any significant changes in percentage of myelinated fibres or neurite densities detected upon CCL2 treatment in PLL-myelinating cultures (Fig 4.7 A&B) or in TnC-myelinating cultures (Fig 4.7 C&D).

The average raw values for myelin sheath percentages detected in control conditions were all above 2.5%. As mentioned above for the other candidates, which were selected as possible regulators of myelination, exogenous CCL2 appeared to be tested on healthy-looking myelinating cultures, where no change in myelination levels could be detected.

4.3.2.4 CCL7 did not affect myelination

Recombinant rat CCL7 (CHM-280, Prospec, USA) was also used at a concentration range of 0.1-100 ng/ml (Fig 4.8). Failing to detect any significant changes in myelination levels upon CCL7 treatment in myelinating cultures on PLL-As (Fig 4.8 A&B) the same concentration range was also applied to the cultures set up on TnC-As (Fig 4.8 C&D). Despite the trend towards decrease in myelination levels upon CCL7 treatment, those changes were not found to be significant using one-way repeated measures ANOVA analysis. Similar to the other cultures mentioned above, the average unstandardised myelination levels for PLL-myelinating cultures were above 2% and those in TnC-myelinating cultures ranged between 5.9-7.3%. The representative images of the cultures (Fig 4.8 E-H) also suggested healthy axonal ensheathment, which did not present increased or decreased levels upon CCL7 treatments.

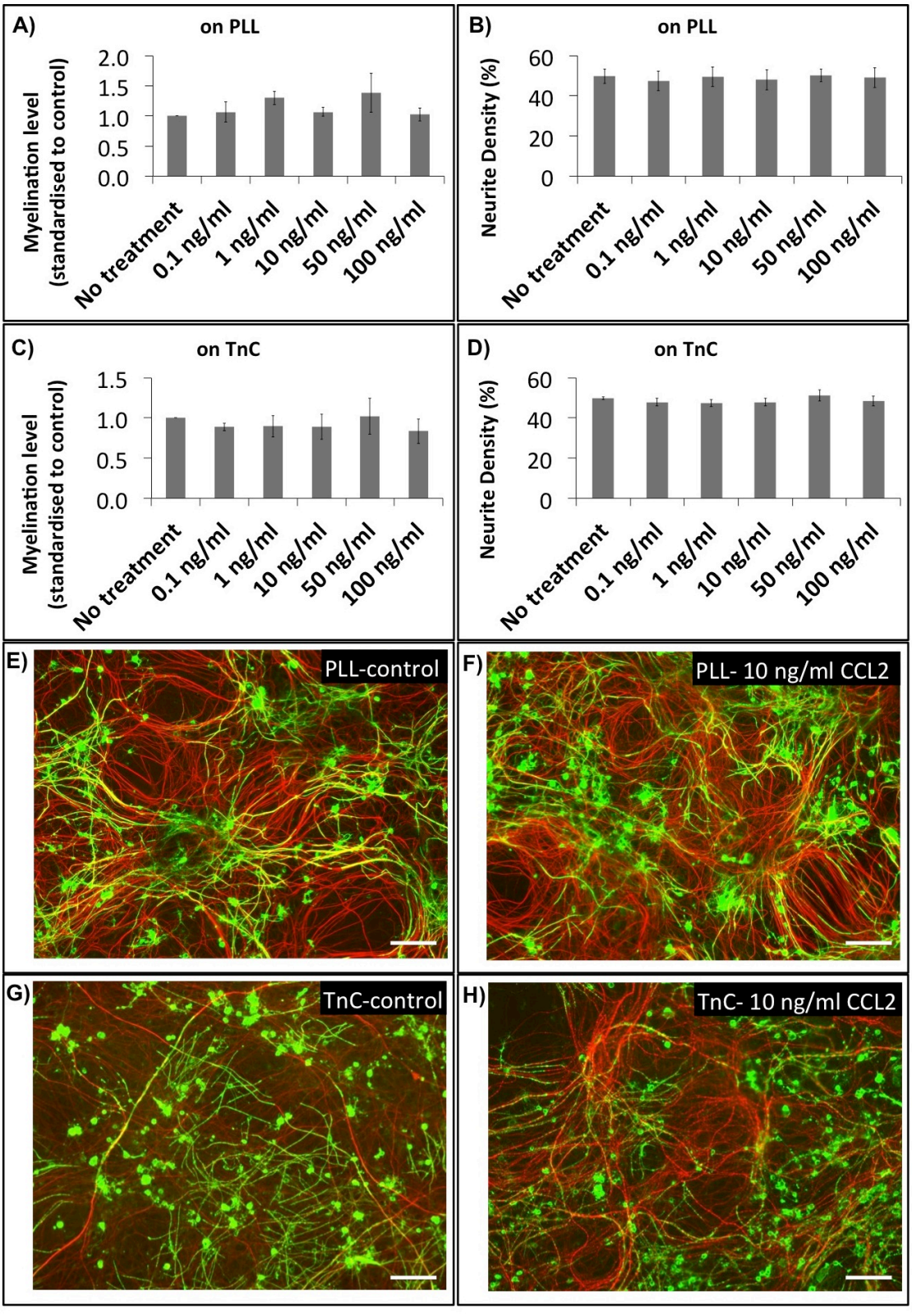

Figure 4. 7 CCL2 does not affect the myelination levels in rat myelinating cultures Embryonic rat spinal cord myelinating cultures, set up using PLL- or TnC-astrocytes, were treated with recombinant rat CCL2 from 12 DIV onwards. The cultures were immunostained at 24-30 DIV using AA3 (PLP, green) and SMI-31 (red) antibody to detect myelin sheaths and neurites, respectively. Myelination percentage is shown as standardised to untreated condition. CCL2 treatment did not lead to any significant change in myelination or neurite percentages in PLL- (**A&B**) or in TnC-myelinating cultures (**C&D**). Representative images for PLL- (**E&F**) and TnC-myelinating cultures (**G&H**) are also presented. PLL- and TnC-experiments were repeated six and three times, respectively. One-way repeated measures ANOVA test was used to detect significance. The error bars represent ± standard error of the mean. DIV: days *in vitro*; PLP: proteolipid protein.

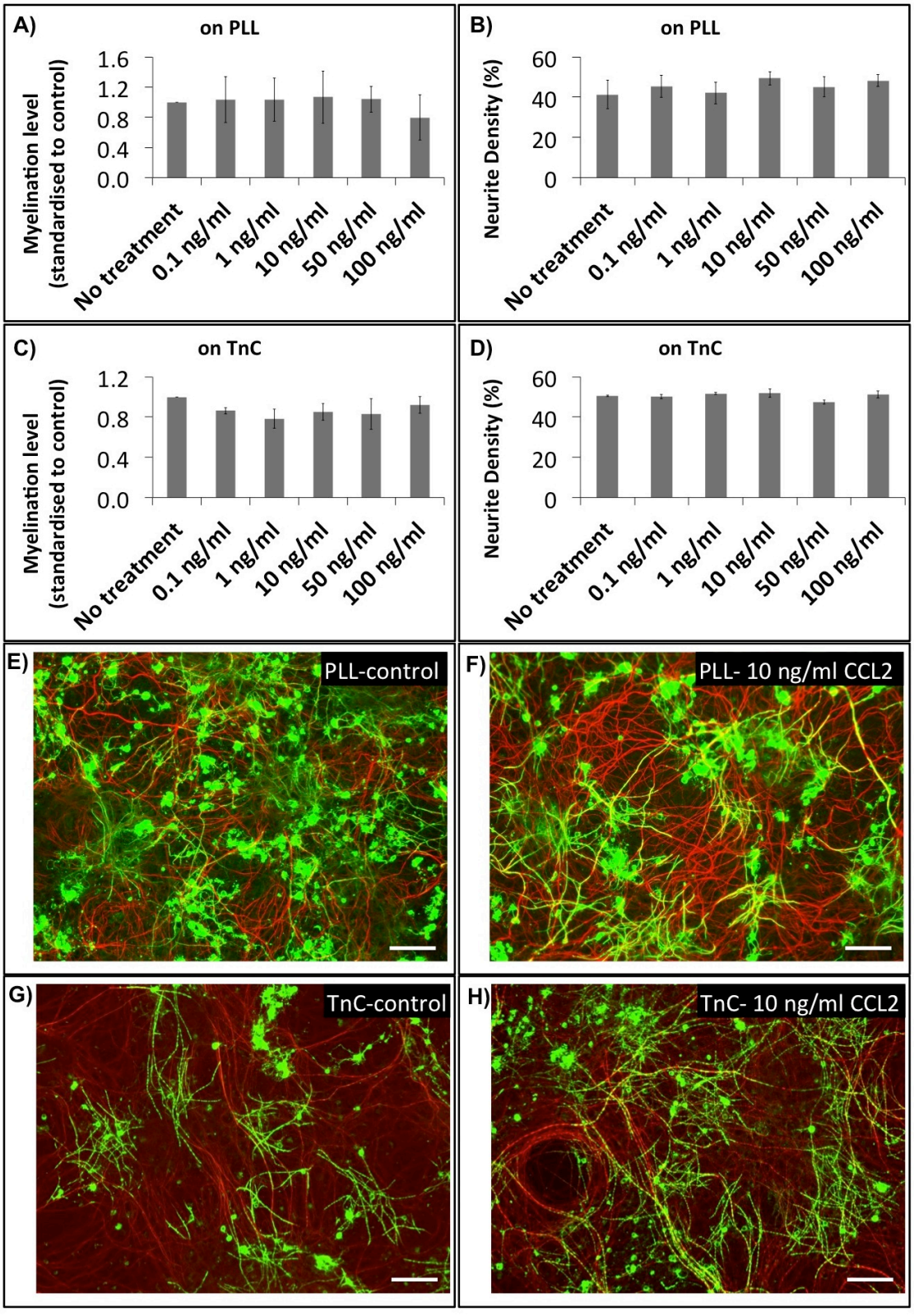

Figure 4. 8 **CCL7 does not affect the myelination levels in rat myelinating cultures** Embryonic rat spinal cord myelinating cultures, set up using PLL- or TnC-astrocytes, were treated with recombinant rat CCL7 from 12 DIV onwards. The cultures were immunostained at 24 DIV using AA3 (PLP, green) and SMI-31 (red) antibody to detect myelin sheaths and neurites, respectively. Myelination percentage is shown as standardised to untreated condition. CCL7 treatment did not lead to any significant change in myelination or neurite percentages in PLL- (**A&B**) or in TnC-myelinating cultures (**C&D**). Representative images for PLL- (**E&F**) and TnC-myelinating cultures (**G&H**) are also presented. The experiments were repeated three times. One-way repeated measures ANOVA test was used to detect significance. The error bars represent ± standard error of the mean. DIV: days *in vitro*; PLP: proteolipid protein.

4.3.2.5 Treatment of myelinating cultures with SERPINB2, CCL2 and CCL7 starting from different time points

Myelinating cultures were treated starting from an earlier time point, 10 DIV, in case the selected candidates affected the axonal ensheathment only when applied to cultures at a specific early time frame. The myelinating cultures that were treated from 10 DIV and 12 DIV onwards with 10 ng/ml of CCL2, CCL7 or SB2 showed average myelination percentages of 7.6-9.2 and 5.8-11.1, respectively, for the control (no treatment) conditions. The average myelination percentages were all standardised to the control values of 10 DIV condition within each experimental repeat. The statistical analysis showed that there were not any significant changes upon the above-mentioned treatments at 10 DIV or 12 DIV within each time point or between the two time points (Fig 4.9). Therefore, it could be concluded that CCL2, CCL7 and SB2 did not affect myelination levels when treated from 10 DIV or 12 DIV onwards.

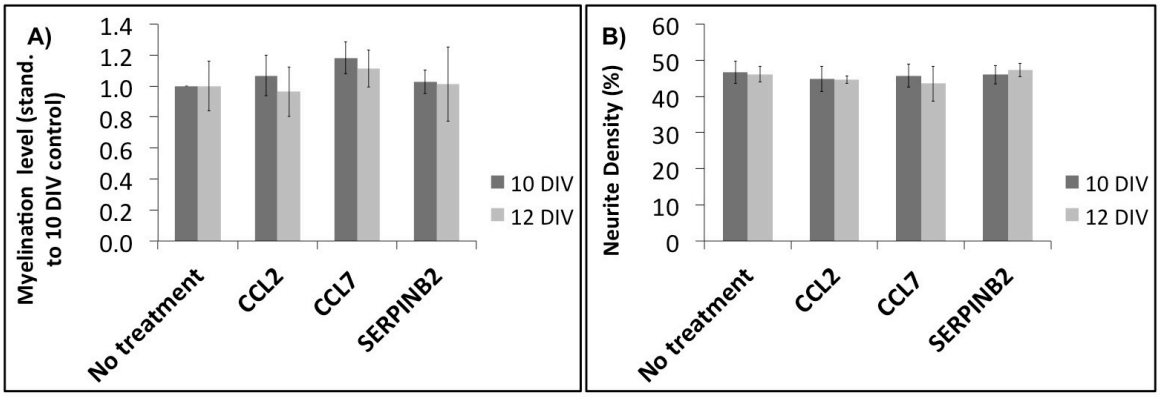

Figure 4. 9 Treatments from 10 DIV onwards did not affect myelination levels Embryonic rat spinal cord myelinating cultures were treated with 10 ng/ml of SERPINB2, CCL2 or CCL7 starting from 10 DIV or 12 DIV onwards. The cultures were set up using PLL-astrocytes. The cultures were immunostained at 24 DIV using AA3 (PLP) and SMI-31 antibody to detect myelin sheaths and neurites, respectively.Statistical analysis did not show any significant changes in myelination (**A**) or neurite (**B**) percentages between the different conditions of the same time point or between the different time points for the same condition. The experiments were carried out in three replicates. One-way repeated measures ANOVA test was applied to the results to detect significance. The error bars represent ± standard error of the mean. DIV: days *in vitro*; PLP: proteolipid protein.

4.4 General conclusions and discussion

The microarray gene expression profiling analysis carried out using samples from untreated and CNTF-treated rat embryonic spinal cord myelinating cultures that were set up using astrocytes plated on PLL or TnC (Array 2, Chapter 3) revealed several candidates that could play a role in myelination. The expressional changes detected in Array 2 for these candidates were validated for *Ccl2*, *Ccl7*, and *Serpinb2* when qRT-PCR

was conducted. Even though such a validation could not be observed for *Ctgf*, it was also included in the list of candidates to apply to the cultures exogenously to observe their effects on myelination since it has been suggested previously to regulate myelination (Nash et al., 2011b). The data demonstrated that these candidates had no effect using neural co-cultures to examine levels of myelination.

Connective tissue growth factor (CTGF) takes part in functions such as angiogenesis, fibrotic and glial scarring, and extracellular matrix remodelling in the central nervous system (Hertel et al., 2000; Schwab et al., 2001). Immunohistochemical studies have presented CTGF protein expression in a subset of neurons in neonatal mouse brains (Hoerder-Suabedissen and Molnar, 2013), in a subpopulation of pyramidal neurons in adult rat cortex, where majority of CTGF immunoreactivity was detected in astrocytes; while, spinal cords showed the immunoreactivity mainly in ependymal cells, tanycytes and gray matter (Kondo et al., 1999). While its expression has been mainly detected in neurons of the human post-mortem brain tissue using immunohistochemistry (Ueberham et al., 2003), another study detected CTGF protein expression mainly in astrocytes of the human post-mortem spinal cords (Spliet et al., 2003). Thus, it is possible that the *Ctgf* expression detected in our rat spinal cord myelinating cultures is provided mainly by the astrocytes. As opposed to the control post-mortem brain tissue, samples from the patients with Alzheimer's Disease presented increased CTGF labelling in both neurons and astrocytes, associated with plaques (Ueberham et al., 2003). Similarly, cryosections from spinal cords of ALS (amyotrophic lateral sclerosis) patients showed elevated CTGF immunereactivity in astrocytes (Spliet et al., 2003). Kainic acid-induced injury in mouse hippocampus and spinal cord injury in rats have also led to increased CTGF protein levels in GFAP positive astrocytes (Hertel et al., 2000; Conrad et al., 2005). Such evidences showing increased levels of CTGF in various types of CNS pathology oppose the suggestion that CTGF could have a supportive role in myelination as concluded at the end of the analysis of Array 2. However, another protein, CXCL13 that has also presented increased levels in CNS pathologies such as EAE and MS has been shown to enhance myelination in cerebellar slice cultures from newborn mice (Yuen et al., 2013). Therefore, CTGF could also demonstrate such a positive effect *in vitro*.

Interestingly, Lamond et al. (2013) reported more than two fold decrease in myelination levels in rat embryonic spinal cord cultures treated with 10 ng/ml of the same source of recombinant CTGF that was used in our experiments. The main difference between their report and my experiments appears to be the quantification of myelination and neurite density. They have more control on the analysis by manually drawing over myelin sheaths in Adobe Photoshop (PS) to allow a specifically designed custom-made macro to quantify these drawn-over pixels. The pipeline I used in the analysis of my

experiments was tailored to quantify overlapping neurite and myelin sheath pixels in the program named Cell Profiler that did not require such manual adjustments and thus facilitated and expedited the analysis. Each method of quantification has its own advantages and therefore one could be preferred over the other based on the personal choice of the investigator. In theory, both methods should provide similar results but as it can be seen in Table 4.2, some differences are observed between the results of the two methods. In those particular experiments analysed in Table 4.2, the Cell Profiler method generally revealed higher standardised myelination levels that were closer to control levels, which would decrease the likelihood of obtaining significance for the treatments analysed. Considering the highest difference of 0.39 seen in that table (for 16 ng/m), it is possible that the Cell Profiler method will reveal the 0.3 value, detected by Lamond et al., as 0.7 for the standardised myelination level, which then might not be significantly different from the control levels.

Lamond et al. have used paired Student's t-test to detect the significant decrease upon CTGF treatment since their experiment consisted of only the control (no treatment) and

Table 4. 2 The comparison of the standardised myelination percentage values detected using methods involving Adobe Photoshop or Cell Profiler upon CTGF treatments

1st titration of CTGF treatments								
Treatment	**Control**	**0.05 ng/ml**	**0.5 ng/ml**	**2.5 ng/ml**	**5.0 ng/ml**	**12.5 ng/ml**	**25 ng/ml**	**50 ng/ml**
Adobe PS	1	1.10	1.00	1.06	0.99	0.59	0.91	0.91
Cell Profiler	1	0.96	0.92	1.08	0.95	0.78	1.11	1.04
Difference	**0.00**	**-0.14**	**-0.08**	**0.03**	**-0.04**	**0.19**	**0.19**	**0.13**
2nd titration of CTGF treatments								
Treatment	**Control**	**4 ng/ml**	**8 ng/ml**	**12 ng/ml**	**16 ng/ml**	**20 ng/ml**		
Adobe PS	1	0.86	0.74	1.00	0.57	0.65		
Cell Profiler	1	0.97	0.99	1.19	0.96	0.99		
Difference	**0.00**	**0.10**	**0.25**	**0.19**	**0.39**	**0.33**		

Embryonic rat spinal cord myelinating cultures were treated with recombinant human CTGF from 12 DIV onwards. In the 1st titration of treatments, concentrations ranged between 0.05-50 ng/ml; whereas, those in the 2nd titration were between 4-20 ng/ml as seen in the table. The cultures were used for immunocytochemistry at 24-28 DIV. Images taken using fluorescence microscopy presented SMI-31 positive neurites in red and PLP positive myelin and oligodendrocytes in green. Myelination levels were quantified in two separate ways from there on. 1) Myelin sheaths were drawn over using a blue brush stroke in Adobe Photoshop (PS) and a custom-made micro was then run on the modified images to detect the pixel value of where blue (myelin sheath) and red overlap with each other. The pixel value from this analysis was used to calculate the myelination percentages together with the values obtained for neurite densities after doing manual adjustments in Image J. 2) A custom-made pipeline in Cell Profiler was run on the unmodified images to detect the pixel values that represent the neurites and the myelin sheaths. These values were then used to calculate the neurite and myelination percentages since the total number of pixels always remained the same. Average myelination levels were standardised to control (no treatment) levels within each experimental repeat of each CTGF titration. Presented in the table are the overall averages of standardised myelination levels obtained from three experimental repeats for each titration. The differences between the values obtained from the method using Cell Profiler and the method using Adobe PS are also presented in the table. CTGF: connective tissue growth factor; DIV: days *in vitro*; PLP: proteolipid protein.

10 ng/ml of CTGF conditions; whereas, I used repeated measures one–way ANOVA test because there were more than two conditions for each titration. When t-test is applied on my CTGF data obtained using manual drawing in PS, significant decrease is seen in myelination levels upon treatments with 12.5 ng/ml CTGF and 16 ng/ml CTGF in the 1st and 2nd titration, respectively (Table 4-2), which is in accordance with the finding of Lamond et al. Nevertheless, the lack of a significant change for 12 ng/ml of CTGF in the 2nd titration despite the presence of one for 12.5 ng/ml CTGF in the 1st titration could suggest a high biological variation among the cultures and thus could require a higher number of experimental repeats to observe a clear effect of the treatment. Such a biological variation could necessitate the use of a stricter statistical test like ANOVA; however, because this test requires the analysis of more than two conditions, it would always be necessary to treat the cultures with a reagent at different concentrations or with different reagents to observe a highly reliable significant effect. Because this is practically difficult, the experiments consisting of myelinating cultures at two conditions (untreated and treated) seem inevitable, in which case t-test will be the major role-player. Therefore, it is very hard to decide which results are more reliable since both types of analysis follow strategies suitable for the design of the experiments. Their finding of CTGF having a negative role in myelination is also supported by the other experiments of Lamond et al. (2013) and another study that has suggested CTGF as an inhibitor of oligodendrocyte precursor cell (OPC) differentiation (Stritt et al. 2009). Because my results are in accordance with these reports when their myelin sheath quantification method and statistical test are used, it can be concluded that CTGF has a negative effect on myelination at specific concentrations and this effect is observed more clearly when the PS method is utilised followed by the Student's t-test.

Stritt et al. (2009) have shown that injection of CTGF into neonatal mouse brain can reduce the number of MBP (myelin basic protein)-positive cells by the time the mice are 6 days old and that CTGF reduces the number of mature oligodendrocytes both in oligodendrocyte-enriched cultures and in mixed neuron/glial cell culture, with a dose-dependent effect in the latter. They also proposed that CTGF could contribute to such inhibition using its insulin growth factor binding protein (IGFBP) domain since pre-incubation of insulin growth factor 1(IGF1) with CTGF antagonised IGF1-stimulated oligodendrocyte maturation by reducing the number of mature oligodendrocytes. However, Lamond et al. (2013) have shown that CTGF can reduce the percentage of mature oligodendrocytes in purified oligodendrocyte cultures even though their CTGF contained only the C-terminus cysteine knot domain, excluding the other three domains; namely, IGFBP domain, Von Willebrand Factor-Type C Repeat, and Thrombospond Type-1 Repeat (UniProt database). Even though the C-terminus domain could be enough to provide signals that will suppress the OPC differentiation and hence

the myelination, the effects of its IGFBP domain could be much stronger, providing clearer results in myelination experiments. It would be interesting to see how a full-length CTGF affects the myelination levels in rat embryonic spinal cord cultures compared to its shorter version containing only the cysteine knot domain.

CTGF could also be applied to myelinating cultures at higher concentrations like 2 μg/ml as Stritt et al. (2009) have tried. Our experiments were carried with treatments at nanogram level to avoid possible cell toxicity (Nash et al., 2011b). However, microgram levels might be more suitable in this particular case. In addition, the rat myelinating cultures could be treated with CTGF starting from earlier time points. Highly branched oligodendrocytes, stained with the O4 antibody, appear to have already been formed by 8 DIV in rat myelinating cultures (Sorensen et al., 2008). Therefore, it could be that the treatment from 12 DIV onwards is less effective in terms of reducing the percentage of mature oligodendrocytes and hence the myelination in the myelinating cultures. Treatments starting before 8 DIV could be more effective.

The myelinating cultures were also treated with CCL2, CCL7, and SERPINB2 to observe their effects on myelination but none of them led to any significant changes in myelination levels. CCL2 is a chemokine that has been shown to play a role in the disease onset of EAE in mice mainly by playing a role in T cell activation (Izikson et al., 2000; Huang et al., 2001; Elhofy et al., 2005). Increased CCL2 expression has been detected in the astrocytes of EAE mice (Glabinski et al., 2003; Santos et al., 2005) and of MS patients around the lesions (Voorn et al., 1999; Tanuma et al., 2006). Even though CCL2 was suggested as a potential positive regulator of myelination due to its up-regulation in PLL-myelinating cultures compared to its expression in TnC-myelinating cultures (Array 2, Chapter 3), above-mentioned observations appear to contradict that. However, it could be that CCL2 has other roles that have not been discovered yet in the CNS. CCL2 was not detected in the healthy human brain or in the normal appearing white matter of MS patients by immunohistochemistry (Voorn et al., 1999, Tanuma et al., 2006), but its presence has been shown in the healthy mouse brain using ELISA (Santos et al., 2005; Gruol et al., 2014), suggesting physiological roles for CCL2 in the normal CNS. Therefore, embryonic rat spinal cord myelinating cultures were treated with CCL2 to examine its effect on myelination level.

CCL7 is another chemokine that has been found to be secreted by astrocytes *in vitro* and *in vivo* (McManus et al., 1998; Thompson et al., 2009, Renner et al., 2011). CCL7 protein is also detected at increased levels in hypertrophic astrocytes in MS lesions (McManus et al., 1998). CCL7 has also been suggested to play a role in chemotaxis of peripheral mononuclear cells into the CNS in pathology (Okada et al., 2009; Renner et

al., 2011). In addition to its immune system-related roles, the presence of CCL7 and its receptor, CCR1, in the midbrain of healthy embryonic and neonatal mice and the fact that it could promote neuronal differentiation and neuriteogenesis in primary cultures (Edman et al., 2008) suggests that CCL7 could have other distinct roles in the CNS in health and pathology. Therefore, rat embryonic spinal cord myelinating cultures were treated with CCL7 in an attempt to observe its stimulatory effects on myelination as we suggested at the end of the microarray gene expression profiling analysis (Array 2, Chapter 3).

The other candidate that was tested in myelinating cultures was SERPINB2, which is a serine protease inhibitor that could inhibit both types of plasminogen activators (PAs), namely tPA and uPA, with a much greater efficiency of inhibition of the latter (Kruithof et al., 1995). Even though PAs could promote neruite extension in the nervous system, it would be important to keep the uPA levels under tight control as the degrading activity of uPA against myelin basic protein has been detected in conditioned media from primary rat microglia cultures, where tPA was also detected but to a smaller extent (Nakajima et al., 1992). In that sense, inhibiting uPA could prevent myelin degradation, in which case the inhibitor of uPA, SERPINB2, could be considered as a potential positive regulator of myelination as also suggested by our microarray gene expression profiling analysis (Array 2). Therefore, embryonic rat spinal cord myelinating cultures were treated with recombinant SERPINB2 to study the effect of this protein on myelination level.

None of the above-mentioned candidates, CCL2, CCL7, or SERPINB2, showed positive or negative effects on myelination levels in the rat embryonic spinal cord myelinating cultures. To investigate their possible roles in myelination further, their effects were observed in purified rat OPC cultures since they have not been tested previously in terms of their effects on OPC differentiation. OPC cultures were treated with 1 ng/ml and 10 ng/ml of CCL2, CCL7 and SERPINB2 and they were immunolabeled with the O4 antibody and anti-PLP at 8-10 DIV to detect the mature oligodendrocytes (Appendix IV) but due to time constraints, only two successful experimental repeats could be carried out. Even though the results present a very high level of variation and are inconclusive, they show a tendency towards inhibition of OPC differentiation with 10 ng/ml of CCL2 and with 1 ng/ml of SERPINB2 (Appendix **IV,** Figure IV.I, Table IV-I). The representative images also appear to support these tendencies (Appendix IV, Fig IV.II&III). However, even if further experiments prove that these candidates do indeed inhibit OPC maturation, that result would propose a negative role for them in the regulation of myelination, which is the opposite of what was suggested at the end of our microarray gene expression profiling analysis (Array 2, Chapter 3). Therefore, another possibility

emerges for the interpretation of their differential regulation at different conditions in Array 2 such as linking those changes with the astrocyte reactivity.

Ccl2, *Ccl7*, and *Serpinb2* were identified as potential positive regulators of myelination due to their increased expression in PLL-myelinating cultures compared to that in TnC-myelinating cultures. However, those two cultures not only differ in terms of myelination levels (Nash et al., 2011b) but possibly also in terms of astrocyte reactivity since differences between the astrocyte monolayers plated on PLL and those on TnC have been observed previously (Holley et al., 2005; Nash et al., 2011b). PLL-astrocytes are larger and express increased nestin levels compared to TnC-astrocytes (Nash et al., 2011b), which resemble a quiescent phenotype, described previously by Holley et al. (2005). If we assume that the astrocyte monolayers will continue to present these differences when used as feeders for spinal cord myelinating cultures, it can be concluded that PLL-myelinating cultures contain activated astrocytes, while TnC-myelinating cultures contain quiescent astrocytes. Therefore, the above-mentioned candidates, CCL2, CCL7 and SERPINB2, could be responsible for increased astrocyte reactivity in these cultures.

Similarly, CTGF might also be playing a role in astrocyte reactivity as it was up-regulated in TnC-myelinating cultures upon CNTF treatment (Array 2), which has also been demonstrated to increase astrocyte reactivity (Levison et al., 1996; Ye et al., 2004; Bechstein et al., 2012;). The fact that the levels of CCL2, CCL7, CTGF and SERPINB2 have all been found to be elevated in various CNS pathologies, where astrocytes were defined as reactive based on their increased GFAP expression and hypertrophy, is in accordance with the suggestion that these proteins could be involved in the regulation of astrocyte reactivity (McManus et al., 1998; Dietzmann et al., 2000; Hertel et al., 2000; Schwab et al., 2001; Spliet et al., 2003; Ueberham et al., 2003; Conrad et al., 2005; Dos santos et al., 2005; Tanuma et al., 2006; Biancotti et al., 2008; McClain et al., 2009; Hidaka et al., 2014; Zheng and Zhang, 2014). These candidates could also be playing a role in the overall reactivity of spinal cord myelinating cultures, i.e., their capacity for how fast and efficiently they can recover from pathological conditions in general or more specifically how well they can show remyelination in demyelinating conditions. CNTF, which has presented elevated mRNA levels during the remyelination phase in mice with cuprizone-induced demyelination (Gudi et al., 2011), increased the levels of expression of the chemokines *Ccl2*, *Ccl7*, and *Cxcl11* in both PLL- and TnC-myelinating cultures, which was detected by qRT-PCR (Fig 4.4). These chemokines could be associated with such a protective CNTF signaling pathway in these myelinating cultures.

Considering their likely association with astrocyte reactivity and/or the reactivity in myelinating cultures in general, it would be interesting to see the roles of these candidates on myelination in a scenario of CNS injury. Boomkamp et al. (2012) have developed such a culture system that allows the observation of the effects of different treatments on myelination in an *in vitro* model that mimics spinal cord injury (SCI). A single cut is made across the embryonic rat spinal cord myelinating cultures on day 22-24 using a razor blade manually. Initially a cell-free area devoid of neurites appears at the site of the cut and it is followed over time with demyelination and reduced neurite density adjacent to the lesion, and infiltration of microglia and reactive astrocytes into the lesion, features that are similar to SCI *in vivo*. The lesion remains devoid of neurites unless treated with known drugs that promote CNS repair *in vivo* (Boomkamp et al., 2012, 2014).

I tried to exploit this system to observe the effects of SERPINB2, CCL2 and CCL7 on myelination during pathology but my inexperience in this model and time constraints did not reveal reliable results (Appendix V). The myelinating cultures were set up using astrocyte monolayers on PLL and were cut at 23 DIV, treated at 24, 26, and 28 DIV, used for immunocytochemistry at 29 DIV. The areas adjacent to cut lesions were used for the quantification of myelination level as described by Boomkamp et al. (2012). For each condition examined on the cut cultures, uncut cultures were also prepared from the same batch of cells to act as controls. The candidates decreased the neurite density in cut cultures compared to both cut and uncut control (untreated) cultures (Fig V.I B), which would suggest neurotoxic effects for them. However, a similar decrease was also seen in uncut cultures (Fig V.I D) that contradicted the previous findings, which were carried out in a higher number of experimental repeats (Fig 4.6-4.9). SERPINB2 increased the level of myelination in both uncut and cut cultures (Fig V.I A&C) but this was likely due to decreased neurite density that would increase the myelination percentage since its calculation is based on the ratio of myelin sheath pixels to that of the neurite pixels. The lack of the decreased myelination level in untreated cultures upon the cut injury, which is one of the main features of this *in vitro* CNS injury model (Boomkamp et al., 2012, 2014), also reduced the reliability of these results. Future experiments by other investigators might provide further insight into the roles of these candidates in CNS pathology.

One other point to consider in terms of why the candidates we selected did not affect myelination in the rat embryonic spinal cord myelinating cultures is the failure to replicate the previous findings of lower myelination levels for mixed neural cells plated on astrocytes on TnC compared to those on PLL-astrocytes (Fig 4.6E). The hypothesis that those candidates would stimulate myelination was based on the fact that they were

up-regulated in PLL-myelination cultures, which present higher myelination levels according to Nash et al. (2011b). The basic difference between my experiments and those of Nash et al. appears to be the way of quantification of myelination as described above. Nevertheless, their representative images present lower levels of myelination in TnC-myelinating cultures very clearly (Nash et al., 2011b). So the difference must be something concerning the way I have carried out the experiments rather than the method of quantification. One clear distinction is that Nash et al. have plated 1 x T75 flask of striatum-derived neurospheres into 1 x 24-well plate to differentiate into astrocytes; whereas, I counted the neurospheres and plated them always at 250,000 cells/ml in each well to start the astrocyte cultures. The concentration of astrocytes could be affecting their capacity to react to different treatments or substrates and thus could be accountable for the above-mentioned opposing results, which will be investigated in the following chapter.

In conclusion, some candidates were validated by qRT-PCR experiments to be potential regulators of myelination as suggested by Array 2 (Table 4.3). These selected candidates did not affect myelination level or neurite density in embryonic rat spinal cord myelinating cultures apart from CTGF that reduced the myelination level when the Adobe PS quantification method and Student's t-test were used for the analysis. CCL2, CCL7, CTGF, and SERPINB2 could be playing more effective roles in astrocyte reactivity or the capacity of myelinating cultures to recover from pathologies rather than in myelination.

Table 4. 3 The candidates selected as potential regulators of myelination after the binary comparisons of Array 2 data and the results of their validations by qRT-PCR and cell culturing

Binary comparison	Candidates selected as possible (+) regulators	Candidates selected as possible (-) regulators	Validated by the 1st qRT-PCR	Validated by the 2nd qRT-PCR	Validated by cell culturing
PLL-control vs PLL+CNTF	CXCL13, LCN2, SERPINB2	-	*Serpinb2*	none	none
TnC-control vs TnC+CNTF	CTGF	THBS2, WIF1	none	none	-
PLL-control vs TnC-control	CCL2, CCL7, SERPINB2	CXCL11, LCN2, WIF1	*Ccl2*, *Ccl7*, *Serpinb2*	*Ccl2*, *Ccl7*	none

Microarray gene expression profiling analysis was carried out using RNA samples from embryonic rat spinal cord mixed cultures (myelinating cultures) at four different conditions: 1) plated on astrocyte monolayers on PLL-coated coverslips (PLL-control), 2) plated on PLL-astrocytes and treated with CNTF (PLL+CNTF), 3) plated on TnC-astrocytes (TnC-control), 4) plated on TnC-astrocytes and treated with CNTF (TnC+CNTF). Differentially expressed transcripts between the cultures shown as binary comparisons in the table were analysed and the candidates presented were selected as possible positive or negative regulators of myelination. The relative expressions of these transcripts between the shown cultural conditions were measured by means of qRT-PCR, where firstly, the original RNA samples from Array 2 were used and secondly, new RNA samples extracted from three biological replicates of new myelinating cultures at the same four conditions were used. The transcripts, for which the expressional regulations were validated by qRT-PCR, are presented in the table. These validated candidates were applied to myelinating cultures as recombinant proteins from 12 DIV onwards. The cultures were stained at 24-28 DIV using the antibodies against SMI-31 and PLP to detect neurites and myelin, respectively. Cell Profiler, followed by microscopy, measured the myelination level and neurite density, which were not affected by any of the candidates examined. CCL2: chemokine (C-C motif) ligand 2; CCL7: chemokine (C-C motif) ligand 7; CXCL11: chemokine (C-X-C motif) ligand 11; CXCL13: chemokine (C-X-C motif) ligand 13; CNTF: ciliary neurotrophic factor; DIV: days *in vitro*; LCN2: lipocalin2; PLL: poly-L-lysine; PLP: proteolipid protein; TnC: tenascin C; THBS2: thrombospondin 2; WIF1: WNT inhibitory factor 1.

Chapter 5

Fine-tuning embryonic rat spinal cord myelinating cultures

5.1 Introduction

The protocol for setting up and maintaining embryonic rat spinal cord myelinating cultures (Sorensen et al., 2008) was developed and modified from a method that was originally used for mouse spinal cord cultures (Thomson et al. 2006; Thomson et al., 2008). Briefly, dissociated spinal cords from Sprague Dawley rat embryos were plated on top of confluent rat astrocyte monolayers, which were differentiated from striatum-derived neurospheres directly on the glass coverslips, coated with PLL or TnC. The astrocytes on PLL- or TnC-coated coverslips will be called as PLL-astrocytes and TnC-astrocytes, respectively, in this chapter. In addition, the spinal cord myelinating cultures that are prepared using PLL- or TnC-astrocytes will be called PLL-myelinating cultures and TnC- myelinating cultures, respectively.

This established protocol (Sorensen et al., 2008) in my opinion could be further modified to be completely optimised as an assay, which can be important to understand how the variability can occur in myelinating cultures and to obtain consistent results when comparing the effects of a treatment on myelination. One such treatment can be provided by CNTF (ciliary neurotrophic factor), which has previously been identified as a pro-myelinating factor in these myelinating cultures (Nash et al., 2011b) and which has been used to generate the samples analysed in our microarray analysis (Array 2, Chapter 3). In the first instance I examined one of the main steps that could produce variations in myelination and which could be optimised further. This step is the plating numbers of the striatum-derived neurospheres on PLL- or TnC-coverslips to generate astrocyte monolayers. Each 75 cm^2 tissue culture flask of neurospheres are prepared from 3-4 rat striata and the entire flask content of cells are plated onto glass coverslips contained in 1-4 x 24-well plates, according to how dense they appear in the flask under the light microscopy. The size and the number of neurosphere clusters may vary depending on the tissue volume of striata used, which would be very difficult to control if required. Therefore, it would be easier to determine an optimal cell number which will generate a constant cell density, at which the neurospheres can be plated down to generate astrocytes at an optimised confluency when they are to be used as monolayers for myelinating cultures, which is usually around 6-9 DIV (Fig 5.1). Such cell density will be referred as “seeding density” in the rest of this chapter. Based on the common dilutions used in our lab (e.g. 1 flask of neurospheres plated into 1-4 x 24-well plates), the following four seeding densities were chosen to work with: 125, 250, 375, and 500 x 10^3 cells/ml.

The original published protocol for the myelinating cultures suggests using astrocyte monolayers at 7-10 DIV prior to the addition of the dissociated spinal cord cells because

this is usually the time point when they form a confluent monolayer (Sorensen et al., 2008). However, personal observations have shown that astrocyte cultures could reach confluency and therefore stop/slow down their proliferation rate sooner than this. Therefore, it is likely that confluent and healthy-looking astrocytes will be used for setting up myelinating cultures by some researchers at earlier time points than 7-10 DIV. The effects of using younger astrocytes on final myelination levels and neurite density will also be examined and data will be presented in this chapter.

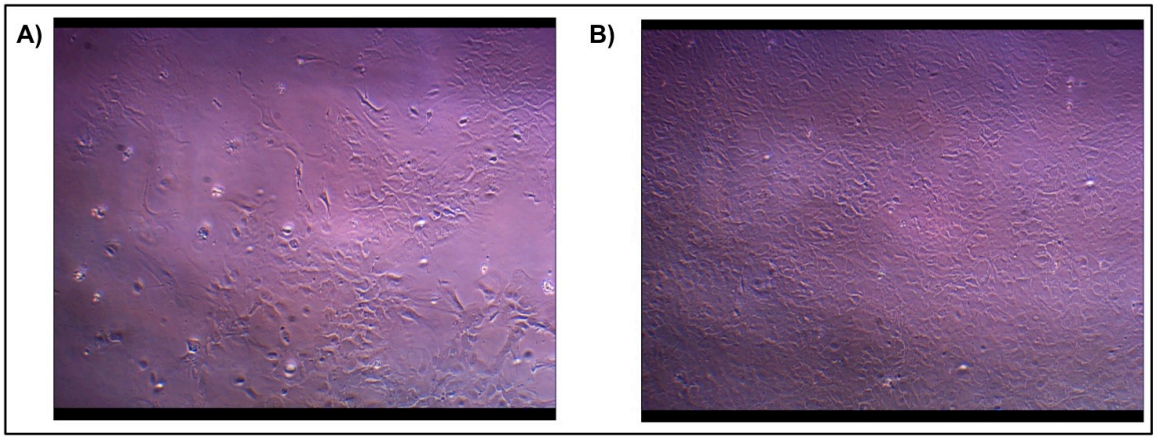

Figure 5. 1 Examples of neurosphere-derived rat astrocyte cultures under phase-contrast microscopy.
Dissociated striata that were isolated from 24-36 hr old Sprague Dawley rats were used to set up neurosphere cell suspensions. These neurospheres were plated down on PLL-coated glass coverslips after 6-9 DIV with different seeding density and allowed to differentiate into astrocytes. The astrocyte cultures were observed under phase-contrast microscopy after 6 DIV. **A)** The cultures do not appear to be confluent. There are several areas devoid of any cells. The cells present different morphology at different locations of the field of view possibly due to the lower cell concentration. The cultures that look like this at 6 DIV generally do not become confluent in the following few three-four days. **B)** The image shows a confluent astrocyte culture, where all of the field of view is covered with a monolayer of cells. The cells appear to be of uniform shape.

5.2 Aims

The overall aim of this chapter is to optimise the protocol for setting up rat spinal cord myelinating cultures further by 1) finding the optimum seeding density of the striatum-derived neurospheres that would generate astrocytes at an optimised confluency and hence less variable spinal cord myelinating cultures and 2) detecting the effect of the astrocyte age on myelination.

These will be carried out specifically as follows:

- To analyse the effects of the seeding density of the striatum-derived neurospheres on the myelinating cultures the following will be assessed:

- the expression of glial fibrillary acidic protein (GFAP) and nestin immunoreactivity of the PLL- and TnC-astrocytes.

- the number/percentage of type-2 astrocytes present in the PLL- and TnC-astrocyte cultures by means of immunocytochemistry using O4 and anti-GFAP antibodies.

- the number/percentage of PLP positive (PLP+) oligodendrocytes present in the PLL- and TnC- astrocyte cultures.

- myelination and neurite density of the neural cells in PLL- and TnC-myelinating cultures.

- myelination and neurite density in CNTF (ciliary neurotrophic factor; a previous identified pro-myelinating factor)-treated PLL-myelinating cultures.

- To examine the effect of PLL-astrocytes at an early time in culture on myelination and neurite density in PLL-myelinating cultures that will be untreated or treated with CNTF starting from different time points onwards.

5.3 Results

The astrocyte cultures were initiated by plating down striatum-derived neurospheres at certain seeding density on PLL- or TnC-coated glass coverslips and the cultures were maintained to confluency for 3-11 DIV. The cultures were observed under phase-contrast microscopy to ensure that the coverslips that appeared to contain cultures at similar densities for each seeding density were used. The astrocyte cultures that were set up using higher and lower concentrations of neurospheres will be called “denser astrocyte cultures” and “less dense astrocyte cultures”, respectively, throughout this chapter. The astrocyte cultures were then either immunostained and analysed separately or were used as a supporting monolayer for spinal cord myelinating cultures. Firstly, the effects of the seeding density of the striatum-derived neurospheres on the morphology of the PLL- and TnC-astrocytes will be examined. Later, the results will be presented for the myelination levels of the untreated and CNTF-treated spinal cord myelinating cultures that were set up using striatum-derived neurospheres at various seeding densities. Finally, the effects of the age of the astrocytes on myelination will be demonstrated in spinal cord myelinating cultures, which were either untreated or treated with CNTF starting from different time points.

The effects of the seeding density of the striatum-derived neurospheres on the morphology of PLL- and TnC-astrocytes will be shown in terms of their GFAP and nestin expressions, detected by fluorescence microscopy. GFAP and nestin are not only intermediate filament proteins that are found in the astrocytes, but they are also used as markers of astrocyte reactivity (Eng et al, 1970; Frisen et al., 1995; Brook et al., 1999; Clarke et al., 1999; Eng et al., 2000; Pekny et al., 2004; Sofroniew et al., 2010; Xue et al, 2011). Monoclonal antibodies will also be used to detect the possible oligodendrocytes and type-2 astrocytes present in the astrocytes cultures. Astrocytes in cultures of developing rat brain have been divided previously into two types (type-1 and 2) based on their morphology and their abilities to bind tetanus toxin and the monoclonal antibody A2B5 (Raff et al., 1983). The stellate type-2 astrocytes have later been shown also to express the sulphatide detected by O4 antibody unlike the epithelioid type-1 astrocytes (Aloisi et al., 1988). Therefore, immunocytochemistry will also be carried out to detect both GFAP and O4 positive cells, which would represent the type-2 astrocytes. O4 antibody can also be used to visualise oligodendrocytes at specific differentiation stages and proteolipid protein (PLP), for which the antibody AA3 (Yamamura et al., 1991) is used, is expressed in more mature stages (Fig 1.1, reviewed in Barateiro and Fernandes, 2014). Thus, O4 and PLP positive cells would represent the mature oligodendrocytes in the astrocyte cultures.

5.3.1 The effects of the seeding density of the striatum-derived neurospheres on the morphology of PLL-astrocytes

Increased GFAP expression is a classical hallmark of pathology (reviewed in Mucke et al., 1993). Its expression previously has been used as an indicator to distinguish astrocyte phenotypes in a way, where low GFAP expression has been associated with quiescent or less active astrocytes and high GFAP expression with reactive astrocytes (reviewed in Sofroniew and Vinters, 2010). Nestin expression has been used for the same purpose but to a lesser extent (Holly et al., 2005). Thus, both GFAP and nestin immunoreactivity were analysed in neurosphere-derived rat astrocytes that were initiated by plating down 500 μl of striatum-derived neurospheres on PLL-coated coverslips at varying densities. The densities were chosen to be 125, 250, and 375 x 10^3 cells/ml. They were immunostained to detect GFAP and nestin expressions at 7-9 DIV when all cultures were observed to be confluent.

Average DAPI positive (DAPI+) cell density differed significantly between the astrocyte cultures that were set up using neurospheres at different seeding density (Fig 5.2 A). The denser cultures presented higher numbers of cells at the end of their culture period, which shows that they did not reach the contact-dependent inhibition earlier

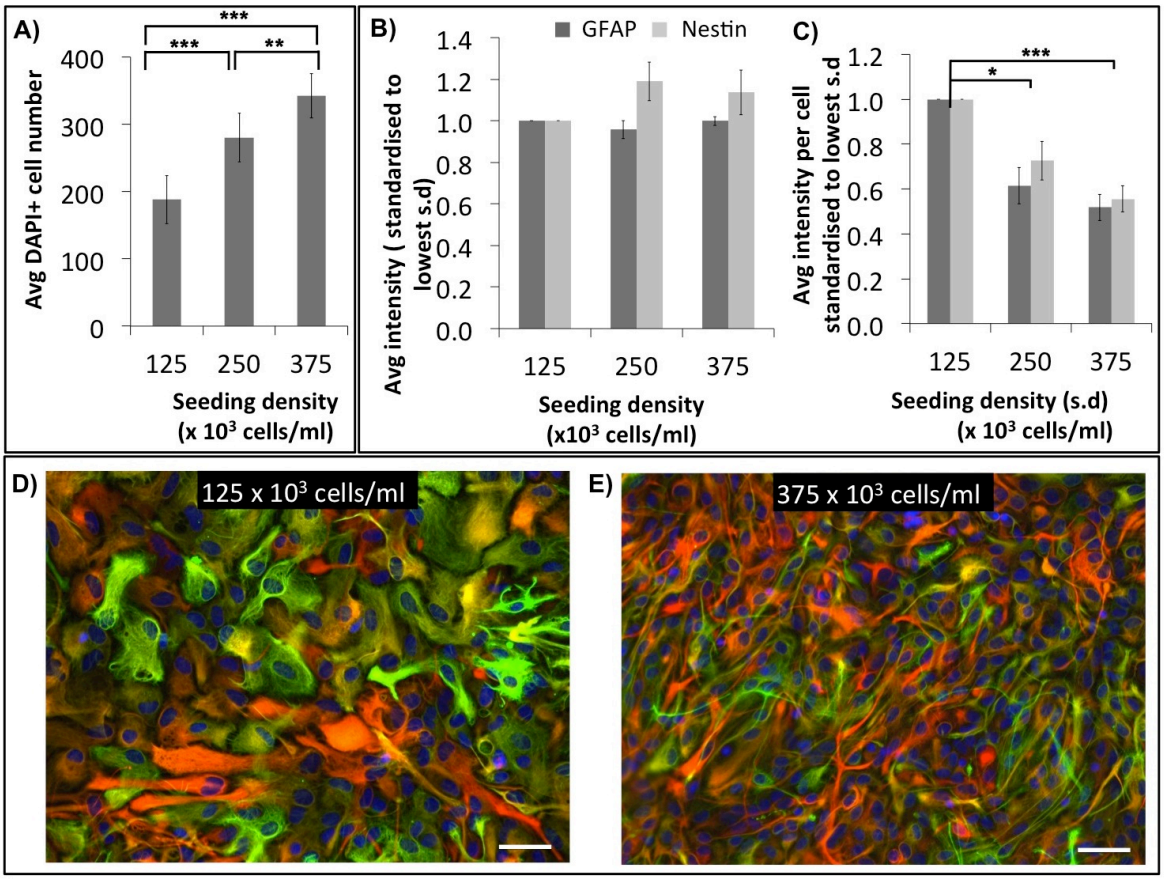

Figure 5. 2 Seeding density of the striatum-derived rat neurospheres appears to induce morphological changes in astrocytes on PLL.

Striatum-derived Sprague Dawley rat neurospheres were plated down (500 μl of cell suspension) on PLL-coated glass coverslips at 5-8 DIV at different seeding density as shown in the graphs above. They were left to differentiate into astrocytes in medium containing 10% FBS and immunocytochemistry was carried out after 7-9 DIV using the primary antibodies to detect GFAP and nestin positive cells. Images were captured using Olympus BX51 fluorescent microscope and Image-Pro imaging software. **A)** Total DAPI positive cell (in blue) number per image was quantified using Cell Profiler and was presented as average DAPI+ cell number, which differed significantly between cultures plated at different seeding density (** $P<0.01$, *** $P<0.001$). The cultures that were initiated with higher seeding density also contained increased cell numbers compared to those initiated with lower seeding density. **B)** Image J was used to quantify the mean intensity of the fluorescence per image detected in green and red channels. This value was multiplied by the whole area of the image to calculate the total intensity of GFAP or nestin fluorescence. The average of all the images captured per condition formed the average intensity values, which were standardised to the values detected in the cultures with the lowest seeding density (125 x 10^3 cells/ml) for both GFAP and nestin separately. Average GFAP or nestin intensity did not show significant changes in cultures with different seeding density. **C)** Average GFAP and nestin intensity per cell was calculated for each image as a ratio of the total intensity to the total cell number of the image. The averages were standardised to the values for the cultures with the lowest seeding density for GFAP and nestin separately. Average intensity per cell decreased significantly for both GFAP and nestin as the seeding density increased (* $P<0.05$, *** $P<0.001$). **D&E)** Representative images of astrocyte cultures are presented for GFAP (green) and nestin (red) immunostainings. Both denser and less dense cultures appear confluent but they present different cell morphology. The cells in the less dense cultures appear larger than those in the denser cultures. Experiments were repeated five times. The error bars represent ± standard error of the mean. One-way repeated measures ANOVA test was applied to the results to detect any possible significance. Scale bar represents 50 μm for all images. Avg: average; DIV: days *in vitro*; FBS: foetal bovine serum; GFAP: glial fibrillary acidic protein; PLL: poly-L-lysine; s.d; seeding density.

despite their increased concentration to begin with. The denser cultures would have to consist of smaller cells to be able to cover the same area (13 mm coverslips) as it can be seen in the representative images, where less dense cultures appeared to consist of cells with larger cell areas (Fig 5.2 D) compared to those found in the denser cultures (Fig 5.2 E).

The GFAP and nestin fluorescence intensities were measured in Image J using the images captured by the fluorescent microscopy. There was no significant difference seen for these intensities between the cultures at different densities (Fig 5.2 B). However, the average intensities per cell were decreased for both GFAP and nestin in denser astrocyte cultures (Fig 5.2 C), which could also be seen in the representative images (Fig 5.2 D & E).

The astrocyte cultures were also immunostained to detect the nature of the spherical, smaller and brighter cells that were seen on top of the astrocytes even after they have generated confluent monolayers after 6 DIV (Fig 5.3). The number of such cells appeared to be increased in denser astrocyte cultures. One possibility was that these were oligodendrocytes or oligodendrocyte progenitor cells (OPCs) since it has been previously observed that some of the progenitor cells, which are present in the neurosphere-derived astrocyte cultures at the initial stages, could differentiate into oligodendrocytes in the same medium, where the majority of the progenitors differentiate into astrocytes (Sorensen et al., 2008). Therefore, the astrocyte cultures were immunostained using the classic oligodendrocyte marker O4 (Sommer and Schachner, 1981) that detects several surface antigens including sulphatide that is expressed at various stages of differentiating oligodendrocytes, starting from OPCs. The cells double-stained for O4 and PLP (Yamamura et al., 1991) would represent the more mature oligodendrocytes compared to those stained with O4 alone (Fig 1.1). On the other hand, O4 can also detect OPCs that could generate oligodendrocytes or type-2 astrocytes depending on the differentiation culture conditions (Raff et al., 1983; Aloisi et al., 1988; Trotter and Schachner, 1989). Because serum-containing medium has been shown to provide a more suitable environment for OPCs to differentiate into type-2 astrocytes *in vitro* rather than into oligodendrocytes (Aloisi et al., 1988; Trotter and Schachner, 1989), the astrocyte cultures were also double stained using the O4 antibody and GFAP antibodies to distinguish the oligodendrocytes from type-2 astrocytes.

The results presented significantly higher numbers and percentages of cells that were labelled with the O4 antibody (O4+) and that were positive both for GFAP and O4 (GFAP&O4+) in denser astrocyte cultures (Fig 5.4). The majority of the O4+ cells were also stained for GFAP, suggesting that these were type-2 astrocytes rather than

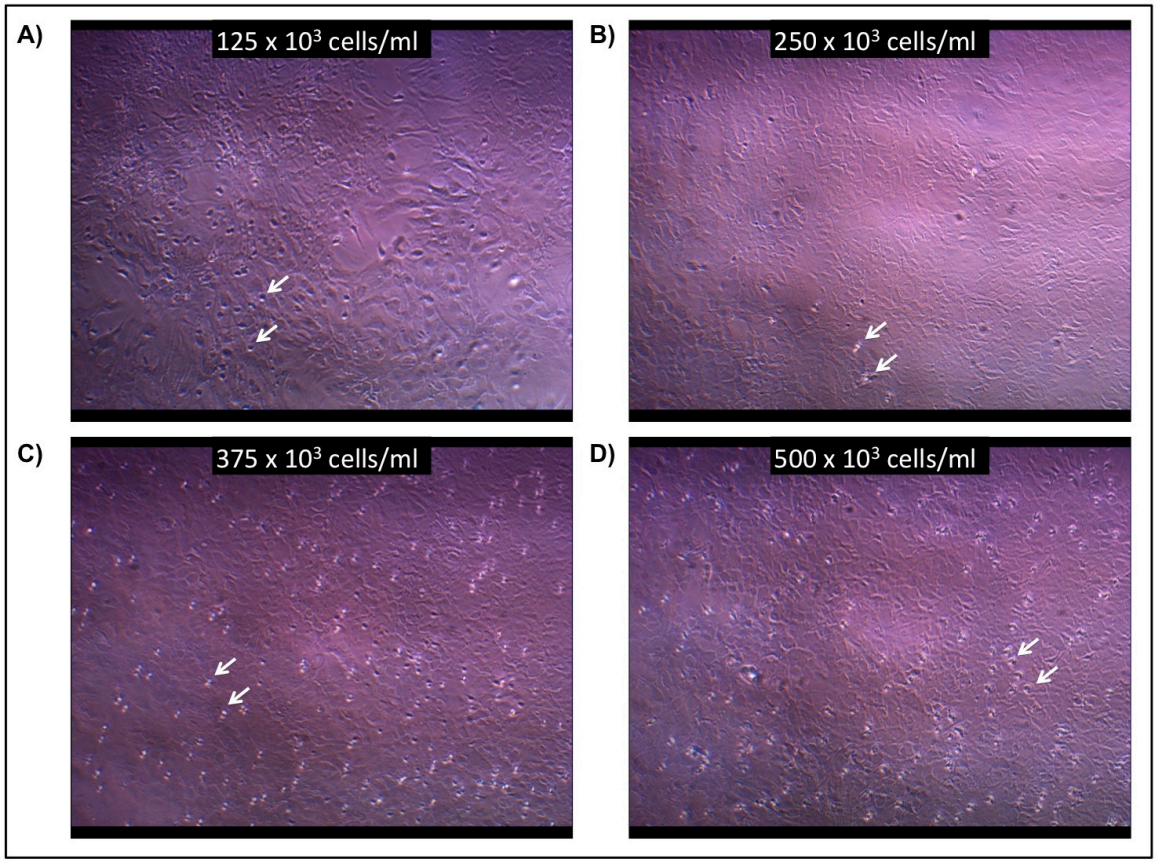

Figure 5. 3 Phase-contrast microscopic image of neurosphere-derived rat astrocyte cultures that were seeded at different concentrations.
Dissociated striata that were isolated from postnatal day 1 Sprague Dawley rats were used to set up neurosphere cell suspensions. These neurospheres were plated down on PLL-coated glass coverslips after 6-9 DIV with a seeding density of **A)** 125 x 10^3 cells/ml, **B)** 250 x 10^3 cells/ml, **C)** 375 x10^3 cells/ml, **D)** 500 x10^3 cells/ml and allowed to differentiate into astrocytes. The astrocyte cultures were observed under phase-contrast microscopy after 6 DIV. There are several blank areas devoid of any cells in the cultures with the lowest seeding density (A). This is not observed in the other cultures (B-D). The sphere-shaped cells that are smaller and brighter compared to the astrocytes underneath are likely to be OPC progenitor cells, oligodendrocytes, and/or type-2 astrocytes as explained in the text. Some of these cells are shown with white arrows. Their number appears to increase as the seeding density of the astrocyte cultures increases. DIV: days *in vitro*; PLL: poly-L-lysine.

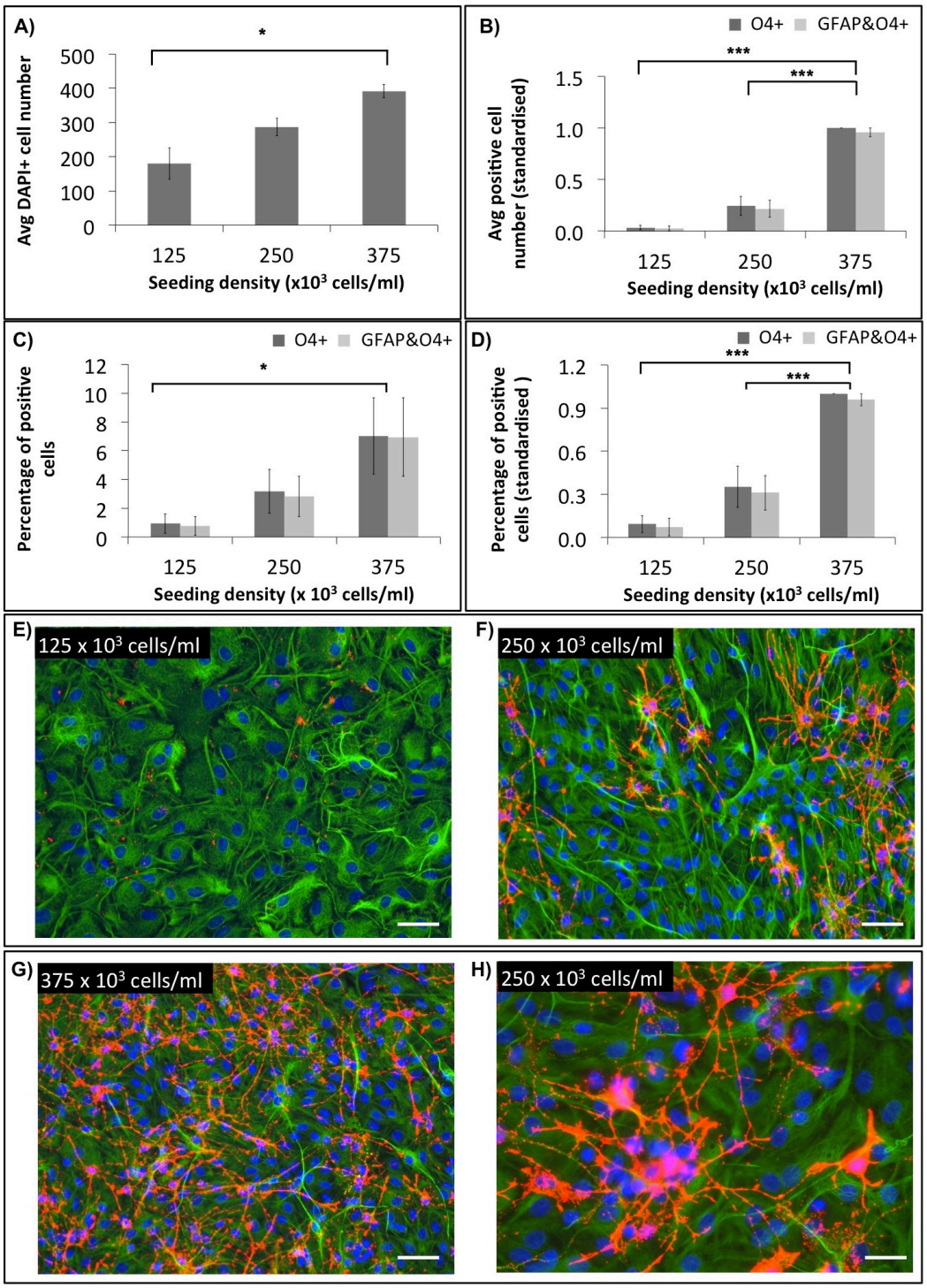

Figure 5. 4 Seeding density of the striatum-derived rat neurospheres leads to a significant increase in the number of type-2 astrocytes in astrocyte cultures on PLL.

Striatum-derived Sprague Dawley rat neurospheres were plated down after 5-8 DIV as 500 μl of cell suspension on PLL-coated glass coverslips at different seeding density as noted above. They were left to differentiate into astrocytes in medium containing 10% FBS. The confluent astrocyte cultures after 7-9 DIV were immunolabelled for O4 antibody and GFAP to detect the type-2 astrocytes. Images were captured using Olympus BX51 fluorescent microscope and Image-Pro imaging software. **A)** Total DAPI positive cell (in blue) number per image was quantified using Cell Profiler and was presented as average DAPI+ cell number per field of view, which differed significantly between cultures plated at seeding density of 125 and 375 x 10^3 cells/ml (* $P<0.05$). The cultures that were initiated with higher seeding density also possessed increased cell numbers when they reached confluency. **B)** The cells, which were positive for O4 and for both O4 and GFAP (GFAP&O4) were counted manually using Image J and were presented as average cell number per seeding density. This was standardised to the O4+ values of the highest seeding density within each experiment. Both O4+ and GFAP&O4+ cell numbers were significantly higher in the astrocyte cultures with the sd. of 375 x 10^3 cells/ml (*** $P<0.001$). **C)** They were also presented as percentages of the total number of cells per image. **D)**

The percentages were standardised to the O4+ values of the highest seeding density within each experiment. **E-H)** Representative images of the astrocyte cultures with different seeding density reflect the changes observed in the graphs. Immunoreactivity of GFAP and the O4 antibody are shown in green and red, respectively. Experiments were repeated three times. The error bars represent ± standard error of the mean. One-way repeated measures ANOVA test was applied to the results to detect any possible significance. Scale bar represents 50 μm in E-G and 25 μm in H. Avg: average; DIV: days *in vitro*; FBS: foetal bovine serum; GFAP: glial fibrillary acidic protein; PLL: poly-L-lysine; s.d; seeding density.

oligodendrocytes. The average percentages of type-2 astrocytes in PLL-astrocytes were 0.8%, 2.8%, and 7.0% in astrocyte cultures with the seeding density of 125, 250, and 375 x 10^3 cells/ml, respectively, with a significance observed between the least dense and densest cultures (Fig 5.4 C). Interestingly, O4+ cells that were found in less dense astrocyte cultures (Fig 5.4 E), did not appear to posses multiple or long cell processes like the ones observed in denser cultures (Fig 5.4 F-G). Therefore, it is possible that these O4+ cells in less dense cultures are at earlier stages of maturation compared to those that reach later stages in denser cultures. Because there was not any significance detected for the difference between the numbers of O4+ cells and GFAP&O4+ cells (Fig 5.4 B), it is likely that the majority of those O4+ cells in Figs 5.4 E-G are type-2 astrocytes and are less mature in less dense PLL-astrocyte cultures.

All the cells that showed PLP expression were also positive for O4 staining (O4&PLP+) in PLL-astrocyte, for which an example is shown in Fig 5.5 H. The percentages of these O4&PLP+ cells were much lower compared to those of type-2 astrocytes, mentioned above. These PLP+ oligodendrocytes presented densities of approximately 0.06%, 0.13%, and 0.22% in astrocyte cultures with the seeding density of 125, 250, and 375 x 10^3 cells/ml, respectively (Fig 5.5 C). Even though there is a trend of increase in the numbers and percentages of PLP+ cells in denser astrocyte cultures, those changes were not found to be significant (Fig 5.5 B&C). Therefore, the number or the percentage of mature oligodendrocytes was not affected by the seeding density of the astrocyte cultures on PLL. The representative images presented PLP+ oligodendrocytes at similar morphologies in astrocyte cultures with different seeding density (Fig 5.5 E-G). The rest of the O4+ cells that were negative for PLP expression (Fig 5.5 H) could be GFAP+ type-2 astrocytes as observed in Fig 5.4 F. Similarly, DAPI+ cell numbers were higher in denser astrocyte cultures (Fig 5.5 A) as seen above (Fig 5.2 A, 5.4A).

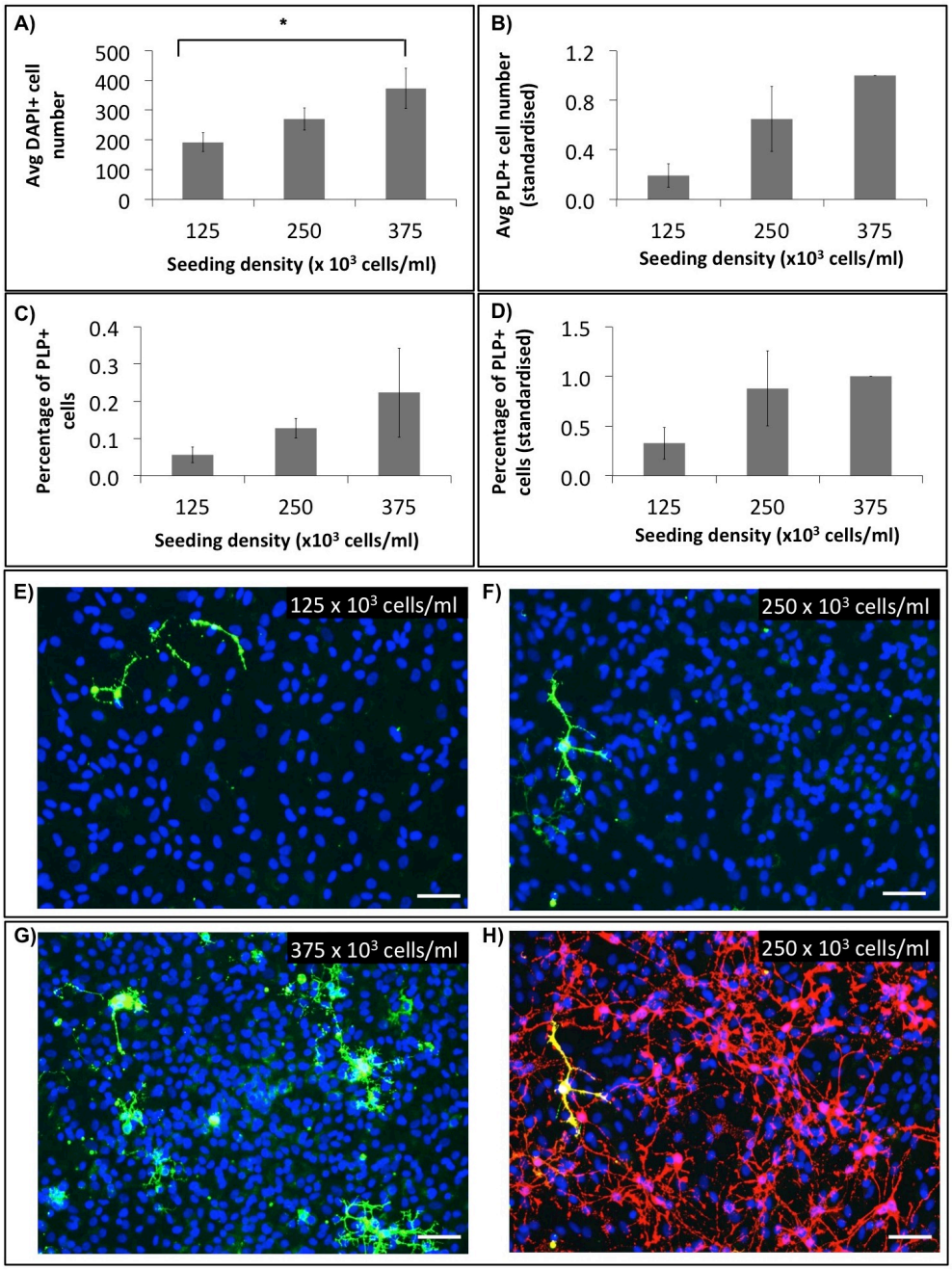

Figure 5. 5 Seeding density of the striatum-derived rat neurospheres does not affect the number of mature oligodendrocytes in astrocyte cultures on PLL.

Striatum-derived Sprague Dawley rat neurospheres were plated down after 5-8 DIV as 500 μl of cell suspension on PLL-coated glass coverslips at different seeding density as stated above. They were left to differentiate into astrocytes in medium containing 10% FBS. The confluent astrocyte cultures after 7-9 DIV were used for immunocytochemistry with antibodies to visualise PLP positive mature oligodendrocytes. Images were captured using Olympus BX51fluorescent microscope and Image-Pro imaging software. **A)** Total DAPI positive cell number per image was quantified using Cell Profiler and was presented as average DAPI+ cell number per field of view, which differed significantly between cultures plated at seeding density of 125 and 375 x 10^3 cells/ml (* $P<0.05$). The cultures that were initiated with higher seeding density showed also increased cell numbers when they reached confluency. **B)** PLP+ cells were counted manually using Image J and were presented as average cell number per seeding density. The results were standardised to the highest seeding density. **C)** PLP+ cells were also presented as percentages of the total number of cells per image. **D)** The percentages were standardised to the highest seeding density. No significant changes were detected in the results presented in B, C and D. **E-G)** Representative images of the astrocyte cultures with different seeding density show DAPI+ cells in blue and PLP+ oligodendrocytes in green. **H)** All PLP positive cells (green) also labelled with the O4 antibody (red). Experiments were repeated three times. The error bars represent ± standard error of the mean. One-way repeated measures ANOVA test was applied to the results to detect any possible significance. Scale bar represents 50 μm in all images. Avg: average; DIV: days *in vitro*; FBS: foetal bovine serum; PLL: poly-L-lysine; PLP: proteolipid protein.

5.3.2 The effects of the seeding density of the striatum-derived neurospheres on the morphology of TnC-astrocytes

Neurosphere-derived rat astrocytes, initiated by plating down striatum-derived neurospheres on TnC-coated coverslips at varying densities, were also analysed in terms of their GFAP and nestin expressions and the percentage of cells that expressed both the O4 antibody and GFAP (GFAP&O4+) known as type-2 astrocytes. The results were not completely similar to those detected in PLL-astrocytes.

A number of coverslips of TnC-astrocytes were immunostained for GFAP and the O4 antibody after 10 DIV; while, the remaining coverslips from the same batch of TnC-astrocytes were used for the double staining of GFAP and nestin after 11 DIV. Both experiments comprised of neurosphere cell suspensions plated down at the concentrations of 125, 250, 375 and 500 x 10^3 cells/ml. Average DAPI+ cell numbers counted at the end of the experiment (10 and 11 DIV) were significantly lower in the less dense cultures, (125 x 10^3 cells/ml), compared to DAPI+ cell numbers in the denser cultures (Fig 5.6 A and 5.7 A). However, the differences between the cultures with the seeding density of 250, 375, and 500 x 10^3 cells/ml were not found to be significant (Fig 5.6 A and 5.7 A). In parallel with that, the representative images presented fewer and larger astrocytes in the cultures initiated with the seeding density of 125 x 10^3 cells/ml (Fig 5.6 D) compared to those in denser cultures (250-500 x 10^3 cells/ml) that appeared to consist of similar number of cells (Fig 5.6 E-G).

Average GFAP fluorescence intensity was not significantly different between the astrocyte cultures with different seeding density but nestin fluorescence intensity was increased in the two highest seeding concentrations compared to the lowest one (Fig 5.6 B). Despite the increase in nestin intensity, the average nestin intensity per cell was still significantly lower in denser cultures (Fig 5.6 C). Consequently, the least dense cultures consisted of astrocytes that appeared to be bigger in cell size (Fig 5.6 D) and that showed higher GFAP and nestin intensities per cell compared to those in denser astrocyte cultures (Fig 5.6 E-G). Because the increased GFAP and nestin expression per cell could be interpreted as increased astrocyte reactivity, it is possible that the astrocytes in the cultures with a seeding density of 125 x 10^3 cells/ml are more reactive compared to those in the cultures with higher seeding density.

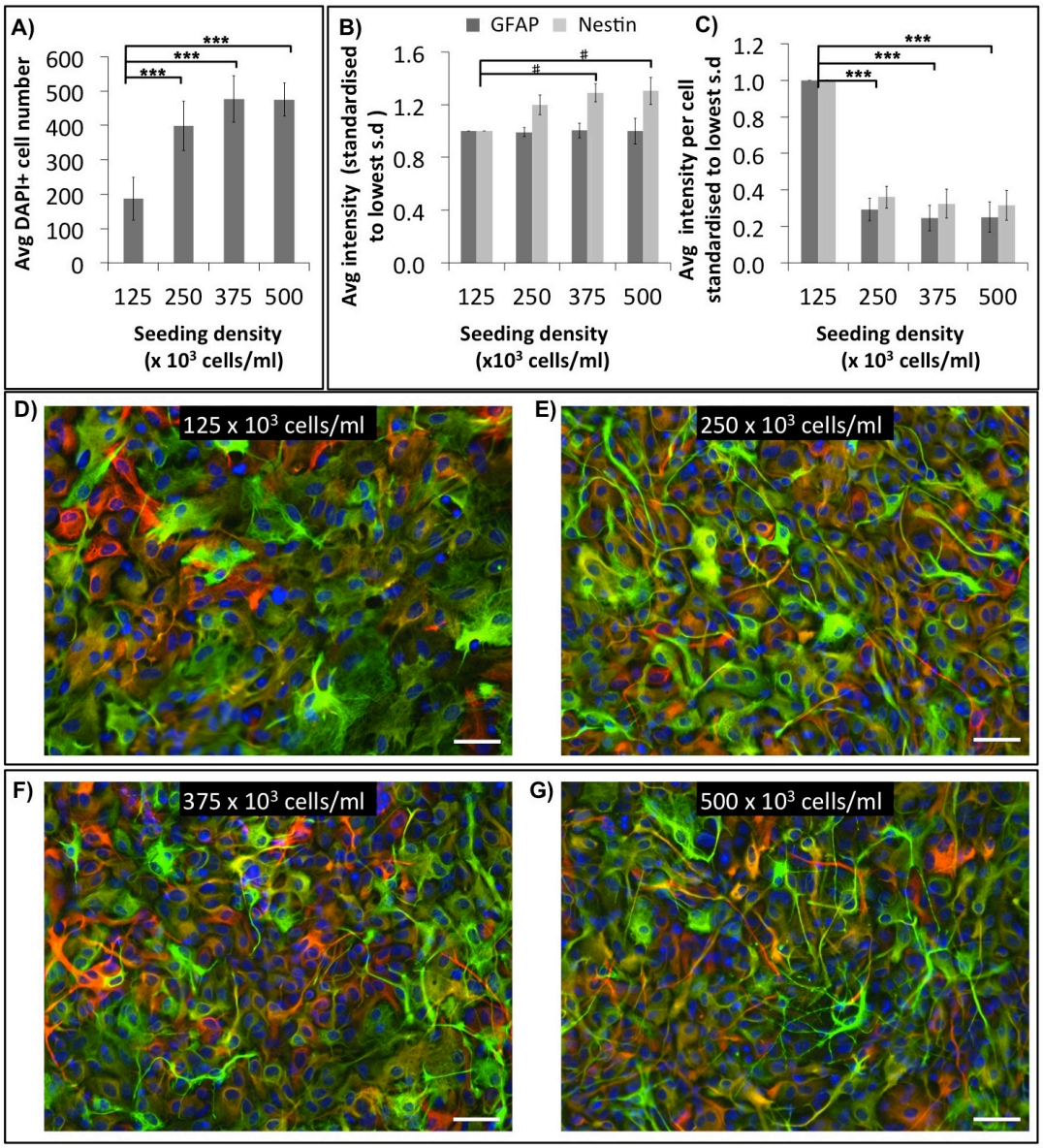

Figure 5. 6 Seeding density of the striatum-derived rat neurospheres appears to stimulate morphological changes in astrocyte cultures on TnC.

Striatum-derived rat neurospheres were plated down in 500 μl on TnC-coated glass coverslips after 11 DIV at different seeding density as stated above. They differentiated into astrocytes in medium containing 10% FBS. The confluent astrocytes were immunolabelled after 11 DIV using antibodies to detect GFAP (green) and nestin (red). **A)** Total DAPI positive cell number per image was quantified using Cell Profiler and was presented as average DAPI+ cell number, which differed significantly between cultures plated at different s.d. (***P<0.001). **B)** Image J was used to quantify the mean intensity of the fluorescence per image for green and red channels, which was multiplied by the whole image area to calculate the total intensity of GFAP or nestin fluorescence per image. The average of all the images captured per condition formed the avg intensity values, which were standardised to the least dense cultures for both GFAP and nestin separately. Avg GFAP intensity did not differ significantly in cultures with different s.d. Avg nestin intensity increased significantly at the s.d. of 375 and 500 x 10^3 cells/ml compared to that of 125 x 10^3 cells/ml (# P<0.05). **C)** Avg GFAP and nestin intensity per cell was calculated for each image as a ratio of the total intensity to the total cell number per image. The averages were standardised to least dense cultures for GFAP and nestin separately. Avg intensity per cell decreased significantly for both GFAP and nestin at higher s.d. compared to the lowest s.d. (***P<0.001). **D-G)** Representative images of astrocyte cultures are presented. Experiments were repeated three times. The error bars represent ± standard error of the mean. One-way repeated measures ANOVA test was used to detect significance. Scale bar represents 50 μm for all images. Avg: average; DIV: days *in vitro*; FBS: foetal bovine serum; GFAP: glial fibrillary acidic protein; s.d; seeding density; TnC: tenascin C.

The average O4+ or GFAP&O4+ cell numbers or percentages did not show any significant changes between the TnC-astrocyte cultures with different seeding density (Fig 5.7) unlike the situation observed for PLL-astrocytes. Therefore, it could be concluded that the number or percentage of type-2 astrocytes is not affected by the seeding density of the TnC-astrocyte cultures. Similar to the observations in PLL-astrocytes, the number of cells that stained with the antibody to O4, which recognises sulphatide, in less dense astrocyte cultures (Fig 5.7 E) did not appear to posses multiple or long cell processes like the ones observed in denser cultures (Fig 5.7 F-H). It is likely that the majority of these O4+ cells in Figs 5.7 E-H are type-2 astrocytes due to the similar levels of cell number and percentage detected for O4+ and GFAP&O4+ cells, and that they are less mature in less dense TnC-astrocyte cultures. DAPI+ cell numbers were also higher in denser astrocyte cultures (Fig 5.7 A) as seen above (Fig 5.6 A).

In conclusion, the seeding density of the striatum-derived neurospheres appears to have an effect on the average DAPI+ cell density, cell size, average GFAP and nestin fluorescence intensity per cell, and morphology of cells (possibly type-2 astrocytes) that stained with the antibody to O4 in rat astrocyte cultures, plated on TnC-coated coverslips. The differences are observed specifically between the cultures, set up at the seeding density of 125 x 10^3 cells/ml, and the denser cultures, as explained above.

5.3.3 The effects of the seeding density of the striatum-derived neurospheres on myelination

After analysing the possible effects of the seeding density of the striatum-derived rat neurospheres on the morphological features of the astrocyte cultures, this effect was also examined on myelination in rat embryonic spinal cord cultures, which were prepared using PLL- or TnC-astrocytes at different densities.

Despite the morphological changes seen above in astrocyte cultures with different seeding density, the myelination levels or the neurite density of the spinal cord myelinating cultures did not appear to be affected by the use of the astrocyte cultures at different densities (Fig 5.8). Both the PLL-myelinating cultures (Fig 5.8 A & B) and TnC-myelinating cultures (Fig 5.8 C & D) contained myelination percentages and neurite density that were at similar levels at all the seeding densities examined. Representative images are also presented for the spinal cord myelinating cultures, prepared with the least and the most dense astrocyte cultures on PLL (Fig 5.8 E & F) and on TnC (Fig 5.8 G & H).

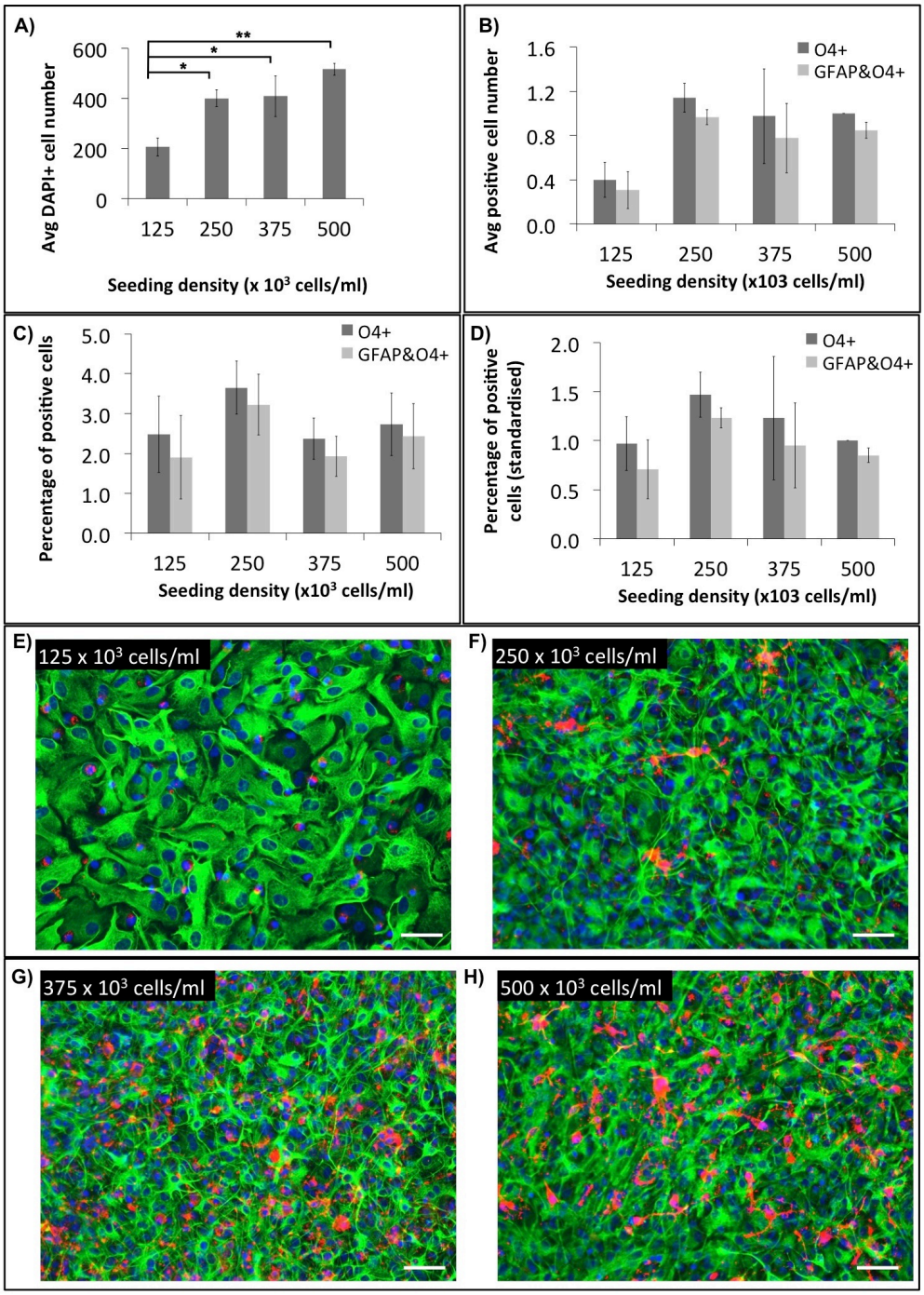

Figure 5. 7 Seeding density of the striatum-derived rat neurospheres does not affect the number of type-2 astrocytes significantly in astrocyte cultures on TnC.

Striatum-derived rat neurospheres were plated down after 11 DIV as 500 μl of cell suspension on TnC-coated glass coverslips at different seeding density as seen above. They differentiated into astrocytes in medium containing 10% FBS. The confluent astrocytes were immunolabelled after 10 DIV to visualise GFAP positive cells (green) and cells the label with the O4 antibody (red) that reflect the type-2 astrocytes. **A)** Average DAPI+ cell number is the total DAPI+ cell number per image that was quantified using Cell Profiler. It was significantly lower in cultures plated at the s.d. of 125 x 10^3 cells/ml compared to that in the cultures with higher s.d. (* P<0.05,** P<0.01). **B)** The cells positive for O4 (O4+) and for both GFAP and O4 (GFAP&O4) were counted manually using Image J and were presented as avg cell number per s.d. **C)** They were also presented as percentages of the total number of cells per image. **D)** The percentages were standardised to the O4+ values of the highest s.d. within each experiment. No significant changes were detected in any of the comparisons. **E-H)** Representative images of astrocyte cultures are presented. Experiments were repeated three times. The error bars represent ± standard error of the mean. One-way repeated measures ANOVA test was used to detect significance. Scale bar represents 50 μm in all the images. Avg: average; DIV: days *in vitro*; FBS: foetal bovine serum; GFAP: glial fibrillary acidic protein; PLL: poly-L-lysine; s.d; seeding density; TnC: tenascin C.

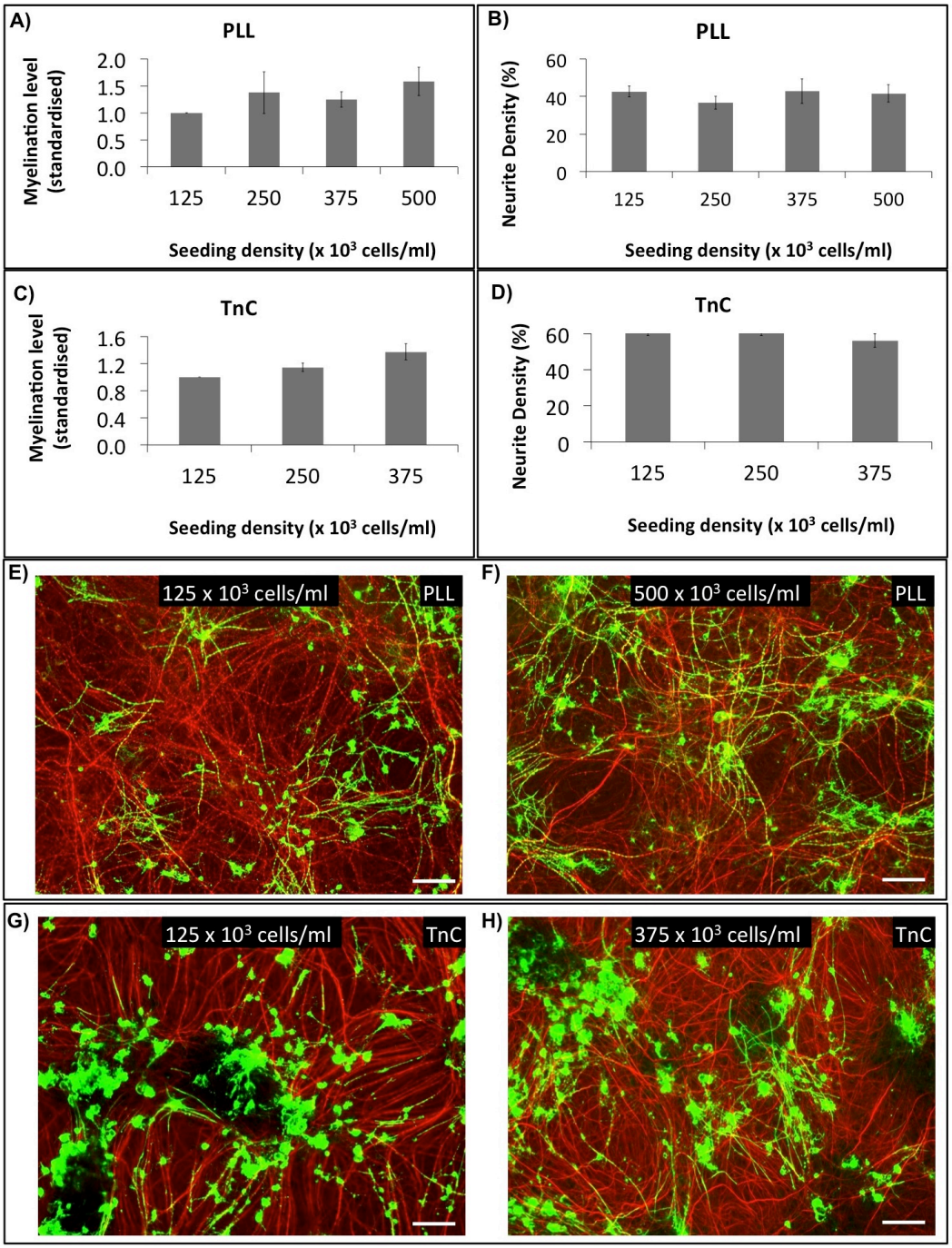

Figure 5. 8 Seeding density of the striatum-derived neurospheres does not affect the myelination levels in rat myelinating cultures on PLL- or TnC-astrocytes.

Embryonic rat spinal cord myelinating cultures were set up on top of neurosphere-derived rat astrocytes, plated on PLL- or TnC-coated glass coverslips. Spinal cord cultures were prepared using astrocytes cultures that were started with neurosphere cell suspensions at different seeding density as shown above in the graphs. The spinal cord cultures were immunostained after 24 DIV using the AA3 antibody to detect PLP (green) and hence mature myelin and using SMI-31 (red) to detect neurites. Myelination percentages and neurite density were quantified using "myelin.cp" pipeline in Cell Profiler using images from fluorescent microscopy. Myelination percentage is standardised to the value in the least dense cultures (125 x 10^3 cells/ml). The initial s.d. of astrocyte cultures did not affect myelination level **(A&C)** or neurite density **(B&D)** significantly. Representative images illustrate cultures on PLL- **(E&F)** or TnC- astrocytes **(G-H)**. The experiments were repeated three times. One-way repeated measures ANOVA test was applied to the results. The error bars represent ± standard error of the mean. Scale bar represents 100 μm for all images. DIV: days *in vitro*; PLL: poly-L-lysine; PLP: proteolipid protein; s.d.: seeding density; TnC: tenascin C.

The PLL-myelinating cultures, which were set up using astrocytes with different densities, were also used to examine the effect of rat recombinant CNTF on myelination. Despite a slight increase in myelination percentages upon CNTF treatment for all the astrocyte densities used, none of them was shown to be significant (Fig 5.9 A). Similarly, CNTF treatment did not lead to any significant changes on neurite density in any of the astrocyte densities used (Fig 5.9 B). Representative images are also given to visualise the untreated (control) and CNTF-treated myelinating cultures (Fig 5.9 C-F). In short, the seeding density of the striatum-derived neurospheres did not affect the myelination levels in untreated or CNTF-treated PLL-myelinating cultures when cell densities between 125-500 x 10^3 cells/ml were used. The CNTF treatment (1ng/ml) did not change the myelination levels in any of the cells densities that were examined.

5.3.4 The effects of the age of the astrocytes on myelination

Because the previously shown stimulatory effect of CNTF on myelination (Nash et al., 2011b) could not be validated in any of the myelinating cultures with varying astrocyte densities (Fig 5.8 & 5.9), the effect of the astrocyte age on myelination was also examined. Since the above-mentioned experiments already presented results from the spinal cord myelinating cultures, where 6-9 DIV old astrocyte cultures were used (Fig 5.8 and 5.9), experiments were carried out this time using astrocytes that had been either 3 DIV or 10 DIV. Astrocyte monolayers are used as support monolayers for spinal cord myelinating cultures after 7-10 DIV as stated in the original study which described these cultures (Sorensen et al., 2008). Therefore, 3 DIV old astrocytes would represent young cultures and 10 DIV old astrocytes would represent older cultures.

PLL-astrocyte cultures were prepared from the striatum-derived neurospheres at the seeding density of 250 x 10^3 cells/ml because the above-mentioned experiments showed that less dense astrocyte cultures consisted of fewer number of cells that were larger, expressed higher GFAP and nestin fluorescence intensities compared to those in denser astrocytes. On the other hand, seeding density between 250-500 x 10^3 cells/ml generated astrocyte cultures with similar morphological properties akin to those astrocytes prepared by plating down 1 x T75 (75 cm^2) tissue culture flask of neurospheres into 1-2 x 24-well plates; the ratio most commonly used in our lab. These myelinating cultures were then treated with CNTF starting from 7, 10, or 12 DIV onwards. Treatments of the spinal cord myelinating cultures are usually initiated after 12 DIV to observe any effects on myelination since 15-18 DIV has been determined to be the time point around which myelin sheath formation begins (Thomson et al., 2008; Nash B., 2010). However, it is also possible that treatments, starting at earlier days, would have an effect on myelination levels at final stages of the cultures. Addition of

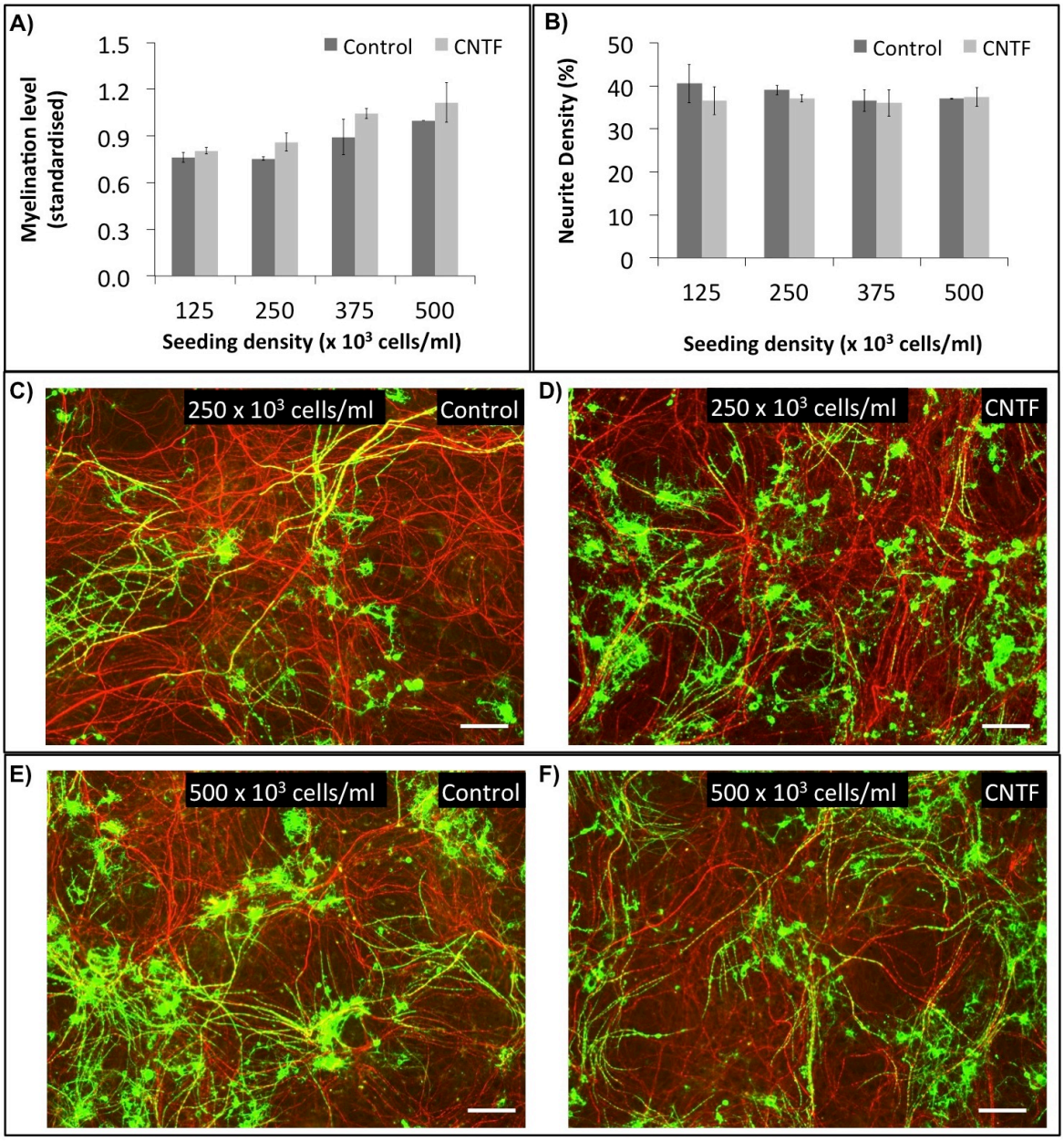

Figure 5. 9 Seeding density of the striatum-derived neurospheres does not affect the myelination levels significantly in CNTF-treated rat myelinating cultures.
Embryonic rat (Sprague Dawley) spinal cord myelinating cultures were plated on neurosphere-derived rat astrocytes, plated on PLL-coated glass coverslips with a range of different seeding density as stated above in the graphs. The spinal cord cultures were treated with 1 ng/ml of recombinant rat CNTF starting from 12 DIV onwards and were immunostained at 24 DIV using AA3 antibody to detect PLP (green) and hence mature myelin and using SMI-31 (red) to detect neurites. Images were captured using Olympus BX51fluorescent microscope and Image-Pro imaging software. Myelination percentages and neurite density were quantified using "myelin.cp" pipeline in Cell Profiler. **A)** Myelination percentage is shown as standardised to the untreated (control) cultures with the highest s.d. of 500 x 10^3 cells/ml. **A&B)** CNTF treatment did not appear to induce a significant effect on myelination levels or on neurite density at any seeding density of astrocytes, which were used to support the spinal cord myelinating cultures. Representative images show the control **(C&E)** and CNTF-treated spinal cord myelinating cultures **(D&F)**, prepared with astrocytes at two different seeding densities. The experiments were repeated three times. One-way repeated measures ANOVA test was applied to the results. The error bars represent mean ± standard deviation for the control cultures with the seeding density of 125 x 10^3 cells/ml (due to the presence of two experimental repeats) and ± standard error of the mean for the other values. Scale bar represents 100 μm for all images. CNTF: ciliary neurotrophic factor; DIV: days *in vitro*; PLL: poly-L-lysine; PLP: proteolipid protein; s.d.: seeding density.

the treatments at 12 DIV are carried out subsequently in a medium, which does not include the insulin hormone. This is to prevent the generation of excessive numbers of oligodendroglia that tend to obscure myelin sheaths and to promote differentiation (Thomson et al., 2006; Thomson et al., 2008). Therefore, treatments starting at earlier time points also had their own control (untreated) cultures, which were fed with medium that did not contain insulin.

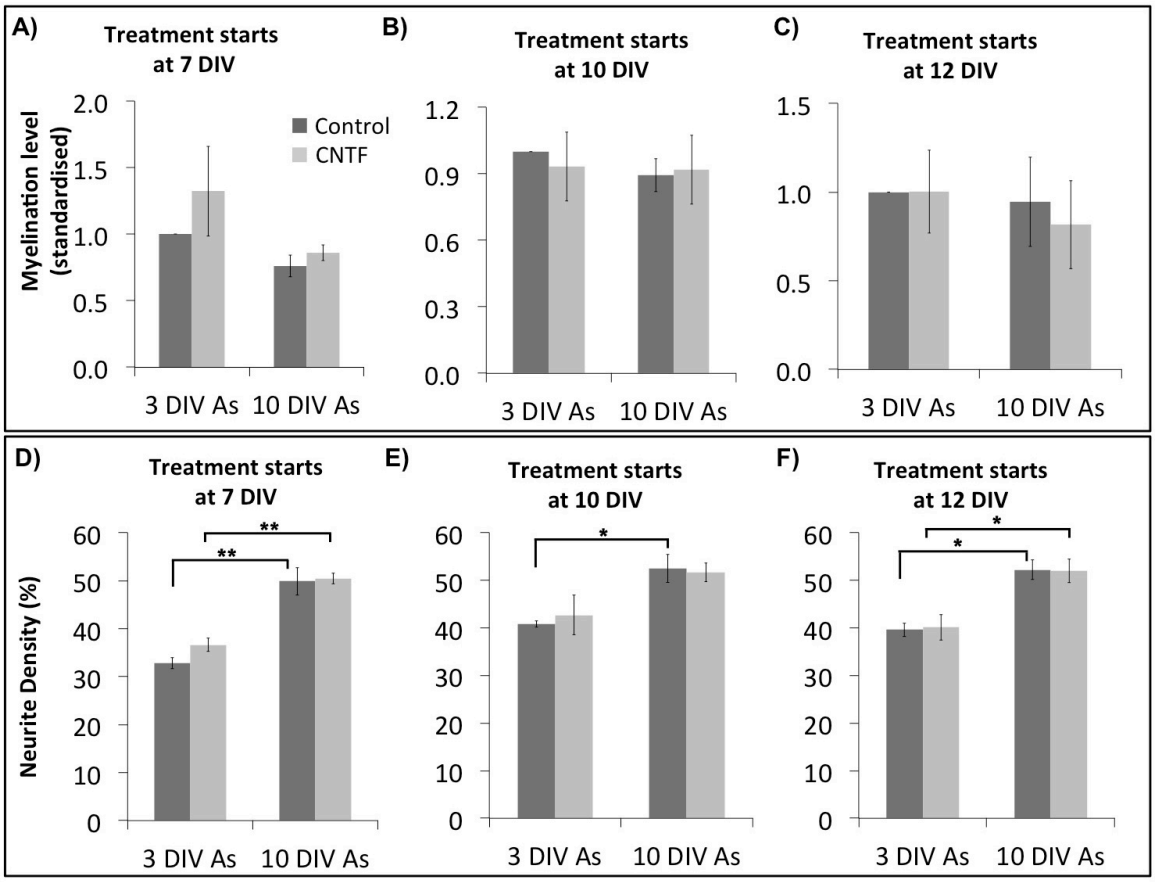

Figure 5. 10 The age of the astrocytes used for rat myelinating cultures affects the neurite density significantly but has no effect on myelination levels.
Embryonic rat (Sprague Dawley) spinal cord myelinating cultures were set up on top of neurosphere-derived rat astrocytes plated on PLL-coated glass coverslips. Spinal cord cultures were prepared using astrocytes that had been either 3 DIV or 10 DIV that were initiated with neurosphere cell suspensions at the seeding density of 250 x 10^3 cells/ml. The spinal cord cultures were treated with 1 ng/ml of recombinant rat CNTF starting from 7 DIV, 10 DIV or 12 DIV onwards and were immunostained at 26 DIV using the AA3 antibody to detect PLP and hence mature myelin and using SMI-31 to detect neurites. Images were captured using Olympus BX51fluorescent microscope and Image-Pro imaging software. Myelination percentages and neurite density were quantified using "myelin.cp" pipeline in Cell Profiler. **A-C)** Myelination percentages were standardised to the values of the untreated (control) spinal cord myelinating cultures, where the supporting astrocyte monolayer had been 3 DIV (young). The myelination level was not affected significantly by the age of astrocytes that were used to set up the spinal cord myelinating cultures. Moreover, CNTF treatment did not show a significant change on myelination levels at any astrocyte age. **D-F)** Neurite density increased significantly in the spinal cord myelinating cultures that were set up using older astrocytes (* $P<0.05$, ** $P<0.01$). CNTF-treated myelinating cultures, prepared with older astrocytes also showed significantly increased neurite density compared to those prepared with younger astrocytes. The experiments were repeated three times. One-way repeated measures ANOVA test was applied to the results to detect any possible significance. The error bars represent ± standard error of the mean. CNTF: ciliary neurotrophic factor; DIV: days *in vitro*; PLL: poly-L-lysine; PLP: proteolipid protein.

The age of the astrocytes did not affect the myelination levels in untreated or CNTF-treated embryonic spinal cord myelinating cultures (Fig 5.10 A-C). CNTF did not change the myelination levels in cultures, set up using young or older astrocytes at the beginning of the experiments. On the other hand, the myelinating cultures that were set up using astrocytes that had been 10 DIV contained significantly higher levels of neurite density compared to those set up using astrocytes that had been 3 DIV (Fig 5.10 D-F). CNTF treatment alone did not affect the neurite density but the CNTF-treated myelinating cultures plated on older astrocytes showed also higher neurite density compared to CNTF-treated cultures plated on younger astrocytes.

5.4 General conclusions and discussion

The protocol for setting up embryonic rat spinal cord myelinating cultures (Sorensen et al., 2008) was optimised further mainly by analysing the effects of the seeding density of the striatum-derived neurospheres on the morphology of PLL- and TnC-astrocytes (Fig 5.2-5.7) and on the myelination of PLL- and TnC-myelinating cultures (Fig 5.8-5.9). The seeding density of 250 x 10^3 cells/ml appeared to be the optimum among the other seeding densities, namely, 125, 375, and 500 x 10^3 cells/ml.

The major differences appeared to be significant between the astrocyte cultures with the seeding density of 125 x 10^3 cells/ml and to those with the seeding density of 250 x 10^3 cells/ml. This difference suggests that starting concentrations of the astrocyte cultures will have an effect on how dense these cultures become once they are ready to be used as supporting monolayers for spinal cord myelinating cultures (6-9 DIV). On the other hand, the differences between the astrocytes with the seeding density of 250, 375, and 500 x 10^3 cells/ml were less obvious. An example is the average density of DAPI+ cells per field of view in astrocytes cultured for 7-11 DIV. Despite the significant increase also in astrocytes with the seeding density of 375 x 10^3 cells/ml compared to those with 250 x 10^3 cells/ml in PLL-astrocytes (Fig 5.2 A), such significance was not detected in the other experiments (Fig 5.4-5.7 A). This suggests that the increase in the average number of DAPI+ cells per field of view is not directly proportional to the seeding density of the striatum-derived neurospheres. The increase appears to reach a plateau at the seeding density of 250 x 10^3 cells/ml in TnC-astrocytes (Fig 5.6 A, 5.7 A). Similar results are seen, but are not observed so clearly in PLL-astrocytes (Fig 5.2 A, 5.4 A, 5.5 A) possibly due to examining three seeding densities (125, 250, 375 x 10^3 cells/ml) there rather than four (125, 250, 375, 500 x 10^3 cells/ml), which can provide a clearer profile for the change in terminal DAPI+ cell numbers per field of view as the initial seeding density of astrocytes increases.

One other example illustrating differences in cell density is seen for the decrease of the average GFAP and nestin intensities per cell in the denser astrocyte cultures compared to that seen for astrocytes seeded at a density of 125 x 10^3 cells/ml (Fig 5.2 C, 5.6 C). Similarly, these intensity per cell values did not differ between the astrocyte cultures with the seeding density of 250, 375, and 500 x 10^3 cells/ml. Because both GFAP and nestin are cytoskeletal proteins, it could be hypothesised that larger astrocytes that attempt to cover a larger area of the glass coverslips despite the lower concentrations they were seeded at would express higher average GFAP and nestin intensities per cell as a consequence of increasing their cell size. Our results agree with this hypothesis in that less dense astrocyte cultures present higher GFAP and nestin intensities per cell. However, these intermediate filament proteins are also associated with astrocyte reactivity. Their increased expressions in individual astrocytes have been detected *in vivo* in rat CNS subjected to tissue insults of different types and *in vitro* in primary astrocytes at the site of mechanical injury (Clarke et al., 1994; Frisen et al., 1995; Levison et al., 1996; Wilhelmsson et al., 2006; Sofroniew et al., 2009; Xue et al., 2011). Therefore, it is possible to consider that astrocytes with the seeding density of 125 x 10^3 cells/ml are more reactive in a sense compared to the denser astrocyte cultures. This may be due to the fact that astrocytes are more stressed in a lower density culture than comparable cultures with more astrocytes and due to presumably an increased autocrine secreted protein environment. Such differences could also lead to the stimulation/inhibition of distinct intracellular pathways and hence change the effects of a treatment in these cultures or in spinal cord myelinating cultures that are generated using these astrocytes.

Phase contrast microscopy illustrates clear differences between the seeding density of cultures at 125 x 10^3 cells/ml to those densities of the other cultures (Fig 5.3). The least dense cultures do not always form confluent monolayers at the same time as the other cultures do. In addition, the number of the smaller and brighter spherical cells observed on top of the PLL-astrocyte monolayers appears to increase as the seeding density increases (Fig 5.3). It is likely that a small percentage of these cells are mature oligodendrocytes (Fig 5.5) and that another small percentage of cells consists of NG2 progenitor cells as detected previously in neurosphere-derived rat astrocyte cultures (Sorensen et al., 2008). OPCs are also likely to constitute part of these cells as previously demonstrated in a study, where immunocytochemistry and electron microscopy have been utilised to show the presence of “small, glossy, and motile” “O2A” progenitors on the astrocyte feeder layers (Asou et al., 1995). The majority of these cells, however, could be type-2 astrocytes as suggested by the GFAP&O4 immunoreactivity (Fig 5.4, 5.7). Type-1 and type-2 astrocytes *in vitro* have been associated in general with the protoplasmic and fibrous astrocytes, respectively, *in vivo*

(Raff et al., 1983; Williams et al., 1985). Both *in vitro* and *in vivo* astrocyte types have presented differences in terms of astrocyte reactivity or sensitivity to injury (Raff et al., 1983; Shannon et al., 2007). Such differences in the type of astrocytes between the astrocyte cultures generated with different seeding densities could also eventually affect the differentiation properties of the spinal cord myelinating cultures plated on top.

Myelination was analysed in PLL- and TnC-myelinating cultures that were set up using the astrocytes with different seeding densities to observe whether the above-mentioned differences between astrocyte cultures could also affect the myelination levels in spinal cord myelinating cultures. No change in myelination levels was observed in PLL- or TnC-myelinating cultures (Fig 5.8). Similarly, the treatment of the myelinating cultures with recombinant CNTF did not affect the myelination levels or neurite density in any of the seeding density experiments (Fig 5.9). CNTF treatments, which were initiated at earlier time points (7 DIV and 10 DIV), did not alter the myelination levels or neurite density, either (Fig 5.10). Conversely, the astrocyte age appeared to have an effect on neurite density of the PLL-myelinating cultures. Myelinating cultures that were set up using astrocytes that were 3 DIV had significantly lower neurite density compared to those cultures prepared using astrocytes that had been 10 DIV (Fig 5.10). Therefore, it appears that even though astrocytes that had been 3 DIV and 10 DIV had originated from the same batch of striatum-derived rat neurospheres and even though they can look like healthy cultures under phase-contrast microscopy and appear as confluent astrocyte monolayers, older astrocytes seem to generate healthier myelinating cultures. Even if the significant decrease in neurite density does not appear to affect the myelination levels (Fig 5.10), higher neurite density is seen as a sign of healthy cultures and hence is preferred. Therefore, these findings are in accordance with the previous suggestions of using astrocytes that had been 7-10 DIV to set up spinal cord myelinating cultures (Sorensen et al., 2008).

In conclusion, the seeding density of the neurosphere-derived astrocytes does not appear to affect myelination or neurite density in PLL- or TnC-myelinating cultures that are prepared using the astrocyte cultures with the seeding density of 125, 250, 375 and 500 x 10^3 cells/ml. Similarly, myelination levels are not changed by the CNTF treatment despite the use of astrocyte monolayers with different seeding densities. The use of astrocytes at different ages or starting the treatments at earlier time points do not provide the right conditions to observe an effect of CNTF on myelination, either. Therefore, it appears unlikely that the reason why elevated myelination levels were not seen in PLL-myelinating cultures compared to TnC-myelinating cultures, or in CNTF-treated cultures compared to untreated ones as published previously (Nash et al.,

2011b) is because of plating down the striatum-derived neurospheres at different densities or using astrocyte cultures at different ages to set up the myelinating cultures. It is more likely that the difference lies within the method used to quantify the myelination levels and neurite density or within the variability of the cultures generated by the two investigators involved.

These further optimisation attempts to fine-tune the rat spinal cord myelinating cultures suggest 250 x 10^3 cells/ml as the optimum seeding density to plate down the striatum-derived neurospheres to differentiate into PLL- or TnC-astrocyte cultures. Astrocytes with this seeding density **1)** appear healthy and confluent under phase-microscopy, **2)** generate average DAPI+ cells at densities that are not significantly different than those of denser astrocyte cultures, **3)** have similar levels of average GFAP and nestin intensities per cell and hence possibly similar levels of astrocyte reactivity when compared to denser astrocyte cultures, **4)** present lower numbers and percentages of type-2 astrocytes and thus show reduced astrocyte heterogeneity compared to denser cultures.

Chapter 6

Further analysis of the role of exogenous CNTF in primary astrocytes and spinal cord myelinating cultures

6.1 Introduction

Ciliary neurotrophic factor (CNTF), an IL-6 family cytokine, has been shown to promote myelination in both PLL- and TnC-myelinating cultures (Nash et al., 2011b) that are the embryonic rat spinal cord myelinating cultures that were set up using rat astrocytes on PLL (PLL-astrocytes) or TnC (TnC-astrocytes) as feeder monolayers. A microarray gene expression profiling analysis was carried out (Array 2, Chapter 3) to identify any potential regulators of myelination based on the observation that myelination levels are reduced in untreated TnC-myelinating cultures compared to PLL-myelinating cultures, and are increased upon CNTF treatment in both PLL- and TnC-myelinating cultures (Nash et al., 2011b). The stimulatory effect of 1 ng/ml of rat recombinant CNTF on myelination could not be validated in the experiments outlined in this thesis, which suggested that this failure was not related to the age of the astrocyte monolayers used or to the seeding density of the striatum-derived rat neurospheres that would differentiate into astrocytes (Chapter 5). Further experiments and analyses were performed to investigate the role of CNTF in neurosphere-derived astrocyte monolayers and on myelination in rat and mouse spinal cord myelinating cultures as will be explained in this chapter.

The positive effects of CNTF on myelination levels have been suggested by a number of studies, where usually this stimulation was attributed to the CNTF properties of being neuroprotective (Barbin et al., 1984; Hagg and Varon, 1993; Naumann et al., 2003; Krady et al, 2008), promoting the survival of oligodendrocyte precursor cells (OPCs) and oligodendrocytes (Barres et al., 1993; Louis et al., 1993), and stimulating the proliferation and maturation of OPCs (Barres et al., 1996; Marmur et al., 1998; Stankoff et al., 2002; Albrecht et al., 2007; Cao et al., 2010). CNTF has also been shown to decrease the severity of disease course and increase the neuronal functional recovery in mice with experimental autoimmune encephalomyelitis (EAE, Butzkueven et al., 2002; Linker et al., 2002; Kuhlmann et al., 2006; Lu et al, 2009). Interestingly, the levels of *Cntf* mRNA have been found to be elevated during the remyelination phase in mice with cuprizone-induced demyelination (Gudi et al., 2011) and the intracranial injections of CNTF have led to increased amounts of MOG (myelin oligodendrocytes glycoprotein) in these animals (Salehi et al., 2013). Moreover, CNTF treatment has also been shown to be related to the increased expression of myelin proteins in mouse oligodendrocytes cultures (Modi et al., 2013).

In addition to the above-mentioned association of CNTF with myelination, other IL-6 family cytokines have also been related to increased myelination levels in myelinating co-cultures (Stankoff et al., 2002), maintenance of neural stem cells *in vivo* (Shimazaki

et al., 2001), immunoregulation and neuroprotection in EAE (Fitzgerald et al., 2007; Gurfein et al., 2009; Yang et al., 2012a; Jafarzadeh et al., 2014), and modulation of the expression of genes involved in the remyelination process in demyelinated sites of ethidium bromide-induced acute demyelination in mice (Glezer et al., 2010). Despite the above-mentioned important roles of these cytokines, mice deficient in one of the members of the IL-6 family have milder phenotypes than expected (reviewed in Fasnacht et al., 2008) such as mild motor neuron degeneration in CNTF-deficient mice (Masu et al., 1993). This has been attributed to the redundancy of IL-6 family cytokines, which bind specific α-receptors that induces the homo- or heterodimerisation of the transmembrane protein, GP130, to complete the IL-6 family cytokine signaling (Fig 1.6, Heinrich et al., 1995; reviewed in Kraakman et al., 2013). Because GP130-deficient mice die in early embryonic stages (Yoshida et al., 1996), conditional transgenic mice were also generated to observe the effects of GP130-dependent signaling. One example is the GFAP-$Cre^{+/-}$$gp130^{fl/fl}$ mouse line (Drogemuller et al., 2008).

Primary cultures from GFAP-$Cre^{+/-}$$gp130^{fl/fl}$ mice were exploited to observe myelination in the absence of the expression of *Gp130* specifically in the supporting astrocyte monolayer. These mice were termed 'Cre positive (Cre+)' in short since these mice harboured the gene for Cre recombinase with expression under the control of the *GFAP* promoter. Cre recombinase inactivates the target gene, *Gp130* in this case, by removing the 'floxed' (fl) DNA sequence flanked by two loxP sites (Lakso et al., 1992; Pichel et al., 1993). On the other hand, the mice, which carried the floxed gene but not the gene for Cre recombinase, were not different to the wild type mice and were termed GFAP-$Cre^{-/-}$$gp130^{fl/fl}$ or 'Cre negative (Cre-)' in short. Embryos from both genotypes were also used to set up spinal cord myelinating cultures, where myelination levels were compared, as described in this chapter.

In addition to the microarray gene expression profiling analysis that revealed potential transcripts to be associated with CNTF signaling in embryonic rat spinal cord myelinating cultures as explained in Chapter 3, those data sets were also used in a web-based program, called oPOSSUM 3.0, in attempt to identify prospective transcription factors associated with CNTF mechanisms in these cultures. Moreover, to gain a deeper insight into the CNTF functions, the metabolites produced in and secreted by astrocyte monolayers were also compared using mass spectrometry-based metabolomics. Thus, the effect of CNTF in neurosphere-derived astrocytes and embryonic rat spinal cord myelinating cultures were analysed from different aspects, some of which were presented in Chapter 3 and the rest of which will be presented in this chapter.

6.2 Aims

The overall aim of this chapter was to determine the mechanism of our previous results of CNTF promoting myelination *in vitro*. Specifically we hypothesised that:

- The seeding density of neurosphere-derived astrocytes would have an effect on the way different concentrations of CNTF treatment affect myelination and neurite density of rat embryonic spinal cord PLL-myelinating cultures.

- The timing of CNTF treatment would affect myelination and neurite density of rat embryonic spinal cord PLL- and TnC-myelinating cultures.

- CNTF treatment would affect astrocyte reactivity as assessed by protein expression of GFAP and nestin and detected by immunocytochemistry in neurosphere-derived rat PLL- and TnC-astrocytes.

- Neurosphere-derived astrocytes obtained from mice lacking *Gp130* expression in astrocytes would present different levels of astrocyte reactivity assessed by GFAP immunoreactivity compared to cultures from wild type mice.

- Embryonic spinal cord myelinating cultures prepared using tissue from mice lacking *Gp130* expression in astrocytes would present a lower level of myelination compared to cultures from wild type mice. CNTF treatment would increase while treatment with neutralising antibody against CNTF would lower the myelination level in wild type cultures; whereas, these treatments would have no effect on myelination in transgenic cultures due to the absence of Gp130 expression.

- The changes CNTF treatment triggers on gene expression in rat myelinating cultures (Array 2) require signaling provided by transcription factors. Thus, a web-based program that detects over-representative conserved transcription factor binding sites was used to detect possible transcription factors involved in CNTF signaling in rat myelinating cultures.

- CNTF treatment would stimulate the neurosphere-derived rat astrocytes to produce and/or secrete metabolites that could play a role in myelination. The metabolites detected by mass spectrometry would be different in PLL-astrocytes and TnC-astrocytes.

6.3 Results

6.3.1 The effects of CNTF on myelination in embryonic rat spinal cord myelinating cultures

Previously our lab had shown that CNTF added to embryonic rat spinal cord myelinating cultures promoted myelination (Nash et al., 2011b). Failing to confirm this observation in my experiments, I hypothesised that one of the factors leading to different results could be the difference in density of the astrocyte monolayers, used as supporting monolayers for the myelinating cultures. However, myelinating cultures treated with 1 ng/ml of rat recombinant CNTF did not have any change in myelination despite using neurosphere-derived astrocytes with different seeding densities (Chapter 5, Fig 5.9). In this chapter, the PLL-myelinating cultures were treated with CNTF at different concentrations to provide a more detailed analysis for the CNTF effect on myelination (Fig 6.1). Even though the astrocyte seeding density of 250 x 10^3 cells/ml was selected to be the optimum cell density to use to prepare astrocyte monolayers to be used for spinal cord myelinating cultures (Chapter 5), astrocytes with different seeding densities were also used in this experiment to clarify whether the concentration of the exogenous CNTF influences the myelination levels differently in cultures with different densities.

As seen in Fig 6.1, CNTF treatment at the concentrations of 0.5, 1, 1.5, and 2 ng/ml did not induce any significant change in myelination levels or neurite density of the spinal cord myelinating cultures, plated on astrocyte monolayers with the seeding density of 125, 250, 375, and 500 x 10^3 cells/ml. Maintaining the myelinating cultures on astrocyte monolayers with different densities did not have an effect on the myelination levels in the presence of exogenous CNTF at any concentrations examined. On the other hand, analysing the myelinating cultures on astrocytes with the seeding density of 250 x 10^3 cells/ml separately showed a significant reduction in myelination levels with 2 ng/ml of CNTF treatment (Fig 6.1 C). Therefore, it is likely that CNTF becomes inhibitory for myelination at higher concentrations without affecting the neurite density. The expected increase in myelination levels was not detected for 0.5, 1, or 1.5 ng/ml of CNTF treatment.

CNTF treatments at 1 ng/ml were also used to condition astrocyte monolayers before spinal cord myelinating cultures were plated on top of them. These cultures were termed ‘pre-treated’ myelinating cultures and they were not treated with CNTF after the dissociated spinal cord cells were plated on top of the conditioned astrocyte monolayers. These pre-treatments appeared to affect myelination levels (Fig 6.2). The pre-treated PLL-myelinating cultures presented significantly higher myelination levels

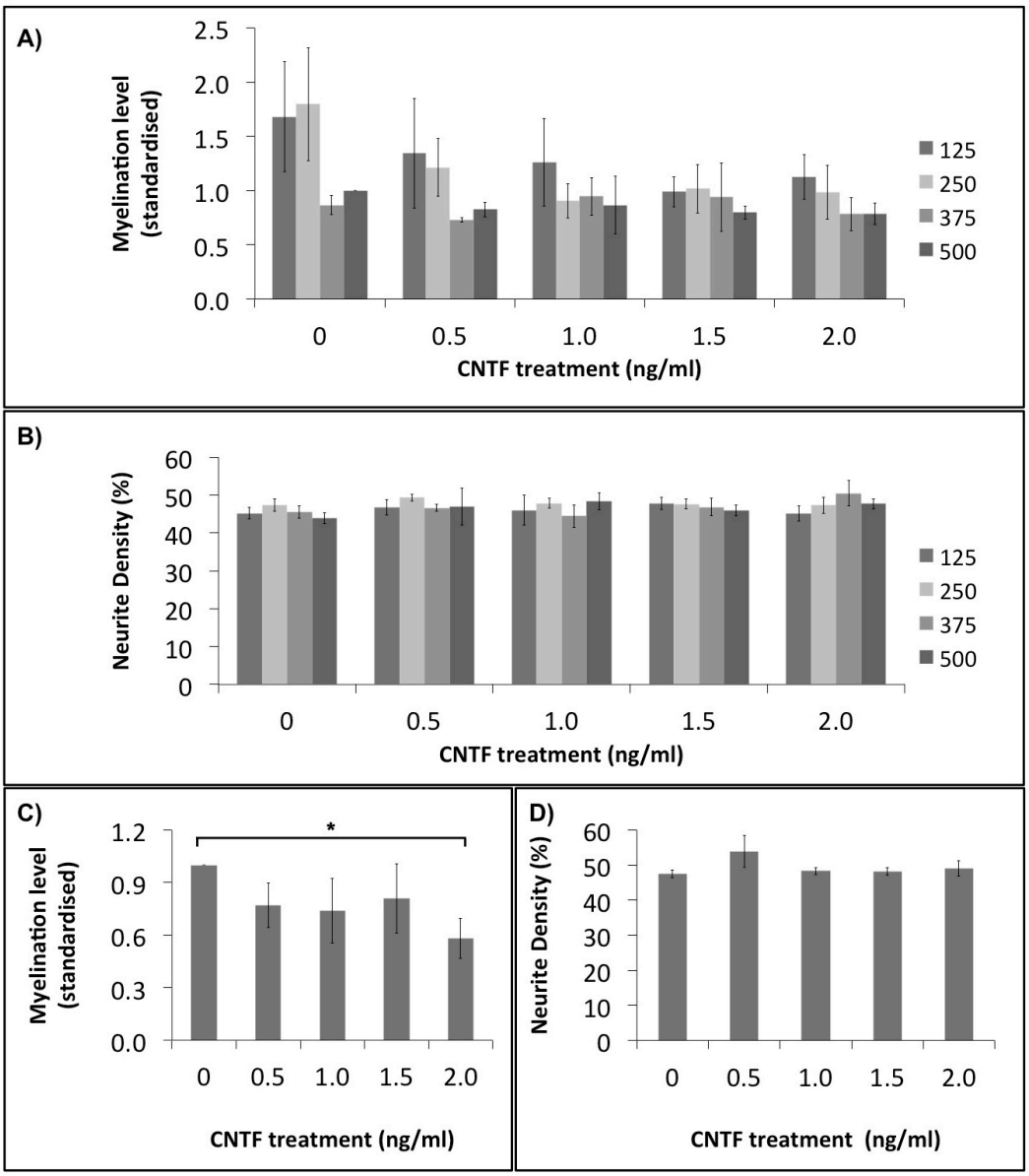

Figure 6. 1 The effects of CNTF on myelination levels in rat spinal cord myelinating cultures appear not to be related to the seeding density of astrocytes.

Embryonic rat spinal cord myelinating cultures were set up using neurosphere-derived rat astrocytes that were plated on PLL-coated glass coverslips and at seeding density of 125, 250, 375 or 500 x 10^3 cells/ml. The spinal cord myelinating cultures were treated with 0.5, 1, 1.5 or 2 ng/ml of recombinant rat CNTF starting from 12 DIV onwards and they were immunostained at 24 DIV using the AA3 antibody to detect PLP and hence mature myelin and SMI-31 to detect neurites. Images were captured using Olympus BX51fluorescent microscope and Image-Pro imaging software. Myelination percentages and neurite density were quantified using "myelin.cp" pipeline in Cell Profiler. **A)** Myelination percentage is shown as standardised to the untreated cultures with the highest seeding density of 500 x 10^3 cells/ml. CNTF does not lead to any significant change on myelination levels (**A**) or neurite density (**B**) in any of the myelinating cultures examined. The seeding density of astrocyte cultures does not have a significant effect on myelination level (**A**) or neurite density (**B**) in untreated or in CNTF-treated myelinating cultures. Experiments in A&B were repeated three times. **C&D)** Spinal cord myelinating cultures that were plated on astrocytes, from neurosphere concentration of 250 x 103 cells/ml, were treated with CNTF at different concentrations. These experiments were repeated four times. Myelination percentage decreases significantly upon CNTF treatment at 2 ng/ml (*P≤0.05); while, no significant change is observed in neurite density. One-way repeated measures ANOVA test was applied to the results to detect any possible significance. The error bars represent ± standard error of the mean. CNTF: ciliary neurotrophic factor; DIV: days *in vitro*; PLL: poly-L-lysine; PLP: proteolipid protein.

compared to 1) untreated PLL-myelinating cultures, 2) untreated TnC-myelinating cultures, 3) pre-treated TnC-myelinating cultures, 4) CNTF-treated TnC-myelinating cultures. Neurite density did not show any significant change between these conditions (Fig 6.2 B). There was a tendency of an increase in myelination levels in CNTF-treated PLL-myelinating cultures compared to untreated PLL-myelinating cultures but it appears that CNTF has a more potent stimulatory effect on myelination when applied to the young, confluent feeder astrocyte monolayers also suggested by Nash et al. (2011b). On the other hand, this effect was not observed in TnC-myelinating cultures. The TnC-myelinating cultures at all three conditions (untreated, pre-treated, CNTF-treated) appeared to show similar myelin levels, which were also not significantly different to those in untreated PLL-myelinating cultures.

In conclusion, embryonic rat spinal cord myelinating cultures did not present significantly different myelination levels when treated with 0.5, 1, and 1.5 ng/ml of CNTF. The seeding density of the astrocyte monolayers that were used for these myelinating cultures did not alter this lack of effect of CNTF, either. A further analysis of the cultures that were set up with astrocyte monolayers with the seeding density of 250 x 10^3 cells/ml showed reduced myelination levels with 2 ng/ml of CNTF treatment. CNTF treatment stimulated the myelination in PLL-myelinating cultures but not in TnC-myelinating cultures only when the astrocyte monolayers were initially pre-treated with 1 ng/ml of CNTF.

6.3.2 The effects of CNTF in neurosphere-derived rat astrocyte cultures

CNTF has previously been reported to activate astrocytes both *in vitro* and *in vivo*, a phenomenon that has been observed mainly based on the increase of GFAP expression and cell hypertrophy (Levison et al., 1996; White and Jakeman, 2008). Therefore, the untreated and CNTF-treated PLL- and TnC-astrocytes were immunostained for GFAP and nestin expressions in an attempt to observe possible differences in astrocyte phenotypes under these conditions. Nestin has also been used as a marker for astrocyte reactivity as explained previously in Chapter 5.

The striatum-derived rat neurospheres were plated down on PLL- or TnC-coated glass coverslips at a seeding density of 250 x 10^3 cells/ml, maintained for 9 DIV and then used for immunocytochemistry. The average DAPI positive (DAPI+) cell numbers did not differ between different conditions at the end of the cultural period (Fig 6.3 A). Because the initial seeding density was the same for all the cultures, it can be concluded that 1 ng/ml of exogenous CNTF did not change the total number of cells detected in astrocyte

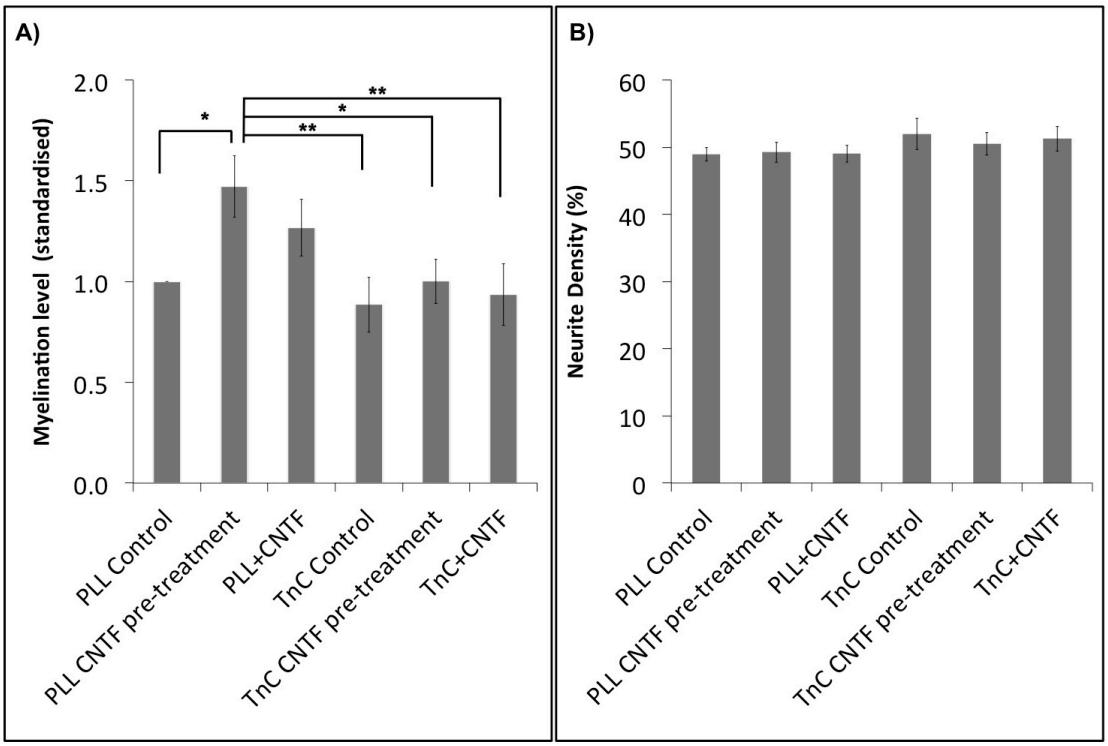

Figure 6. 2 The effects of CNTF treatments on myelination levels in embryonic rat spinal cord myelinating cultures.

Embryonic rat spinal cord myelinating cultures were plated on neurosphere-derived astrocytes that were seeded on PLL- or TnC-coated glass coverslips. Some of astrocytes were previously treated with 1 ng/ml of recombinant rat CNTF before they were used to set up the spinal cord myelinating cultures. Those myelinating cultures were termed “pre-treated” and were not treated later with CNTF. The spinal cord myelinating cultures that were set up using untreated astrocytes were treated with 1 ng/ml of CNTF from 12 DIV onwards. The cultures were immunostained at 24 DIV using the AA3 antibody to detect PLP and hence mature myelin and SMI-31 to detect neurites. Images were captured using Olympus BX51fluorescent microscope and Image-Pro imaging software. Myelination percentages and neurite density were quantified using “myelin.cp” pipeline in Cell Profiler. A) Myelination percentage is shown as standardised to the untreated cultures on PLL-astrocytes (PLL-control). CNTF treatment increases the myelination level in PLL-myelinating cultures only when pre-treated astrocytes are used (* P≤0.05). Pre-treated PLL-myelinating cultures also present a significantly higher myelination level compared to untreated, CNTF pre-treated, and CNTF-treated TnC-myelinating cultures (* P≤0.05, ** P≤ 0.01). B) CNTF pre-treatments or treatments do not affect the neurite density significantly. The experiments were repeated five times. One-way repeated measures ANOVA test was applied to the results to detect any possible significance. The error bars represent ± standard error of the mean. CNTF: ciliary neurotrophic factor; DIV: days *in vitro*; PLL: poly-L-lysine; PLP: proteolipid protein; TnC: tenascin C.

monolayers hence the rate of proliferation. CNTF did not appear to affect the average GFAP and nestin intensities detected per image, either, which were measured in Image J using the images captured by the fluorescent microscopy (Fig 6.3 B). Similarly, all the cultures showed comparable levels for the average GFAP and nestin intensities per cell (Fig 6.3 C), which could also be observed in the representative images (Fig 6.3 D-G). In conclusion, CNTF did not appear to activate astrocytes based on their GFAP and nestin expressions detected by immunocytochemistry.

6.3.3 The effects of CNTF in astrocytic-Gp130 knockout mouse astrocytes and spinal cord myelinating cultures

The effects of exogenous CNTF on myelination were also investigated in embryonic mouse spinal cord myelinating cultures. Transgenic C57BL/6 mice that lacked the astrocytic expression of *Gp130*, a component of the CNTF receptor complex, have been previously shown to present reduced numbers of GFAP positive astrocytes and an aggravated disease course when infected with *Toxoplasma gondii* or when immunised with MOG_{35-55} to generate encephalitis or EAE, respectively (Drogemuller et al., 2008; Haroon et al., 2011). Especially due to severe demyelination observed in these animals, CNTF signaling in astrocytes has been suggested to have positive effects on myelination (Haroon et al., 2011). In addition, CNTF-treated astrocytes were shown to increase the myelination levels in rat spinal cord myelinating cultures as explained above (Fig 6.2). Therefore, both neurosphere-derived astrocyte cultures and spinal cord myelinating cultures, generated from the CNS of these transgenic mice, were analysed to observe the effects of the absence of the astrocytic CNTF signaling.

The heterozygous mice that carried the allele for the Cre recombinase (GFAP-$Cre^{+/-}$ $gp130^{fl/fl}$, Cre positive) and the homozygous mice that lacked this gene (GFAP-$Cre^{-/-}$ $gp130^{fl/fl}$, Cre negative) were crossed to obtain a litter that would consist of Cre negative (Cre-) and Cre positive (Cre+, knockout) pups with a 50% possibility of occurrence for each genotype (Fig 2.1). The striatum tissue obtained from each pup was treated and cultured separately. The striatum-derived neurospheres that were generated from the pups with the same *Cre* genotype were pulled down together to generate astrocyte monolayers. These astrocytes were immunostained for GFAP and with the O4 antibody to observe morphological differences between the Cre- and Cre+ mouse astrocyte cultures (Fig 6.4).

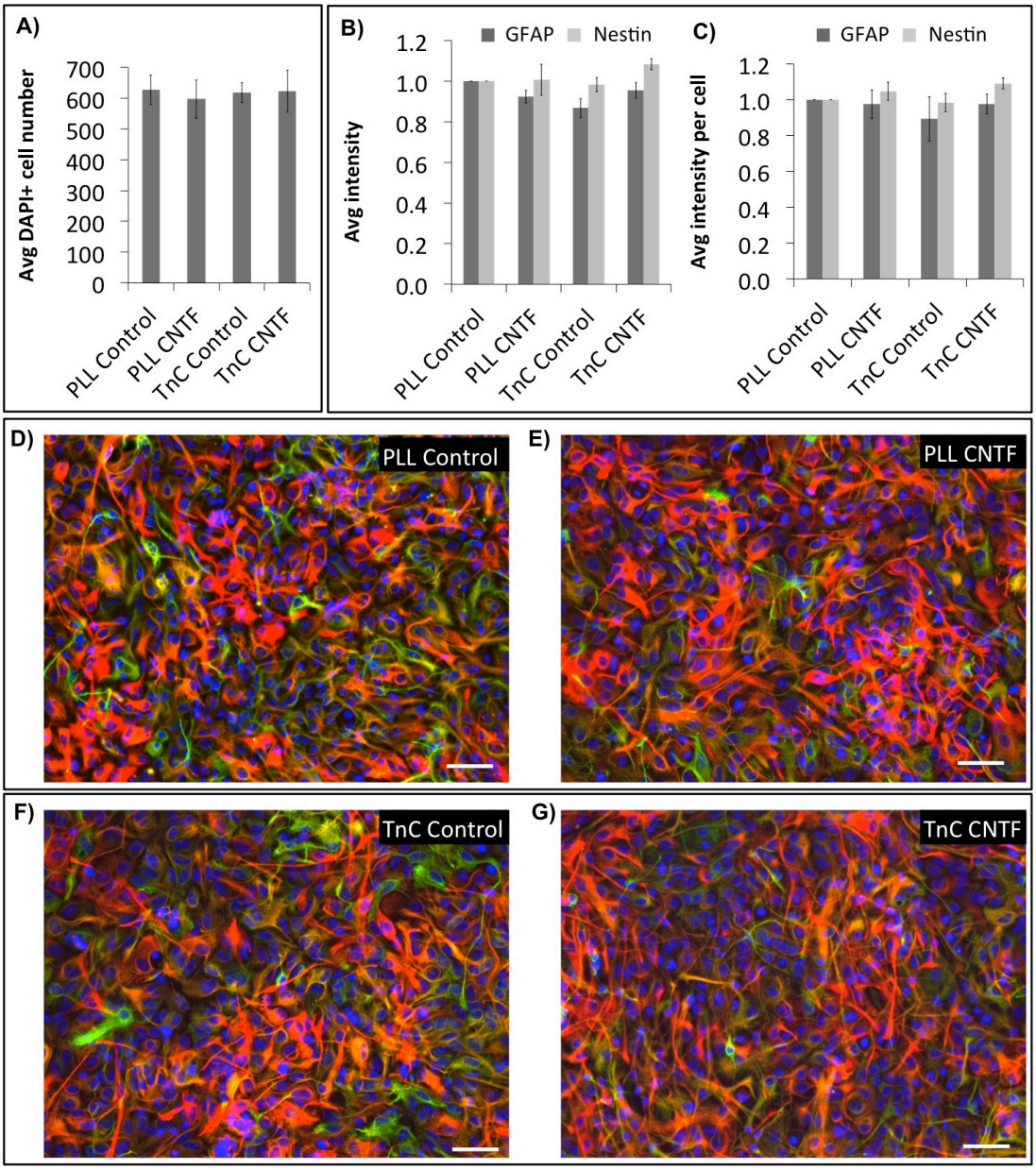

Figure 6. 3 CNTF treatment does not affect GFAP and nestin intensities detected in the neurosphere-derived rat astrocyte cultures.

Striatum-derived rat neurospheres were plated down on PLL- or TnC-coated glass coverslips at 5 DIV at a concentration of 250 x 10^3 cells/ml and were left to differentiate into astrocytes in medium containing 10% FBS. Astrocytes were treated with 1 ng/ml of recombinant rat CNTF after 5 and 7 DIV. The confluent astrocyte cultures were used for immunocytochemistry at 9 DIV to detect GFAP and nestin expressions. **A)** The number of total DAPI positive cells was quantified using Cell Profiler and was presented as average (avg) cell number per filed of view, which did not differ significantly between astrocytes at different conditions. **B)** Image J was used to quantify the mean brightness of the fluorescence detected in green (GFAP) and red (nestin) channels per image. This value was multiplied by the whole image area to calculate the total intensity of GFAP or nestin fluorescence. Avg intensity per image values were standardised to the untreated PLL-astrocytes for GFAP and nestin separately. CNTF treatment or the use of different glass-coating substrates did not affect avg GFAP or nestin intensity per image significantly. **C)** Avg GFAP and nestin intensity per cell was calculated for each image as a ratio of the total intensity to the total cell number of the image. The averages were standardised to the values of the untreated PLL-astrocytes for GFAP and nestin separately and were not affected significantly by the CNTF treatment or the use of different substrates. Representative images present untreated and CNTF-treated astrocytes on PLL- **(D, E)** or TnC-coated coverslips **(F, G)**. Experiments were repeated three times. The error bars represent ± standard error of the mean. One-way repeated measures ANOVA test was used to detect any possible significance. Scale bar represents 50 μm for all images. Avg: average; CNTF: ciliary neurotrophic factor; DIV: days *in vitro*; FBS: foetal bovine serum; GFAP: glial fibrillary acidic protein; TnC: tenascin C.

Both Cre- and Cre+ astrocytes were generated by plating down neurospheres at a seeding density of 250 x 10^3 cells/ml. Therefore, both astrocyte cultures were expected to present similar average DAPI+ cell numbers at the end of their cultural period unless the distinct genotypes affected the cell numbers. As expected, there was no significant difference between the average DAPI+ cell numbers of the astrocyte cultures (Fig 6.4 A). Similarly, the average GFAP intensity per image or per cell did not differ between the Cre- and Cre+ astrocytes, either (Fig 6.4 B), suggesting that inhibition of GP130 signaling in mouse astrocytes may not affect the astrocyte reactivity based on their GFAP expressions detected by immunocytochemistry.

The number of cells labelled with the O4 antibody termed O4 positive (O4+) cells were also detected using immunocytochemistry. The majority of these cells appeared to be also positive for GFAP staining (Fig 6.4 C-E), which suggested that they were type-2 astrocytes rather than oligodendrocytes (Raff et al, 1983; Aloisi et al., 1988). Even though the number and the standardised percentage of these GFAP and O4+ (GFAP&O4+) cells presented a trend towards an increase in Cre+ astrocytes, the change was not found to be significant (Fig 6.4 C&E). The representative images of the immunostained cultures correlate with the above-mentioned findings and also show that O4 negative and O4 positive astrocytes between the Cre- and Cre+ astrocyte cultures do not appear to be different in terms of cell size or the number/length of the cell processes (Fig 6.4 F-I).

Cre- and Cre+ astrocytes were also used as feeder monolayers for dissociated spinal cords that were obtained from wild type C57BL/6 mouse embryos. These spinal cord myelinating cultures were treated with CNTF to observe the effect of exogenous CNTF on myelination. As seen in Fig 6.5, CNTF did not alter the myelination levels significantly in Cre- or Cre+ mouse myelinating cultures. Therefore, the presence or the absence of the expression of the astrocytic *Gp130* does not appear to affect myelination in these mouse myelinating cultures. In addition, the myelinating cultures were also treated with a neutralising antibody against endogenous CNTF starting from 12 DIV onwards (Fig 6.5 C&D). This treatment did not affect the myelination levels or the neurite density, either.

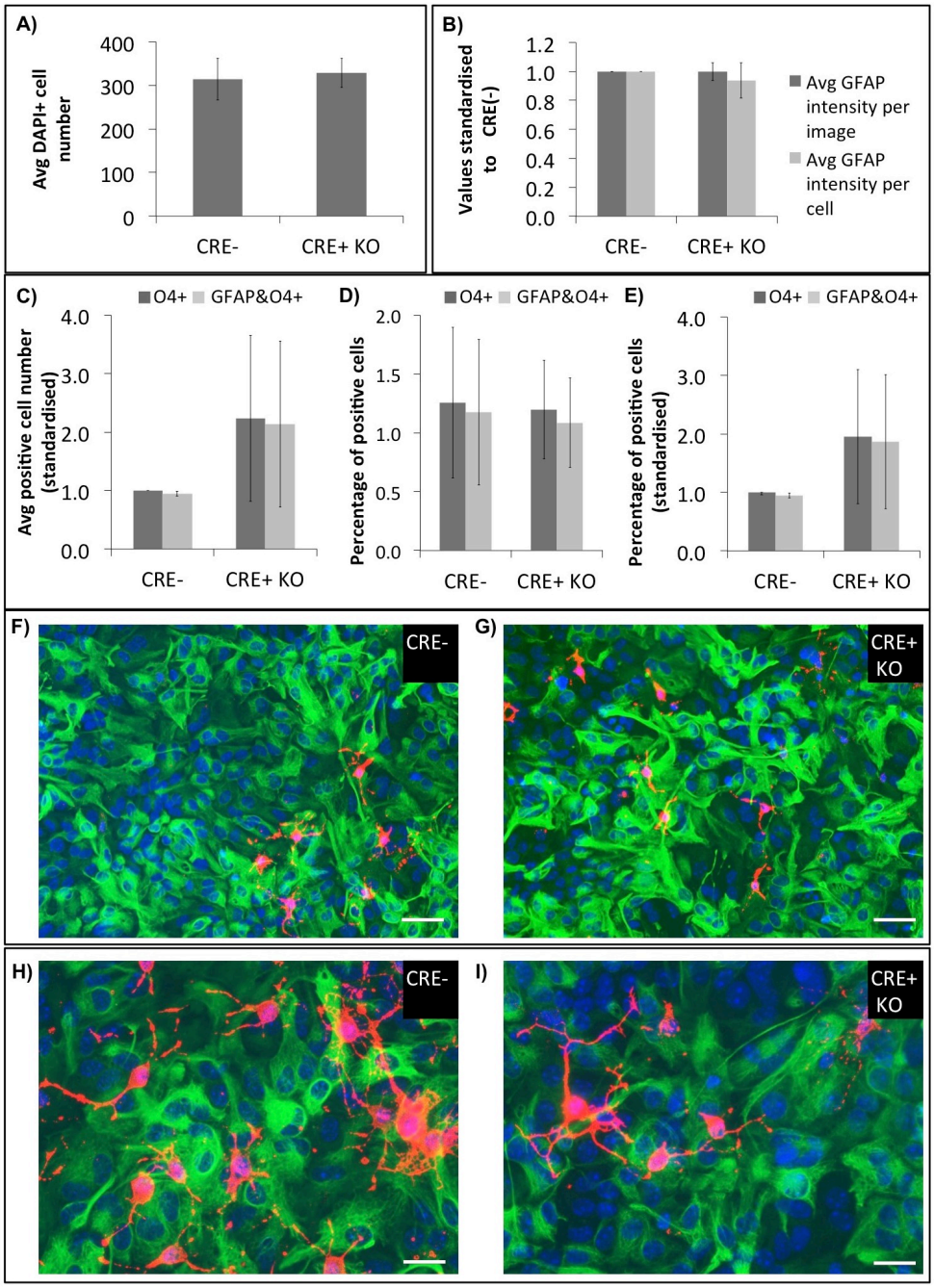

Figure 6. 4 Astrocytes from wild type and astrocytic-gp130 knockout mice do not differ in terms of GFAP intensity.

Striatum-derived mouse neurospheres, obtained from GFAP-Cre$^{-/-}$gp130$^{fl/fl}$ (Cre negative, wild type) and from GFAP-Cre$^{+/-}$gp130$^{fl/fl}$ (Cre positive, knockout) transgenic mice on a C57BL/6 background, were plated down on PLL-coated glass coverslips at 5 DIV at a concentration of 250 x 10^3 cells/ml. They were left to differentiate into astrocytes in medium containing 10% FBS. The confluent astrocyte cultures were immunolabelled for O4 antibody (red) and GFAP (green). **A)** The number of total DAPI positive cells was quantified using Cell Profiler and was presented as average cell number per field of view, which did not differ significantly between astrocytes from mice of the two genotypes. **B)** Image J was used to quantify the mean brightness of the fluorescence detected in green channel, representing GFAP expression. This value was multiplied by the whole image area to calculate the total intensity of GFAP per image. Average GFAP intensity per cell was calculated for each image as a ratio of the total intensity to the total cell number of the image. Both averages were standardised to the values detected in the Cre negative mice. A significant change was not observed in average GFAP intensity per cell or in average GFAP intensity per image between the mouse astrocytes of two genotypes. **C)** The cells, which were positive for O4 and for both O4 and GFAP (GFAP&O4) were counted manually using Image J and were presented as average cell number. This was standardised to the O4+ values of Cre negatives. **D)** They were also presented as percentages of the total number of cells per image. **E)** The percentages were standardised to the O4+ values of the Cre negatives. Representative images present astrocytes from Cre negative **(F, H)** or Cre positive mice **(G, I)**. Experiments were repeated three

times. The error bars represent ± standard error of the mean. One-way repeated measures ANOVA test was applied to the results to detect any possible significance. Scale bar represents 50 μm for F&G and 25 μm for H&I. Avg: average; DIV: days *in vitro*; FBS: foetal bovine serum; GFAP: glial fibrillary acidic protein; KO: knockout; PLL: poly-L-lysine; WT; wild type.

Mouse myelinating cultures were also set up by plating down dissociated spinal cords from Cre- and Cre+ transgenic mouse embryos on top of PLL-coated glass coverslips without including any feeder astrocyte monolayers. A Cre- mouse and a Cre+ mouse were mated to obtain a litter that would consist of Cre- and Cre+ embryos with a 50% possibility of occurrence for each genotype (Fig 2.1). Therefore, the spinal cord from each embryo was treated separately to set up the myelinating cultures. The myelinating cultures from each embryo had its own control and its own CNTF treatments. The embryos were genotyped for *Cre* expression using tail DNA after the myelinating cultures were set up. Thus, the results obtained from Cre- and Cre+ embryos were later pulled down to obtain average values for myelination levels and neurite density at different conditions. This was considered as one experimental repeat because embryos were used from the same litter.

Unfortunately, the analysis could only be done using Cre+ myelinating cultures (Cre+ spinal cords on PLL-coated coverslips) without being able to compare them with the Cre- myelinating cultures. The healthy myelinating cultures that could be maintained until 24 DIV and analysed successfully consisted of Cre+ samples only. The majority of the mouse litters (35 out of 44) contained more than 50% Cre+ embryos (Fig 6.6 A&B). There were even 10 litters, where all the embryos (100%) were found to be Cre+. The most likely explanation for this observation is that at least one of the GFAP-Cre$^{+/-}$ animals must have been mislabelled as GFAP-Cre$^{-/-}$ due the absence of a clear band in agarose gel electrophoresis possibly due to a failed PCR resulting from a degraded or contaminated DNA sample. Breeding GFAP-Cre$^{+/-}$ with another GFAP-Cre$^{+/-}$ due to mislabelling would result in 25% GFAP-Cre$^{+/+}$, 50% GFAP-Cre$^{+/-}$, and 25% GFAP-Cre$^{-/-}$ leading to a litter with 75% Cre+ genotype that can be seen for some litters in Fig 6.6 B. Crossing a GFAP-Cre$^{+/+}$ animal with GFAP-Cre$^{-/-}$ would then result in litters with 100% Cre+ genotype. Some of the 44 litters, for which the details were presented in Fig 6.6 B, were used 1) to set up astrocyte monolayers, 2) to generate spinal cord myelinating cultures, 3) for optimisation purposes like identifying the best PLL solution that would help the spinal cord cultures stick better to the glass coverslips and thus generate healthier cultures, 4) to practise setting up myelinating cultures since working with such small mouse embryos required an adaptation period, during which the cultures did not appear healthy enough to be used for analyses. In addition, the spinal cords from the

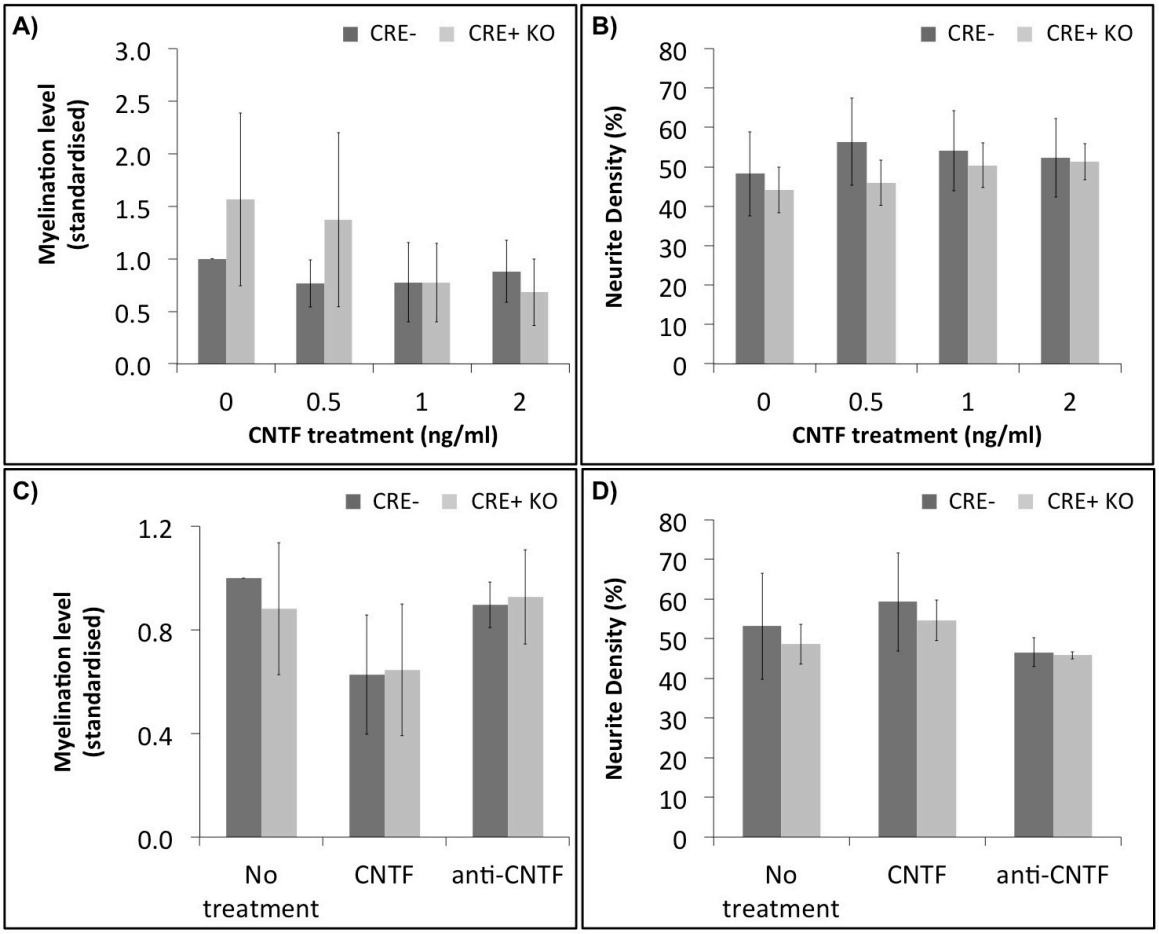

Figure 6. 3 CNTF does not affect myelination levels in wild type or astrocytic-gp130 knockout mouse spinal cord myelinating cultures

Wild type (GFAP-Cre$^{-/-}$gp130$^{fl/fl}$, Cre negative) and astrocytic-gp130 knockout (GFAP-Cre$^{+/-}$gp130$^{fl/fl}$, Cre positive) C57BL/6 mice were used to set up neurosphere-derived astrocyte cultures, plated on PLL-coated glass coverslips at a seeding density of 250 x 10^3 cells/ml. Dissociated spinal cords, obtained from wild type C57BL/6 mouse embryos, were plated on these astrocytes to form the spinal cord myelinating cultures. The myelinating cultures were treated with 0.5, 1, or 2 ng/ml of recombinant rat CNTF starting from 12 DIV onwards and they were immunostained at 24 DIV using the AA3 antibody to detect PLP and hence mature myelin and using SMI-31 to detect neurites. Images were captured using Olympus BX51fluorescent microscope and Image-Pro imaging software. Myelin percentages and neurite densities were quantified using "myelin.cp" pipeline in Cell Profiler. **A&B)** Myelination percentage is shown as standardised to untreated wild type cultures. CNTF does not appear to affect myelination levels or neurite densities in the Cre negative or Cre positive mouse spinal cord myelinating cultures significantly. The myelination levels and neurite density between the wild type and knockout mouse myelinating cultures do not differ significantly, either. **C&D)** Wild type and knockout mouse spinal cord myelinating cultures were also treated with 1 ng/ml of CNTF and 2 μg/ml of rat anti-CNTF neutralising antibody, which did not show any significant effects on the myelin levels or the neurite density. All experiments were repeated three times. One-way repeated measures ANOVA test was applied to the results to detect any possible significance. The error bars represent ± standard error of the mean. CNTF: ciliary neurotrophic factor; DIV: days *in vitro*; PLL: poly-L-lysine; PLP: proteolipid protein.

few Cre- embryos in some litters did not reveal a high cell yield probably due to only dissecting out smaller pieces of tissue and therefore, the cell suspension was not dense enough to generate enough number of coverslips to complete the experiments. Consequently, there were only three litters that could be used to present the effect of CNTF in embryonic mouse myelinating cultures, consisting of transgenic spinal cords on top of PLL-coated coverslips, and these cultures did not contain any samples from Cre- embryos, which would be the controls for the experiments (Fig 6.6 C&D). CNTF treatments did not show any significant changes on myelination levels in these astrocytic *Gp130* deficient mouse cultures. The average myelination level was found to be 3.8% in these cultures, which is not very different from 4.7% that was the average myelination percentage in the mouse myelinating cultures, which were set up using wild type spinal cords on top of transgenic astrocytes (Fig 6.5 A&B). On the other hand, CNTF treatments appeared to increase the neurite density in the Cre+ spinal cord myelinating cultures on PLL-coverslips (Fig 6.6 D).

In conclusion, the inactivation of the *Gp130* gene using the Cre/loxP system under the control of the *GFAP* promoter in astrocytes of C57BL/6 mice did not affect **1)** the morphology of the astrocyte cultures based on their GFAP expressions detected by immunocytochemistry, and the amount of contaminating type-2 astrocytes, **2)** the potency of these astrocyte cultures to promote myelination. The myelinating cultures consisting of transgenic spinal cords on PLL-coated coverslips could only be analysed using Cre+ samples, which showed that neurite density increased upon CNTF treatments despite the inhibition of astrocytic CNTF signaling via GP130 receptor, but presented no difference in myelination levels.

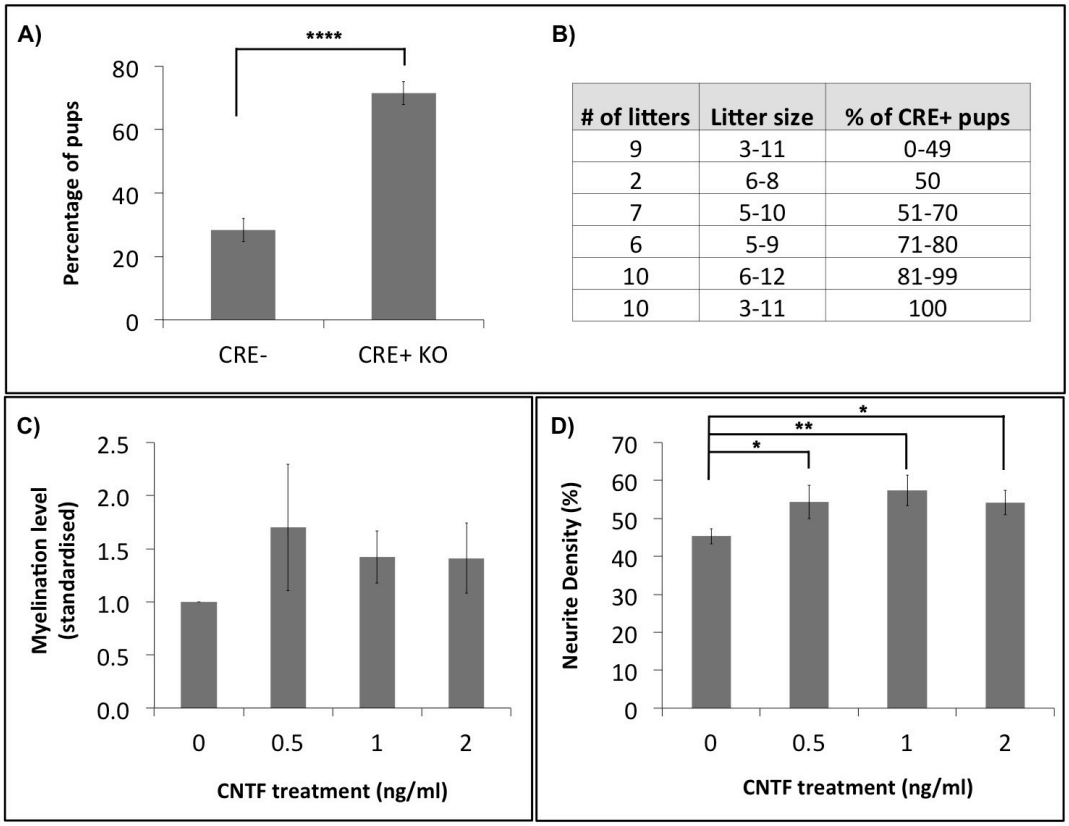

Figure 6. 4 CNTF titration in astrocytic-gp130 knockout mouse spinal cord cultures does not show a significant effect on myelination level.

The mouse embryos from the mating of GFAP-Cre$^{-/-}$gp130$^{fl/fl}$ (Cre negative) and GFAP-Cre$^{+/-}$gp130$^{fl/fl}$ (Cre positive) transgenic strains were used to obtain dissociated spinal cords that were plated on PLL-coated glass coverslips. The embryonic tissue was later used for genotyping the mouse litters. **A)** The number of Cre positive and negative transgenic mouse pups were expressed as percentages within each litter. When 44 litters were analysed, the percentage of Cre positive pups was found to be significantly higher than the percentage of Cre negative pups (**** P≤0.0001). The statistical significance was detected using paired Student's t-test. **B)** In 10 litters with varying litter sizes, all of the mouse pups were Cre positive. **C&D)** Spinal cord myelinating cultures obtained from three litters provided healthy cultures to analyse myelination. The cultures were treated with 0.5, 1, or 2 ng/ml of rat recombinant CNTF starting from 12 DIV onwards and the cultures were immunostained at 24 DIV using the AA3 antibody to detect PLP and hence mature myelin and using SMI-31 to detect neurites. Images were captured using Olympus BX51 fluorescent microscope and Image-Pro imaging software. Myelination percentages and neurite density were quantified using "myelin.cp" pipeline in Cell Profiler. Myelination percentage is shown as standardised to the value of untreated cultures. CNTF did not affect myelination levels significantly in Cre positive transgenic mouse spinal cord cultures. However, it appeared to increase neurite density significantly compared to the untreated cultures (* P<0.05, ** P<0.01). One-way repeated measures ANOVA test was applied to the results to detect any possible significance. The error bars represent ± standard error of the mean. CNTF: ciliary neurotrophic factor; DIV: days *in vitro*; PLL: poly-L-lysine; PLP: proteolipid protein.

6.3.4 The possible transcription factors that could play a role in CNTF signaling in rat spinal cord myelinating cultures

A microarray gene expression profiling was carried out previously to identify the transcriptional changes between untreated or CNTF-treated embryonic rat spinal cord cultures plated on either PLL- or TnC-astrocytes (Array 2, Chapter 3). To further analyse the possible roles of CNTF in myelinating cultures, the data obtained from Array 2 were used to form a list of putative transcription factors (TFs) involved in CNTF-signaling. The transcripts, which were differentially regulated upon CNTF treatment 4 and 24 hours later, were entered into a web-based program called oPOSSUM 3.0 that detects over-represented conserved transcription factor binding sites (TFBSs) in the *cis*-regulatory regions (non-coding DNA) of a set of human, mouse, fly, worm and yeast genes (Kwon et al., 2012). This process has been named as Single Site Analysis (SSA) in the program and the JASPAR database has been used as the source of DNA-binding profiles (Portales-Casamar et al., 2010). Because mouse is the closest species to the rat among the alternatives provided in the program, SSA was carried out on mouse genes.

The up-regulated and down-regulated transcripts between two conditions were analysed separately as presented in Table 6.1. The TFBS hits were searched maximum 10,000 bp upstream/downstream from the Ensembl-annotated transcription start sites since this sequence length was adjusted by the developers of the program to reflect the intergenic distances. The analysis was carried out for all six DNA sequence distances available in the program; namely, 2000/0, 2000/2000, 5000/2000, 5000/5000, 10000/5000, and 10000/1000 bp (Table 6.1). The TFs, whose DNA-binding sites were detected in the genes analysed at high enough levels to be statistically significant, are presented in Table 6.1 separately for each DNA sequence length. These results were based on the values with Z-score≥10 and Fisher score≥7 (Kwon et al., 2012). Z-score and Fisher score reflect **1)** the change in the relative number of TFBS motifs and **2**) the number of genes with the TFBS motifs, respectively, in the foreground set *vs*. the background set. The results in Table 6.1 are significant in terms of both of the scoring methods and hence comparisons.

The transcripts that were differentially regulated upon CNTF treatment in PLL-myelinating cultures did not reveal any possible TFs involved with their differential expression (Table 6.1). In contrast, the analysis of down-regulated transcripts 4 hour after CNTF treatment in TnC-myelinating cultures presented CTCF, E2F1, INSM1, KLF4, MZF1_1-4, RREB1, SP1, SRF, STAT3, TCFCP2L1, and the protein complexes PPARG::RXRA and TLX1::NFIC as putative TFs that could be responsible for the CNTF-associated changes in these cultures (Table 6.1). These TFs contain different types of DNA-binding

domains such as zinc coordinating (CTCF, INSM1, KLF4, MZF1, PPARγ:RXRα, RREB1, SP1), basic helix-loop-helix (E2F1), helix-turn-helix (TLX1::NFIC), alpha-helix (SRF), beta-scaffold (STAT3), and TCFCP2L1. Most of these transcription factors have been associated with different functions in the CNS including neurogenesis, neuronal survival, neuronal and/or glial differentiation, and regulation of cell apoptosis in health and pathology as summarised in Table 6.2.

Table 6. 1 Possible transcription factors that are triggered by CNTF treatment in embryonic rat spinal cord myelinating cultures.

	PLL-CNTF 4 h vs PLL-Con 4 h		PLL-CNTF 24 h vs PLL-Con 24 h	
Sequence Length	**Up**	**Down**	**Up**	**Down**
All	-	-	-	-
	TnC-CNTF 4 h vs TnC-Con 4 h		**TnC-CNTF 24 h vs TnC-Con 24 h**	
Sequence Length	**Up**	**Down**	**Up**	**Down**
2000/0	-	INSM1, KLF4, SP1, SRF	-	-
2000/2000	-	CTCF, KLF4, MZF1_1-4, RREB1, SP1,	-	-
5000/2000	-	CTCF, INSM1, KLF4, SP1	-	-
5000/5000	-	CTCF, E2F1, INSM1, KLF4, SP1, TCFCP2L1	-	-
10000/5000	-	E2F1, PPARγ::RXRα, SP1, TLX1::NFIC	-	-
10000/10000	-	CTCF, E2F1, INSM1, PPARγ::RXRα, SP1,	-	-
Common	-	**SP1**	-	-
All	-	CTCF, E2F1, INSM1, KLF4, MZF1_1-4,	-	-

Microarray gene expression profiling analysis (Array 2) was carried out using embryonic rat myelinating spinal cord cultures that were set up using neurosphere-derived rat astrocytes, plated on PLL- or TnC-coated glass coverslips. The cultures were either untreated (control, con) or treated with rat recombinant CNTF for 4 h or 24 h. The transcripts that were differentially expressed between the untreated and CNTF-treated cultures were entered into the web-based program called oPOSSUM 3.0 for single site analysis that detects over-represented conserved transcription factor binding sites in a set of mouse genes. The conservation cut off value was left as 0.4 and matrix score threshold as 85%. The analysis was run for all the possible upstream/downstream sequence lengths. The results with Z-score≥10 and Fisher score≥7 are shown in the table. The transcription factors detected from the analysis of the up- and down-regulated transcripts in CNTF-treated cultures compared to control cultures are shown in the table under the columns named “Up” and “Down”, respectively. CNTF: ciliary neurotrophic factor; CTCF: CCCTC-binding factor; Hand1: heart and neural crest derivatives expressed 1: INSM1: insulinoma-associated 1; Klf4: Kruppel-like factor 4; MZF1: myeloid zing finger 1; PLL: poly-L-lysine; Tcfe2a: transcription factor E2a; TnC: tenascin C.

Table 6. 2 Previously reported functions of the putative transcription factors that could be playing role in CNTF-signaling in rat embryonic TnC-myelinating cultures.

TF	Reported functions related to CNS
CTCF	• Ubiquitous deletion of *Ctcf* in the mouse leads to lethality before embryonic day 3.5 (E3.5). • Important for functional neural networks and regulation of neuronal diversity in the brain. • Conditional knockout of *Ctcf* in anterior retina and forebrain caused extensive apoptosis at E8.5 resulting in profound loss of telenchephalic and anterior retina tissue by E13.5. • Early neuroepithelial cells are more sensitive to CTCF loss than the neuroprogenitors present slightly later in development. • A transcription factor-binding site was found in the regulatory region of golli-Mbp gene, expressed in the CNS. • *De novo* mutations were identified in *Ctcf* in individuals with intellectual disability, microcephaly, and growth retardation. • **References:** Baruch et al., 2009; Hirayama et al., 2012; Gregor et al., 2013; Watson et al., 2014
E2F1	• Is involved in neurogenesis. *E2f1*-deficient adolescent mice show decreased stem cell and progenitor division, and reduced production of newborn neurons in their proliferative brain zones. • Plays a role in the generation of granule cells in the postnatal and adult CNS by affecting proliferation and cell death. • Modulates neuronal apoptosis *in vitro*. Cortical neuronal cultures from *E2f1*-deficient mice are resistant to induced apoptosis. Overexpression of *E2f1* in cortical neuron cultures leads to neuronal cell apoptosis. • Nuclear E2F1 levels decrease during differentiation of rodent OPCs into oligodendrocytes in developing rat white matter tracts and in cultured cells. • E2F1 might have novel roles in neuronal apoptosis of neurons in temporal lobe epilepsy due to its abnormal location in neuronal cytoplasm. • Apoptotic neuronal cell death in hippocampus is reduced in *E2f1* knockout mice with acute pneumococcal meningitis compared to in wild types. • Affects neuronal apoptosis, neuronal death and axonal damage in cerebral ischemia. E2f1 knockout mice show smaller infarcts and less neuronal damage. • E2F1 expression increases in cortex of adult rats with traumatic brain injury, which also leads to neuronal loss, and microglial and astrocyte activation. • Increases transiently 1 day after spinal cord injury in mouse hippocampus. • *E2f1* levels decrease in NGF-induced differentiating PC12 cells. • E2F1 up-regulation is associated with VEGF-induced neuroproliferation and dopamine-induced apoptosis in rat cortical cultures. • **References:** Hou et al., 2000; Hou et al., 2001; Cooper et al., 2002; MacManus et al., 2003; Zhu et al., 2003; Jiang et al., 2007; Braun et al., 2008; Zhou et al., 2008; Suzuki et al., 2011; Fiala et al., 2013; Kabadi et al., 2014; Magri et al., 2014; Wu et al., 2014

INSM1	• Is expressed in developing mouse brain. • INSM1 is suggested to be expressed transiently during terminal neurogenic divisions, from late progenitors to nascent neurons, and particularly during symmetric neurogenic divisions. *Insm1* expression is lower in adult CNS. • It is suggested that transient expression of INSM1 at the appropriate developmental window functions as a differentiation factor by facilitating cell cycle exit and entrance into normal neuroendocrine cell differentiation. • Promotes the transition of progenitors from apical and proliferative to basal, terminal and neuronogenic state. • Regulates the synthesis of monoaminergic neurotransmitters. • **References:** Beslin et al., 2003; Duggan et al., 2008; Jacob et al., 2009; Lan et al., 2009; Rosenbaum et al., 2011
KLF4	• Plays role in reprogramming of pluripotent stem cells. • The precise regulation of KLF4 expression is critical to neuronal differentiation and migration during the formation of cerebral cortex. • Regulates axon regeneration. KLF4 is suggested as a suppressor for neurite outgrowth. • *Klf4* is down-regulated in porcine neural progenitor cells when treated with CNTF, which stimulates the proliferation and differentiation of these cells into a oligodendrocyte-like morphology. • Plays role in transient forebrain ischemia, where its expression increases in reactive astrocytes in adult rat brains. • Plays role in microglial activation and subsequent release of pro-inflammatory cytokines *in vitro* and *in vivo*. It can also suppress the anti-inflammatory action of drugs. • An association has been found between high levels of KLF4 and shorter survival in high-grade astrocytomas. • **References:** Moore et al., 2009; Kaushik et al., 2010; Nori et al., 2011; Kaushik et al., 2012; Qin et al., 2012; Shimojima et al., 2012; Yang et al., 2012b; Elsir et al., 2013; Park et al., 2014
MZF1	• Regulates the expression of an APP-cleaving enzyme that is responsible for the generation of beta-amyloid peptides in Alzheimer's disease and of a brain kinase. • It is suggested to play role in drug-stimulated FGF-2 expression in striatal rat astrocytes. • **References:** Nomato et al. 1999; Lange-Dohna et al., 2003; Luo et al., 2009
PPARγ:: **RXRα** **PPARγ::**	• **PPARγ:** • PPARs have been detected in brain and spinal cord. They have been shown to be expressed in neurons, astrocytes and oligodendrocytes. • Administration of PPARγ agonists before and at the time of cerebral infarction reduces infarction volume and improves neurological function following ischemic injury in rats. PPARγ is suggested to provide these positive effects by i) decreasing the cerebral oxidative stress, ii) inhibiting ischemia-induced inflammatory markers, and iii) preventing ischemia-induced vascular expression of adhesion molecules and metalloproteinases. • PPARγ agonists reduce glial activation and show a neuroprotective effect in

RXRα (cont'd)	animal models of Alzheimer's disease and Parkinson's disease. • Activation of PPARγ signaling reduces the severity of motor symptoms in EAE possibly through the regulation of the inflammatory pathway and modulation of the maturation and differentiation of oligodendrocytes. • **RXRα:** • RXRα is expressed in various cells of brain tissue. • RXRγ is suggested as a positive regulator of endogenous OPC differentiation and remyelinaton in rats. • RXRα agonists are suggested to have beneficial roles in ameliorating Alzheimer's disease pathogenesis. • **PPARγ:: RXRα:** • PPARγ and RXRα form heterodimers to regulate target gene expression. • The PPARγ-RXRα heterodimer can be activated by the ligands of PPARγ or of RXRα. The maximal receptor activity is provided by the binding of both. • Co-treatment of primary cortical neuron cultures with the combination of PPARγ and RXRα ligands protects the cells from oxygen depravation-induced damage more robustly than each of the ligands alone. • Primary rat microglia demonstrate a higher phagocytosis efficacy toward erythrocytes in response to combined PPARγ activator and RXRα activator. • Combinatorial administration of PPARγ and RXRα ligands provides a higher reduction in behavioural dysfunction in EAE. • **References: PPARγ:** Cullingford et al., 1998; Feinstein et al., 2002; Breidert et al., 2002; Kielian et al., 2003; Moreno et al., 2004; Heneka et al., 2005; Pereira et al., 2005; Shimazu et al., 2005; Sundararajan et al., 2005; Zhao et al., 2005a; reviewed in Bordet et al., 2006; Lin et al., 2006a; Schintu et al., 2009 **/ RXRα:** Kojo et al., 2004; Huang et al., 2011; Kawahara et al., 2014; Zhao et al., 2014 **/ PPARγ:: RXRα:** Leblanc et al., 1995; Mangelsdorf et al., 1995; Mukherjee et al., 1997; Tontonoz et al., 1997; Diab et al., 2004
RREB1	• RREB1 has been shown to play role in pancreatic, prostate and thyroid cancers, in tumoral calcinosis, in DNA damage repair through regulation of p53 transcription, and to repress *HLA-G* expression. However, it has not been reported to play role in the CNS in a direct way. • References: Thiagalingam et al., 1996; Flajollet et al., 2009; Liu et al., 2009; Milon et ak., 2010; Jiang et al., 2011; Franklin et al., 2014
SP1	• Is suggested to play role in development due to increased expression in differentiating cells. • SP1 is associated with MBP and PLP expressions in rat brain. Increased SP1 expression is associated with enhanced activation of MBP. The binding of SP1 to a regulatory region activates *Mbp* promoter. • Its phosphorylation is important for MBP transcription and oligodendrocyte differentiation *in vitro*. • SP1 plays role in TGFβ-modulated OPC cell cycle withdrawal and differentiation. • Primary astrocytes treated with ammonium chloride showed decreased mRNA and protein levels of both CNTF and SP1. • **References:** Tamura et al., 1988; Saffer et al., 1991; Zawia et al., 1998; Tretiakova

	et al., 1999; Wei et al., 2003; Wei et al., 2004; Wei et al., 2005; Paez et al., 2006; Bodega et al., 2007; Calatayud et al., 2009; Guo et al., 2010; Palazuelos et al 2014
SRF	• Plays role in neuronal development, plasticity, learning and memory. • Suggested to be important for early post-natal development of the CNS based on its progressive increased expression in neurons of the rat cerebral and cerebellar cortices and in selective subcortical regions from birth through post-natal day 28. • Regulates astrocyte and oligodendrocyte specification in neural precursor cells (NPCs) *in vitro* and *in vivo*. *Srf*-deficient NPCs generate fewer astrocytes and oligodendrocytes in response to lineage-specific differentiation factors. • Neuronal *Srf*-deficient mouse brains present lower expressions of several myelin genes, reduced myelination, pathological axonal morphology, and increased numbers of astrocytes. • OPCs derived from neuronal *Srf*-deficient mice have been shown to produce no oligodendrocytes unlike those from wild type mice. Hippocampal mixed cultures generated using these conditional *Srf*-deficient mice also present reduced oligodendrocyte maturation. • Mediates the immediate early response and actin cytoskeletal gene transcription in primary mouse CNS neurons, stimulated with several axon growth inhibitors. • **References:** Stringer et al., 2002; Knoll and Nordheim, 2009; Stritt et al., 2009; Johnson et al., 2011; Lu et al., 2012; Stern and Knoll, 2014
STAT3	• Is involved in neuroprotection, promotion of axon growth, and optic nerve regeneration upon inflammatory stimulation in rodents. • Its phosphorylation increases upon CNTF treatment, which presents neuroprotective effects in a rat model of multiple sclerosis. • CNTF-responsive elements are present within the *Gfap* gene promoter. • *S*-nitrosoglutahtione-induced-astrocytes secrete higher levels of CNTF that increases their GFAP expression via STAT3 activation. • Phosphorylated STAT3 levels increase during spinal cord injury in precursor cells, oligodendrocytes and astrocytes of rats. • CNTF treatment promotes neuroepithelial stem cells to differentiate into astrocytes in the presence of increased STAT3 activation. • **References:** Kahn et al., 1997; Rajan et al., 1998; Maier et al., 2004; Muller et al., 2007; Tripathi et al., 2008; Leibinger et al., 2013; Paintlia et al., 2013
TCFCP2L1	• Is important for establishing and maintaining pluripotent cell identity and self-renewal in embryonic stem cells. • **References:** Pelton et al., 2001; van den Berg et al., 2010; Ye et al., 2013
TLX1::NFIC **TLX1::NFIC (cont'd)**	• **TLX1:** • Expressed by neural stem/progenitor cells in the adult brain. • Plays role in neurogenesis and differentiation of neurons in mouse brain. It is an intrinsic regulator in the decision to proliferate or differentiate. • Mediates proliferation and pluripotency of neural progenitors upon hypoxia. • Determines excitatory neurotransmission over inhibitory one in embryonic dorsal

	mouse spinal cord. • Represses cell cycle and glial differentiation but activates neuronal lineage commitment in adult rat hippocampus-derived progenitors. • **NFIC:** • NFI proteins bind to target sequences as either hetero- or homodimers. • Relatively low NFIC levels are present in the brain compared to those of NFIA, NFIB, and NFIX, in the absence of which the mice present aberrant brain development. *Nfic*-deficient mice show mainly abnormal root (tooth) formation. • NFIC binds to and regulates the expression of GFAP *in vitro*. • NFIC regulates the expression of the human secretin (a neuropeptide) gene in response to retinoic acid treatment *in vitro*. • **References: TLX1:** Roy et al., 2002; Land et al., 2003; Stenman et al., 2003; Cheng et al., 2004; Miyawaki et al., 2004; Roy et al., 2004; Shi et al., 2004; Li et al., 2008b; Liu et al., 2008a; Zhang et al., 2008; Elmi et al., 2010; Qu et al., 2010; Chavali et al., 2011; Ryan et al., 2013; Murai et al., 2014 **NFIC:** Kruse et al., 1994: Chaudhry et al., 1997; das Neves et al., 1999; Shu et al., 2003; Steele-Perkins et al., 2003; Lee et al., 2005; Steele-Perkins et al., 2005; Driller et al., 2007; Campbell et al., 2008; Braun et al., 2009

A microarray gene expression profiling analysis was carried out using samples from rat embryonic spinal cord myelinating cultures (Array 2). The down-regulated transcripts upon CNTF treatment in myelinating cultures plated on rat astrocytes on TnC-coated coverslips were analysed in oPOSSUM 3.0 to detect over-represented conserved transcription factor binding sites. The conservation cut off value was left as 0.4 and matrix score threshold as 85%. The results with Z-score≥10 and Fisher score≥7 are shown in the table together with their previously reported functions in the central nervous system (CNS) or *in vitro* that could be related to CNS, as well. CNTF: ciliary neurotrophic factor; cont'd: continued; CTCF: CCCTC-binding factor; EAE: experimental autoimmune encephalomyelitis; GFAP: glial fibrillary acidic protein; HLA-G: major histocompatibility complex, class I, G; INSM1: insulinoma-associated 1; KLF4: Kruppel-like factor 4; MBP: myelin basic protein; MZF1: myeloid zinc finger 1; NFI: Nuclear factor I; OPC: oligodendrocyte precursor cell; PPAR: peroxisome proliferator-activated receptor; RREB1: ras responsive element binding protein 1; RXR: retinoid X receptor; SP1: specificity protein 1; SRF: serum response factor; STAT3: signal transducer and activator of transcription 3; TCFCP2L1: transcription factor CP2-like 1; TGF: transforming growth factor; TLX: tailless; TnC: tenascin C; VEGF: vascular endothelial growth factor

The results from the analysis of the down-regulated transcripts upon CNTF treatment in TnC-myelinating cultures were also presented as scatter plots, where the x and y coordinate planes represented Z-score and Fisher score values, respectively. Each graph is divided into four quadrants as seen in Fig 6.7 A. **Quadrant II** represents the TFBSs, for which the enrichment is due to a majority of DNA regions carrying a TFBS but at a low frequency per sequence (Fischer score high rank, Z-score low rank). **Quadrant IV** represents the TFs, for which the enrichment is due to a high frequency of TFBSs in some of the sequences and absence in others (Z-score high rank, Fisher score low rank). On the other hand, **Quadrant III** shows the TFBSs, which were not found to be enriched in the genes analysed. We were interested in **Quadrant I**, where Z-score and Fisher score of TFBS hits were both equal or higher than the significance threshold values (10 and 7, respectively), showing that the significant enrichment of the binding sites of the

suggested TFs is due to both facts explained above for quadrants II and IV (Kwon et al., 2012). TFBS for SP1 (specificity protein 1) appeared to have the highest Z-score for most of the sequence lengths scanned (Fig 6.7 A, C-F) and the highest Fisher score for half of them (Fig 6.7 A-C, F). It was also the only common TF detected at all sequence lengths.

SP1 has been previously shown to posses binding sites for some genes, which also contain recognition sites for CTCF (CCCTC-binding factor) or MZF1 (myeloid zinc finger protein 1) in a way that their recognition sequences do not interfere with that of each other (Yang et al., 1999; Yin et al., 1999; Hikichi et al., 2003; Lange-dohna et al., 2003). These observations are in accordance with our findings, which suggest that all of the above-mentioned TFs contain conserved binding sites for shared genes (Table 6.3). For example, at the end of the analysis of the 2000/2000 bp regulatory DNA region, both SP1 and CTCF appeared to contain TFBSs for the genes of *Col5a1*, *Cyp1b1*, *Ngfr*, *Pdlim7*, *Lox*, *Megf6*, and *Wif1*; whereas, the genes that were likely to be regulated by both SP1 and MZF1 seemed to be *Col5a1*, *Cyp1b1*, *Ngfr*, *Pdlim7*, *Fstl1*, *Lox*, *Megf6*, and *Wif1* (Table 6.3). Such similarities were also seen for other TFs.

The microarray gene expression profiling analysis (Array 2) also revealed differentially expressed transcripts between spinal cord myelinating cultures at two time points (4 hr and 24 hr) and between cultures on different substrates (PLL or TnC). The up- and down-regulated transcripts between these two sets of different conditions were also analysed in oPOSSUM 3.0 (Tables 6.4 and 6.5). The TFs that appeared to be responsible for down-regulated transcripts over time in PLL-myelinating cultures were CREB1, NFKB, NFKB1, REL, RELA, SRF, USF1; while, the protein complex RXR::RAR_DR5 was detected as the TF associated with the down-regulations over time in TnC-myelinating cultures (Table 6.4). The TFs, which were detected in the analysis of the up-regulation of the transcripts in PLL-myelinating cultures compared to TnC-myelinating cultures at 4 hr, were CREB1, GFI, HLF, MZF1_5-13, NFKB1, REL, REST, SPIB, SRF, STAT1, TBP, and USF1; and at 24 hr were MZF1_1-4, MZF1_5-13, REST, TBP. In addition to being detected for the down-regulated transcripts upon CNTF-treatment in TnC-myelinating cultures, SRF appeared to play a role in the intracellular signaling pathways associated with the change of time from 4 hr to 24 hr and with the use of different coverslips-coating substrates (Table 6.4, 6.5), and MZF1 emerged as a putative TF to take part in the up-regulations of transcripts in PLL-myelinating cultures compared to TnC-myelinating cultures (Table 6.5).

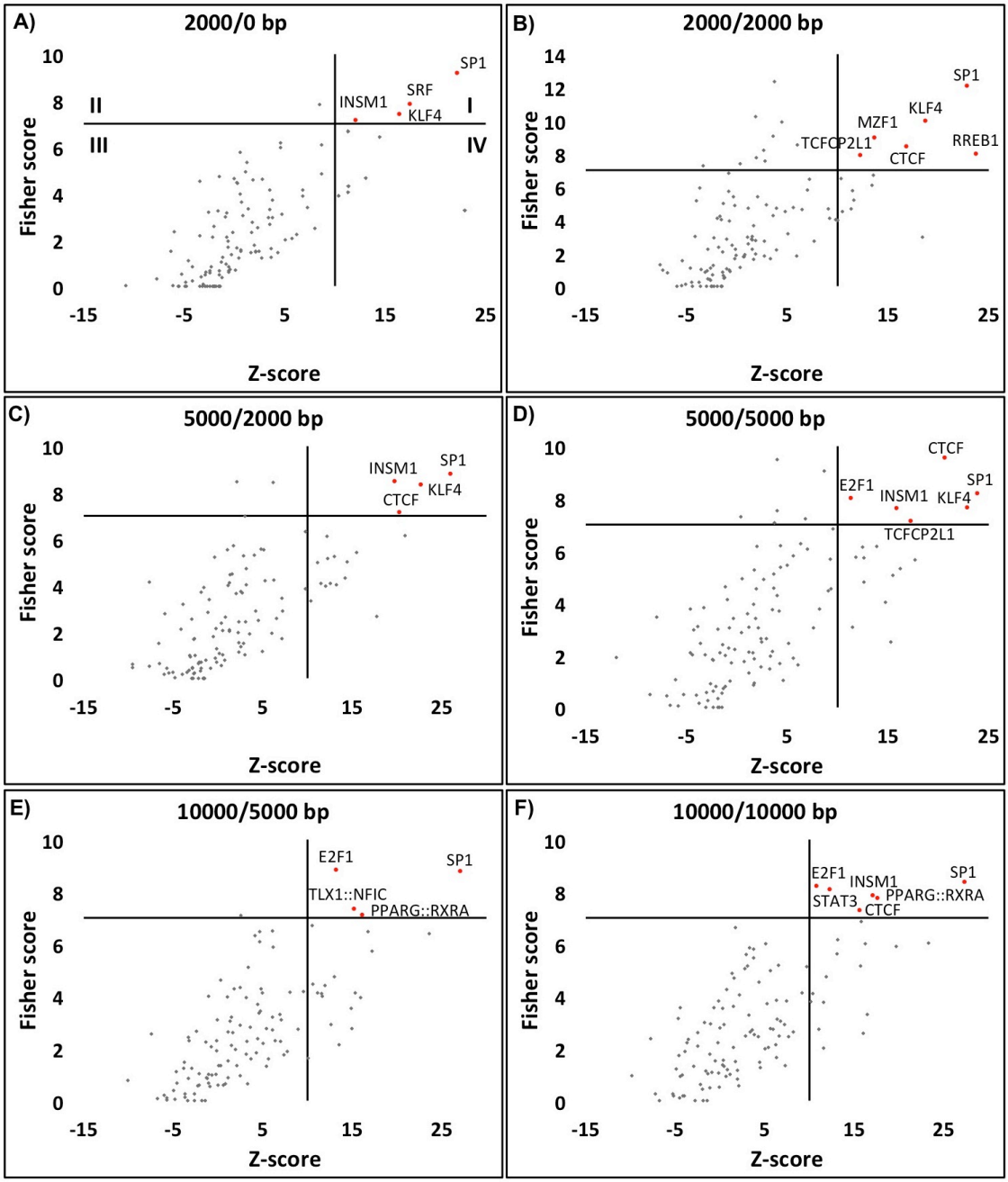

Figure 6. 7 Several transcription factors were suggested to play a role in CNTF-signaling in rat embryonic spinal cord myelinating cultures on TnC-astrocytes.
A microarray gene expression profiling analysis (Array 2) was carried out using RNA samples from embryonic rat spinal cord myelinating cultures, which were plated on rat astrocytes on TnC-coated glass coverslips. After 12 DIV, samples were collected 4 hours after treatment with CNTF to be used for a rat Illumina array. False discovery rate was designated as 5% and a list of up- and down-regulated transcripts upon CNTF was generated using Rank Products statistical analysis. The down-regulated transcripts upon CNTF treatment were entered into the web-based software, named oPOSSUM 3.0 to detect the highly conserved transcription factor-binding sites in those genes. The conservation cut off value was left at 0.40 and matrix score threshold as 85% as suggested by the developers of the program. Analysis was carried out for each DNA sequence length (2000/0, 2000/2000, 5000/2000, 5000/5000, 10000/5000, and 10000/10000 bp), provided in the program. The results were presented as Fisher score vs Z-score scatter plots using Microsoft Excel for each sequence length as seen above. The values with Z-score≥10 and Fisher score≥7 were considered statistically significant as directed by the developers of the program. These values for the binding sites are shown in red in Quadrant I with the corresponding transcription factor names next to them. CNTF: ciliary neurotrophic factor; DIV: days *in vitro*; TnC: tenascin C.

Table 6. 3 The genes that appeared to be enriched with the transcription factor binding sites for the transcription factors detected at the end of the analysis using oPOSSUM 3.0.

Seq. Length	The genes enriched with TFBSs for the TFs shown in bold
2000/ 0 bp	**INSM1:** *Cd248, Igf2, Nfatc4, Colec12, Col5a1, Cyp1b1, Pdlim7, Fstl1, Fbn2, Col18a1, Msx1* **KLF4:** *Cd248, Igf2, Nfatc4, Loxl2, Colec12, Emp1, Col5a1, Cyp1b1, Ngfr, Pdlim7, Fstl1, Fbn2, Igfbp2, Slc14a2, Loxl1, Wif1, Col18a1, Msx1* **SP1:** *Cd248, Igf2, Nfatc4, Loxl2, Thbs2, Colec12, Col5a1, Cyp1b1, Ngfr, Pdlim7, Lox, Fbn2, Igfbp2, Slc14a2, Megf6, Loxl1, Wif1, Col18a1, Msx1* **SRF:** *Cd248, Igf2, Pdlim7, Msx1*
2000/ 2000 bp	**CTCF:** *Col5a1, Cyp1b1, Ngfr, Pdlim7, Fstl1, Lox, Megf6, Wif1* **KLF4:** *Cd248, Igf2, Nfatc4, Loxl2, Colec12, Emp1, Col5a1, Cyp1b1, Ngfr, Pdlim7, Fstl1, Lox, Fbn2, Boc, Igfbp2, Slc14a2, Megf6, Loxl1, Wif1, Fmod, Col18a1, Msx1* **MZF1:** *Cd248, Igf2, Nfatc4, Loxl2, Thbs2, Colec12, Emp1, Col5a1, Cyp1b1, Ngfr, Pdlim7, Fstl1, Lox, Fbn2, Boc, Igfbp2, Slc14a2, Megf6, Col3a1, Loxl1, Wif1, Fmod, Col18a1, Msx1* **RREB1:** *Igf2, Nfatc4, Pdlim7, Boc, Igfbp2, Col18a1* **SP1:** *Cd248, Igf2, Nfatc4, Loxl2, Thbs2, Colec12, Col5a1, Cyp1b1, Ngfr, Pdlim7, Lox, Fbn2, Igfbp2, Slc14a2, Megf6, Loxl1, Wif1, Col18a1, Msx1* **TCFCP2L1:** *Cd248, Igf2, Nfatc4, Loxl2, Colec12, Emp1, Col5a1, Pdlim7, Fbn2, Boc, Igfbp2, Megf6, Col3a1, Loxl1, Fmod, Col18a1, Msx1*
10000/5000 bp	**E2F1:** *Cd248, Igf2, Nfatc4, Loxl2, Colec12, Emp1, Cyp1b1, Ngfr, Pdlim7, Fstl1, Lox, Fbn2, Boc, Slc14a2, Col3a1, Loxl1, Wif1, Col18a1, Msx1, Cckar* **PPARG::RXRA:** *Cd248, Igf2, Nfatc4, Emp1, col5a1, Ngfr, Pdlim7, Fstl1, Fbn2, Boc, Igfbp2, Slc14a2, Loxl1, Fmod, Col18a1, Msx1, Cckar* **SP1:** *Cd248, Igf2, Nfatc4, Loxl2, Thbs2, Colec12, Emp1, Col5a1, Cyp1b1, Ngfr, Pdlim7, Fstl1, Lox, Fbn2, Boc, Igfbp2, Slc14a2, Megf6, Col3a1, Loxl1, Wif1, Fmod, Col18a1, Msx1* **TLX1::NFIC:** *Igf2, Col5a1, Pdlim7, Boc, Igfbp2, Col3a1, Col18a1*
10000/10000 bp	**CTCF:** *Nfatc4, Emp1, Col5a1, Cyp1b1, Ngfr, Pdlim7, Fstl1, Lox, Megf6, Col3a1, Wif1, Fmod* **E2F1:** *Cd248, Igf2, Nfatc4, Loxl2, Colec12, Emp1, Cyp1b1, Ngfr, Pdlim7, Fstl1, Lox, Fbn2, Boc, Slc14a2, Col3a1, Loxl1, Wif1, Col18a1, Msx1, Cckar* **INSM1:** *Cd248, Igf2, Nfatc4, Loxl2, Thbs2, Colec12, Col5a1, Cyp1b1, Ngfr, Pdlim7, Fstl1, Fbn2, Boc, Igfbp2, Slc14a2, Col13a1, Wif1, Col18a1, Msx1* **PPARG::RXRA:** *Cd248, Igf2, Nfatc4, Loxl2, Emp1, Col5a1, Ngfr, Pdlim7, Fstl1, Fbn2, Boc, Igfbp2, Slc14a2, Loxl1,,Fmod, Col18a1, Msx1, Cckar* **SP1:** *Cd248, Igf2, Nfatc4, Loxl2, Thbs2, Colec12, Emp1, Col5a1, Cyp1b1, Ngfr, Pdlim7, Fstl1, Lox, Fbn2, Boc, Igfbp2, Slc14a2, Megf6, Col3a1, Loxl1, Wif1, Fmod, Col18a1, Msx1* **STAT3:** *Cd248, Igf2, Nfatc4, Loxl2, Colec12, Emp1, Col5a1, Cyp1b1, Ngfr, Pdlim7, Fstl1, Lox, Fbn2, Boc, Igfbp2, Slc14a2, Megf6, Col3a1, Loxl1, Wif1, Fmod, Col18a1, Msx1*

A microarray gene expression profiling (Array 2) was carried out using embryonic rat spinal cord myelinating cultures on astrocytes, plated on PLL or TnC-coated coverslips. The analysis revealed a number of differentially regulated transcripts upon CNTF treatment. The down-regulated transcripts upon CNTF treatment in TnC-myelinating cultures were entered into oPOSSUM 3.0, a web-based program that detects over-represented conserved transcription factor binding sites (TFBSs) in the regulatory DNA regions of mouse genes. TFBS hits were searched at different base pair (bp) distances upstream and downstream from the Ensembl-annotated transcription start sites. Examples are given from the sequence lengths of 2000/0, 2000/2000, 10000/5000, 10000/10000 to cover all the TFBS hits detected for this set of genes. Transcription factors (TFs) for the TFBS hits with values of Z-score≥10 and Fisher score≥7 for each sequence length are presented in bold above. These TFBS hits appear to be present in the regulatory regions of the genes shown in the table. PLL: poly-l-lysine; TnC: tenascin C.

Table 6. 4 Possible transcription factors that are stimulated over time in untreated and CNTF-treated embryonic rat spinal cord myelinating cultures.

	PLL-Con 24 h vs PLL-Con 4 h		PLL-CNTF 24 h vs PLL-CNTF 4 h	
Sequence Length	**Up**	**Down**	**Up**	**Down**
2000/0	-	CREB1, NFKB, REL, RELA, SRF, USF1	-	SRF
2000/2000	-	CREB1, NFKB, NFKB1, REL, RELA, SRF	-	-
5000/2000	-	MEF2A, NFKB, NFKB1, REL, RELA, SRF	-	-
5000/5000	-	NFKB, NFKB1, REL, RELA, SRF	-	-
10000/5000	-	NFKB1, RELA	-	-
10000/10000	-	NFKB1	-	-
Common		NFKB	-	-
All	-	CREB1, NFKB, NFKB1, REL, RELA, SRF,	-	SRF

	TnC-Con 24 h vs TnC-Con 4 h		TnC-CNTF 24 h vs TnC-CNTF 4 h	
Sequence Length	**Up**	**Down**	**Up**	**Down**
2000/0	-	RXR::RAR_DR5	-	-
2000/2000	-	RXR::RAR_DR5	-	-
5000/2000	-	-	-	-
5000/5000	-	-	-	-
10000/5000	-	-	-	-
10000/10000	-	-	-	-
All	-	RXR::RAR_DR5	-	-

Microarray gene expression profiling analysis (Array 2) was carried out using embryonic rat myelinating spinal cord cultures that were set up using neurosphere-derived rat astrocytes, plated on PLL- or TnC-coated glass coverslips. The cultures were either untreated (control, con) or treated with rat recombinant CNTF for 4 h or 24 h. The transcripts that were differentially expressed over time (24 h versus 4 h) in control and CNTF-treated cultures were entered into the web-based program called oPOSSUM 3.0 for single site analysis that detects over-represented conserved transcription factor binding sites in a set of mouse genes. The conservation cut off value was left as 0.4 and matrix score threshold as 85%. The analysis was run for all the possible upstream/downstream sequence lengths. The results with Z-score≥10 and Fisher score≥7 are shown in the table. The transcription factors detected from the analysis of the up- and down-regulated transcripts in 24 h samples compared to 4 h samples are shown in the table under the columns named “Up” and “Down”, respectively. Ar: androgen receptor; CNTF: ciliary neurotrophic factor; CREB1: cyclic AMP-responsive element-binding protein 1; NFKB1: nuclear factor kappa B 1; PLL: poly-L-lysine; REL: reticuloendotheliosis oncogene; REST: RE1-silencing transcription factor; RAR: retinoic acid receptor; RXR: retinoic X receptor; SRF: serum response factor; TnC: tenascin C.

Table 6. 5 Possible transcription factors that could take part in the cellular mechanisms stimulated by the substrates, on which embryonic rat spinal cord myelinating cultures are plated.

	PLL-Con 4 h vs TnC-Con 4 h		PLL Con 24 h vs TnC Con 24 h	
Sequence Length	**Up**	**Down**	**Up**	**Down**
2000/0	CREB1, GFI, MZF1_5-13, REL,	-	-	-
2000/2000	CREB1, HLF, NFKB1, REL, REST,	-	REST, TBP	-
5000/2000	GFI, REST, SPIB, SRF, TBP	-	MZF1_1-4, MZF1_5-13, REST	-
5000/5000	REST, SRF, STAT1, TBP, USF1	-	MZF1_1-4, MZF1_5-13, REST	-
10000/5000	REL, REST	-	MZF1_5-13, REST	-
10000/10000	REL	-	MZF1_5-13, REST	-
Common	-	-	-	-
All	CREB1, GFI, HLF, MZF1_5-13,	-	MZF1_1-4, MZF1_5-13,	-

Microarray gene expression profiling analysis (Array 2) was carried out using embryonic rat myelinating spinal cord cultures that were set up using neurosphere-derived rat astrocytes, plated on PLL- or TnC-coated glass coverslips. The transcripts that were differentially expressed between the PLL- and TnC-cultures were entered into the web-based program called oPOSSUM 3.0 for single site analysis that detects over-represented conserved transcription factor binding sites in a set of mouse genes. The conservation cut off value was left as 0.4 and matrix score threshold as 85%. The analysis was run for all the possible upstream/downstream sequence lengths. The results with Z-score≥10 and Fisher score≥7 are shown in the table. The transcription factors detected from the analysis of the up- and down-regulated transcripts in PLL-cultures compared to TnC-cultures are shown in the table under the columns named "Up" and "Down", respectively. CNTF: ciliary neurotrophic factor; CREB1: cyclic AMP-responsive element-binding protein 1; PLL: poly-L-lysine; REL: reticuloendotheliosis oncogene; REST: RE1-silencing transcription factor; SRF: serum response factor; STAT1: signal transducer and activator of transcription 1; TBP: TATA box binding protein; TnC: tenascin C.

6.3.5 Metabolomics of CNTF signaling in embryonic rat spinal cord myelinating cultures

Further experiments were carried out to understand the pathways CNTF triggers in neurosphere-derived rat astrocyte cultures. Metabolite samples were collected from untreated and CNTF-treated PLL- and TnC-astrocytes to be analysed by Glasgow University Metabolomics Facility. Metabolite levels in spent culture medium (secreted metabolites) and those contained in cells were both compared between above-mentioned culture conditions. Q-Exactive Hybrid Quadrupole-Orbitrap mass spectrometer (Q-Exactive MS) was used to process the samples for the purposes of lipid chromatography tandem mass spectrometry (LC-MS/MS). Quality control (QC) pooled standards, which are the aliquots of the total mixture of all the untreated and CNTF-treated culture samples, were also run in between the culture samples so that the data could be normalised after the run to correct the drift in the measured signal based on the assumption that all QC samples should be identical (Dunne et al., 2011).

Thermo MetQuest metabolic stability screening application was used to process high-resolution accurate mass data gathered from Q-Exactive MS and to produce ".raw" files that were converted to "mzXML" files to present positive and negative total ion current (TIC) chromatograms. These TIC plots present signal intensities against retention times

in the three biological repeats for each astrocyte culture condition (Appendix VI). Consistency of the signal intensity values at the same retention times between the biological replicates is interpreted as a successful sample preparation with little or no technical variance and this is observed by the overlay of three colours in TIC plots. Our results showed such high consistency between the biological replicates for all of the samples (Appendix VI).

The data collected from Q-Exactive MS were condensed in an IDEOM file, which is a Microsoft Excel template with a collection of macros that enable automated data processing of mass spectrometry data (Creek et al., 2012). The signal intensities detected at each retention time for each biological replicate were used to obtain the average signal intensity for each culture condition. The average intensities of control (untreated) and CNTF-treated conditions were compared to generate fold changes (FCs), for which unpaired t-test was applied to detect the significance in binary comparisons. The results for CNTF-treated PLL- and TnC-cells and -cell medium were compared to those of control ones. The putative metabolites, for which the FCs were found to be statistically significant, are shown in Tables 6.6, 6,7, 6.8, and 6.9 from the highest to the lowest FC. The metabolites highlighted in yellow with a bold font were the ones identified with authentic standards; whereas, the other metabolites were putatively identified from the database based on accurate mass to charge ratio (m/z value) but predicted retention times. Those metabolites with matching values to the authentic standards were **inosine** and **dGMP** in astrocyte cells on PLL (PLL-As, Table 6.6), and **phthalate** and **l-lysine** in the medium of PLL-As (Table 6.7). There were no such metabolites detected in spent medium from PLL- or TnC-As (Tables 6.7 & 6.9). Inosine and dGMP levels increased significantly in PLL-astrocytes upon CNTF treatment (Table 6.6); whereas, the treatment decreased the levels of phthalate and l-lysine in TnC-astrocytes.

Table 6. 6 Putative metabolites that were produced at different levels upon CNTF treatment in neurosphere-derived rat astrocytes on PLL.

Mass	RT	Formula	Isomers	Putative Metabolites	Confidence	Metaobolism	FC: PLL Con	FC: PLL CNTF
192	9.0	C6H12N2O5	1	Ser-Ser	5	Peptide -di	1.0	**5.9**
226	4.0	C14H26O2	12	(9Z)-Tetradecenoic acid	5	Lipids: F. A.	1.0	**1.9**
341	3.9	C19H35NO4	1	trans-2-Dodecenoylcarnitine	5	0	1.0	**1.7**
224	6.5	C15H12O2	7	(2S)-Flavanone	7	0	1.0	**1.5**
338	3.9	C18H26O6	2	Pinolidoxin	5	0	1.0	**1.5**
268	9.0	C10H12N4O5	3	**Inosine**	10	Nucl.	1.0	**1.5**
689	4.2	C38H77N2O6P	1	[SP (18:0/14:0)] N-(octade canoyl)-tetradecasphing-4-en ine-1-phosphoethanolamine	5	Lipids: Sph.	1.0	**1.4**
182	3.5	C14H14	1	1,2-Dihydrostilbene	5	0	1.0	**1.3**
347	9.2	C10H14N5O7P	7	**dGMP**	10	Nucl.	1.0	**1.2**
332	3.6	C20H28O4	20	[FA oxo,hydroxy(4:0)] 9-oxo-15S-hydroxy-5Z,10Z,13E,17Z-prostatetraenoic acid	5	Lipids: F. A.	1.0	**1.2**
208	5.0	C15H12O	2	Chalcone	7	0	1.0	**1.2**
387	3.8	C56H86O	1	2-decaprenylphenol	7	Cof. & Vit.	1.0	**1.2**
247	9.0	C10H17NO6	2	Linamarin	5	0	1.0	**1.1**
729	4.2	C41H81N2O6P	2	SM(d18:1/18:1(9Z))	5	Lipids: Sph.	1.0	**1.1**
283	4.2	C15H25NO4	2	Amabiline	7	0	1.0	**0.9**
99	5.0	C5H9NO	3	N-Methyl-2-pyrrolidinone	7	0	1.0	**0.9**
408	4.3	C23H36O6	2	[FA methyl,oxo,hydroxy(2:0)] methyl 9-oxo-11R-hydroxy-15R-acetoxy-5Z,13E-prostadienoate	5	Lipids: F. A.	1.0	**0.8**
192	4.3	C11H12O3	6	Carpacin	5	0	1.0	**0.8**
766	3.9	C43H76NO8P	28	PE(20:2(11Z,14Z)/18:3(6Z,9Z,12Z)	5	Lipids: Gly.	1.0	**0.7**
133	7.2	C4H7NO2S	1	L-thiazolidine-4-carboxylate	5	0	1.0	**0.7**
399	4.5	C23H45NO4	1	[FA] O-Palmitoyl-R-carnitine	8	Lipids: F. A.	1.0	**0.6**
788	4.0	C44H86NO8P	24	[PC (18:0/18:1)] 1-octade canoyl-2-(9Z-octadecenoyl)-sn-glycero-3-phosphocholine	5	Lipids: Gly.	1.0	**0.6**

241	4.5	C12H19NO4	2	N-(3-Oxooctanoyl) homoserine lactone	5	Lipids: F. A.	1.0	**0.4**

Confluent neurosphere-derived rat astrocyte monolayers plated on PLL-coated glass coverslips were washed with PBS and lysed with a mixture of chloroform/methanol/water at 9 DIV. The lysates were centrifuged and the supernatant was sent to Glasgow University Metabolomics Facility for the analysis using a Q-Exactive Hybrid Quadrupole-Orbitrap mass spectrometer. Using a Microsoft Excel interface named IDEOM, R statistical packages XCMS and Mzmatch were run to detect peaks, combine data and annotate related peaks. The fold changes (FCs) between the signal intensities of metabolites detected in untreated PLL-astrocytes (PLL Con) and CNTF-treated PLL-astrocytes (PLL CNTF) were calculated and unpaired t-test was used to detect the significance between these FCs in IDEOM. Presented in bold are the statistically significant ($p \leq 0.05$) increased (highlighted in red) and reduced (highlighted in blue) fold changes in "PLL CNTF" astrocytes. The putative metabolites highlighted in yellow (**Inosine** and **dGMP**) were matched within 3 ppm of the mass and 5% of the retention time of an authentic standard, run prior to every batch of samples. Confidence scores of 8 or lower are identifications based on accurate mass but predicted retention time. The isomers column shows the number of different compounds that have identical chemical formulas, but different structures. Mass is the accurate monoisotropic mass and RT is the chromatographic retention time (RT) of the compound. Masses are highlighted according to the polarity mode of detection (red, blue, and white for positive, negative, and both types of ionisation, respectively). CNTF: ciliary neurotrophic factor; Cof. & Vit.: cofactors and vitamins; DIV: day *in vitro*; F.A.: fatty acyls; Gly.: glycerophospholipids; Nucl.: nucleotide; PLL: poly-L-lysine; ppm: parts per million; Sph.: sphingolipids

Table 6. 7 Putative metabolites that were secreted at different levels upon CNTF treatment by the neurosphere-derived rat astrocytes on PLL.

Mass	RT	Formula	Isomers	Putative Metabolite	Confidence	Metaobolism	FC: m PLL Con	FC: m PLL CNTF
196	7.2	C8H12N4O2	1	3,5-dihydro-5-methyl idene-4H-imidazol-4-one	5	0	1.0	**1.78**
521	4.6	C26H52NO7P	11	1-Oleoylglycero phosphocholine	5	0	1.0	**1.46**
84	9.4	HO3Cl	1	Chlorate	5	0	1.0	**1.41**
316	3.8	C19H24O4	6	3,4-Dihydroxy-9,10-secoandrosta-1,3,5(10)-triene-9,17-dione	5	Lipids: Sterol lipids	1.0	**1.35**
246	8.7	C9H14N2O6	2	5-6-Dihydrouridine	5	0	1.0	**1.34**
271	4.0	C15H29NO3	1	Tridecanoylglycine	7	0	1.0	**1.27**
224	6.5	C15H12O2	7	(2S)-Flavanone	7	0	1.0	**1.26**
523	4.5	C26H54NO7P	9	[PC (18:0)] 1-octadecano yl-sn-glycero-3-phosphocholine	5	Lipids: Gly.	1.0	**1.24**
151	7.3	C6H9N5	1	N3-Metyladenine	5	0	1.0	**1.19**
101	8.0	C4H7NO2	5	Diacetylmonoxime	7	0	1.0	**1.19**
195	10.4	C6H13NO4S	1	MES	7	M.C.	1.0	**1.19**
184	4.2	C10H16O3	9	4,5-dihydro-5,5-dimethyl -4-(3-oxobutyl)furan-2(3H)-one	5	0	1.0	**0.94**
166	9.6	C8H6O4	7	**Phthalate**	9	Xenobiotic	1.0	**0.89**
262	4.0	C16H22O3	2	3''-hydroxy-geranylhydroquinone	5	0	1.0	**0.84**
238	4.5	C16H14O2	1	[Fv Methox] 4'-Methoxychalcone	5	Lipids: Polyketide	1.0	**0.81**
146	18.4	C6H14N2O2	8	**L-Lysine**	10	A. A.	1.0	**0.80**
238	3.8	C15H26O2	9	[FA (15:0)] 3-pentadecynoic acid	5	Lipids: F. A.	1.0	**0.66**
248	3.8	C15H20O3	20	Tomentosin	5	0	1.0	**0.63**
133	7.2	C4H7NO2S	1	L-thiazolidine-4-carboxylate	5	0	1.0	**0.39**
103	10.7	C4H9NO2	14	N,N-Dimethylglycine	8	A. A.	1.0	**0.34**

Spent medium was collected from confluent neurosphere-derived rat astrocyte monolayers, plated on PLL-coated glass coverslips, into a mixture of chloroform/methanol/water at 9 DIV. The samples were sent to Glasgow University Metabolomics Facility for the analysis using a Q-Exactive Hybrid Quadrupole-Orbitrap mass spectrometer. Using a Microsoft Excel interface named IDEOM, R statistical packages XCMS and Mzmatch were run to detect peaks, combine data and annotate related peaks. The fold changes (FCs) between the signal intensities of secreted metabolites from untreated PLL-astrocytes (PLL Con) and CNTF-treated PLL-astrocytes (PLL CNTF) were calculated and unpaired t-test was used to detect the significance between these FCs in IDEOM. Presented in bold are the statistically significant ($p \leq 0.05$) increased (highlighted in red) and reduced (highlighted in blue) fold changes of the intensities of secreted metabolites

from “PLL CNTF” astrocytes. The putative metabolites highlighted in yellow (**phthalate** and **l-lysine**) were matched within 3 ppm of the mass and 5% of the retention time of an authentic standard, run prior to every batch of samples. Confidence scores of 8 or lower are identifications based on accurate mass but predicted retention time. The isomers column shows the number of different compounds that have identical chemical formulas, but different structures. Mass is the accurate monoisotropic mass and RT is the chromatographic retention time (RT) of the compound. Masses are highlighted according to the polarity mode of detection (red, blue, and white for positive, negative, and both types of ionisation, respectively). A.A.: amino acid; CNTF: ciliary neurotrophic factor; DIV: day *in vitro*; F.A.: fatty acyls; Gly.: glycerophospholipids; M.C.: medium component; PLL: poly-L-lysine; ppm: parts per million.

Table 6. 8 Putative metabolites that were produced at different levels upon CNTF treatment in neurosphere-derived rat astrocytes on TnC.

Mass	RT	Formula	Isomers	Putative Metabolite	Confidence	Metaobolism	FC: TnC Con	FC: TnC CNTF
165	9.5	C9H11NO2	7	D-Phenylalanine	8	A. A.	1.00	**2.35**
159	10.1	C8H17NO2	4	DL-2-Aminooctanoicacid	5	0	1.00	**0.87**
122	7.3	C6H6N2O	4	Picolinamide	7	0	1.00	**0.84**
101	8.0	C4H7NO2	5	Diacetylmonoxime	7	0	1.00	**0.82**
300	3.8	C20H28O2	25	[PR] Tretinoin/All-Trans Retinoic Acid	5	Lipids: Prenols	1.00	**0.82**
131	11.1	C4H9N3O2	2	Creatine	8	A. A.	1.00	**0.82**
314	3.6	C18H34O4	12	[FA hydroxy(18:1)] 9,10-dihydroxy-12Z-octadecenoic acid	5	Lipids: F. A.	1.00	**0.81**
106	7.3	C4H10O3	1	Diethylene glycol	5	0	1.00	**0.78**
226	7.2	C12H22N2O2	1	1,8-Diazacyclotetradecane-2,9-dione	5	0	1.00	**0.78**
133	10.4	C5H11NO3	4	1-deoxyxylonojirimycin	7	0	1.00	**0.77**
176	4.8	C8H16O4	2	[FA hydroxy(8:0)] 6,8-dihydroxy-octanoic acid	7	Lipids: F. A.	1.00	**0.77**
363	4.0	C19H29N3O4	1	Phe-Val-Val	5	Peptide tri	1.00	**0.77**
158	8.3	C6H10N2O3	2	4-Methylene-L-glutamine	8	Carb.	1.00	**0.73**
191	8.1	C7H13NO3S	1	N-Acetylmethionine	7	0	1.00	**0.68**
152	9.7	C9H12O2	4	3-Isopropylcatechol	7	0	1.00	**0.66**
175	7.3	C10H9NO2	12	Indole-3-acetate	6	A. A.	1.00	**0.66**
302	11.7	C11H22N6O4	2	Ala-Gly-Arg	5	Peptide tri	1.00	**0.66**
216	10.1	C10H20N2O3	1	Val-Val	5	Peptide di	1.00	**0.65**
247	8.5	C9H17N3O5	3	Ala-Ala-Ser	7	Peptide tri	1.00	**0.64**
146	10.6	C4H6N2O2S	1	ZAPA	5	0	1.00	**0.64**
140	7.7	C6H8N2O2	7	Methylimidazoleacetic acid	8	A. A.	1.00	**0.64**
116	4.7	C6H12O2	16	Hexanoic acid	5	Lipids: F. A.	1.00	**0.55**
133	7.2	C4H7NO2S	1	L-thiazolidine-4-carboxylate	5	0	1.00	**0.46**

Confluent neurosphere-derived rat astrocyte monolayers plated on TnC-coated glass coverslips were washed with PBS and lysed with a mixture of chloroform/methanol/water at 9 DIV. The lysates were centrifuged and the supernatant was sent to Glasgow University Metabolomics Facility for the analysis using a Q-Exactive Hybrid Quadrupole-Orbitrap mass spectrometer. Using a Microsoft Excel interface named IDEOM, R statistical packages XCMS and Mzmatch were run to detect peaks, combine data and annotate related peaks. The fold changes (FCs) between the signal intensities of the metabolites detected in untreated TnC -astrocytes (TnC

Con) and CNTF-treated TnC -astrocytes (TnC CNTF) were calculated and unpaired t-test was used to detect the significance between these FCs in IDEOM. Presented in bold are the statistically significant ($p \leq 0.05$) increased (highlighted in red) and reduced (highlighted in blue) fold changes in "PLL CNTF" astrocytes. Confidence scores of 8 or lower are identifications based on accurate mass but predicted retention time. The isomers column shows the number of different compounds that have identical chemical formulas, but different structures. Mass is the accurate monoisotropic mass and RT is the chromatographic retention time (RT) of the compound. Masses are highlighted according to the polarity mode of detection (red, blue, and white for positive, negative, and both types of ionisation, respectively). A.A.: amino acids; Carb.: carbohydrate; CNTF: ciliary neurotrophic factor; DIV: day *in vitro*; F.A.: fatty acyls; ppm: parts per million; TnC: tenascin C.

Table 6. 9 Putative metabolites that were secreted at different levels upon CNTF treatment by the neurosphere-derived rat astrocytes on TnC.

Mass	RT	Formula	Isomers	Putative Metabolite	Confidence	Metaobolism	FC: m TnC Con	FC: m TnC CNTF
299	5.3	C18H37NO2	7	[SP] 3-dehydrosphinganine	5	Lipids: Sph.	1.00	**4.79**
103	10.7	C4H9NO2	14	N,N-Dimethylglycine	8	A. A.	1.00	**2.57**
146	4.9	C6H10O4	16	[FA oxo,hydroxy(6:0)] 2-oxo-4-hydroxy-hexanoic acid	5	Lipids: F. A.	1.00	**1.42**
141	7.3	C7H11NO2	3	L-Hypoglycin	7	0	1.00	**1.34**
192	4.3	C11H12O3	6	Carpacin	5	0	1.00	**1.23**
411	3.3	C23H41NO5	1	3-Hydroxyhexadecadienoylcarnitine	5	0	1.00	**1.20**
346	3.6	C20H26O5	8	Microhelenin C	5	0	1.00	**0.85**
238	4.5	C16H14O2	1	[Fv Methox] 4'-Methoxychalcone	5	Lipids: Polyketi des	1.00	**0.82**
171	7.7	C7H9NO4	3	2,3,4,5-Tetrahydrodipicolinate	8	A. A.	1.00	**0.75**
188	7.8	C7H12N2O4	2	L-glycyl-L-hydroxyproline	7	Peptide	1.00	**0.71**
191	10.7	C6H9NO4S	1	a Cysteine adduct	7	M. C.	1.00	**0.70**
283	8.9	C11H17N5O4	2	Ala-Gly-His	5	Peptide tri	1.00	**0.61**
240	3.8	C15H28O2	5	[FA dimethyl(13:0)] 2,5-dimethyl-2E-tridecenoic acid	7	Lipids: F. A.	1.00	**0.59**
189	7.6	C6H11N3O4	3	Asn-Gly	5	Peptide di	1.00	**0.53**

Spent medium was collected from confluent neurosphere-derived rat astrocyte monolayers, which were plated on PLL-coated glass coverslips, into a mixture of chloroform/methanol/water at 9 DIV. The samples were sent to Glasgow University Metabolomics Facility for the analysis using a Q-Exactive Hybrid Quadrupole-Orbitrap mass spectrometer. Using a Microsoft Excel interface named IDEOM, R statistical packages XCMS and Mzmatch were run to detect peaks, combine data and annotate related peaks. The fold changes (FCs) between the signal intensities of the secreted metabolites from untreated TnC-astrocytes (TnC Con) and CNTF-treated TnC -astrocytes (TnC CNTF) were calculated and unpaired t-test was used to detect the significance between these FCs in IDEOM. Presented in bold are the statistically significant ($p \leq 0.05$) increased (highlighted in red) and reduced (highlighted in blue) fold changes of the intensities of secreted metabolites from "TnC CNTF" astrocytes. Confidence scores of 8 or lower are identifications based on accurate mass but predicted retention time. The isomers column shows the number of different compounds that have identical chemical formulas, but different structures. Mass is the accurate monoisotropic mass and RT is the chromatographic retention time (RT) of the compound. Masses are highlighted according to the polarity mode of detection (red, blue, and white for positive, negative, and both types of ionisation, respectively). A.A.: amino acid; CNTF: ciliary neurotrophic factor; DIV: day *in vitro*; F.A.: fatty acyls; M.C.: medium component; ppm: parts per million; Sph.: sphingolipids; TnC: tenascin C.

The putative metabolites that were produced in or secreted by PLL- and TnC-astrocytes at different levels upon CNTF treatment (Tables 6.6-6.9) appeared to be mostly involved in lipid metabolisms. Among the subtypes of lipid metabolism were the metabolisms of fatty acyls, glycerophospholipids, sphingolipids, sterol lipids, polyketides and prenols. Fatty acyl metabolism was the only common one between all four comparisons (Tables 6.6-6.9). The other groups of metabolites appeared to be involved in the metabolisms of amino acids, nucleotides, peptides, cofactors and vitamins, and xenobiotics. **N,N-Dimethylglycine** was the only common putative metabolite that was found to be secreted at significantly different levels upon CNTF treatment by both PLL- and TnC-astrocytes (Tables 6.7, 6.9). On the other hand, CNTF treatment lowered the levels of **L-thiazolidine-4-carboxylate** in both PLL- and TnC-astrocyte cells (Tables 6.6, 6.8). **L-thiazolidine-4-carboxylate** and **(2S)-flavanone** were detected at lower levels in the presence of exogenous CNTF in both PLL-astrocyte cells and spent medium (Tables 6.6, 6.7); whereas, such a common metabolite was not seen between the cells and spent medium of TnC-astrocytes.

All the putative metabolites that were presented in the IDEOM file after the mass spectrometry analysis were also used to generate volcano plots to narrow down the list to those presenting the highest fold changes (≥2) and significance values (≤0.05) when CNTF-treatment and control conditions were compared (Fig 6.8). According to these plots, CNTF treatment seemed to increase the production of the dipeptide **ser-ser** (serinyl-serine) and the amino acid **D-phenylalanine** (DPh) in PLL- and TnC-astrocytes, respectively (Fig 6.8 A&B). On the other hand, CNTF treatment reduced the levels of **N-(3-Oxooctanoyl) homoserine lactone** (N3OHL) and **L-thiazolidine-4-carboxylate** (LT4C) in PLL- and TnC-astrocytes, respectively (Fig 6.8 A&B). In addition, L4TC levels were decreased upon CNTF treatment also in the PLL-astrocyte medium. Conversely, the level of the amino acid derivative **N,N-Dimethylglycine** (NNDG) was reduced in the spent medium of PLL-astrocytes even though it was increased in that of TnC-astrocytes (Fig 6.8 C&D). Therefore, CNTF treatment could affect the levels of the same metabolites in the opposite way based on the substrate the rat astrocytes were plated on. Lastly, the sphingolipid **3-dehydrosphinganine** (3DS) levels were increased upon CNTF treatment in TnC-astrocyte medium (Fig 6.8D). These changes in the signal intensities could be seen more clearly in the column bars in Fig 6.9, where the levels of the metabolites could also be compared between the cells and the spent cell medium (dark and light gray bars, respectively). The majority of serinyl-serine produced by astrocyte cultures appeared to be secreted into the culture medium (Fig 6.9 B); while, the opposite was seen for NNDG and 3DS (Fig 6.9 E&F).

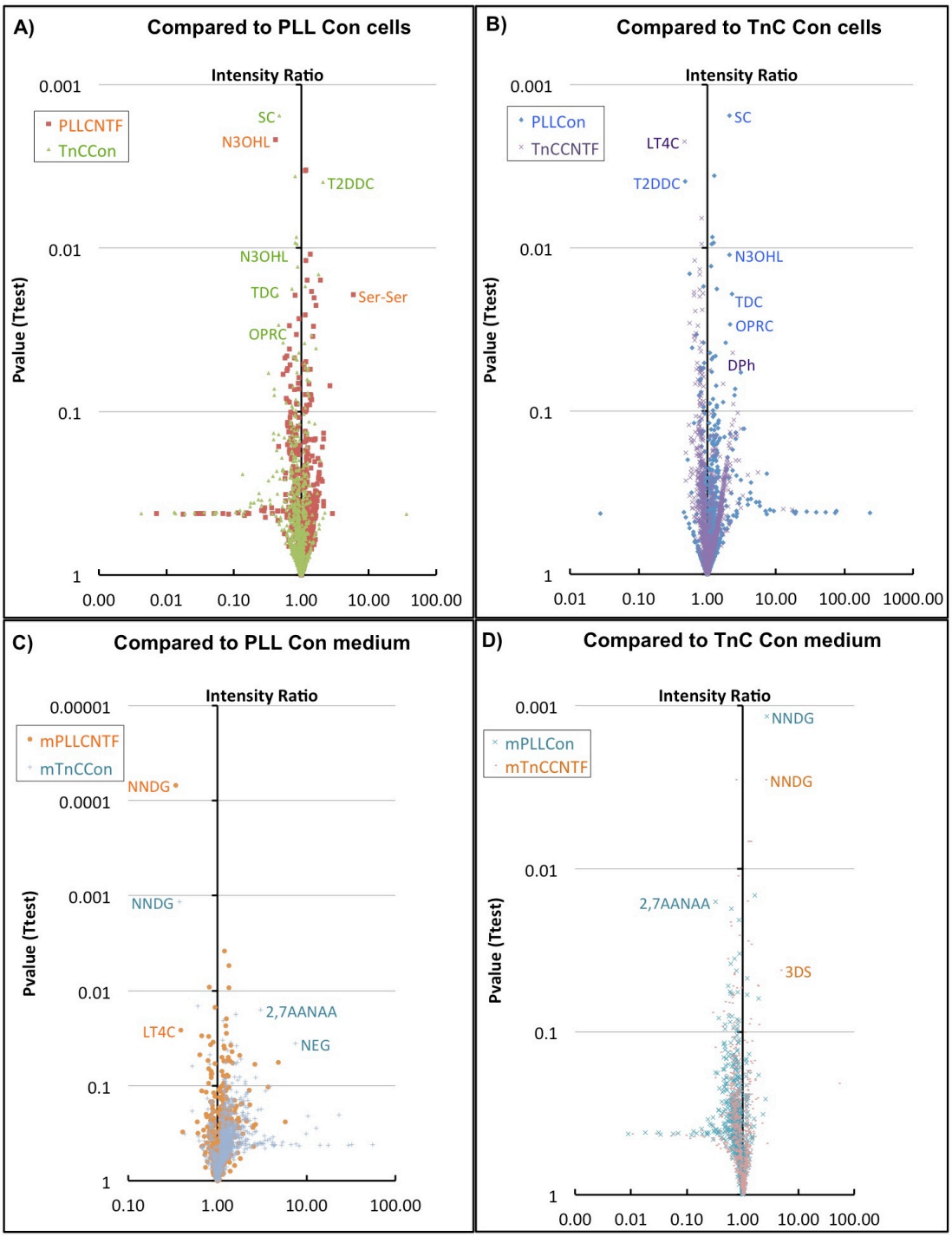

Figure 6. 8 Volcano plots presented several putative metabolites that could be important for CNTF signaling in rat astrocyte cultures.

Metabolite samples extracted from untreated and CNTF-treated neurosphere-derived rat astrocyte cells and spent culture medium were analysed using Q-Exactive Hybrid Quadrupole-Orbitrap mass spectrometer. The signal intensities for each metabolite was measured over 1400 seconds of a period of retention time. The results were presented in an IDEOM file, where volcano plots were generated. Presented in the y-axis are the statistical significance values (unpaired t-test) and in the x-axis are the fold changes (FCs) between the average values of the signal intensities of three biological repeats for different culture conditions. The points with a fold change of ≥ 2 and with a P value of ≤ 0.05 were labelled. The results are presented as compared to different controls. Each control was compared to two other conditions within each volcano plot (shown boxed on top left corners). **A)** N3OHL was decreased and Ser-Ser was increased upon CNTF treatment in astrocyte cells, plated on PLL-coated coverslips (PLL-As). **B)** L4TC was decreased and DPh was increased upon CNTF treatment in TnC-As. **C)** NNDG and LT4C were both decreased after CNTF treatment in the spent medium from PLL-As; whereas NNDG and 3DS were both increased with the addition of CNTF in the spent medium of TnC-As. The metabolites that showed the highest fold changes when their levels were compared between untreated PLL- and TnC- cultures are also shown in the graphs in green (A) and blue (B-D). 2,7AANAA: 2,7-

Anhydro-alpha-N-acetylneuraminic acid; 3DS: [SP] 3-dehydrosphinganine; CNTF: ciliary neurotrophic factor; DPh: D-Phenylalanine; LT4C: L-thiazolidine-4-carboxylate; N3OHL: N-(3-Oxooctanoyl)homoserine lactone; NEG: N-Ethylglycocyamine; NNDG: N,N-Dimethylglycine; OPRC: [FA] O-Palmitoyl-R-carnitine; PLL: poly-L-lysine; SC: stearoylcarnitine; T2DDC: trans-2-dodecenoylcarnitine; TDC: tetradecanoylcarnitine; TnC: tenascin C.

The volcano plots also showed the metabolites with the highest fold changes when their levels were compared between the untreated PLL- and TnC-cultures (Fig 6.8). The level of **trans-2-dodecenoylcarnitine** (T2DDC) was increased and the levels of **N-3-oxooctanoyl-homoserine lactone** (N3OHL), **o-palmitoyl-r-carnitine** (OPRC), **stearoylcarnitine** (SC), and **tetradecanoylcarnitine** (TDC) were decreased in untreated TnC-astrocytes compared to their levels in PLL-astrocytes, which can also be seen in Table 6.10. The secreted metabolites that were detected in TnC-culture spent medium in higher levels were **2,7-Anhydro-alpha-N-acetylneuraminic acid** (2,7AANAA) and **N-ethylglycocyamine** (NEG); while, the level of **N,N-dimethylglycine** (NNDG) was higher in PLL-culture spent medium (Fig 6.8, Table 6.11).

In conclusion, the mass spectrometry analysis identified a list of putative metabolites that could be involved in CNTF-signaling in neurosphere-derived rat astrocyte cultures, plated on PLL- or TnC-coated coverslips. Those that showed the highest signal intensities upon CNTF treatment compared to control levels were **serinyl-serine** in PLL-astrocyte cultures and **3-dehydrosphinganine**, **D-phenylalanine**, **N,N-Dimethylglycine** (NNDG) in TnC-astrocyte cultures; whereas, the levels of NNDG and **N-(3-Oxooctanoyl) homoserine lactone** decreased after conditioning with CNTF in PLL-As cultures and the level of **L-thiazolidine-4-carboxylate** was reduced in both types of astrocyte cultures.

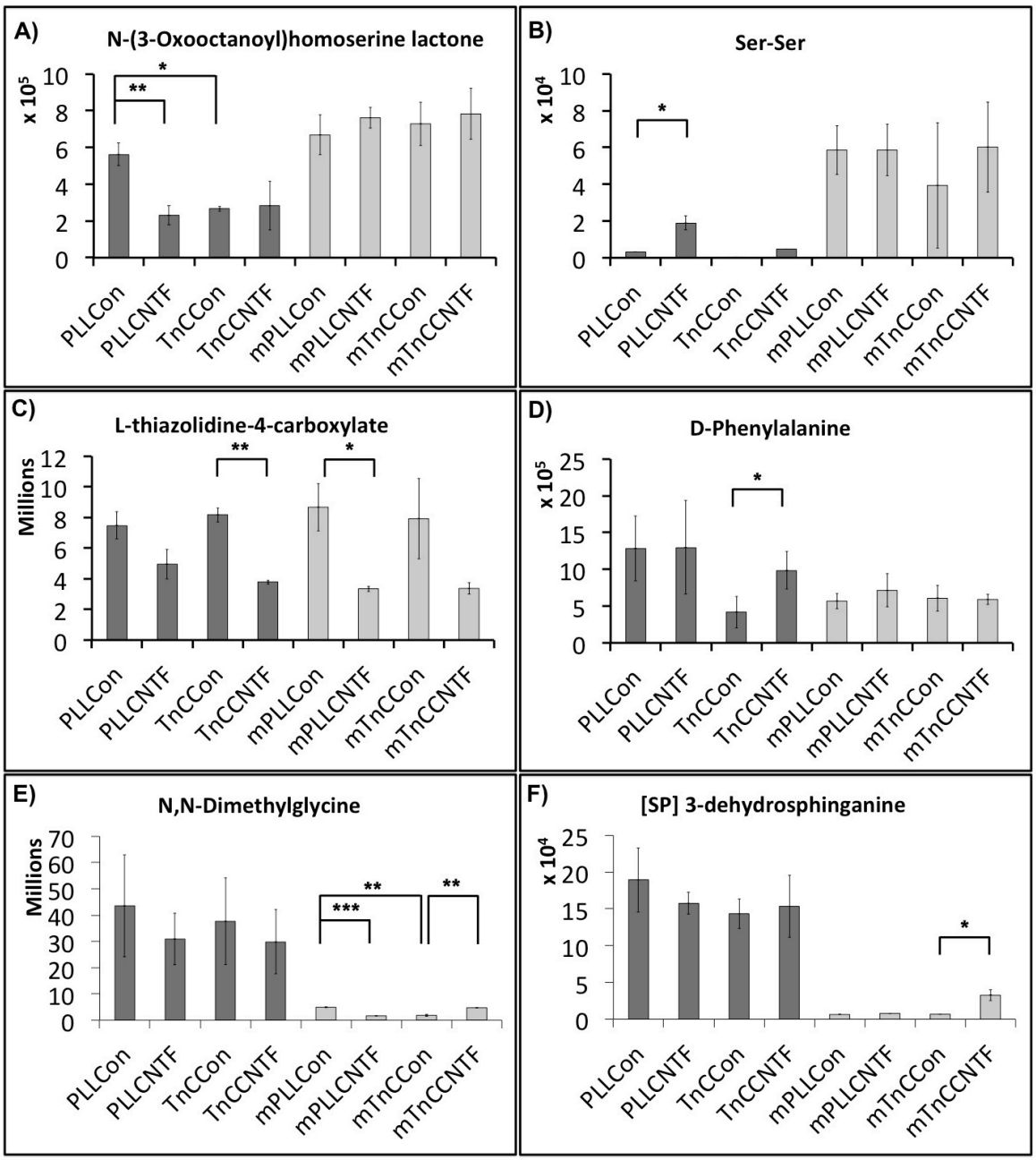

Figure 6. 9 Signal intensities of the putative metabolites that were previously identified to be possibly involved in CNTF-signaling using volcano plots.

Metabolite samples extracted from untreated and CNTF-treated neurosphere-derived rat astrocyte cells and spent culture medium were analysed using Q-Exactive Hybrid Quadrupole-Orbitrap mass spectrometer. The signal intensities for each metabolite was measured over 1400 seconds of a period of retention time. The results were presented in an IDEOM file, where volcano plots were generated showing P value of significance test (unpaired t-test) vs fold change between the average values of the signal intensities of three biological repeats. The points with a fold change of ≥ 2 and with a P value of ≤ 0.05 were labelled. The signal intensities of putative metabolites (PMs) that were found to be produced at different levels upon CNTF treatment are shown in arbitrary units. The PMs that showed different levels upon CNTF treatment in the cells of astrocyte cultures on PLL (**A&B**) and on TnC (**C&D**) and in the spent medium of astrocyte cultures on PLL (**C&E**) and on TnC (**E&F**) are presented above. * P ≤0.05, ** P ≤0.01, *** P ≤0.001. CNTF: ciliary neurotrophic factor; PLL: poly-L-lysine; TnC: tenascin C.

Table 6. 10 Putative metabolites that were produced at different levels in neurosphere-derived rat astrocytes on TnC compared to those on PLL.

Mass	RT	Formula	Isomers	Putative Metabolites	Confidence	Metaobolism	FC: PLL Con	FC: TnC Con
341	3.9	C19H35NO4	1	trans-2-Dodecenoylcarnitine	5	0	1.0	**2.1**
338	3.9	C18H26O6	2	Pinolidoxin	5	0	1.0	**1.8**
226	4.0	C14H26O2	12	(9Z)-Tetradecenoic acid	5	Lipids: F.A.	1.0	**1.7**
155	10.0	C3H10NO4P	3	N-Methylethanolamine phosphate	8	Lipid	1.0	**1.4**
159	7.3	C7H13NO3	10	N-α-acetyl-DL-norvaline	5	0	1.0	**1.1**
332	3.6	C20H28O4	20	[FA oxo,hydroxy(4:0)] 9-oxo-15S-hydroxy 5Z, 10Z,13E,17Z-prostatetraenoic acid	5	Lipids: F. A.	1.0	**1.1**
97	7.4	C4H7N3	1	Deoxycytosine	5	0	1.0	**0.9**
182	7.3	C10H14O3	8	5-Oxo-1,2-campholide	5	0	1.0	**0.9**
310	4.1	C20H22O3	4	[Fv] Dihydrocordoin	5	Lipids: Polyke.	1.0	**0.9**
509	4.6	C25H52NO7P	8	LysoPC(17:0)	5	Lipids: Gly.	1.0	**0.9**
240	3.8	C15H28O2	5	[FA dimethyl(13:0)] 2,5-dimethyl-2E-tridecenoic acid	7	Lipids: F.A.	1.0	**0.8**
282	3.5	C17H30O3	4	[FA hydroxy(17:0)] 12S-hydroxy-16-heptadecynoic acid	5	Lipids: F.A.	1.0	**0.8**
292	4.0	C19H32O2	17	[FA hydroxy(18:1)] 8-hydroxy-11E-octadecen-9-ynoic acid	5	Lipids: F.A.	1.0	**0.8**
315	3.7	C17H33NO4	2	[FA (10:0)] O-decanoyl-R-carnitine	5	Lipids: F.A.	1.0	**0.8**
193	8.2	C6H11NO4S	1	γ-thiomethyl glutamate	5	0	1.0	**0.8**
192	4.3	C11H12O3	6	Carpacin	5	0	1.0	**0.7**
146	10.0	C6H10O4	16	(R)-3-Hydroxy-3-methyl-2-oxopentanoate	8	A. A.	1.0	**0.5**
427	4.4	C25H49NO4	1	Stearoylcarnitine	7	0	1.0	**0.5**
241	4.5	C12H19NO4	2	N-(3-Oxooctanoyl) homoserine lactone	5	Lipids: F.A.	1.0	**0.5**
399	4.5	C23H45NO4	1	[FA] O-Palmitoyl-R-carnitine	8	Lipids: F.A.	1.0	**0.5**
371	4.7	C21H41NO4	1	Tetradecanoylcarnitine	5	0	1.0	**0.4**

Confluent neurosphere-derived rat astrocyte monolayers, which were plated on PLL- or TnC-coated glass coverslips were washed with PBS and lysed with a mixture of chloroform/methanol/ water at 9 DIV. The lysates were centrifuged and the supernatant was sent to Glasgow University Metabolomics Facility for the analysis using a Q-Exactive Hybrid Quadrupole-Orbitrap mass spectrometer. Using a Microsoft Excel interface named IDEOM, R statistical packages XCMS and Mzmatch were run to detect peaks, combine data and annotate related peaks. The fold changes (FCs) between the signal intensities of the metabolites detected in PLL-astrocytes (PLL Con) and TnC-astrocytes (TnC Con) were calculated and unpaired t-test was used to detect the significance between these FCs in IDEOM. Presented in bold are the statistically significant ($p \leq 0.05$) increased (highlighted in red) and reduced (highlighted in blue) fold changes in “TnC Con” astrocytes.

Confidence scores of 8 or lower are identifications based on accurate mass but predicted retention time. The isomers column shows the number of different compounds that have identical chemical formulas, but different structures. Mass is the accurate monoisotropic mass and RT is the chromatographic retention time (RT) of the compound. Masses are highlighted according to the polarity mode of detection (red, blue, and white for positive, negative, and both types of ionisation, respectively). A.A.: amino acid metabolism; Carb.: carbohydrate; DIV: day *in vitro*; F.A.: fatty acyls; Gly.: glycerophospholipids; PLL: poly-L-lysine; ppm: parts per million; Polyke.: polyketides; TnC: tenascin C.

Table 6. 11 Putative metabolites that were secreted at different levels by the neurosphere-derived rat astrocytes on TnC compared to those on PLL.

Mass	RT	Formula	Isomers	Putative Metabolites	Confidence	Metaobolism	FC: mPLL Con	FC: mTnC Con
207	7.3	C8H17NO5	3	N-Ethylglycocyamine	5	0	1.0	**7.5**
291	9.6	C11H17NO8	3	2,7-Anhydro-alpha-N-acetylneuraminic acid	7	0	1.0	**3.1**
278	3.8	C17H26O3	4	[FA hydroxy(17:2)] 7-hydroxy-10E,16-heptadecadien-8-ynoic acid	5	Lipids: F.A.	1.0	**1.6**
82	9.4	H3O3P	1	Phosphonate	5	0	1.0	**1.6**
116	7.9	C4H4O4	3	Maleic acid	10	Carb.	1.0	**1.4**
268	3.9	C26H32O12	1	[Fv Hydroxy,methoxy(5:0/9:1)] 5-Hydroxy-6,7,3',4',5'-pentamethoxyflavanone 5-O-rhamnoside	7	Lipids: Polyketides	1.0	**1.3**
308	3.8	C20H36O2	12	Icosadienoic acid	6	Lipid	1.0	**1.2**
154	4.2	C9H14O2	11	[FA (9:2)] 2,6-nonadienoic acid	5	Lipids: F.A.	1.0	**1.1**
132	9.8	C3H8N4O2	1	Methylenediurea	5	0	1.0	**0.8**
136	7.2	C7H8N2O	3	Pralidoxime	5	0	1.0	**0.6**
103	10.7	C4H9NO2	14	N,N-Dimethylglycine	8	A. A.	1.0	**0.4**

Spent medium was collected from confluent neurosphere-derived rat astrocyte monolayers, which were plated on PLL- or TnC-coated glass coverslips, into a mixture of chloroform/methanol/water at 9 DIV. The samples were centrifuged and the supernatant was sent to Glasgow University Metabolomics Facility for the analysis using a Q-Exactive Hybrid Quadrupole-Orbitrap mass spectrometer. Using a Microsoft Excel interface named IDEOM, R statistical packages XCMS and Mzmatch were run to detect peaks, combine data and annotate related peaks. The fold changes (FCs) between the signal intensities of secreted metabolites from PLL-astrocytes (mPLL Con) and TnC-astrocytes (mTnC Con) were calculated and unpaired t-test was used to detect the significance between these FCs in IDEOM. Presented in bold are the statistically significant ($p \leq 0.05$) increased (highlighted in red) and reduced (highlighted in blue) fold changes of the intensities of secreted metabolites from "TnC Con" astrocytes. Confidence scores of 8 or lower are identifications based on accurate mass but predicted retention time. The isomers column shows the number of different compounds that have identical chemical formulas, but different structures. Mass is the accurate monoisotropic mass and RT is the chromatographic retention time (RT) of the compound. Masses are highlighted according to the polarity mode of detection (red and blue for positive and negative type of ionisation, respectively). A.A.: amino acid metabolism; Carb.: carbohydrate metabolism; DIV: day *in vitro*; F.A.: fatty acyls; PLL: poly-L-lysine; ppm: parts per million; Polyke.: polyketides; TnC: tenascin C.

6.4 General conclusions and discussion

The cytokine CNTF has previously been reported to play a stimulatory role in myelination as explained above. Even though exogenous recombinant rat CNTF has been demonstrated to increase the myelination levels in embryonic rat spinal cord myelinating cultures, plated on neurosphere-derived astrocytes on PLL-coated coverslips (Nash et al., 2011b), my experiments did not show any significant effect of CNTF treatment on myelination levels in these cultures. CNTF titrations in PLL-myelinating cultures using astrocyte monolayers at different seeding densities did not present a significantly different effect, either. Therefore, it is likely that the difference observed between the two studies is due to the methods followed to quantify myelination levels. In addition, because the fold changes of increased myelination levels were not very high in the other study, either (Nash et al., 2011b), it is also possible that biological variation observed in these rat spinal cord myelinating cultures requires a much higher number of samples to be analysed and failing that makes it more difficult to observe a change in myelination levels upon CNTF treatment. However, my results also showed that pre-treatment of astrocyte cultures with CNTF before using them for PLL-myelinating cultures did increase the myelination levels, which suggests the importance of the activation of astrocytes by CNTF to be able to increase their ability to support myelination. Despite the fact that CNTF treatment did not change the GFAP or nestin fluorescence signal intensities of the PLL- or TnC-astrocytes in my experiments, the positive role of astrocytes on myelination upon increased CNTF levels is in agreement with the other examples in the literature (Albrecht et al., 2003; Reviewed in Liberto et al., 2004; Ye et al., 2004; Albrecht et al., 2007; Escartin et al., 2007; Bechstein et al., 2012; Modi et al., 2013).

Treatments of embryonic mouse spinal cord PLL-myelinating cultures with CNTF from 12 DIV onwards did not affect myelination levels significantly. Considering the fact that CNTF could be playing a role in myelination as explained above, transgenic mice were also used to demonstrate the effects of the inhibition of the signaling of CNTF together with the other IL-6 family cytokines on myelination. GFAP-$Cre^{+/-}$gp$130^{fl/fl}$ mice contained the gene for Cre recombinase with an expression under the control of *Gfap* promoter, allowing the conditional knockout of *Gp130* gene in their astrocytes (Drogemuller et al., 2008). Despite the previous findings showing increased levels of demyelination accompanied by more severe disease course in GFAP-$Cre^{+/-}$gp$130^{fl/fl}$ mice with EAE (Haroon et al., 2011), no significant difference was observed between the myelination levels of the spinal cord PLL-myelinating cultures, generated using Cre negative or Cre positive mice. In addition, the treatment with neither recombinant

CNTF nor the neutralising antibody anti-CNTF showed an effect in these Cre+ or Cre- myelinating cultures. This could be due to the differences between *in vitro* and *in vivo* systems since primary cultures do not always parallel the results observed *in vivo* (Reviewed in Reichardt and Gunzer, 2006; in Yin and Chen, 2008; in LeRoux et al., 2009). Alternatively, the stimulatory effect of CNTF signaling on myelination could be more prominent in the presence of demyelination as seen in EAE (Haroon et al., 2011) compared to that in normal conditions. It would be interesting to observe how Cre+ myelinating cultures would behave compared to Cre-myelinating cultures in an *in vitro* model of CNS pathology. One example could be the model developed by Boomkamp et al., (2012) that mimics spinal cord injury in spinal cord myelinating cultures, where a cut is made across using a razor blade manually to generate the lesion, around which myelination levels stay lower than the controls till the end of the cultural period.

Embryonic rat spinal cord cultures were also used to identify potential transcription factors (TFs) that could be involved in CNTF signaling mechanisms. The data obtained from the microarray gene expression profiling analysis (Array 2, Chapter 3) were analysed online using a program that detects the over-representative conserved TF binding sites (TFBSs). The analysis of the differentially regulated transcripts in the presence of exogenous CNTF in PLL-myelinating cultures did not reveal any significant results possibly due to the small number of transcripts available. Significant results were seen only for the list of down-regulated transcripts 4 hr after CNTF treatment in TnC-myelinating cultures. The analysis was run for each length of regulatory DNA region separately and the results obtained from all of the runs were put together to present a general picture. The putative TFs that could be responsible for the repression of certain genes upon CNTF treatment in these cultures were identified to be CTCF, E2F1, INSM1, KLF4, MZF1_1-4, RREB1, SP1, SRF, STAT3, TCFCP2L1, TLX1::NFIC.

Among these TFs, SRF and MZF1 were also suggested to play a role in non-CNTF-related mechanisms such as gene expression regulations between cultures on different substrates (PLL *vs* TnC) and/or regulations over time. SRF could be a repressor of the genes that were down-regulated over time in PLL-myelinating cultures (Table 6.4); however, it could be a transcriptional activator of the genes that were up-regulated in PLL-myelinating cultures compared to TnC-myelinating cultures or a transcriptional repressor of the genes that were down-regulated in TnC- cultures compared to PLL-cultures (Table 6.5). Similarly, MZF1 was detected as a putative transcriptional factor when the transcripts that were up-regulated in PLL-myelinating cultures compared to TnC-myelinating cultures were analysed (Table 6.5)

SP1 (specificity protein 1) was the common TF detected for all the sequence lengths analysed. Some genes have previously been shown to posses separate binding sites for SP1 and CTCF, and others for SP1 and MZF1 (Yang et al., 1999; Yin et al., 1999; Hikichi et al., 2003; Lange-dohna et al., 2003). Some of these TFs, SP1 and KLF4, have also been reported to be associated with CNTF-signaling. For example, SP1 mRNA and protein levels have been shown to decrease in primary rat astrocyte cultures, where the reduction of CNTF levels was induced by an exogenous reagent (Bodega et al., 2007). In addition, SP1 has been shown to play a role in the expressional regulations that are induced by GP130 family cytokines other than CNTF such as leptin and oncostatin M (Botelho et al., 1998; Lin et al., 2012). Another such cytokine, LIF, has also been shown to up-regulate *Klf4* expression in neural precursor cultures (Buono et al., 2012) and to contain DNA-binding motifs for SP1 in the regulatory regions of its gene (Chambers et al., 1997). These observations are in accordance with our findings and therefore they strengthen the possibility of these TFs being involved in CNTF-signaling in spinal cord myelinating cultures.

As another attempt to gain insights into the CNTF-signaling, samples from the cells and the spent medium of neurosphere-derived PLL- and TnC-astrocyte cultures were analysed by lipid chromatography tandem mass spectrometry (LC-MS/MS). The analysis suggested the following putative metabolites to be important for CNTF-signaling in astrocyte cultures: serinyl-serine, 3-dehydrosphinganine (3DS), D-phenylalanine (DPh), N,N-Dimethylglycine (NNDG), N-(3-Oxooctanoyl) homoserine lactone (N3OHL), L-thiazolidine-4-carboxylate (LT4C). The direction of change upon CNTF treatment for each of these metabolites in the astrocyte cultures is presented in Table 6.10. Interestingly, CNTF appears to regulate NNDG in opposite directions in astrocyte cultures on PLL or TnC. This may not be surprising considering that NNDG has been associated with both positive and negative roles in the CNS. A synthetic derivative of NNDG has reduced neurologic dysfunction and brain edema in mice suffering from glioblastoma (Jones-Bolin et al., 2006) and therapeutic effects of NNDG in combined treatments of seizure disorders have also been reported (Jones-Bolin et al., 2006). Conversely, a case report has presented abnormal peripheral nervous system myelination in addition to abnormally slow myelination and atrophy in white matter of an infant male with a mutation in a hydrolase gene, which also has resulted in elevated levels of NNDG in plasma (Baric et al., 2004). Therefore, it is possible that the different signaling pathways regulated by CNTF in PLL- and TnC-astrocytes (as also suggested by Array 2, Chapter 3) change the levels of production/hydrolysis of NNDG in opposite ways.

Table 6. 12 The putative metabolites that showed the highest fold changes upon CNTF treatment in neurosphere-derived rat astrocyte cultures.

Changes in the levels of the metabolites upon CNTF treatment			
in PLL-astrocyte cultures		in TnC-astrocyte cultures	
In cells	**In spent medium**	**In cells**	**In spent medium**
serinyl-serine ↑	NNDG ↓	DPh ↑	NNDG ↑
N3OHL ↓	LT4C ↓	LT4C ↓	3DS ↑

3DS: [SP] 3-dehydrosphinganine; CNTF: ciliary neurotrophic factor; DPh: D-Phenylalanine; LT4C: L-thiazolidine-4-carboxylate; N3OHL: N-(3-Oxooctanoyl)homoserine lactone; NNDG: N,N-Dimethylglycine; PLL: poly-L-lysine; TnC: tenascin C.

LT4C was the other common metabolite that was shown to present lower levels upon CNTF treatment in both PLL- and TnC-astrocyte cultures. Its levels were reduced in both the cells and the spent medium of both types of cultures even though the significance was detected for some of them (Fig 6.9, Table 6.10). LT4C is a brain metabolite that has been reported to have *in vivo* antioxidant effects and to improve the immune response in aged mice (De la Fuente et al., 1998). LT4C-supplemented diet has also presented decrease of the age-dependent oxidative damage in brain and liver mitochondria of adult mice followed by improved neurological functions (Navarro et al., 2007). In addition, it has been demonstrated to be a therapeutic agent for some tumours and a scavenging agent for reactive nitrosamines (Deutch et al., 1992). Considering these positive effects of LT4C *in vivo*, it appears that CNTF would be generating an environment with increased oxidative stress by decreasing the levels of LT4C in the astrocyte cultures. However, over dosage of LT4C has also been observed to be neurotoxic, leading to convulsions in children (Garnier et al., 1982; Wlodek et al., 1993). CNTF might be preventing the accumulation of LT4C and hence the neurotoxicity, which could be associated with the neuroprotective roles of CNTF (Barbin et al., 1984; Hagg and Varon, 1993; Naumann et al., 2003; Krady et al, 2008). LT4C could be a metabolite, via which CNTF regulates the homeostasis of the environment to provide less cell toxicity.

The levels of the metabolites secreted by astrocytes with and without CNTF treatment were compared in attempt to identify astrocytic regulators that could contribute to the elevated myelination levels in spinal cord myelinating cultures. Even though CNTF was suggested to stimulate myelination in both PLL- and TnC-myelinating cultures (Nash et al., 2011b), I could show the stimulatory effects only for the PLL-astrocytes that were pre-treated before they were used as feeder monolayers for the spinal cord myelinating cultures (Fig 6.2). No such effect was observed with TnC-astrocytes. Nevertheless, the

secreted metabolites that presented significantly different levels upon CNTF treatment in both types of astrocyte cultures (Tables 6.7, 6.9) could be investigated further in future studies in an attempt to identify any potential metabolites or metabolic pathways involved in previously-shown CNTF roles such as neuroprotection, stimulation of the OPC proliferation and maturation, and myelination, as explained above. For example, the increase of 3-dehydrosphinganine (3DS) levels after CNTF treatment in TnC-astrocyte cultures (Table 6.10) is very interesting since 3DS takes place in the first step of the sphingolipid biosynthesis (Mandon et al., 1992), which eventually leads to the production of sphingomyelin (Fig 6.10). Because sphingomyelin is particularly found in the myelin sheaths (reviewed in O'Brien, 1965; in Jana and Pahan, 2010), the increase in the levels of 3DS due to CNTF treatment suggests another association between CNTF and stimulation of myelination.

In summary, recombinant rat CNTF treatment triggered different metabolic changes compared to untreated astrocyte monolayers, which were less supportive for myelination but were not different in terms of fluorescent expression of GFAP. A list of putative transcription factors that were associated with CNTF signaling in TnC-myelinating cultures was also identified.

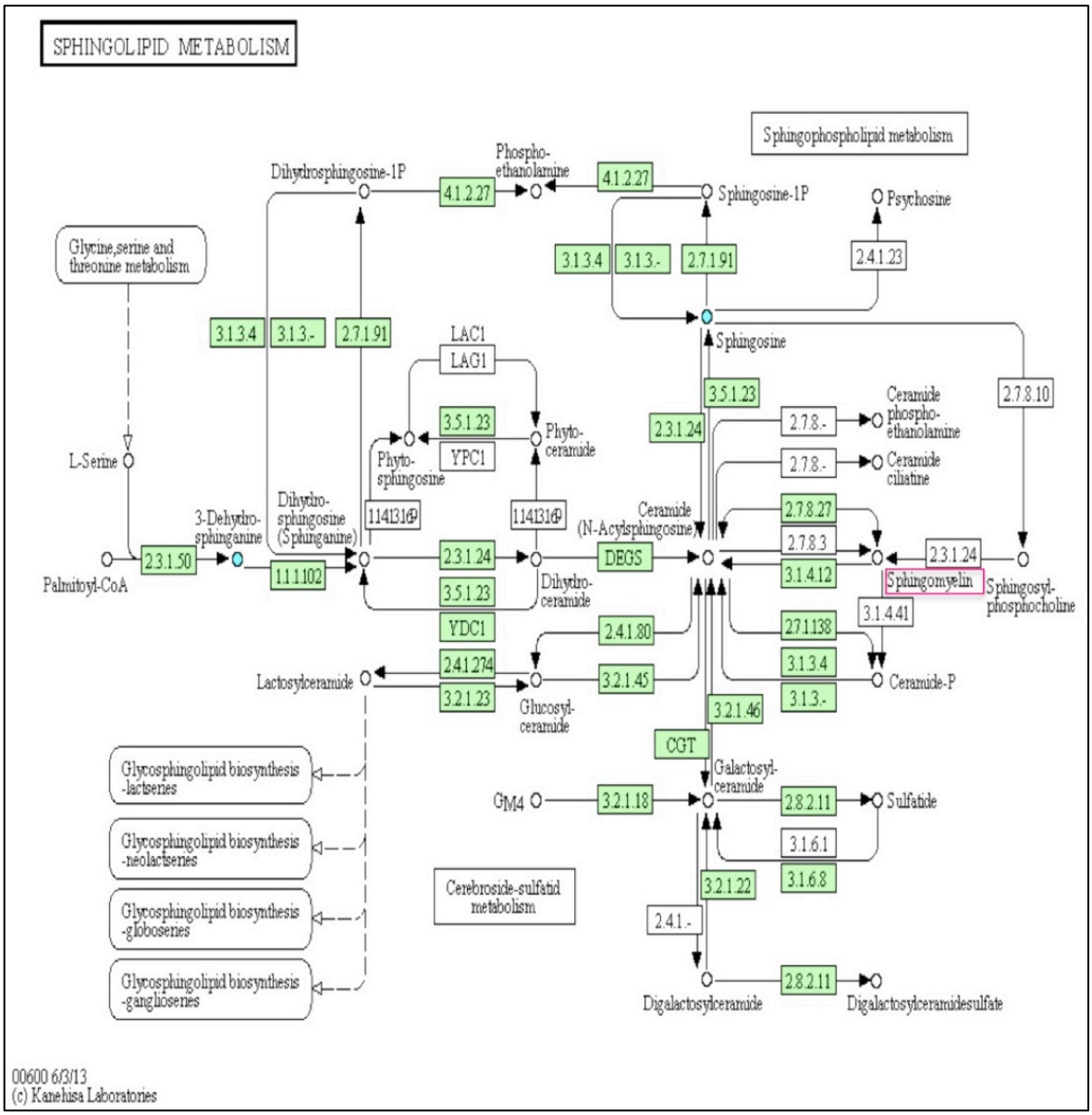

Figure 6. 10 KEGG map showing the pathways involved in sphingolipid metabolism. Samples extracted from neurosphere-derived rat astrocyte cultures, plated on TnC-coated glass coverslips, were analysed by means of lipid chromatography tandem mass spectrometry. Q-Exactive Hybrid Quadrupole-Orbitrap was used for the analysis. The signal intensity (abundance) was found to be increased upon CNTF treatment for the metabolite 3-dehydrosphinganine, which was identified putatively based on accurate m/z but a predicted retention time. The isomer 3-dehydrosphinganine and sphingosin, which is another possible isomer with the same chemical formula, are both shown in blue in the map above. The map was obtained from the web-based software named Pathos (Burgess et al., 2011, http://motif.gla.ac.uk/Pathos/). Sphingomyelin, which is a sphingolipid found particularly in the myelin sheaths, is highlighted in a box with pink borders. CNTF: ciliary neurotrophic factor; KEGG: Kyoto Encyclopedia of Genes and Genomes; m/z: mass to charge ratio; TnC: tenascin C.

Chapter 7

Discussion

Differences were observed by means of microarray analysis in terms of gene expression between spinal cord myelinating cultures under different conditions; conditions that were previously shown by Nash et al. (2011) to induce distinct levels of myelination. The candidates selected from those lists of differentially regulated genes (Ccl2, Ccl7, and Serpinb2) could not be validated to affect myelination when the myelinating cultures were treated with recombinant proteins. Our hypothesis was not supported, in that up-regulated genes in cultures that were previously shown to be more supportive for myelination did not enhance myelination in myelinating cultures. Therefore, it is likely that the differential regulation of these transcripts is not associated with myelination but with another difference between these cultures such as astrocyte reactivity. Some of the transcripts that were associated with elevated astrocyte reactivity *in vivo* in the presence of LPS-induced neuroinflammation or a mouse model of ischemia (Zamanian et al., 2012) were found to be differentially expressed between PLL- and TnC-myelinating cultures, and between untreated and CNTF-treated cultures in a way that suggested that TnC-astrocytes might not be as "quiescent" as previously suggested (Holley et al., 2005). TnC-astrocytes were categorised as "quiescent" based on their lowered nestin expression compared to PLL-astrocytes . However our results suggest that nestin expression is not a highly reliable method to identify astrocyte reactivity since spinal cord mixed cells on TnC-astrocytes expressed higher levels of Cxcl10 and Lcn2, which were shown to be elevated in both above-mentioned models of *in vivo* injury (Zamanian et al., 2012).

This thesis also provides a list of transcription factors (CTCF, E2F1, INSM1, KLF4, MZF1_1-4, PPARγ::RXRα, RREB1, SP1, SRF, STAT3, TCFCP2L1, TLX1::NFIC) that could be involved in CNTF signalling in myelinating cultures, which could be responsible for the previously reported stimulatory roles of CNTF on neuronal survival, oligodendrocyte proliferation and maturation, and myelination (Barbin et al., 1984; Barres et al., 1996; Albrecht et al., Messersmith et al., 2000; 2003; Krady et al., 2008; Cao et al., 2010) and/or for its role in activating astrocytes (Winter et al., 1995; Levison et al., 1996; 1998; Hudgins and Levison, 1998).

Lastly, we detected several metabolites produced by astrocytes that were previously shown to be supportive for myelination at varying degrees. Those metabolites found in increased levels in PLL-astrocyte cultures compared to TnC-astrocytes, and in CNTF-treated astrocytes compared to untreated cultures may therefore be stimulatory for myelination and/or astrocyte reactivity. Among these metabolites, 3-dehydrosphinganine stands out as a strong candidate to be stimulatory for myelination based on the fact that it takes place in sphingolipid biosynthesis (Mandon et al., 1992) leading to the production of sphingomyelin, which is particularly found in the myelin

sheaths (reviewed in O'Brien, 1965; in Jana and Pahan, 2010). Further analysis is required to validate this hypothesis in the future. However, the list of metabolites presented in this thesis provides a basis to inspire future studies to identify different metabolic roles of astrocytes.

7.1 Advantages and disadvantages of the techniques used in this thesis

7.1.1 Embryonic rat spinal cord myelinating cultures

The embryos obtained from one pregnant female rat allow the generation of myelinating cultures at a number enough to be treated, in duplicate, with up to approximately 15 different factors in one experiment. Therefore, the number of animals to be used for three experimental repeats is reduced compared to *in vivo* studies. The spinal cord myelinating cultures are advantageous compared to DRG/OPC co-cultures since they mimic the *in vivo* situation more closely due to the fact that they contain all the major cell types of the CNS. They are also easy to manipulate once generated, and unlike organotypic slice cultures, do not require the use of tissue choppers to initiate the cultures. On the other hand, these cultures appear to be variable in terms of myelination levels observed, which could be due to technical variations and/or biological variation of the animals that provide the tissue for the cultures although the latter is minimised by using in-bred animals. However, standardising the data to control levels solves this problem in terms of myelination levels. As for mRNA expression levels detected by qRT-PCR, normalising the data does not always appear to be enough to overcome the problem of variation in these cultures as also seen in this thesis.

7.1.2 Microarray gene expression analysis and qRT-PCR

Microarray gene expression profiling analysis allows comparison between the expression of over 22,000 genes between myelinating cultures under different conditions in one experiment, carried out with three biological repeats. However, using mixed neural cultures as samples makes it more difficult to identify which cells are responsible for the differential regulation detected in the microarray analysis. Moreover, it is also possible that the differential regulation of some genes in certain cell types will be masked by the expression of those genes by other cell types at much higher levels under all culture conditions tested. Using purified astrocytes (Array 1, Nash et al., 2011), oligodendrocytes, or microglia alone for microarray analysis could overcome this problem but this method will lose the complex crosstalk between the different CNS cell types provided in spinal cord myelinating cultures. Microarray also needs to be validated

by other studies because the statistics become more complicated and the possibility of false positives increases in microarray experiments due to the very high numbers of variables.

To validate microarrays, usually qRT-PCR experiments are conducted and because the comparative expression of one gene is measured in one experiment, the statistics involved in the experiment are less complicated and less prone to false positives. However, qRT-PCR can lead to large differences between biological replicates (Willems et al., 2008), which was also seen in this thesis. Using a strict test such as repeated measures one-way ANOVA followed by Bonferroni correction to obtain statistical significance still ensures that the data are more reliable.

7.1.3 Immunocytochemistry

Immunocytochemistry (ICC) allowed the visualisation of GFAP and nestin proteins in astrocyte cultures in this thesis, which was compared in an attempt to observe differences in astrocyte reactivity. This method is not only easy and fast to carry out but also allows the observation of general astrocyte cell morphology in the cultures. As GFAP staining can sometimes fail to detect astrocytes that express lower levels of this protein (Bushong et al., 2002; Cahoy et al., 2008), western blotting might be a more advantageous technique to compare levels of GFAP protein between cultures under different conditions. However, western blotting does not allow the detection of GFAP protein level expressed per cell unlike ICC. ICC performed in this thesis was also used to visualise myelinated axons in spinal cord myelinating cultures in a way where specifically myelin sheaths that wrap around axons could be quantified rather than all membrane detected by PLP antibody. This antibody provides a very strong signal in ICC and thus makes the visualisation and quantification processes easier. However, other myelin markers such as MOG or MBP that would provide a more specific localisation to myelin sheaths could also be used.

7.1.4 Cell Profiler to quantify myelination level

The software Cell Profiler was used to quantify myelination level present in spinal cord myelinating cultures in this thesis. It provides an unbiased quantification of myelination compared to manual quantification such as where myelin sheaths are manually drawn over in Adobe Photoshop (Nash et al., 2011; Lamond et al; 2013) but sometimes includes cell bodies in the analysis. Despite this disadvantage, Cell Profiler has recently been shown to be a technique sensitive enough to detect significant differences in myelination level in spinal cord myelinating cultures under different conditions (Lindner

et al., 2015). In addition, carrying out the ICC using an antibody against MOG (myelin oligodendrocyte glycoprotein), which is expressed at later stages in oligodendrocyte maturation and stains the cell bodies far less than PLP antibody does (Lindner et al., 2015) can provide a stronger method to quantify myelination more precisely. Cell Profiler also facilitates the quantification process highly, both compared to Adobe Photoshop manual quantification and to methods where myelin sheaths are observed using electron microscopy.

7.1.5 Cre-loxP transgenic mice

The Cre-loxP system facilitates the generation of conditional knockout animals especially when ubiquitous knockouts do not live long enough to obtain tissue for experimental procedures. As Gp130 knockout mice die in early embryonic stages (Yoshida et al., 1996), astrocytic Gp130 knockout mice provide a tool to study Gp130 deficiency and hence CNTF and other IL-6 family cytokine signalling in astrocytes of these animals. However, the major handicap in using these animals is that there is no PCR product in the absence of a transgene, and a homozygous Cre transgene is indistinguishable from the hemizygous Cre transgene. Since a failed PCR produces the same outcome as an absent transgene, the newborn GFAP-$Cre^{+/-}$$gp130^{fl/fl}$ pups to continue the colony can be mislabelled as GFAP-$Cre^{-/-}$$gp130^{fl/fl}$, which eventually can lead to the generation of GFAP-$Cre^{+/+}$$gp130^{fl/fl}$ since the colony is maintained by breeding GFAP-$Cre^{+/-}$$gp130^{fl/fl}$ with GFAP-$Cre^{-/-}$$gp130^{fl/fl}$ genotype. Crossing GFAP-$Cre^{+/+}$$gp130^{fl/fl}$ with GFAP-$Cre^{+/-}$$gp130^{fl/fl}$ will then lead to litters with 100% Cre+ genotype, which will not be able to be used due to absence of a Cre- control sample.

7.2 Future Experiments

In order to further elucidate CNTF mechanisms on myelination, the astrocytic metabolites detected upon CNTF treatment (Chapter 6) could be used as a basis for future experiments, which might identify enzymes and metabolic steps crucial and specific for CNTF signalling in these astrocyte cultures and hence myelination. These experiments could even identify metabolic markers to be used for the diagnosis of demyelinating neurodegenerative diseases (Francis et al., 2012; Blasco et al., 2013). The involvement of CNTFaR-mediated signalling could also be investigated in these cultures as suggested above to clarify whether astrocytic CNTFaR levels are enough to initiate the transcriptional and metabolic changes that would lead to increased myelination levels or whether these levels are minimal and would require the crosstalk between astrocytes and other neural cells to become elevated. The presence of CNTFaR

could be shown using a series of experiments including immunocytochemistry, western blotting, and qRT-PCR using astrocyte cells and also samples from their spent medium to detect the soluble form of the receptor.

The microarray analysis (Array 2) was carried out using samples from myelinating cultures at 12 days *in vitro* (DIV), which is usually considered to be the time point when oligodendrocyte processes begin to interact with axons (Sorensen et al., 2008; Nash B, 2010). However, it is not until 15-18 DIV that myelin sheaths around axons form in these cultures (Sorensen et al., 2008; Nash B, 2010). As eight different culture conditions (8x3=24 samples) were used in Array 2, it was not practical to conduct a study with a higher number of time points. Nevertheless, later time points such as 15 DIV, 18 DIV, and 21 DIV, where myelination appears to be more active, could also be analysed in the future to gain more insight into the CNTF effect on myelination. On the other hand, the results in this thesis showed that CNTF enhanced myelination only when astrocytes were pre-treated 4-5 days before they were used as monolayers for spinal cord myelinating cultures but did not show an effect when the myelinating cultures were treated starting from 12 DIV onwards. This suggests that CNTF effect might be stronger at early time points such as 6-8 DIV, which could also be included in the microarray analysis. To make the experiment more manageable by reducing the number of samples, the experiment could be performed using TnC-astrocytes alone since TnC is found in the CNS unlike PLL, which is a bacterial product. This thesis showed a much higher percentage of type-2 astrocytes, when neurospheres were plated on PLL. However, type 2-astrocytes have not been detected *in vivo* (Skoff, 1990; Fulton et al., 1992; Franklin and Blakemore, 1995; Franklin, 2002; Noble et al., 2004). Therefore, TnC-astrocytes appear to reflect *in vivo* better and could be chosen over PLL-astrocytes when required. The microarray analysis could also be repeated using purified oligodendrocyte cultures or microglia cultures alone to overcome the problem of higher expression levels by other cell types in the mixed neural cultures that could mask the differential changes occurring in specific cell types with lower expression levels.

The transcription factors and metabolites identified in this thesis could be investigated further in the future to understand the roles of CNTF in myelinating cultures especially on myelination. Transgenic animals overexpressing or knockout for one or more of the transcription factors or key enzymes that are found in the astrocytic pathways of production of those metabolites identified here could provide tools for such studies. Similarly, transgenic animals could also be used to investigate the role of GP130 further by conducting the same myelination studies performed here on transgenic mice that lack oligodendroglial Gp130 expression, provided by Cre-loxP system, where the expression of Cre is driven by a mature oligodendroglial gene promoter such as *PLP*,

MBP, or MOG. This will provide a tool to observe the importance of oligodendroglial CNTF signalling on myelination. Analysis of myelination could also be undertaken in tissue samples taken from these transgenic mice.

7.3 Astrocyte diversity: subtypes and reactivity states/ phenotypes

Astrocytes are mainly divided into two subgroups, namely protoplasmic and fibrous (Cajal, 1909), and have been visualised generally using antibodies against the cytoskeletal protein GFAP for more than four decades (Eng et al., 1970). This widely used astrocyte marker has later been shown to be absent from some astrocyte populations, which have been detected by other astrocytic markers, discovered more recently (Cahoy et al., 2008). The discovery of the fact that astrocytes originate in the CNS as different subpopulations, which present distinct expressions of transcription factors also suggests that there might be various astrocyte subtypes that are still awaiting to be explored (Hochstim et al., 2008; Garcia-Marques and Lopez-Mascaraque, 2013). Differences observed in the developmental origin, morphology, and location of the protoplasmic and fibrous astrocyte subtypes and newly emerged pial astrocytes have been interpreted as each subgroup playing different roles during development and mostly likely in adulthood (Molofsky et al., 2014; reviewed in Bayraktar, et al., 2015). Considering the possible variability of astrocyte subclasses and hence of their numerous vital functions in the CNS during homeostasis and in reaction to pathologies, the identification of the differences between the astrocyte subtypes appears crucial.

The diversity of astrocytes in the CNS can increase even more when these cells go through activation upon CNS pathology, which will generate astrocytes with different reactive phenotypes with distinct cell morphology and proliferation rate, and cytokine/chemokine expression profiles (reviewed in Sofroniew and Vinters, 2010). We have used an *in vitro* model that allows the comparison of relatively "quiescent" astrocytes on tenascin C (TnC) with more "activated" ones on poly-L-lysine (PLL, Holley et al., 2005; Nash et al., 2011b), their reactivity being based on the increased immunofluorescence detected for nestin protein expression. I showed that these astrocyte cultures consist primarily of type-1 astrocytes, which have been associated with protoplasmic astrocytes found mainly in the grey matter (Raff et al., 1983; Peters et al., 1991). Even though multiple sclerosis (MS) is generally considered as a disease affecting the white matter, demyelination in grey matter and specifically within the cerebral cortex has been shown to be extensive particularly in patients with progressive disease (Kidd et al., 1999; Peterson et al., 2001; reviewed in Kutzelnigg and Lassmann, 2014). Therefore these PLL- and TnC-astrocyte cultures might represent grey matter

astrocytes *in vivo* and also provide an *in vitro* model to study the effects of grey matter astrocytes on the myelination of **i)** white matter neural cells such as embryonic spinal cord mixed cells (Thomson et al., 2006, 2008; Sorensen et al., 2008) or **ii)** grey matter neural cells like cortical cells if methods could be developed in the future to generate and maintain healthy cortical myelinating cultures.

It is likely that type-1 astrocytes in neurosphere-derived astrocyte cultures secrete factors to stimulate the generation of type-2 astrocytes in the same cultures in much smaller numbers as also suggested by other studies (Lillien et al., 1988). Type-2 astrocytes were shown to develop from oligodendrocyte precursor cells (OPCs) and were associated with *in vivo* fibrous astrocytes by Raff et al. (1983) but it has so far not proved possible to identify cells with the antigenic phenotype of type-2 astrocytes *in vivo* (Skoff, 1990; Fulton et al., 1992; Franklin and Blakemore, 1995; Franklin, 2002; Noble et al., 2004). The substrate on which neurosphere-derived astrocytes are plated appears to affect their ability to generate type-2 astrocytes. As the density at which the striatum-derived neurospheres are seeded on PLL-coated glass coverslips increases, the percentage of type-2 astrocytes formed is also elevated as shown in this thesis (Chapter 5) probably due to raised concentrations of stimulatory factors secreted by type-1 astrocytes. However, the percentage of type-2 astrocytes in TnC-astrocyte cultures is not affected by the increasing seeding density of neurospheres and hence by the total cell number in these cultures, which suggests that TnC-astrocytes might exhibit a negative feedback for type-2 astrocyte stimulatory factors and keep their concentrations at a constant level possibly to provide homeostasis as it would be expected from their "quiescent" phenotype. Identification of such factors, which can stimulate the generation of type-2 astrocytes, can give more insight into the regulation of differentiation of astrocytes *in vitro*, which might be later linked to *in vivo*. Members of the BMP (bone morphogenetic protein) family other than BMP4, which is already used in serum-free medium to stimulate the differentiation of both types of astrocytes *in vitro* (Chen et al., 2012; Hu et al., 2012; Fan et al., 2014), and/or smaller CNTF-like proteins (Lillien et al., 1988) could be among such factors. Even though cells with similar antigenic profiles to type-2 astrocytes have not been detected so far *in vivo*, the fact that OPCs can give rise to astrocyte-like glia (pituicytes) during development of rat neurihypophysis, a CNS structure located at the base of the brain (Virard et al., 2006), suggests that type-2 astrocytes might have similarities with some *in vivo* glial cells to some extent.

Astrocytes were in general thought to be reactive and play negative roles in CNS pathology but later they were also presented to have stimulatory effects that can contribute to recovery (Williams et al., 2007). The emerging view suggests that there is

a continuum of astrocyte reactive phenotypes present (Sofroniew and Vinters, 2010; Nash et al., 2011a) suggesting greater astrocyte diversity in the CNS than previously anticipated. Therefore, identifying a range of factors to manipulate the astrocyte cultures to mimic *in vivo* astrocytes in different stages of various CNS pathologies allows the distinct astrocyte reactivity profiles to be studied. This simple *in vitro* model can be diversified by changing the factors such as the substrate on which astrocyte cultures are plated and the treatment of cultures with relevant cytokines/chemokines or other secreted factors not yet identified. Using this system, we have compared TnC-astrocytes with PLL-astrocytes, which were previously shown to exhibit "quiescent" and more reactive phenotypes, respectively (Holley et al., 2005). Even though their GFAP and nestin expressions, detected by immunocytochemistry, did not differ in our experiments, unlike other reported studies (Holley et al., 2005; Nash et al., 2011b), differences have been observed between PLL- and TnC-astrocytes in other ways, which could also be associated with their reactive phenotypes. GFAP or nestin expression might not always be appropriate markers to detect the changes in astrocyte reactivity if for example astrocytes obtain an activated phenotype closer to quiescence than to high reactivity, in which case other markers will gain importance. In addition to previously conducted transcriptomics analyses (Cahoy et al., 2008; Nash et al., 2011b; Zamanian et al., 2012), we showed for the first time that lipid chromatography tandem mass spectrometry (LC-MS/MS) could be an adequate method to identify metabolites that might be used as markers for specific astrocyte phenotypes in the future and provide insights into differences between their metabolisms. PLL- and TnC-astrocytes showed differences mainly in lipid metabolism, which were altered even more after treatment with CNTF. The changes observed for secreted metabolites suggest that astrocytes with presumably distinct reactive phenotypes can alter the composition of the medium they are cultured in principally in terms of lipid content, which in turn can affect the functions of other neural cells plated on top of these astrocyte monolayers as seen in spinal cord myelinating cultures (Nash et al., 2011b).

7.4 How do *in vitro* astrocytes reflect *in vivo* astrocytes?

PLL is a modified amino acid that is widely used in tissue culturing due to its adhesive properties allowing the attachment, proliferation, and maintenance of cells from different tissue sources (Mazia et al., 1975; Gebicke-Harter et al., 1981). Even though the majority of cells in PLL-astrocyte cultures appear similar to protoplasmic astrocytes as shown in Chapter 5, the absence of PLL in eukaryotes makes it difficult to estimate what state of reactivity astrocytes will gain on this substrate. Attempts have been made to generate astrocyte cultures that do not display a reactive phenotype and thus resemble the *in vivo* quiescent phenotype more closely compared to conventional PLL-

astrocytes. These attempts have revealed the coverslip-coating molecule TnC as a substrate that leads to decreased expression of reactive markers in neurosphere-derived astrocyte monolayers compared to those plated on PLL (Holley et al., 2005; Nash et al., 2011b). However, despite their seemingly "quiescent" phenotype, TnC-astrocytes are likely to contain a denser extracellular matrix (ECM) environment, which they continue to provide when they are used as supporting monolayers for mixed neural cells. In addition to the up-regulation of ECM molecules such as ***Col6a1*** (collagen), ***Omd*** (osteomodulin, a keratan sulphate proteoglycan), ***Ltbp2*** (latent TGF-ß1 binding protein 2), and ***Mfap5*** (microfibrillar associated protein 5, involved in elastic fibre formation) in TnC-astrocytes (Array 1, Nash et al., 2011b); the ECM components of collagen (**Col1a2**), and ficolin (**Fcnb**) were also up-regulated in mixed neural cells supported by TnC-astrocytes, where an ECM-modifying protease *Mmp3* was down-regulated compared to PLL-cultures (Array 2, Chapter 3). Interestingly, expressions of several structural proteins were also promoted in mixed neural cells on TnC-astrocytes as presented in Chapter 3.

The detection of elevated levels for other glial scar markers in cultures on TnC also supports the suggestion that TnC-astrocytes might not be as "quiescent" as originally thought. The increased mRNA expression of the ECM glycoprotein **fibronectin 1 (Fn1)** in TnC-astrocytes and in mixed neural cells, supported by these astrocytes, suggests that TnC-astrocytes could be creating an inhibitory environment such as seen in lesions of MS and EAE, where FN1 protein specifically localises in areas of demyelination and inhibits oligodendrocyte differentiation and remyelination (Stoffels et al., 2013). FN1 is proposed to play a role in the formation of the glial scar due to its increased expression in microglia /macrophages and reactive astrocytes of injured CNS (Camand et al., 2004; Stenzel et al., 2011; Kim et al., 2013) similar to **transgelin (Tagln)** that presents increased expression after spinal cord injury in rats (Lin et al., 2005) and was detected also to be up-regulated in astrocytes and mixed neural cultures on TnC as shown in Chapter 3. Therefore, it is likely that the three glial scar markers (eNCAM, EGFR, bFGF) used by Holley et al. (2005) to compare the reactivity of astrocytes on different substrates are not enough to provide a general profile for distinct astrocyte reactive phenotypes.

Considering the likelihood of a wide spectrum of astrocyte reactive states, a more comprehensive study should be carried out, where immunocytochemistry and western blotting analysis for various glial scar/CNS injury markers can be used to differentiate astrocytes on TnC from those plated on PLL or other coating substrates. It is possible that some of these markers will present raised levels in TnC-astrocytes while others will be lowered, such as seen for ***Serpinb2*** (Dietzmann et al., 2000) in this thesis.

Therefore, to be able to refer to one *in vitro* astrocyte phenotype as more reactive than another one with more certainty, a panel of reactivity markers should be graded according to the associated CNS disease/pathology severity, after which levels of these markers can be compared between two astrocyte phenotypes and those that express markers of higher reactivity could be termed more "reactive". Such an extensive investigation can also reveal reactivity markers that can be grouped together based on their similar spatial and temporal expressions upon various CNS pathologies and common association with pathology severity, which might reduce the large list of markers into several basic groups to allow higher practicality when carrying out the future experiments.

Zamanian et al. (2012) have carried out such an extensive study, where they compared transcriptional changes in reactive astrocytes upon two different injury models in mice. Transient ischemia and neuroinflammation were induced by occluding the middle cerebral artery (MCAO) and by a single intraperitoneal injection of the bacterial endotoxin LPS, respectively. Both injury models presented increased mRNA expression for astrocyte reactivity markers GFAP and vimentin by 1 day; whereas, nestin expression was induced only in MCAO astrocytes. The increase in the expression of these markers resolved gradually over time, measured up to 7 days. Having established that they had isolated purified populations of reactive astrocytes from injured animals in addition to less reactive ("quiescent") astrocytes from sham-operated and saline-injected control animals, they carried out a gene expression profiling microarray analysis to compare "quiescent" astrocytes with reactive astrocytes within each injury scenario. They showed that reactive astrocyte transcriptome could depend on the nature of the inducing stimulus. Some of the transcripts that were up-regulated specifically upon the type of injury were also detected in the myelinating cultures (Table 7.1). Zamanian et al. (2012) suggested that reactive astrocytes in ischemia could be beneficial due to their increased expression of neurotrophic factors and cytokines; while, LPS reactive astrocytes could be detrimental with their up-regulated expression of complement factors. It is difficult to predict which type of *in vivo* reactive astrocytes PLL- and TnC astrocytes might be reflecting since some ischemia-associated transcripts (*Anxa3* and *Icam1*) were up-regulated in TnC-cultures; while others were up-regulated in PLL-cultures (*Hmox1*, *Ptgs2*, *Vgf*). Therefore, both PLL- and TnC-astrocytes might be reactive to some extent, which would require another *in vitro* phenotype to mimic *in vivo* "quiescent" astrocytes more closely.

Zamanian et al. (2012) also identified common transcripts that were up-regulated in reactive astrocytes from both injuries (*Cxcl10*, *Lcn2*, and *Serpina3n*), which we found to be expressed in embryonic rat spinal cord myelinating cultures (Table 7.1) that were set

Table 7. 1 Possible astrocyte reactivity markers that were detected both *in vivo* and *in vitro*.

In vivo markers	The injury model	Astrocyte cultures (no CNTF) Array 1	Mixed neural cells (no CNTF)	Mixed neural cells (+ CNTF)	Differential expression of markers in mixed neural cells a) on a different substrate, b) upon treatment, c) over time
Anxa3	MCAO	-	TnC	TnC	**a)** PLL-Con-4 vs TnC-Con-4 ↑ **a)** PLL-CNTF-24 vs TnC-CNTF- 24 ↑
Chi3l1	LPS	-	-	PLL	**a)**↑PLL-CNTF-24 vs TnC-CNTF-24
Ctgf	MCAO	TnC	-	TnC	**a)** PLL-CNTF-24 vs TnC-CNTF-24 ↑ **b)** ↑TnC-CNTF-24 vs TnC-Con-24
Cxcl1	LPS	-	-	PLL	**a)** ↑PLL-CNTF-4 vs TnC-CNTF-4 **c)** PLL-CNTF-24 vs PLL-CNTF-4 ↑
Cxcl10	LPS, MCAO	TnC	TnC	-	**a)** PLL-Con-4 vs TnC-Con-4 ↑
Emp1	MCAO	-	-	TnC	**a)** PLL-CNTF-24 vs TnC-CNTF-24 ↑ **b)** TnC-CNTF-4 vs TnC-Con-4 ↑ **c)** PLL-CNTF-24 vs PLL-CNTF-4 ↑ **c)** TnC-Con-24 vs TnC-Con-4 ↑
Hmox1	MCAO	-	PLL	-	**a)** ↑PLL-Con-4 vs TnC-Con-4 **c)** PLL-Con-24 vs PLL-Con-4 ↑ **c)** TnC-CNTF-24 vs TnC-CNTF-4 ↑
Icam1	MCAO	-	TnC	-	**a)** PLL-Con-4 vs TnC-Con-4 ↑
Lcn2	LPS, MCAO	-	TnC	PLL	**a)** PLL-Con-4 vs TnC-Con-4 ↑ **a)** ↑PLL-CNTF-24 vs TnC-CNTF-24 **b)** ↑PLL-CNTF-24 vs PLL-Con-24 **c)** PLL-Con-24 vs PLL-Con-4 ↑ **c)** PLL-CNTF 24 vs PLL-CNTF-4 ↑ **c)** TnC-Con-24 vs TnC-Con-4 ↑
Ptgs2	MCAO	-	PLL	PLL	**a)** ↑PLL-Con-4 vs TnC-Con-4 **a)** ↑PLL-CNTF-4 vs TnC-CNTF-4 **c)** PLL-Con-24 vs PLL-Con-4 ↑ **c)** PLL-CNTF-24 vs PLL-CNTF-4 ↑
Serpina3n	LPS, MCAO	-	-	PLL	**a)**↑ PLL-CNTF-4 vs TnC-CNTF-4
Vgf	MCAO	-	PLL	PLL	**a)**↑ PLL-Con-4 vs TnC-Con-4 **a)** ↑PLL-Con-24 vs TnC-Con-24 **a)** ↑PLL-CNTF-24 vs TnC-CNTF-24

Astrocytic transcripts that were shown to be up-regulated in an animal model of ischemia and neuroinflammation (Zamanian et al., 2012) were compared with **i)** transcripts that were differentially regulated between neurosphere-derived astrocyte monolayers plated on PLL or TnC and **ii)** transcripts that were differentially regulated in embryonic rat mixed spinal cord cultures (mixed neural cells) at different conditions. Zamanin et al. (2012) identified several transcripts (*in vivo* markers) that could be associated with astrocytic reactivity due to their up-regulation in neuroinflammation, induced by intraperitoneal injection of LPS, and ischemia, which was initiated by occluding the middle cerebral artery (MCAO). Markers that were up-regulated in both injury models are shown as highlighted in yellow. The coverslip-coating substrates (PLL or TnC) on which astrocytes (Array 1, Nash et al., 2011b) and mixed neural cells showed increased expression for *in vivo*

markers with or without the presence of CNTF treatment are presented in the table. Binary comparisons, where *in vivo* markers present up-regulated expression in one of two conditions (underlined and shown with ↑), are also shown above. Expressions were compared in mixed neural cells between cultures **a)** on PLL and TnC, **b)** untreated or treated with CNTF, **c)** over time (4 hr vs 24 hr). Anxa3: annexin A3; Chi3l1: chitinase 3-like 1; CNTF: ciliary neurotrophic factor; Ctgf: connective tissue growth factor; Cxcl1: chemokine (C-X-C motif) ligand 1; Cxcl10: chemokine (C-X-C motif) ligand 10; Emp1: epithelial membrane protein 1; Hmox1: heme oxygenase 1; Icam1: intercellular adhesion molecule 1; Lcn2: lipocalin2; PLL: poly-L-lysine; Ptgfs2: prostaglandin-endoperoxide synthase 2; Serpina3n: serine (or cysteine) peptidase inhibitor, clade A, member 3 NTnC: tenascin C; Vgf: VGF nerve growth factor.

up using PLL- or TnC-astrocytes. *Cxcl10* and *Lcn2* were detected to be up-regulated in TnC-myelinating cultures compared to PLL-myelinating cultures, which would parallel the discussion above that TnC-cultures could be more reactive despite their reduced nestin expression (Holley et al., 2005). CNTF treatment, on the other hand, increased *Lcn2* expression in PLL-myelinating cultures, which suggests that CNTF could make PLL-astrocytes more reactive through signaling cascades involving Lcn2 while the same signaling pathway will not be activated in TnC-astrocytes. This is not surprising as our microarray analysis (Array 2) proposed that CNTF shows its pro-myelinating effects in PLL- and TnC-myelinating cultures through different transcriptional changes (Chapter 3). Serpina3n was also up-regulated in PLL-cultures in the presence of CNTF treatment compared to TnC-cultures; however, it is difficult to interpret this change due to the absence of any other significant transcriptional changes detected between untreated PLL- and TnC-cultures, or between untreated and CNTF-treated cultures. Because astrocyte reactivity can be present not only to different degrees (based on their expression of reactivity markers) but also with opposing roles on CNS biology (positive vs negative), CNTF-induced reactivity in PLL-astrocytes could be of a kind that is beneficial as evidenced by its stimulatory effect on myelination levels (Chapter 3, Nash et al., 2011b). In contrast, TnC-astrocytes could be more reactive compared to PLL-astrocytes in a different way, where they actively suppress myelination rather than just being quiescent as suggested earlier (Holley et al., 2005).

The inhibitory roles of TnC-astrocytes on myelination in mixed embryonic spinal cord myelinating cultures (Nash et al., 2011b) could be due to their more compact ECM that physically and chemically can hinder axonal ensheathment process (Mohan et al., 2010) and increased levels of other suppressing cues such as markers of reactivity as explained above and possibly due to increased immunological signaling as evidenced by the microarray analysis (Chapter 3). The interaction of astrocytes with TnC *in vitro* might be stimulating intrinsic mechanisms in astrocytes to prepare a denser ECM and a more reactive environment to some extent, possibly with the help of other neural cells plated on top, in an attempt to patch a hypothetical scar, stop inflammation and initiate other repair mechanisms before re/myelination can take place. Despite this comparatively

reactive environment, astrocytes might not be reactive enough to increase their GFAP expression due to lack of activating signals that can be provided by macrophages and/or other peripheral leukocytes that can infiltrate into the CNS upon demyelination-inducing signals even in the presence of an intact blood brain barrier (Kondo et al., 1987; Hiremath et al., 1981; McMahon et al., 2002). Therefore, culturing astrocytes with activated macrophages might lead to a much higher increase in GFAP expression on TnC compared to that on PLL due to potentially more reactive environment present in TnC-astrocyte cultures.

The previously detected down-regulation of nestin in TnC-astrocytes (Holley et al., 2005; Nash et al., 2011b) could be associated with the differentiation stage of astrocytes rather than their reactive state especially considering the fact that both PLL- and TnC-astrocytes present similar levels of GFAP (Holley et al., 2005), a widely used astrocyte marker of reactivity (Axelsson et al., 2011) as mentioned above. A lower nestin expression might represent the presence of more mature astrocytes (Frederiksen and McKay, 1988; Lendahl et al., 1990) on TnC. Astrocytes on TnC might reduce their nestin expression while increasing GFAP levels as they mature, which would be similar to their differentiation during *in vivo* CNS development (Wiese et al., 2012). On the other hand, PLL-astrocytes might be able to initiate GFAP expression as they become more differentiated without lowering their nestin expression first, which would probably create mature astrocytes with some properties of immature astrocytes. This could be an artefact of the interaction between astrocytes and PLL that is not found in the CNS. The up-regulation of several developmental proteins in mixed neural cells on PLL-astrocytes such as ***Arc***, ***Ascl1***, ***Dlx1***, and ***Gadd45g*** (Array 2, Chapter 3) also supports this suggestion. The increased capacity of PLL-astrocytes to support myelination could thus also be related to their more regenerative environment possibly allowing the development and the process of oligodendrocyte differentiation more efficiently as also evidenced by their up-regulated levels of **tenascin R (*TnR*)**, which has been shown to promote oligodendrocyte differentiation *in vitro* as opposed to TnC (Czopka et al., 2009).

Future experiments can be conducted to investigate cell differentiation and astrocyte reactivity on PLL- and TnC-astrocytes by comparing these cultures to astrocyte monolayers on tenascin R (TnR)-coated coverslips (Czopka et al., 2009) or neural ECM (nECM)-coated coverslips that are covered with a mixture of ECM molecules (laminin, collagen IV, entacin, and heparin sulphate proteoglycan, Garcia-Parra et al., 2012), which could be more similar to *in vivo* conditions. Moreover, coverslips coated with nECM have been shown to increase neuronal survival and neuronal differentiation of rat hippocampal cells compared to that seen in cultures on PLL-coverslips (Garcia-Parra et

al., 2013). Astrocytes isolated from adult animals could also be used to obtain a "quiescent" phenotype that resembles the *in vivo* adult quiescence more closely compared to astrocyte cultures generated using neonatal tissue (Wu et al., 1998). In my opinion, neurosphere-derived astrocytes on TnC reflect adult astrocytes, which would be in contact with the reactive ECM environment *in vivo* in the absence of activating signals from macrophages, as explained above. Because TnC levels increase upon CNS pathology *in vivo* possibly to contribute to the recovery of the injury (Chen et al., 2010; reviewed in Jakovcevski et al., 2013), it is not surprising that mature astrocytes will have intrinsic mechanisms triggered by TnC to initiate repair mechanisms rather than giving the priority to generating an environment to promote axonal ensheathment. However, further experiments are required to elucidate this hypothesis. Embryonic spinal cord myelinating cultures on PLL- and TnC could be compared, for example, in terms of the way they will react to a single cut made using a razor blade manually to mimic spinal cord injury (Boomkamp et al., 2012). If TnC-astrocytes are indeed programmed to initiate recovery at a higher level than PLL-astrocytes, they will most likely patch the cut faster and more efficiently. It would also be interesting to observe these changes in the presence of activated macrophages that can provide signals to activate astrocytes as proposed above.

7.5 Crosstalk between neural cells and astrocytes

We have used astrocyte cultures as supporting monolayers for embryonic mixed spinal cord cells, where it is possible to follow neuronal survival, neurite outgrowth, oligodendrocyte precursor cell proliferation and extension of their processes to myelinate axons. The astrocytic lipids detected after the LC-MS/MS analysis could be sources of energy for highly active neurons or possibly monomers for lipid-rich myelinogenesis process in oligodendrocytes as suggested by previous studies showing that astrocytes play an important role in supplying fatty acids to neurons and other cells (Moore et al., 1991, 2001; Bernoud et al., 1998). These lipids could be secreted with apolipoproteins to provide intercellular trafficking of fatty acids from astrocytes to other neural cells (Innis and Dyer, 2002) or transported to axonal mitochondria via "carnitine-transporters" from astrocytic peroxisomes as hypothesised for the transfer of fatty acids from oligodendrocytes to neurons (reviewed in Kassmann, 2014). Astrocytic peroxisomes perform ß-oxidation of especially very long chain fatty acids (VLCFAs) and thereby may provide the monomer acetyl-CoA for *de novo* fatty acid and cholesterol synthesis in the brain, which might be important for remyelination and the maintenance of the myelin structure in the CNS (Morita et al., 2012). Consequently, the metabolic changes observed in astrocyte monolayers could be important for the regulation of myelination in embryonic spinal cord myelinating cultures.

Nash et al. (2011b) have suggested that the reason why only two transcripts were differentially expressed upon CNTF treatment in PLL-astrocytes, detected by microarray analysis (Array 1), could be the lack of the crosstalk between astrocytes and other neural cells. This suggestion was in parallel with the previous observations showing that intracranial CNTF injection can induce astrogliotic response in neonatal rat brains, where CNTF-alpha receptor (CNTF-αR, Fig 1.6) mRNA and protein expression was detected in neurons but not in S100α-expressing astrocytes (Kahn et al., 1997). Despite the lack of neurons in the astrocyte cultures I have used, CNTF treatment did change the levels of various metabolites in these PLL- and TnC-astrocyte monolayers, where CNTF-αR might have been expressed by astrocytes and allowed the CNTF signaling that would lead to those metabolic changes. Another possibility is that CNTF signals through currently unknown receptors/receptor complexes that do not involve CNTF-αR, which can be confirmed in the future through a series of experiments involving immunocytochemistry, qRT-PCR, and/or western blotting by using the astrocyte cultures. It is also possible that astrocytes express CNTF-αR subunit at low levels that might be enough to initiate CNTF signaling and thereby a few transcriptional changes, which might be involved in complex signaling pathways and lead to various metabolic changes.

The CNTF effect observed in the metabolomics analysis might also be attributed to possible mechanisms allowing CNTF to regulate the activity of enzymes in the astrocyte cultures without directly involving transcriptional changes. One example is that CNTF has recently been shown to stimulate enzyme activity of tyrosine hydroxylase in rat and mouse neuronal cultures, where CNTF was suggested to alter the phosphorylation state of the enzyme during post-translation modification (Shi et al., 2012). CNTF was proposed to activate ERK 1/2 (Dziennis and Habecker, 2003), which would phosphorylate the enzyme at a specific serine residue that would allow increased enzymatic activity; whereas, the phosphorylation observed at another serine residue upon CNTF treatment was associated with targeting of the enzyme for proteasomal degradation (Shi et al., 2012). CNTF might therefore be leading to metabolic changes in astrocyte cultures by activating the phosphorylation of different amino acid residues of potentially distinct enzymes through possibly GP130 receptor signalling (Fig 1.6, Shi and Habecker, 2012), where the binding of CNTF to astrocytic CNTF-αR is a prerequisite or other receptors are involved in the initiation of CNTF signalling.

The crosstalk between astrocyte monolayers and neural mixed cells in cocultures on PLL revealed increased numbers of transcripts that were differentially regulated upon CNTF treatment possibly due to the elevated CNTF-αR levels, secreted by neurons, as Nash et al. (2011b) have predicted and as explained above. Interestingly, even in the presence

of the crosstalk, 13 transcriptional changes were detected after CNTF treatment in PLL-myelinating cultures (Array 2) as opposed to 2 changes detected previously in PLL-astrocytes (Array 1). On the other hand, 43 transcripts were differentially regulated upon CNTF treatment in mixed neural cells on TnC. It might be that higher levels of CNTF-αR will lead to a higher number of transcriptional changes, in which case CNTF-αR would need to be present in mixed neural cells on TnC at elevated levels compared to those on PLL, which was not detected in Array 2. Another explanation could be that CNTF-αR levels are not directly associated with the number of transcriptional changes CNTF will stimulate in myelinating cultures. The stimulation of CNTF on myelination levels appears to be more efficient in mixed neural cells on TnC compared to those on PLL (Nash et al., 2011b). This higher increase in myelination levels in TnC-cultures might be due to a more complex CNTF signaling that triggers a higher number of transcriptional changes rather than due to increased levels of CNTF-αR. However, to speculate about the importance of CNTF-αR levels on the transcriptional changes in these cultures, TnC-astrocytes should also be compared before and after the CNTF treatment by means of microarray (not carried out in Array 1). If CNTF differentially regulates a high number of transcripts in TnC-astrocytes and if these transcripts show similarities with those detected in mixed neural cells on TnC, it could be concluded that CNTF signalling is almost as efficient in astrocyte monolayers as it could be in mixed neural cells. Otherwise, the production of CNTF-αR subunit by other neural cells might be considered important.

7.6 CNTF effect on neural cultures

Myelination levels were increased in spinal cord mixed neural cultures seeded on astrocytes that were pretreated with CNTF (Chapter 6) as also shown by others (Nash et al., 2011b). Despite stimulating different signaling pathways in mixed neural cultures on PLL and TnC as discussed in Chapter 3, CNTF appears to regulate ECM in both of these myelinating cultures in the same direction. The expressions of several ECM proteins were down-regulated while the expression of an ECM-modifying protease was up-regulated upon CNTF treatment in both PLL- and TnC-cultures (Array 2, Chapter 3). Therefore, its stimulating role on myelination could involve mechanisms that create a more permissive environment for oligodendrocyte process extension and axon ensheathment. Furthermore, metabolomics studies showed that CNTF increased the levels of several fatty acids and sphingolipids that might be important for myelinogenesis as explained in Chapter 6. Thus, CNTF may be included in disease-modifying combination therapies in the future to treat neurodegenerative diseases such as multiple sclerosis, where it could help to constrain the excessive enlargement of glial scar and facilitate recovery (Fang et al., 2013).

The failure to show increased myelination levels in neural mixed cells on TnC-astrocytes upon CNTF treatment in this thesis could be related to the timing of the treatments. Neither pre-conditioning astrocyte monolayers with CNTF nor treatments initiated 12 DIV after neural mixed cells were plated on astrocyte monolayers presented a significant change on axonal ensheathment (Chapter 6) unlike previous observations (Nash et al., 2011b). Considering the possible "adult phenotype" of TnC-astrocytes as discussed above, conditioning astrocyte monolayers and continuing with the CNTF treatment once spinal cord mixed cells are plated on top could provide a more efficient strategy to alter the myelination-inhibitory conditions in TnC-cultures. I might have missed the critical time frame for CNTF to initiate its positive effects by depriving the cultures from CNTF treatment during 12 DIV after they had been set up, which might not have made a difference in the other study (Nash et al., 2011b) maybe due to the differentiation stage of the astrocytes used. Because TnC-astrocytes might constitute a relatively non-permissive environment with their increased levels of ECM proteins as discussed above, neural mixed cells on these astrocytes might require more time and energy to down-regulate those ECM molecules and then stimulate processes leading to myelination such as oligodendrocyte proliferation, maturation, and process extension. One of the ways to save energy upon CNTF treatment could be halting myelination-related processes temporarily as can be evidenced by the down-regulation of a tight junction protein, **Claudin 11** (Chapter 3), which promotes the proliferation and migration of oligodendrocytes and takes place on myelin sheaths (Morita et al., 1999; Bronstein et al., 2000a, 2000b; Tiwari-Woodruff et al., 2001). This transcript was up-regulated over time (4 hr vs 24 hr) in untreated mixed neural cultures on TnC (Chapter 3), which suggests that CNTF inhibits such an increase rather than reducing *Cldn11* expression continuing until then. Resuming and facilitating the myelination-promoting functions could be very sensitive and prone to errors unless the very right conditions are provided, which is why high variations were observed for myelination levels in TnC+CNTF myelinating cultures even in the original study that did present significant increase in axonal ensheathment (Nash et al., 2011b).

7.7 General conclusions

Astrocytes not only constitute the majority of cells in the CNS but also take part in various vital functions to maintain homeostasis in normal conditions and to repair damaged tissue upon distinct pathologies as explained earlier in Chapter 1. The potential of reactive astrocytes to exert both beneficial and detrimental effects in CNS disorders (Williams et al., 2007) underlines the importance of the necessity to identify different activated astrocyte phenotypes and conditions required to generate them. This identification might allow the manipulation of astrocytes in a way to stimulate

their favourable roles to be exploited in therapies for numerous neurodegenerative diseases (Buffo et al., 2010; Hamby and Sofroniew, 2010), including multiple sclerosis, Alzheimer's disease, amyotrophic lateral sclerosis (ALS), and Parkinson's disease (Holley et al., 2003; Rothstein et al., 2005; Mena and de Yebenes, 2008; Fuller et al., 2009). This thesis provides examples for different *in vitro* astrocyte phenotypes, which were associated with *in vivo* astrocyte subtypes and phenotypes as discussed above, and also presents specific transcriptional and metabolic changes associated with their roles on myelination. Similar studies comparing other astrocyte phenotypes, possibly generated by being plated on different coverslip-coating reagents or stimulated by distinct cytokines/chemokines, can provide further insights into astrocytic roles that could be employed in modifying current treatments or in developing new therapies for neurodegenerative diseases.

Appendix

Appendix I

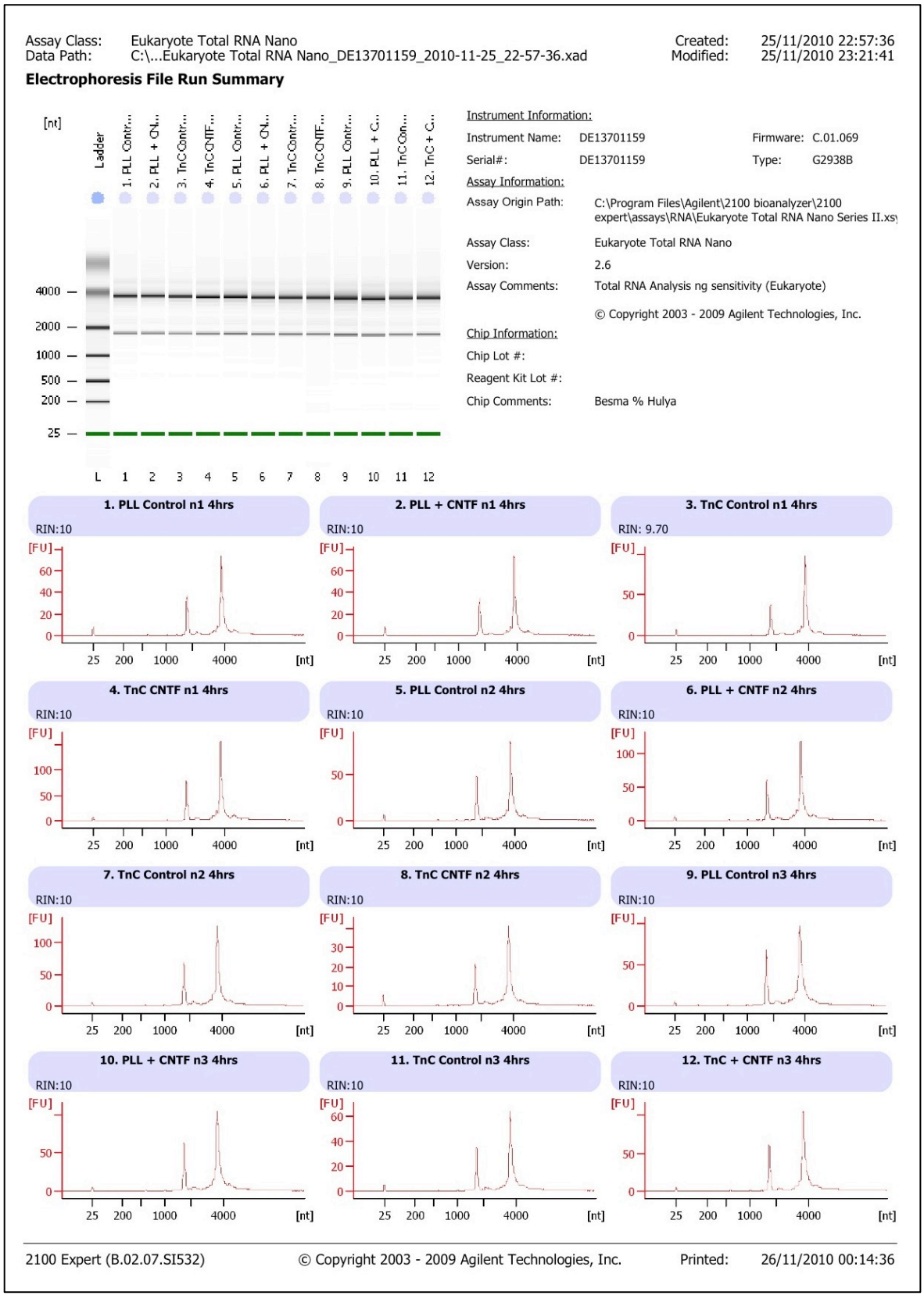

Figure I. l Electropherograms and RIN values, obtained using the Agilent 2100 Bioanalyser, for total RNA samples, used for microarray gene expression profiling analysis.
Only 4 hr samples are presented.

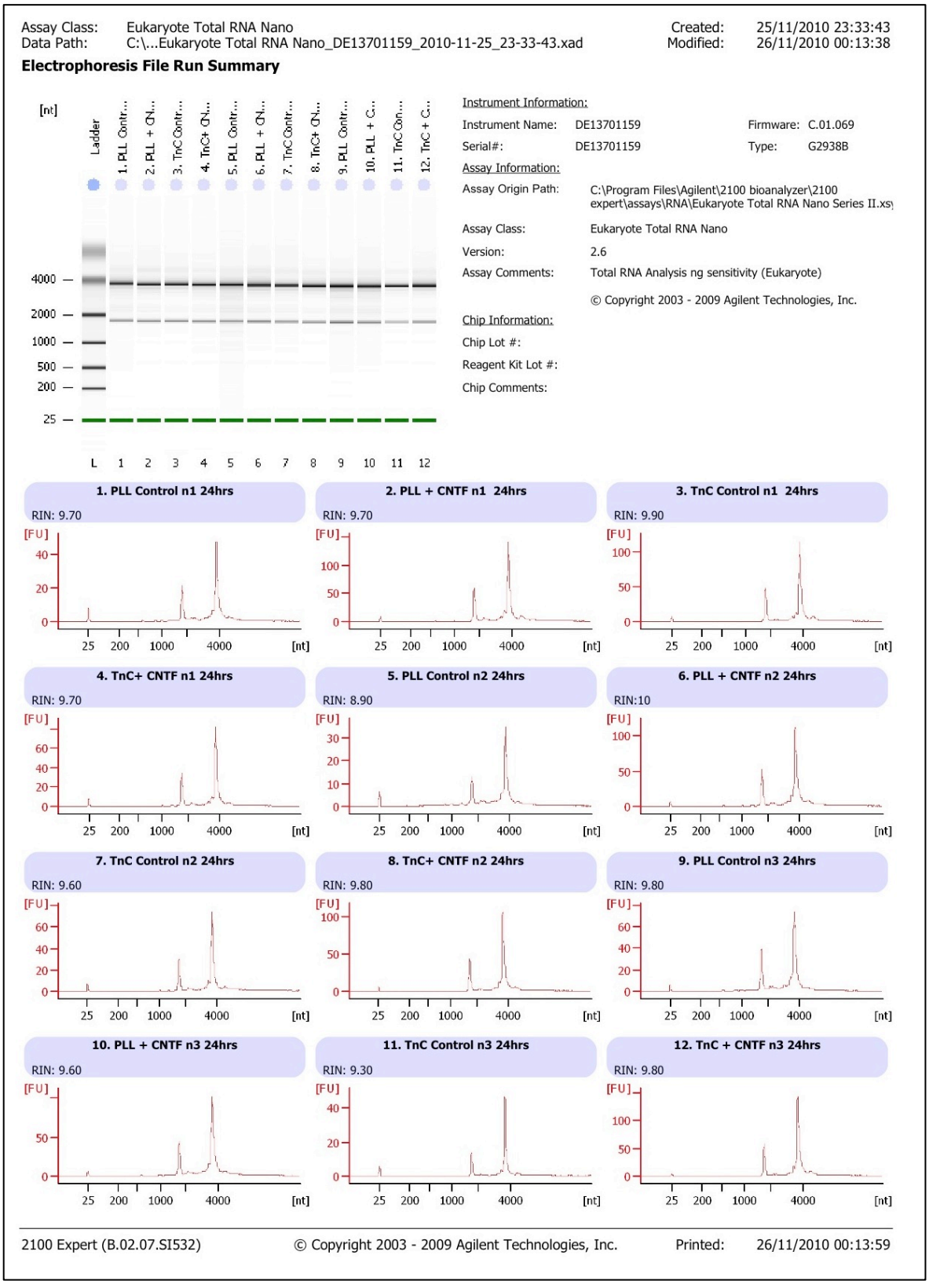

Figure I. II Electropherograms and RIN values, obtained using the Agilent 2100 Bioanalyser, for total RNA samples, used for microarray gene expression profiling analysis.
Only 24 hr samples are presented.

Appendix II

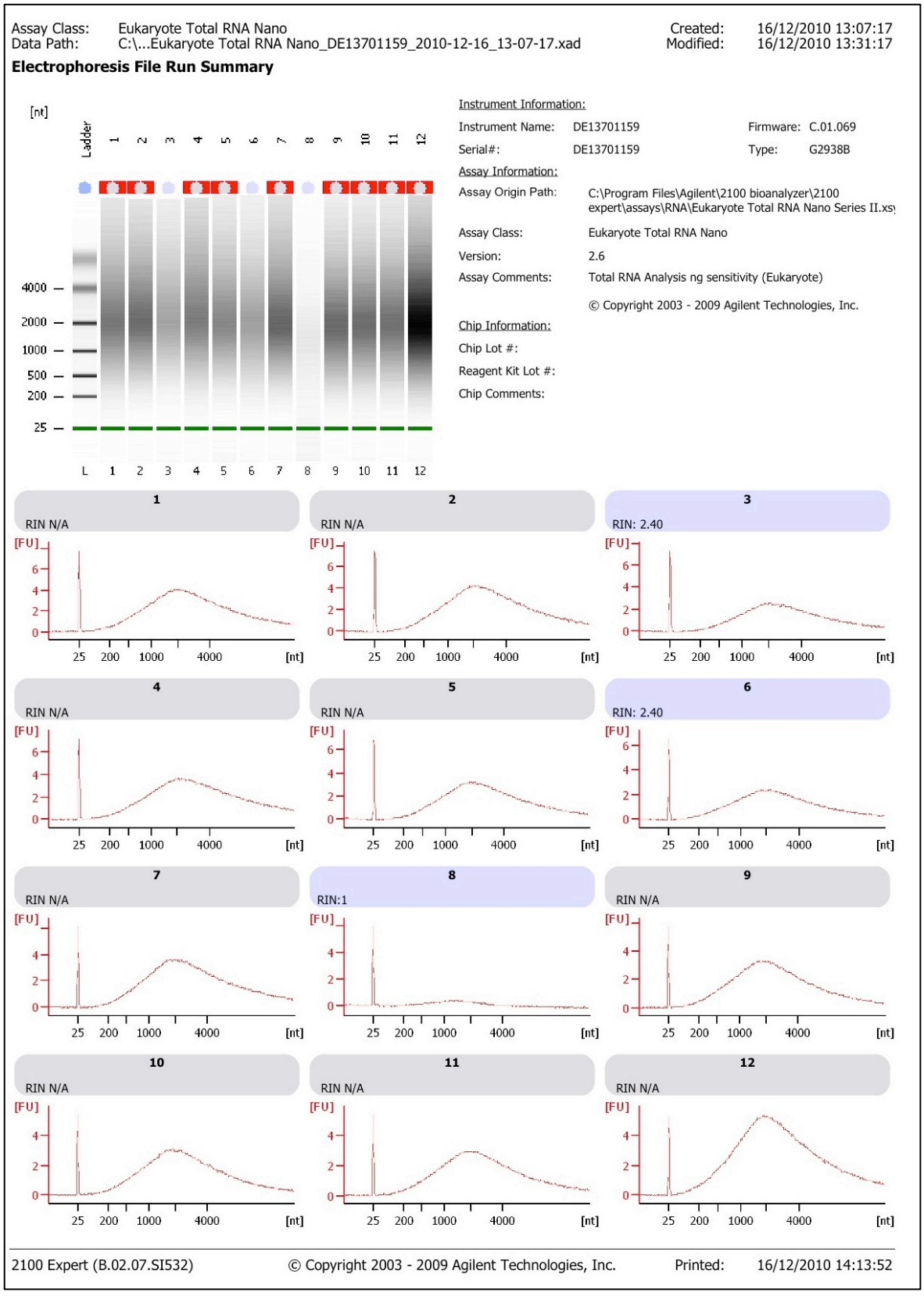

Figure II. I Electropherograms, obtained using the Agilent 2100 Bioanalyser, for cRNA samples, used for microarray gene expression profiling analysis.
Only 4 hr samples are presented. 1: PLL-control-n1; 2: PLL-CNTF-n1; 3:TnC-control-n1; 4:TnC-CNTF-n1; 5: PLL-control-n2; 6: PLL-CNTF-n2; 7:TnC-control-n2; 8:TnC-CNTF-n2; 9: PLL-control-n3; 10: PLL-CNTF-n3; 11:TnC-control-n3; 12:TnC-CNTF-n3.

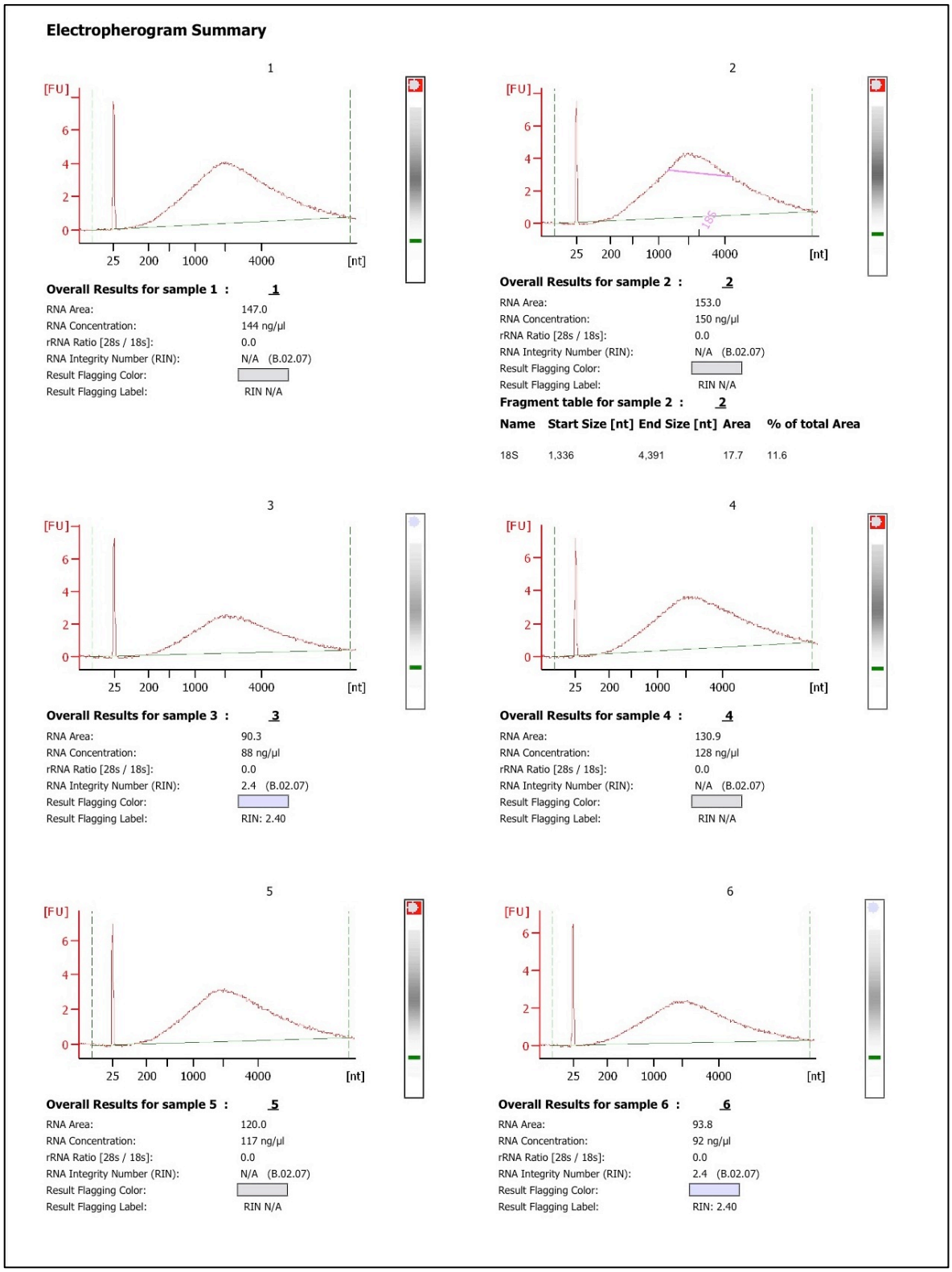

Figure II. II Details of the electropherograms, obtained using the Agilent 2100 Bioanalyser, for cRNA samples, used for microarray gene expression profiling analysis.
Only 4 hr samples are presented. 1: PLL-control-n1; 2: PLL-CNTF-n1; 3:TnC-control-n1; 4:TnC-CNTF-n1; 5: PLL-control-n2; 6: PLL-CNTF-n2.

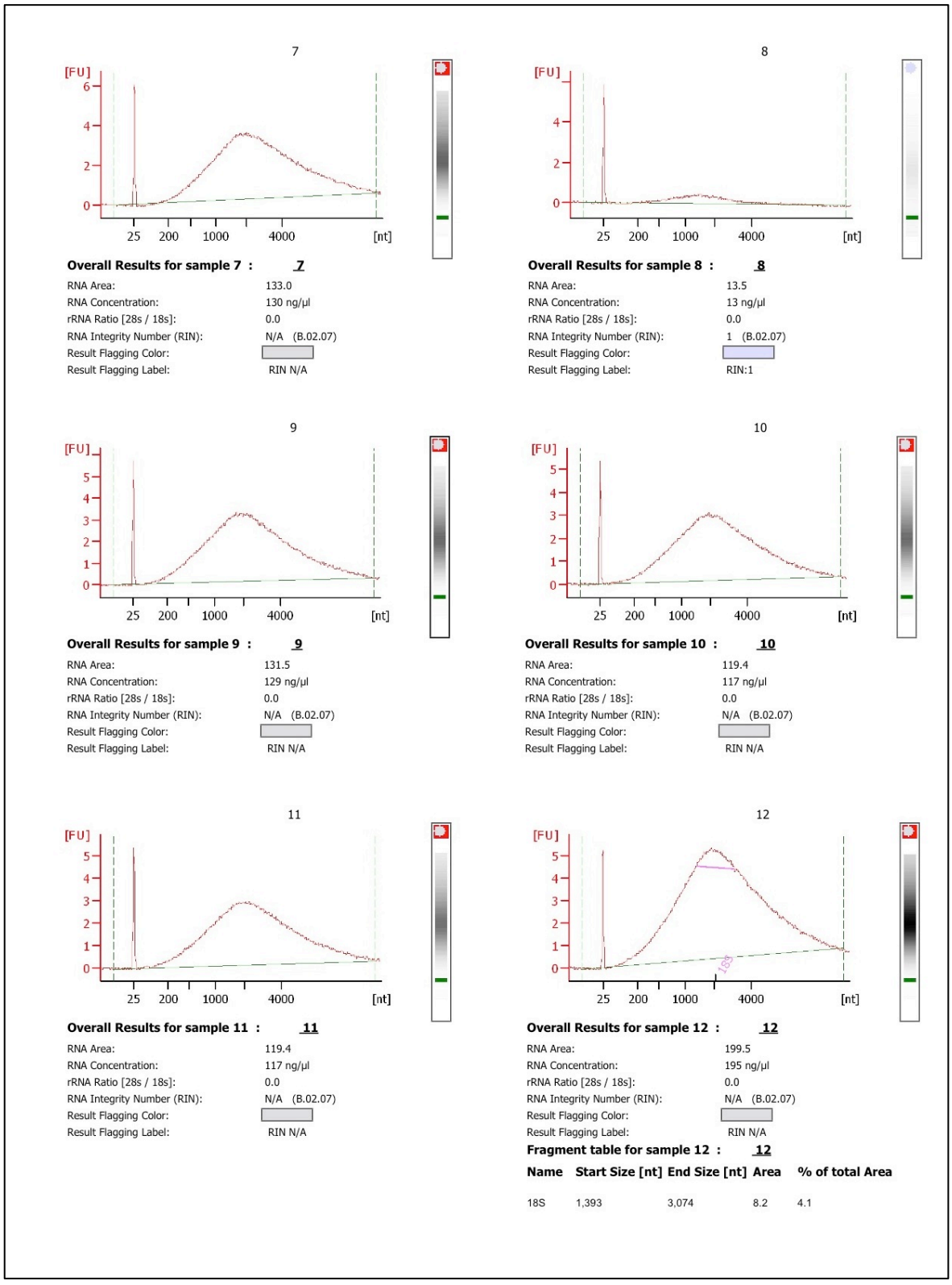

Figure II. III Details of the electropherograms, obtained using the Agilent 2100 Bioanalyser, for cRNA samples, used for microarray gene expression profiling analysis.
Only 4 hr samples are presented. 7:TnC-control-n2; 8:TnC-CNTF-n2; 9: PLL-control-n3; 10: PLL-CNTF-n3; 11:TnC-control-n3; 12:TnC-CNTF-n3.

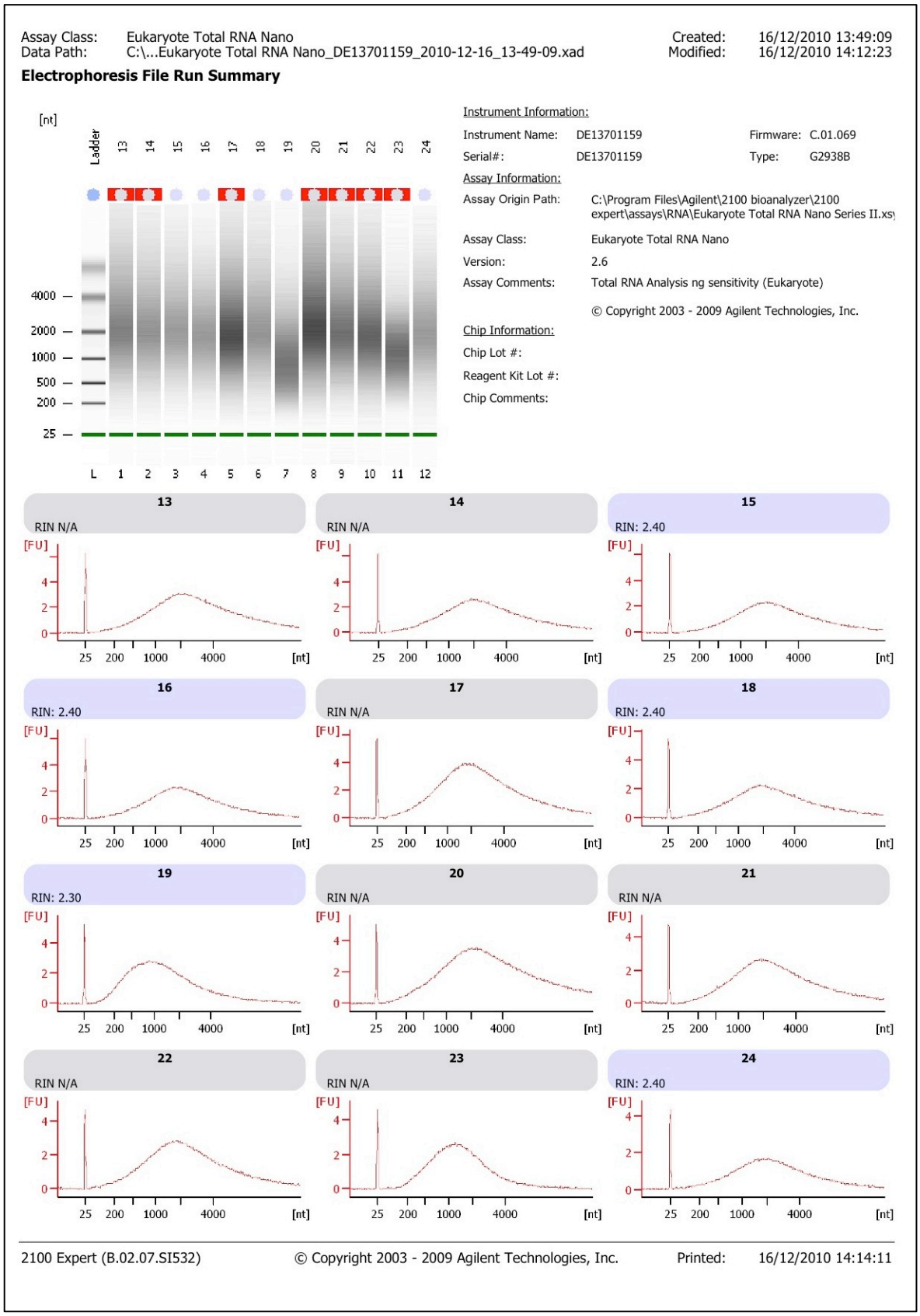

Figure II. IV Electropherograms, obtained using the Agilent 2100 Bioanalyser, for cRNA samples, used for microarray gene expression profiling analysis.
Only 24 hr samples are presented. 13: PLL-control-n1; 14: PLL-CNTF-n1; 15:TnC-control-n1; 16:TnC-CNTF-n1; 17: PLL-control-n2; 18: PLL-CNTF-n2; 19:TnC-control-n2; 20:TnC-CNTF-n2; 21: PLL-control-n3; 22: PLL-CNTF-n3; 23:TnC-control-n3; 24:TnC-CNTF-n3.

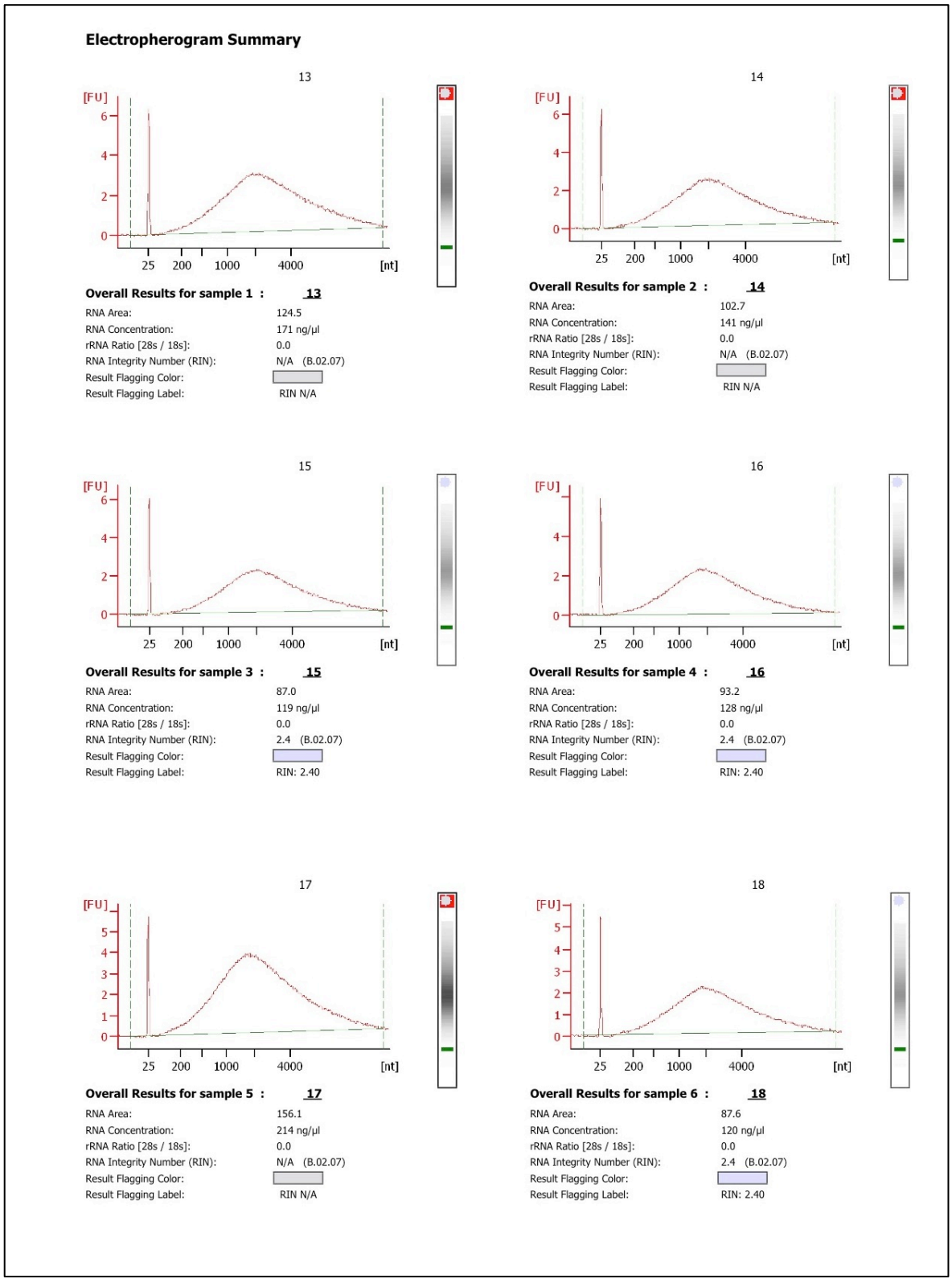

Figure II. V Details of the electropherograms, obtained using the Agilent 2100 Bioanalyser, for cRNA samples, used for microarray gene expression profiling analysis.
Only 24 hr samples are presented. 13: PLL-control-n1; 14: PLL-CNTF-n1; 15:TnC-control-n1; 16:TnC-CNTF-n1; 17: PLL-control-n2; 18: PLL-CNTF-n2.

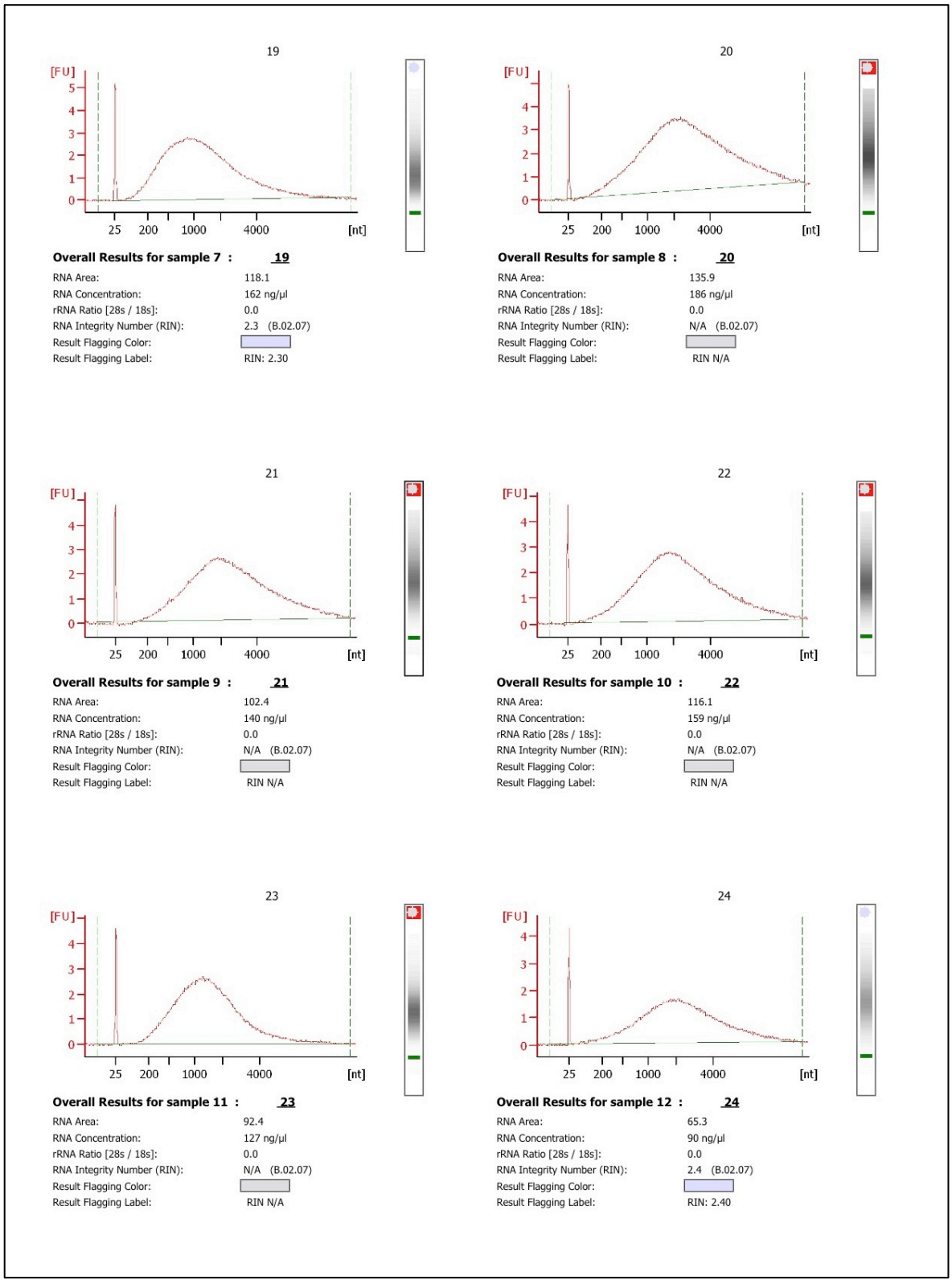

Figure II. VI Details of the electropherograms, obtained using the Agilent 2100 Bioanalyser, for cRNA samples, used for microarray gene expression profiling analysis.
Only 24 hr samples are presented. 19:TnC-control-n2; 20:TnC-CNTF-n2; 21: PLL-control-n3; 22: PLL-CNTF-n3; 23:TnC-control-n3; 24:TnC-CNTF-n3.

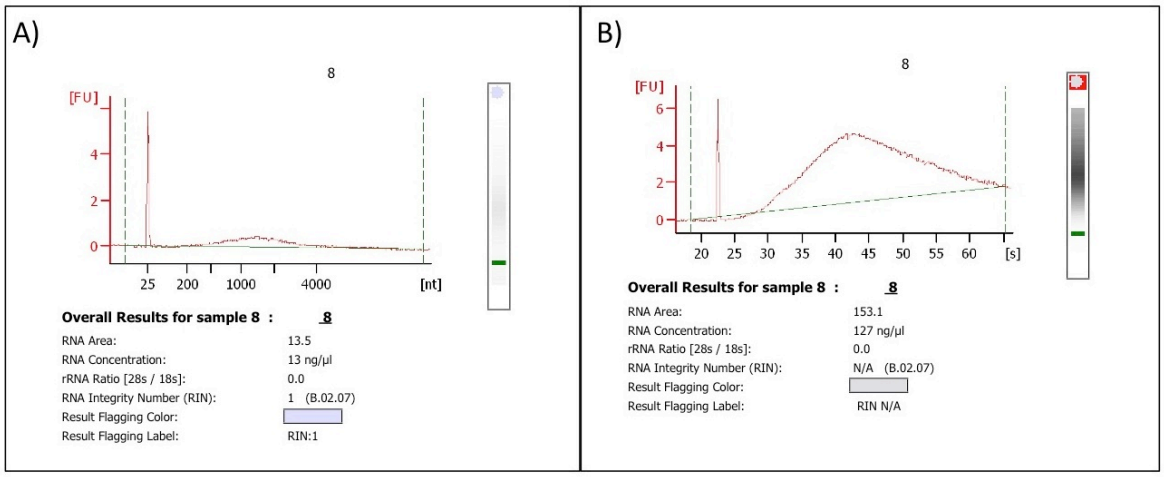

Figure II. VII Details of the electropherograms, obtained using the Agilent 2100 Bioanalyser, for cRNA sample of #8.
The electropherograms were obtained either before (A) or after (B) the samples were centrifuged at high-speed vacuum centrifuge. #8 sample is TnC-CNTF-n2.

Appendix III

Table III. I The concentrations of biotinylated RNA samples, which were used for microarray gene expression profiling, before and after they were concentrated using a high-speed vacuum centrifuge.

Sample #	Sample Name	Time point	n	Concentration (ng/µl)	Concentration (ng/µl) after centrifugation
1	PLL Control	4 hours	1	144	640
2	PLL + CNTF	4 hours	1	153	595
3	TnC Control	4 hours	1	88	461
4	TnC + CNTF	4 hours	1	128	415
5	PLL Control	4 hours	2	117	442
6	PLL + CNTF	4 hours	2	92	343
7	TnC Control	4 hours	2	130	557
8	TnC + CNTF	4 hours	2	13/ 75	261
9	PLL Control	4 hours	3	129	732
10	PLL + CNTF	4 hours	3	117	417
11	TnC Control	4 hours	3	117	434
12	TnC + CNTF	4 hours	3	195	409
13	PLL Control	24 hours	1	171	452
14	PLL + CNTF	24 hours	1	141	392
15	TnC Control	24 hours	1	119	418
16	TnC + CNTF	24 hours	1	128	358
17	PLL Control	24 hours	2	214	595
18	PLL + CNTF	24 hours	2	120	352
19	TnC Control	24 hours	2	162	422
20	TnC + CNTF	24 hours	2	186	413
21	PLL Control	24 hours	3	140	438
22	PLL + CNTF	24 hours	3	159	417
23	TnC Control	24 hours	3	127	189
24	TnC + CNTF	24 hours	3	90	231

Appendix IV

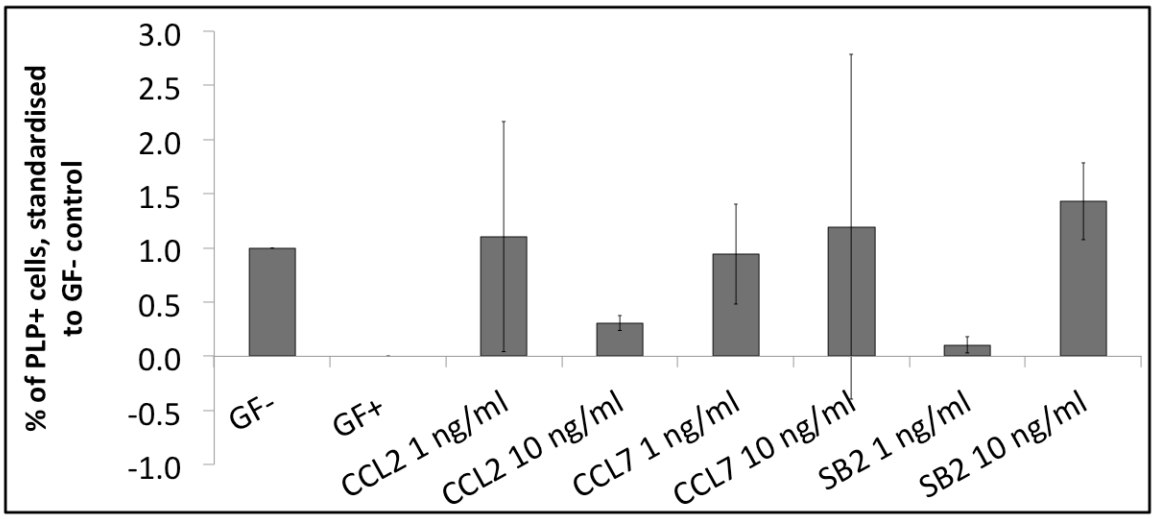

Figure IV. I The effcts of different treatments on the maturation of oligodendrocytes. Oligodendrocyte precursor cells (OPC) were purified from the rat cerebral cortical astrocyte cultures. They were initially maintained in medium containing the growth factors (GF) PDGF and FGF2, known mitogens that inhibit oligodendrocyte maturation. After 4-5 DIV, the cultures were treated with CCL2, CCL7 or SERPINB2 (SB2) at 1 ng/ml or 10 ng/ml. GF+ control cultures were always fed with medium containing PDGF and FGF2; whereas, GF- control cultures were fed with standard oligodendrocyte medium without GFs after the initial period of 4-5 DIV to allow the maturation of OPCs. The cultures were stained using the O4 and anti-PLP antibodies together with DAPI at 8-10 DIV to detect the number of mature oligodendrocytes. The cells were counted in Image J using 15-20 images per coverslip from fluorescent microscopy. Total number of cells were quantified using "dapi.cp" pipeline in Cell Profiler. PLP positive cells were expressed as a percentage of the total number of cells per coverslip. All PLP+ cells were also positive for the O4 antibody. Two coverslips were used per condition. The averages shown here are from two experimental repeats. The error bars present the ±standard deviation. Statistical analysis could not be carried on the data due to the lack of the minimum required number of experimental repeats. DIV: days *in vitro*; FGF2: fibroblast growth factor 2; GF: growth factor; PDGF: platelet-derived growth factor; PLP: proteolipid protein.

Table IV. I Percentage of PLP positive mature oligodendrocytes upon treatments with CCL2, CCL7 or SERPINB2

Percentage of PLP+ cells								
	GF-	**GF+**	**CCL2 1 ng/ml**	**CCL2 10 ng/ml**	**CCL7 1 ng/ml**	**CCL7 10 ng/ml**	**SB2 1 ng/ml**	**SB2 10 ng/ml**
n=1	4.9	0.0	9.0	1.3	6.2	0.3	0.3	5.7
n=2	2.2	0.0	0.8	0.8	1.4	5.2	0.4	3.8
Avg.	3.6	0.0	4.9	1.0	3.8	2.8	0.3	4.8
SD	1.9	0.0	5.8	0.3	3.4	3.4	0.1	1.4
Percentage of PLP+ cells, standardised to control within each biological replicate.								
	GF-	**GF+**	**CCL2 1 ng/ml**	**CCL2 10 ng/ml**	**CCL7 1 ng/ml**	**CCL7 10 ng/ml**	**SB2 1 ng/ml**	**SB2 10 ng/ml**
n=1	1.0	0.0	1.9	0.3	1.3	0.1	0.1	1.2
n=2	1.0	0.0	0.4	0.4	0.6	2.3	0.2	1.7
Avg.	1.0	0.0	1.1	0.3	0.9	1.2	0.1	1.4
SD	0.0	0.0	1.1	0.1	0.5	1.6	0.1	0.4

Purified rat oligodendrocyte precursor cells (OPCs) were treated with 1 ng/ml or 10 ng/ml of CCL2, CCL7 or SERPINB2 (SB2). Control cultures consisted of GF+ cultures that were always fed with medium containing the growth factors (GF) PDGF and FGF2; whereas, GF- control cultures were fed with standard oligodendrocyte medium without GFs after the initial period of 4-5 DIV to allow the maturation of OPCs**.** The number of PLP positive (+) cells are expressed as a percentage of the total number of cells per coverslips. Two coverslips were used per condition. The averages presented in the table are from two experimental repeats. These averages are also shown as values standardised to GF- controls within each experimental repeat (biological replicate). Avg: average; GF: growth factor; SD: standard deviation.

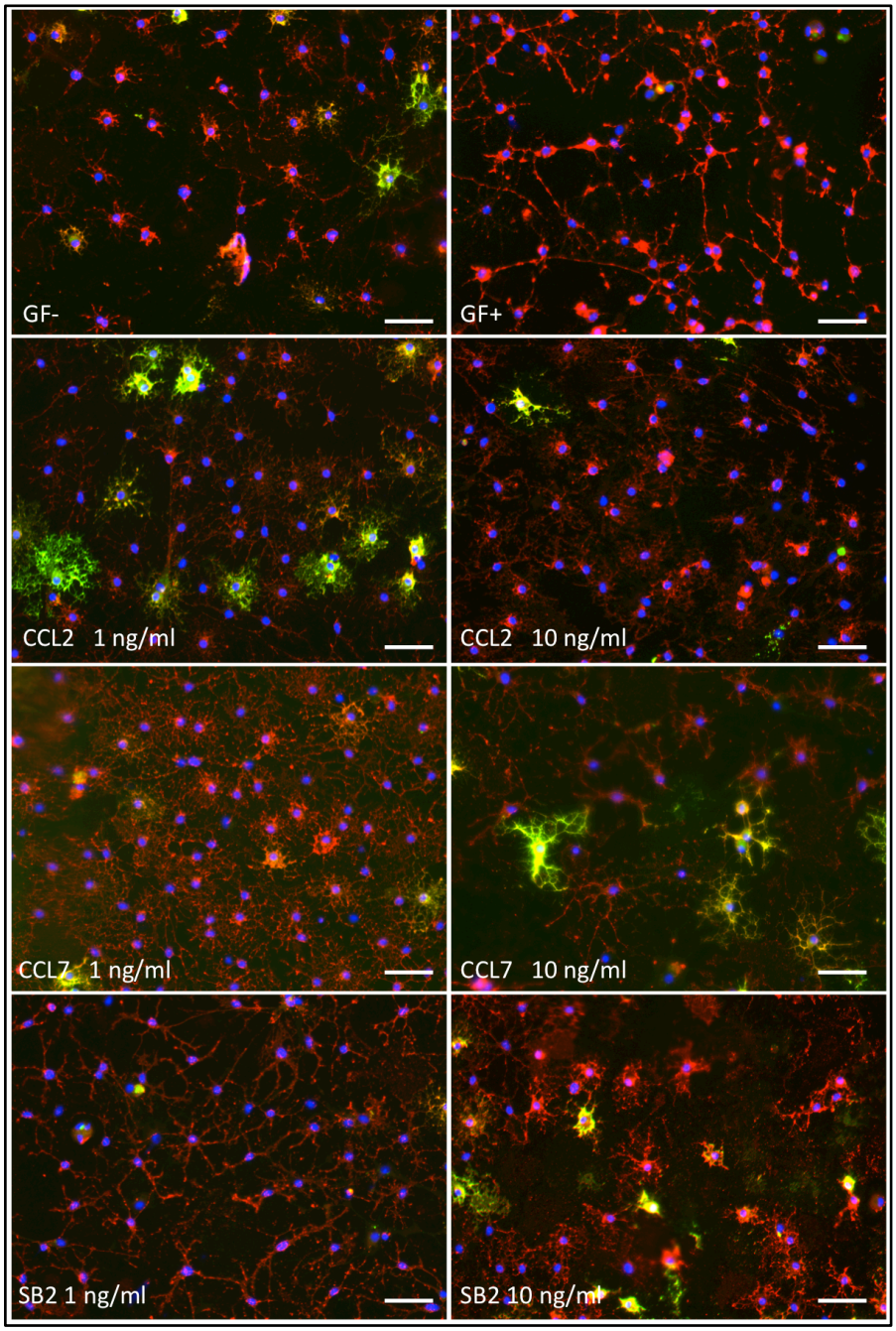

Figure IV. II Representative images from the 1st experimental repeat of the effects of different treatments on oligodendrocyte maturation.
Purified rat oligodendrocyte precursor cells were initially maintained in medium containing the growth factors (GF) PDGF and FGF2, known mitogens that inhibit oligodendrocyte maturation. After 4-5 DIV, the cultures were treated with CCL2, CCL7 or SERPINB2 (SB2) at 1 ng/ml or 10 ng/ml. GF+ control cultures were always maintained in medium with GFs; whereas GFs were not added to the GF- control cultures after 4-5 DIV to allow oligodendrocyte maturation. The cultures were stained using the O4 and anti-PLP antibodies together with DAPI at 8-10 DIV to detect the number of mature oligodendrocytes. The O4 antibody, PLP and DAPI are shown in red, green and blue, respectively. All scale bars represent 50 μm. DIV: days *in vitro*; FGF2: fibroblast growth factor 2; GF: growth factor; PDGF: platelet-derived growth factor; PLP: proteolipid protein.

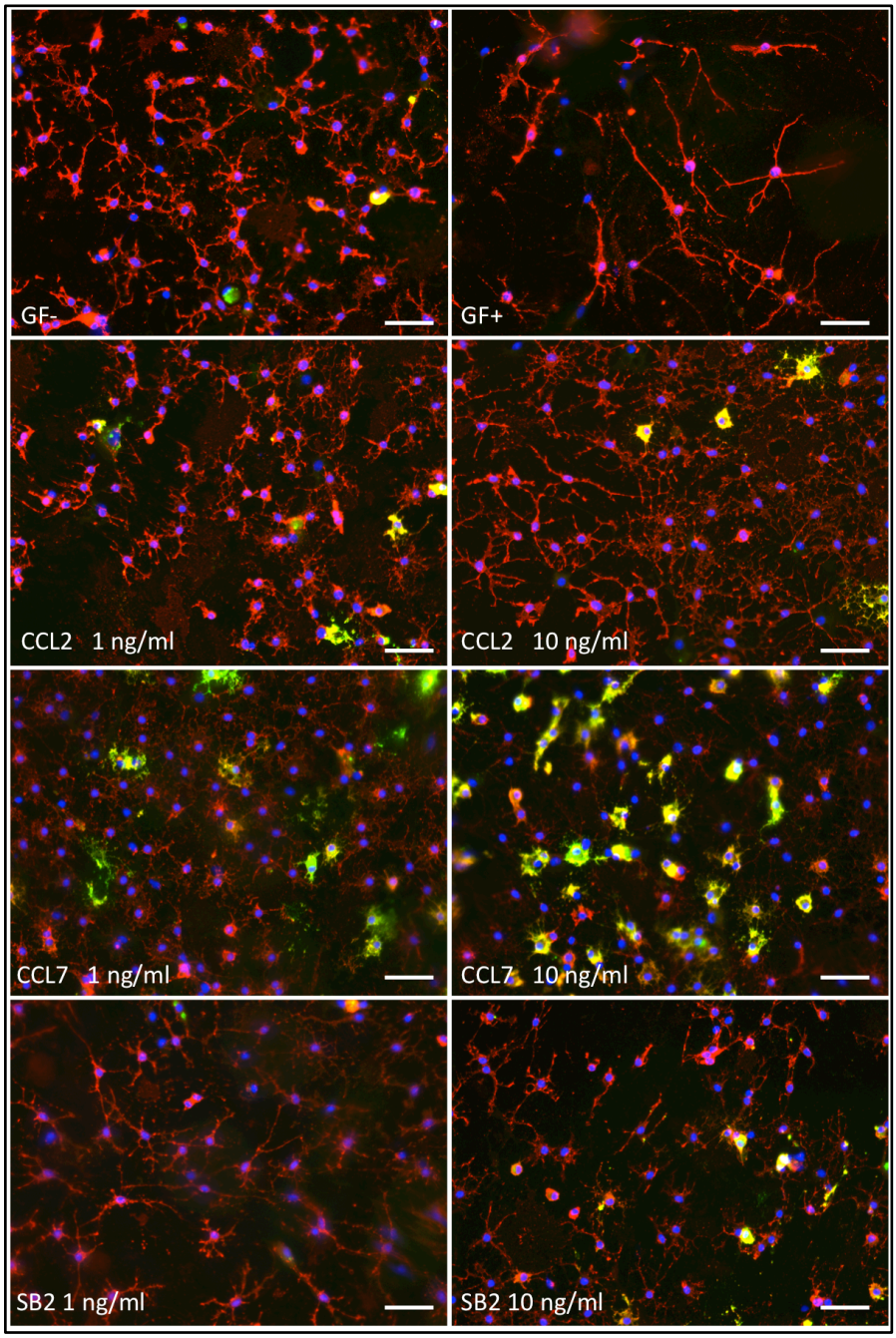

Figure IV. III Representative images from the 2nd experimental repeat of the effects of different treatments on oligodendrocyte maturation.
Purified rat oligodendrocyte precursor cells were initially maintained in medium containing the growth factors (GF) PDGF and FGF2, known mitogens that inhibit oligodendrocyte maturation. After 4-5 DIV, the cultures were treated with CCL2, CCL7 or SERPINB2 (SB2) at 1 ng/ml or 10 ng/ml. GF+ control cultures were always maintained in medium with GFs; whereas GFs were not added to the GF- control cultures after 4-5 DIV to allow oligodendrocyte maturation. The cultures were stained using the O4 and anti-PLP antibodies together with DAPI at 8-10 DIV to detect the number of mature oligodendrocytes. The O4 antibody, PLP and DAPI are shown in red, green and blue, respectively. All scale bars represent 50 μm. DIV: days *in vitro*; FGF2: fibroblast growth factor 2; GF: growth factor; PDGF: platelet-derived growth factor; PLP: proteolipid protein.

Appendix V

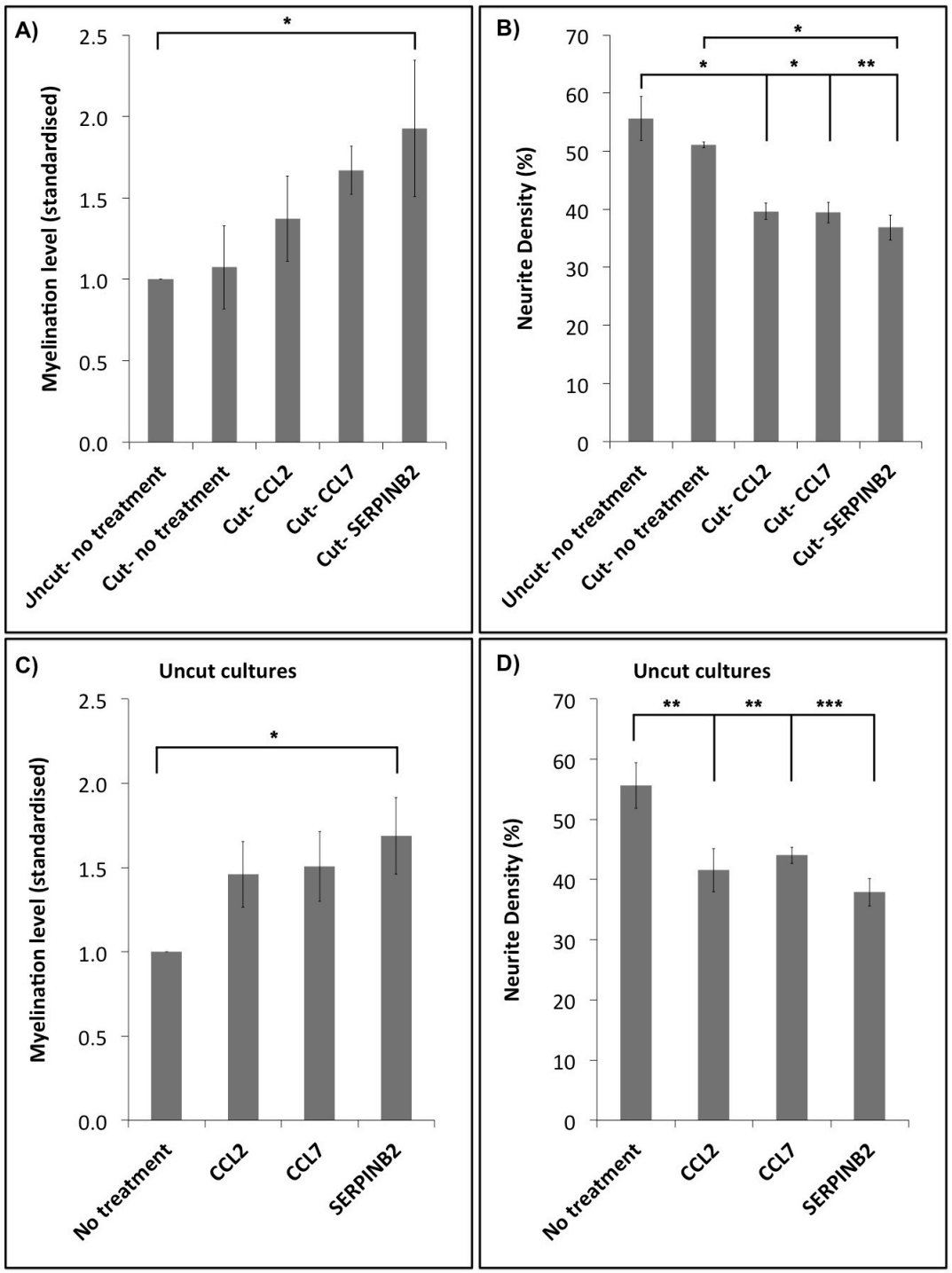

Figure V. I Treatment of cut myelinating cultures with SERPINB2, CCL2 or CCL7
Embryonic rat spinal cord myelinating cultures, set up using PLL-astrocytes, were cut manually using a razor blade at 23 DIV to initiate an *in vitro* model of CNS pathology. They were treated with 10 ng/ml of recombinant SERPINB2, CCL2 or CCL7 at the time points of 24, 26 and 28 DIV and were immunostained at 29 DIV. In each experimental repeat, there was also a batch of cells that were not cut (uncut) but treated with the same reagents at the same time points. The areas adjacent to cut lesions were used for the quantification of myelination in cut cultures. Myelination was presented as standardised to untreated uncut cultures. The experiment was repeated three times. One-way repeated measures ANOVA test was applied to the results to detect any possible significance. The error bars represent ± standard error of the mean. *P<0.05; **P<0.01; ***P<0.001. CNS: central nervous system; DIV: days *in vitro*; PLL: poly-L-lysine.

Appendix VI

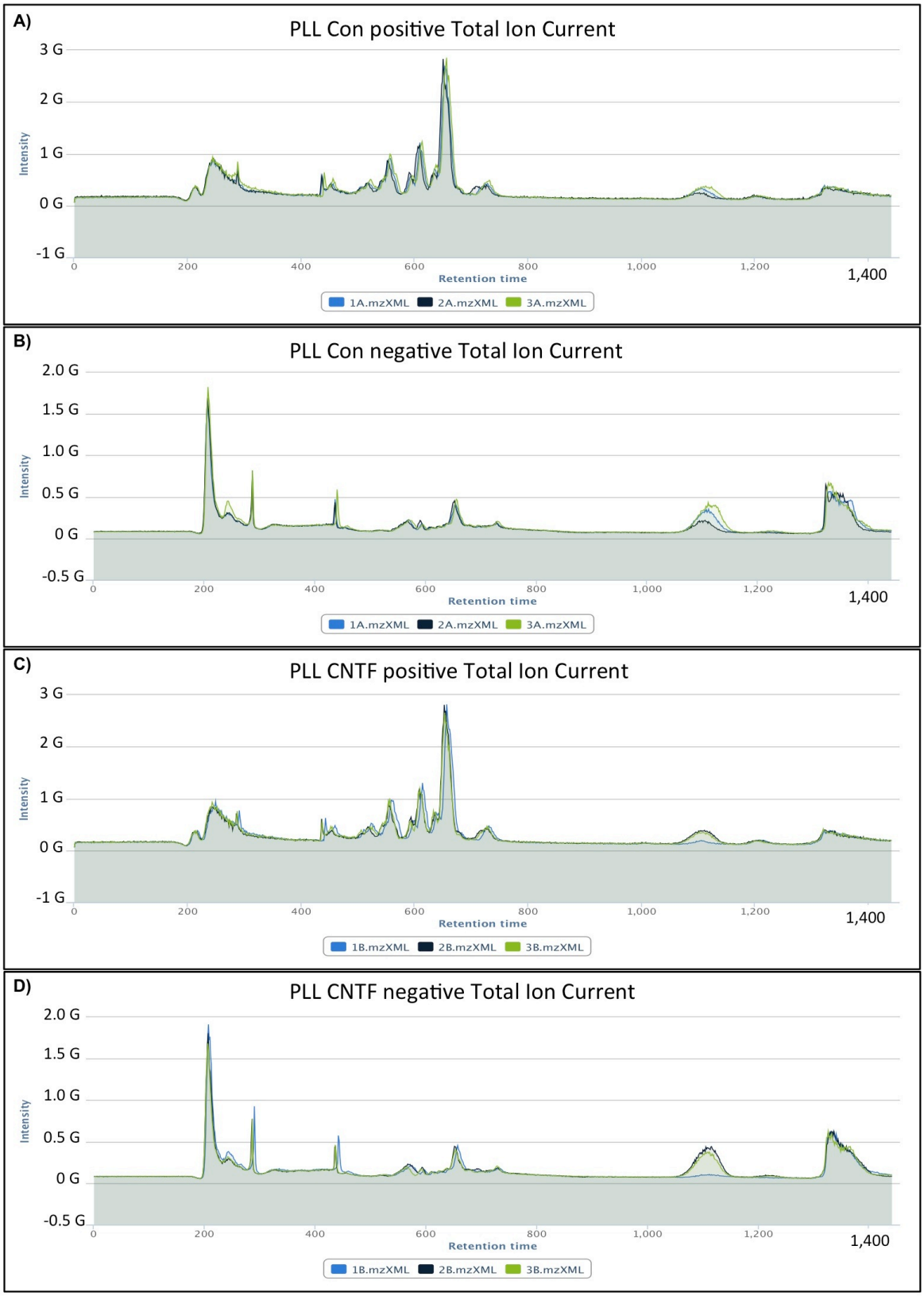

Figure VI. I Positive and negative total ion current (TIC) chromatograms of control and CNTF-treated PLL-astrocyte samples.

The samples extracted from confluent astrocytes, which were plated on PLL-coated coverslips, were analysed by Q-Exactive Hybrid Quadrupole-Orbitrap mass spectrometry. Y-axis presents the signal intensity in billions (G) as arbitrary units and x-axis presents the retention time in seconds. TIC plot for each biological replicate is shown in a different colour: blue, black, or green.

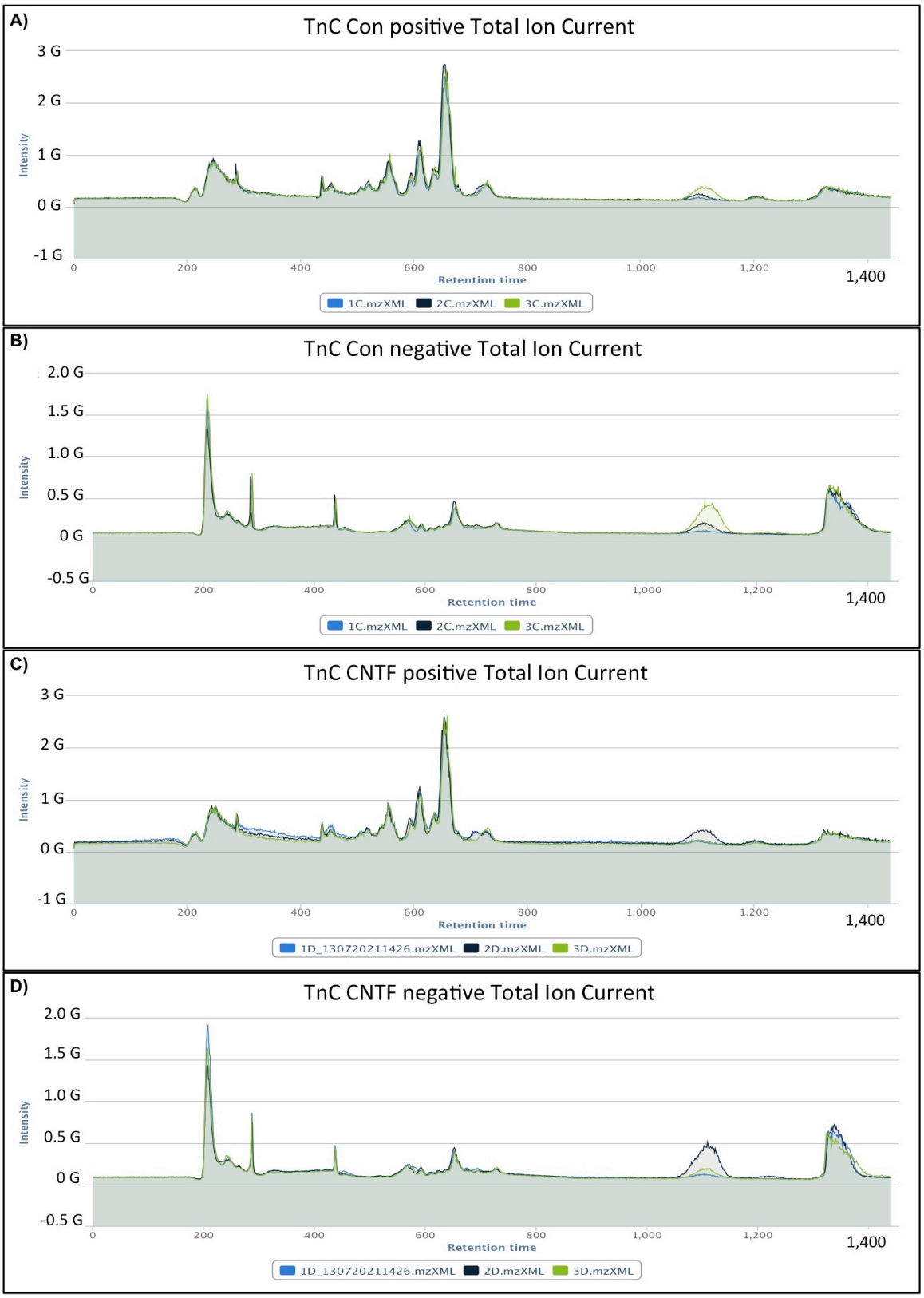

Figure VI. II Positive and negative total ion current (TIC) chromatograms of control and CNTF-treated TnC-astrocyte samples.
The samples extracted from confluent astrocytes, which were plated on TnC-coated coverslips, were analysed by Q-Exactive Hybrid Quadrupole-Orbitrap mass spectrometry. Y-axis presents the signal intensity in billions (G) as arbitrary units and x-axis presents the retention time in seconds. TIC plot for each biological replicate is shown in a different colour: blue, black, or green.

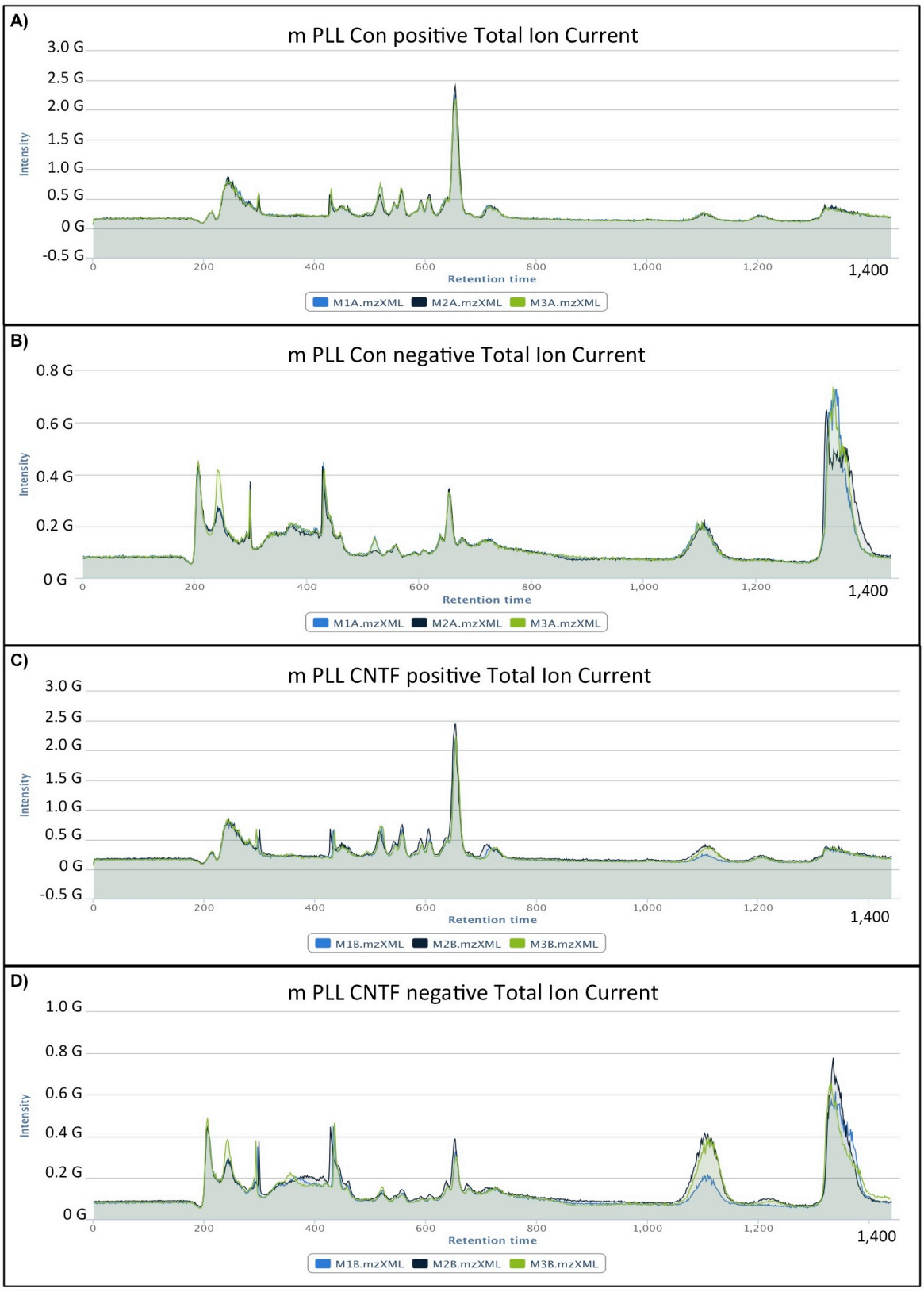

Figure VI. III Positive and negative total ion current (TIC) chromatograms of control and CNTF-treated PLL-astrocyte culture medium samples.
The samples extracted from the spent medium of confluent astrocytes, plated on PLL-coated coverslips, were analysed by Q-Exactive Hybrid Quadrupole-Orbitrap mass spectrometry. Y-axis presents the signal intensity in billions (G) as arbitrary units and x-axis presents the retention time in seconds. TIC plot for each biological replicate is shown in a different colour: blue, black, or green.

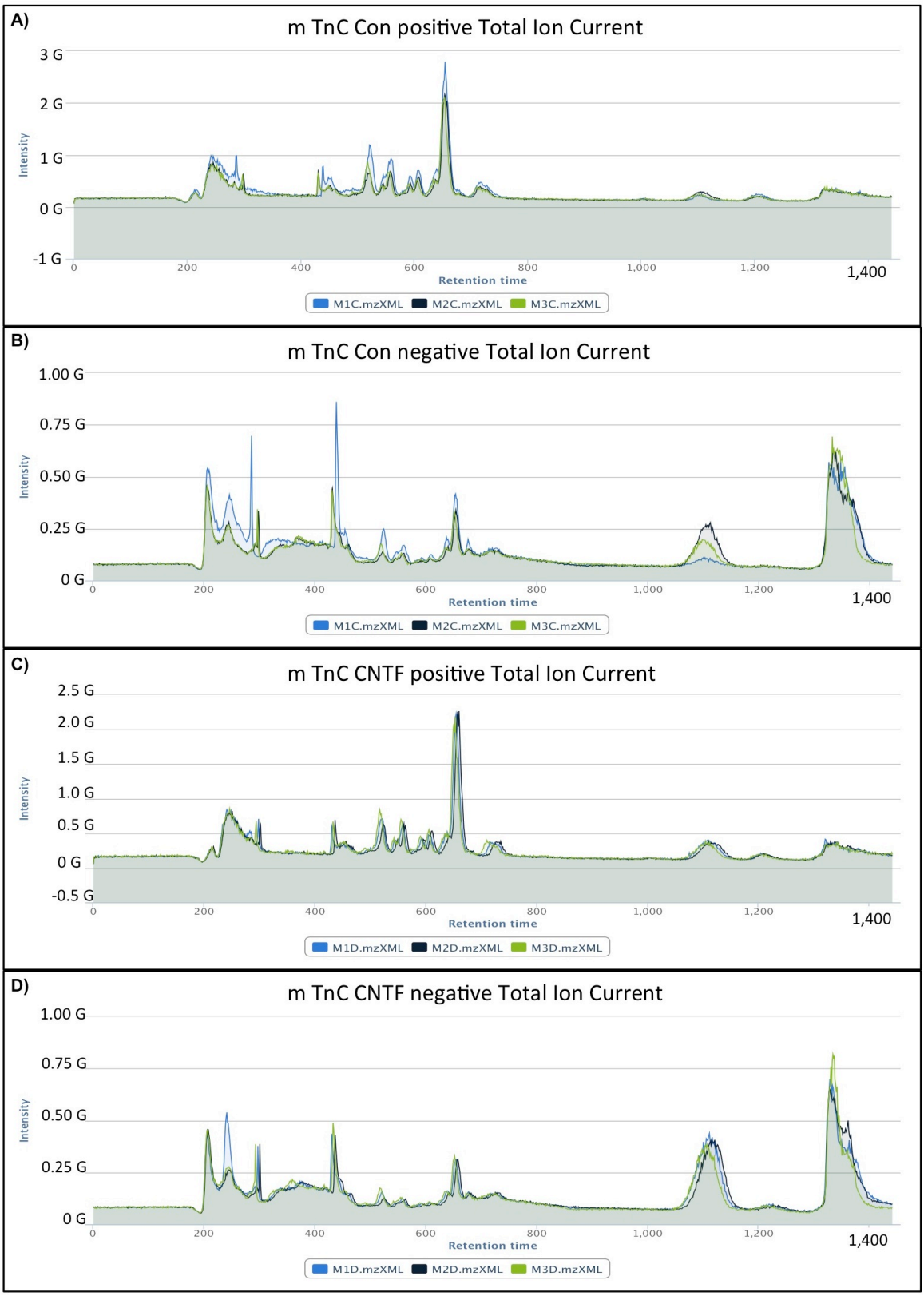

Figure VI. IV Positive and negative total ion current (TIC) chromatograms of control and CNTF-treated TnC-astrocyte culture medium samples.
The samples extracted from the spent medium of confluent astrocytes, plated on TnC-coated coverslips, were analysed by Q-Exactive Hybrid Quadrupole-Orbitrap mass spectrometry. Y-axis presents the signal intensity in billions (G) as arbitrary units and x-axis presents the retention time in seconds. TIC plot for each biological replicate is shown in a different colour: blue, black, or green.

Appendix VII

List of genes detected in Array 2

Ace2	Angiotensin-converting enzyme 2
Acot1	acyl-CoA thioesterase 1
Acsbg1	acyl-CoA synthetase bubblegum family member 1
Adamts1	ADAM metallopeptidase with thrombospondin type 1 motif, 1
Adcy8	adenylate cyclase 8
Adcyap1	adenylate cyclase activating polypeptide 1
Adora2a	Adenosine receptor A2a
Aff4	AF4/FMR2 family, member 4 (Predicted)
Agpat7	lysophosphatidylcholine acyltransferase 4
Agt	angiotensinogen (serpin peptidase inhibitor, clade A, member 8)
Agtr1a	Type-1A angiotensin II receptor
Aif1	allograft inflammatory factor 1
Aldh1a1	aldehyde dehydrogenase 1 family, member A1
Alk	anaplastic lymphoma receptor tyrosine kinase
Anxa3	annexin A3
AP-1	activator protein-1
APOC1	Apolipoprotein C-I
Arc	activity-regulated cytoskeleton-associated protein
Arhgdib	Rho, GDP dissociation inhibitor (GDI) beta
Arhgef19	Rho guanine nucleotide exchange factor (GEF) 19
Ascl1	Achaete-scute homolog 1
Asgr1	Asialoglycoprotein receptor 1
Atp1a2	Sodium/potassium-transporting ATPase subunit alpha-2
Axl	Axl receptor tyrosine kinase
Baalc	brain and acute leukemia, cytoplasmic
BAMBI	BMP and activin membrane-bound inhibitor homolog
Bcl2a1d	BCL2-related protein A1
Bdnf	brain-derived neurotrophic factor
Boc	BOC cell adhesion associated, oncogene regulated
Brunol6	Bruno-like 6, RNA binding protein (Drosophila) (Predicted)
Bub1	budding uninhibited by benzimidazoles 1 homolog
Cartptp	CART prepropeptide
Casp1	Caspase-1, Interleukin-1 beta convertase
Cbs	cystathionine beta synthase
Ccdc67	Coiled-coil domain-containing protein 67
Cckar	cholecystokinin A receptor
Ccl	chemokine (C-C motif) ligand
Ccna2	Ccna2 protein
Ccr1	chemokine (C-C motif) receptor 1
Cd248	CD248 molecule, endosialin
Cd37	CD37 antigen
CD53	Leukocyte surface antigen CD53
Cd68	CD68 antigen
Cd93	CD93 antigen
Ch25h	cholesterol 25-hydroxylase
Chgb	chromogranin B (secretogranin 1)
Chi3l1	Chitinase-3-like protein 1
Cldn11	claudin 11
Col16a1	collagen, type XVI, alpha 1
Col18a1	collagen, type XVIII, alpha 1

Col1a2	collagen, type I, alpha 2
Col3a1	collagen, type III, alpha 1
Col5a1	collagen, type V, alpha 1
Colec12	collectin sub-family member 12
Coq10b	coenzyme Q10 homolog B
Creb	cAMP responsive element binding protein
Crem	cAMP responsive element modulator
Crh	corticotropin releasing hormone
Cryab	crystallin, alpha B
CSC2	CRISPR-associated protein Csc2
Ctgf	connective tissue growth factor
Cth	cystathionine gamma-lyase
Cxcl	chemokine (C-X-C motif) ligand
Cxcr	chemokine (C-X-C motif) receptor
Cyp1b1	cytochrome P450, family 1, subfamily B, polypeptide 1
Cyr61	cysteine-rich, angiogenic inducer, 61
Dclk1	Serine/threonine-protein kinase DCLK1
Ddit4l	DNA-damage-inducible transcript 4-like
Dlx1	distal-less homeobox 1
Dlx2	distal-less homeobox 2
Dusp1	dual specificity phosphatase 1
Dynlrb2	Dynein light chain roadblock-type 2
Egr1	early growth response 1
Ell2	elongation factor, RNA polymerase II, 2
Emd	emerin
Emp1	epithelial membrane protein 1
Entpd5	Ectonucleoside triphosphate diphosphohydrolase 5
Fabp4	fatty acid binding protein 4, adipocyte
Fbn2	fibrillin 2
Fcgr3	Fc receptor, IgG, low affinity III
Fcnb	ficolin B
Fn1	fibronectin 1
Fmod	fibromodulin
Fos	FBJ osteosarcoma oncogene
Fstl1	follistatin-like 1
G0S2	G0/G1 switch protein 2
Gadd45g	growth arrest and DNA-damage-inducible, gamma
Gapdh	glyceraldehyde-3-phosphate dehydrogenase
Gda	Guanine deaminase
Gdf15	growth differentiation factor 15
Gem	GTP binding protein overexpressed in skeletal muscle
Gldc	glycine dehydrogenase
Glipr1	GLI pathogenesis-related 1
Gp130	glycoprotein 130
Gpr103	pyroglutamylated RFamide peptide receptor
GPR37L1	Endothelin B receptor-like protein 2, G protein-coupled receptor 37-like 1, isoform CRA_a
GPC4	Glypican 4
Gstm1	glutathione S-transferase mu 1
Gstm7	glutathione S-transferase mu 7
GSTP2	Glutathione S-transferase P 2
H19	H19, imprinted maternally expressed transcript
Hbb	hemoglobin, beta
Hbegf	heparin-binding EGF-like growth factor
Hcrt	hypocretin
HLA-DMB	Major histocompatibility complex, class II, DM beta, isoform CRA_a

Hmox1	heme oxygenase (decycling) 1
HTRA1	Serine protease HTRA1
Icam1	intercellular adhesion molecule 1
ICER	inducible cAMP early repressor
Igf2	insulin-like growth factor 2
Igfbp2	insulin-like growth factor binding protein 2
Inpp5d	Phosphatidylinositol 3,4,5-trisphosphate 5-phosphatase 1
Irf5	interferon regulatory factor 5
Irf7	interferon regulatory factor 7
Isg12(b)	interferon, alpha-inducible protein 27
Kcnc2	Potassium voltage-gated channel subfamily C member 2
Kcnn4	potassium intermediate/small conductance calcium-activated channel, subfamily N, member 4
Kif11	kinesin family member 11
Klf4	Kruppel-like factor 4
Krt19	keratin 19
Laptm5	lysosomal protein transmembrane 5
Lcn2	lipocalin 2
Lcp1	lymphocyte cytosolic protein 1
Lipa	lipase A, lysosomal acid, cholesterol esterase
Lgi2	leucine-rich repeat LGI family, member 2
Lgi4	leucine-rich repeat LGI family, member 4
Loxl	lysyl oxidase-like
Lpl	lipoprotein lipase
LY86	Lymphocyte antigen 86 (Predicted)
Maff	v-maf avian musculoaponeurotic fibrosarcoma oncogene homolog F
Map1b	Microtubule-associated protein 1B
Mat2a	methionine adenosyltransferase II, alpha
Megf6	multiple EGF-like-domains 6
Mfhas1	Malignant fibrous histiocytoma amplified sequence 1 (Predicted), isoform CRA_a
Mmd2	Monocyte to macrophage differentiation-associated 2
Mmp	matrix metalloproteinase
Mrc1	mannose receptor, C type 1
Mrps10	28S ribosomal protein S10, mitochondrial
Msr2	myosuppressin receptor 2
Msx1	Msh homeobox 1
Mt1a	Metallothionein-1
Mx1	MX dynamin-like GTPase 1
Negr1	Neuronal growth regulator 1
Nfatc4	Nuclear factor of activated T-cells, cytoplasmic, calcineurin-dependent 4
Nfil3	nuclear factor, interleukin 3, regulated
Nfkbia	nuclear factor of kappa light polypeptide gene enhancer in B-cells inhibitor, alpha
Ngfr	nerve growth factor receptor
Nmbr	neuromedin B receptor
Nmu	Neuromedin-U
Npas4	neuronal PAS domain protein 4
Nptx2	neuronal pentraxin II
Npy	Pro-neuropeptide Y
Nr4a2	nuclear receptor subfamily 4, group A, member 2
Nr4a3	nuclear receptor subfamily 4, group A, member 3
Nqo1	NAD(P)H dehydrogenase, quinone 1
NTS	Neurotensin/neuromedin N
Oas1a	2'-5' oligoadenylate synthetase 1A
Ocil	C-type lectin domain family 2 member D5

Ogn	Mimecan, Osteoglycin
Omd	osteomodulin
Osgin1	oxidative stress induced growth inhibitor 1
Oxnad1	oxidoreductase NAD-binding domain containing 1
P2ry12	P2Y purinoceptor 12
P2ry14	purinergic receptor P2Y, G-protein coupled, 14
Pax3	paired box 3
PBS	phosphate-buffered saline
Pdlim7	PDZ and LIM domain 7
Penk1	proenkephalin
Per1	period circadian clock 1
Pik3ap1	phosphoinositide-3-kinase adaptor protein 1
Pkm2	pyruvate kinase, muscle
Plagl1	pleiomorphic adenoma gene-like 1
Plcd4	phospholipase C, delta 4
Plec1	Plectin-1
Plek	pleckstrin
Pnoc	Prepronociceptin
Porf1	preoptic regulatory factor 1
Postn	periostin, osteoblast specific factor
Ppp1r1b	protein phosphatase 1, regulatory (inhibitor) subunit 1B
Pqlc1	PQ-loop repeat-containing protein 1
Prph1	peripherin
Ptgs2	prostaglandin-endoperoxide synthase 2
Ptp4a1	protein tyrosine phosphatase type IVA, member 1
Ptpn6	Tyrosine-protein phosphatase non-receptor type 6, Protein-tyrosine phosphatase SHP-1
Ptprn	protein tyrosine phosphatase, receptor type, N
Rab27b	RAB27B, member RAS oncogene family
Rac2	RAS-related C3 botulinum substrate 2
Rasd1	RAS, dexamethasone-induced 1
Rbm3	RNA binding motif protein 3
RBP1	Retinol-binding protein 1
Reg3b	regenerating islet-derived 3 beta
Rgs4	Regulator of G-protein signaling 4
Rib43a	coiled-coil protein associated with protofilament ribbons
Ribc2	RIB43A domain with coiled-coils 2
Rilp	Rab interacting lysosomal protein
Rom1	retinal outer segment membrane protein 1
Rpe65	retinal pigment epithelium 65
S100A11	S100 calcium-binding protein A11
S100a13	S100 calcium binding protein A13
S100a3	S100 calcium binding protein A3
Scd1	Acyl-CoA desaturase 1
Scg2	secretogranin II
Serpina3n	Serine protease inhibitor A3N
Serpinb2	serpin peptidase inhibitor
Serpinf1	serpin peptidase inhibitor, clade F (alpha-2 antiplasmin, pigment epithelium derived factor), member 1
Sfxn5	Sideroflexin-5
Slamf9	SLAM family member 9 [
SLC	solute carrier
Slc14a2	urea transporter member 2
Slc2a5	solute carrier family 2 (facilitated glucose transporter), member 5
Slc38a1	solute carrier family 38, member 1
Slc7A5	Large neutral amino acids transporter small subunit 1

Slc7A11	solute carrier family 7 (anionic amino acid transporter light chain, xc- system), member 11
Slco1c1	solute carrier organic anion transporter family, member 1c1
Slco2b1	solute carrier organic anion transporter family, member 2b1
Snap25	Synaptosomal-associated protein 25
Snf1lk	salt-inducible kinase 1
Sorl1	Protein Sorl1
Sostdc1	sclerostin domain containing 1
Spag4	sperm associated antigen 4
Spbc24	Kinetochore protein Spc25
Spp1	Osteopontin
Srrm2	serine/arginine repetitive matrix 2
Ssg1	steroid sensitive gene 1
Stc1	stanniocalcin 1
Sult1a1	Sulfotransferase 1A1
Tagln	transgelin
Tbc1d17	TBC1 domain family, member 17
Tbx15	T-box 15
Th1	T helper cell type 1
Thbs2	thrombospondin 2
Thrsp	thyroid hormone responsive
Tlr	toll-like receptor
Tmem37	Voltage-dependent calcium channel gamma-like subunit, Transmembrane protein 37
Tnnc2	troponin C2, fast
Tpm4	Tropomyosin alpha-4 chain
Traf4af1	kinetochore-localized astrin/SPAG5 binding protein
Trem2	triggering receptor expressed on myeloid cells 2
Tsp2	thrombospondin 2
Ttk	Ttk protein kinase (Predicted)
Ube1c	ubiquitin-like modifier activating enzyme 3
Usp2	ubiquitin specific peptidase 2
Vgf	similar to viral growth factor, nerve growth factor inducible
Vif	Vif protein
Vip	vasoactive intestinal polypeptide
Vmp	Vacuole membrane protein 1
Wif1	WNT inhibitory factor 1
Ypel4	yippee-like 4
Zbp1	Z-DNA binding protein 1
Zdhhc20	zinc finger, DHHC-type containing 20

References

Abbott NJ, Rönnbäck L, Hansson E. Astrocyte-endothelial interactions at the blood-brain barrier. Nat Rev Neurosci. 2006;7(1):41-53.

Abbott NJ. Astrocyte-endothelial interactions and blood-brain barrier permeability. J Anat. 2002;200(6):629-38.

Adam SA, Schnell O, Pöschl J, Eigenbrod S, Kretzschmar HA, Tonn JC, Schüller U. ALDH1A1 is a marker of astrocytic differentiation during brain development and correlates with better survival in glioblastoma patients. Brain Pathol. 2012;22(6):788-97.

Afshari FS, Chu AK, Sato-bigbee C. Effect of cyclic AMP on the expression of myelin basic protein species and myelin proteolipid protein in committed oligodendrocytes: differential involvement of the transcription factor CREB. J Neurosci Res. 2001;66(1):37-45.

Agulhon C, Petravicz J, McMullen AB, Sweger EJ, Minton SK, Taves SR, Casper KB, Fiacco TA, McCarthy KD. What is the role of astrocyte calcium in neurophysiology?. Neuron. 2008;59(6):932-46.

Albrecht PJ, Dahl JP, Stoltzfus OK, Levenson R, Levison SW. Ciliary neurotrophic factor activates spinal cord astrocytes, stimulating their production and release of fibroblast growth factor-2, to increase motor neuron survival. Exp Neurol. 2002;173(1):46-62.

Albrecht PJ, Enterline JC, Cromer J, Levison SW. CNTF-activated astrocytes release a soluble trophic activity for oligodendrocyte progenitors. Neurochem Res. 2007;32(2):263-71.

Albrecht PJ, Murtie JC, Ness JK, Redwine JM, Enterline JR, Armstrong RC, Levison SW. Astrocytes produce CNTF during the remyelination phase of viral-induced spinal cord demyelination to stimulate FGF-2 production. Neurobiol Dis. 2003;13(2):89-101.

Alfonsi F, Filippi P, Salaun D, Delapeyrière O, Durbec P. LIFR beta plays a major role in neuronal identity determination and glial differentiation in the mouse facial nucleus. Dev Biol. 2008;313(1):267-78.

Alliot F, Godin I, Pessac B. Microglia derive from progenitors, originating from the yolk sac, and which proliferate in the brain. Brain Res. Dev. Brain Res. 1999;117:145–52.

Aloisi F, Agresti C, Levi G. Establishment, characterization, and evolution of cultures enriched in type-2 astrocytes. J Neurosci Res. 1988;21(2-4):188-98.

Aloisi F, Rosa S, Testa U, Bonsi P, Russo G, Peschle C, Levi G. Regulation of leukemia inhibitory factor synthesis in cultured human astrocytes. J Immunol. 1994;152(10):5022-31.

Alvarez-maubecin V, Garcia-hernandez F, Williams JT, Van bockstaele EJ. Functional coupling between neurons and glia. J Neurosci. 2000;20(11):4091-8.

Amiry-moghaddam M, Williamson A, Palomba M, Eid T, de Lanerolle NC, Nagelhus EA, Adams ME, Froehner SC, Agre P, Ottersen OP. Delayed K+ clearance associated with aquaporin-4 mislocalization: phenotypic defects in brains of alpha-syntrophin-null mice. Proc Natl Acad Sci USA. 2003;100(23):13615-20.

Anandatheerthavarada HK, Shankar SK, Ravindranath V. Rat brain cytochromes P-450: catalytic, immunochemical properties and inducibility of multiple forms. Brain Res. 1990;536(1-2):339-43.

Anderson CM, Nedergaard M. Astrocyte-mediated control of cerebral microcirculation. Trends Neurosci. 2003;26(7):340-4.

Arai K, Lo EH. Astrocytes protect oligodendrocyte precursor cells via MEK/ERK and PI3K/Akt signaling. J Neurosci Res. 2010;88(4):758-63.

Araque A, Parpura V, Sanzgiri RP, Haydon PG. Glutamate-dependent astrocyte modulation of synaptic transmission between cultured hippocampal neurons. Eur J Neurosci. 1998;10(6):2129-42.

Araque A, Parpura V, Sanzgiri RP, Haydon PG. Tripartite synapses: glia, the unacknowledged partner. Trends Neurosci. 1999;22(5):208-15.

Araujo DM, Cotman CW. Basic FGF in astroglial, microglial, and neuronal cultures: characterization of binding sites and modulation of release by lymphokines and trophic factors. J. Neurosci.1992;12:1668–78.

Argaw AT, Gurfein BT, Zhang Y, Zameer A, John GR. VEGF-mediated disruption of endothelial CLN-5 promotes blood-brain barrier breakdown. Proc Natl Acad Sci USA. 2009;106(6):1977-82.

Armstrong RC, Dorn HH, Kufta CV, Friedman E, Dubois-dalcq ME. Pre-oligodendrocytes from adult human CNS. J Neurosci. 1992;12(4):1538-47.

Asou H, Hamada K, Miyazaki T, Sakota T, Hayashi K, Takeda Y, Marret S, Delpech B, Itoh K, Uyemura K. CNS myelinogenesis *in vitro*: time course and pattern of rat oligodendrocyte development. J Neurosci Res. 1995;40(4):519-34.

Auron PE. The interleukin 1 receptor: ligand interactions and signal transduction. Cytokine Growth Factor Rev. 1998;9(3-4):221-37.

Axelsson M, Malmeström C, Nilsson S, Haghighi S, Rosengren L, Lycke J. Glial fibrillary acidic protein: a potential biomarker for progression in multiple sclerosis. J Neurol. 2011;258(5):882-8.

Azevedo FA, Carvalho LR, Grinberg LT, Farfel JM, Ferretti RE, Leite RE, Jacob Filho W, Lent R, Herculano-Houzel S. Equal numbers of neuronal and nonneuronal cells make the human brain an isometrically scaled-up primate brain. J Comp Neurol. 2009;513(5):532-41.

Bagaeva LV, Rao P, Powers JM, Segal BM. CXC chemokine ligand 13 plays a role in experimental autoimmune encephalomyelitis. J Immunol. 2006;176(12):7676-85.

Bajetto A, Bonavia R, Barbero S, Florio T, Schettini G. Chemokines and their receptors in the central nervous system. Front Neuroendocrinol. 2001;22(3):147-84.

Baklaushev VP, Kardashova KSh, Gurina OI, Yusubaliyeva GM, Zorkina YA, Chekhonin VP. Organ, cellular, and subcellular localization of brain-specific anion transporter BSAT1. Bull Exp Biol Med. 2013;155(4):491-7.

Balasingam V, Tejada-berges T, Wright E, Bouckova R, Yong VW. Reactive astrogliosis in the neonatal mouse brain and its modulation by cytokines. J Neurosci. 1994;14(2):846-56.

Baluchnejadmojarad T, Roghani M. Coenzyme q10 ameliorates neurodegeneration, mossy fiber sprouting, and oxidative stress in intrahippocampal kainate model of temporal lobe epilepsy in rat. J Mol Neurosci. 2013;49(1):194-201.

Bannerman P, Hahn A, Soulika A, Gallo V, Pleasure D. Astrogliosis in EAE spinal cord: derivation from radial glia, and relationships to oligodendroglia. Glia. 2007;55(1):57-64.

Barateiro A, Fernandes A. Temporal oligodendrocyte lineage progression: *in vitro* models of proliferation, differentiation and myelination. Biochim Biophys Acta. 2014;1843(9):1917-29.

Barbin G, Manthorpe M, Varon S. Purificationofthechickeyeciliary neuronotrophic factor. J Neurochem. 1994;43:1468-78.

Baric I, Fumic K, Glenn B, Cuk M, Schulze A, Finkelstein JD, James SJ, Mejaski-Bosnjak V, Pazanin L, Pogribny IP, Rados M, Sarnavka V, Scukanec-Spoljar M, Allen RH, Stabler S, Uzelac L, Vugrek O, Wagner C, Zeisel S, Mudd SH. S-adenosylhomocysteine hydrolase deficiency in a human: a genetic disorder of methionine metabolism. Proc Natl Acad Sci USA. 2004;101(12):4234-9.

Barnabé-heider F, Wasylnka JA, Fernandes KJ, Porsche C, Sendtner M, Kaplan DR, Miller FD. Evidence that embryonic neurons regulate the onset of cortical gliogenesis via cardiotrophin-1. Neuron. 2005;48(2):253-65.

Barnett MH, Prineas JW. Relapsing and remitting multiple sclerosis: pathology of the newly forming lesion. Ann Neurol. 2004;55(4):458-68.

Barnett SC, Linington C. Myelination: do astrocytes play a role?. Neuroscientist. 2013;19(5):442-50.

Barres BA, Burne JF, Holtmann B, Thoenen H, Sendtner M, Raff MC. Ciliary neurotrophic factor enhances the rate of oligodendrocyte generation. Mol Cell Neurosci. 1996; 8:146-56.

Barres BA, Schmid R, Sendnter M, Raff MC. Multiple extracellular signals are required for long-term oligodendrocyte survival. Development. 1993;118:283-95.

Barres BA. The mystery and magic of glia: a perspective on their roles in health and disease. Neuron. 2008;60(3):430-40.

Baruch K, Silberberg G, Aviv A, Shamir E, Bening-Abu-Shach U, Baruch Y, Darvasi A, Navon R. Association between golli-MBP and schizophrenia in the Jewish Ashkenazi population: are regulatory regions involved?. Int J Neuropsychopharmacol. 2009;12(7):885-94.

Baxter RC, Martin JL. Binding proteins for the insulin-like growth factors: structure, regulation and function. Prog Growth Factor Res. 1989;1(1):49-68.

Baxter RC. Insulin-like growth factor (IGF)-binding proteins: interactions with IGFs and intrinsic bioactivities. Am J Physiol Endocrinol Metab. 2000;278(6):E967-76.

Bayraktar OA, Fuentealba LC, Alvarez-buylla A, Rowitch DH. Astrocyte development and heterogeneity. Cold Spring Harb Perspect Biol. 2015;7(1):a020362.

Bechstein M, Häussler U, Neef M, Hofmann HD, Kirsch M, Haas CA. CNTF-mediated preactivation of astrocytes attenuates neuronal damage and epileptiform activity in experimental epilepsy. Exp Neurol. 2012;236(1):141-50.

Bekar LK, He W, Nedergaard M. Locus coeruleus alpha-adrenergic-mediated activation of cortical astrocytes *in vivo*. Cereb Cortex. 2008;18(12):2789-95.

Benjamini Y, Hochberg Y. Controlling the false discovery rate: A practical and powerful approach to multiple testing. Journal of the Royal Statistical Society, Series B (Methodological). 1995;57(1):289-300.

Bennett MV, Contreras JE, Bukauskas FF, Sáez JC. New roles for astrocytes: gap junction hemichannels have something to communicate. Trends Neurosci. 2003;26(11):610-7.

Berard JL, Zarruk JG, Arbour N, Prat A, Yong VW, Jacques FH, Akira S, David S. Lipocalin 2 is a novel immune mediator of experimental autoimmune encephalomyelitis pathogenesis and is modulated in multiple sclerosis. Glia. 2012;60(7):1145-59.

Berger T, Walz W, Schnitzer J, Kettenmann H. GABA- and glutamate-activated currents in glial cells of the mouse corpus callosum slice. J Neurosci Res. 1992;31(1):21-7.

Bergles DE, Jahr CE. Synaptic activation of glutamate transporters in hippocampal astrocytes. Neuron. 1997;19(6):1297-308.

Bernoud N, Fenart L, Bénistant C, Pageaux JF, Dehouck MP, Molière P, Lagarde M, Cecchelli R, Lecerf J. Astrocytes are mainly responsible for the polyunsaturated fatty acid enrichment in blood-brain barrier endothelial cells *in vitro*. J Lipid Res. 1998;39(9):1816-24.

Bezzi P, Carmignoto G, Pasti L, Vesce S, Rossi D, Rizzini BL, Pozzan T, Volterra A. Prostaglandins stimulate calcium-dependent glutamate release in astrocytes. Nature. 1998;391(6664):281-5.

Bi F, Huang C, Tong J, Qiu G, Huang B, Wu Q, Li F, Xu Z, Bowser R, Xia XG, Zhou H. Reactive astrocytes secrete lcn2 to promote neuron death. Proc Natl Acad Sci USA. 2013;110(10):4069-74.

Bi Y, Ehirchiou D, Kilts TM, Inkson CA, Embree MC, Sonoyama W, Li L, Leet AI, Seo BM, Zhang L, Shi S, Young MF. Identification of tendon stem/progenitor cells and the role of the extracellular matrix in their niche. Nat Med. 2007;13(10):1219-27.

Biancotti JC, Kumar S, De vellis J. Activation of inflammatory response by a combination of growth factors in cuprizone-induced demyelinated brain leads to myelin repair. Neurochem Res. 2008;33(12):2615-28.

Billings-gagliardi S, Adcock LH, Schwing GB, Wolf MK. Hypomyelinated mutant mice. II. Myelination *in vitro*. Brain Res. 1980;200(1):135-50.

Bitsch A, Kuhlmann T, Da costa C, Bunkowski S, Polak T, Brück W. Tumour necrosis factor alpha mRNA expression in early multiple sclerosis lesions: correlation with demyelinating activity and oligodendrocyte pathology. Glia. 2000;29(4):366-75.

Bittman K, Becker DL, Cicirata F, Parnavelas JG. Connexin expression in homotypic and heterotypic cell coupling in the developing cerebral cortex. J Comp Neurol. 2002;443(3):201-12.

Blasco H, Corcia P, Pradat PF, Bocca C, Gordon PH, Veyrat-Durebex C, Mavel S, Nadal-Desbarats L, Moreau C, Devos D, Andres CR, Emond P. Metabolomics in cerebrospinal fluid of patients with amyotrophic lateral sclerosis: an untargeted approach via high-resolution mass spectrometry. J Proteome Res. 2013;12(8):3746-54.

Bleasel JM, Wong JH, Halliday GM, Kim WS. Lipid dysfunction and pathogenesis of multiple system atrophy. Acta Neuropathol Commun. 2014;2(1):15.

Boche D, Perry VH, Nicoll JA. Review: activation patterns of microglia and their identification in the human brain. Neuropathol Appl Neurobiol. 2013;39(1):3-18.

Bodega G, Suárez I, Almonacid L, Ciordia S, Beloso A, Lopez-Fernandez LA, Zaballos A, Fernandez B. Effect of ammonia on ciliary neurotrophic factor mRNA and protein expression and its upstream signalling pathway in cultured rat astroglial cells: possible implication of c-fos, Sp1 and p38MAPK. Neuropathol Appl Neurobiol. 2007;33(4):420-30.

Bögler O, Wren D, Barnett SC, Land H, Noble M. Cooperation between two growth factors promotes extended self-renewal and inhibits differentiation of oligodendrocyte-type-2 astrocyte (O-2A) progenitor cells. Proc Natl Acad Sci USA. 1990;87(16):6368-72.

Bondy C, Werner H, Roberts CT, Leroith D. Cellular pattern of type-I insulin-like growth factor receptor gene expression during maturation of the rat brain: comparison with insulin-like growth factors I and II. Neuroscience. 1992;46(4):909-23.

Boomkamp SD, Mcgrath MA, Houslay MD, Barnett SC. Epac and the high affinity rolipram binding conformer of PDE4 modulate neurite outgrowth and myelination using an *in vitro* spinal cord injury model. Br J Pharmacol. 2014;171(9):2385-98.

Boomkamp SD, Riehle MO, Wood J, Olson MF, Barnett SC. The development of a rat *in vitro* model of spinal cord injury demonstrating the additive effects of Rho and ROCK inhibitors on neurite outgrowth and myelination. Glia. 2012;60(3):441-56.

Bordet R, Ouk T, Petrault O, Gelé P, Gautier S, Laprais M, Deplanque D, Duriez P, Staels B, Fruchart JC, Bastide M. PPAR: a new pharmacological target for neuroprotection in stroke and neurodegenerative diseases. Biochem Soc Trans. 2006;34(Pt 6):1341-6.

Borlikova G, Endo S. Inducible cAMP early repressor (ICER) and brain functions. Mol Neurobiol. 2009;40(1):73-86.

Bornstein P. Thrombospondins as matricellular modulators of cell function. J Clin Invest. 2001;107(8):929-34.

Borroni EM, Buracchi C, De la torre YM, Galliera E, Vecchi A, Bonecchi R, Mantovani A, Locati M. The chemoattractant decoy receptor D6 as a negative regulator of inflammatory responses. Biochem Soc Trans. 2006;34(Pt 6):1014-7.

Bos PD, Zhang XH, Nadal C, Shu W, Gomis RR, Nguyen DX, Minn AJ, van de Vijver MJ, Gerald WL, Foekens JA, Massagué J. Genes that mediate breast cancer metastasis to the brain. Nature. 2009;459(7249):1005-9.

Botelho FM, Edwards DR, Richards CD. Oncostatin M stimulates c-Fos to bind a transcriptionally responsive AP-1 element within the tissue inhibitor of metalloproteinase-1 promoter. J Biol Chem. 1998;273(9):5211-8.

Bottenstein JE, Sato GH. Growth of a rat neuroblastoma cell line in serum-free supplemented medium. Proc Natl Acad Sci USA. 1979;76(1):514-7.

Boyle EA, Mcgeer PL. Cellular immune response in multiple sclerosis plaques. Am J Pathol. 1990;137(3):575-84.

Boyles JK, Pitas RE, Wilson E, Mahley RW, Taylor JM. Apolipoprotein E associated with astrocytic glia of the central nervous system and with nonmyelinating glia of the peripheral nervous system. J Clin Invest. 1985;76(4):1501-13.

Bradbury MW. The blood-brain barrier. Exp Physiol. 1993;78(4):453-72.

Brambilla R, Bracchi-ricard V, Hu WH, Frydel B, Bramwell A, Karmally S, Green EJ, Bethea JR. Inhibition of astroglial nuclear factor kappaB reduces inflammation and improves functional recovery after spinal cord injury. J Exp Med. 2005;202(1):145-56.

Brambilla R, Persaud T, Hu X, Karmally S, Shestopalov VI, Dvoriantchikova G, Ivanov D, Nathanson L, Barnum SR, Bethea JR. Transgenic inhibition of astroglial NF-kappa B improves functional outcome in experimental autoimmune encephalomyelitis by suppressing chronic central nervous system inflammation. J Immunol. 2009;182(5):2628-40.

Brask J, Kristensson K, Hill RH. Exposure to interferon-gamma during synaptogenesis increases inhibitory activity after a latent period in cultured rat hippocampal neurons. Eur J Neurosci. 2004;19(12):3193-201.

Braun JS, Herzog KH. E2F1 mediates pneumococcal-induced brain damage. Acta Neuropathol. 2008;116(1):133-4.

Breidert T, Callebert J, Heneka MT, Landreth G, Launay JM, Hirsch EC. Protective action of the peroxisome proliferator-activated receptor-gamma agonist pioglitazone in a mouse model of Parkinson's disease. J Neurochem.

Breitling, R. Armengaud P, Amtmann A, Herzyk P. Rank products: a simple, yet powerful, new method to detect differentially regulated genes in replicated microarray experiments. FEBS Lett. 2004;573: 83–92.

Brenneman DE, Gozes I. A femtomolar-acting neuroprotective peptide. J Clin Invest. 1996;97(10):2299-307.

Brenner M, Johnson AB, Boespflug-tanguy O, Rodriguez D, Goldman JE, Messing A. Mutations in GFAP, encoding glial fibrillary acidic protein, are associated with Alexander disease. Nat Genet. 2001;27(1):117-20.

Breslin MB, Zhu M, Lan MS. NeuroD1/E47 regulates the E-box element of a novel zinc finger transcription factor, IA-1, in developing nervous system. J Biol Chem. 2003;278(40):38991-7.

Brini E, Ruffini F, Bergami A, Brambilla E, Dati G, Greco B, Cirillo R, Proudfoot AE, Comi G, Furlan R, Zaratin P, Martino G. Administration of a monomeric CCL2 variant to EAE mice inhibits inflammatory cell recruitment and protects from demyelination and axonal loss. J Neuroimmunol. 2009;209(1-2):33-9.

Bronstein JM, Chen K, Tiwari-woodruff S, Kornblum HI. Developmental expression of OSP/claudin-11. J Neurosci Res. 2000;60(3):284-90.

Bronstein JM, Tiwari-woodruff S, Buznikov AG, Stevens DB. Involvement of OSP/claudin-11 in oligodendrocyte membrane interactions: role in biology and disease. J Neurosci Res. 2000;59(6):706-11.

Brook GA, Pérez-bouza A, Noth J, Nacimiento W. Astrocytes re-express nestin in deafferented target territories of the adult rat hippocampus. Neuroreport. 1999;10(5):1007-11.

Brown AM, Ransom BR. Astrocyte glycogen and brain energy metabolism. Glia. 2007;55(12):1263-71.

Brun M, Coles JE, Monckton EA, Glubrecht DD, Bisgrove D, Godbout R. Nuclear factor I regulates brain fatty acid-binding protein and glial fibrillary acidic protein gene expression in malignant glioma cell lines. J Mol Biol. 2009;391(2):282-300.

Buffo A, Rite I, Tripathi P, Lepier A, Colak D, Horn AP, Mori T, Götz M. Origin and progeny of reactive gliosis: A source of multipotent cells in the injured brain. Proc Natl Acad Sci USA. 2008;105(9):3581-6.

Buffo A, Rolando C, Ceruti S. Astrocytes in the damaged brain: molecular and cellular insights into their reactive response and healing potential. Biochem Pharmacol. 2010;79(2):77-89.

Bugga L, Gadient RA, Kwan K, Stewart CL, Patterson PH. Analysis of neuronal and glial phenotypes in brains of mice deficient in leukemia inhibitory factor. J Neurobiol. 1998;36(4):509-24.

Bunge RP, Wood P. Studies on the transplantation of spinal cord tissue in the rat. I. The development of a culture system for hemisections of embryonic spinal cord. Brain Res. 1973;57(2):261-76.

Buono KD, Vadlamuri D, Gan Q, Levison SW. Leukemia inhibitory factor is essential for subventricular zone neural stem cell and progenitor homeostasis as revealed by a novel flow cytometric analysis. Dev Neurosci. 2012;34(5):449-62.

Burdakov D. Electrical signaling in central orexin/hypocretin circuits: tuning arousal and appetite to fit the environment. Neuroscientist. 2004;10(4):286-91.

Bush TG, Puvanachandra N, Horner CH, Polito A, Ostenfeld T, Svendsen CN, Mucke L, Johnson MH, Sofroniew MV. Leukocyte infiltration, neuronal degeneration, and neurite outgrowth after ablation of scar-forming, reactive astrocytes in adult transgenic mice. Neuron. 1999;23:297-308.

Bushong EA, Martone ME, Jones YZ, Ellisman MH. Protoplasmic astrocytes in CA1 stratum radiatum occupy separate anatomical domains. J Neurosci. 2002;22(1):183-92.

Butzkueven H, Zhang JG, Soilu-hanninen M, Hochrein H, Chionh F, Shipham KA, Emery B, Turnley AM, Petratos S, Ernst M, Bartlett PF, Kilpatrick TJ. LIF receptor signaling limits immune-mediated demyelination by enhancing oligodendrocyte survival. Nat Med. 2002;8(6):613-9.

Byravan S, Foster LM, Phan T, Verity AN, Campagnoni AT. Murine oligodendroglial cells express nerve growth factor. Proc Natl Acad Sci USA. 1994;91:8812-6.

Cahoy JD, Emery B, Kaushal A, Foo LC, Zamanian JL, Christopherson KS, Xing Y, Lubischer JL, Krieg PA, Krupenko SA, Thompson WJ, Barres BA. A transcriptome database for astrocytes, neurons, and oligodendrocytes: a new resource for understanding brain development and function. J Neurosci. 2008;28(1):264-78.

Cajal, SR. Histologie du systeme nerveux de l'homme et des vertebres, Maloine, Paris, France, 1909.

Calatayud CA, García CI, Paez PM, Pasquini JM, Soto EF, Pasquini LA. Partial inhibition of the proteasome enhances the activity of the myelin basic protein promoter. Dev Neurosci. 2009;31(3):169-80.

Camacho-arroyo I, López-griego L, Morales-montor J. The role of cytokines in the regulation of neurotransmission. Neuroimmunomodulation. 2009;16(1):1-12.

Camand E, Morel MP, Faissner A, Sotelo C, Dusart I. Long-term changes in the molecular composition of the glial scar and progressive increase of serotoninergic fibre sprouting after hemisection of the mouse spinal cord. Eur J Neurosci. 2004;20(5):1161-76.

Camargo N, Brouwers JF, Loos M, Gutmann DH, Smit AB, Verheijen MH. High-fat diet ameliorates neurological deficits caused by defective astrocyte lipid metabolism. FASEB J. 2012;26(10):4302-15.

Cambron M, D'haeseleer M, Laureys G, Clinckers R, Debruyne J, De keyser J. White-matter astrocytes, axonal energy metabolism, and axonal degeneration in multiple sclerosis. J Cereb Blood Flow Metab. 2012;32(3):413-24.

Cammer W, Zhang H. Maturation of oligodendrocytes is more sensitive to TNF alpha than is survival of precursors and immature oligodendrocytes. J Neuroimmunol. 1999;97(1-2):37-42.

Cammer W. Glutamine synthetase in the central nervous system is not confined to astrocytes. J Neuroimmunol. 1990;26:173-8.

Cammer W. Protection of cultured oligodendrocytes against tumor necrosis factor-alpha by the antioxidants coenzyme Q(10) and N-acetyl cysteine. Brain Res Bull. 2002;58(6):587-92.

Campbell CE, Piper M, Plachez C, Yeh YT, Baizer JS, Osinski JM, Litwack ED, Richards LJ, Gronostajski RM. The transcription factor Nfix is essential for normal brain development. BMC Dev Biol. 2008;8:52.

Campbell CE, Piper M, Plachez C, Yeh YT, Baizer JS, Osinski JM, Litwack ED, Richards LJ, Gronostajski RM. The transcription factor Nfix is essential for normal brain development. BMC Dev Biol. 2008;8:52.

Candela P, Gosselet F, Saint-pol J, Sevin E, Boucau MC, Boulanger E, Cecchelli R, Fenart L. Apical-to-basolateral transport of amyloid-ß peptides through blood-brain barrier cells is mediated by the receptor for advanced glycation end-products and is restricted by P-glycoprotein. J Alzheimers Dis. 2010;22(3):849-59.

Canning DR, Höke A, Malemud CJ, Silver J. A potent inhibitor of neurite outgrowth that predominates in the extracellular matrix of reactive astrocytes. Int J Dev Neurosci. 1996;14(3):153-75.

Cao Q, He Q, Wang Y, Cheng X, Howard RM, Zhang Y, DeVries WH, Shields CB, Magnuson DS, Xu XM, Kim DH, Whittemore SR. Transplantation of ciliary neurotrophic factor-expressing adult oligodendrocyte

precursor cells promotes remyelination and functional recovery after spinal cord injury. J Neurosci. 2010;30(8):2989-3001.

Carlén M, Meletis K, Göritz C, et al. Forebrain ependymal cells are Notch-dependent and generate neuroblasts and astrocytes after stroke. Nat Neurosci. 2009;12(3):259-67.

Carpenter AE, Jones TR, Lamprecht MR, Clarke C, Kang IH, Friman O, Guertin DA, Chang JH, Lindquist RA, Moffat J, Golland P, Sabatini DM. CellProfiler: image analysis software for identifying and quantifying cell phenotypes. Genome Biol. 2006;7(10):R100.

Carter SL, Müller M, Manders PM, Campbell IL. Induction of the genes for Cxcl9 and Cxcl10 is dependent on IFN-gamma but shows differential cellular expression in experimental autoimmune encephalomyelitis and by astrocytes and microglia *in vitro*. Glia. 2007;55(16):1728-39.

Cătălin B, Cupido A, Iancău M, Albu CV, Kirchhoff F. Microglia: first responders in the central nervous system. Rom J Morphol Embryol. 2013;54(3):467-72.

Cepko CL, Austin CP, Yang X, Alexiades M, Ezzeddine D. Cell fate determination in the vertebrate retina. Proc Natl Acad Sci USA. 1996;93(2):589-95.

Chambers I, Cozens A, Broadbent J, Robertson M, Lee M, Li M, Smith A. Structure of the mouse leukaemia inhibitory factor receptor gene: regulated expression of mRNA encoding a soluble receptor isoform from an alternative 5' untranslated region. Biochem J. 1997;328(Pt 3):879-88.

Chan JR, Watkins TA, Cosgaya JM, Zhang C, Chen L, Reichardt LF, Shooter EM, Barres BA. NGF controls axonal receptivity to myelination by Schwann cells or oligodendrocytes. Neuron. 2004;43(2):183-91.

Chandler S, Coates R, Gearing A, Lury J, Wells G, Bone E. Matrix metalloproteinases degrade myelin basic protein. Neurosci Lett. 1995;201(3):223-6.

Chandler S, Cossins J, Lury J, Wells G. Macrophage metalloelastase degrades matrix and myelin proteins and processes a tumour necrosis factor-alpha fusion protein. Biochem Biophys Res Commun. 1996;228(2):421-9.

Chao CC, Hu S, Tsang M, Weatherbee J, Molitor TW, Anderson WR, Peterson PK. Effects of transforming growth factor-beta on murine astrocyte glutamine synthetase activity. Implications in neuronal injury. J Clin Invest. 1992;90(5):1786-93.

Chaudhry AZ, Lyons GE, Gronostajski RM. Expression patterns of the four nuclear factor I genes during mouse embryogenesis indicate a potential role in development. Dev Dyn. 1997;208(3):313-25.

Chaudhry FA, Schmitz D, Reimer RJ, Larsson P, Gray AT, Nicoll R, Kavanaugh M, Edwards RH. Glutamine uptake by neurons: interaction of protons with system a transporters. J Neurosci. 2002;22(1):62-72.

Chavali PL, Saini RK, Matsumoto Y, Ågren H, Funa K. Nuclear orphan receptor TLX induces Oct-3/4 for the survival and maintenance of adult hippocampal progenitors upon hypoxia. J Biol Chem. 2011;286(11):9393-404.

Chen C, Daugherty D, Jiang P, Deng W. Oligodendrocyte progenitor cells derived from mouse embryonic stem cells give rise to type-1 and type-2 astrocytes *in vitro*. Neurosci Lett. 2012;523(2):180-5.

Chen HL, Chew LJ, Packer RJ, Gallo V. Modulation of the Wnt/beta-catenin pathway in human oligodendroglioma cells by Sox17 regulates proliferation and differentiation. Cancer Lett. 2013;335(2):361-71.

Chen J, Joon Lee H, Jakovcevski I, Shah R, Bhagat N, Loers G, Liu HY, Meiners S, Taschenberger G, Kügler S, Irintchev A, Schachner M. The extracellular matrix glycoprotein tenascin-C is beneficial for spinal cord regeneration. Mol Ther. 2010;18(10):1769-77.

Chen SK, Tvrdik P, Peden E, Cho S, Wu S, Spangrude G, Capecchi MR. Hematopoietic origin of pathological grooming in Hoxb8 mutant mice. Cell.2010;141:775–85.

Chen Y, Vartiainen NE, Ying W, Chan PH, Koistinaho J, Swanson RA. Astrocytes protect neurons from nitric oxide toxicity by a glutathione-dependent mechanism. J Neurochem. 2001;77(6):1601-10.

Cheng L, Arata A, Mizuguchi R, Qian Y, Karunaratne A, Gray PA, Arata S, Shirasawa S, Bouchard M, Luo P, Chen CL, Busslinger M, Goulding M, Onimaru H, Ma Q.Tlx3 and Tlx1 are post-mitotic selector genes

determining glutamatergic over GABAergic cell fates. Nat Neurosci. 2004;7(5):510-7.

Cherry JD, Olschowka JA, O'banion MK. Neuroinflammation and M2 microglia: the good, the bad, and the inflamed. J Neuroinflammation. 2014;11(1):98.

Chesik D, De keyser J, Wilczak N. Insulin-like growth factor binding protein-2 as a regulator of IGF actions in CNS: implications in multiple sclerosis. Cytokine Growth Factor Rev. 2007;18(3-4):267-78.

Chesik D, Kühl NM, Wilczak N, De keyser J. Enhanced production and proteolytic degradation of insulin-like growth factor binding protein-2 in proliferating rat astrocytes. J Neurosci Res. 2004;77(3):354-62.

Chiang MK, Flanagan JG. PTP-NP, a new member of the receptor protein tyrosine phosphatase family, implicated in development of nervous system and pancreatic endocrine cells. Development. 1996;122(7):2239-50.

Chojnacki A, Shimazaki T, Gregg C, Weinmaster G, Weiss S. Glycoprotein 130 signaling regulates Notch1 expression and activation in the self-renewal of mammalian forebrain neural stem cells. J Neurosci. 2003;23(5):1730-41.

Choudhury A, Derkow K, Daneshmanesh AH, Mikaelsson E, Kiaii S, Kokhaei P, Osterborg A, Mellstedt H. Silencing of ROR1 and FMOD with siRNA results in apoptosis of CLL cells. Br J Haematol. 2010;151(4):327-35.

Christopherson KS, Ullian EM, Stokes CC, Mullowney CE, Hell JW, Agah A, Lawler J, Mosher DF, Bornstein P, Barres BA. Thrombospondins are astrocyte-secreted proteins that promote CNS synaptogenesis. Cell. 2005;120(3):421-33.

Ciccarelli O, Barkhof F, Bodini B, De Stefano N, Golay X, Nicolay K, Pelletier D, Pouwels PJ, Smith SA, Wheeler-Kingshott CA, Stankoff B, Yousry T, Miller DH. Pathogenesis of multiple sclerosis: insights from molecular and metabolic imaging. Lancet Neurol. 2014;13(8):807-22.

Clarke SR, Shetty AK, Bradley JL, Turner DA. Reactive astrocytes express the embryonic intermediate neurofilament nestin. Neuroreport. 1999;10:1885–88.

Clarke SR, Shetty AK, Bradley JL, Turner DA. Reactive astrocytes express the embryonic intermediate neurofilament nestin. Neuroreport. 1994;5(15):1885-8.

Coco S, Calegari F, Pravettoni E, Pozzi D, Taverna E, Rosa P, Matteoli M, Verderio C. Storage and release of ATP from astrocytes in culture. J Biol Chem. 2003;278(2):1354-62.

Collett-solberg PF, Cohen P. The role of the insulin-like growth factor binding proteins and the IGFBP proteases in modulating IGF action. Endocrinol Metab Clin North Am. 1996;25(3):591-614.

Colodner KJ, Montana RA, Anthony DC, Folkerth RD, De girolami U, Feany MB. Proliferative potential of human astrocytes. J Neuropathol Exp Neurol. 2005;64(2):163-9.

Compston, A., Confavreux, C., Lassmann, H., McDonald, I., Miller, D., Noseworthy, J., Smith, K., Wekerle, H. McAlpine's Multiple Sclerosis. Churchill Livingstone Elsevier. China. 2006. 5.

Conrad S, Schluesener HJ, Adibzahdeh M, Schwab JM. Spinal cord injury induction of lesional expression of profibrotic and angiogenic connective tissue growth factor confined to reactive astrocytes, invading fibroblasts and endothelial cells. J Neurosurg Spine. 2005;2(3):319-26.

Cooper-kuhn CM, Vroemen M, Brown J, Ye H, Thompson MA, Winkler J, Kuhn HG. Impaired adult neurogenesis in mice lacking the transcription factor E2F1. Mol Cell Neurosci. 2002;21(2):312-23.

Corbin JG, Kelly D, Rath EM, Baerwald KD, Suzuki K, Popko B. Targeted CNS expression of interferon-gamma in transgenic mice leads to hypomyelination, reactive gliosis, and abnormal cerebellar development. Mol Cell Neurosci. 1996;7(5):354-70.

Cotrina ML, Gao Q, Lin JH, Nedergaard M. Expression and function of astrocytic gap junctions in aging. Brain Res. 2001;901(1-2):55-61.

Creek DJ, Jankevics A, Burgess KE, Breitling R, Barrett MP. IDEOM: an Excel interface for analysis of LC-MS-based metabolomics data. Bioinformatics. 2012;28(7):1048-9.

Cruz NF, Ball KK, Dienel GA. Astrocytic gap junctional communication is reduced in amyloid-ß-treated cultured astrocytes, but not in Alzheimer's disease transgenic mice. ASN Neuro. 2010;2(4):e00041.

Cuadros MA, Martin C, Coltey P, Almendros A, Navascues J. First appearance, distribution, and origin of macrophages in the early development of the avian central nervous system. J. Comp. Neurol. 1993;330:113-29.

Cullingford TE, Bhakoo K, Peuchen S, Dolphin CT, Patel R, Clark JB. Distribution of mRNAs encoding the peroxisome proliferator-activated receptor alpha, beta, and gamma and the retinoid X receptor alpha, beta, and gamma in rat central nervous system. J Neurochem 1998;70:1366–75.

Cuzner ML, Gveric D, Strand C, Loughlin AJ, Paemen L, Opdenakker G, Newcombe J. The expression of tissue-type plasminogen activator, matrix metalloproteases and endogenous inhibitors in the central nervous system in multiple sclerosis: comparison of stages in lesion evolution. J Neuropathol Exp Neurol. 1996;55(12):1194-204.

Czopka T, Von holst A, Schmidt G, Ffrench-constant C, Faissner A. Tenascin C and tenascin R similarly prevent the formation of myelin membranes in a RhoA-dependent manner, but antagonistically regulate the expression of myelin basic protein via a separate pathway. Glia. 2009;57(16):1790-801.

D'souza CA, Moscarello MA. Differences in susceptibility of MBP charge isomers to digestion by stromelysin-1 (MMP-3) and release of an immunodominant epitope. Neurochem Res. 2006;31(8):1045-54.

Dai X, Qu P, Dreyfus CF. Neuronal signals regulate neurotrophin expression in oligodendrocytes of the basal forebrain. Glia 2001;34:234-9.

Dallner C, Woods AG, Deller T, Kirsch M, Hofmann HD. CNTF and CNTF receptor alpha are constitutively expressed by astrocytes in the mouse brain. Glia. 2002;37(4):374-8.

Das neves L, Duchala CS, Tolentino-Silva F, Haxhiu MA, Colmenares C, Macklin WB, Campbell CE, Butz KG, Gronostajski RM. Disruption of the murine nuclear factor I-A gene (Nfia) results in perinatal lethality, hydrocephalus, and agenesis of the corpus callosum. Proc Natl Acad Sci USA. 1999;96(21):11946-51.

De cesare D, Sassone-corsi P. Transcriptional regulation by cyclic AMP-responsive factors. Prog Nucleic Acid Res Mol Biol. 2000;64:343-69.

De la Fuente M, Ferrandez MD, Del Rio M, Sol BM, Miquel J. Enhancement of leukocyte functions in aged mice supple- mented with the antioxidant thioproline. Mech Ageing Dev. 1998;104:213–225.

Derecki NC, Cronk JC, Lu Z, Xu E, Abbott SB, Guyenet PG, Kipnis J. Wild-type microglia arrest pathology in a mouse model of Rett syndrome. Nature. 2012;484:105–9.

Derouiche A, Haseleu J, Korf HW. Fine Astrocyte Processes Contain Very Small Mitochondria: Glial Oxidative Capability May Fuel Transmitter Metabolism. Neurochem Res. 2015.

Derouet D, Rousseau F, Alfonsi F, Froger J, Hermann J, Barbier F, Perret D, Diveu C, Guillet C, Preisser L, Dumont A, Barbado M, Morel A, deLapeyrière O, Gascan H, Chevalier S. Neuropoietin, a new IL-6-related cytokine signaling through the ciliary neurotrophic factor receptor. Proc Natl Acad Sci USA. 2004;101(14):4827-32.

Deutch CE. Oxidation of L-thiazolidine-4-carboxylate by L-proline dehydrogenase in Escherichia coli. J Gen Microbiol. 1992;138 Pt 8:1593-8.

Deverman BE, Patterson PH. Cytokines and CNS development. Neuron. 2009;64(1):61-78.

Di Giorgio FP, Carrasco MA, Siao MC, Maniatis T, Eggan K. Non-cell autonomous effect of glia on motor neurons in an embryonic stem cell-based ALS model. Nat Neurosci. 2007;10(5):608-14.

Diab A, Hussain RZ, Lovett-Racke AE, Chavis JA, Drew PD, Racke MK. Ligands for the peroxisome proliferator-activated receptor-gamma and the retinoid X receptor exert additive anti-inflammatory effects on experimental autoimmune encephalomyelitis. J Neuroimmuno 2004;148(1-2):116-26.

Díaz JL, Asai M. Dominant mice show much lower concentrations of methionine-enkephalin in brain tissue than subordinates: cause or effect?. Behav Brain Res. 1990;39(3):275-80.

Dibaj P, Nadrigny F, Steffens H, Scheller A, Hirrlinger J, Schomburg ED, Neusch C, Kirchhoff F. NO mediates microglial response to acute spinal cord injury under ATP control *in vivo*. Glia. 2010;58(9):1133-44.

Dietzmann K, Von bossanyi P, Krause D, Wittig H, Mawrin C, Kirches E. Expression of the plasminogen activator system and the inhibitors PAI-1 and PAI-2 in posttraumatic lesions of the CNS and brain injuries following dramatic circulatory arrests: an immunohistochemical study. Pathol Res Pract. 2000;196(1):15-21.

Dogan RN, Elhofy A, Karpus WJ. Production of CCL2 by central nervous system cells regulates development of murine experimental autoimmune encephalomyelitis through the recruitment of TNF- and iNOS-expressing macrophages and myeloid dendritic cells. J Immunol. 2008;180(11):7376-84.

Domercq M, Perez-samartin A, Aparicio D, Alberdi E, Pampliega O, Matute C. P2X7 receptors mediate ischemic damage to oligodendrocytes. Glia. 2010;58(6):730-40.

Dos santos AC, Barsante MM, Arantes RM, Bernard CC, Teixeira MM, Carvalho-tavares J. CCL2 and CCL5 mediate leukocyte adhesion in experimental autoimmune encephalomyelitis--an intravital microscopy study. J Neuroimmunol. 2005;162(1-2):122-9.

Dreyfus CF, Dai X, Lercher LD, Racey BR, Friedman WJ, Black IB. Expression of neurotrophins in the adult spinal cord *in vivo*. J Neurosci Res. 1999;56(1):1-7.

Driller K, Pagenstecher A, Uhl M, Omran H, Berlis A, Grunder A, Sippel AE. Nuclear factor I X deficiency causes brain malformation and severe skeletal defects. Mol Cell Biol. 2007;27(10):3855-3867.

Dringen R, Wiesinger H, Hamprecht B. Uptake of L-lactate by cultured rat brain neurons. Neurosci Lett. 1993;163(1):5-7.

Drögemüller K, Helmuth U, Brunn A, Sakowicz-Burkiewicz M, Gutmann DH, Mueller W, Deckert M, Schlüter D. Astrocyte gp130 expression is critical for the control of Toxoplasma encephalitis. J Immunol. 2008;181(4):2683-93.

Dubois-dalcq M, Murray K. Why are growth factors important in oligodendrocyte physiology?. Pathol Biol. 2000;48(1):80-6.

Duggan A, Madathany T, De castro SC, Gerrelli D, Guddati K, García-añoveros J. Transient expression of the conserved zinc finger gene INSM1 in progenitors and nascent neurons throughout embryonic and adult neurogenesis. J Comp Neurol. 2008;507(4):1497-520.

Dunn WB, Broadhurst D, Begley P, Zelena E, Francis-McIntyre S, Anderson N, Brown M, Knowles JD, Halsall A, Haselden JN, Nicholls AW, Wilson ID, Kell DB, Goodacre R. Procedures for large-scale metabolic profiling of serum and plasma using gas chromatography and liquid chromatography coupled to mass spectrometry. Nat Protoc. 2011;6(7):1060-83.

Dunn WB, Erban A, Weber RJM, Creek DJ, Brown M, Breitling R, Hankemeier T, Goodacre R, Neumann S, Kopka J, Viant MR. Mass appeal: metabolite identification in mass spectrometry-focused untargeted metabolomics. Metabolomics. 2012:9(S1);44-66.

Dziennis S, Habecker BA. Cytokine suppression of dopamine-beta-hydroxylase by extracellular signal-regulated kinase-dependent and -independent pathways. J Biol Chem. 2003;278(18):15897-904.

Dziewulska D, Jamrozik Z, Podlecka A, Rafałowska J. Do astrocytes participate in rat spinal cord myelination?. Folia Neuropathol. 1999;37(2):81-6.

East E, Golding JP, Phillips JB. A versatile 3D culture model facilitates monitoring of astrocytes undergoing reactive gliosis. J Tissue Eng Regen Med. 2009;3(8):634-46.

Eddie SL, Childs AJ, Jabbour HN, Anderson RA. Developmentally regulated IL6-type cytokines signal to germ cells in the human fetal ovary. Mol Hum Reprod. 2012;18(2):88-95.

Eddleston M, Mucke L. Molecular profile of reactive astrocytes--implications for their role in neurologic disease. Neuroscience. 1993;54(1):15-36.

Edgar JM, Mcculloch MC, Montague P, Brown AM, Thilemann S, Pratola L, Gruenenfelder FI, Griffiths IR, Nave KA. Demyelination and axonal preservation in a transgenic mouse model of Pelizaeus-Merzbacher disease. EMBO Mol Med. 2010;2(2):42-50.

Edgar JM, Mclaughlin M, Yool D, Zhang SC, Fowler JH, Montague P, Barrie JA, McCulloch MC, Duncan ID, Garbern J, Nave KA, Griffiths IR. Oligodendroglial modulation of fast axonal transport in a mouse model of hereditary spastic paraplegia. J Cell Biol. 2004;166(1):121-31.

Edman LC, Mira H, Arenas E. The beta-chemokines CCL2 and CCL7 are two novel differentiation factors for midbrain dopaminergic precursors and neurons. Exp Cell Res. 2008;314(10):2123-30.

Eglitis MA, Mezey E´. Hematopoietic cells differentiate into both microglia and macroglia in the brains of adult mice. Proc. Natl. Acad. Sci. USA.1997;94:4080-5.

Elhofy A, Wang J, Tani M, Fife BT, Kennedy KJ, Bennett J, Haung D, Ransohoff RM, Karpus WJ. Transgenic expression of CCL2 in the central nervous system prevents experimental autoimmune encephalomyelitis. J Leukoc Biol. 2005;77(2):229-37.

Elmi M, Matsumoto Y, Zeng ZJ, Lakshminarasimhan P, Yang W, Uemura A, Nishikawa S, Moshiri A, Tajima N, Agren H, Funa K. TLX activates MASH1 for induction of neuronal lineage commitment of adult hippocampal neuroprogenitors. Mol Cell Neurosci. 2010;45(2):121-31.

Elsir T, Edqvist PH, Carlson J, Ribom D, Bergqvist M, Ekman S, Popova SN, Alafuzoff I, Ponten F, Nistér M, Smits A. A study of embryonic stem cell-related proteins in human astrocytomas: identification of Nanog as a predictor of survival. Int J Cancer. 2014;134(5):1123-31.

Emery B. Regulation of oligodendrocyte differentiation and myelination. Science. 2010;330(6005):779-82.

Eng DL, Lee YL, Lal PG. Expression of glutamate uptake transporters after dibutyryl cyclic AMP differentiation and traumatic injury in cultured astrocytes. Brain Res. 1997;778(1):215-21.

Eng LF, Gerstl B, Vanderhaeghen JJ. A study of proteins in old mutliple sclerosis plaques. Trans Am Soc Neurochem. 1970;1:42.

Eng LF, Ghirnikar RS, Lee YL. Glial fibrillary acidic protein: GFAP-thirty-one years (1969-2000). Neurochem Res. 2000;25(9-10):1439-51.

Engelhardt B. Development of the blood-brain barrier. Cell Tissue Res. 2003;314(1):119-29.

Eroglu C, Allen NJ, Susman MW, O'Rourke NA, Park CY, Ozkan E, Chakraborty C, Mulinyawe SB, Annis DS, Huberman AD, Green EM, Lawler J, Dolmetsch R, Garcia KC, Smith SJ, Luo ZD, Rosenthal A, Mosher DF, Barres BA. Gabapentin receptor alpha2delta-1 is a neuronal thrombospondin receptor responsible for excitatory CNS synaptogenesis. Cell. 2009;139(2):380-92.

Escartin C, Pierre K, Colin A, Brouillet E, Delzescaux T, Guillermier M, Dhenain M, Déglon N, Hantraye P, Pellerin L, Bonvento G. Activation of astrocytes by CNTF induces metabolic plasticity and increases resistance to metabolic insults. J Neurosci. 2007;27(27):7094-104.

Esen N, Kielian T. Central role for MyD88 in the responses of microglia to pathogen-associated molecular patterns. J Immunol. 2006;176(11):6802-11.

Faden AI, Demediuk P, Panter SS, Vink R. The role of excitatory amino acids and NMDA receptors in traumatic brain injury. Science. 1989;244(4906):798-800.

Fan C, Wang H, Chen D, Cheng X, Xiong K, Luo X, Cao Q. Effect of type-2 astrocytes on the viability of dorsal root ganglion neurons and length of neuronal processes. Neural Regen Res. 2014;9(2):119-28.

Fan J, Zhang YQ, Li P, Hou M, Tan L, Wang X, Zhu YS. Interaction of plasminogen activator inhibitor-2 and proteasome subunit, beta type 1. Acta Biochim Biophys Sin (Shanghai). 2004;36(1):42-6.

Fancy SP, Baranzini SE, Zhao C, Yuk DI, Irvine KA, Kaing S, Sanai N, Franklin RJ, Rowitch DH. Dysregulation of the Wnt pathway inhibits timely myelination and remyelination in the mammalian CNS. Genes Dev. 2009;23(13):1571-85.

Fancy SP, Harrington EP, Yuen TJ, Silbereis JC, Zhao C, Baranzini SE, Bruce CC, Otero JJ, Huang EJ, Nusse R, Franklin RJ, Rowitch DH. Axin2 as regulatory and therapeutic target in newborn brain injury and remyelination. Nat Neurosci. 2011;14(8):1009-16.

Fang M, He D, Zhang F, Hu Z, Yang J, Jiang H, Han S. Antineuroinflammatory and neurotrophic effects of CNTF and C16 peptide in an acute experimental autoimmune encephalomyelitis rat model. Front Neuroanat. 2013;7:44.

Farina C, Aloisi F, Meinl E. Astrocytes are active players in cerebral innate immunity. Trends Immunol. 2007;28(3):138-45.

Fasnacht N, Müller W. Conditional gp130 deficient mouse mutants. Semin Cell Dev Biol. 2008;19(4):379-84.

Faulkner JR, Herrmann JE, Woo MJ, Tansey KE, Doan NB, Sofroniew MV. Reactive astrocytes protect tissue and preserve function after spinal cord injury. J Neurosci. 2004;24(9):2143-55.

Faustino JV, Wang X, Johnson CE, Klibanov A, Derugin N, Wendland MF, Vexler ZS. Microglial cells contribute to endogenous brain defenses after acute neonatal focal stroke. J Neurosci. 2011;31(36):12992-3001.

Feigenson K, Reid M, See J, Crenshaw EB, Grinspan JB. Wnt signaling is sufficient to perturb oligodendrocyte maturation. Mol Cell Neurosci. 2009;42(3):255-65.

Feinstein DL, Galea E, Gavrilyuk V, Brosnan CF, Whitacre CC, Dumitrescu-Ozimek L, Landreth GE, Pershadsingh HA, Weinberg G, Heneka MT. Peroxisome proliferator-activated receptor-gamma agonists prevent experimental autoimmune encephalomyelitis. Ann Neurol. 2002;51(6):694-702.

Fellin T, Pascual O, Gobbo S, Pozzan T, Haydon PG, Carmignoto G. Neuronal synchrony mediated by astrocytic glutamate through activation of extrasynaptic NMDA receptors. Neuron. 2004;43(5):729-43.

Fiala M, Avagyan H, Merino JJ, Bernas M, Valdivia J, Espinosa-Jeffrey A, Witte M, Weinand M. Chemotactic and mitogenic stimuli of neuronal apoptosis in patients with medically intractable temporal lobe epilepsy. Pathophysiology. 2013;20(1):59-69.

Fields RD, Stevens-graham B. New insights into neuron-glia communication. Science. 2002;298(5593):556-62.

Fife BT, Kennedy KJ, Paniagua MC, Lukacs NW, Kunkel SL, Luster AD, Karpus WJ. CXCL10 (IFN-gamma-inducible protein-10) control of encephalitogenic CD4+ T cell accumulation in the central nervous system during experimental autoimmune encephalomyelitis. J Immunol. 2001;166(12):7617-24.

Figley CR, Stroman PW. The role(s) of astrocytes and astrocyte activity in neurometabolism, neurovascular coupling, and the production of functional neuroimaging signals. Eur J Neurosci. 2011;33(4):577-88.

Filous AR, Miller JH, Coulson-thomas YM, Horn KP, Alilain WJ, Silver J. Immature astrocytes promote CNS axonal regeneration when combined with chondroitinase ABC. Dev Neurobiol. 2010;70(12):826-41.

Fisher M. Injuries to the vascular endothelium: vascular wall and endothelial dysfunction. Rev Neurol Dis. 2008;5 Suppl 1:S4-11.

Fitzgerald DC, Ciric B, Touil T, Harle H, Grammatikopolou J, Das Sarma J, Gran B, Zhang GX, Rostami A. Suppressive effect of IL-27 on encephalitogenic Th17 cells and the effector phase of experimental autoimmune encephalomyelitis. J Immunol. 2007;179(5):3268-75.

Fitzner D, Simons M. Chronic progressive multiple sclerosis - pathogenesis of neurodegeneration and therapeutic strategies. Curr Neuropharmacol. 2010;8(3):305-15.

Flajollet S, Poras I, Carosella ED, Moreau P. RREB-1 is a transcriptional repressor of HLA-G. J Immunol. 2009;183(11):6948-59.

Fletcher L, Isgor E, Sprague S, Williams LH, Alajajian BB, Jimenez DF, Digicaylioglu M. Spatial distribution of insulin-like growth factor binding protein-2 following hypoxic-ischemic injury. BMC Neurosci. 2013;14:158.

Flynn G, Maru S, Loughlin J, Romero IA, Male D. Regulation of chemokine receptor expression in human microglia and astrocytes. J Neuroimmunol. 2003;136(1-2):84-93.

Fogarty M, Richardson WD, Kessaris N. A subset of oligodendrocytes generated from radial glia in the dorsal spinal cord. Development. 2005;132(8):1951-9.

Foo LC, Allen NJ, Bushong EA, Ventura PB, Chung WS, Zhou L, Cahoy JD, Daneman R, Zong H, Ellisman MH, Barres BA. Development of a method for the purification and culture of rodent astrocytes. Neuron. 2011;71(5):799-811.

Fowlkes JL, Serra DM, Bunn RC, Thrailkill KM, Enghild JJ, Nagase H. Regulation of insulin-like growth factor (IGF)-I action by matrix metalloproteinase-3 involves selective disruption of IGF-I/IGF-binding protein-3 complexes. Endocrinology. 2004;145(2):620-6.

Frade JM, Barde YA. Microglia-derived nerve growth factor causes cell death in the developing retina. Neuron. 1998;20:35–41.

Francis JS, Strande L, Markov V, Leone P. Aspartoacylase supports oxidative energy metabolism during myelination. J Cereb Blood Flow Metab. 2012;32(9):1725–36.

Franklin RB, Zou J, Costello LC. The cytotoxic role of RREB1, ZIP3 zinc transporter, and zinc in human pancreatic adenocarcinoma. Cancer Biol Ther. 2014;15(10):1431–7.

Franklin RJ, Blakemore WF. Glial-cell transplantation and plasticity in the O-2A lineage--implications for CNS repair. Trends Neurosci. 1995;18(3):151–6.

Franklin RJ, Crang AJ, Blakemore WF. Transplanted type-1 astrocytes facilitate repair of demyelinating lesions by host oligodendrocytes in adult rat spinal cord. J Neurocytol. 1991;20(5):420–30.

Franklin RJ. Remyelination of the demyelinated CNS: the case for and against transplantation of central, peripheral and olfactory glia. Brain Res Bull. 2002;57(6):827–32.

Frederiksen K, Mckay RD. Proliferation and differentiation of rat neuroepithelial precursor cells *in vivo*. J Neurosci. 1988;8(4):1144–51.

Friedman WJ, Lärkfors L, Ayer-lelievre C, Ebendal T, Olson L, Persson H. Regulation of beta-nerve growth factor expression by inflammatory mediators in hippocampal cultures. J Neurosci Res. 1990;27(3):374–82.

Frisén J, Johansson CB, Török C, Risling M, Lendahl U. Rapid, widespread, and longlasting induction of nestin contributes to the generation of glial scar tissue after CNS injury. J Cell Biol. 1995;131(2):453–64.

Fróes MM, Correia AH, Garcia-abreu J, Spray DC, Campos de carvalho AC, Neto MV. Gap-junctional coupling between neurons and astrocytes in primary central nervous system cultures. Proc Natl Acad Sci USA. 1999;96(13):7541–6.

Froger N, Orellana JA, Calvo CF, Amigou E, Kozoriz MG, Naus CC, Sáez JC, Giaume C. Inhibition of cytokine-induced connexin43 hemichannel activity in astrocytes is neuroprotective. Mol Cell Neurosci. 2010;45(1):37–46.

From R, Eilam R, Bar-Lev DD, Levin-Zaidman S, Tsoory M, LoPresti P, Sela M, Arnon R, Aharoni R. Oligodendrogenesis and myelinogenesis during postnatal development effect of glatiramer acetate. Glia. 2014;62(4):649–65.

Fujita H, Sato K, Wen TC, Peng Y, Sakanaka M. Differential expressions of glycine transporter 1 and three glutamate transporter mRNA in the hippocampus of gerbils with transient forebrain ischemia. J Cereb Blood Flow Metab. 1999;19(6):604–15.

Fuller S, Münch G, Steele M. Activated astrocytes: a therapeutic target in Alzheimer's disease?. Expert Rev Neurother. 2009;9(11):1585–94.

Fulton BP, Burne JF, Raff MC. Visualization of O-2A progenitor cells in developing and adult rat optic nerve by quisqualate-stimulated cobalt uptake. J Neurosci. 1992;12(12):4816–33.

Funari VA, Herrera VL, Freeman D, Tolan DR. Genes required for fructose metabolism are expressed in Purkinje cells in the cerebellum. Brain Res Mol Brain Res. 2005;142(2):115–22.

Gadea A, Schinelli S, Gallo V. Endothelin-1 regulates astrocyte proliferation and reactive gliosis via a JNK/c-Jun signaling pathway. J Neurosci. 2008;28(10):2394–408.

Gao X, Arlotta P, Macklis JD, Chen J. Conditional knock-out of beta-catenin in postnatal-born dentate gyrus granule neurons results in dendritic malformation. J Neurosci. 2007;27(52):14317–25.

García-marqués J, López-mascaraque L. Clonal identity determines astrocyte cortical heterogeneity. Cereb Cortex. 2013;23(6):1463–72.

García-marqués J, López-mascaraque L. Clonal identity determines astrocyte cortical heterogeneity. Cereb Cortex. 2013;23(6):1463–72.

García-parra P, Cavaliere F, Maroto M, Bilbao L, Obieta I, Lopez de Munain A, Alava JI, Izeta A. Modeling

neural differentiation on micropatterned substrates coated with neural matrix components. Front Cell Neurosci. 2012;6:10.

García-parra P, Maroto M, Cavaliere F, Naldaiz-Gastesi N, Álava JI, García AG, López de Munain A, Izeta A. A neural extracellular matrix-based method for *in vitro* hippocampal neuron culture and dopaminergic differentiation of neural stem cells. BMC Neurosci. 2013;14(1):48.

Gard AL, Pfeiffer SE. Oligodendrocyte progenitors isolated directly from developing telencephalon at a specific phenotypic stage: myelinogenic potential in a defined environment. Development. 1989;106(1):119-32.

Garg S, Md syed M, Kielian T. Staphylococcus aureus-derived peptidoglycan induces Cx43 expression and functional gap junction intercellular communication in microglia. J Neurochem. 2005;95(2):475-83.

Garnier R, Efthymiou ML, Fournier E. Acute thioproline poisoning. J Toxicol Clin Toxicol. 1982;19(3):289-95.

Garré JM, Retamal MA, Cassina P, Barbeito L, Bukauskas FF, Sáez JC, Bennett MV, Abudara V. FGF-1 induces ATP release from spinal astrocytes in culture and opens pannexin and connexin hemichannels. Proc Natl Acad Sci USA. 2010;107(52):22659-64.

Ge WP, Miyawaki A, Gage FH, Jan YN, Jan LY. Local generation of glia is a major astrocyte source in postnatal cortex. Nature. 2012;484(7394):376-80.

Gebicke-härter PJ, Althaus HH, Schwartz P, Neuhoff V. Oligodendrocytes from postnatal cat brain in cell culture. I. Regeneration and maintenance. Brain Res. 1981;227(4):497-518.

Ghosh A, Manrique-hoyos N, Voigt A, Schulz JB, Kreutzfeldt M, Merkler D, Simons M. Targeted ablation of oligodendrocytes triggers axonal damage. PLoS ONE. 2011;6(7):e22735.

Ghoumari AM, Ibanez C, El-etr M, Leclerc P, Eychenne B, O'Malley BW, Baulieu EE, Schumacher M. Progesterone and its metabolites increase myelin basic protein expression in organotypic slice cultures of rat cerebellum. J Neurochem. 2003;86(4):848-59.

Giaume C, Leybaert L, Naus CC, Sáez JC. Connexin and pannexin hemichannels in brain glial cells: properties, pharmacology, and roles. Front Pharmacol. 2013;4:88.

Giaume C. Astroglial Wiring is Adding Complexity to Neuroglial Networking. Front Neuroenergetics. 2010;2:129

Gilad GM, Kagan HM, Gilad VH. Evidence for increased lysyl oxidase, the extracellular matrix-forming enzyme, in Alzheimer's disease brain. Neurosci Lett. 2005;376(3):210-4.

Gilad GM, Kagan HM, Gilad VH. Lysyl oxidase, the extracellular matrix-forming enzyme, in rat brain injury sites. Neurosci Lett. 2001;310(1):45-8.

Gilbert P, Kettenmann H, Schachner M. gamma-Aminobutyric acid directly depolarizes cultured oligodendrocytes. J Neurosci. 1984;4(2):561-9.

Ginhoux F, Greter M, Leboeuf M, Nandi S, See P, Gokhan S, Mehler MF, Conway SJ, Ng LG, Stanley ER, Samokhvalov IM, Merad M. Fate mapping analysis reveals that adult microglia derive from primitive macrophages. Science. 2010;330:841-5.

Glabinski AR, Bielecki B, Ransohoff RM. Chemokine upregulation follows cytokine expression in chronic relapsing experimental autoimmune encephalomyelitis. Scand J Immunol. 2003;58(1):81-8.

Glabinski AR, Tani M, Strieter RM, Tuohy VK, Ransohoff RM. Synchronous synthesis of alpha- and beta-chemokines by cells of diverse lineage in the central nervous system of mice with relapses of chronic experimental autoimmune encephalomyelitis. Am J Pathol. 1997;150(2):617-30.

Glezer I, Rivest S. Oncostatin M is a novel glucocorticoid-dependent neuroinflammatory factor that enhances oligodendrocyte precursor cell activity in demyelinated sites. Brain Behav Immun. 2010;24(5):695-704.

Godiska R, Chantry D, Dietsch GN, Gray PW. Chemokine expression in murine experimental allergic encephalomyelitis. J Neuroimmunol. 1995;58(2):167-76.

Goncalves CA, Leite MC, Nardin P. Biological and methodological features of the measurement of S100B, a putative marker of brain injury. Clin Biochem. 2008;41: 755-63.

Goodwin CR, Lal B, Zhou X, Ho S, Xia S, Taeger A, Murray J, Laterra J. Cyr61 mediates hepatocyte growth factor-dependent tumor cell growth, migration, and Akt activation. Cancer Res. 2010;70(7):2932-41.

Gotow T, Leterrier JF, Ohsawa Y, Watanabe T, Isahara K, Shibata R, Ikenaka K, Uchiyama Y. Abnormal expression of neurofilament proteins in dysmyelinating axons located in the central nervous system of jimpy mutant mice. Eur J Neurosci. 1999;11(11):3893-903.

Götz M, Huttner WB. The cell biology of neurogenesis. Nat Rev Mol Cell Biol. 2005;6(10):777-88.

Götz M, Huttner WB. The cell biology of neurogenesis. Nat Rev Mol Cell Biol. 2005;6(10):777-88.

Gozes I, Bardea A, Reshef A, Zamostiano R, Zhukovsky S, Rubinraut S, Fridkin M, Brenneman DE. Neuroprotective strategy for Alzheimer disease: intranasal administration of a fatty neuropeptide. Proc Natl Acad Sci USA. 1996;93(1):427-32.

Gozes I, Bassan M, Zamostiano R, Pinhasov A, Davidson A, Giladi E, Perl O, Glazner GW, Brenneman DE. A novel signaling molecule for neuropeptide action: activity-dependent neuroprotective protein. Ann N Y Acad Sci. 1999;897:125-35.

Greer JM, Capecchi MR. Hoxb8 is required for normal grooming behavior in mice. Neuron. 2002;33:23–34.

Gregg C, Weiss S. CNTF/LIF/gp130 receptor complex signaling maintains a VZ precursor differentiation gradient in the developing ventral forebrain. Development. 2005;132(3):565-78.

Gregor A, Oti M, Kouwenhoven EN, Hoyer J, Sticht H, Ekici AB, Kjaergaard S, Rauch A, Stunnenberg HG, Uebe S, Vasileiou G, Reis A, Zhou H, Zweier C. *De novo* mutations in the genome organizer CTCF cause intellectual disability. Am J Hum Genet. 2013;93(1):124-31.

Griffiths I, Klugmann M, Anderson T, Yool D, Thomson C, Schwab MH, Schneider A, Zimmermann F, McCulloch M, Nadon N, Nave KA. Axonal swellings and degeneration in mice lacking the major proteolipid of myelin. Science. 1998;280(5369):1610-3.

Grinspan JB, Franceschini B. Platelet-derived growth factor is a survival factor for PSA-NCAM+ oligodendrocyte pre-progenitor cells. J Neurosci Res. 1995;41(4):540-51.

Gruol DL, Vo K, Bray JG. Increased astrocyte expression of IL-6 or CCL2 in transgenic mice alters levels of hippocampal and cerebellar proteins. Front Cell Neurosci. 2014;8:234.

Gudi V, Škuljec J, Yildiz Ö, Frichert K, Skripuletz T, Moharregh-Khiabani D, Voss E, Wissel K, Wolter S, Stangel M. Spatial and temporal profiles of growth factor expression during CNS demyelination reveal the dynamics of repair priming. PLoS ONE. 2011;6(7):e22623.

Guengerich FP, Liebler DC. Enzymatic activation of chemicals to toxic metabolites. Crit Rev Toxicol. 1985;14(3):259-307.

Gundersen V, Ottersen OP, Storm-mathisen J. Selective excitatory amino acid uptake in glutamatergic nerve terminals and in glia in the rat striatum: quantitative electron microscopic immunocytochemistry of exogenous (D)-aspartate and endogenous glutamate and GABA. Eur J Neurosci. 1996;8(4):758-65.

Guo L, Eviatar-ribak T, Miskimins R. Sp1 phosphorylation is involved in myelin basic protein gene transcription. J Neurosci Res. 2010;88(15):3233-42.

Gurfein BT, Zhang Y, López CB, Argaw AT, Zameer A, Moran TM, John GR. IL-11 regulates autoimmune demyelination. J Immunol. 2009;183(7):4229-40.

Guthrie KM, Woods AG, Nguyen T, Gall CM. Astroglial ciliary neurotrophic factor mRNA expression is increased in fields of axonal sprouting in deafferented hippocampus. J Comp Neurol. 1997;386(1):137-48.

Guthrie PB, Knappenberger J, Segal M, Bennett MV, Charles AC, Kater SB. ATP released from astrocytes mediates glial calcium waves. J Neurosci. 1999;19(2):520-8.

Hagg T, Varon S. Ciliary neurotrophic factor prevents degeneration of adult rat substantia nigra dopaminergic neurons *in vivo*. Proc Natl Acad Sci USA. 1993;90(13):6315-9.

Halassa MM, Fellin T, Haydon PG. The tripartite synapse: roles for gliotransmission in health and disease. Trends Mol Med. 2007;13(2):54-63.

Hamann I, Zipp F, Infante-duarte C. Therapeutic targeting of chemokine signaling in Multiple Sclerosis. J Neurol Sci. 2008;274(1-2):31-8.

Hamby ME, Hewett JA, Hewett SJ. TGF-beta1 potentiates astrocytic nitric oxide production by expanding the population of astrocytes that express NOS-2. Glia. 2006;54(6):566-77.

Hamby ME, Sofroniew MV. Reactive astrocytes as therapeutic targets for CNS disorders. Neurotherapeutics. 2010;7(4):494-506.

Hamilton NH, Banyer JL, Hapel AJ, Mahalingam S, Ramsay AJ, Ramshaw IA, Thomson SA. IFN-gamma regulates murine interferon-inducible T cell alpha chemokine (I-TAC) expression in dendritic cell lines and during experimental autoimmune encephalomyelitis (EAE). Scand J Immunol. 2002;55(2):171-7.

Hanafy KA, Sloane JA. Regulation of remyelination in multiple sclerosis. FEBS Lett. 2011;585(23):3821-8.

Hao J, Liu R, Piao W, Zhou Q, Vollmer TL, Campagnolo DI, Xiang R, La Cava A, Van Kaer L, Shi FD. Central nervous system (CNS)-resident natural killer cells suppress Th17 responses and CNS autoimmune pathology. J Exp Med. 2010;207(9):1907-21.

Haroon F, Drögemüller K, Händel U, Brunn A, Reinhold D, Nishanth G, Mueller W, Trautwein C, Ernst M, Deckert M, Schlüter D. Gp130-dependent astrocytic survival is critical for the control of autoimmune central nervous system inflammation. J Immunol. 2011;186(11):6521-31.

Haseley A, Boone S, Wojton J, Yu L, Yoo JY, Yu J, Kurozumi K, Glorioso JC, Caligiuri MA, Kaur B. Extracellular matrix protein CCN1 limits oncolytic efficacy in glioma. Cancer Res. 2012;72(6):1353-62.

Hawkins SA, Mcdonnell GV. Benign multiple sclerosis? Clinical course, long term follow up, and assessment of prognostic factors. J Neurol Neurosurg Psychiatr. 1999;67(2):148-52.

Hayashi K, Fong KS, Mercier F, Boyd CD, Csiszar K, Hayashi M. Comparative immunocytochemical localization of lysyl oxidase (LOX) and the lysyl oxidase-like (LOXL) proteins: changes in the expression of LOXL during development and growth of mouse tissues. J Mol Histol. 2004;35(8-9):845-55.

He F, Ge W, Martinowich K, Becker-Catania S, Coskun V, Zhu W, Wu H, Castro D, Guillemot F, Fan G, de Vellis J, Sun YE. A positive autoregulatory loop of Jak-STAT signaling controls the onset of astrogliogenesis. Nat Neurosci. 2005;8(5):616-25.

Heinrich PC, Graeve L, Rose-John S, Schneider-Mergener J, Dittrich E, Erren A, Gerhartz C, Hemann U, Lütticken C, Wegenka U, Weiergräber O, Horn F. Membrane-bound and soluble interleukin-6 receptor: studies on structure, regulation of expression, and signal transduction. Ann N Y Acad Sci 1995; 762:222–36.

Heneka MT, Nadrigny F, Regen T, Martinez-Hernandez A, Dumitrescu-Ozimek L, Terwel D, Jardanhazi-Kurutz D, Walter J, Kirchhoff F, Hanisch UK, Kummer MP. Locus ceruleus controls Alzheimer's disease pathology by modulating microglial functions through norepi- nephrine. Proc. Natl. Acad. Sci. USA. 2010;107:6058–63.

Heneka MT, Sastre M, Dumitrescu-ozimek L, Hanke A, Dewachter I, Kuiperi C, O'Banion K, Klockgether T, Van Leuven F, Landreth GE. Acute treatment with the PPARgamma agonist pioglitazone and ibuprofen reduces glial inflammation and Abeta1-42 levels in APPV717I transgenic mice. Brain. 2005;128(Pt 6):1442-53.

Heo JH, Lucero J, Abumiya T, Koziol JA, Copeland BR, Del zoppo GJ. Matrix metalloproteinases increase very early during experimental focal cerebral ischemia. J Cereb Blood Flow Metab. 1999;19(6):624-33.

Herber DL, Maloney JL, Roth LM, Freeman MJ, Morgan D, Gordon MN. Diverse microglial responses after intra- hippocampal administration of lipopolysaccharide. Glia. 2006;53:382-91.

Herculano-houzel S. The glia/neuron ratio: how it varies uniformly across brain structures and species and what that means for brain physiology and evolution. Glia. 2014;62(9):1377-91.

Herrmann JE, Imura T, Song B, Qi J, Ao Y, Nguyen TK, Korsak RA, Takeda K, Akira S, Sofroniew MV. STAT3 is a critical regulator of astrogliosis and scar formation after spinal cord injury. J Neurosci. 2008;28(28):7231-43.

Hertel M, Tretter Y, Alzheimer C, Werner S. Connective tissue growth factor: a novel player in tissue reorganization after brain injury?. Eur J Neurosci. 2000;12(1):376-80.

Herx LM, Rivest S, Yong VW. Central nervous system-initiated inflammation and neurotrophism in trauma: IL-1 beta is required for the production of ciliary neurotrophic factor. J Immunol. 2000;165(4):2232-9.

Hickey WF, Kimura H. Perivascular microglial cells of the CNS are bone marrow-derived and present antigen *in vivo*. Science.1988;239:290-2.

Hickman SE, Allison EK, El Khoury J. Microglial dysfunction and defective ß-amyloid clearance pathways in aging Alzheimer's disease mice. J. Neurosci. 2008;28:8354–60.

Hidaka Y, Inaba Y, Matsuda K, Itoh M, Kaneyama T, Nakazawa Y, Koh CS, Ichikawa M. Cytokine production profiles in chronic relapsing-remitting experimental autoimmune encephalomyelitis: IFN-γ and TNF-α are important participants in the first attack but not in the relapse. J Neurol Sci. 2014;340(1-2):117-22.

Hikichi T, Kohda T, Kaneko-ishino T, Ishino F. Imprinting regulation of the murine Meg1/Grb10 and human GRB10 genes; roles of brain-specific promoters and mouse-specific CTCF-binding sites. Nucleic Acids Res. 2003;31(5):1398-406.

Hild W.Myelin formation in central nervous system tissue cultures. Verh Anat Ges. 1956;53:315–317.

Hirayama T, Tarusawa E, Yoshimura Y, Galjart N, Yagi T. CTCF is required for neural development and stochastic expression of clustered Pcdh genes in neurons. Cell Rep. 2012;2(2):345-57.

Hiremath MM, Saito Y, Knapp GW, Ting JP, Suzuki K, Matsushima GK. Microglial/macrophage accumulation during cuprizone-induced demyelination in C57BL/6 mice. J Neuroimmunol. 1998;92(1-2):38-49.

Hochstim C, Deneen B, Lukaszewicz A, Zhou Q, Anderson DJ. Identification of positionally distinct astrocyte subtypes whose identities are specified by a homeodomain code. Cell. 2008;133(3):510-22.

Hoerder-suabedissen A, Molnár Z. Molecular diversity of early-born subplate neurons. Cereb Cortex. 2013;23(6):1473-83.

Holley JE, Gveric D, Newcombe J, Cuzner ML, Gutowski NJ. Astrocyte characterization in the multiple sclerosis glial scar. Neuropathol Appl Neurobiol. 2003;29(5):434-44.

Holley JE, Gveric D, Whatmore JL, Gutowski NJ. Tenascin C induces a quiescent phenotype in cultured adult human astrocytes. Glia. 2005;52(1):53-8.

Holzer P, Maggi CA. Dissociation of dorsal root ganglion neurons into afferent and efferent-like neurons. Neuroscience. 1998;86(2):389-98.

Horgan RP, Kenny LC. 'Omic' technologies: genomics, transcriptomics, proteomics and metabolomics. The Obstetrician & Gynaecologist. 2011;13:189-195.

Horikoshi Y, Sasaki A, Taguchi N, Maeda M, Tsukagoshi H, Sato K, Yamaguchi H. Human GLUT5 immunolabeling is useful for evaluating microglial status in neuropathological study using paraffin sections. Acta Neuropathol. 2003;105(2):157-62.

Hou ST, Callaghan D, Fournier MC, Hill I, Kang L, Massie B, Morley P, Murray C, Rasquinha I, Slack R, MacManus JP. The transcription factor E2F1 modulates apoptosis of neurons. J Neurochem. 2000;75(1):91-100.

Hou ST, Cowan E, Dostanic S, Rasquinha I, Comas T, Morley P, MacManus JP. Increased expression of the transcription factor E2F1 during dopamine-evoked, caspase-3-mediated apoptosis in rat cortical neurons. Neurosci Lett. 2001;306(3):153-6.

Howe CL, Kaptzan T, Magaña SM, Ayers-ringler JR, Lafrance-corey RG, Lucchinetti CF. Neuromyelitis optica IgG stimulates an immunological response in rat astrocyte cultures. Glia. 2014;62(5):692-708.

Hristova M, Cuthill D, Zbarsky V, Acosta-Saltos A, Wallace A, Blight K, Buckley SM, Peebles D, Heuer H, Waddington SN, Raivich G. Activation and deactivation of periventricular white matter phagocytes during postnatal mouse development. Glia. 2010;58:11–28.

Hu JG, Zhang YX, Qi Q, Wang R, Shen L, Zhang C, Xi J, Zhou JS, Lu HZ. Expression of BMP-2 and BMP-4 proteins by type-1 and type-2 astrocytes induced from neural stem cells under different differentiation conditions. Acta Neurobiol Exp (Wars). 2012;72(1):95-101.

Hu YA, Gu X, Liu J, Yang Y, Yan Y, Zhao C. Expression pattern of Wnt inhibitor factor 1(Wif1) during the development in mouse CNS. Gene Expr Patterns. 2008;8(7-8):515-22.

Huang D, Wujek J, Kidd G, He TT, Cardona A, Sasse ME, Stein EJ, Kish J, Tani M, Charo IF, Proudfoot AE, Rollins BJ, Handel T, Ransohoff RM. Chronic expression of monocyte chemoattractant protein-1 in the central nervous system causes delayed encephalopathy and impaired microglial function in mice. FASEB J. 2005;19(7):761-72.

Huang DR, Wang J, Kivisakk P, Rollins BJ, Ransohoff RM. Absence of monocyte chemoattractant protein 1 in mice leads to decreased local macrophage recruitment and antigen-specific T helper cell type 1 immune response in experimental autoimmune encephalomyelitis. J Exp Med. 2001;193(6):713-26.

Huang J, Zhou L, Wang H, Luo J, Zeng L, Xiong K, Chen D. Distribution of thrombospondins and their neuronal receptor α2δ1 in the rat retina. Exp Eye Res. 2013;111:36-49.

Huang JK, Jarjour AA, Nait oumesmar B, Kerninon C, Williams A, Krezel W, Kagechika H, Bauer J, Zhao C, Baron-Van Evercooren A, Chambon P, Ffrench-Constant C, Franklin RJ. Retinoid X receptor gamma signaling accelerates CNS remyelination. Nat Neurosci. 2011;14(1):45-53.

Hudgins SN, Levison SW. Ciliary neurotrophic factor stimulates astroglial hypertrophy *in vivo* and *in vitro*. Exp Neurol. 1998;150(2):171-82.

Hüppi PS, Warfield S, Kikinis R, Barnes PD, Zientara GP, Jolesz FA, Tsuji MK, Volpe JJ. Quantitative magnetic resonance imaging of brain development in premature and mature newborns. Ann Neurol. 1998;43(2):224-35.

Iglesias R, Dahl G, Qiu F, Spray DC, Scemes E. Pannexin 1: the molecular substrate of astrocyte "hemichannels". J Neurosci. 2009;29(21):7092-7.

Innis SM, Dyer RA. Brain astrocyte synthesis of docosahexaenoic acid from n-3 fatty acids is limited at the elongation of docosapentaenoic acid. J Lipid Res. 2002;43(9):1529-36.

Ishibashi T, Dakin KA, Stevens B, Lee PR, Kozlov SV, Stewart CL, Fields RD. Astrocytes promote myelination in response to electrical impulses. Neuron. 2006;49(6):823-32.

Izikson L, Klein RS, Charo IF, Weiner HL, Luster AD. Resistance to experimental autoimmune encephalomyelitis in mice lacking the CC chemokine receptor (CCR)2. J Exp Med. 2000;192(7):1075-80.

Jacob J, Storm R, Castro DS, Milton C, Pla P, Guillemot F, Birchmeier C, Briscoe J. Insm1 (IA-1) is an essential component of the regulatory network that specifies monoaminergic neuronal phenotypes in the vertebrate hindbrain. Development. 2009;136(14):2477-85.

Jaerve A, Müller HW. Chemokines in CNS injury and repair. Cell Tissue Res. 2012;349(1):229-48.

Jafarzadeh A, Mohammadi-kordkhayli M, Ahangar-parvin R, et al. Ginger extracts influence the expression of IL-27 and IL-33 in the central nervous system in experimental autoimmune encephalomyelitis and ameliorates the clinical symptoms of disease. J Neuroimmunol. 2014;276(1-2):80-8.

Jakovcevski I, Miljkovic D, Schachner M, Andjus PR. Tenascins and inflammation in disorders of the nervous system. Amino Acids. 2013;44(4):1115-27.

Jana A, Pahan K. Sphingolipids in multiple sclerosis. Neuromolecular Med. 2010;12(4):351-61.

Jang E, Kim JH, Lee S, Kim JH, Seo JW, Jin M, Lee MG, Jang IS, Lee WH, Suk K. Phenotypic polarization of activated astrocytes: the critical role of lipocalin-2 in the classical inflammatory activation of astrocytes. J Immunol. 2013a;191(10):5204-19.

Jang E, Lee S, Kim JH, Kim JH, Seo JW, Lee WH, Mori K, Nakao K, Suk K. Secreted protein lipocalin-2 promotes microglial M1 polarization. FASEB J. 2013b;27(3):1176-90.

Jansen LA, Uhlmann EJ, Crino PB, Gutmann DH, Wong M. Epileptogenesis and reduced inward rectifier potassium current in tuberous sclerosis complex-1-deficient astrocytes. Epilepsia. 2005;46(12):1871-80.

Jaworski J, Mioduszewska B, Sánchez-capelo A, Figiel I, Habas A, Gozdz A, Proszynski T, Hetman M, Mallet J, Kaczmarek L. Inducible cAMP early repressor, an endogenous antagonist of cAMP responsive element-binding protein, evokes neuronal apoptosis *in vitro*. J Neurosci. 2003;23(11):4519-26.

Jernås M, Malmeström C, Axelsson M, Olsson C, Nookaew I, Wadenvik H, Zetterberg H, Blennow K, Lycke J, Rudemo M, Olsson B. MS risk genes are transcriptionally regulated in CSF leukocytes at relapse. Mult Scler. 2013;19(4):403-10.

Ji K, Akgul G, Wollmuth LP, Tsirka SE. Microglia actively regulate the number of functional synapses. PLoS ONE. 2013;8(2):e56293.

Ji K, Miyauchi J, Tsirka SE. Microglia: an active player in the regulation of synaptic activity. Neural Plast. 2013;2013:627325.

Jian J, Zheng Z, Zhang K, Rackohn TM, Hsu C, Levin A, Enjamuri DR, Zhang X, Ting K, Soo C. Fibromodulin promoted *in vitro* and *in vivo* angiogenesis. Biochem Biophys Res Commun. 2013;436(3):530-5.

Jiang HR, Milovanović M, Allan D, Niedbala W, Besnard AG, Fukada SY, Alves-Filho JC, Togbe D, Goodyear CS, Linington C, Xu D, Lukic ML, Liew FY. IL-33 attenuates EAE by suppressing IL-17 and IFN-γ production and inducing alternatively activated macrophages. Eur J Immunol. 2012;42(7):1804-14.

Jiang Q, Quaynor B, Sun A, Li Q, Matsui H, Honda H, Inaba T, Sprecher E, Uitto J. The Samd9L gene: transcriptional regulation and tissue-specific expression in mouse development. J Invest Dermatol. 2011;131(7):1428-34.

Jiang S, Avraham HK, Kim TA, Rogers RA, Avraham S. Receptor-type PTP-NP inhibition of Dynamin-1 GTPase activity is associated with neuronal depolarization. Cell Signal. 2006;18(9):1439-46.

Jiang S, Tulloch AG, Kim TA, Fu Y, Rogers R, Gaskell A, White RA, Avraham H, Avraham S. Characterization and chromosomal localization of PTP-NP-2, a new isoform of protein tyrosine phosphatase-like receptor, expressed on synaptic boutons. Gene. 1998;215(2):345-59.

Jiang SX, Sheldrick M, Desbois A, Slinn J, Hou ST. Neuropilin-1 is a direct target of the transcription factor E2F1 during cerebral ischemia-induced neuronal death *in vivo*. Mol Cell Biol. 2007;27(5):1696-705.

Jiménez AJ, Domínguez-pinos MD, Guerra MM, Fernández-llebrez P, Pérez-fígares JM. Structure and function of the ependymal barrier and diseases associated with ependyma disruption. Tissue Barriers. 2014;2:e28426.

John GR, Lee SC, Brosnan CF. Cytokines: powerful regulators of glial cell activation. Neuroscientist. 2003;9(1):10-22.

Johnson AW, Crombag HS, Smith DR, Ramanan N. Effects of serum response factor (SRF) deletion on conditioned reinforcement. Behav Brain Res. 2011;220(2):312-8.

Jones EV, Bouvier DS. Astrocyte-secreted matricellular proteins in CNS remodelling during development and disease. Neural Plast. 2014;2014:321209.

Jones JI, Clemmons DR. Insulin-like growth factors and their binding proteins: biological actions. Endocr Rev. 1995;16(1):3-34.

Jones-bolin S, Zhao H, Hunter K, Klein-szanto A, Ruggeri B. The effects of the oral, pan-VEGF-R kinase inhibitor CEP-7055 and chemotherapy in orthotopic models of glioblastoma and colon carcinoma in mice. Mol Cancer Ther. 2006;5(7):1744-53.

Jordan CA, Friedrich VL, Godfraind C, Cardellechio CB, Holmes KV, Dubois-dalcq M. Expression of viral and myelin gene transcripts in a murine CNS demyelinating disease caused by a coronavirus. Glia. 1989;2(5):318-29.

Kabadi SV, Stoica BA, Loane DJ, Luo T, Faden AI. CR8, a novel inhibitor of CDK, limits microglial activation, astrocytosis, neuronal loss, and neurologic dysfunction after experimental traumatic brain injury. J Cereb Blood Flow Metab. 2014;34(3):502-13.

Kagan HM, Vaccaro CA, Bronson RE, Tang SS, Brody JS. Ultrastructural immunolocalization of lysyl oxidase in vascular connective tissue. J Cell Biol. 1986;103(3):1121-8.

Kagan HM. Lysyl oxidase: mechanism, regulation and relationship to liver fibrosis. Pathol Res Pract. 1994;190(9-10):910-9.

Kahn MA, De Vellis J. Regulation of an oligodendrocyte progenitor cell line by the interleukin-6 family of cytokines. Glia. 1994;12(2):87-98.

Kahn MA, Ellison JA, Chang RP, Speight GJ, De vellis J. CNTF induces GFAP in a S-100 alpha brain cell population: the pattern of CNTF-alpha R suggests an indirect mode of action. Brain Res Dev Brain Res. 1997;98(2):221-33.

Kahn MA, Huang CJ, Caruso A, Barresi V, Nazarian R, Condorelli DF, de Vellis J. Ciliary neurotrophic factor activates JAK/Stat signal transduction cascade and induces transcriptional expression of glial fibrillary acidic protein in glial cells. J Neurochem. 1997;68(4):1413-23.

Kamakura S, Oishi K, Yoshimatsu T, Nakafuku M, Masuyama N, Gotoh Y. Hes binding to STAT3 mediates crosstalk between Notch and JAK-STAT signalling. Nat Cell Biol. 2004;6(6):547-54.

Kang J, Jiang L, Goldman SA, Nedergaard M. Astrocyte-mediated potentiation of inhibitory synaptic transmission. Nat Neurosci. 1998;1(8):683-92.

Káradóttir R, Cavelier P, Bergersen LH, Attwell D. NMDA receptors are expressed in oligodendrocytes and activated in ischaemia. Nature. 2005;438:1162–6.

Karpuk N, Burkovetskaya M, Fritz T, Angle A, Kielian T. Neuroinflammation leads to region-dependent alterations in astrocyte gap junction communication and hemichannel activity. J Neurosci. 2011;31(2):414-25.

Kassmann CM. Myelin peroxisomes - essential organelles for the maintenance of white matter in the nervous system. Biochimie. 2014;98:111-8.

Kaushik DK, Gupta M, Das S, Basu A. Krüppel-like factor 4, a novel transcription factor regulates microglial activation and subsequent neuroinflammation. J Neuroinflammation. 2010;7(1):68.

Kaushik DK, Mukhopadhyay R, Kumawat KL, Gupta M, Basu A. Therapeutic targeting of Krüppel-like factor 4 abrogates microglial activation. J Neuroinflammation. 2012;9(1):57.

Kawahara K, Suenobu M, Ohtsuka H, Kuniyasu A, Sugimoto Y, Nakagomi M, Fukasawa H, Shudo K, Nakayama H. Cooperative therapeutic action of retinoic acid receptor and retinoid x receptor agonists in a mouse model of Alzheimer's disease. J Alzheimers Dis. 2014;42(2):587-605.

Kawano T, Morimoto K, Uemura Y. Partial purification and properties of urokinase inhibitor from human placenta. J Biochem. 1970;67(3):333-42.

Kazazoglou T, Fleischer-lambropoulos E, Geladopoulos T, Kentroti S, Stefanis C, Vernadakis A. Differential responsiveness of late passage C-6 glial cells and advanced passages of astrocytes derived from aged mouse cerebral hemispheres to cytokines and growth factors: glutamine synthetase activity. Neurochem Res. 1996;21(5):609-14.

Kessaris N, Fogarty M, Iannarelli P, Grist M, Wegner M, Richardson WD. Competing waves of oligodendrocytes in the forebrain and postnatal elimination of an embryonic lineage. Nat Neurosci. 2006;9(2):173-9.

Kessaris N, Pringle N, Richardson WD. Specification of CNS glia from neural stem cells in the embryonic neuroepithelium. Philos Trans R Soc Lond, B, Biol Sci. 2008;363(1489):71-85.

Kidd D, Barkhof F, Mcconnell R, Algra PR, Allen IV, Revesz T. Cortical lesions in multiple sclerosis. Brain. 1999;122 (Pt 1):17-26.

Kielian T, Drew PD. Effects of peroxisome proliferator-activated receptor-gamma agonists on central nervous system inflammation. J Neurosci Res. 2003;71(3):315-25.

Kielty CM, Sherratt MJ, Shuttleworth CA. Elastic fibres. J Cell Sci. 2002;115(Pt 14):2817-28.

Kienitz MC, Bender K, Dermietzel R, Pott L, Zoidl G. Pannexin 1 constitutes the large conductance cation channel of cardiac myocytes. J Biol Chem. 2011;286(1):290-8.

Kierdorf K, Erny D, Goldmann T, Sander V, Schulz C, Perdiguero EG, Wieghofer P, Heinrich A, Riemke P, Hölscher C, Müller DN, Luckow B, Brocker T, Debowski K, Fritz G, Opdenakker G, Diefenbach A, Biber K, Heikenwalder M, Geissmann F, Rosenbauer F, Prinz M. Microglia emerge from ery- thromyeloid precursors via Pu.1- and Irf8-dependent pathways. Nat. Neurosci. 2013;16:273–80.

Kim DW, Chang JH, Park SW, Jeon GS, Seo JH, Cho SS. Activated cyclic AMP-response element binding protein (CREB) is expressed in a myelin-associated protein in chick. Neurochem Res. 2005;30(9):1133-7.

Kim H, Ahn M, Choi S, Kim M, Sim KB, Kim J, Moon C, Shin T. Potential role of fibronectin in microglia/macrophage activation following cryoinjury in the rat brain: an immunohistochemical study. Brain Res. 2013;1502:11-9.

Kim H, Moon C, Ahn M, Lee Y, Kim S, Matsumoto Y, Koh CS, Kim MD, Shin T. Increased phosphorylation of cyclic AMP response element-binding protein in the spinal cord of Lewis rats with experimental autoimmune encephalomyelitis. Brain Res. 2007;1162:113-20.

Kimber SJ, Sneddon SF, Bloor DJ, El-Bareg AM, Hawkhead JA, Metcalfe AD, Houghton FD, Leese HJ, Rutherford A, Lieberman BA, Brison DR. Expression of genes involved in early cell fate decisions in human embryos and their regulation by growth factors. Reproduction. 2008;135(5):635-47.

Kirsch M, Lee MY, Meyer V, Wiese A, Hofmann HD. Evidence for multiple, local functions of ciliary neurotrophic factor (CNTF) in retinal development: expression of CNTF and its receptors and *in vitro* effects on target cells. J Neurochem. 1997;68(3):979-90.

Kirsch M, Trautmann N, Ernst M, Hofmann HD. Involvement of gp130-associated cytokine signaling in Müller cell activation following optic nerve lesion. Glia. 2010;58(7):768-79.

Knöll B, Nordheim A. Functional versatility of transcription factors in the nervous system: the SRF paradigm. Trends Neurosci. 2009;32(8):432-42.

Koblar SA, Turnley AM, Classon BJ, Reid KL, Ware CB, Cheema SS, Murphy M, Bartlett PF. Neural precursor differentiation into astrocytes requires signaling through the leukemia inhibitory factor receptor. Proc Natl Acad Sci USA. 1998;95(6):3178-81.

Koehler RC, Roman RJ, Harder DR. Astrocytes and the regulation of cerebral blood flow. Trends Neurosci. 2009;32(3):160-9.

Koistinaho M, Lin S, Wu X, Esterman M, Koger D, Hanson J, Higgs R, Liu F, Malkani S, Bales KR, Paul SM. Apolipoprotein E promotes astrocyte colocalization and degradation of deposited amyloid-beta peptides. Nat Med. 2004;10(7):719-26.

Kojima N, Borlikova G, Sakamoto T, Yamada K, Ikeda T, Itohara S, Niki H, Endo S. Inducible cAMP early repressor acts as a negative regulator for kindling epileptogenesis and long-term fear memory. J Neurosci. 2008;28(25):6459-72.

Kojo H, Tajima K, Fukagawa M, Isogai T, Nishimura S. Molecular cloning and characterization of two novel human RXR alpha splice variants. J Steroid Biochem Mol Biol. 2004;92(1-2):19-28.

Kondo A, Nakano T, Suzuki K. Blood-brain barrier permeability to horseradish peroxidase in twitcher and cuprizone-intoxicated mice. Brain Res. 1987;425(1):186-90.

Kondo Y, Nakanishi T, Takigawa M, Ogawa N. Immunohistochemical localization of connective tissue growth factor in the rat central nervous system. Brain Res. 1999;834(1-2):146-51.

König M, Zimmer AM, Steiner H, Holmes PV, Crawley JN, Brownstein MJ, Zimmer A. Pain responses, anxiety and aggression in mice deficient in pre-proenkephalin. Nature. 1996;383(6600):535-8.

Kotter MR, Li WW, Zhao C, Franklin RJ. Myelin impairs CNS remyelination by inhibiting oligodendrocyte precursor cell differentiation. J Neurosci. 2006;26(1):328-32.

Koulakoff A, Ezan P, Giaume C. Neurons control the expression of connexin 30 and connexin 43 in mouse cortical astrocytes. Glia. 2008;56(12):1299-311.

Kraakman MJ, Allen TL, Whitham M, Iliades P, Kammoun HL, Estevez E, Lancaster GI, Febbraio MA. Targeting gp130 to prevent inflammation and promote insulin action. Diabetes Obes Metab. 2013;15 Suppl 3:170-5.

Kraakman MJ, Allen TL, Whitham M, Iliades P, Kammoun HL, Estevez E, Lancaster GI, Febbraio MA. Targeting gp130 to prevent inflammation and promote insulin action. Diabetes Obes Metab. 2013;15 Suppl 3:170-5.

Krabbe G, Halle A, Matyash V, Rinnenthal JL, Eom GD, Bernhardt U, Miller KR, Prokop S, Kettenmann H, Heppner FL. Functional impairment of microglia coincides with ß-amyloid deposition in mice with Alzheimer-like pathology. PLoS ONE. 2013;8(4):e60921.

Krady JK, Lin HW, Liberto CM, Basu A, Kremlev SG, Levison SW. Ciliary neurotrophic factor and interleukin-6 differentially activate microglia. J Neurosci Res. 2008;86(7):1538-47.

Krsmanovic LZ, Mores N, Navarro CE, Arora KK, Catt KJ. An agonist-induced switch in G protein coupling of the gonadotropin-releasing hormone receptor regulates pulsatile neuropeptide secretion. Proc Natl Acad Sci USA. 2003;100(5):2969-74.

Kruithof EK, Baker MS, Bunn CL. Biological and clinical aspects of plasminogen activator inhibitor type 2. Blood. 1995;86(11):4007-24.

Krum JM, Phillips TM, Rosenstein JM. Changes in astroglial GLT-1 expression after neural transplantation or stab wounds. Exp Neurol. 2002;174(2):137-49.

Krumbholz M, Theil D, Cepok S, Hemmer B, Kivisäkk P, Ransohoff RM, Hofbauer M, Farina C, Derfuss T, Hartle C, Newcombe J, Hohlfeld R, Meinl E. Chemokines in multiple sclerosis: CXCL12 and CXCL13 up-regulation is differentially linked to CNS immune cell recruitment. Brain. 2006;129(Pt 1):200-11.

Kruse U, Sippel AE. Transcription factor nuclear factor I proteins form stable homo- and heterodimers. FEBS Lett. 1994;348(1):46-50.

Kuchibhotla KV, Lattarulo CR, Hyman BT, Bacskai BJ. Synchronous hyperactivity and intercellular calcium waves in astrocytes in Alzheimer mice. Science. 2009;323(5918):1211-5.

Kühl NM, De keyser J, De vries H, Hoekstra D. Insulin-like growth factor binding proteins-1 and -2 differentially inhibit rat oligodendrocyte precursor cell survival and differentiation *in vitro*. J Neurosci Res. 2002;69(2):207-16.

Kuhlmann T, Remington L, Cognet I, Bourbonniere L, Zehntner S, Guilhot F, Herman A, Guay-Giroux A, Antel JP, Owens T, Gauchat JF. Continued administration of ciliary neurotrophic factor protects mice from inflammatory pathology in experimental autoimmune encephalomyelitis. Am J Pathol. 2006;169(2):584-98.

Kuhn HG, Winkler J, Kempermann G, Thal LJ, Gage FH. Epidermal growth factor and fibroblast growth factor-2 have different effects on neural progenitors in the adult rat brain. J Neurosci. 1997;17(15):5820-9.

Kurumada S, Onishi A, Imai H, Ishii K, Kobayashi T, Sato SB. Stage-specific association of apolipoprotein A-I and E in developing mouse retina. Invest Ophthalmol Vis Sci. 2007;48(4):1815-23.

Kutzelnigg A, Lassmann H. Pathology of multiple sclerosis and related inflammatory demyelinating diseases. Handb Clin Neurol. 2014;122:15-58.

Kwon AT, Arenillas DJ, Worsley Hunt R, Wasserman WW. oPOSSUM-3: advanced analysis of regulatory motif over-representation across genes or ChIP-Seq datasets. G3 (Bethesda). 2012;2(9):987-1002.

Lakso M, Sauer B, Mosinger B, Lee EJ, Manning RW, Yu SH, Mulder KL, Westphal H. Targeted oncogene activation by site-specific recombination in transgenic mice. Proc Natl Acad Sci USA. 1992;89(14):6232-6.

Lalor SJ, Segal BM. Lymphoid chemokines in the CNS. J Neuroimmunol. 2010;224(1-2):56-61.

Lamond R, Barnett SC. Schwann cells but not olfactory ensheathing cells inhibit CNS myelination via the secretion of connective tissue growth factor. J Neurosci. 2013;33(47):18686-97.

Lan MS, Breslin MB. Structure, expression, and biological function of INSM1 transcription factor in neuroendocrine differentiation. FASEB J. 2009;23(7):2024-33.

Land PW, Monaghan AP. Expression of the transcription factor, tailless, is required for formation of superficial cortical layers. Cereb Cortex. 2003;13(9):921-31.

Lange-dohna C, Zeitschel U, Gaunitz F, Perez-polo JR, Bigl V, Rossner S. Cloning and expression of the rat BACE1 promoter. J Neurosci Res. 2003;73(1):73-80.

Larsen PH, Dasilva AG, Conant K, Yong VW. Myelin formation during development of the CNS is delayed in matrix metalloproteinase-9 and -12 null mice. J Neurosci. 2006;26(8):2207-14.

Latronico T, Branà MT, Gramegna P, Fasano A, Di bari G, Liuzzi GM. Inhibition of myelin-cleaving poteolytic activities by interferon-beta in rat astrocyte cultures. Comparative analysis between gelatinases and calpain-II. PLoS ONE. 2013;8(2):e49656.

Lawson LJ, Perry VH, Dri P, Gordon S. Heterogeneity in the distribution and morphology of microglia in the normal adult mouse brain. Neuroscience. 1990;39(1):151-70.

Leader DP, Burgess K, Creek D, Barrett MP. Rapid Commun. Mass Spectrom. 2011;25: 3422–6.

Leblanc BP, Stunnenberg HG. 9-cis retinoic acid signaling: Changing partners causes some excitement. Genes Dev 1995;9:1811-16.

Lee HY, Kléber M, Hari L, Brault V, Suter U, Taketo MM, Kemler R, Sommer L. Instructive role of Wnt/beta-catenin in sensory fate specification in neural crest stem cells. Science. 2004;303(5660):1020-3.

Lee LT, Tan-un KC, Lin MC, Chow BK. Retinoic acid activates human secretin gene expression by Sp proteins and nuclear factor I in neuronal SH-SY5Y cells. J Neurochem. 2005;93(2):339-50.

Lee S, Lee WH, Lee MS, Mori K, Suk K. Regulation by lipocalin-2 of neuronal cell death, migration, and morphology. J Neurosci Res. 2012a;90(3):540-50.

Lee S, Park JY, Lee WH, Kim H, Park HC, Mori K, Suk K. Lipocalin-2 is an autocrine mediator of reactive astrocytosis. J Neurosci. 2009;29(1):234-49.

Lee Y, Morrison BM, Li Y, Lengacher S, Farah MH, Hoffman PN, Liu Y, Tsingalia A, Jin L, Zhang PW, Pellerin L, Magistretti PJ, Rothstein JD. Oligodendroglia metabolically support axons and contribute to neurodegeneration. Nature. 2012;487(7408):443-8.

Lee Y, Morrison BM, Li Y, Lengacher S, Farah MH, Hoffman PN, Liu Y, Tsingalia A, Jin L, Zhang PW, Pellerin L, Magistretti PJ, Rothstein JD. Oligodendroglia metabolically support axons and contribute to neurodegeneration. Nature. 2012b;487(7408):443-8.

Lee YH, Schiemann WP. Fibromodulin suppresses nuclear factor-kappaB activity by inducing the delayed degradation of IKBA via a JNK-dependent pathway coupled to fibroblast apoptosis. J Biol Chem. 2011;286(8):6414-22.

Lehmann HC, Köhne A, Bernal F, Jangouk P, Meyer Zu Hörste G, Dehmel T, Hartung HP, Previtali SC, Kieseier BC. Matrix metalloproteinase-2 is involved in myelination of dorsal root ganglia neurons. Glia. 2009;57(5):479-89.

Leibinger M, Müller A, Gobrecht P, Diekmann H, Andreadaki A, Fischer D. Interleukin-6 contributes to CNS axon regeneration upon inflammatory stimulation. Cell Death Dis. 2013;4:e609.

Lendahl U, Zimmerman LB, Mckay RD. CNS stem cells express a new class of intermediate filament protein. Cell. 1990;60(4):585-95.

Leroux M, Lakshmanan V, Daily JP. Plasmodium falciparum biology: analysis of *in vitro* versus *in vivo* growth conditions. Trends Parasitol. 2009;25(10):474-81.

Levi G, Meyer. Nouvelles recherches sur le tissu nerveux cultiv_e *in vitro*. Morphologie, croissance et relations r_eciproques des neurones. Arch Biol(Paris) 1941;52:133–278.

Levison SW, Ducceschi MH, Young GM, Wood TL. Acute exposure to CNTF *in vivo* induces multiple components of reactive gliosis. Exp Neurol. 1996;141(2):256-68.

Levison SW, Hudgins SN, Crawford JL. Ciliary neurotrophic factor stimulates nuclear hypertrophy and increases the GFAP content of cultured astrocytes. Brain Res. 1998;803(1-2):189-93.

Li F, Chong ZZ, Maiese K. Vital elements of the Wnt-Frizzled signaling pathway in the nervous system. Curr Neurovasc Res. 2005;2(4):331-40.

Li L, Lundkvist A, Andersson D, Wilhelmsson U, Nagai N, Pardo AC, Nodin C, Ståhlberg A, Aprico K, Larsson K, Yabe T, Moons L, Fotheringham A, Davies I, Carmeliet P, Schwartz JP, Pekna M, Kubista M, Blomstrand F, Maragakis N, Nilsson M, Pekny M. Protective role of reactive astrocytes in brain ischemia. J Cereb Blood Flow Metab. 2008a;28(3):468-81.

Li PA, He Q, Cao T, Yong G, Szauter KM, Fong KS, Karlsson J, Keep MF, Csiszar K. Up-regulation and altered distribution of lysyl oxidase in the central nervous system of mutant SOD1 transgenic mouse model of amyotrophic lateral sclerosis. Brain Res Mol Brain Res. 2004;120(2):115-22.

Li R, Messing A, Goldman JE, Brenner M. GFAP mutations in Alexander disease. Int J Dev Neurosci. 2002;20(3-5):259-68.

Li W, Quigley L, Yao DL, Hudson LD, Brenner M, Zhang BJ, Brocke S, McFarland HF, Webster HD. Chronic relapsing experimental autoimmune encephalomyelitis: effects of insulin-like growth factor-I treatment on clinical deficits, lesion severity, glial responses, and blood brain barrier defects. J Neuropathol Exp Neurol. 1998;57(5):426-38.

Li W, Sun G, Yang S, Qu Q, Nakashima K, Shi Y. Nuclear receptor TLX regulates cell cycle progression in neural stem cells of the developing brain. Mol Endocrinol. 2008b;22(1):56-64.

Liauw J, Hoang S, Choi M, Eroglu C, Choi M, Sun GH, Percy M, Wildman-Tobriner B, Bliss T, Guzman RG, Barres BA, Steinberg GK. Thrombospondins 1 and 2 are necessary for synaptic plasticity and functional recovery after stroke. J Cereb Blood Flow Metab. 2008;28(10):1722-32.

Liberto CM, Albrecht PJ, Herx LM, Yong VW, Levison SW. Pro-regenerative properties of cytokine-activated astrocytes. J Neurochem. 2004;89(5):1092-100.

Liedtke W, Edelmann W, Bieri PL, Chiu FC, Cowan NJ, Kucherlapati R, Raine CS. GFAP is necessary for the integrity of CNS white matter architecture and long-term maintenance of myelination. Neuron. 1996;17(4):607-15.

Lillien LE, Sendtner M, Rohrer H, Hughes SM, Raff MC. Type-2 astrocyte development in rat brain cultures is initiated by a CNTF-like protein produced by type-1 astrocytes. Neuron. 1988;1(6):485-94.

Lin CT, Xu YF, Wu JY, Chan L. Immunoreactive apolipoprotein E is a widely distributed cellular protein. Immunohistochemical localization of apolipoprotein E in baboon tissues. J Clin Invest. 1986;78(4):947-58.

Lin JH, Lou N, Kang N, Takano T, Hu F, Han X, Xu Q, Lovatt D, Torres A, Willecke K, Yang J, Kang J, Nedergaard M. A central role of connexin 43 in hypoxic preconditioning. J Neurosci. 2008;28(3):681-95.

Lin TN, Cheung WM, Wu JS, Chen JJ, Lin H, Chen JJ, Liou JY, Shyue SK, Wu KK. 15d-prostaglandin J2 protects brain from ischemia-reperfusion injury. Arterioscler Thromb Vasc Biol. 2006a;26(3):481-7.

Lin TN, Kim GM, Chen JJ, Cheung WM, He YY, Hsu CY. Differential regulation of thrombospondin-1 and thrombospondin-2 after focal cerebral ischemia/reperfusion. Stroke. 2003;34(1):177-86.

Lin W, Kemper A, Dupree JL, Harding HP, Ron D, Popko B. Interferon-gamma inhibits central nervous system remyelination through a process modulated by endoplasmic reticulum stress. Brain. 2006b;129(Pt 5):1306-18.

Lin W, Kunkler PE, Harding HP, Ron D, Kraig RP, Popko B. Enhanced integrated stress response promotes myelinating oligodendrocyte survival in response to interferon-gamma. Am J Pathol. 2008;173(5):1508-17.

Lindberg RL, De groot CJ, Montagne L, Freitag P, van der Valk P, Kappos L, Leppert D. The expression profile of matrix metalloproteinases (MMPs) and their inhibitors (TIMPs) in lesions and normal appearing white matter of multiple sclerosis. Brain. 2001;124(Pt 9):1743-53.

Lindner M, Thümmler K, Arthur A, Brunner S, Elliott C, McElroy D, Mohan H, Williams A, Edgar JM, Schuh C, Stadelmann C, Barnett SC, Lassmann H, Mucklisch S, Mudaliar M, Schaeren-Wiemers N, Meinl E, Linington C. Fibroblast growth factor signalling in multiple sclerosis: inhibition of myelination and induction of pro-inflammatory environment by FGF9. Brain. 2015;138(Pt 7):1875-93.

Linker RA, Maurer M, Gaupp S, Martini R, Holtmann B, Giess R, Rieckmann P, Lassmann H, Toyka KV, Sendtner M, Gold R. CNTF is a major protective factor in demyelinating CNS disease: a neurotrophic cytokine as modulator in neuroinflammation. Nat Med. 2002;8:620-4.

Liu H, Hew HC, Lu ZG, Yamaguchi T, Miki Y, Yoshida K. DNA damage signalling recruits RREB-1 to the p53 tumour suppressor promoter. Biochem J. 2009;422(3):543-51.

Liu HK, Belz T, Bock D, Takacs A, Wu H, Lichter P, Chai M, Schütz G. The nuclear receptor tailless is required for neurogenesis in the adult subventricular zone. Genes Dev. 2008a;22(18):2473-8.

Liu L, Huang D, Matsui M, He TT, Hu T, Demartino J, Lu B, Gerard C, Ransohoff RM. Severe disease, unaltered leukocyte migration, and reduced IFN-gamma production in CXCR3-/- mice with experimental autoimmune encephalomyelitis. J Immunol. 2006a;176(7):4399-409.

Liu Q, Zerbinatti CV, Zhang J, Hoe HS, Wang B, Cole SL, Herz J, Muglia L, Bu G. Amyloid precursor protein regulates brain apolipoprotein E and cholesterol metabolism through lipoprotein receptor LRP1. Neuron. 2007;56(1):66-78.

Liu Y, Wang X, Lu CC, Kerman R, Steward O, Xu XM, Zou Y. Repulsive Wnt signaling inhibits axon regeneration after CNS injury. J Neurosci. 2008b;28(33):8376-82.

Locovei S, Wang J, Dahl G. Activation of pannexin 1 channels by ATP through P2Y receptors and by cytoplasmic calcium. FEBS Lett. 2006;580(1):239-44.

Logan A, Gonzalez AM, Hill DJ, Berry M, Gregson NA, Baird A. Coordinated pattern of expression and localization of insulin-like growth factor-II (IGF-II) and IGF-binding protein-2 in the adult rat brain. Endocrinology. 1994;135(5):2255-64.

Loret C, Laeng P, Sensenbrenner M, Labourdette G. Acidic and basic fibroblast growth factors similarly regulate the rate of biosynthesis of rat astroblast proteins. FEBS Lett. 1989;257(2):324-8.

Louis JC, Magal E, Takayama S, Varon S. CNTF protection of oligodendrocytes against natural and tumor necrosis factor-induced death. Science. 1993;259:689-92.

Lovatt D, Sonnewald U, Waagepetersen HS, Schousboe A, He W, Lin JH, Han X, Takano T, Wang S, Sim FJ, Goldman SA, Nedergaard M. The transcriptome and metabolic gene signature of protoplasmic astrocytes in the adult murine cortex. J Neurosci. 2007;27(45):12255-66.

Lu PP, Ramanan N. A critical cell-intrinsic role for serum response factor in glial specification in the CNS. J Neurosci. 2012;32(23):8012-23.

Lu Z, Hu X, Zhu C, Wang D, Zheng X, Liu Q. Overexpression of CNTF in Mesenchymal Stem Cells reduces demyelination and induces clinical recovery in experimental autoimmune encephalomyelitis mice. J Neuroimmunol. 2009;206(1-2):58-69.

Lubetzki C, Demerens C, Anglade P, Villarroya H, Frankfurter A, Lee VM, Zalc B. Even in culture, oligodendrocytes myelinate solely axons. Proc Natl Acad Sci USA. 1993;90(14):6820-4.

Luckman SM, Cox HJ. Expression of inducible cAMP early repressor (ICER) in hypothalamic magnocellular neurons. Brain Res Mol Brain Res. 1995;34(2):231-8.

Luo D, Liu K, Zhu B, Xu X. Expression profiling in glaucomatous human lamina cribrosa cells based on graph-clustering approach. Curr Eye Res. 2013;38(7):767-73.

Luo X, Zhang X, Shao W, Yin Y, Zhou J. Crucial roles of MZF-1 in the transcriptional regulation of apomorphine-induced modulation of FGF-2 expression in astrocytic cultures. J Neurochem. 2009;108(4):952-61.

Lutz SE, Zhao Y, Gulinello M, Lee SC, Raine CS, Brosnan CF. Deletion of astrocyte connexins 43 and 30 leads to a dysmyelinating phenotype and hippocampal CA1 vacuolation. J Neurosci. 2009;29(24):7743-52.

Ma S, Kwon HJ, Huang Z. A functional requirement for astroglia in promoting blood vessel development in the early postnatal brain. PLoS ONE. 2012a;7(10):e48001.

Ma W, Compan V, Zheng W, Martin E, North RA, Verkhratsky A, Surprenant A. Pannexin 1 forms an anion-selective channel. Pflugers Arch. 2012b;463(4):585-92.

MacManus JP, Jian M, Preston E, Rasquinha I, Webster J, Zurakowski B. Absence of the transcription factor E2F1 attenuates brain injury and improves behavior after focal ischemia in mice. J Cereb Blood Flow Metab. 2003;23(9):1020-8.

Maeda A, Sobel RA. Matrix metalloproteinases in the normal human central nervous system, microglial nodules, and multiple sclerosis lesions. J Neuropathol Exp Neurol.1996;55(3):300-9.

Magistretti PJ. Neuron-glia metabolic coupling and plasticity. J Exp Biol. 2006;209(Pt 12):2304-11.

Maglione M, Tress O, Haas B, Karram K, Trotter J, Willecke K, Kettenmann H. Oligodendrocytes in mouse corpus callosum are coupled via gap junction channels formed by connexin47 and connexin32. Glia. 2010;58(9):1104-17.

Magliozzi R, Columba-cabezas S, Serafini B, Aloisi F. Intracerebral expression of CXCL13 and BAFF is accompanied by formation of lymphoid follicle-like structures in the meninges of mice with relapsing experimental autoimmune encephalomyelitis. J Neuroimmunol. 2004;148(1-2):11-23.

Magnus T, Carmen J, Deleon J, Xue H, Pardo AC, Lepore AC, Mattson MP, Rao MS, Maragakis NJ. Adult glial precursor proliferation in mutant SOD1G93A mice. Glia. 2008;56(2):200-8.

Magri L, Swiss VA, Jablonska B, Lei L, Pedre X, Walsh M, Zhang W, Gallo V, Canoll P, Casaccia P. E2F1 coregulates cell cycle genes and chromatin components during the transition of oligodendrocyte progenitors from proliferation to differentiation. J Neurosci. 2014;34(4):1481-93.

Maier K, Rau CR, Storch MK, Sättler MB, Demmer I, Weissert R, Taheri N, Kuhnert AV, Bähr M, Diem R. Ciliary neurotrophic factor protects retinal ganglion cells from secondary cell death during acute autoimmune optic neuritis in rats. Brain Pathol. 2004;14(4):378-87.

Maki T, Liang AC, Miyamoto N, Lo EH, Arai K. Mechanisms of oligodendrocyte regeneration from ventricular-subventricular zone-derived progenitor cells in white matter diseases. Front Cell Neurosci. 2013;7:275.

Malhotra, S. K., Shnitka, T.K. Diversity in reactive astrocytes, Humana Press, New Jersey, 2002, 17 pp.

Mancuso M, Orsucci D, Volpi L, Calsolaro V, Siciliano G. Coenzyme Q10 in neuromuscular and neurodegenerative disorders. Curr Drug Targets. 2010;11(1):111-21.

Mandon EC, Ehses I, Rother J, Van echten G, Sandhoff K. Subcellular localization and membrane topology of serine palmitoyltransferase, 3-dehydrosphinganine reductase, and sphinganine N-acyltransferase in mouse liver. J Biol Chem. 1992;267(16):11144-8.

Marin-Teva JL, Dusart I, Colin C, Gervais A, van Rooijen N, Mallat M. Microglia promote the death of developing Purkinje cells. Neuron. 2004;41:535–47.

Marmur R, Kessler JA, Zhu G, Gokhan S, Mehler MF. Differentiation of oligodendroglial progenitors derived from cortical multipotent cells requires extrinsic signals including activation of gp130/LIFb receptors. J Neurosci. 1998;18:9800-11.

Maronde E, Pfeffer M, Olcese J, Molina CA, Schlotter F, Dehghani F, Korf HW, Stehle JH. Transcription factors in neuroendocrine regulation: rhythmic changes in pCREB and ICER levels frame melatonin synthesis. J Neurosci. 1999;19(9):3326-36.

Marques F, Mesquita SD, Sousa JC, Coppola G, Gao F, Geschwind DH, Columba-Cabezas S, Aloisi F, Degn M, Cerqueira JJ, Sousa N, Correia-Neves M, Palha JA. Lipocalin 2 is present in the EAE brain and is modulated by natalizumab. Front Cell Neurosci. 2012;6:33.

Martinez FO, Helming L, Gordon S. Alternative activation of macrophages: an immunologic functional perspective. Annu Rev Immunol. 2009;27:451-83.

März P, Heese K, Dimitriades-schmutz B, Rose-john S, Otten U. Role of interleukin-6 and soluble IL-6 receptor in region-specific induction of astrocytic differentiation and neurotrophin expression. Glia. 1999;26(3):191-200.

Masliah E, Ho G, Wyss-coray T. Functional role of TGF beta in Alzheimer's disease microvascular injury: lessons from transgenic mice. Neurochem Int. 2001;39(5-6):393-400.

Masos T, Miskin R. mRNAs encoding urokinase-type plasminogen activator and plasminogen activator inhibitor-1 are elevated in the mouse brain following kainate-mediated excitation. Brain Res Mol Brain Res. 1997;47(1-2):157-69.

Masu Y, Wolf E, Holtmann B, Sendtner M, Brem G, Thoenen H. Disruption of the CNTF gene results in motor neuron degeneration. Nature. 1993;365(6441):27-32.

May P, Rohlmann A, Bock HH, Zurhove K, Marth JD, Schomburg ED, Noebels JL, Beffert U, Sweatt JD, Weeber EJ, Herz J. Neuronal LRP1 functionally associates with postsynaptic proteins and is required for normal motor function in mice. Mol Cell Biol. 2004;24(20):8872-83.

Mayer M, Bhakoo K, Noble M. Ciliary neurotrophic factor and leukemia inhibitory factor promote the generation, maturation and survival of oligodendrocytes *in vitro*. Development. 1994;120(1):143-53.

Mayr C, Bund D, Schlee M, Moosmann A, Kofler DM, Hallek M, Wendtner CM. Fibromodulin as a novel tumor-associated antigen (TAA) in chronic lymphocytic leukemia (CLL), which allows expansion of specific CD8+ autologous T lymphocytes. Blood. 2005;105(4):1566-73.

Mazia D, Schatten G, Sale W. Adhesion of cells to surfaces coated with polylysine. Applications to electron microscopy. J Cell Biol. 1975;66(1):198-200.

McAlpine D. The Benign Form of Multiple Sclerosis: Results of a Long-Term Study. Br Med J. 1964;2(5416):1029-32.

McAlpine D. The benign form of multiple sclerosis. A study based on 241 cases seen within three years of onset and followed up until the tenth year or more of the disease. Brain. 1961;84:186-203.

McAlpine, D., Lumsden, C.E., Acheson, E.D. Multiple Sclerosis: A Reappraisal, Churcill Livingstone, Edinburgh. 1972.

Mccawley LJ, Matrisian LM. Matrix metalloproteinases: they're not just for matrix anymore!. Curr Opin Cell Biol. 2001;13(5):534-40.

Mcclain JA, Phillips LL, Fillmore HL. Increased MMP-3 and CTGF expression during lipopolysaccharide-induced dopaminergic neurodegeneration. Neurosci Lett. 2009;460(1):27-31.

Mccoll SR, Mahalingam S, Staykova M, Tylaska LA, Fisher KE, Strick CA, Gladue RP, Neote KS, Willenborg DO. Expression of rat I-TAC/CXCL11/SCYA11 during central nervous system inflammation: comparison with other CXCR3 ligands. Lab Invest. 2004;84(11):1418-29.

Mcconnell SK. The control of neuronal identity in the developing cerebral cortex. Curr Opin Neurobiol. 1992;2(1):23-7.

Mcdonnell GV, Hawkins SA. Primary progressive multiple sclerosis: a distinct syndrome?. Mult Scler. 1996;2(3):137-41.

Mcfarland HF, Martin R. Multiple sclerosis: a complicated picture of autoimmunity. Nat Immunol. 2007;8(9):913-9.

McGeer PL, Itagaki S, Boyes BE, McGeer EG. Reactive microglia are positive for HLA-DR in the substantia nigra of Parkinson's and Alzheimer's disease brains. Neurology. 1988;38:1285–91.

McMahon EJ, Bailey SL, Castenada CV, Waldner H, Miller SD. Epitope spreading initiates in the CNS in two mouse models of multiple sclerosis. Nat Med. 2005;11(3):335-9.

Mcmahon EJ, Suzuki K, Matsushima GK. Peripheral macrophage recruitment in cuprizone-induced CNS demyelination despite an intact blood-brain barrier. J Neuroimmunol. 2002;130(1-2):32-45.

Mcmanus C, Berman JW, Brett FM, Staunton H, Farrell M, Brosnan CF. MCP-1, MCP-2 and MCP-3 expression in multiple sclerosis lesions: an immunohistochemical and in situ hybridization study. J Neuroimmunol. 1998;86(1):20-9.

Medcalf RL. Plasminogen activator inhibitor type 2: still an enigmatic serpin but a model for gene regulation. Meth Enzymol. 2011;499:105-34.

Meeuwsen S, Persoon-deen C, Bsibsi M, Ravid R, Van noort JM. Cytokine, chemokine and growth factor gene profiling of cultured human astrocytes after exposure to proinflammatory stimuli. Glia. 2003;43(3):243-53.

Mei X, Ezan P, Giaume C, Koulakoff A. Astroglial connexin immunoreactivity is specifically altered at ß-amyloid plaques in ß-amyloid precursor protein/presenilin1 mice. Neuroscience. 2010;171(1):92-105.

Melone M, Quagliano F, Barbaresi P, Varoqui H, Erickson JD, Conti F. Localization of the glutamine transporter SNAT1 in rat cerebral cortex and neighboring structures, with a note on its localization in human cortex. Cereb Cortex. 2004;14(5):562-74.

Mena MA, García de Yébenes J. Glial cells as players in parkinsonism: the "good," the "bad," and the "mysterious" glia. Neuroscientist. 2008;14(6):544-60.

Menichella DM, Goodenough DA, Sirkowski E, Scherer SS, Paul DL. Connexins are critical for normal myelination in the CNS. J Neurosci. 2003;23(13):5963-73.

Mennerick S, Benz A, Zorumski CF. Components of glial responses to exogenous and synaptic glutamate in rat hippocampal microcultures. J Neurosci. 1996;16(1):55-64.

Mesnil M, Testa B, Jenner P. Xenobiotic metabolism by brain monooxygenases and other cerebral enzymes. AdvDrug Res. 1984;13:95–207.

Messersmith DJ, Murtie JC, Le TQ, Frost EE, Armstrong RC. Fibroblast growth factor 2 (FGF2) and FGF receptor expression in an experimental demyelinating disease with extensive remyelination. J Neurosci Res. 2000;62(2):241-56.

Miller RH, Ono K. Morphological analysis of the early stages of oligodendrocyte development in the vertebrate central nervous system. Microsc Res Tech. 1998;41(5):441-53.

Milligan ED, Watkins LR. Pathological and protective roles of glia in chronic pain. Nat Rev Neurosci. 2009;10(1):23-36.

Mills JC, Nelson D, Erecińska M, Pittman RN. Metabolic and energetic changes during apoptosis in neural cells. J Neurochem. 1995;65(4):1721-30.

Milon BC, Agyapong A, Bautista R, Costello LC, Franklin RB. Ras responsive element binding protein-1 (RREB-1) down-regulates hZIP1 expression in prostate cancer cells. Prostate. 2010;70(3):288-96.

Mioduszewska B, Jaworski J, Kaczmarek L. Inducible cAMP early repressor (ICER) in the nervous system--a transcriptional regulator of neuronal plasticity and programmed cell death. J Neurochem. 2003;87(6):1313-20.

Miskimins R, Miskimins WK. A role for an AP-1-like site in the expression of the myelin basic protein gene during differentiation. Int J Dev Neurosci. 2001;19(1):85-91.

Misund K, Steigedal TS, Laegreid A, Thommesen L. Inducible cAMP early repressor splice variants ICER I and IIgamma both repress transcription of c-fos and chromogranin A. J Cell Biochem. 2007;101(6):1532-44.

Mitew S, Hay CM, Peckham H, Xiao J, Koenning M, Emery B. Mechanisms regulating the development of oligodendrocytes and central nervous system myelin. Neuroscience. 2013.

Mithen FA, Wood PM, Agrawal HC, Bunge RP. Immunohistochemical study of myelin sheaths formed by oligodendrocytes interacting with dissociated dorsal root ganglion neurons in culture. Brain Res. 1983;262(1):63-9.

Miyata T, Kawaguchi A, Okano H, Ogawa M. Asymmetric inheritance of radial glial fibers by cortical neurons. Neuron. 2001;31(5):727-41.

Miyawaki T, Uemura A, Dezawa M, Yu RT, Ide C, Nishikawa S, Honda Y, Tanabe Y, Tanabe T. Tlx, an orphan nuclear receptor, regulates cell numbers and astrocyte development in the developing retina. J Neurosci. 2004;24(37):8124-34.

Modi KK, Sendtner M, Pahan K. Up-regulation of ciliary neurotrophic factor in astrocytes by aspirin: implications for remyelination in multiple sclerosis. J Biol Chem. 2013;288(25):18533-45.

Mohan H, Krumbholz M, Sharma R, Eisele S, Junker A, Sixt M, Newcombe J, Wekerle H, Hohlfeld R, Lassmann H, Meinl E. Extracellular matrix in multiple sclerosis lesions: Fibrillar collagens, biglycan and decorin are upregulated and associated with infiltrating immune cells. Brain Pathol. 2010;20(5):966-75.

Molofsky AV, Kelley KW, Tsai HH, Redmond SA, Chang SM, Madireddy L, Chan JR, Baranzini SE, Ullian EM, Rowitch DH. Astrocyte-encoded positional cues maintain sensorimotor circuit integrity. Nature. 2014;509(7499):189-94.

Monaco L, Sassone-corsi P. Cross-talk in signal transduction: Ras-dependent induction of cAMP-responsive transcriptional repressor ICER by nerve growth factor. Oncogene. 1997;15(20):2493-500.

Montoliu C, Sancho-tello M, Azorin I, Burgal M, Vallés S, Renau-Piqueras J, Guerri C. Ethanol increases cytochrome P4502E1 and induces oxidative stress in astrocytes. J Neurochem. 1995;65(6):2561-70.

Moore CS, Abdullah SL, Brown A, Arulpragasam A, Crocker SJ. How factors secreted from astrocytes impact myelin repair. J Neurosci Res. 2011;89(1):13-21.

Moore DL, Blackmore MG, Hu Y, Kaestner KH, Bixby JL, Lemmon VP, Goldberg JL. KLF family members regulate intrinsic axon regeneration ability. Science. 2009;326(5950):298-301.

Moore SA, Yoder E, Murphy S, Dutton GR, Spector AA. Astrocytes, not neurons, produce docosahexaenoic acid (22:6 omega-3) and arachidonic acid (20:4 omega-6). J Neurochem. 1991;56(2):518-24.

Moore SA. Polyunsaturated fatty acid synthesis and release by brain-derived cells *in vitro*. J Mol Neurosci. 2001;16(2-3):195-200.

Moreno S, Farioli-vecchioli S, Cerù MP. Immunolocalization of peroxisome proliferator-activated receptors and retinoid X receptors in the adult rat CNS. Neuroscience. 2004;123(1):131-45.

Morgan D, Gordon MN, Tan J, Wilcock D, Rojiani AM. Dynamic complexity of the microglial activation response in transgenic models of amyloid deposition: implications for Alzheimer therapeutics. J Neuropathol Exp Neurol. 2005;64:743-53.

Morita K, Sasaki H, Fujimoto K, Furuse M, Tsukita S. Claudin-11/OSP-based tight junctions of myelin sheaths in brain and Sertoli cells in testis. J Cell Biol. 1999;145(3):579-88.

Morita M, Saruta C, Kozuka N, Okubo Y, Itakura M, Takahashi M, Kudo Y. Dual regulation of astrocyte gap junction hemichannels by growth factors and a pro-inflammatory cytokine via the mitogen-activated protein kinase cascade. Glia. 2007;55(5):508-15.

Morita M, Shinbo S, Asahi A, Imanaka T. Very long chain fatty acid ß-oxidation in astrocytes: contribution of the ABCD1-dependent and -independent pathways. Biol Pharm Bull. 2012;35(11):1972-9.

Mothet JP, Parent AT, Wolosker H, Brady RO Jr, Linden DJ, Ferris CD, Rogawski MA, Snyder SH. D-serine is an endogenous ligand for the glycine site of the N-methyl-D-aspartate receptor. Proc Natl Acad Sci USA. 2000;97(9):4926-31.

Mucke L, Eddleston M. Astrocytes in infectious and immune-mediated diseases of the central nervous system. FASEB J. 1993;7(13):1226-32.

Mukherjee R, Jow L, Croston GE, Paterniti JR Jr. Identification, characterization, and tissue distribution of human peroxisome proliferator-activated receptor (PPAR) isoforms PPARgamma2 versus PPARgamma1 and activation with retinoid X receptor agonists and antagonists. J Biol Chem 1997;272:8071–76.

Müller A, Hauk TG, Fischer D. Astrocyte-derived CNTF switches mature RGCs to a regenerative state following inflammatory stimulation. Brain. 2007;130(Pt 12):3308-20.

Murai K, Qu Q, Sun G, Ye P, Li W, Asuelime G, Sun E, Tsai GE, Shi Y. Nuclear receptor TLX stimulates hippocampal neurogenesis and enhances learning and memory in a transgenic mouse model. Proc Natl Acad Sci USA. 2014;111(25):9115-20.

Myer DJ, Gurkoff GG, Lee SM, Hovda DA, Sofroniew MV. Essential protective roles of reactive astrocytes in traumatic brain injury. Brain. 2006;129(Pt 10):2761-72.

N Engl J Med, Vol. 346, No. 3 · January 17, 2002 Chang

Nagy JI, Li W, Hertzberg EL, Marotta CA. Elevated connexin43 immunoreactivity at sites of amyloid plaques in Alzheimer's disease. Brain Res. 1996;717(1-2):173-8.

Nait-oumesmar B, Picard-riera N, Kerninon C, Decker L, Seilhean D, Hoglinger GU. Activation of the subventricular zone in multiple sclerosis: evidence for early glial progenitors. Proc Natl Acad Sci USA. 2007;104(11):4694-9.

Nakajima K, Honda S, Tohyama Y, Imai Y, Kohsaka S, Kurihara T. Neurotrophin secretion from cultured microglia. J. Neurosci. Res. 2001;65:322–31.

Nakajima K, Tsuzaki N, Shimojo M, Hamanoue M, Kohsaka S. Microglia isolated from rat brain secrete a urokinase-type plasminogen activator. Brain Res. 1992;577(2):285-92.

Nakashima K, Wiese S, Yanagisawa M, Arakawa H, Kimura N, Hisatsune T, Yoshida K, Kishimoto T, Sendtner M, Taga T. Developmental requirement of gp130 signaling in neuronal survival and astrocyte differentiation. J Neurosci. 1999;19(13):5429-34.

Narita M, Bu G, Holtzman DM, Schwartz AL. The low-density lipoprotein receptor-related protein, a multifunctional apolipoprotein E receptor, modulates hippocampal neurite development. J Neurochem. 1997;68(2):587-95.

Nash B, Ioannidou K, Barnett SC. Astrocyte phenotypes and their relationship to myelination. J Anat. 2011a;219(1):44-52.

Nash B, Thomson CE, Linington C, Arthur, A.T., McClure, J.D., McBride, M.W., Barnett, S.C. Functional duality of astrocytes in myelination. J Neurosci. 2011b;31(37):13028-38.

Nash B. The dual role of astrocytes in myelination. PhD. Thesis. University of Glasgow:UK. 2010.

Naumann T, Schnell O, Zhi Q, Kirsch M, Schubert KO, Sendtner M, Hofmann HD. Endogenous ciliary neurotrophic factor protects GABAergic, but not cholinergic, septohippocampal neurons following fimbria-fornix transection. Brain Pathol. 2003;13(3):309-21.

Navarro A, Sánchez-pino MJ, Gómez C, Bández MJ, Cadenas E, Boveris A. Dietary thioproline decreases spontaneous food intake and increases survival and neurological function in mice. Antioxid Redox Signal. 2007;9(1):131-41.

Nayak D, Roth TL, Mcgavern DB. Microglia development and function. Annu Rev Immunol. 2014;32:367-402.

Nedergaard M. Direct signaling from astrocytes to neurons in cultures of mammalian brain cells. Science. 1994;263(5154):1768-71.

Niederreither K, Fraulob V, Garnier JM, Chambon P, Dollé P. Differential expression of retinoic acid-synthesizing (RALDH) enzymes during fetal development and organ differentiation in the mouse. Mech Dev. 2002;110(1-2):165-71.

Nielsen S, Nagelhus EA, Amiry-moghaddam M, Bourque C, Agre P, Ottersen OP. Specialized membrane domains for water transport in glial cells: high-resolution immunogold cytochemistry of aquaporin-4 in rat brain. J Neurosci. 1997;17(1):171-80.

Nieweg K, Schaller H, Pfrieger FW. Marked differences in cholesterol synthesis between neurons and glial cells from postnatal rats. J Neurochem. 2009;109(1):125-34.

Noble M, Murray K. Purified astrocytes promote the *in vitro* division of a bipotential glial progenitor cell. EMBO J. 1984;3(10):2243-7.

Noble M, Proschel C, Mayer-Proschel M. 2004. Getting a GRiP on oligo- dendrocyte development. Dev Biol 265:33–52.

Noctor SC, Flint AC, Weissman TA, Dammerman RS, Kriegstein AR. Neurons derived from radial glial cells establish radial units in neocortex. Nature. 2001;409(6821):714-20.

Nomoto S, Tatematsu Y, Takahashi T, Osada H. Cloning and characterization of the alternative promoter regions of the human LIMK2 gene responsible for alternative transcripts with tissue-specific expression. Gene. 1999;236(2):259-71.

Norenberg MD, Rama Rao KV, Jayakumar AR. Signaling factors in the mechanism of ammonia neurotoxicity. Metab Brain Dis. 2009;24(1):103-17.

Norenberg MD. Distribution of glutamine synthetase in the rat central nervous system. J Histochem Cytochem. 1979;27:756-62.

Nori S, Okada Y, Yasuda A, Tsuji O, Takahashi Y, Kobayashi Y, Fujiyoshi K, Koike M, Uchiyama Y, Ikeda E, Toyama Y, Yamanaka S, Nakamura M, Okano, H. Grafted human-induced pluripotent stem-cell-derived neurospheres promote motor functional recovery after spinal cord injury in mice. Proc Natl Acad Sci USA. 2011;108(40):16825-30.

Noseworthy J, Paty D, Wonnacott T, Feasby T, Ebers G. Multiple sclerosis after age 50. Neurology. 1983;33(12):1537-44.

O'brien JS. STABILITY OF THE MYELIN MEMBRANE. Science. 1965;147(3662):1099-107.

O'donnell SL, Frederick TJ, Krady JK, Vannucci SJ, Wood TL. IGF-I and microglia/macrophage proliferation in the ischemic mouse brain. Glia. 2002;39(1):85-97.

Obayashi S, Tabunoki H, Kim SU, Satoh J. Gene expression profiling of human neural progenitor cells following the serum-induced astrocyte differentiation. Cell Mol Neurobiol. 2009;29(3):423-38.

Ocrant I, Fay CT, Parmelee JT. Characterization of insulin-like growth factor binding proteins produced in the rat central nervous system. Endocrinology. 1990;127(3):1260-7.

Odermatt B, Wellershaus K, Wallraff A, Seifert G, Degen J, Euwens C, Fuss B, Büssow H, Schilling K, Steinhäuser C, Willecke K. Connexin 47 (Cx47)-deficient mice with enhanced green fluorescent protein reporter gene reveal predominant oligodendrocytic expression of Cx47 and display vacuolized myelin in the CNS. J Neurosci. 2003;23(11):4549-59.

Ogata K, Kosaka T. Structural and quantitative analysis of astrocytes in the mouse hippocampus. Neuroscience. 2002;113:221-33.

Okada M, Saio M, Kito Y, Ohe N, Yano H, Yoshimura S, Iwama T, Takami T. Tumor-associated macrophage/microglia infiltration in human gliomas is correlated with MCP-3, but not MCP-1. Int J Oncol. 2009;34(6):1621-7.

Okada S, Nakamura M, Katoh H, Miyao T, Shimazaki T, Ishii K, Yamane J, Yoshimura A, Iwamoto Y, Toyama Y, Okano H. Conditional ablation of Stat3 or Socs3 discloses a dual role for reactive astrocytes after spinal cord injury. Nat Med. 2006;12(7):829-34.

Olah M, Amor S, Brouwer N, Vinet J, Eggen B, Biber K, Boddeke HW. Identification of a microglia phenotype supportive of remyelination. Glia. 2012;60(2):306-21.

Oluich LJ, Stratton JA, Xing YL, Ng SW, Cate HS, Sah P, Windels F, Kilpatrick TJ, Merson TD. Targeted ablation of oligodendrocytes induces axonal pathology independent of overt demyelination. J Neurosci. 2012;32(24):8317-30.

Omari KM, John GR, Sealfon SC, Raine CS. CXC chemokine receptors on human oligodendrocytes: implications for multiple sclerosis. Brain. 2005;128(Pt 5):1003-15.

Omary MB, Ku NO, Toivola DM. Keratins: guardians of the liver. Hepatology. 2002;35(2):251-7.

Orellana JA, Díaz E, Schalper KA, Vargas AA, Bennett MV, Sáez JC. Cation permeation through connexin 43 hemichannels is cooperative, competitive and saturable with parameters depending on the permeant species. Biochem Biophys Res Commun. 2011a;409(4):603-9.

Orellana JA, Sáez PJ, Cortés-campos C, Elizondo RJ, Shoji KF, Contreras-Duarte S, Figueroa V, Velarde V, Jiang JX, Nualart F, Sáez JC, García MA. Glucose increases intracellular free Ca(2+) in tanycytes via ATP released through connexin 43 hemichannels. Glia. 2012;60(1):53-68.

Orellana JA, Sáez PJ, Shoji KF, Schalper KA, Palacios-Prado N, Velarde V, Giaume C, Bennett MV, Sáez JC. Modulation of brain hemichannels and gap junction channels by pro-inflammatory agents and their possible role in neurodegeneration. Antioxid Redox Signal. 2009;11(2):369-99.

Orellana JA, Shoji KF, Abudara V, Ezan P, Amigou E, Sáez PJ, Jiang JX, Naus CC, Sáez JC, Giaume C. Amyloid ß-induced death in neurons involves glial and neuronal hemichannels. J Neurosci. 2011b;31(13):4962-77.

Orellana JA, Stehberg J. Hemichannels: new roles in astroglial function. Front Physiol. 2014;5:193.

Ozawa K, Suchanek G, Breitschopf H, Brück W, Budka H, Jellinger K, Lassmann H. Patterns of oligodendroglia pathology in multiple sclerosis. Brain. 1994;117 (Pt 6):1311-22.

Paez PM, García CI, Pasquini JM. Expression of myelin basic protein in two oligodendroglial cell lines is modulated by apotransferrin through different transcription factors. J Neurosci Res. 2006;83(4):606-18.

Paez PM, Spreuer S, Handley V, Feng JM, Campagnoni C, Campagnoni AT. Increased expression of golli myelin basic proteins enhances calcium influx into oligodendroglial cells. J Neurosci. 2007;27:12690–9.

Paintlia MK, Paintlia AS, Singh AK, Singh I. S-nitrosoglutathione induces ciliary neurotrophic factor expression in astrocytes, which has implications to protect the central nervous system under pathological conditions. J Biol Chem. 2013;288(6):3831-43.

Pakhotin P, Verkhratsky A. Electrical synapses between Bergmann glial cells and Purkinje neurones in rat cerebellar slices. Mol Cell Neurosci. 2005;28(1):79-84.

Palazuelos J, Klingener M, Aguirre A. TGFβ signaling regulates the timing of CNS myelination by modulating oligodendrocyte progenitor cell cycle exit through SMAD3/4/FoxO1/Sp1. J Neurosci. 2014;34(23):7917-30.

Panchin Y, Kelmanson I, Matz M, Lukyanov K, Usman N, Lukyanov S. A ubiquitous family of putative gap junction molecules. Curr Biol. 2000;10(13):R473-4.

Pannasch U, Vargová L, Reingruber J, Ezan P, Holcman D, Giaume C, Syková E, Rouach N. Astroglial networks scale synaptic activity and plasticity. Proc Natl Acad Sci USA. 2011;108(20):8467-72.

Paolicelli RC, Bolasco G, Pagani F, Maggi L, Scianni M, Panzanelli P, Giustetto M, Ferreira TA, Guiducci E, Dumas L, Ragozzino D, Gross CT. Synaptic pruning by microglia is necessary for normal brain development. Science. 2011;333:1456-8.

Pardo B, Rodrigues TB, Contreras L, Garzón M, Llorente-Folch I, Kobayashi K, Saheki T, Cerdan S, Satrústegui J. Brain glutamine synthesis requires neuronal-born aspartate as amino donor for glial glutamate formation. J Cereb Blood Flow Metab. 2011;31(1):90-101.

Park J, Park HH, Choi H, Kim YS, Yu HJ, Lee KY, Lee YJ, Kim SH, Koh SH. Coenzyme Q10 protects neural stem cells against hypoxia by enhancing survival signals. Brain Res. 2012;1478:64-73.

Park JH, Riew TR, Shin YJ, Park JM, Cho JM, Lee MY. Induction of Krüppel-like factor 4 expression in reactive astrocytes following ischemic injury *in vitro* and *in vivo*. Histochem Cell Biol. 2014;141(1):33-42.

Parpura V, Basarsky TA, Liu F, Jeftinija K, Jeftinija S, Haydon PG. Glutamate-mediated astrocyte-neuron signalling. Nature. 1994;369(6483):744-7.

Pasquali L, Lucchesi C, Pecori C, Metelli MR, Pellegrini S, Iudice A, Bonuccelli U. A clinical and laboratory study evaluating the profile of cytokine levels in relapsing remitting and secondary progressive multiple sclerosis. J Neuroimmunol. 2015;278:53-9.

Paterson EK, Ho H, Kapadia R, Ganesan AK. 9-cis retinoic acid is the ALDH1A1 product that stimulates melanogenesis. Exp Dermatol. 2013;22(3):202-9.

Paul D, Ge S, Lemire Y, Jellison ER, Serwanski DR, Ruddle NH, Pachter JS. Cell-selective knockout and 3D confocal image analysis reveals separate roles for astrocyte-and endothelial-derived CCL2 in neuroinflammation. J Neuroinflammation. 2014;11:10.

Pekny M, Pekna M. Astrocyte intermediate filaments in CNS pathologies and regeneration. J Pathol. 2004;204(4):428-37.

Pellegri G, Rossier C, Magistretti PJ, Martin JL. Cloning, localization and induction of mouse brain glycogen synthase. Brain Res Mol Brain Res. 1996;38(2):191-9.

Pellerin L, Bouzier-sore AK, Aubert A, Serres S, Merle M, Costalat R, Magistretti PJ. Activity-dependent regulation of energy metabolism by astrocytes: an update. Glia. 2007;55(12):1251-62.

Pelton TA, Sharma S, Schulz TC, Rathjen J, Rathjen PD. Transient pluripotent cell populations during primitive ectoderm formation: correlation of *in vivo* and *in vitro* pluripotent cell development. J Cell Sci. 2002;115(Pt 2):329-39.

Pereira MP, Hurtado O, Cárdenas A, Alonso-Escolano D, Boscá L, Vivancos J, Nombela F, Leza JC, Lorenzo P, Lizasoain I, Moro MA. The nonthiazolidinedione PPARgamma agonist L-796,449 is neuroprotective in experimental stroke. J Neuropathol Exp Neurol. 2005;64(9):797-805.

Perry VH, Teeling J. Microglia and macrophages of the central nervous system: the contribution of microglia priming and systemic inflammation to chronic neurodegeneration. Semin Immunopathol. 2013;35(5):601-12.

Peters A, Palay SL, Webster HD. The fine structure of the nervous system, Third ed., Oxford University Press, New York, 1991.

Peters O, Schipke CG, Philipps A, Haas B, Pannasch U, Wang LP, Benedetti B, Kingston AE, Kettenmann H. Astrocyte function is modified by Alzheimer's disease-like pathology in aged mice. J Alzheimers Dis. 2009;18(1):177-89.

Peterson JW, Bö L, Mörk S, Chang A, Trapp BD. Transected neurites, apoptotic neurons, and reduced inflammation in cortical multiple sclerosis lesions. Ann Neurol. 2001;50(3):389-400.

Pfeffer M, Maronde E, Molina CA, Korf HW, Stehle JH. Inducible cyclic AMP early repressor protein in rat pinealocytes: a highly sensitive natural reporter for regulated gene transcription. Mol Pharmacol. 1999;56(2):279-89.

Pfeiffer-Guglielmi B, Fleckenstein B, Jung G, Hamprecht B. Immunocytochemical localization of glycogen phosphorylase isozymes in rat nervous tissues by using isozyme-specific antibodies. J Neurochem. 2003;85(1):73-81.

Pfrieger FW, Ungerer N. Cholesterol metabolism in neurons and astrocytes. Prog Lipid Res. 2011;50(4):357-71.

Phelps CH. Barbiturate-induced glycogen accumulation in brain. An electron microscopic study. Brain Res. 1972;39(1):225-34.

Piccio L, Naismith RT, Trinkaus K, Klein RS, Parks BJ, Lyons JA, Cross AH. Changes in B- and T-lymphocyte and chemokine levels with rituximab treatment in multiple sclerosis. Arch Neurol. 2010;67(6):707-14.

Pichel JG, Lakso M, Westphal H. Timing of SV40 oncogene activation by site-specific recombination determines subsequent tumor progression during murine lens development. Oncogene. 1993;8(12):3333-42.

Pohl HB, Porcheri C, Mueggler T, Bachmann LC, Martino G, Riethmacher D, Franklin RJ, Rudin M, Suter U. Genetically induced adult oligodendrocyte cell death is associated with poor myelin clearance, reduced remyelination, and axonal damage. J Neurosci. 2011;31(3):1069-80.

Poliak S, Peles E. The local differentiation of myelinated axons at nodes of Ranvier. Nat Rev Neurosci. 2003;4(12):968-80.

Portales-casamar E, Thongjuea S, Kwon AT, Arenillas D, Zhao X, Valen E, Yusuf D, Lenhard B, Wasserman WW, Sandelin A. JASPAR 2010: the greatly expanded open-access database of transcription factor binding profiles. Nucleic Acids Res. 2010;38(Database issue):D105-10.

Prasad SS, Russell M, Nowakowska M, Williams A, Yauk C. Gene expression analysis to identify molecular correlates of pre- and post-conditioning derived neuroprotection. J Mol Neurosci. 2012;47(2):322-39.

Prineas JW, Barnard RO, Kwon EE, Sharer LR, Cho ES. Multiple sclerosis: remyelination of nascent lesions. Ann Neurol. 1993;33(2):137-51.

Proost P, Van damme J, Opdenakker G. Leukocyte gelatinase B cleavage releases encephalitogens from human myelin basic protein. Biochem Biophys Res Commun. 1993;192(3):1175-81.

Pugliatti M, Sotgiu S, Solinas G, Castiglia P, Rosati G. Multiple sclerosis prevalence among Sardinians: further evidence against the latitude gradient theory. Neurol Sci. 2001;22(2):163-5.

Qin S, Zhang CL. Role of Kruppel-like factor 4 in neurogenesis and radial neuronal migration in the developing cerebral cortex. Mol Cell Biol. 2012;32(21):4297-305.

Qu Q, Sun G, Li W, Yang S, Ye P, Zhao C, Yu RT, Gage FH, Evans RM, Shi Y. Orphan nuclear receptor TLX activates Wnt/beta-catenin signalling to stimulate neural stem cell proliferation and self-renewal. Nat Cell Biol. 2010;12(1):31-40.

Raff MC, Abney ER, Cohen J, Lindsay R, Noble M. Two types of astrocytes in cultures of developing rat white matter: differences in morphology, surface gangliosides, and growth characteristics. J Neurosci. 1983;3(6):1289-1300.

Raine CS, Wu E. Multiple sclerosis: remyelination in acute lesions. J Neuropathol Exp Neurol. 1993;52(3):199-204.

Rainey-barger EK, Rumble JM, Lalor SJ, Esen N, Segal BM, Irani DN. The lymphoid chemokine, CXCL13, is dispensable for the initial recruitment of B cells to the acutely inflamed central nervous system. Brain Behav Immun. 2011;25(5):922-31.

Rajan P, Mckay RD. Multiple routes to astrocytic differentiation in the CNS. J Neurosci. 1998;18(10):3620-9.

Ramos C, Martinez A, Robert B, Soriano E. Msx1 expression in the adult mouse brain: characterization of populations of beta-galactosidase-positive cells in the hippocampus and fimbria. Neuroscience. 2004;127(4):893-900.

Rankin LL, Chvapil M, Misiorowski R, Johnson P, Weinstein PR. Diffusion characteristics of beta-aminopropionitrile in peripheral nerve. Exp Neurol. 1983;79(1):97-105.

Ransohoff RM, Brown MA. Innate immunity in the central nervous system. J Clin Invest. 2012;122(4):1164-71.

Ransohoff RM, Hamilton TA, Tani M, et al. Astrocyte expression of mRNA encoding cytokines IP-10 and JE/MCP-1 in experimental autoimmune encephalomyelitis. FASEB J. 1993;7(6):592-600.

Ransohoff RM, Perry VH. Microglial physiology: unique stimuli, specialized responses. Annu Rev Immunol. 2009;27:119-45.

Ransom BR, Kettenmann H. Electrical coupling, without dye coupling, between mammalian astrocytes and oligodendrocytes in cell culture. Glia. 1990;3(4):258-66.

Rao KV, Panickar KS, Jayakumar AR, Norenberg MD. Astrocytes protect neurons from ammonia toxicity. Neurochem Res. 2005;30(10):1311-8.

Rash JE, Yasumura T, Hudson CS, Agre P, Nielsen S. Direct immunogold labeling of aquaporin-4 in square arrays of astrocyte and ependymocyte plasma membranes in rat brain and spinal cord. Proc Natl Acad Sci USA. 1998;95(20):11981-6.

Rathore KI, Berard JL, Redensek A, Chierzi S, Lopez-Vales R, Santos M, Akira S, David S. Lipocalin 2 plays an immunomodulatory role and has detrimental effects after spinal cord injury. J Neurosci. 2011;31(38):13412-9.

Ravera S, Bartolucci M, Calzia D, Aluigi MG, Ramoino P, Morelli A, Panfoli I. Tricarboxylic acid cycle-sustained oxidative phosphorylation in isolated myelin vesicles. Biochimie. 2013;95(11):1991-8.

Redwine JM, Blinder KL, Armstrong RC. In situ expression of fibroblast growth factor receptors by oligodendrocyte progenitors and oligodendrocytes in adult mouse central nervous system. J Neurosci Res. 1997;50(2):229-37.

Reichardt P, Gunzer M. The biophysics of T lymphocyte activation *in vitro* and *in vivo*. Results Probl Cell Differ. 2006;43:199-218.

Renner NA, Ivey NS, Redmann RK, Lackner AA, Maclean AG. MCP-3/CCL7 production by astrocytes: implications for SIV neuroinvasion and AIDS encephalitis. J Neurovirol. 2011;17(2):146-52.

Retamal MA, Schalper KA, Shoji KF, Bennett MV, Sáez JC. Opening of connexin 43 hemichannels is increased by lowering intracellular redox potential. Proc Natl Acad Sci USA. 2007;104(20):8322-7.

Rieder CR, Ramsden DB, Williams AC. Cytochrome P450 1B1 mRNA in the human central nervous system. MP, Mol Pathol. 1998;51(3):138-42.

Robinson SR, Hampson EC, Munro MN, Vaney DI. Unidirectional coupling of gap junctions between neuroglia. Science. 1993;262(5136):1072-4.

Rodgers JM, Robinson AP, Miller SD. Strategies for protecting oligodendrocytes and enhancing remyelination in multiple sclerosis. Discov Med. 2013;16(86):53-63.

Roghani M, Lassarre C, Zapf J, Povoa G, Binoux M. Two insulin-like growth factor (IGF)-binding proteins are responsible for the selective affinity for IGF-II of cerebrospinal fluid binding proteins. J Clin Endocrinol Metab. 1991;73(3):658-66.

Roques BP. Novel approaches to targeting neuropeptide systems. Trends Pharmacol Sci. 2000;21(12):475-83.

Rosenbaum JN, Duggan A, García-añoveros J. Insm1 promotes the transition of olfactory progenitors from apical and proliferative to basal, terminally dividing and neuronogenic. Neural Dev. 2011;6(1):6.

Rothe T, Müller HW. Uptake of endoneurial lipoprotein into Schwann cells and sensory neurons is mediated by low density lipoprotein receptors and stimulated after axonal injury. J Neurochem. 1991;57(6):2016-25.

Rothstein JD, Dykes-hoberg M, Pardo CA, Bristol LA, Jin L, Kuncl RW, Kanai Y, Hediger MA, Wang Y, Schielke JP, Welty DF. Knockout of glutamate transporters reveals a major role for astroglial transport in excitotoxicity and clearance of glutamate. Neuron. 1996;16(3):675-86.

Rothstein JD, Patel S, Regan MR, Haenggeli C, Huang YH, Bergles DE, Jin L, Dykes Hoberg M, Vidensky S, Chung DS, Toan SV, Bruijn LI, Su ZZ, Gupta P, Fisher PB. Beta-lactam antibiotics offer neuroprotection by increasing glutamate transporter expression. Nature. 2005;433(7021):73-7.

Rouach N, Koulakoff A, Abudara V, Willecke K, Giaume C. Astroglial metabolic networks sustain hippocampal synaptic transmission. Science. 2008;322(5907):1551-5.

Roumier A, Bechade C, Poncer JC, Smalla KH, Tomasello E, Vivier E, Gundelfinger ED, Triller A, Bessis A. Impaired synaptic function in the microglial KARAP/DAP12-deficient mouse. J. Neurosci. 2004;24:11421-8.

Roy K, Kuznicki K, Wu Q, Sun Z, Bock D, Schutz G, Vranich N, Monaghan AP. The Tlx gene regulates the timing of neurogenesis in the cortex. J Neurosci. 2004;24(38):8333-45.

Roy K, Thiels E, Monaghan AP. Loss of the tailless gene affects forebrain development and emotional behavior. Physiol Behav. 2002;77(4-5):595-600.

Roybon L, Hjalt T, Christophersen NS, Li JY, Brundin P. Effects on differentiation of embryonic ventral midbrain progenitors by Lmx1a, Msx1, Ngn2, and Pitx3. J Neurosci. 2008;28(14):3644-56.

Rudge JS, Pasnikowski EM, Holst P, Lindsay RM. Changes in neurotrophic factor expression and receptor activation following exposure of hippocampal neuron/astrocyte cocultures to kainic acid. J Neurosci. 1995;15(10):6856-67.

Ruminot I, Gutiérrez R, Peña-Münzenmayer G, Añazco C, Sotelo-Hitschfeld T, Lerchundi R, Niemeyer MI, Shull GE, Barros LF. NBCe1 mediates the acute stimulation of astrocytic glycolysis by extracellular K+. J Neurosci. 2011;31(40):14264-71.

Ryan SM, O'keeffe GW, O'connor C, Keeshan K, Nolan YM. Negative regulation of TLX by IL-1β correlates with an inhibition of adult hippocampal neural precursor cell proliferation. Brain Behav Immun. 2013;33:7-13.

Sáez JC, Schalper KA, Retamal MA, Orellana JA, Shoji KF, Bennett MV. Cell membrane permeabilization via connexin hemichannels in living and dying cells. Exp Cell Res. 2010;316(15):2377-89.

Saffer JD, Jackson SP, Annarella MB. Developmental expression of Sp1 in the mouse. Mol Cell Biol. 1991;11(4):2189-99.

Sage EH, Bornstein P. Extracellular proteins that modulate cell-matrix interactions. SPARC, tenascin, and thrombospondin. J Biol Chem. 1991;266(23):14831-4.

Salehi Z, Hadiyan SP, Navidi R. Ciliary neurotrophic factor role in myelin oligodendrocyte glycoprotein expression in Cuprizone-induced multiple sclerosis mice. Cell Mol Neurobiol. 2013;33(4):531-5.

Salem M, Mony JT, Løbner M, Khorooshi R, Owens T. Interferon regulatory factor-7 modulates experimental autoimmune encephalomyelitis in mice. J Neuroinflammation. 2011;8:181.

Salinas PC, Zou Y. Wnt signaling in neural circuit assembly. Annu Rev Neurosci. 2008;31:339-58.

Sanoobar M, Eghtesadi S, Azimi A, Khalili M, Khodadadi B, Jazayeri S, Gohari MR, Aryaeian N. Coenzyme Q10 supplementation ameliorates inflammatory markers in patients with multiple sclerosis: a double blind, placebo, controlled randomized clinical trial. Nutr Neurosci. 2014.

Sato-bigbee C, Devries GH. Treatment of oligodendrocytes with antisense deoxyoligonucleotide directed against CREB mRNA: effect on the cyclic AMP-dependent induction of myelin basic protein expression. J Neurosci Res. 1996;46(1):98-107.

Sattler R, Rothstein JD. Regulation and dysregulation of glutamate transporters. Handb Exp Pharmacol. 2006;(175):277-303.

Schintu N, Frau L, Ibba M, Caboni P, Garau A, Carboni E, Carta AR. PPAR-gamma-mediated neuroprotection in a chronic mouse model of Parkinson's disease. Eur J Neurosci 2009;29(5):954-63.

Schmidt H, Raasch J, Merkler D, Klinker F, Krauss S, Brück W, Prinz M. Type I interferon receptor signalling is induced during demyelination while its function for myelin damage and repair is redundant. Exp Neurol. 2009;216(2):306-11.

Schmitz T, Chew LJ. Cytokines and myelination in the central nervous system. ScientificWorldJournal. 2008;8:1119-47.

Schulz C, Gomez Perdiguero E, Chorro L, Szabo-Rogers H, Cagnard N, Kierdorf K, Prinz M, Wu B, Jacobsen SE, Pollard JW, Frampton J, Liu KJ, Geissmann F. A lineage of myeloid cells independent of Myb and hematopoietic stem cells. Science. 2012;336:86–90.

Schwab JM, Beschorner R, Nguyen TD, Meyermann R, Schluesener HJ. Differential cellular accumulation of connective tissue growth factor defines a subset of reactive astrocytes, invading fibroblasts, and endothelial cells following central nervous system injury in rats and humans. J Neurotrauma. 2001;18(4):377-88.

Schwartz JP, Nishiyama N. Neurotrophic factor gene expression in astrocytes during development and following injury. Brain Res Bull. 1994;35(5-6):403-7.

Seifert G, Schilling K, Steinhäuser C. Astrocyte dysfunction in neurological disorders: a molecular perspective. Nat Rev Neurosci. 2006;7(3):194-206.

Seil FJ, Herndon RM. Myelination and glial ensheathment of Purkinje cells in cerebellar cultures are not inhibited by antibodies to the neural cell adhesion molecule, N-CAM. Int J Dev Neurosci. 1991;9(6):587-96.

Seiler N, Sarhan S. Synergistic anticonvulsant effects of GABA-T inhibitors and glycine. Naunyn Schmiedebergs Arch Pharmacol. 1984;326(1):49-57.

Selmaj K, Raine CS. Tumor necrosis factor mediates myelin damage in organotypic cultures of nervous tissue. Ann N Y Acad Sci. 1988;540:568-70.

Shah BH, Farshori MP, Catt KJ. Neuropeptide-induced transactivation of a neuronal epidermal growth factor receptor is mediated by metalloprotease-dependent formation of heparin-binding epidermal growth factor. J Biol Chem. 2004;279(1):414-20.

Shannon C, Salter M, Fern R. GFP imaging of live astrocytes: regional differences in the effects of ischaemia upon astrocytes. J Anat. 2007;210(6):684-92.

Sharon R, Abramovitz R, Miskin R. Plasminogen mRNA induction in the mouse brain after kainate excitation: codistribution with plasminogen activator inhibitor-2 (PAI-2) mRNA. Brain Res Mol Brain Res. 2002;104(2):170-5.

Sherman DL, Brophy PJ. Mechanisms of axon ensheathment and myelin growth. Nat Rev Neurosci. 2005;6(9):683-90.

Shi X, Habecker BA. Gp130 cytokines stimulate proteasomal degradation of tyrosine hydroxylase via extracellular signal regulated kinases 1 and 2. J Neurochem. 2012;120(2):239-47.

Shi X, Woodward WR, Habecker BA. Ciliary neurotrophic factor stimulates tyrosine hydroxylase activity. J Neurochem. 2012;121(5):700-4.

Shi Y, Chichung lie D, Taupin P, Nakashima K, Ray J, Yu RT, Gage FH, Evans RM. Expression and function of orphan nuclear receptor TLX in adult neural stem cells. Nature. 2004;427(6969):78-83.

Shih AY, Johnson DA, Wong G, Kraft AD, Jiang L, Erb H, Johnson JA, Murphy TH. Coordinate regulation of glutathione biosynthesis and release by Nrf2-expressing glia potently protects neurons from oxidative stress. J Neurosci. 2003;23(8):3394-406.

Shimazu T, Inoue I, Araki N, Asano Y, Sawada M, Furuya D, Nagoya H, Greenberg JH. A peroxisome proliferator-activated receptor-gamma agonist reduces infarct size in transient but not in permanent ischemia. Stroke. 2005;36(2):353-9.

Shimizu T, Kagawa T, Wada T, Muroyama Y, Takada S, Ikenaka K. Wnt signaling controls the timing of oligodendrocyte development in the spinal cord. Dev Biol. 2005;282(2):397-410.

Shimojima K, Inoue T, Imai Y, Arai Y, Komoike Y, Sugawara M, Fujita T, Ideguchi H, Yasumoto S, Kanno H, Hirose S, Yamamoto T. Reduced PLP1 expression in induced pluripotent stem cells derived from a Pelizaeus-Merzbacher disease patient with a partial PLP1 duplication. J Hum Genet. 2012;57(9):580-6.

Shimojo H, Ohtsuka T, Kageyama R. Dynamic expression of notch signaling genes in neural stem/progenitor cells. Front Neurosci. 2011;5:78.

Shiryaev SA, Savinov AY, Cieplak P, Ratnikov BI, Motamedchaboki K, Smith JW, Strongin AY. Matrix metalloproteinase proteolysis of the myelin basic protein isoforms is a source of immunogenic peptides in autoimmune multiple sclerosis. PLoS ONE. 2009;4(3):e4952.

Shrager P, Novakovic SD. Control of myelination, axonal growth, and synapse formation in spinal cord explants by ion channels and electrical activity. Brain Res Dev Brain Res. 1995;88(1):68-78.

Shu T, Butz KG, Plachez C, Gronostajski RM, Richards LJ. Abnormal development of forebrain midline glia and commissural projections in Nfia knock-out mice. J Neurosci. 2003;23(1):203-12.

Silver J, Miller JH. Regeneration beyond the glial scar. Nat Rev Neurosci. 2004;5(2):146-56.

Sim SE, Chung YH, Jeong JH, Yun SW, Lim HS, Kim D, Kim SS, Lee WB, Cha CI. Immunohistochemical localization of insulin-like growth factor binding protein 2 in the central nervous system of SOD1(G93A) transgenic mice. J Mol Histol. 2009;40(2):157-63.

Simard AR, Rivest S. Bone marrow stem cells have the ability to populate the entire central nervous system into fully differentiated parenchymal microglia. FASEB J. 2004;18:998–1000.

Simpson JE, Ince PG, Lace G, et al. Astrocyte phenotype in relation to Alzheimer-type pathology in the ageing brain. Neurobiol Aging. 2010;31(4):578-90.

Sin WC, Bechberger JF, Rushlow WJ, Naus CC. Dose-dependent differential upregulation of CCN1/Cyr61 and CCN3/NOV by the gap junction protein Connexin43 in glioma cells. J Cell Biochem. 2008;103(6):1772-82.

Sindern E, Haas J, Stark E, Wurster U. Early onset MS under the age of 16: clinical and paraclinical features. Acta Neurol Scand. 1992;86(3):280-4.

Skinner RA, Gibson RM, Rothwell NJ, Pinteaux E, Penny JI. Transport of interleukin-1 across cerebromicrovascular endothelial cells. Br J Pharmacol. 2009;156(7):1115-23.

Skoff RP. Gliogenesis in rat optic nerve: astrocytes are generated in a single wave before oligodendrocytes. Dev Biol. 1990;139(1):149-68.

Skripuletz T, Hackstette D, Bauer K, Gudi V, Pul R, Voss E, Berger K, Kipp M, Baumgärtner W, Stangel M. Astrocytes regulate myelin clearance through recruitment of microglia during cuprizone-induced demyelination. Brain. 2013;136(Pt 1):147-67.

Skuljec J, Gudi V, Ulrich R, Frichert K, Yildiz O, Pul R, Voss EV, Wissel K, Baumgärtner W, Stangel M. Matrix metalloproteinases and their tissue inhibitors in cuprizone-induced demyelination and remyelination of brain white and gray matter. J Neuropathol Exp Neurol. 2011;70(9):758-69.

Sleeman MW, Anderson KD, Lambert PD, Yancopoulos GD, Wiegand SJ. The ciliary neurotrophic factor and its receptor, CNTFR alpha. Pharm Acta Helv. 2000;74(2-3):265-72.

Sofroniew MV, Vinters HV. Astrocytes: biology and pathology. Acta Neuropathol. 2010;119(1):7-35.

Sofroniew MV. Molecular dissection of reactive astrogliosis and glial scar formation. Trends Neurosci. 2009;32(12):638-47.

Sofroniew MV. Reactive astrocytes in neural repair and protection. Neuroscientist. 2005;11(5):400-7.

Solenov E, Watanabe H, Manley GT, Verkman AS. Sevenfold-reduced osmotic water permeability in primary astrocyte cultures from AQP-4-deficient mice, measured by a fluorescence quenching method. Am J Physiol, Cell Physiol. 2004;286(2):C426-32.

Somjen GG. Nervenkitt: notes on the history of the concept of neuroglia. Glia. 1988;1(1):2-9.

Sommer I, Schachner M. Monoclonal antibodies (O1 to O4) to oligodendrocyte cell surfaces: an immunocytological study in the central nervous system. Dev Biol. 1981;83(2):311-27.

Song F, Bandara M, Deol H, Loeb JA, Benjamins J, Lisak RP. Complexity of trophic factor signaling in experimental autoimmune encephalomyelitis: differential expression of neurotrophic and gliotrophic factors. J Neuroimmunol. 2013;262(1-2):11-8.

Song H, Stevens CF, Gage FH. Astroglia induce neurogenesis from adult neural stem cells. Nature. 2002;417(6884):39-44.

Sorensen A, Moffat K, Thomson C, Barnett SC. Astrocytes, but not olfactory ensheathing cells or Schwann cells, promote myelination of CNS axons *in vitro*. Glia. 2008;56(7):750-63.

Spliet WG, Aronica E, Ramkema M, Aten J, Troost D. Increased expression of connective tissue growth factor in amyotrophic lateral sclerosis human spinal cord. Acta Neuropathol. 2003;106(5):449-57.

Spranger M, Lindholm D, Bandtlow C, Heumann R, Gnahn H, Näher-Noé M, Thoenen H. Regulation of Nerve Growth Factor (NGF) Synthesis in the Rat Central Nervous System: Comparison between the Effects of Interleukin-1 and Various Growth Factors in Astrocyte Cultures and *in vivo*. Eur J Neurosci. 1990;2(1):69-76.

Stanhope GB, Wolf MK, Billings-gagliardi S. Genotype-specific myelin formation around normal axons in cytosine arabinoside-treated organotypic cultures injected with normal or shiverer optic nerve. Brain Res. 1986;389(1-2):109-16.

Stankoff B, Aigrot MS, Noël F, Wattilliaux A, Zalc B, Lubetzki C. Ciliary neurotrophic factor (CNTF) enhances myelin formation: a novel role for CNTF and CNTF-related molecules. J Neurosci. 2002;22(21):9221-7.

Steele-Perkins G, Butz KG, Lyons GE, Zeichner-David M, Kim HJ, Cho MI, Gronostajski RM. Essential role for NFI-C/CTF transcription-replication factor in tooth root development. Mol Cell Biol. 2003;23(3):1075-84.

Steele-Perkins G, Plachez C, Butz KG, Yang G, Bachurski CJ, Kinsman SL, Litwack ED, Richards LJ, Gronostajski RM. The transcription factor gene Nfib is essential for both lung maturation and brain development. Mol Cell Biol. 2005;25(2):685-98.

Stefanova N, Fellner L, Reindl M, Masliah E, Poewe W, Wenning GK. Toll-like receptor 4 promotes α-synuclein clearance and survival of nigral dopaminergic neurons. Am. J. Pathol. 2011;179:954–63.

Steinhäuser C, Jabs R, Kettenmann H. Properties of GABA and glutamate responses in identified glial cells of the mouse hippocampal slice. Hippocampus. 1994;4(1):19-35.

Stenman JM, Wang B, Campbell K. Tlx controls proliferation and patterning of lateral telencephalic progenitor domains. J Neurosci. 2003;23(33):10568-76.

Stenzel D, Lundkvist A, Sauvaget D, Busse M, Graupera M, van der Flier A, Wijelath ES, Murray J, Sobel M, Costell M, Takahashi S, Fässler R, Yamaguchi Y, Gutmann DH, Hynes RO, Gerhardt H. Integrin-dependent and -independent functions of astrocytic fibronectin in retinal angiogenesis. Development. 2011;138(20):4451-63.

Stern S, Knöll B. CNS axon regeneration inhibitors stimulate an immediate early gene response via MAP kinase-SRF signaling. Mol Brain. 2014;7(1):86.

Stevens B, Porta S, Haak LL, Gallo V, Fields RD. Adenosine: a neuron-glial transmitter promoting myelination in the CNS in response to action potentials. Neuron. 2002;36(5):855-68.

Stichel CC, Müller HW. The CNS lesion scar: new vistas on an old regeneration barrier. Cell Tissue Res. 1998;294(1):1-9.

Stöckli KA, Lillien LE, Näher-noé M, Breitfeld G, Hughes RA, Raff MC, Thoenen H, Sendtner M. Regional distribution, developmental changes, and cellular localization of CNTF-mRNA and protein in the rat brain. J Cell Biol. 1991;115(2):447-59.

Stoffels JM, De jonge JC, Stancic M, Nomden A, van Strien ME, Ma D, Sisková Z, Maier O, Ffrench-Constant C, Franklin RJ, Hoekstra D, Zhao C, Baron W. Fibronectin aggregation in multiple sclerosis lesions impairs remyelination. Brain. 2013;136(Pt 1):116-31.

Storvik M, Lindén AM, Kontkanen O, Lakso M, Castrén E, Wong G. Induction of cAMP response element modulator (CREM) and inducible cAMP early repressor (ICER) expression in rat brain by uncompetitive N-methyl-D-aspartate receptor antagonists. J Pharmacol Exp Ther. 2000;294(1):52-60.

Stringer B, Udofa EA, Antalis TM. Regulation of the human plasminogen activator inhibitor type 2 gene: cooperation of an upstream silencer and transactivator. J Biol Chem. 2012;287(13):10579-89.

Stringer JL, Belaguli NS, Iyer D, Schwartz RJ, Balasubramanyam A. Developmental expression of serum response factor in the rat central nervous system. Brain Res Dev Brain Res. 2002;138(1):81-6.

Stritt C, Stern S, Harting K, Manke T, Sinske D, Schwarz H, Vingron M, Nordheim A, Knöll B. Paracrine control of oligodendrocyte differentiation by SRF-directed neuronal gene expression. Nat Neurosci. 2009;12(4):418-27.

Suh SW, Bergher JP, Anderson CM, Treadway JL, Fosgerau K, Swanson RA. Astrocyte glycogen sustains neuronal activity during hypoglycemia: studies with the glycogen phosphorylase inhibitor CP-316,819 ([R-R*,S*]-5-chloro-N-[2-hydroxy-3-(methoxymethylamino)-3-oxo-1-(phenylmethyl)propyl]-1H-indole-2-carboxamide). J Pharmacol Exp Ther. 2007;321(1):45-50.

Sun T, Pringle NP, Hardy AP, Richardson WD, Smith HK. Pax6 influences the time and site of origin of glial precursors in the ventral neural tube. Mol Cell Neurosci. 1998;12(4-5):228-39.

Sun Y, Wu S, Bu G, Onifade MK, Patel SN, LaDu MJ, Fagan AM, Holtzman DM. Glial fibrillary acidic protein-apolipoprotein E (apoE) transgenic mice: astrocyte-specific expression and differing biological effects of astrocyte-secreted apoE3 and apoE4 lipoproteins. J Neurosci. 1998;18(9):3261-72.

Sundararajan S, Gamboa JL, Victor NA, Wanderi EW, Lust WD, Landreth GE. Peroxisome proliferator-activated receptor-gamma ligands reduce inflammation and infarction size in transient focal ischemia. Neuroscience. 2005;130(3):685-96.

Sunnemark D, Eltayeb S, Wallström E, Appelsved L, Malmberg A, Lassmann H, Ericsson-Dahlstrand A, Piehl F, Olsson T. Differential expression of the chemokine receptors CX3CR1 and CCR1 by microglia and macrophages in myelin-oligodendrocyte-glycoprotein-induced experimental autoimmune encephalomyelitis. Brain Pathol. 2003;13(4):617-29.

Suzuki DE, Ariza CB, Porcionatto MA, Okamoto OK. Upregulation of E2F1 in cerebellar neuroprogenitor cells and cell cycle arrest during postnatal brain development. *In vitro* Cell Dev Biol Anim. 2011;47(7):492-9.

Suzuki K, Ikegaya Y, Matsuura S, Kanai Y, Endou H, Matsuki N. Transient upregulation of the glial glutamate transporter GLAST in response to fibroblast growth factor, insulin-like growth factor and epidermal growth factor in cultured astrocytes. J Cell Sci. 2001;114(Pt 20):3717-25.

Suzuki R, Watanabe J, Arata S, Funahashi H, Kikuyama S, Shioda S. A transgenic mouse model for the detailed morphological study of astrocytes. Neurosci Res. 2003;47(4):451-4.

Svenningsen AF, Shan WS, Colman DR, Pedraza L. Rapid method for culturing embryonic neuron-glial cell cocultures. J Neurosci Res. 2003;72(5):565-73.

Svensson L, Närlid I, Oldberg A. Fibromodulin and lumican bind to the same region on collagen type I fibrils. FEBS Lett. 2000;470(2):178-82.

Swanson RA, Ying W, Kauppinen TM. Astrocyte influences on ischemic neuronal death. Curr Mol Med. 2004;4(2):193-205.

Szczuciński A, Kalinowska A, Losy J. CXCL11 (Interferon-inducible T-cell alpha chemoattractant) and interleukin-18 in relapsing-remitting multiple sclerosis patients treated with methylprednisolone. Eur Neurol. 2007;58(4):228-32.

Tabira T, Chui DH, Fan JP, Shirabe T, Konishi Y. Interleukin-3 and interleukin-3 receptors in the brain. Ann N Y Acad Sci. 1998;840:107-16.

Takahashi K, Rochford CD, Neumann H. Clearance of apoptotic neurons without inflammation by microglial triggering receptor expressed on myeloid cells-2. J. Exp. Med. 2005;201:647–57.

Takano T, Kang J, Jaiswal JK, Simon SM, Lin JH, Yu Y, Li Y, Yang J, Dienel G, Zielke HR, Nedergaard M. Receptor-mediated glutamate release from volume sensitive channels in astrocytes. Proc Natl Acad Sci USA. 2005;102(45):16466-71.

Takebayashi H, Nabeshima Y, Yoshida S, Chisaka O, Ikenaka K, Nabeshima Y. The basic helix-loop-helix factor olig2 is essential for the development of motoneuron and oligodendrocyte lineages. Curr Biol. 2002;12(13):1157-63.

Tamura T, Miura M, Ikenaka K, Mikoshiba K. Analysis of transcription control elements of the mouse myelin basic protein gene in HeLa cell extracts: demonstration of a strong NFI-binding motif in the upstream region. Nucleic Acids Res. 1988;16(24):11441-59.

Tanaka T, Murakami K, Bando Y, Yoshida S. Minocycline reduces remyelination by suppressing ciliary neurotrophic factor expression after cuprizone-induced demyelination. J Neurochem. 2013;127(2):259-70.

Tanner DC, Cherry JD, Mayer-pröschel M. Oligodendrocyte progenitors reversibly exit the cell cycle and give rise to astrocytes in response to interferon-γ. J Neurosci. 2011;31(16):6235-46.

Tanuma N, Sakuma H, Sasaki A, Matsumoto Y. Chemokine expression by astrocytes plays a role in microglia/macrophage activation and subsequent neurodegeneration in secondary progressive multiple sclerosis. Acta Neuropathol. 2006;112(2):195-204.

Taupenot L, Harper KL, O'connor DT. The chromogranin-secretogranin family. N Engl J Med. 2003;348(12):1134-49.

Tawk M, Makoukji J, Belle M, Fonte C, Trousson A, Hawkins T, Li H, Ghandour S, Schumacher M, Massaad C. Wnt/beta-catenin signaling is an essential and direct driver of myelin gene expression and myelinogenesis. J Neurosci. 2011;31(10):3729-42.

Theparambil SM, Ruminot I, Schneider HP, Shull GE, Deitmer JW. The electrogenic sodium bicarbonate cotransporter NBCe1 is a high-affinity bicarbonate carrier in cortical astrocytes. J Neurosci. 2014;34(4):1148-57.

Thiagalingam A, De bustros A, Borges M, Jasti R, Compton D, Diamond L, Mabry M, Ball DW, Baylin SB, Nelkin BD. RREB-1, a novel zinc finger protein, is involved in the differentiation response to Ras in human medullary thyroid carcinomas. Mol Cell Biol. 1996;16(10):5335-45.

Thompson DS, Nelson LM, Burns A, Burks JS, Franklin GM. The effects of pregnancy in multiple sclerosis: a retrospective study. Neurology. 1986;36(8):1097-9.

Thompson WL, Van eldik LJ. Inflammatory cytokines stimulate the chemokines CCL2/MCP-1 and CCL7/MCP-3 through NFkB and MAPK dependent pathways in rat astrocytes [corrected]. Brain Res. 2009;1287:47-57.

Thomson CE, Hunter AM, Griffiths IR, Edgar JM, Mcculloch MC. Murine spinal cord explants: a model for evaluating axonal growth and myelination *in vitro*. J Neurosci Res. 2006;84(8):1703-15.

Thomson CE, Mcculloch M, Sorenson A, Barnett SC, Seed BV, Griffiths IR, McLaughlin M. Myelinated, synapsing cultures of murine spinal cord--validation as an *in vitro* model of the central nervous system. Eur J Neurosci. 2008;28(8):1518-35.

Tian GF, Azmi H, Takano T, Xu Q, Peng W, Lin J, Oberheim N, Lou N, Wang X, Zielke HR, Kang J, Nedergaard M. An astrocytic basis of epilepsy. Nat Med. 2005;11(9):973-81.

Tian L, Ma L, Kaarela T, Li Z. Neuroimmune crosstalk in the central nervous system and its significance for neurological diseases. J Neuroinflammation. 2012;9:155.

Tian W, Kyriakides TR. Thrombospondin 2-null mice display an altered brain foreign body response to polyvinyl alcohol sponge implants. Biomed Mater. 2009;4(1):015010.

Tiwari-woodruff SK, Buznikov AG, Vu TQ, Micevych PE, Chen K, Kornblum HI, Bronstein JM. OSP/claudin-11 forms a complex with a novel member of the tetraspanin super family and beta1 integrin and regulates proliferation and migration of oligodendrocytes. J Cell Biol. 2001;153(2):295-305.

Toledo EM, Colombres M, Inestrosa NC. Wnt signaling in neuroprotection and stem cell differentiation. Prog Neurobiol. 2008;86(3):281-96.

Tontonoz P, Singer S, Forman BM, Sarraf P, Fletcher JA, Fletcher CD, Brun RP, Mueller E, Altiok S, Oppenheim H, Evans RM, Spiegelman BM. Terminal differentiation of human liposarcoma cells induced by ligands for peroxisome proliferator-activated receptor gamma and the retinoid X receptor. Proc Natl Acad Sci U S A 1997;94:237–41.

Toru-delbauffe D, Baghdassarian-chalaye D, Gavaret JM, Courtin F, Pomerance M, Pierre M. Effects of transforming growth factor beta 1 on astroglial cells in culture. J Neurochem. 1990;54(3):1056-61.

Trang T, Beggs S, Salter MW. Brain-derived neurotrophic factor from microglia: a molecular substrate for neuropathic pain. Neuron Glia Biol. 2011;7:99–108.

Traugott U, Lebon P. Interferon-gamma and Ia antigen are present on astrocytes in active chronic multiple sclerosis lesions. J Neurol Sci. 1988;84(2-3):257-64.

Tremblay ME, Lowery RL, Majewska AK. Microglial interactions with synapses are modulated by visual experience. PLoS Biol. 2010;8(11):e1000527.

Tremblay MÈ, Lowery RL, Majewska AK. Microglial interactions with synapses are modulated by visual experience. PLoS Biol. 2010;8(11):e1000527.

Tress O, Maglione M, May D, Pivneva T, Richter N, Seyfarth J, Binder S, Zlomuzica A, Seifert G, Theis M, Dere E, Kettenmann H, Willecke K. Panglial gap junctional communication is essential for maintenance of myelin in the CNS. J Neurosci. 2012;32(22):7499-518.

Tretiakova A, Steplewski A, Johnson EM, Khalili K, Amini S. Regulation of myelin basic protein gene transcription by Sp1 and Puralpha: evidence for association of Sp1 and Puralpha in brain. J Cell Physiol. 1999;181(1):160-8.

Tripathi RB, Mctigue DM. Chronically increased ciliary neurotrophic factor and fibroblast growth factor-2 expression after spinal contusion in rats. J Comp Neurol. 2008;510(2):129-44.

Trotter J, Schachner M. Cells positive for the O4 surface antigen isolated by cell sorting are able to differentiate into astrocytes or oligodendrocytes. Brain Res Dev Brain Res. 1989;46(1):115-22.

Tsukada N, Miyagi K, Matsuda M, Yanagisawa N, Yone K. Tumor necrosis factor and interleukin-1 in the CSF and sera of patients with multiple sclerosis. J Neurol Sci. 1991;104(2):230-4.

Uchida K, Baba H, Maezawa Y, Furukawa S, Furusawa N, Imura S. Histological investigation of spinal cord lesions in the spinal hyperostotic mouse (twy/twy): morphological changes in anterior horn cells and immunoreactivity to neurotropic factors. J Neurol. 1998;245(12):781-93.

Ueberham U, Ueberham E, Gruschka H, Arendt T. Connective tissue growth factor in Alzheimer's disease. Neuroscience. 2003;116(1):1-6.

Ueno M, Fujita Y, Tanaka T, Nakamura Y, Kikuta J, Ishii M, Yamashita T. Layer V cortical neurons require microglial support for survival during postnatal development. Nat. Neurosci. 2013;16:543–51.

Ullian EM, Sapperstein SK, Christopherson KS, Barres BA. Control of synapse number by glia. Science. 2001;291(5504):657-61.

Ullian EM, Sapperstein SK, Christopherson KS, Barres BA. Control of synapse number by glia. Science. 2001;291(5504):657-61.

Van den berg DL, Snoek T, Mullin NP, Yates A, Bezstarosti K, Demmers J, Chambers I, Poot RA. An Oct4-centered protein interaction network in embryonic stem cells. Cell Stem Cell. 2010;6(4):369-81.

Van der voorn P, Tekstra J, Beelen RH, Tensen CP, Van der valk P, De groot CJ. Expression of MCP-1 by reactive astrocytes in demyelinating multiple sclerosis lesions. Am J Pathol. 1999;154(1):45-51.

Van hove I, Lemmens K, Van de velde S, Verslegers M, Moons L. Matrix metalloproteinase-3 in the central nervous system: a look on the bright side. J Neurochem. 2012;123(2):203-16.

Van zwam M, Wierenga-wolf AF, Melief MJ, Schrijver B, Laman JD, Boven LA. Myelin ingestion by macrophages promotes their motility and capacity to recruit myeloid cells. J Neuroimmunol. 2010;225(1-2):112-7.

Varin A, Gordon S. Alternative activation of macrophages: immune function and cellular biology. Immunobiology. 2009;214(7):630-41.

Venance L, Cordier J, Monge M, Zalc B, Glowinski J, Giaume C. Homotypic and heterotypic coupling mediated by gap junctions during glial cell differentiation *in vitro*. Eur J Neurosci. 1995;7(3):451-61.

Vernerey J, Macchi M, Magalon K, Cayre M, Durbec P. Ciliary neurotrophic factor controls progenitor migration during remyelination in the adult rodent brain. J Neurosci. 2013;33(7):3240-50.

Vialou V, Balasse L, Callebert J, Launay JM, Giros B, Gautron S. Altered aminergic neurotransmission in the brain of organic cation transporter 3-deficient mice. J Neurochem. 2008;106(3):1471-82.

Vikman KS, Owe-larsson B, Brask J, Kristensson KS, Hill RH. Interferon-gamma-induced changes in synaptic activity and AMPA receptor clustering in hippocampal cultures. Brain Res. 2001;896(1-2):18-29.

Villarroya H, Violleau K, Ben younes-chennoufi A, Baumann N. Myelin-induced experimental allergic encephalomyelitis in Lewis rats: tumor necrosis factor alpha levels in serum and cerebrospinal fluid immunohistochemical expression in glial cells and macrophages of optic nerve and spinal cord. J Neuroimmunol. 1996;64(1):55-61.

Vincent AJ, Taylor JM, Choi-lundberg DL, West AK, Chuah MI. Genetic expression profile of olfactory ensheathing cells is distinct from that of Schwann cells and astrocytes. Glia. 2005;51(2):132-47.

Virchow, R. Die Cellularpathologie in ihrer Begrundung auf physiologische und pathologische Gewebelehre. Berlin. 1859. Verlag von August Hirschfeld.

Vogel KG, Paulsson M, Heinegård D. Specific inhibition of type I and type II collagen fibrillogenesis by the small proteoglycan of tendon. Biochem J. 1984;223(3):587-97.

Volterra A, Meldolesi J. Astrocytes, from brain glue to communication elements: the revolution continues. Nat Rev Neurosci. 2005;6(8):626-40.

Vom Berg J, Prokop S, Miller KR, Obst J, Kalin RE, Lopategui-Cabezas I, Wegner A, Mair F, Schipke CG, Peters O, Winter Y, Becher B, Heppner FL. Inhibition of IL-12/IL-23 signaling reduces Alzheimer's disease-like pathology and cognitive decline. Nat. Med. 2012;18:1812–19.

Vos CM, Van haastert ES, De groot CJ, Van der valk P, De vries HE. Matrix metalloproteinase-12 is expressed in phagocytotic macrophages in active multiple sclerosis lesions. J Neuroimmunol. 2003;138(1-2):106-14.

Voskuhl RR, Peterson RS, Song B, Ao Y, Morales LB, Tiwari-Woodruff S, Sofroniew MV. Reactive astrocytes form scar-like perivascular barriers to leukocytes during adaptive immune inflammation of the CNS. J Neurosci. 2009;29(37):11511-22.

Wake H, Moorhouse AJ, Jinno S, Kohsaka S, Nabekura J. Resting microglia directly monitor the functional state of synapses *in vivo* and determine the fate of ischemic terminals. J. Neurosci. 2009;29:3974–80.

Wakselman S, Bechade C, Roumier A, Bernard D, Triller A, Bessis A. Developmental neuronal death in hippocampus requires the microglial CD11b integrin and DAP12 immunoreceptor. J. Neurosci. 2008;28:8138–43.

Wallraff A, Köhling R, Heinemann U, Theis M, Willecke K, Steinhäuser C. The impact of astrocytic gap junctional coupling on potassium buffering in the hippocampus. J Neurosci. 2006;26(20):5438-47.

Walz W, Mukerji S. Lactate release from cultured astrocytes and neurons: a comparison. Glia. 1988;1(6):366-70.

Wang K, Walz W. Unusual topographical pattern of proximal astrogliosis around a cortical devascularizing lesion. J Neurosci Res. 2003;73:497-506.

Wang N, De Vuyst E, Ponsaerts R, Boengler K, Palacios-Prado N, Wauman J, Lai CP, De Bock M, Decrock E, Bol M, Vinken M, Rogiers V, Tavernier J, Evans WH, Naus CC, Bukauskas FF, Sipido KR, Heusch G, Schulz R, Bultynck G, Leybaert L. Selective inhibition of Cx43 hemichannels by Gap19 and its impact on myocardial ischemia/reperfusion injury. Basic Res Cardiol. 2013;108(1):309.

Wasseff SK, Scherer SS. Cx32 and Cx47 mediate oligodendrocyte:astrocyte and oligodendrocyte:oligodendrocyte gap junction coupling. Neurobiol Dis. 2011;42(3):506-13.

Watkins TA, Emery B, Mulinyawe S, Barres BA. Distinct stages of myelination regulated by gamma-secretase and astrocytes in a rapidly myelinating CNS coculture system. Neuron. 2008;60(4):555-69.

Watson LA, Wang X, Elbert A, Kernohan KD, Galjart N, Bérubé NG. Dual effect of CTCF loss on neuroprogenitor differentiation and survival. J Neurosci. 2014;34(8):2860-70.

Wei Q, Miskimins WK, Miskimins R. Sox10 acts as a tissue-specific transcription factor enhancing activation of the myelin basic protein gene promoter by p27Kip1 and Sp1. J Neurosci Res. 2004;78(6):796-802.

Wei Q, Miskimins WK, Miskimins R. Stage-specific expression of myelin basic protein in oligodendrocytes involves Nkx2.2-mediated repression that is relieved by the Sp1 transcription factor. J Biol Chem. 2005;280(16):16284-94.

Wei Q, Miskimins WK, Miskimins R. The Sp1 family of transcription factors is involved in p27(Kip1)-mediated activation of myelin basic protein gene expression. Mol Cell Biol. 2003;23(12):4035-45.

Wen TC, Tanaka J, Peng H, Desaki J, Matsuda S, Maeda N, Fujita H, Sato K, Sakanaka M. Interleukin 3 prevents delayed neuronal death in the hippocampal CA1 field. J Exp Med. 1998;188(4):635-49.

Wender R, Brown AM, Fern R, Swanson RA, Farrell K, Ransom BR. Astrocytic glycogen influences axon function and survival during glucose deprivation in central white matter. J Neurosci. 2000;20(18):6804-10.

White RE, Jakeman LB. Don't fence me in: harnessing the beneficial roles of astrocytes for spinal cord repair. Restor Neurol Neurosci. 2008;26(2-3):197-214.

Wiedermann CJ. Secretoneurin: a functional neuropeptide in health and disease. Peptides. 2000;21(8):1289-98.

Wiese S, Karus M, Faissner A. Astrocytes as a source for extracellular matrix molecules and cytokines. Front Pharmacol. 2012;3:120.

Wilhelmsson U, Bushong EA, Price DL, Smarr BL, Phung V, Terada M, Ellisman MH, Pekny M. Redefining the concept of reactive astrocytes as cells that remain within their unique domains upon reaction to injury. Proc Natl Acad Sci USA. 2006;103(46):17513-8.

Willems E, Leyns L, Vandesompele J. Standardization of real-time PCR gene expression data from independent biological replicates. Anal Biochem. 2008;379(1):127-9.

Williams A, Piaton G, Lubetzki C. Astrocytes--friends or foes in multiple sclerosis?. Glia. 2007;55(13):1300-12.

Williams BP, Abney ER, Raff MC. Macroglial cell development in embryonic rat brain: studies using monoclonal antibodies, fluorescence activated cell sorting, and cell culture. Dev Biol. 1985;112(1):126-34.

Williams JL, Holman DW, Klein RS. Chemokines in the balance: maintenance of homeostasis and protection at CNS barriers. Front Cell Neurosci. 2014;8:154.

Winter CG, Saotome Y, Levison SW, Hirsh D. A role for ciliary neurotrophic factor as an inducer of reactive gliosis, the glial response to central nervous system injury. Proc Natl Acad Sci USA. 1995;92(13):5865-9.

Włodek L, Radomski J, Wróbel M. The effect of 2-substituted thiazolidine-4(R)-carboxylic acids on non-protein sulphydryl levels and sulphurtransferase activities in mouse liver and brain. Biochem Pharmacol. 1993;46(1):190-3.

Wolswijk, 1998, vol 117 oligo regeneration in adult failure process in ms

Won R, Lee KH, Lee BH. Coenzyme Q10 protects neurons against neurotoxicity in hippocampal slice culture. Neuroreport. 2011;22(14):721-6.

Wood PM, Bunge RP. Myelination of cultured dorsal root ganglion neurons by oligodendrocytes obtained from adult rats. J Neurol Sci. 1986;74(2-3):153-69.

Wood PM, Williams AK. Oligodendrocyte proliferation and CNS myelination in cultures containing dissociated embryonic neuroglia and dorsal root ganglion neurons. Brain Res. 1984;314(2):225-41.

Wu J, Fang J, Yang Z, Chen F, Liu J, Wang Y. Wnt inhibitory factor-1 regulates glioblastoma cell cycle and proliferation. J Clin Neurosci. 2012a;19(10):1428-32.

Wu J, Zhao Z, Sabirzhanov B, Stoica BA, Kumar A, Luo T, Skovira J, Faden AI. Spinal cord injury causes brain inflammation associated with cognitive and affective changes: role of cell cycle pathways. J Neurosci. 2014;34(33):10989-1006.

Wu VW, Schwartz JP. Cell culture models for reactive gliosis: new perspectives. J Neurosci Res. 1998;51(6):675-81.

Wyss MT, Jolivet R, Buck A, Magistretti PJ, Weber B. *In vivo* evidence for lactate as a neuronal energy source. J Neurosci. 2011;31(20):7477-85.

Xie C, Li Z, Zhang GX, Guan Y. Wnt Signaling in Remyelination in Multiple Sclerosis: Friend or Foe?. Mol Neurobiol. 2013.

Xu Q, Bernardo A, Walker D, Kanegawa T, Mahley RW, Huang Y. Profile and regulation of apolipoprotein E (ApoE) expression in the CNS in mice with targeting of green fluorescent protein gene to the ApoE locus. J Neurosci. 2006;26(19):4985-94.

Xue L, Ding P, Xiao L, Hu M, Hu Z. Nestin is induced by hypoxia and is attenuated by hyperoxia in Müller glial cells in the adult rat retina. Int J Exp Pathol. 2011;92(6):377-81.

Yamagata T, Muroya K, Mukasa T, Igarashi H, Momoi M, Tsukahara T, Arahata K, Kumagai H, Momoi T. Hepatocyte growth factor specifically expressed in microglia activated Ras in the neurons, similar to the action of neurotrophic factors. Biochem. Biophys. Res. Commun. 1995;210:231-7.

Yamamura T, Konola JT, Wekerle H, Lees MB. Monoclonal antibodies against myelin proteolipid protein: identification and characterization of two major determinants. J Neurochem. 1991;57(5):1671-80.

Yamamuro A, Ago Y, Takuma K, Maeda S, Sakai Y, Baba A, Matsuda T. Possible involvement of astrocytes in neuroprotection by the cognitive enhancer T-588. Neurochem Res. 2003;28(12):1779-83.

Yamazaki Y, Hozumi Y, Kaneko K, Fujii S, Goto K, Kato H. Oligodendrocytes: facilitating axonal conduction by more than myelination. Neuroscientist. 2010;16(1):11-8.

Yamazaki Y, Hozumi Y, Kaneko K, Sugihara T, Fujii S, Goto K, Kato H. Modulatory effects of oligodendrocytes on the conduction velocity of action potentials along axons in the alveus of the rat hippocampal CA1 region. Neuron Glia Biol. 2007;3(4):325-34.

Yang J, Jiang Z, Fitzgerald DC, et al. Adult neural stem cells expressing IL-10 confer potent immunomodulation and remyelination in experimental autoimmune encephalitis. J Clin Invest. 2009;119(12):3678-91.

Yang JF, Tao HQ, Liu YM, Zhan XX, Liu Y, Wang XY, Wang JH, Mu LL, Yang LL, Gao ZM, Kong QF, Wang GY, Han JH, Sun B, Li HL.Characterization of the interaction between astrocytes and encephalitogenic lymphocytes during the development of experimental autoimmune encephalitomyelitis (EAE) in mice. Clin Exp Immunol. 2012a;170(3):254-65.

Yang P, Yang Z. Enhancing intrinsic growth capacity promotes adult CNS regeneration. J Neurol Sci. 2012b;312(1-2):1-6.

Yang Y, Quitschke WW, Vostrov AA, Brewer GJ. CTCF is essential for up-regulating expression from the amyloid precursor protein promoter during differentiation of primary hippocampal neurons. J Neurochem. 1999;73(6):2286-98.

Yang Y, Vidensky S, Jin L, Jie C, Lorenzini I, Frankl M, Rothstein JD. Molecular comparison of GLT1+ and ALDH1L1+ astrocytes *in vivo* in astroglial reporter mice. Glia. 2011;59(2):200-7.

Yang Z, Strickland DK, Bornstein P. Extracellular matrix metalloproteinase 2 levels are regulated by the low density lipoprotein-related scavenger receptor and thrombospondin 2. J Biol Chem. 2001;276(11):8403-8.

Yang Z, Wang Y, Fang J, Chen F, Liu J, Wu J, Wang Y, Song T, Zeng F, Rao Y. Downregulation of WIF-1 by hypermethylation in astrocytomas. Acta Biochim Biophys Sin (Shanghai). 2010;42(6):418-25.

Yao DL, Liu X, Hudson LD, Webster HD. Insulin-like growth factor-I given subcutaneously reduces clinical deficits, decreases lesion severity and upregulates synthesis of myelin proteins in experimental autoimmune encephalomyelitis. Life Sci. 1996;58(16):1301-6.

Yao Y, Tsirka SE. Truncation of monocyte chemoattractant protein 1 by plasmin promotes blood-brain barrier disruption. J Cell Sci. 2011;124(Pt 9):1486-95.

Ye F, Chen Y, Hoang T, Montgomery RL, Zhao XH, Bu H, Hu T, Taketo MM, van Es JH, Clevers H, Hsieh J, Bassel-Duby R, Olson EN, Lu QR. HDAC1 and HDAC2 regulate oligodendrocyte differentiation by disrupting the beta-catenin-TCF interaction. Nat Neurosci. 2009;12(7):829-38.

Ye J, Cao L, Cui R, Huang A, Yan Z, Lu C, He C. The effects of ciliary neurotrophic factor on neurological function and glial activity following contusive spinal cord injury in the rats. Brain Res. 2004;997(1):30-9.

Ye S, Li P, Tong C, Ying QL. Embryonic stem cell self-renewal pathways converge on the transcription factor Tfcp2l1. EMBO J. 2013;32(19):2548-60.

Yin D, Chave KJ, Macaluso CR, Galivan J, Yao R. Structural organization of the human gamma-glutamyl hydrolase gene. Gene. 1999;238(2):463-70.

Yin J, Chen JD. Roles of interstitial cells of Cajal in regulating gastrointestinal motility: *in vitro* versus *in vivo* studies. J Cell Mol Med. 2008;12(4):1118-29.

Yong VW, Krekoski CA, Forsyth PA, Bell R, Edwards DR. Matrix metalloproteinases and diseases of the CNS. Trends Neurosci. 1998;21(2):75–80.

Yong VW, Moumdjian R, Yong FP, Ruijs TC, Freedman MS, Cashman N, Antel JP. Gamma-interferon promotes proliferation of adult human astrocytes *in vitro* and reactive gliosis in the adult mouse brain *in vivo*. Proc Natl Acad Sci USA. 1991;88(16):7016-20.

Yoshida K, Taga T, Saito M, Suematsu S, Kumanogoh A, Tanaka T, Fujiwara H, Hirata M, Yamagami T, Nakahata T, Hirabayashi T, Yoneda Y, Tanaka K, Wang WZ, Mori C, Shiota K, Yoshida N, Kishimoto T. Targeted disruption of gp130, a common signal transducer for the interleukin 6 family of cytokines, leads to myocardial and hematological disorders. Proc Natl Acad Sci USA 1996;93(1):407–11.

Yoshida M, Saito H, Katsuki H. Neurotrophic effects of conditioned media of astrocytes isolated from different brain regions on hippocampal and cortical neurons. Experientia. 1995;51(2):133-6.

Yoshimatsu T, Kawaguchi D, Oishi K, Takeda K, Akira S, Masuyama N, Gotoh Y. Non-cell-autonomous action of STAT3 in maintenance of neural precursor cells in the mouse neocortex. Development. 2006;133(13):2553-63.

Young N, Pearl DK, Van brocklyn JR. Sphingosine-1-phosphate regulates glioblastoma cell invasiveness through the urokinase plasminogen activator system and CCN1/Cyr61. Mol Cancer Res. 2009;7(1):23-32.

Yu L, Guan Y, Wu X, Chen Y, Liu Z, Du H, Wang X. Wnt Signaling is altered by spinal cord neuronal dysfunction in amyotrophic lateral sclerosis transgenic mice. Neurochem Res. 2013;38(9):1904-13.

Yuen TJ, Johnson KR, Miron VE, Zhao C, Quandt J, Harrisingh MC, Swire M, Williams A, McFarland HF, Franklin RJ, Ffrench-Constant C. Identification of endothelin 2 as an inflammatory factor that promotes central nervous system remyelination. Brain. 2013;136(Pt 4):1035-47.

Zador Z, Stiver S, Wang V, Manley GT. Role of aquaporin-4 in cerebral edema and stroke. Handb Exp Pharmacol. 2009;(190):159-70.

Zaheer S, Wu Y, Yang X, Ahrens M, Sahu SK, Zaheer A. Clinical course of myelin oligodendrocyte glycoprotein 35-55 induced experimental autoimmune encephalomyelitis is aggravated by glia maturation factor. Neurochem Int. 2012;60(3):215-9.

Zamanian JL, Xu L, Foo LC, Nouri N, Zhou L, Giffard RG, Barres BA. Genomic analysis of reactive astrogliosis. J Neurosci. 2012;32(18):6391-410.

Zappalà A, Li volti G, Serapide MF, Pellitteri R, Falchi M, La Delia F, Cicirata V, Cicirata F. Expression of pannexin2 protein in healthy and ischemized brain of adult rats. Neuroscience. 2007;148(3):653-67.

Zawia NH, Sharan R, Brydie M, Oyama T, Crumpton T. Sp1 as a target site for metal-induced perturbations of transcriptional regulation of developmental brain gene expression. Brain Res Dev Brain Res. 1998;107(2):291-8.

Zelenaia O, Schlag BD, Gochenauer GE, Ganel R, Song W, Beesley JS, Grinspan JB, Rothstein JD, Robinson MB. Epidermal growth factor receptor agonists increase expression of glutamate transporter GLT-1 in astrocytes through pathways dependent on phosphatidylinositol 3-kinase and transcription factor NF-kappaB. Mol Pharmacol. 2000;57(4):667-78.

Zhan H, Moore CS, Chen B, Zhou X, Ma XM, Ijichi K, Bennett MV, Li XJ, Crocker SJ, Wang ZW. Stomatin inhibits pannexin-1-mediated whole-cell currents by interacting with its carboxyl terminal. PLoS ONE. 2012;7(6):e39489.

Zhang B, Ma JX. Wnt pathway antagonists and angiogenesis. Protein Cell. 2010;1(10):898-906.

Zhang CL, Zou Y, He W, Gage FH, Evans RM. A role for adult TLX-positive neural stem cells in learning and behaviour. Nature. 2008;451(7181):1004-7.

Zhang H, Jarjour AA, Boyd A, Williams A. Central nervous system remyelination in culture--a tool for multiple sclerosis research. Exp Neurol. 2011;230(1):138-48.

Zhang SC. Defining glial cells during CNS development. Nat Rev Neurosci. 2001;2(11):840-3.

Zhang SJ, Zou M, Lu L, Lau D, Ditzel DA, Delucinge-Vivier C, Aso Y, Descombes P, Bading H. Nuclear calcium signaling controls expression of a large gene pool: identification of a gene program for acquired neuroprotection induced by synaptic activity. PLoS Genet. 2009;5(8):e1000604.

Zhao J, Fu Y, Liu CC, Shinohara M, Nielsen HM, Dong Q, Kanekiyo T, Bu G. Retinoic acid isomers facilitate apolipoprotein E production and lipidation in astrocytes through the retinoid X receptor/retinoic acid receptor pathway. J Biol Chem. 2014;289(16):11282-92.

Zhao Y, Patzer A, Gohlke P, Herdegen T, Culman J. The intracerebral application of the PPARgamma-ligand pioglitazone confers neuroprotection against focal ischaemia in the rat brain. Eur J Neurosci. 2005a;22(1):278-82.

Zhao Z, Ho L, Wang J, Qin W, Festa ED, Mobbs C, Hof P, Rocher A, Masur S, Haroutunian V, Pasinetti GM. Connective tissue growth factor (CTGF) expression in the brain is a downstream effector of insulin resistance- associated promotion of Alzheimer's disease beta-amyloid neuropathology. FASEB J. 2005b;19(14):2081-2.

Zheng MM, Zhang XH. Cross-reactivity between human cytomegalovirus peptide 981-1003 and myelin oligodendroglia glycoprotein peptide 35-55 in experimental autoimmune encephalomyelitis in Lewis rats. Biochem Biophys Res Commun. 2014;443(3):1118-23.

Zheng Z, Jian J, Zhang X, Zara JN, Yin W, Chiang M, Liu Y, Wang J, Pang S, Ting K, Soo C. Reprogramming of human fibroblasts into multipotent cells with a single ECM proteoglycan, fibromodulin. Biomaterials. 2012;33(24):5821-31.

Zheng Z, Nguyen C, Zhang X, Khorasani H, Wang JZ, Zara JN, Chu F, Yin W, Pang S, Le A, Ting K, Soo C. Delayed wound closure in fibromodulin-deficient mice is associated with increased TGF-ß3 signaling. J Invest Dermatol. 2011;131(3):769-78.

Zheng Z, Nguyen K, Wang JZ, Zhang X, Ting K, Soo C. Differential expression of transforming growth factor (TGF)-betas and TGF-beta receptors during skin wound healing in adult mice with fibromodulin (FMOD) deficiency. Wound Repair Regen. 2008;16: A28-A28.

Zhong J, Kim HT, Lyu J, Yoshikawa K, Nakafuku M, Lu W. The Wnt receptor Ryk controls specification of GABAergic neurons versus oligodendrocytes during telencephalon development. Development. 2011;138(3):409-19.

Zhou F, Zhang L, Wang A, Song B, Gong K, Zhang L, Hu M, Zhang X, Zhao N, Gong Y. The association of GSK3 beta with E2F1 facilitates nerve growth factor-induced neural cell differentiation. J Biol Chem. 2008;283(21):14506-15.

Zhu Y, Jin K, Mao XO, Greenberg DA. Vascular endothelial growth factor promotes proliferation of cortical neuron precursors by regulating E2F expression. FASEB J. 2003;17(2):186-93.

Zhu ZH, Yang R, Fu X, Wang YQ, Wu GC. Astrocyte-conditioned medium protecting hippocampal neurons in

primary cultures against corticosterone-induced damages via PI3-K/Akt signal pathway. Brain Res. 2006;1114(1):1-10.

Zoidl G, Dermietzel R. On the search for the electrical synapse: a glimpse at the future. Cell Tissue Res. 2002;310(2):137-42.

Zonta M, Angulo MC, Gobbo S, Rosengarten B, Hossmann KA, Pozzan T, Carmignoto G. Neuron-to-astrocyte signaling is central to the dynamic control of brain microcirculation. Nat Neurosci. 2003;6(1):43-50.